

In this Issue

Highlights from this issue of *A&R* | By Lara C. Pullen, PhD

Gene Expression Biomarkers as a Classifier of Methotrexate Nonresponse

In this issue, Plant et al (p. 678) report the results of gene expression profiling in samples of whole blood collected from patients with rheumatoid arthritis (RA) at pretreatment and

p. 678 4 weeks following the initiation of methotrexate (MTX) therapy. When the investigators looked at gene expression in patients starting MTX treatment, they found that changes in gene expression could provide an early classifier of the MTX treatment response.

The researchers were able to use the ratio of transcript values and L2-regularized

logistic regression to develop a highly predictive classifier of MTX nonresponse. They then compared the classifier to models that included clinical covariates and found that the classifier was superior to these earlier models. The authors suggest that their classifier should be able to identify those patients who are unlikely to benefit from MTX over a 6-month course of treatment. Such patients could then have their treatment escalated more rapidly, potentially improving clinical response. These findings emphasize the important role of

early treatment biomarker monitoring when patients with RA are started on MTX.

The investigators then performed a pathway analysis of their identified gene networks and found that at pretreatment and at 4 weeks after treatment initiation, nonresponders had significant overrepresentation of type I interferon signaling pathway genes. The authors explain in their discussion that type I interferon signaling activates the JAK/STAT pathway and influences the development of both innate and adaptive immune responses.

Evaluating Pulmonary Hypertension in Patients With Systemic Sclerosis

Pulmonary arterial compliance (PAC), the ratio of stroke volume to pulse pressure, and cardiac index are means of measuring right ventricular output reserve. This parameter is increasingly being regarded as an important prognostic indicator in patients

p. 805 with pulmonary hypertension (PH). In this issue, Nagel et al (p. 805) report the results of the first prospective study to assess and compare right ventricular output reserve and PAC in patients with systemic sclerosis (SSc) who have normal mean pulmonary artery pressure (PAP), those with mildly elevated mean PAP, and those with manifest PH.

The investigators found that patients with mildly elevated mean PAP had a lower 6-minute walking distance, lower cardiac index, higher pulmonary vascular resistance during exercise, and lower PAC at rest and during different stages of exercise compared to patients with normal mean PAP. Patients with SSc, mildly elevated mean PAP, and impaired 6-minute walking distance also were more likely to have reduced PAC during exercise and reduced right ventricular output reserve. In contrast, mean right ventricle cardiac index at rest was normal in patients with mildly elevated PAP and did not differ from that seen in

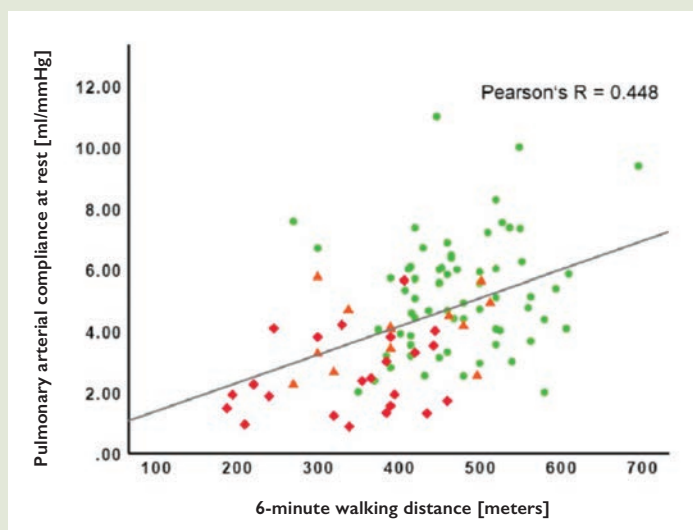


Figure 1. Significant correlation between pulmonary arterial compliance at rest and 6-minute walking distance, determined by Pearson's correlation analysis. Circles represent patients with mean pulmonary artery pressure (PAP) of <20 mm Hg, triangles represent patients with mean PAP of 21–24 mm Hg, and squares represent patients with mean PAP of >25 mm Hg.

patients with normal mean PAP. The investigators concluded that the reduced PAC during exercise may be the result of impaired coupling between the right ventricle and the pulmonary vasculature. They also note that their data reinforce the clinical relevance of mildly elevated mean PAP in patients with SSc.

IgG Autoantibody Repertoire in Established Systemic Lupus Erythematosus

Scientists consider epitope spreading to be an important aspect of the development of systemic autoimmune diseases. In this issue, Vordenbäumen et al (p. 736) report the results of their investigation of the role of epitope spreading in established systemic lupus erythematosus (SLE). The investigators performed a 6-year longitudinal surveillance of the IgG autoantibody repertoire in patients with established SLE and compared it to that seen in healthy

p. 736

controls. They found that patients had a higher total number of autoantibodies, mean fluorescence intensity (MFI), and number of autoantibodies in epitope fine mapping. While the total number of autoantibodies to distinct autoantigens in patients remained stable over time, the mean MFI decreased. However, the researchers identified 22 individual autoantibodies in patients with SLE that, after Bonferroni correction, had higher time-averaged MFIs compared to controls. Thus, patients sustained the breadth of their

autoantibody repertoire without significantly expanding it.

Although the total number of recognized autoepitopes did not correlate with disease activity, new organ involvement was associated with more clones of the anti-U1 RNP autoantibody. Moreover, mean MFI was higher in patients with lupus nephritis. The authors also confirmed the associations of disease activity with antibodies to double-stranded DNA and with histone cluster 2 H3c.

Chronic Opioid Use and Arthritis

Since the early 2000s, the medical community has recognized the increasing rate of opioid prescribing and the resulting opioid epidemic as major public health concerns. Unfortunately, even though arthritis is one of the most common sources of chronic pain in the US, long-term prescription opioid use is not well-studied in this population. In this issue, 2 articles explore the use of opioids in the treatment of arthritis.

p. 712

Desai et al (p. 712) sought to determine whether or not there was variation in long-term opioid use in patients with osteoarthritis (OA) according to geography and health care access. The researchers report that there is a substantial statewide variation in rates of treatment with long-term opioids in patients with OA. Their large observational cohort study of Medicare enrollees with OA ($n = 358,121$; mean age 74 years) undergoing total joint replacement included patients from 4,080 primary care service areas (PCSAs). The unadjusted mean percentage of long-term opioid use varied from 8.9% in Minnesota to 26.4% in Alabama, and this variation persisted in adjusted models.

The study demonstrated that the variation in long-term opioid use could not be fully explained by the differences in access to health care providers, varying case-mix, or state-level policies. The only factor even modestly associated with rates of long-term opioid use between PCSAs was access to primary care providers (PCPs). Specifically, the adjusted mean difference between PCSAs with the highest (>8.6) versus lowest (<3.6) concentration of PCPS was 1.4%. In contrast, access to rheumatologists was not associated with long-term opioid use.

Lee et al (p. 670) report that, from 2002 to 2015, chronic opioid use doubled (from 7.4% to 16.9%) among patients with

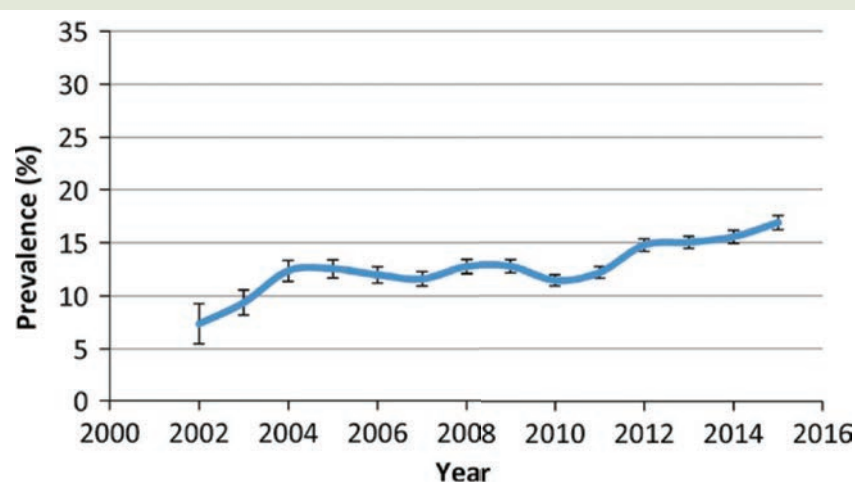


Figure 1. Trend in chronic opioid use (defined as >2 consecutive report of opioid use) among 33,739 rheumatoid arthritis patients with >90 days of follow-up. Bars show the 95% confidence interval (Lee et al, 2019).

rheumatoid arthritis (RA). In their discussion, the investigators state that self-reported chronic opioid use among their population of patients with RA continued to increase from 2010 to 2015. When the investigators looked to identify clinical predictors of chronic opioid use in this group, they found that pain and use of antidepressants were the strongest predictors of use, followed by high disease activity and high level of disability. In contrast, Asian ethnicity was most strongly associated with a decreased risk of chronic opioid use.

Both of these studies show that strategies for stringent control of RA disease activity and management of pain and depression should be research priorities. Such an approach should help to curb the rise of chronic opioid use in these populations.

Arthritis & Rheumatology

An Official Journal of the American College of Rheumatology
www.arthritisrheum.org and wileyonlinelibrary.com

Editor

Richard J. Bucala, MD, PhD
Yale University School of Medicine, New Haven

Deputy Editor

Daniel H. Solomon, MD, MPH, *Boston*

Co-Editors

Joseph E. Craft, MD, *New Haven*
David T. Felson, MD, MPH, *Boston*
Richard F. Loeser Jr., MD, *Chapel Hill*
Peter A. Nigrovic, MD, *Boston*
Janet E. Pope, MD, MPH, FRCPC, *London, Ontario*
Christopher T. Ritchlin, MD, MPH, *Rochester*
John Varga, MD, *Chicago*

Co-Editor and Review Article Editor

Robert Terkeltaub, MD, *San Diego*

Clinical Trials Advisor

Michael E. Weinblatt, MD, *Boston*

Social Media Editor

Paul H. Sufka, MD, *St. Paul*

Journal Publications Committee

Shervin Assassi, MD, MS, *Chair, Houston*
Vivian Bykerk, MD, FRCPC, *New York*
Cecilia P. Chung, MD, MPH, *Nashville*
Meenakshi Jolly, MD, MS, *Chicago*
Kim D. Jones, RN, PhD, FNP, *Portland*
Maximilian Konig, MD, *Baltimore*
Linda C. Li, PT, MSc, PhD, *Vancouver*
Uyen-Sa Nguyen, MPH, DSc, *Worcester*

Editorial Staff

Jane S. Diamond, MPH, *Managing Editor, Atlanta*
Maggie Parry, *Assistant Managing Editor, Atlanta*
Lesley W. Allen, *Senior Manuscript Editor, Atlanta*
Kelly Barraza, *Manuscript Editor, Atlanta*
Jessica Hamilton, *Manuscript Editor, Atlanta*
Ilani S. Lorber, MA, *Manuscript Editor, Atlanta*
Emily W. Wehby, MA, *Manuscript Editor, Atlanta*
Sara Omer, *Editorial Coordinator, Atlanta*
Brittany Swett, *Assistant Editor, New Haven*
Carolyn Roth, *Senior Production Editor, Boston*

Associate Editors

Daniel Aletaha, MD, MS, *Vienna*
Heather G. Allore, PhD, *New Haven*
Lenore M. Buckley, MD, MPH, *New Haven*
Daniel J. Clauw, MD, *Ann Arbor*
Robert A. Colbert, MD, PhD, *Bethesda*
Karen H. Costenbader, MD, MPH, *Boston*
Nicola Dalbeth, MD, FRACP, *Auckland*
Kevin D. Deane, MD, *Denver*
Patrick M. Gaffney, MD, *Oklahoma City*

Mark C. Genovese, MD, *Palo Alto*
Insoo Kang, MD, *New Haven*
Wan-Uk Kim, MD, PhD, *Seoul*
S. Sam Lim, MD, MPH, *Atlanta*
Anne-Marie Malfait, MD, PhD, *Chicago*
Paul A. Monach, MD, PhD, *Boston*
Chester V. Oddis, MD, *Pittsburgh*
Andras Perl, MD, PhD, *Syracuse*
Jack Porrino, MD, *New Haven*

Timothy R. D. J. Radstake, MD, PhD, *Utrecht*
William Robinson, MD, PhD, *Palo Alto*
Georg Schett, MD, *Erlangen*
Nan Shen, MD, *Shanghai*
Betty P. Tsao, PhD, *Charleston*
Ronald van Vollenhoven, MD, PhD, *Amsterdam*
Fredrick M. Wigley, MD, *Baltimore*

Advisory Editors

Abhishek Abhishek, MD, PhD, *Nottingham*
Tom Appleton, MD, PhD, *London, Ontario*
Charles Auffray, PhD, *Lyon*
André Ballesteros-Tato, PhD, *Birmingham*
Lorenzo Beretta, MD, *Milan*
Bryce A. Binstadt, MD, PhD, *Minneapolis*
Jaime Calvo-Alen, MD, *Vitoria*
Scott Canna, MD, *Pittsburgh*
Niek de Vries, MD, PhD, *Amsterdam*

Liana Fraenkel, MD, MPH, *New Haven*
Monica Guma, MD, PhD, *La Jolla*
Nigil Haroon, MD, PhD, *Toronto*
Erica Herzog, MD, PhD, *New Haven*
Hui-Chen Hsu, PhD, *Birmingham*
Mariana J. Kaplan, MD, *Bethesda*
Jonathan Kay, MD, *Worcester*
Francis Lee, MD, PhD, *New Haven*
Sang-Il Lee, MD, PhD, *Jinju*

Rik Lories, MD, PhD, *Leuven*
Bing Lu, PhD, *Boston*
Suresh Mahalingam, PhD, *Southport, Queensland*
Tony R. Merriman, PhD, *Otago*
Yukinori Okada, MD, PhD, *Osaka*
Aridaman Pandit, PhD, *Utrecht*
Kevin Winthrop, MD, MPH, *Portland*
Raghunatha Yammani, PhD, *Winston-Salem*
Kazuki Yoshida, MD, MPH, MS, *Boston*

AMERICAN COLLEGE OF RHEUMATOLOGY

Paula Marchetta, MD, MBA, *New York*, **President**
Ellen M. Gravallese, MD, *Worcester*, **President-Elect**
David R. Karp, MD, PhD, *Dallas*, **Treasurer**

Kenneth G. Saag, MD, MSc, *Birmingham*, **Secretary**
Mark Andrejeski, *Atlanta*, **Executive Vice-President**

© 2019 American College of Rheumatology. All rights reserved. No part of this publication may be reproduced, stored or transmitted in any form or by any means without the prior permission in writing from the copyright holder. Authorization to copy items for internal and personal use is granted by the copyright holder for libraries and other users registered with their local Reproduction Rights Organization (RRO), e.g. Copyright Clearance Center (CCC), 222 Rosewood Drive, Danvers, MA 01923, USA (www.copyright.com), provided the appropriate fee is paid directly to the RRO. This consent does not extend to other kinds of copying such as copying for general distribution, for advertising or promotional purposes, for creating new collective works or for resale. Special requests should be addressed to: permissions@wiley.com

Access Policy: Subject to restrictions on certain backfiles, access to the online version of this issue is available to all registered Wiley Online Library users 12 months after publication. Subscribers and eligible users at subscribing institutions have immediate access in accordance with the relevant subscription type. Please go to onlinelibrary.wiley.com for details.

The views and recommendations expressed in articles, letters, and other communications published in Arthritis & Rheumatology are those of the authors and do not necessarily reflect the opinions of the editors, publisher, or American College of Rheumatology. The publisher and the American College of Rheumatology do not investigate the information contained in the classified advertisements in this journal and assume no responsibility concerning them. Further, the publisher and the American College of Rheumatology do not guarantee, warrant, or endorse any product or service advertised in this journal.

Cover design: Todd Machen

©This journal is printed on acid-free paper.

Arthritis & Rheumatology

An Official Journal of the American College of Rheumatology
www.arthritisrheum.org and wileyonlinelibrary.com

VOLUME 71 • May 2019 • NO. 5

In This Issue	A15
Clinical Connections	A17
Special Articles	
Editorial: Prescribing Opioids for Severe Hip and Knee Osteoarthritis Varies Widely in the United States: The Devil Is in the Details <i>Janet E. Pope</i>	659
Editorial: Casting a Spotlight on the Right Ventricle in Systemic Sclerosis <i>Steven Hsu</i>	662
ACR Presidential Address: Building on the Strengths of Our Unique Specialty <i>David I. Daikh</i>	664
Rheumatoid Arthritis	
Chronic Opioid Use in Rheumatoid Arthritis: Prevalence and Predictors <i>Yvonne C. Lee, Joel Kremer, Hongshu Guan, Jeffrey Greenberg, and Daniel H. Solomon</i>	670
Profiling of Gene Expression Biomarkers as a Classifier of Methotrexate Nonresponse in Patients With Rheumatoid Arthritis <i>Darren Plant, Mateusz Maciejewski, Samantha Smith, Nisha Nair, the Maximising Therapeutic Utility in Rheumatoid Arthritis Consortium, the RAMS Study Group, Kimme Hyrich, Daniel Ziemek, Anne Barton, and Suzanne Verstappen</i>	678
Evaluation of the Short-, Mid-, and Long-Term Effects of Tofacitinib on Lymphocytes in Patients With Rheumatoid Arthritis <i>Ronald van Vollenhoven, Eun Bong Lee, Sander Strengholt, Christopher Mojcik, Hernan Valdez, Sriram Krishnaswami, Pinaki Biswas, Irina Lazariciu, Anasuya Hazra, James D. Clark, Jennifer Hodge, Lisy Wang, and Ernest Choy</i>	685
Brief Report: Association of Baseline Peptidylarginine Deiminase 4 Autoantibodies With Favorable Response to Treatment Escalation in Rheumatoid Arthritis <i>Erika Darrah, Fang Yu, Laura C. Cappelli, Antony Rosen, James R. O'Dell, and Ted R. Mikuls</i>	696
Ibuprofen Inhibits Chemokine Expression in Rheumatoid Arthritis Synovial Fibroblasts and Exhibits Immunomodulatory Activity in Experimental Arthritis <i>Felix I. L. Clancy and Richard O. Williams</i>	703
Osteoarthritis	
Association of Geography and Access to Health Care Providers With Long-Term Prescription Opioid Use in Medicare Patients With Severe Osteoarthritis: A Cohort Study <i>Rishi J. Desai, Yinzhu Jin, Patricia D. Franklin, Yvonne C. Lee, Brian T. Bateman, Joyce Lii, Daniel H. Solomon, Jeffrey N. Katz, and Seoyoung C. Kim</i>	712
Spondyloarthritis	
Progression of Structural Damage in the Sacroiliac Joints in Patients With Early Axial Spondyloarthritis During Long-Term Anti-Tumor Necrosis Factor Treatment: Six-Year Results of Continuous Treatment With Etanercept <i>Valeria Rios Rodriguez, Kay-Geert Hermann, Anja Weiß, Joachim Listing, Hildrun Haibel, Christian Althoff, Fabian Proft, Olaf Behmer, Joachim Sieper, and Denis Poddubnyy</i>	722
Sensitivity and Specificity of Autoantibodies Against CD74 in Nonradiographic Axial Spondyloarthritis <i>Elke Riechers, Niklas Baerlecken, Xenofon Baraliakos, Katrin Achilles-Mehr Bakhsh, Peer Aries, Bettina Bannert, Klaus Becker, Jan Brandt-Jürgens, Jürgen Braun, Boris Ehrenstein, Hans-Hartwig Euler, Martin Fleck, Reinhard Hein, Kirsten Karberg, Lars Köhler, Torsten Matthias, Regina Max, Adelheid Melzer, Dirk Meyer-Olson, Jürgen Rech, Karin Rockwitz, Martin Rudwaleit, Reinhold E. Schmidt, Eva Schweikhard, Joachim Sieper, Carsten Stille, Ulrich von Hinüber, Peter Wagoner, Heike-Franziska Weidemann, Silke Zinke, and Torsten Witte</i>	729
Systemic Lupus Erythematosus	
Comprehensive Longitudinal Surveillance of the IgG Autoantibody Repertoire in Established Systemic Lupus Erythematosus <i>Stefan Vordenbäumen, Ralph Brinks, Annika Hoyer, Rebecca Fischer-Betz, Georg Pongratz, Torsten Lowin, Hans-Dieter Zucht, Petra Budde, Ellen Bleck, Peter Schulz-Knappe, and Matthias Schneider</i>	736
Identification of Low-Abundance Urinary Biomarkers in Lupus Nephritis Using Electrochemiluminescence Immunoassays <i>Samantha Stanley, Chi Chiu Mok, Kamala Vanarsa, Deena Habazi, Jennifer Li, Claudia Pedroza, Ramesh Saxena, and Chandra Mohan</i>	744
Monitoring Disease Activity in Systemic Lupus Erythematosus With Single-Molecule Array Digital Enzyme-Linked Immunosorbent Assay Quantification of Serum Interferon- α <i>Alexis Mathian, Suzanne Mouries-Martin, Karim Dorgham, Hervé Devilliers, Laura Barnabei, Elyès Ben Salah, Fleur Cohen-Aubart, Laura Garrido Castillo, Julien Haroche, Miguel Hie, Marc Pineton de Chambrun, Makoto Miyara, Delphine Sterlin, Micheline Pha, Du Lê Thi Huong, Frédéric Rieux-Laucat, Flore Rozenberg, Guy Gorochov, and Zahir Amoura</i>	756

Brief Report: Promotion of Calcium/Calmodulin-Dependent Protein Kinase 4 by GLUT1-Dependent Glycolysis in Systemic Lupus Erythematosus <i>Tomohiro Koga, Tomohito Sato, Kaori Furukawa, Shimpei Morimoto, Yushiro Endo, Masataka Umeda, Remi Sumiyoshi, Shoichi Fukui, Shin-ya Kawashiri, Naoki Iwamoto, Kunihiko Ichinose, Mami Tamai, Tomoki Origuchi, Hideki Nakamura, and Atsushi Kawakami</i>	766
Adenosine 2a Receptor Signal Blockade of Murine Autoimmune Arthritis via Inhibition of Pathogenic Germinal Center–Follicular Helper T Cells <i>Shirdi E. Schmiel, Lokesh A. Kalekar, Na Zhang, Thomas W. Blankespoor, Londyn J. Robinson, and Daniel L. Mueller</i>	773
Vasculitis	
Effect of Disease Activity at Three and Six Months After Diagnosis on Long-Term Outcomes in Antineutrophil Cytoplasmic Antibody–Associated Vasculitis <i>Seerapani Gopaluni, Oliver Flossmann, Mark A. Little, Paul O'Hara, Pirow Bekker, and David Jayne, on behalf of the European Vasculitis Society</i>	784
Monocyte-Derived Interleukin-1 β As the Driver of S100A12-Induced Sterile Inflammatory Activation of Human Coronary Artery Endothelial Cells: Implications for the Pathogenesis of Kawasaki Disease <i>Giulia Armaroli, Emely Verweyen, Carolin Pretzer, Katharina Kessel, Keiichi Hirono, Fukiko Ichida, Mako Okabe, David A. Cabral, Dirk Foell, Kelly L. Brown, and Christoph Kessel</i>	792
Systemic Sclerosis	
Reduced Right Ventricular Output Reserve in Patients With Systemic Sclerosis and Mildly Elevated Pulmonary Artery Pressure <i>Christian Nagel, Alberto M. Marra, Nicola Benjamin, Norbert Blank, Antonio Cittadini, Gerry Coghlan, Oliver Distler, Christopher P. Denton, Benjamin Egenlauf, Christoph Fiehn, Christine Fischer, Satenik Harutyunova, Marius M. Hoeper, Hanns-Martin Lorenz, Panagiota Xanthouli, Eduardo Bossone, and Ekkehard Grünig</i>	805
Autoimmunity	
Association of Dendritic Cell Signatures With Autoimmune Inflammation Revealed by Single-Cell Profiling <i>Michelle P. Ashton, Anne Eugster, Sevina Dietz, Doreen Loebel, Annett Lindner, Denise Kuehn, Anna E. Taranko, Babett Heschel, Anita Gavrisan, Anette-Gabriele Ziegler, Martin Aringer, and Ezio Bonifacio</i>	817
Concise Communication	
Efficacy of Baricitinib in the Treatment of Chilblains Associated With Aicardi-Goutières Syndrome, a Type I Interferonopathy <i>Kornvalee Meesilpavikkai, Willem A. Dik, Benjamin Schrijver, Cornelia G. van Helden-Meeuwssen, Marjan A. Versnel, P. Martin van Hagen, Emilia K. Bijlsma, Claudia A. L. Ruivenkamp, Margreet J. Oele, and Virgil A. S. H. Dalm</i>	829
Clinical Images	
Heel Pain in a Young Patient—Calcaneal Involvement in Juvenile Spondyloarthritis <i>Stacey Lallemand and Jean-Denis Laredo</i>	831
Letters	
Galectin 9: Friend or Foe of Systemic Lupus Erythematosus? Comment on the Article by Zeggar et al <i>Wang-Dong Xu, Lin-Chong Su, and An-Fang Huang</i>	832
Reply <i>Jun Wada and Sonia Zeggar</i>	832
More Comprehensive Considerations in Assessing the Safety of Treatments During Pregnancy: Comment on the Editorial by Pope <i>Olga Sánchez-Pernaute</i>	833
Reply <i>Janet E. Pope</i>	834
Childhood- Versus Adult-Onset Takayasu Arteritis: Are They Really Different? Comment on the Article by Aeschlimann et al <i>Sergey Moiseev, Ilya Smitienko, Alexander Kulikov, and Pavel Novikov</i>	835
Reply <i>Florence A. Aeschlimann, Rae S. M. Yeung, Lillian Barra, and Susanne M. Benseler</i>	836
ACR Announcements	A19

Cover image: The figure on the cover (from Desai et al, page 712) summarizes long-term opioid use in patients with severe osteoarthritis in the year leading up to their total joint replacement surgery across the US. Proportions of long-term opioid users were generally higher in the South (darker blue) and lower in the Northeast and the Midwest (light blue).

EDITORIAL

Prescribing Opioids for Severe Hip and Knee Osteoarthritis Varies Widely in the United States: The Devil Is in the Details

Janet E. Pope

In this issue of *Arthritis & Rheumatology*, Desai et al report on a study in which they examined regional variation in opioid prescribing and found marked variation in long-term prescribing practices for severe hip and knee osteoarthritis (OA) in senior adults who are awaiting joint replacement surgery (1). The study was conducted using data from 2010 through 2014, and prescribing patterns may now be different as the awareness of the “opioid crisis” is likely higher than 4–8 years ago. The generalizability of the authors’ findings to younger patients is unknown, as only patients who were age ≥ 65 years were studied. The appropriateness of prescribing opioids for those awaiting a joint replacement is uncertain. The American College of Rheumatology 2012 guidelines have no recommendations with respect to opioid prescribing for treatment of symptomatic OA of the hip(s) and/or knee(s) (2). Desai et al suggest that targeted strategies for safe opioid prescribing should be regional, as the Southern states have more narcotic prescriptions compared to the Northeast and Midwest (1). This variation implies that the rate of prescribing in some areas is too high. However, their study doesn’t examine patient outcomes such as surgical success for those taking versus not taking opioids in the year prior to joint replacement, and harms were also not studied.

The authors did find that 7.5% of long-term narcotic users took more than twice as many very high doses of opioids (average daily dose >90 mg/day of morphine milligram equivalent) versus short-term users taking very high doses (2.8%). Tramadol, which may be a safer narcotic, was prescribed more commonly in long-term users (45.8%) versus short-term users (36.8%), whereas fentanyl, which is less safe and is reserved in guidelines for use after failure of safer narcotics (3), was also prescribed more often in long-term users (6.2%) compared to short-term users (0.5%). Assuming the medication is a temporary measure before a more definitive pain-reducing procedure is performed, a prescriber may be more apt to suggest opioids for a patient on the surgical wait-

ing list. In the study by Desai et al there is no control group of patients with OA who are not receiving surgery, so it is difficult to know if this pattern of prescribing is consistent in other OA patients who don’t receive surgery within a year.

Patients may have a far longer wait time for joint replacement surgery in some regions of the country compared to others. Also, patients who are denied surgery may have a different chronic usage of narcotics in different states, but these patients were not part of the study and can’t be compared.

More women were long-term narcotic users, as were those eligible for both Medicaid and Medicare, which implies patients with lower income. The long-term users had more concomitant pain conditions such as rheumatoid arthritis, neuropathic pain, mechanical back pain, migraines, and anxiety and depression, as well as slightly more comorbidities, as would be expected. Those awaiting hip replacement surgeries showed more use of narcotics, which could be due to lack of other easily accessible treatments; e.g., intraarticular steroids are administered to knee OA patients in the clinic, but require fluoroscopic or ultrasound guidance for administration to hip OA patients.

Desai et al found that access to a rheumatologist did not affect the prescribing rate for opioids (1). Another study showed that patients with knee and hip OA who saw orthopedic surgeons were less likely to be exposed to nonsteroidal antiinflammatory drugs (NSAIDs) versus patients seeing a rheumatologist, but there could be a channeling bias with respect to severity of OA, and opioid prescriptions were not studied (4).

An important question to ask is what is the “right” amount of prescriptions for opioids in significant lower-extremity large-joint OA? Pain is a prominent feature in patients awaiting joint surgery. Opioid-prescribing guidelines are meant to reduce prescribing, including the overall daily amount of narcotics, and the guidelines often suggest random drug testing and a signed contract with the

Janet E. Pope, MD, MPH, FRCPC: St. Joseph’s Health Care, University of Western Ontario, London, Ontario, Canada.

No potential conflicts of interest relevant to this article were reported.

Address correspondence to Janet E. Pope, MD, MPH, FRCPC, Division of Rheumatology, St. Joseph’s Health Care, 268 Grosvenor Street,

London, Ontario N6A 4V2, Canada. E-mail: janet.pope@sjhc.london.on.ca.

Submitted for publication December 28, 2018; accepted in revised form January 3, 2019.

patient (3,5). This is due to the unintended consequences of opioid use such as addiction, overdose, death, and diversion. However, there are benefits of narcotic analgesics in some patients. A systematic review determined that the side effects (such as nausea) outweigh the benefits of chronic narcotic prescribing in noncancer pain, unless there is a significant benefit (>2 points on a 10-point scale) (6).

Despite the opioid epidemic in the US, chronic narcotic misuse rates haven't changed; rather, the substance of choice has changed (7). In 2005, overdoses from narcotics were mostly from oxycontin. Approximately 5 years later, overdoses were primarily from heroin and fentanyl, with deaths rising rapidly from overdoses of heroin, which is not a prescription opioid (7,8). There will always be a small proportion of chronic pain patients who become addicted to their narcotics and become drug-seeking or purchase narcotics illegally, but these numbers are small (9). This low number may be due to screening out of patients with a substance abuse history and identifying other high-risk patients prior to prescribing. In 2011, there was an oxycontin crisis in North Carolina. An intervention resulted in an 80% reduction in deaths despite no change in opioid prescribing. The intervention was likely successful due to education, including safe storage of controlled medications and a public awareness campaign about substance abuse, addiction, and not driving while impaired (10). Also, perhaps the increased availability of naloxone has lowered "recreational" overdoses that could have been lethal.

The elephant in the room may be that people with chronic pain are discriminated against. Health care providers in general don't like seeing these patients, as treatment is often not very effective and regular visits are needed if narcotics are prescribed. In addition, other problems such as depression and work disability are associated with chronic pain, and there may be clustering with socioeconomic determinants of poor health, as is seen in the study by Desai et al (1). Physicians may have their state license suspended if they are overprescribing opioids, and in some jurisdictions a special application is needed to prescribe certain opioids, which may act as a deterrent. Prohibition is likely not the answer to stopping the opioid crisis, as heroin is the largest cause of overdose-related deaths (8). Designer opioids, for which no antidote works in the case of respiratory depression, are now available, so one can predict that opioid-related deaths will continue to rise.

There is no drug class for chronic pain that is highly effective and has no safety issues. NSAIDs may not be adequately effective in chronic OA, and the mortality rate in nonselective NSAID users is 48 per 1,000 person-years, which is slightly lower than the 75 per 1,000 person-years in opioid users (11). There is now abuse of gabapentin and pregabalin, which are other treatment options. Even duloxetine can be responsible

for overdose-related deaths (12). In Canada and some states there may be another epidemic with the use of medical cannabis for the treatment of musculoskeletal pain and possible side effects (13).

It is noteworthy that large variation occurs in the surgical treatment of hip and knee OA, and this cannot be fully explained by risk factors (14,15). Therefore it is not surprising that wide variation is seen in the prescribing of opioids for treatment of pain in patients destined to receive joint replacement surgery. Over time the unmet need of pain control in these patients will hopefully be addressed and the safe prescribing practices for opioids be widely adopted, but until then, large regional variation will continue.

AUTHOR CONTRIBUTIONS

Dr. Pope drafted the article, revised it critically for important intellectual content, and approved the final version to be published.

REFERENCES

- Desai R, Yinzu J, Franklin PD, Lee YC, Bateman BT, Lii J, et al. Association of geography and access to health care providers with long-term prescription opioid use in Medicare patients with severe osteoarthritis: a cohort study. *Arthritis Rheumatol* 2019;71:712–21.
- Hochberg MC, Altman RD, April KT, Benkhalti M, Guyatt G, McGowan J, et al. American College of Rheumatology 2012 recommendations for the use of nonpharmacologic and pharmacologic therapies in osteoarthritis of the hand, hip, and knee. *Arthritis Care Res (Hoboken)* 2012;64:465–74.
- Dowell D, Haegerich TM, Chou R. CDC guideline for prescribing opioids for chronic pain: United States, 2016. *JAMA* 2016;315:1624–45.
- Pope J, McCrea K, Stevens A, Ouimet JM. The relationship between NSAID use and osteoarthritis (OA) severity in patients with hip and knee OA: results of a case control study of NSAID use comparing those requiring hip and knee replacements to those in whom surgery was not recommended. *Med Sci Monit* 2008;14:CR604–10.
- Busse JW, Craigie S, Juurlink DN, Buckley N, Wang L, Couban RJ, et al. Guideline for opioid therapy and chronic noncancer pain. *CMAJ* 2017;189:E659–66.
- Goshua A, Craigie S, Guyatt GH, Agarwal A, Li R, Bhullar JS, et al. Patient values and preferences regarding opioids for chronic non-cancer pain: a systematic review. *Pain Med* 2018;19:2469–80.
- Jalal H, Buchanich JM, Roberts MS, Balmert LC, Zhang K, Burke DS. Changing dynamics of the drug overdose epidemic in the United States from 1979 through 2016. *Science* 2018;361:eaau1184.
- Cicero TJ, Ellis MS, Kasper ZA. Increased use of heroin as an initiating opioid of abuse. *Addict Behav* 2017;74:63–6.
- Salsitz EA. Chronic pain, chronic opioid addiction: a complex nexus. *J Med Toxicol* 2016;12:54–7.
- Albert S, Brason FW II, Sanford CK, Dasgupta N, Graham J, Lovette B. Project Lazarus: community-based overdose prevention in rural North Carolina. *Pain Med* 2011;12 Suppl 2:S77–85.
- Solomon DH, Rassen JA, Glynn RJ, Lee J, Levin R, Schneeweiss S. The comparative safety of analgesics in older adults with arthritis. *Arch Intern Med* 2010;170:1968–76.

12. Pilgrim JL, Gerostamoulos D, Drummer OH. The prevalence of duloxetine in medico-legal death investigations in Victoria, Australia (2009-2012). *Forensic Sci Int* 2014;234:165–73.
13. Curran HV, Freeman TP, Mokrysz C, Lewis DA, Morgan CJ, Parsons LH. Keep off the grass? Cannabis, cognition and addiction. *Nat Rev Neurosci* 2016;17:293–306.
14. Bederman SS, Rosen CD, Bhatia NN, Kiester PD, Gupta R. Drivers of surgery for the degenerative hip, knee, and spine: a systematic review. *Clin Orthop Relat Res* 2012;470:1090–105.
15. Katz BP, Freund DA, Heck DA, Dittus RS, Paul JE, Wright J, et al. Demographic variation in the rate of knee replacement: a multi-year analysis. *Health Serv Res* 1996;31:125–40.

EDITORIAL

Casting a Spotlight on the Right Ventricle in Systemic Sclerosis

Steven Hsu 

Pulmonary arterial hypertension (PAH) and other pulmonary issues such as interstitial fibrosis have emerged as the leading causes of mortality in systemic sclerosis (SSc) (1). Whereas scleroderma renal crisis was once the leading cause of mortality among SSc patients, PAH now accounts for 26% of SSc-related mortalities (1). This is in part because, among those with World Health Organization group I PAH, the subset of patients with SSc-associated PAH experiences disproportionately worse morbidity, mortality, and response to pulmonary vasodilator therapy. Recent studies have revealed that the key factor in this discrepancy is likely inadequate compensation of the right ventricle in SSc-associated PAH. Right ventricular compensation is paramount in PAH, and failure of right ventricular adaptation leads to inadequate coupling between right ventricular contractility and the increased pulmonary arterial afterload of PAH. Our group and others have shown that patients with SSc-associated PAH demonstrate decreased right ventricular contractile function, both at rest (2) and during exercise (3), when compared to those with idiopathic PAH. Furthermore, we recently showed that this *in vivo* right ventricular contractile dysfunction closely correlates with underlying defects in right ventricular sarcomere contractility, directly measured from right ventricular myocytes isolated from patients with SSc-associated PAH (4).

Why is the right ventricle so vulnerable to PAH in SSc? A growing body of work suggests that SSc patients either have underlying right ventricular dysfunction or are vulnerable to early right ventricular decompensation in the face of elevated pulmonary pressures. This would not be surprising given the microangiopathy and fibrosis of SSc. Even in the absence of any pulmonary vascular disease, SSc patients exhibit evidence of right ventricular functional defects on strain-based echocardiographic imaging (5). Interestingly, these clinical findings extend to underlying right ventricular myocyte function in SSc as well. In the study of right ventricular myocytes from patients with SSc-associated PAH described above, we found intermediate decreases in right

ventricular myofilament contractility in SSc patients without PAH (4). These underlying right ventricle deficits likely impact the ability of the right ventricle in SSc patients to compensate in the face of pulmonary vascular disease, even in its earliest stages.

In this issue of *Arthritis & Rheumatology*, Nagel and colleagues cast further light on the role of the right ventricle in SSc (6). They prospectively studied right ventricular and pulmonary vascular hemodynamics at rest and during exercise in SSc patients with borderline elevations in pulmonary artery pressure (PAP) (mean PAP 21–24 mm Hg), before the onset of pulmonary hypertension (PH), and compared them to findings in SSc patients with normal mean PAP (mean PAP \leq 20 mm Hg) and those with full-fledged PH (mean PAP \geq 25 mm Hg). On the surface, SSc patients with borderline mean PAP did not have any overt right ventricular dysfunction; resting right atrium and right ventricle size and function as determined by echocardiography, and most hemodynamic measures including cardiac output, were indistinguishable from those in the cohort with normal mean PAP. The only differences between SSc patients with borderline mean PAP and SSc patients with normal mean PAP at rest were mild pulmonary vascular derangements, which included a slightly elevated pulmonary vascular resistance (PVR), and slightly decreased pulmonary arterial compliance (PAC) (6). Given the mild increase in mean PAP, without a statistically evident increase in left-sided filling pressure, mild derangements in PVR and PAC were to be expected.

It was not until patients with SSc with borderline mean PAP *stressed* their system that significant right ventricular and pulmonary vascular abnormalities arose. SSc patients with borderline mean PAP were found to have decreased functional capacity when compared to controls, as measured by decreased 6-minute walking distance. Consistent with this finding, during exercise with invasive hemodynamic monitoring, SSc patients with borderline mean PAP also showed diminished augmentation in right ventricular cardiac output. Left-sided heart disease was ruled out as a culprit since there were no significant differences in systemic and

Steven Hsu, MD, FACC: Johns Hopkins University School of Medicine, Baltimore, Maryland.

No potential conflicts of interest relevant to this article were reported.

Address correspondence to Steven Hsu, MD, FACC, Division of Cardiology, Department of Medicine, Johns Hopkins University School of Medicine, 600

North Wolfe Street, Carnegie 591A, Baltimore, MD 21205. E-mail: steven.hsu@jhmi.edu.

Submitted for publication December 9, 2018; accepted December 13, 2018.

pulmonary capillary wedge pressure throughout exercise. Importantly, the authors found that PAC was closely correlated with both 6-minute walking distance and right ventricular cardiac output reserve, no matter the SSc subtype (6). Decreased PAC has been shown to be an early marker of pulmonary vascular disease, and predictive of outcomes in PH. The findings of Nagel et al thus indicate that right ventricular cardiac output reserve and functional capacity in SSc patients are very sensitive to even small increases in pulmonary vascular disease. Their findings also support the notion that SSc patients with borderline mean PAP have more similarities with patients with overt SSc-associated PAH than they do with patients with normal mean PAP. The patients with borderline mean PAP and those with PH had similar increases in pulmonary pressures and insufficiency of cardiac flow reserve during exercise, rightfully leading the authors to suppose that many of the SSc patients with borderline mean PAP likely had so-called exercise-induced PH as well (6).

Nagel and colleagues add an important piece to the growing body of evidence showing that the right ventricle in SSc behaves very differently from the right ventricle in other populations at risk of developing PAH, and seems particularly ill-equipped to handle the stressors of pulmonary vascular disease. Their work makes a strong argument, founded in carefully obtained clinical, echocardiographic, and hemodynamic data, that the SSc population with even mild increases in mean PAP constitutes a clear intermediate phenotype in the spectrum of PH in SSc. Their findings are also consistent with the results of other studies of borderline pressures in other cohorts. Thus, the current study adds considerable weight to recommendations from the recent 6th World Symposium on Pulmonary Hypertension, which suggested that a mean PAP >20 mm Hg should serve as the new threshold for diagnosing PH (7). Importantly, among the many patients these new guidelines will affect, the SSc borderline group will likely be impacted the most, since these patients are known to have early, underlying right ventricular dysfunction.

What do these findings collectively mean for the treatment of pulmonary vascular disease in this vulnerable population? If the right ventricle is especially vulnerable in patients with SSc, perhaps we need to rethink our screening and treatment paradigms for SSc-associated PAH, with an eye toward better screening, targeting, and treatment of right ventricular dysfunction. Screening for PH remains an important part of the longitudinal management of SSc, and future studies may do well to investigate exercise stress testing of the right ventricle, since stressing the right ventricle can elicit abnormalities better than studies of patients at rest (8). More aggressive upfront treatment with dual vasodilator therapy has already been shown to be beneficial in SSc-associated PAH (9). It stands to reason that a similar tack toward earlier treatment in SSc-associated PAH, and new studies of treatment in SSc patients

with borderline mean PAP, may be of further benefit to the right ventricle in SSc. In fact, treatment of exercise-induced PH in SSc patients was recently tested and found to be both safe and beneficial (10). Last, current therapies in PAH are almost exclusively directed toward alleviating pulmonary vascular disease, but perhaps the missing link in treating SSc-associated PAH is some type of augmentation of right ventricular compensation. Future studies and randomized trials are needed on all these fronts. Over the last several decades, we have been able to understand and better treat scleroderma renal disease and greatly reduce mortality due to renal crisis. Hopefully, with a better appreciation for and treatment of the right ventricle in SSc, we can do the same for SSc-associated PAH.

AUTHOR CONTRIBUTIONS

Dr. Hsu drafted the article, revised it critically for important intellectual content, and approved the final version to be published.

REFERENCES

1. Tyndall AJ, Bannert B, Vonk M, Airò P, Cozzi F, Carreira PE, et al. Causes and risk factors for death in systemic sclerosis: a study from the EULAR Scleroderma Trials and Research (EUSTAR) database. *Ann Rheum Dis* 2010;69:1809–15.
2. Tedford RJ, Mudd JO, Girgis RE, Mathai SC, Zaiman AL, Houston-Harris T, et al. Right ventricular dysfunction in systemic sclerosis-associated pulmonary arterial hypertension. *Circ Heart Fail* 2013;6:953–63.
3. Hsu S, Houston BA, Tampakakis E, Bacher AC, Rhodes PS, Mathai SC, et al. Right ventricular functional reserve in pulmonary arterial hypertension. *Circulation* 2016;133:2413–22.
4. Hsu S, Kokkonen-Simon KM, Kirk JA, Kolb TM, Damico RL, Mathai SC, et al. Right ventricular myofilament functional differences in humans with systemic sclerosis-associated versus idiopathic pulmonary arterial hypertension. *Circulation* 2018;137:2360–70.
5. Mukherjee M, Chung SE, Ton VK, Tedford RJ, Hummers LK, Wigley FM, et al. Unique abnormalities in right ventricular longitudinal strain in systemic sclerosis patients. *Circ Cardiovasc Imaging* 2016;9:e003792.
6. Nagel C, Marra AM, Benjamin N, Blank N, Cittadini A, Coghlan G, et al. Reduced right ventricular output reserve in patients with systemic sclerosis and mildly elevated pulmonary artery pressure. *Arthritis Rheumatol* 2019;5:805–16.
7. Simonneau G, Montani D, Celermajer DS, Denton CP, Gatzoulis MA, Krowka M, et al. Haemodynamic definitions and updated clinical classification of pulmonary hypertension. *Euro Respir J* 2018;53:1–13.
8. Grünig E, Tiede H, Enyimayew EO, Ehlken N, Seyfarth HJ, Bossone E, et al. Assessment and prognostic relevance of right ventricular contractile reserve in patients with severe pulmonary hypertension. *Circulation* 2013;128:2005–15.
9. Hassoun PM, Zamanian RT, Damico R, Lechtzin N, Khair R, Kolb TM, et al. Ambrisentan and tadalafil upfront combination therapy in scleroderma-associated PAH. *Am J Respir Crit Care Med* 2015;192:1102–10.
10. Segrera SA, Lawler L, Opatowsky AR, Systrom D, Waxman AB. Open label study of ambrisentan in patients with exercise pulmonary hypertension. *Pulm Circ* 2017;7:531–8.

ACR PRESIDENTIAL ADDRESS

Building on the Strengths of Our Unique Specialty

David I. Daikh

I am both honored and humbled to deliver this address as the President of the ACR. The honor does not come from the title, but rather from the precedents, performance, and professionalism that define those in the field of rheumatology. I am extremely proud to be a rheumatologist. Although I always wanted to be a doctor, I didn't always want to be a rheumatologist. Fortunately, I was exposed to the essential features of this profession as a medical student, allowing me to start what has become a great life journey. I credit 3 wonderful teachers with opening the amazing world of rheumatology to a bright-eyed young medical student. Steve Campbell, Mike Davey, and Jim Rosenbaum at the Oregon Health Sciences University showed me, through their teaching and their skills, the essential features of our profession, just as they have for many other generations of medical and graduate students.

What are these essential features that define rheumatology professionals? They can be found at the very beginnings of the specialty. The ways in which rheumatology has grown from its beginnings as a brand new field to its current standing as a subspecialty of internal medicine say a lot about who we are. One thing we are is young. Compared to the long-established branches and specialties of medicine based on technical approach or organ system, rheumatology is still a young field. It was born from attempts to understand and define conditions that defied traditional understanding (Figure 1), and this origin continues to define us.

Despite the ancient roots of the word “rheum,” the first descriptions of the role of antibody in RA that provided a new serologic test and fundamental recognition of immune mechanisms of disease were really quite recent in the history of science. And although we are witnessing a subsequent revolution in biologic therapy today, I think it is quite telling that the very name of our specialty continues to defy simple meaning and understanding. Rheumatologists are attracted to the unknown.

Those new developments in science and medicine that would lead in a relatively short time to the targeted treatments we take for granted today began in academic centers around the world. In the United States, a handful of early rheumatologists established the

first departments of rheumatology and, given where we are today, it is remarkable that the first department of rheumatology in the United States was established less than 100 years ago. These first centers (Figure 2) trained the early cohort of academic rheumatologists that would go on to establish departments of rheumatology across the country. This partial evolutionary tree also illustrates another truism about our field: Every practicing rheumatologist was born in an academic division, and this training heritage has indelibly defined our field (Figure 3). These are the defining and essential features of our profession and the attributes that attract new members to the field.

When I see my colleagues in action across the country and around the world I am continually reminded that these characteristics are not restricted to one segment of the profession, but are shared by all. These characteristics define rheumatology the world over. Unfortunately, the academic divisions of rheumatology that incubate our rheumatology trainees and the new science in our field currently face significant challenges to their survival, precipitated by a workforce shortage, decreased research funding, and barriers to the physician-scientist career pathway. There is an urgent need to support the survival of our rheumatology training programs, and this must be an issue of focus for the ACR.

I have come to see the admirable features of rheumatology in so many aspects of the profession during my time as a volunteer with the ACR, which has been one of the most rewarding aspects of my professional career. This stems from the opportunity to meet and work with truly remarkable people who share the values of which I speak and who give their time and energy to these goals. The character of this organization truly reflects that of the profession that it serves. From a very small and uncertain beginning as a professional society, the ACR has grown into a large and diverse organization that works to meet the needs of the many kinds of rheumatology professionals in their work to improve the lives of people with rheumatic and musculoskeletal disease. In fact, we can point to many areas of effectiveness and success.

Presented at the 82nd Annual Meeting of the American College of Rheumatology, Chicago, IL, October 20, 2018.

David I. Daikh, MD, PhD: University of California, San Francisco and San Francisco Veterans Administration Medical Center, San Francisco, California; President, American College of Rheumatology, 2017–2018.

Address correspondence to David I. Daikh, MD, PhD, Immunology 111R, Veterans Affairs Medical Center, 4150 Clement Street, San Francisco, CA 94121. E-mail: david.daikh@ucsf.edu.

Submitted for publication January 24, 2019; accepted January 24, 2019.



Figure 1. The origins of rheumatology.

One recent example is the development and growth of the RISE registry. RISE, the Rheumatology Information System for Effectiveness, was originally developed to provide clinicians a means for reporting quality data from their practice as required by the new Merit-based Incentive Payment System. In the first year of reporting from RISE to the Centers for Medicare and Medicaid Services, 100% of participating practices successfully reported and achieved an exceptional or better rating. Not only is this a service to participating practices, but it underscores that rheumatologists are providing the highest-quality care to their patients. Under the leadership of Dino Kazi and Jinoos Yazdany, the first

chairs of the ACR Registries and Health IT Committee, and from Rachel Myslinski, ACR Vice President for Practice and Advocacy and Quality, RISE has grown to become the largest registry of rheumatology clinical data in the world. This registry provides an unparalleled resource not only for practice quality management, but for all kinds of research on the entire range of rheumatic diseases. Such research is now starting to be done and is enabled through RISE data analytic centers led by Gabby Schmajuk at the University of California, San Francisco, Jeff Curtis at the University of Alabama, Birmingham, and Megan Clowse at Duke University. Notably, a number of oral and poster presentations of RISE data

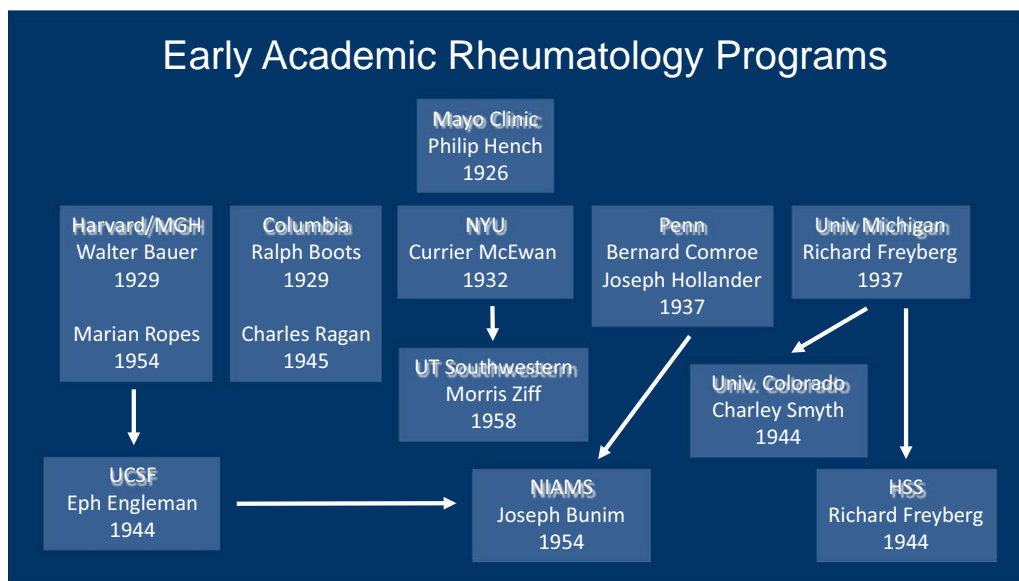


Figure 2. Roots of academic rheumatology in the United States.

Characteristics of Rheumatology

- An interest in understanding the unknown
- A scientific and evidence-based approach
- Devising new ways to treat and cure disease
- Helping others
- A love for education - We like to teach

Figure 3. The essential features of rheumatology and rheumatology professionals.

are being presented at the 2018 Annual Meeting. If your practice has not yet signed up with RISE, I urge you to consider it.

This organization has achieved remarkable effectiveness by combining the efforts of experienced and committed volunteer rheumatology professionals with the work of a highly dedicated professional staff. In fact, the ACR—and the ACR staff—mirror the defining characteristics of rheumatology on which I focused earlier. The ACR supports science and innovation, as well as the training of young rheumatology professionals, through the Rheumatology Research Foundation. The Foundation was born from the vision of our first leaders that the profession could provide financial resources for research and education. From that small beginning as a nonprofit charitable organization, the RRF has grown to support \$10–13 million annually in grants to young physician-scientists, established researchers, and rheumatology clinical trainees. The Foundation funds and manages its diverse portfolio of awards under the direction of its own board of directors comprising rheumatology professionals and lay community members led by President Abby Abelson, Vice President Lou Bridges, and Executive Director Mary Wheatley—and through the work of an army of volunteers working with a professional and highly committed development, communications, and program staff. The most important individual donors to the Foundation have always been our practicing rheumatologists. This fact emphasizes the value that rheumatology professionals place on research and training to ensure the future of the discipline. If you are working in rheumatology in the United States, I urge you to support the Rheumatology Research Foundation and to tell your patients about its great work.

The Foundation is just one of many examples of how the ACR works to support people. As highlighted earlier, rheumatologists like to learn and to teach. The quality of educational activities and products provided by the ACR is best exemplified by this annual meeting, which is the largest of its kind in the world. I would like to acknowledge Vicki Shanmugam, as Meeting Chair and the many volunteers of the Annual Meeting Planning Committee, along with the Committee on Education and Vice President for Education Donna Hoyne and her staff, as well as the professional meetings staff for organizing yet another spectacular

annual scientific meeting in 2018. A new innovation for our educational meetings is ACR Beyond. This program provides attendees access to many of the high-quality sessions after the meeting, so that you can see sessions online that you were unable to attend in person or that you wish to review again in detail. ACR Beyond also can provide access to our meeting for those who are unable to attend in person. Another recent development in our annual meeting is attendance by patients. I offer a warm welcome to the patients attending this year's meeting, along with thanks for helping us learn more about the conditions we seek to improve.

I would also like to acknowledge and thank the many international attendees at this meeting. You make this a truly worldwide meeting. Your presence significantly enhances our proceedings and is greatly appreciated. Your attendance also emphasizes that the ACR has itself become an international organization of rheumatology professionals. The most recent example of our efforts to reach our international colleagues is our first international educational meeting, organized this year in collaboration with the Emirates Society of Rheumatology (Figure 4). The goal of this meeting was to provide rheumatology professionals who are unable to travel all the way to North America the opportunity to learn about the newest advances directly from leaders in the field. This first meeting was a truly collaborative effort and a great success. I thank our colleagues in the United Arab Emirates for their collegiality, and we are already looking forward to this meeting taking place again next year.

Our meeting, with all of its diverse attendees, emphasizes another of the essential features of rheumatology. We are inclusive. From its very beginning, the specialty of rheumatology has emphasized the importance of interdisciplinary care across the lifetime of the patient. The importance of the interprofessional team is a concept and a buzzword that has recently become common in medical schools and training programs in this country. While this certainly is important, it is not a new concept for us. Rheumatology care and research have emphasized this fact about quality rheumatologic care for decades. Accordingly, the ACR is an inclusive organization. The ACR includes adult and pediatric rheumatologists. Through the Association of Rheumatology Professionals (ARP), the ACR supports the work of a wide variety of health care professionals, researchers, and other



Figure 4. ACR faculty at the Emirates Society of Rheumatology/ACR conference in Dubai, UAE.

important members of the health care team, such as practice managers. The many international rheumatology professionals who are here, many of whom are ACR members, as well as our international outreach also speak to such inclusion. This is the fabric of which rheumatology is made.

In this vein, I think that the longstanding association between community practice-based rheumatologists and academic research-oriented rheumatologists in the ACR is also particularly noteworthy—and extremely important. In fact, the collegiality I witnessed as a medical student in the regular meetings attended by community and university rheumatologists was another one of the features that really attracted me to the specialty. The fact that the ACR is a single organization representing all rheumatology professionals mirrors this reality. I believe that this is probably the single most important feature of our organization—and it is the most important one to foster and maintain. This is the basis of our strength, and it has allowed us to have an impact in many aspects of medicine that surpass the size of our specialty. I would further emphasize the value of this union because we are currently witnessing many disturbing examples of polarization and inability to reach agreement in our society. In the face of this fundamental challenge, the ACR is not divided. While we may have different jobs and different needs and priorities in accomplishing them, we also share many needs and goals. We must continue to focus on our shared goals and needs, and stay unified as a single organization to ensure that our organization can effectively help us achieve our goals.

A very important avenue for achieving our goals is through advocacy. The development of an active and effective advocacy program has been one of the most important initiatives of the

ACR over the past decade. Now, a cadre of staff and volunteers on the ACR Government Affairs Committee tirelessly monitors and advocates with Congress and government agencies on behalf of rheumatology professionals and their patients. It has been very encouraging to see increasingly large groups of ACR members, including the ACR Board of Directors and fellows in training, make their way to Capitol Hill each year. As we enter those increasingly divided halls, we are reminded that advocacy for our goals in rheumatology requires unity of purpose and effort among ourselves. We also see that participation in advocacy can provide lessons in tolerance and accommodation. If we are not active and united in advocating for rheumatology, we will have no chance of preserving and expanding the gains we have made and continuing to advance our mission to improve the lives of patients with rheumatic disease. Thus, I encourage all of our members to become more involved in advocacy for our field and for your work. This includes those of you who work in areas that have not traditionally engaged in advocacy, like academics and research, because we can no longer take support for these crucial activities for granted.

I am compelled to emphasize these themes tonight as I end my term as ACR President because we are at an inflection point in our evolution as an organization. The political landscape is treacherous, and policy changes can have direct and rapid effects on our profession. Our members are under increasing pressure in their jobs to do more with less time and fewer resources. An emerging workforce shortage threatens to further reduce access to care for patients with rheumatic disease. Advocating for more support for rheumatology training to meet this workforce shortage is perhaps our most urgent need.

Counteracting these forces that would serve to bend our curve of success downward are a number of opportunities that can help continue our upward success. The good news is that the rising wave of the millennial generation that is beginning to contribute to the workforce is motivated by the same values that define rheumatology—innovation, care for others, education, and inclusivity. This demographic shift, coupled with recent survey results indicating that rheumatologists are among the most satisfied and happiest of all physicians, bodes well for our specialty. In fact, we may already be seeing this effect. Over the last 2–3 years, we have seen a marked increase in interest in rheumatology training in the United States, with a rise in highly qualified applicants applying for rheumatology fellowship: so much so, that last year obtaining a training position in rheumatology was almost as competitive as for cardiology training. The arrival of large numbers of young people and their movement into rheumatology is an incredibly positive development. When I see the quality and commitment of our trainees and their enthusiasm for advancing the scientific progress we have already made, I am reminded of that song by Timbuk 3—“The future’s so bright, I gotta wear shades!” My daughter certainly makes me feel this way! I am proud of the recent efforts that the ACR has made to move younger rheumatology professionals into leadership positions in the organization, and it is our responsibility to keep the ACR relevant to this young generation.

The other reason that the ACR is at an inflection point is that our long-time Executive Vice President will retire in the coming year. Mark Andrejeski is the first and only executive the ACR has ever had. The remarkable growth and success that the ACR has experienced over the 31 years that Mark has been in this position are very significantly attributable to his work, skill, and vision. The fact that the ACR has been named one of Atlanta’s Best Places to Work for the past 2 years emphasizes the great work that he has done to build and retain a world-class staff for the organization. Mr. Andrejeski’s work has been acknowledged in many other circles as well, including here in Chicago. A Proclamation from Chicago Mayor Rahm Emanuel cites many of his accomplishments and proclaims October 24, 2018 as Mark Andrejeski Day in Chicago. On behalf of the organization, including all of the many volunteers, staff, and stakeholders who have worked with the ACR, as well as rheumatology professionals around the world, I would like to acknowledge Mr. Mark Andrejeski. We thank you eternally.

Over this past year in anticipation of Mark’s retirement, the ACR Board of Directors, staff, and stakeholders have undertaken an organizational review to determine the future needs of the organization with respect to a new executive, and a national search for that person is underway. Based on this thoughtful, strategic review, the strong foundation that has been built, and the current successful operations of the College, I am confident that we will soon have a new and outstanding executive staff leader to help move us forward to meet the needs and challenges of the future.

I would also like to thank the many people with whom I have worked over the past year and who have made this work both possible and extremely enjoyable. While they are innumerable, I want to highlight a few of them. The Board of Directors has steadily guided the ACR through sometimes choppy waters this past year. They, along with the ACR committee chairs, are a remarkable group of leaders, and I have greatly appreciated the honest and careful deliberation that they have brought to every issue. I have especially appreciated working closely with the ACR Executive Committee. Your guidance, support, and friendship have been invaluable and will stay with me always. The ACR staff is the best that there is. They make all of the volunteers look good and have provided a solid rock of hard work, support, and professionalism for me to stand on this year. I love working with all of you! I would also like to particularly thank Mark Andrejeski for his support and friendship, and Julie Anderson, ACR Director of Governance, who has been my right hand for the past year. She made that hand work better than it ever did, and I could not have done the job without her. I have also learned much from past leaders of the College, and I am particularly indebted to the ACR Presidents who have mentored me directly, including Stan Cohen, Jim O’Dell, Bill St.Clair, Audrey Uknis, Joseph Flood, Joan Von Feldt, and Sharad Lakhanpal.

I mentioned at the beginning of this address that it is humbling to be standing here. I do so with the ever-present knowledge that it is only because of the support of many people who have taught and believed in me. My parents gave me the values that I have tried to carry forward in this work. Thus, I do not think it is an accident that my brother also became a rheumatologist or that my sister works in preschool education. I am pleased that my mother and sister are able to join me here today. And although my father is no longer with us, my presence before you is testament to the sacrifices and faith he exhibited in coming to the United States alone as a college student from Baghdad to build a life and support a family of 5 as a teacher—and it is testament that anyone and everyone in this world has the potential to achieve success if given the opportunity. My work and life would not be possible without the love and support of my wife Wendy and daughter Clara, who thankfully have also joined me here today. They have given a lot to allow me to spend time with the ACR, and I am forever grateful.

My opportunities for success in rheumatology have been provided by my mentors and colleagues at the University of California, San Francisco, where I have had the privilege to work in a division with a long tradition of excellence and to observe and learn from giants in the field, beginning with Eph Engleman and Wally Epstein. Like all of our fellows at UCSF, I learned clinical rheumatology from many people, but first among them were Ken Fye and Ken Sack, who epitomize what it means to be a rheumatologist. I cannot imagine a more outstanding and collegial group than my colleagues at UCSF. I feel so fortunate to have spent my professional career with them and thank them all for


their friendship and support. We also have a tradition of working closely with our community-based colleagues, and I am truly thankful for the teaching I received from volunteer faculty who devoted their time to teach me—and I appreciate the critical role that they continue to play in our fellowship program today. These community- and industry-based rheumatology professionals who give their time to students, residents, and fellows—at UCSF and around the country—are the unsung heroes of rheumatology training in this country. We also learn much from our students, and the rheumatology fellows with whom I have worked at UCSF and beyond have enriched my professional life and made it fun.

Most important, however, have been my mentors. Few are as lucky to have a role model like David Wofsy. David was one of the people who attracted me to stay at UCSF for rheumatology training, mentored me for postdoctoral research, and nominated me for my first ACR committee. I have learned much from David and will forever cherish the experience of having him as a role model

and friend. He is a prince in much more than name. Bill Seaman has also been a valuable mentor to me, as he has for many others around the world. Bill is a mentor's mentor and truly epitomizes this noble role. He also has great taste in music!

Finally, I would like to acknowledge and thank my UCSF colleagues at the VA Medical Center in San Francisco with whom I work most closely. Mary Nakamura has been a colleague and friend at the VA over the entire time I have worked there. And I am most appreciative of the collegiality and support I have received from Mimi Margaretten, Lianne Gensler, and Gabby Schmajuk during this past year. They, along with our nurse practitioners Jo Dana and Gina Vitulano, have taken up the slack I have left in the line this year, and they have done so with incredible grace and ability. I could not have done this job without them. Their kindness, skill, and collegiality amaze me and make my own job at UCSF and the VA a true pleasure. And finally, to conclude, I thank you for your attention, for your support of the ACR, and for your work in rheumatology.

Chronic Opioid Use in Rheumatoid Arthritis: Prevalence and Predictors

Yvonne C. Lee,¹  Joel Kremer,² Hongshu Guan,³ Jeffrey Greenberg,⁴ and Daniel H. Solomon³

Objective. The opioid epidemic is a major public health concern. However, little is known about opioid use among rheumatoid arthritis (RA) patients. We undertook this study to examine trends in chronic opioid use in RA patients in 2002–2015 and to identify clinical predictors.

Methods. RA patients were identified from the Corrona registry. Opioid use was ascertained from surveys obtained at clinical visits as often as every 3 months. Chronic opioid use was defined as any opioid use reported during ≥ 2 consecutive study visits. Annual prevalence of chronic opioid use was calculated using data from 33,739 RA patients with information on opioid use from ≥ 2 visits. Among the 26,288 individuals who were not taking opioids at baseline, Cox proportional hazards models identified associations between patient characteristics and incident chronic opioid use. Hazard ratios (HRs) and 95% confidence intervals (95% CIs) were calculated.

Results. Chronic opioid use increased from 7.4% in 2002 to 16.9% in 2015. Severe pain (HR 2.53 [95% CI 2.19–2.92]) and antidepressant use (HR 1.79 [95% CI 1.64–1.92]) were associated with an increased risk of chronic opioid use. High disease activity (HR 1.55 [95% CI 1.30–1.84]) and a high level of disability (HR 1.45 [95% CI 1.27–1.65]) were also associated with chronic opioid use, whereas Asian ethnicity (HR 0.49 [95% CI 0.36–0.68]) was associated with a decreased risk of chronic opioid use.

Conclusion. Among RA patients, chronic opioid use doubled from 2002 to 2015. Pain and antidepressant use were the strongest predictors of chronic opioid use. To curb the rise in chronic opioid use, strategies for stringent control of RA disease activity and management of pain and depression should be research priorities.

INTRODUCTION

Over the past decade, physicians, patients, and policy makers have expressed increasing concern about the high frequency of opioids being prescribed and the association between opioid use and poor outcomes. Rates of opioid prescriptions in the general population rose considerably from the 1990s through 2010, with a plateau in the early 2010s (1–4). In 2015, 38% of US adults reported using opioids, and, of these individuals, 17% had an opioid use disorder (5). Compared to other medications for chronic pain (e.g., anticonvulsants, tricyclic antidepressants), opioids were associated

with significantly increased risk of overdose-related mortality, as well as non-overdose deaths, particularly cardiovascular deaths (6).

Rheumatoid arthritis (RA) is a systemic inflammatory disease associated with an increased risk of chronic opioid use (2,7). Claims-based studies indicate that the prevalence of opioid prescriptions for individuals with RA increased substantially in the late 1990s and early 2000s, with rates stabilizing in the mid-2000s to mid-2010s (8,9). While there is weak evidence that opioids are efficacious for the treatment of pain in RA (10–12), there is growing evidence that opioids are associated with serious risks, including nonvertebral fractures and serious infections (13,14). These

The Corrona Rheumatoid Arthritis registry is supported by AbbVie, Amgen, AstraZeneca, Bristol-Myers Squibb, Crescendo, Eli Lilly, Genentech, GlaxoSmithKline, Horizon Pharma, Janssen, Momenta Pharmaceuticals, Novartis, Pfizer, Roche, and UCB.

¹Yvonne C. Lee, MD, MMSc: Northwestern University Feinberg School of Medicine, Chicago, Illinois, and Brigham and Women's Hospital, Boston, Massachusetts; ²Joel Kremer, MD: Corrona, LLC, Waltham, Massachusetts, and Albany Medical College, Center for Rheumatology, Albany, New York; ³Hongshu Guan, MS, Daniel H. Solomon, MD, MPH: Brigham and Women's Hospital, Boston, Massachusetts; ⁴Jeffrey Greenberg, MD: Corrona, LLC, Waltham, Massachusetts, and New York University School of Medicine, New York, New York.

Dr. Lee has served on the advisory board of Eli Lilly, has received research support from Pfizer, and owns stock or stock options in Express Scripts. Dr. Kremer has received consulting fees and/or honoraria from AbbVie, Gilead, Eli Lilly, and Pfizer (less than \$10,000 each), has received research support from AbbVie, Eli Lilly, Novartis, and Pfizer, and owns stock or stock options in Corrona. Dr. Greenberg owns stock or stock options in Corrona. Dr. Solomon has received research support from AbbVie, Amgen, Janssen, Genentech, and Pfizer. No other disclosures relevant to this article were reported.

Address correspondence to Yvonne C. Lee, MD, MMSc, Division of Rheumatology, Northwestern Medicine, 633 North St. Clair Street, 18-093, Chicago, IL 60611. E-mail: yvonne.lee@northwestern.edu.

Submitted for publication December 2, 2017; accepted in revised form November 20, 2018.

observations highlight the importance of understanding the prevalence and predictors of chronic opioid use in RA.

The objective of the present study was to examine trends in patient-reported opioid use in 2002–2015 and to identify clinical factors, particularly RA-related factors (e.g., inflammatory disease activity, disability, and pain), associated with increased risk of chronic opioid use.

PATIENTS AND METHODS

Study cohort. We examined data from the Corrona RA registry. Since 2002, Corrona has enrolled over 42,000 individuals with RA, through 650 academic and community rheumatologists across 40 states in the US (15). Patients and rheumatologists provide data at the time of routine clinical visits, as often as once every 3 months. For the analyses examining prevalence of opioid use over time, we included all participants with RA who had ≥ 90 days of follow-up. For the analyses examining predictors of chronic opioid use, we excluded those who reported prevalent opioid use at study entry. Follow-up began with the baseline Corrona visit and continued through December 31, 2016, the end point defined as chronic opioid use, or loss to follow-up, whichever came first. All subjects provided written informed consent, and the study protocol was approved by the appropriate institutional review boards.

Study end point. The primary outcome measure was chronic opioid use, defined as the documentation of opioid use on patient questionnaires from ≥ 2 consecutive Corrona visits. We chose this definition because the median time between follow-up visits was 156 days, with an interquartile range (IQR) of 113–209 days, and other studies have commonly used intervals between 90 and 180 days as the cutoff for long-term opioid use (16–19). Of note, the questions pertaining to opioid use changed as versions of the Corrona patient questionnaires were updated. In versions 4–7 (used from October 2001 to August 2011), participants were asked if they had taken any of the following drugs in the past 8 weeks: Ultram, Darvon, Tylenol with codeine, Lortab, Vicodin, or Percocet. In versions 8–12 (used from April 2010 to May 2015), opioid use was assessed using the following question: “Do you take a narcotic pain medication?” Participants were provided examples of narcotic pain medications (specifically, Lortab, Vicodin, Percocet, and Darvocet). Darvocet was removed as an example in 2010, when it was taken off the market. In version 13 (used from June 2004 to December 2015), the Corrona questionnaire was changed to ask participants to “check the medications you are taking as of today,” with answer choices including narcotic pain medications (e.g., Lortab, Vicodin, Percocet) and tramadol (e.g., Ultram). If participants answered yes to any of the above questions, they were categorized as current opioid users at the time the survey was administered.

Potential predictors. Demographic information (e.g., age, sex, ethnicity), RA disease characteristics (e.g., seropositivity, RA

duration, disease activity), and medication use were recorded at the time of enrollment. Disease activity was measured using the Clinical Disease Activity Index (CDAI) score, which combines tender and swollen joint counts, patient global assessment of arthritis activity, and physician global assessment of arthritis activity (20). Disability was assessed using the Health Assessment Questionnaire (HAQ) (21,22). Pain intensity was assessed on a scale of 0–100 by the question, “How much pain have you had because of your arthritis in the past week?” Glucocorticoid and disease-modifying antirheumatic drug (DMARD) use data were obtained from the physician questionnaires. DMARDs were categorized as nonbiologic or biologic. Tofacitinib was categorized as a biologic DMARD. Data on nonsteroidal antiinflammatory drug (NSAID) and antidepressant use were obtained by patient report.

Statistical analysis. Baseline descriptive statistics (e.g., medians, frequencies) were calculated. To determine the annual prevalence of chronic opioid use, we performed 2 calculations. In both calculations, the numerator was the number of participants who reported opioid use in ≥ 2 consecutive questionnaires in a given year. In the primary analysis, the denominator was the total number of individuals who contributed data in that year. In the sensitivity analysis, the denominator was the number of individuals who contributed ≥ 2 data points in that year. To characterize the effects of using different questions to ask about chronic opioid use, a sensitivity analysis was performed, excluding data from versions 8–12, in which tramadol was not specifically mentioned as an opioid medication.

Missing data were imputed. For most variables, we assumed these data were missing at random, and missing variables were imputed using MI and MIANALYZE procedures (SAS Institute). For medication data, we set all missing data to 0 (i.e., not taking that particular medication). For insurance categories, missing data among individuals ≥ 65 years were set to “Medicare.”

To estimate hazard ratios (HRs) and 95% confidence intervals (95% CIs) for the relationship between patient characteristics and incident chronic opioid use, we constructed unadjusted Cox proportional hazards models and multivariable Cox proportional hazards models. Covariates included calendar year and all variables with *P* values less than 0.1 in the unadjusted models. The final model for analysis of associations with incident chronic opioid use consisted of individual level variables (age group, sex, ethnicity, insurance status, RA duration, CDAI category, HAQ category, pain level, number of DMARDs used historically, biologic DMARD use, glucocorticoid use, and antidepressant use) after adjusting for intracluster correlations within physicians and physicians’ practices. We performed a sensitivity analysis using a more stringent definition of chronic opioid use, requiring ≥ 3 reports of consecutive opioid use. A subgroup analysis was performed among RA patients who reported ≥ 1 instance of opioid use during the follow-up period. Two-sided *P* values less than 0.05 were considered significant. All analyses were performed using SAS version 9.4.

RESULTS

Prevalence of chronic opioid use over time. Among the 33,739 participants with RA who had ≥ 90 days of follow-up, chronic opioid use increased from 7.4% in 2002 to 16.9% in 2015 (Figure 1). Among RA patients who contributed ≥ 2 data points in a given year, chronic opioid use increased from 14.1% in 2002 to 31.3% in 2015 (see Supplementary Figure 1, on the *Arthritis & Rheumatology* web site at <http://onlinelibrary.wiley.com/doi/10.1002/art.40789/abstract>). Similar results were obtained when we excluded data obtained from survey versions 8–12, which did not specifically list tramadol as an opioid medication.

Characteristics of the incident study cohort. Of the 33,739 RA patients with data on opioid use, 26,288 were not taking opioids at their baseline visit and were included in the analyses examining associations between clinical characteristics and incident chronic opioid use. The median age was 59 years (IQR 49–68), and 75.9% were female (Table 1). Most patients (83.0%) were white. The median CDAI was 9.2 (IQR 3.5–18.0), and the median HAQ score was 0.1 (IQR 0–0.5). Median pain intensity was 24 (IQR 8–50) on a 100-point scale. Biologic DMARDs were received by 40.4% of patients, 27.1% were receiving glucocorticoids, and 17.7% were receiving antidepressants. The median number of DMARDs previously used was 2 (IQR 1–3).

Predictors of incident chronic opioid use. Severe pain (HR 2.53 [95% CI 2.19–2.92]) and antidepressant use (HR 1.79 [95% CI 1.64–1.92]) were the strongest predictors of incident chronic opioid use (Table 2). High disease activity (HR 1.55 [95% CI 1.30–1.84]), high level of disability (HR 1.45 [95% CI 1.27–1.65]), Medicaid insurance (HR 1.30 [95% CI 1.09–1.55]), and Medicare insurance (HR 1.27 [95% CI 1.12–1.44]) were also significantly associated with incident chronic opioid use. In addition, medications for RA, specifically glucocorticoids (HR 1.14 [95% CI 1.04–1.25]) and number of previous DMARDs (HR 1.08 [95% CI 1.04–1.11]), were associated with a risk of incident chronic opioid use. Conversely, Asian ethnicity was associated with a lower risk

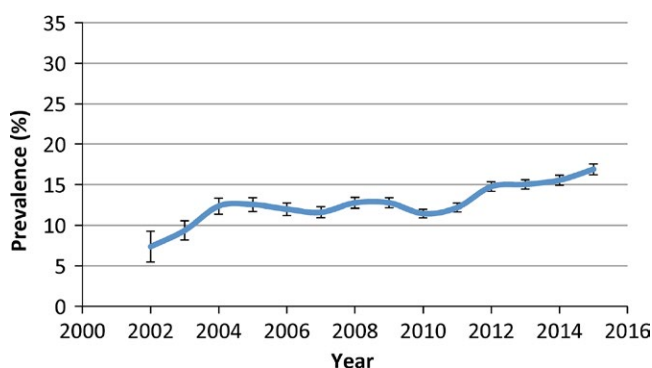


Figure 1. Trend in chronic opioid use (defined as ≥ 2 consecutive reports of opioid use) among 33,739 rheumatoid arthritis patients with ≥ 90 days of follow-up. Bars show the 95% confidence interval.

Table 1. Baseline patient characteristics (n = 26,288) at entry into analyses*

Demographic data	
Age, median (IQR) years	59 (49–68)
Female sex	19,942 (75.9)
Ethnicity	
White	21,819 (83.0)
Hispanic	1,669 (6.4)
Black	1,789 (6.8)
Asian	500 (1.9)
Other	511 (1.9)
Duration of follow-up, median (IQR) years	3.1 (1.3–5.7)
Insurance status	
None	721 (2.7)
Medicaid	1,501 (5.7)
Medicare	8,299 (31.6)
Medicaid and Medicare	523 (2.0)
Private	15,244 (58.0)
RA-related variables	
RA duration, median (IQR) years	5 (1–13)
CDAI score (range 0–76), median (IQR)	9.2 (3.5–18.0)
HAQ DI score (range 0–3), median (IQR)	0.1 (0–0.5)
Pain intensity score (range 0–100), median (IQR)	24 (8–50)
Medication use	
No. of DMARDs previously taken, median (IQR)	2 (1–3)
Current medications	
Nonbiologic DMARDs	21,530 (81.9)
Biologic DMARDs†	10,617 (40.4)
Glucocorticoids	7,134 (27.1)
Antidepressants‡	3,992 (17.7)

* Except where indicated otherwise, values are the number (%) of patients. IQR = interquartile range; RA = rheumatoid arthritis; CDAI = Clinical Disease Activity Index; HAQ DI = Health Assessment Questionnaire disability index.

† Tofacitinib was categorized as a biologic disease-modifying anti-rheumatic drug (DMARD).

‡ Total number of patients with data on antidepressant treatment was 22,498.

of chronic opioid use (HR 0.49 [95% CI 0.36–0.68]). In a sensitivity analysis with a more stringent definition of chronic opioid use (≥ 3 documentations of consecutive opioid use), similar results were observed (Table 2).

Subgroup analyses among RA patients who reported ≥ 1 instance of opioid use. To determine whether similar factors were associated with chronic opioid use among RA patients exposed to opioids at least once during follow-up,

Table 2. Unadjusted and multivariable adjusted HRs for the association between patient characteristics and chronic opioid use among RA patients*

Patient characteristic	Reported opioid use ≥ 2 times		Reported opioid use ≥ 3 times	
	Unadjusted HR (95% CI)	Multivariable adjusted HR (95% CI)†	Unadjusted HR (95% CI)	Multivariable adjusted HR (95% CI)†
Demographic data				
Age				
<50 years	1.00‡	1.00‡	1.00‡	1.00‡
≥ 50 –59 years	1.24 (1.15–1.35)	1.14 (1.04–1.25)	1.30 (1.16–1.45)	1.20 (1.06–1.34)
≥ 60 –69 years	1.17 (1.08–1.28)	1.06 (0.97–1.17)	1.11 (1.00–1.23)	1.00 (0.89–1.13)
≥ 70 years	1.10 (0.98–1.24)	1.02 (0.88–1.17)	0.92 (0.79–1.07)	0.84 (0.71–1.00)
Female sex	1.18 (1.08–1.29)	1.04 (0.96–1.14)	1.15 (1.03–1.29)	0.99 (0.89–1.10)
Ethnicity				
White	1.00‡	1.00‡	1.00‡	1.00‡
Hispanic	1.12 (0.94–1.33)	1.00 (0.82–1.23)	1.07 (0.89–1.30)	0.96 (0.77–1.20)
Black	1.11 (0.93–1.33)	1.04 (0.86–1.25)	1.05 (0.84–1.32)	1.01 (0.81–1.26)
Asian	0.45 (0.33–0.63)	0.49 (0.36–0.68)	0.51 (0.34–0.76)	0.56 (0.37–0.84)
Other	1.26 (1.02–1.55)	1.16 (0.93–1.45)	1.38 (1.08–1.75)	1.27 (0.99–1.63)
Insurance status				
Private	1.00‡	1.00‡	1.00‡	1.00‡
Medicaid	1.52 (1.26–1.83)	1.30 (1.09–1.55)	1.42 (1.16–1.73)	1.13 (0.94–1.37)
Medicare	1.26 (1.15–1.38)	1.27 (1.12–1.44)	1.14 (1.02–1.27)	1.26 (1.11–1.44)
Medicaid and Medicare	1.66 (1.32–2.09)	1.18 (0.91–1.52)	1.45 (1.06–1.99)	1.10 (0.78–1.54)
None	1.14 (0.82–1.56)	1.01 (0.75–1.37)	1.09 (0.76–1.55)	0.99 (0.70–1.40)
RA-related variables				
RA duration				
≤ 5 years	1.00‡	1.00‡	1.00‡	1.00‡
>5–10 years	0.97 (0.86–1.09)	0.93 (0.83–1.05)	1.00 (0.87–1.16)	0.97 (0.84–1.11)
>10 years	1.14 (1.03–1.27)	1.02 (0.91–1.13)	1.18 (1.05–1.32)	1.05 (0.94–1.18)
CDAI score				
Remission (≤ 2.8)	1.00‡	1.00‡	1.00‡	1.00‡
Low (>2.8–10)	1.81 (1.56–2.10)	1.31 (1.14–1.51)	1.82 (1.54–2.16)	1.30 (1.10–1.54)
Moderate (>10–22)	2.52 (2.15–2.95)	1.51 (1.31–1.74)	2.66 (2.21–3.22)	1.56 (1.30–1.86)
High (>22)	3.40 (2.90–3.99)	1.55 (1.30–1.84)	3.69 (3.04–4.47)	1.67 (1.36–2.04)
HAQ DI score				
≤ 0.5	1.00‡	1.00‡	1.00‡	1.00‡
>0.5–1.0	2.24 (2.05–2.44)	1.36 (1.24–1.48)	2.24 (2.01–2.51)	1.32 (1.18–1.48)
>1.0	2.85 (2.54–3.20)	1.45 (1.27–1.65)	2.69 (2.30–3.15)	1.30 (1.09–1.55)
Pain level				
None (<10)	1.00‡	1.00‡	1.00‡	1.00‡
Low (10–40)	1.91 (1.67–2.18)	1.56 (1.37–1.78)	2.11 (1.83–2.43)	1.68 (1.45–1.94)
Moderate (>40–60)	3.37 (2.93–3.88)	2.23 (1.93–2.57)	3.57 (3.04–4.18)	2.30 (1.96–2.71)
Severe (>60)	4.40 (3.86–5.01)	2.53 (2.19–2.92)	4.83 (4.13–5.64)	2.70 (2.26–3.21)
Medication use				
No. of DMARDs previously taken	1.13 (1.09–1.16)	1.08 (1.04–1.11)	1.15 (1.10–1.91)	1.08 (1.04–1.12)
Current medications				
Biologic DMARDs	1.26 (1.13–1.40)	1.09 (0.99–1.20)	1.30 (1.13–1.48)	1.10 (0.97–1.24)
Glucocorticoids	1.34 (1.22–1.48)	1.14 (1.04–1.25)	1.42 (1.27–1.69)	1.21 (1.08–1.35)
Antidepressants	2.12 (1.97–2.29)	1.79 (1.64–1.92)	2.25 (2.03–2.48)	1.86 (1.68–2.07)

* Values are based on a patient population of 26,288. HRs = hazard ratios; 95% CI = 95% confidence interval (see Table 1 for other definitions).

† All multivariable models were also adjusted for calendar year and intracluster correlations within physicians and physicians' practices.

‡ Referent.

Table 3. Unadjusted and multivariable adjusted HRs for the association between patient characteristics and chronic opioid use among a subgroup of RA patients who reported ≥ 1 instance of opioid use during the follow-up period*

Patient characteristic	Unadjusted HR (95% CI)	Multivariable adjusted HR (95% CI)†	Patient characteristic	Unadjusted HR (95% CI)	Multivariable adjusted HR (95% CI)†
Demographic data			CDAI score		
Age			Remission (≤ 2.8)		
<50 years	1.00‡	1.00‡	Low (>2.8–10)	1.30 (1.14–1.49)	1.13 (0.98–1.29)
≥ 50 –59 years	1.12 (1.03–1.21)	1.07 (0.98–1.17)	Moderate (>10–22)	1.43 (1.24–1.66)	1.16 (1.00–1.33)
≥ 60 –69 years	1.04 (0.96–1.13)	0.98 (0.89–1.08)	High (>22)	1.69 (1.46–1.95)	1.21 (1.03–1.42)
≥ 70 years	1.03 (0.92–1.16)	0.98 (0.86–1.10)	HAQ DI score		
Female sex	1.02 (0.94–1.10)	0.97 (0.89–1.05)	≤ 0.5	1.00‡	1.00‡
Ethnicity			>0.5–1.0	1.48 (1.35–1.62)	1.17 (1.07–1.28)
White	1.00‡	1.00‡	>1.0	1.62 (1.44–1.84)	1.18 (1.04–1.34)
Hispanic	1.09 (0.92–1.30)	1.04 (0.90–1.21)	Pain level		
Black	0.96 (0.81–1.15)	0.90 (0.76–1.08)	None (<10)	1.00‡	1.00‡
Asian	0.80 (0.59–1.09)	0.79 (0.58–1.07)	Low (10–40)	1.36 (1.20–1.54)	1.29 (1.14–1.46)
Other	0.97 (0.79–1.20)	1.04 (0.83–1.31)	Moderate (>40–60)	1.78 (1.56–2.04)	1.52 (1.32–1.75)
Insurance status			Severe (>60)	2.11 (1.85–2.42)	1.65 (1.42–1.92)
Private	1.00‡	1.00‡	Medication use		
Medicaid	0.99 (0.86–1.14)	1.21 (1.06–1.39)	No. of DMARDs previously taken	1.03 (1.00–1.06)	1.03 (1.00–1.06)
Medicare	1.08 (1.00–1.17)	1.13 (1.02–1.26)	Current medications		
Medicaid and Medicare	1.10 (0.87–1.40)	0.94 (0.72–1.23)	Biologic DMARDs	1.10 (1.00–1.21)	0.98 (0.90–1.06)
None	1.16 (0.92–1.47)	1.08 (0.89–1.32)	Glucocorticoids	1.08 (0.99–1.19)	1.05 (0.97–1.14)
RA-related variables			Antidepressants	1.39 (1.29–1.50)	1.24 (1.15–1.34)
RA duration					
≤ 5 years	1.00‡	1.00‡			
>5–10 years	0.88 (0.79–0.99)	0.93 (0.83–1.03)			
>10 years	0.97 (0.88–1.07)	1.02 (0.92–1.14)			

* Values are based on a subgroup patient population of 7,137. HRs = hazard ratios; 95% CI = 95% confidence interval (see Table 1 for other definitions).

† All multivariable models were also adjusted for calendar year and intracluster correlations within physicians and physicians' practices.

‡ Referent.

we performed a subgroup analysis ($n = 7,137$). Within this subgroup, 3,446 patients (48.3%) ultimately reached the end point defined as chronic opioid use. The strongest predictors of incident chronic opioid use were severe pain at baseline (HR 1.65 [95% CI 1.42–1.92]) and antidepressant use (HR 1.24 [95% CI 1.15–1.34]) (Table 3). In addition, there was an increased risk of chronic opioid use among individuals with high disease activity (HR 1.21 [95% CI 1.03–1.42]), a higher disability index (HR 1.18 [95% CI 1.04–1.34]), and those with Medicaid insurance (HR 1.21 [95% CI 1.06–1.39]) or Medicare insurance (HR 1.13 [95% CI 1.02–1.26]). Specific medications for RA (e.g., biologic DMARDs, glucocorticoids) were not associated with risk of incident chronic opioid use, although the number of DMARDs previously taken remained weakly associated with chronic opioid use (HR 1.03 [95% CI 1.00–1.06]) (Table 3).

DISCUSSION

Among individuals with RA, the annual prevalence of chronic opioid use has more than doubled, from 7.4% in 2002 to 16.9% in 2015. Severe pain and antidepressant use were the strongest independent predictors of incident chronic opioid use, whereas Asian ethnicity was most strongly associated with a decreased risk of chronic opioid use. In the subgroup of individuals who reported ≥ 1 instance of opioid use during follow-up, severe pain at baseline and antidepressant use continued to be strongly associated with an increased risk of chronic opioid use.

These findings are important to consider within the context of the opioid epidemic, which gained recognition in the early 2000s. Initial studies showed an increase in overall opioid prescriptions between the 1990s and 2010, followed by a plateau or decrease in

rates of opioid prescriptions in recent years (1,9,23,24). In chronic disease populations, similar increases were observed in the late 1990s to early 2000s. Using data from the National Ambulatory Medical Care Survey and the National Hospital Ambulatory Medical Care Survey, Mafi et al showed that opioid pain medication use for back pain increased from 19.3% in 1999 to 29.1% in 2010 (25). Similarly, Wright et al reported that the percentage of patients with knee osteoarthritis receiving opioids increased from 31% in 2003 to 40% in 2009 (26). However, no data after 2010 were available from these studies.

Considering these findings, our results are particularly interesting, because we continued to observe increases in self-reported chronic opioid use among our population of RA patients from 2010 to 2015. The majority of studies showing a plateau in opioid prescription rates after 2010 included data from the general population, rather than from a specific chronic disease population, indicating that factors influencing the decrease in opioid prescriptions in the general population (e.g., withdrawal of propoxyphene from the market, increased physician and patient education on the risks of opioid use) may be less influential when considering opioid prescriptions for chronic pain populations, such as RA patients. In addition, our study focused on patient-reported use of opioids, which may be uncoupled from opioid prescriptions if patients use opioids left over from previous prescriptions or those prescribed to family members or friends.

Although the prevalence of chronic opioid use continued to increase in the 2010s, annual frequencies of opioid use in this study were lower than the frequencies of opioid prescriptions reported in claims data. A study using data from Tennessee Medicaid databases reported rates ranging from 38% to 55% from 1995 to 2004 (8), and a more recent study of RA patients with Medicare insurance showed estimated percentages in the low 40s between 2007 and 2014 (9). A potential explanation for this discrepancy is the difference in the outcome measure, specifically, patient self-reported opioid use versus opioid prescription data. Participants may not use all of their medication at the time of prescription. In addition, some participants may not be comfortable reporting opioid use. In a study linking the Quebec Pain Registry to Quebec prescription claims databases, the κ coefficient for agreement on opioid use was 0.57–0.67, which is in the weak-to-moderate range (27,28). According to the authors, the discordance was predominantly due to lower rates of patient-reported medication use compared to prescription claims, which is consistent with what we observed in the present study. Additional studies linking clinical registry data to claims data are needed to shed light on the discrepancies between prescription data versus self-reported opioid consumption data.

In RA patients, severe pain was the strongest predictor of incident chronic opioid use, independent of disease activity and disability. High disease activity and high disability levels were also associated with chronic opioid use, independent of pain. Notably, biologic DMARD use was associated with chronic opioid use

only in unadjusted analyses, and not in adjusted analyses that included disease activity as a covariate. This finding indicates that the association between biologic DMARD use and chronic opioid use was not independent of disease activity, suggesting that biologic DMARD use may have served as a marker for high disease activity in unadjusted analyses.

These data complement results from 2 previous studies: a study using Medicare claims data (9) and a study using data from a population-based incidence cohort of RA patients (the Rochester Epidemiology Project) (29). While the latter study included information about some RA disease characteristics (e.g., rheumatoid factor/anti-citrullinated peptide antibody positivity, erythrocyte sedimentation rate, erosions), neither study included information on pain and/or RA disease activity, which may be more likely to drive patient behaviors. Our results suggest that RA disease activity should be treated aggressively, as with a treat-to-target strategy (30), and, in addition to treating inflammation with DMARDs, physicians should be mindful of evaluating and managing pain caused by other etiologies (e.g., osteoarthritis, noninflammatory back pain, fibromyalgia). An evaluation of possible comorbid conditions should be pursued, and, if diagnosed, treated accordingly, preferably without the use of opioid analgesics.

In addition to pain, antidepressant use was associated with an increased risk (1.79-fold) of chronic opioid use in this study. The association between depression and chronic opioid use has been well documented in the postsurgical population (31–33) and in chronic disease populations (34), including in the above-mentioned study of an RA cohort identified from Medicare claims data (9). In contrast, the Rochester Epidemiology Project study did not show an association between treatment for depression and chronic opioid use (29). The authors hypothesized that other factors related to RA may have outweighed the effects of depression on chronic opioid use among individuals with RA. In our cohort, we continued to see a statistically significant relationship between antidepressant use and chronic opioid use in multivariable analyses, though the magnitude of the HR decreased from 2.12 in unadjusted analyses to 1.79 in the fully adjusted model, which included RA-related factors as covariates.

We were particularly interested in the risk of chronic opioid use in RA patients who reported ≥ 1 instance of opioid use in the follow-up period, because these data provide information regarding the risk of chronic opioid use among those who were exposed to opioids. Results of this analysis were similar to results of the overall analysis, though the strengths of association were diminished.

A major strength of the present study is the large Corrona registry, which includes a wealth of data on clinical variables related to RA from tens of thousands of RA patients recruited from academic and community-based clinics around the country. Thus, data from the Corrona registry have the advantage of being more generalizable than single-center studies or studies based solely at academic centers. It also includes detailed patient-level informa-

tion, such as disease activity, pain, and disability, which are not available in claims databases. In addition, while claims databases necessarily draw from prescription data, Corrona includes information on patient-reported medication use.

Limitations of our study include possible selection bias and the absence of a concurrent control population. To identify predictors of chronic opioid use, it was necessary to exclude those taking opioids at the time of registry enrollment. However, the remaining participants may have been at a lower risk of chronic opioid use since they had lived many years without taking opioids according to the definition of chronic use. Therefore, observed associations in this population may not be generalizable to a younger population. In addition, without a control population, it remains unclear whether the observed changes in prevalence are specific to RA or whether they reflect a general trend. However, most general population studies have revealed a plateau or decrease in the prevalence of chronic opioid use after 2010, suggesting that the continued increases seen in this study may be specific to RA (4,23,24).

Another limitation of this study is the absence of information on specific types and dosages of opioids. As a result, we were unable to compare the use of different types of opioids or determine changes in the amount of opioids used. In addition, the questions about opioid use evolved as versions of the Corrona patient questionnaires were updated. The most notable difference was that tramadol was not specifically highlighted as an example of an opioid in survey versions 8–12. When data from these surveys were excluded in the assessment of trends in chronic opioid use over time, no substantive changes were observed, indicating that most participants recognized Ultram as an opioid medication, even if it was not explicitly identified as such in the question itself. There was also overlap in the use of different questionnaire versions across time, making it less likely that the observed changes were an artifact of changing questionnaires alone.

Finally, the focus of this study was to identify independent predictors of chronic opioid use and not to test a specific hypothesis (e.g., that pain intensity predicts chronic opioid use). Although we examined the association between multiple patient-related variables and chronic opioid use, it is likely that unmeasured confounders exist; thus, the coefficients presented in this article may not represent unconfounded estimates of risk. In particular, standardized radiographic scores, such as Sharp/van der Heijde scores (35), were not available in this data set. Therefore, we were not able to assess the extent to which RA damage, rather than disease activity, drove opioid pain medication use, although an earlier study of 501 RA patients did not show a statistically significant association between radiographically evident erosions/destructive changes and chronic opioid use (29).

In conclusion, we demonstrated that, among RA patients, self-reported opioid use increased from 2002 to 2015. Our study also identified important potential drivers of opioid use among individu-

als with RA. In particular, severe pain at baseline and antidepressant use were strongly associated with chronic opioid use, independent of RA disease activity, and baseline RA disease activity and disability were associated with chronic opioid use, independent of baseline pain. These data highlight the importance of aggressively treating inflammatory disease activity with a treat-to-target strategy, and of evaluating and treating pain and mental health problems, before prescribing opioid medications and in addition to treating with DMARDs. Future research is needed to identify alternative pain management strategies for patients with RA.

AUTHOR CONTRIBUTIONS

All authors were involved in drafting the article or revising it critically for important intellectual content, and all authors approved the final version to be published. Dr. Lee had full access to all of the data in the study and takes responsibility for the integrity of the data and the accuracy of the data analysis.

Study conception and design. Lee, Solomon.

Acquisition of data. Kremer, Greenberg.

Analysis and interpretation of data. Lee, Guan, Solomon.

REFERENCES

- Dart RC, Surratt HL, Cicero TJ, Parrino MW, Severtson SG, Bucher-Bartelson B, et al. Trends in opioid analgesic abuse and mortality in the United States. *N Engl J Med* 2015;372:241–8.
- Kuo YF, Raji MA, Chen NW, Hasan H, Goodwin JS. Trends in opioid prescriptions among part D Medicare recipients from 2007 to 2012. *Am J Med* 2016;129:e21–30.
- Guy GP Jr, Zhang K, Bohm MK, Losby J, Lewis B, Young R, et al. Vital signs: changes in opioid prescribing in the United States, 2006–2015. *MMWR Morb Mortal Wkly Rep* 2017;66:697–704.
- Axeen S. Trends in opioid use and prescribing in Medicare, 2006–2012. *Health Serv Res* 2018;53:3309–28.
- Han B, Compton WM, Blanco C, Crane E, Lee J, Jones CM. Prescription opioid use, misuse, and use disorders in U.S. adults: 2015 national survey on drug use and health. *Ann Intern Med* 2017;167:293–301.
- Ray WA, Chung CP, Murray KT, Hall K, Stein CM. Prescription of long-acting opioids and mortality in patients with chronic noncancer pain. *JAMA* 2016;315:2415–23.
- Hamina A, Taipale H, Tanskanen A, Tolppanen AM, Karttunen N, Pylkanen L, et al. Long-term use of opioids for nonmalignant pain among community-dwelling persons with and without Alzheimer disease in Finland: a nationwide register-based study. *Pain* 2017;158:252–60.
- Grijalva CG, Chung CP, Stein CM, Mitchel EF Jr, Griffin MR. Changing patterns of medication use in patients with rheumatoid arthritis in a Medicaid population. *Rheumatology (Oxford)* 2008;47:1061–4.
- Curtis JR, Xie F, Smith C, Saag KG, Chen L, Beukelman T, et al. Changing trends in opioid use among patients with rheumatoid arthritis in the United States. *Arthritis Rheumatol* 2017;69:1733–40.
- Whittle SL, Richards BL, Husni E, Buchbinder R. Opioid therapy for treating rheumatoid arthritis pain. *Cochrane Database Syst Rev* 2011:CD003113.
- Whittle SL, Richards BL, van der Heijde DM, Buchbinder R. The efficacy and safety of opioids in inflammatory arthritis: a Cochrane systematic review. *J Rheumatol Suppl* 2012;90:40–6.
- Whittle SL, Richards BL, Buchbinder R. Opioid analgesics for rheumatoid arthritis pain. *JAMA* 2013;309:485–6.

13. Acurcio FA, Moura CS, Bernatsky S, Bessette L, Rahme E. Opioid use and risk of nonvertebral fractures in adults with rheumatoid arthritis: a nested case-control study using administrative databases. *Arthritis Rheumatol* 2016;68:83–91.
14. Wiese AD, Griffin MR, Stein CM, Mitchel EF Jr, Grijalva CG. Opioid analgesics and the risk of serious infections among patients with rheumatoid arthritis: a self-controlled case series study. *Arthritis Rheumatol* 2016;68:323–31.
15. Kremer JM. The Corrona US registry of rheumatic and autoimmune diseases. *Clin Exp Rheumatol* 2016;34 Suppl 101:S96–9.
16. Jena AB, Goldman D, Karaca-Mandic P. Hospital prescribing of opioids to Medicare beneficiaries. *JAMA Intern Med* 2016;176:990–7.
17. Dunn KM, Saunders KW, Rutter CM, Banta-Green CJ, Merrill JO, Sullivan MD, et al. Opioid prescriptions for chronic pain and overdose: a cohort study. *Ann Intern Med* 2010;152:85–92.
18. Braden JB, Russo J, Fan MY, Edlund MJ, Martin BC, DeVries A, et al. Emergency department visits among recipients of chronic opioid therapy. *Arch Intern Med* 2010;170:1425–32.
19. Barnett ML, Olenski AR, Jena AB. Opioid-prescribing patterns of emergency physicians and risk of long-term use. *N Engl J Med* 2017;376:663–73.
20. Aletaha D, Nell VP, Stamm T, Uffmann M, Pflugbeil S, Machold K, et al. Acute phase reactants add little to composite disease activity indices for rheumatoid arthritis: validation of a clinical activity score. *Arthritis Res Ther* 2005;7:R796–806.
21. Bruce B, Fries JF. The Health Assessment Questionnaire (HAQ). *Clin Exp Rheumatol* 2005;23 Suppl 39:S14–8.
22. Fries JF, Spitz P, Kraines RG, Holman HR. Measurement of patient outcome in arthritis. *Arthritis Rheum* 1980;23:137–45.
23. Boudreau D, Von Korff M, Rutter CM, Saunders K, Ray GT, Sullivan MD, et al. Trends in long-term opioid therapy for chronic non-cancer pain. *Pharmacoepidemiol Drug Saf* 2009;18:1166–75.
24. Larochelle MR, Zhang F, Ross-Degnan D, Wharam JF. Rates of opioid dispensing and overdose after introduction of abuse-deterrent extended-release oxycodone and withdrawal of propoxyphene. *JAMA Intern Med* 2015;175:978–87.
25. Mafi JN, McCarthy EP, Davis RB, Landon BE. Worsening trends in the management and treatment of back pain. *JAMA Intern Med* 2013;173:1573–81.
26. Wright EA, Katz JN, Abrams S, Solomon DH, Losina E. Trends in prescription of opioids from 2003–2009 in persons with knee osteoarthritis. *Arthritis Care Res (Hoboken)* 2014;66:1489–95.
27. Lacasse A, Ware MA, Bourgault P, Lanctot H, Dorais M, Boulanger A, et al. Accuracy of self-reported prescribed analgesic medication use: linkage between the Quebec Pain Registry and the Quebec administrative prescription claims databases. *Clin J Pain* 2016;32:95–102.
28. McHugh ML. Interrater reliability: the κ statistic. *Biochem Med (Zagreb)* 2012;22:276–82.
29. Zamora-Legoff JA, Achenbach SJ, Crowson CS, Krause ML, Davis JM III, Matteson EL. Opioid use in patients with rheumatoid arthritis 2005–2014: a population-based comparative study. *Clin Rheumatol* 2016;35:1137–44.
30. Grigor C, Capell H, Stirling A, McMahon AD, Lock P, Vallance R, et al. Effect of a treatment strategy of tight control for rheumatoid arthritis (the TICORA study): a single-blind randomised controlled trial. *Lancet* 2004;364:263–9.
31. Schoenfeld AJ, Nwosu K, Jiang W, Yau AL, Chaudhary MA, Scully RE, et al. Risk factors for prolonged opioid use following spine surgery, and the association with surgical intensity, among opioid-naïve patients. *J Bone Joint Surg Am* 2017;99:1247–52.
32. Sun EC, Darnall BD, Baker LC, Mackey S. Incidence of and risk factors for chronic opioid use among opioid-naïve patients in the postoperative period. *JAMA Intern Med* 2016;176:1286–93.
33. Inacio MC, Hansen C, Pratt NL, Graves SE, Roughead EE. Risk factors for persistent and new chronic opioid use in patients undergoing total hip arthroplasty: a retrospective cohort study. *BMJ Open* 2016;6:e010664.
34. Merlin JS, Tamhane A, Starrels JL, Kertesz S, Saag M, Cropsey K. Factors associated with prescription of opioids and co-prescription of sedating medications in individuals with HIV. *AIDS Behav* 2016;20:687–98.
35. Van der Heijde DM. How to read radiographs according to the Sharp/van der Heijde method [corrected and republished in *J Rheumatol* 2000;27:261–3]. *J Rheumatol* 1999;26:743–5.

Profiling of Gene Expression Biomarkers as a Classifier of Methotrexate Nonresponse in Patients With Rheumatoid Arthritis

Darren Plant,¹ Mateusz Maciejewski,² Samantha Smith,³ Nisha Nair,³ the Maximising Therapeutic Utility in Rheumatoid Arthritis Consortium, the RAMS Study Group, Kimme Hyrich,¹ Daniel Ziemek,² Anne Barton,¹ and Suzanne Verstappen¹

Objective. Approximately 30–40% of rheumatoid arthritis (RA) patients who are initially started on low-dose methotrexate (MTX) will not benefit from the treatment. To date, no reliable biomarkers of MTX inefficacy in RA have been identified. The aim of this study was to analyze whole blood samples from RA patients at 2 time points (pretreatment and 4 weeks following initiation of MTX), to identify gene expression biomarkers of the MTX response.

Methods. RA patients who were about to commence treatment with MTX were selected from the Rheumatoid Arthritis Medication Study. Using European League Against Rheumatism (EULAR) response criteria, 42 patients were categorized as good responders and 43 as nonresponders at 6 months following the initiation of MTX treatment. Data on whole blood transcript expression were generated, and supervised machine learning methods were used to predict a EULAR nonresponse. Models in which transcript levels were included were compared to models in which clinical covariates alone (e.g., baseline disease activity, sex) were included. Gene network and ontology analysis was also performed.

Results. Based on the ratio of transcript values (i.e., the difference in \log_2 -transformed expression values between 4 weeks of treatment and pretreatment), a highly predictive classifier of MTX nonresponse was developed using L2-regularized logistic regression (mean \pm SEM area under the receiver operating characteristic [ROC] curve [AUC] 0.78 ± 0.11). This classifier was superior to models that included clinical covariates (ROC AUC 0.63 ± 0.06). Pathway analysis of gene networks revealed significant overrepresentation of type I interferon signaling pathway genes in nonresponders at pretreatment ($P = 2.8 \times 10^{-25}$) and at 4 weeks after treatment initiation ($P = 4.9 \times 10^{-26}$).

Conclusion. Testing for changes in gene expression between pretreatment and 4 weeks post-treatment initiation may provide an early classifier of the MTX treatment response in RA patients who are unlikely to benefit from MTX over 6 months. Such patients should, therefore, have their treatment escalated more rapidly, which would thus potentially impact treatment pathways. These findings emphasize the importance of a role for early treatment biomarker monitoring in RA patients started on MTX.

INTRODUCTION

Low-dose methotrexate (MTX) is the key therapy for the majority of patients with rheumatoid arthritis (RA). However, in ~30–40% of patients treated with MTX, disease activity is not adequately controlled (1), but current guidelines suggest that MTX treatment be administered for 6 months before a decision

is made as to its efficacy (2). It is now well-established that early, effective therapy prevents long-term joint damage and disability (3), and the availability of biologic agents emphasizes the importance of identifying those patients who will not do well with MTX therapy, and who should, therefore, be fast-tracked to more targeted therapies in order to protect against progressive and irreversible joint damage.

Supported by Arthritis Research UK (grants 20385, 20380, and 20670), the Medical Research Council (MR/K015346/1), and Pfizer (I-CRP).

¹Darren Plant, PhD, Kimme Hyrich, MD, PhD, FRCPC, Anne Barton, FRCP, PhD, Suzanne Verstappen, PhD: Manchester University NHS Foundation Trust, Manchester, UK; ²Mateusz Maciejewski, PhD, Daniel Ziemek, PhD: Pfizer, Cambridge, Massachusetts; ³Samantha Smith, PhD, Nisha Nair, PhD: University of Manchester, Manchester, UK.

Drs. Plant and Maciejewski contributed equally to this work.

Drs. Maciejewski and Ziemek are full-time employees of Pfizer and own stock or stock options in Pfizer. No other disclosures relevant to this article were reported.

Address correspondence to Anne Barton, FRCP, PhD, Division of Musculoskeletal and Dermatological Sciences, University of Manchester, Manchester, M13 9PT, UK. E-mail: anne.barton@manchester.ac.uk.

Submitted for publication July 11, 2018; accepted in revised form December 4, 2018.

Although MTX has been used for more than 2 decades to treat RA, our ability to predict who will experience a good response versus nonresponse remains very limited. Clinical and demographic factors are only moderately predictive of the clinical response to MTX. For example, age and seropositivity (e.g., seropositive for rheumatoid factor, anti-cyclic citrullinated peptide antibodies [ACPAs]) are not robustly associated with MTX response (4–6), whereas male patients tend to respond better than female patients (7). Furthermore, patients with low levels of disease activity tend to respond better than those with higher disease activity. Finally, patients who take non-steroidal antiinflammatory drugs tend to respond better to MTX than those who do not (7), while prior treatment with disease-modifying antirheumatic drugs has been associated with MTX nonresponse (8).

Several studies have tested whether genetic and genomic factors can predict the response to MTX (9). However, many of the published studies have been small and have assessed a limited number of genes, with limited coverage. Moreover, the results of those studies have not been validated.

Expression microarrays have been investigated as a potential source of biomarkers that may be predictive of the treatment response in RA (10). The majority of studies have focused on response to biologic therapies, and not MTX (11,12), and there has been little consistency in the findings. These inconsistencies could be attributable to differences in study design and inclusion criteria, the time point assessed, the sample sizes investigated, lack of appropriate model validation, the drugs studied, and the assessment of individual, rather than combined, groups of related transcripts (10). Nonetheless, in other diseases, gene expression has been used to stratify the underlying disease into subgroups with differing responses to treatments. For example, several markers that can predict the responsiveness to endocrine therapies in patients with breast cancer have been identified (13–17).

Therefore, the aim of the current study was to identify gene transcripts in patients with recent-onset RA that could potentially be used to classify nonresponse to MTX at 6 months following the initiation of treatment, when tested either before MTX is initiated or at a time point (4 weeks) shortly after treatment initiation.

PATIENTS AND METHODS

Patients and samples. Patients in this study were participants in the Rheumatoid Arthritis Medication Study (RAMS), a national multicenter, longitudinal observational study in the UK that recruits patients with RA who have commenced MTX monotherapy for the first time. MTX was prescribed according to local practice. Patients were seen by a research nurse prior to commencement of MTX and at 3, 6, and 12 months thereafter. Clinical assessments included 28-joint counts of swollen and tender joints. Patients completed health status questionnaires,

including a self-report of current functional disability using the Health Assessment Questionnaire (HAQ) (a score of ≤ 1 was considered low) (18). Blood samples were obtained at each visit, and serum was stored at -80°C prior to measuring the C-reactive protein (CRP) level and ACPAs. The Disease Activity Score in 28 joints using CRP level (DAS28-CRP) was calculated at baseline and at 6 months, and established European League Against Rheumatism (EULAR) response criteria were applied (19) to categorize patients as either MTX good responders or MTX nonresponders over the course of 6 months of treatment.

Samples of whole blood from the patients was drawn into Tempus blood tubes at the pretreatment and 4-week time points, before being shipped to the central processing laboratory at the Arthritis Research UK Centre for Genetics and Genomics. The samples were logged onto a laboratory information management system and stored at -80°C .

Expression profiling. Total RNA was extracted using a Tempus Spin RNA isolation kit, according to the manufacturer's protocol. After extraction, RNA was quantified using a Thermo Scientific Nanodrop ND-1000 spectrophotometer, and RNA integrity was assessed using an Agilent Technologies 2100 Bioanalyzer. An optical density at 260/280 nm ($\text{OD}_{260/280\text{ nm}}$) of ~ 2 and an $\text{OD}_{260/230\text{ nm}}$ of 2–2.2 suggests that no contaminants were present within a sample, and an RNA integrity number of >6 was deemed to indicate sufficient RNA quality.

RNA samples were labeled with biotin and amplified using an Illumina TotalPrep RNA amplification kit. Following labeling and amplification, the RNA was re-quantified and 750 ng was hybridized onto Illumina HumanHT-12-v4 Expression BeadChips (which target 47,000 probes), in accordance with the direct hybridization protocol. Scanning was performed using an Illumina iScan system, in order to collect raw intensity data from the expression BeadChips prior to export into GenomeStudio for further analysis.

Data quality control. GenomeStudio software was used to assess control probe summary statistics and summarize bead-level expression data. Quality control was performed using the limma Bioconductor package (20). Probes not expressed on any array or probe sequences with undesirable properties (e.g., poor mapping) were removed, and data were quantile normalized and \log_2 transformed. Potential batch effects were assessed by visual inspection of multidimensional scaling plots, and principal components analysis and hierarchical clustering of samples was performed to identify sample outliers.

Statistical analysis. Classifier performance. We built statistical machine learning models to distinguish therapeutic nonresponders from responders (assessed at 6 months) using gene expression data at pretreatment and 4 weeks, and using the ratio

of gene expression (i.e., the difference in \log_2 -transformed transcript expression intensity between 4 weeks of treatment and pretreatment [a total of 6 contrasts]). In addition, we built models based on clinical variables at pretreatment and 3 month. These models included sex, age at disease onset, HAQ score, smoking habits, ACPA positivity (titer >10 units/ml), number of swollen joints, number of tender joints, CRP levels, and patient's assessment of overall well-being (on 100-mm visual analog scale [VAS]).

For each contrast, we employed 3 state-of-the-art machine learning methods with different characteristics: a linear method (regularized logistic regression), a nonlinear method (random forest), and, in the case of the contrasts using gene expression data, a pathway-supported approach (21). Standardization was applied to all input data, and each method was run under a 10-fold nested cross-validation scheme (where hyperparameters were computed in each of the strata using an inner 5-fold cross-validation loop) to give accurate estimates of predicted performance. The performance of resulting models was reported using balanced accuracy and receiver operating characteristic (ROC) curves. Balanced accuracy and area under the ROC curves (AUCs) are reported as the mean \pm SEM. To estimate feature importance, we averaged the model regression coefficients (mean \pm SD) from across the cross-validation runs.

Weighted genetic coexpression network analysis (WGCNA). For modular analysis by WGCNA (details on the workflow are provided in ref. 22), we first calculated Pearson's correlations between all genes present in the data set. Next, an adjacency matrix was calculated by raising the absolute values of the

correlation matrix to a power β , to penalize weak correlations and preserve stronger ones. The β value for the soft thresholding was chosen in each data set using the "scale-free topology criterion." Topologic overlap was then calculated to quantify gene coexpression relationships, considering each pair of genes in relation to all of the other genes in the coexpression network.

Hierarchical clustering was then used to construct a dendrogram with branches corresponding to genes within modules, determined using a dynamic tree-cutting approach (22). For visualization, gene modules were given arbitrary color labels. Genes that were unassigned (i.e., not coexpressed) during network construction were arbitrarily labeled with a grey color. Gene counts in the intersection of corresponding modules between nonresponders and the consensus group of good responders and nonresponders at pretreatment and at 4 weeks were compared using the hypergeometric test P value for the overlap of the 2 modules.

In order to identify hub genes from the gene modules, an adjacency matrix was constructed for each gene, and connectivity was calculated as the sum of the adjacency to all other genes. Genes were then ranked by connectivity, and the top 20% of genes were selected from each module, the rationale being that only a fraction of genes in modules are likely to relate to the main biologic function (23).

Pathway analysis. Functional analysis of hub genes derived from the modules were analyzed by hypergeometric testing on gene ontology terms (24). In addition, previous evi-

Table 1. Pretreatment characteristics of the patients with rheumatoid arthritis*

Characteristic	EULAR good responders (n = 42)	EULAR nonresponders (n = 43)	<i>P</i>
Female, no. (%)	32 (76)	33 (77)	0.95
Age at onset, mean \pm SD years	59 \pm 15	55 \pm 14	0.28
HAQ score, median (IQR)	1.18 (0.9–1.7)	1.0 (0.3–1.6)	0.07
MTX start dose, median (IQR) mg	12.5 (10–15)	10 (10–15)	0.87
Taking oral steroids, no. (%)	5 (12)	12 (27)	0.07
Disease duration, median (IQR) months	9.1 (4.2–15.3)	5.8 (3.1–21.7)	0.94
Smoking habits, no. never/past/current	23/11/8	16/17/10	0.25
ACPA positive, no. (%)	27 (64)	25 (58)	0.56
DAS28, mean \pm SD	4.8 \pm 1.0	4.0 \pm 1.3	0.001
CRP, mean \pm SD mg/liter	2.2 \pm 1	1.7 \pm 1	0.01
28-joint swollen joint count, median (IQR)	5 (3–11)	3 (2–8)	0.02
28-joint tender joint count, median (IQR)	8 (6–15)	6 (1–13)	0.05
Patient's assessment of overall well-being, median (IQR) VAS score	44 (25–64)	32 (15–59)	0.07

* EULAR = European League Against Rheumatism; HAQ = Health Assessment Questionnaire; IQR = interquartile range; MTX = methotrexate; ACPA = anti-cyclic citrullinated peptide antibody; DAS28 = Disease Activity Score in 28 joints; CRP = C-reactive protein; VAS = 100-mm visual analog scale.

† P values were derived by t -test, Mann-Whitney U test, and chi-square test for comparisons of variables expressed as the mean, median, and number (%), respectively.

dence of coexpression was investigated using data from Gene Expression Omnibus (25,26).

RESULTS

Samples. Following application of data quality control, 22,771 probes were identified and available for analysis at the 2 time points in samples of whole blood from 82 RA patients. The patients were categorized as either good responders (n = 42) or poor responders/nonresponders (n = 43) following 6 months of treatment with MTX. The pretreatment demographic and clinical characteristics of the patients are shown in Table 1.

Classifier performance. In the models based on transcriptomics data, a high level of prediction of MTX nonresponse was observed with the L2-regularized logistic regression (linear method) model of the gene expression ratio between 4 weeks and pretreatment (Figures 1 and 2). Using this model, the balanced accuracy was a mean ± SEM 0.61 ± 0.10, and the ROC AUC was 0.78 ± 0.11. A very limited predictive utility was observed at the pretreatment time point. In contrast, the network-based models had a good degree of predictive utility at the 4-week time point (balanced accuracy 0.68 ± 0.06, ROC AUC 0.78 ± 0.06).

Very limited predictive utility was observed in the models based on the clinical data alone, either at baseline or at 3 months (e.g., with the linear method, at baseline, balanced accuracy 0.58 ± 0.5, ROC AUC 0.65 ± 0.06; at 3 months, balanced accuracy 0.62 ± 0.04, ROC AUC 0.70 ± 0.05) (see Supplementary Figure 1, available on the *Arthritis & Rheumatology* web site at <http://onlinelibrary.wiley.com/doi/10.1002/art.40810/abstract>). The transcripts with the largest positive impact on the performance of the models, based on the transcript ratio analysis, are presented in Supplementary Figure 2 (available on the *Arthritis & Rheumatology* web site at <http://onlinelibrary.wiley.com/doi/10.1002/art.40810/abstract>).

Modular analysis using WGCNA. In samples of whole blood from RA patients at pretreatment, 9 modules (arbitrarily labeled in midnight blue, light green, royal blue, magenta, grey60, black, salmon, green-yellow, and light-yellow colors in Supplementary Figure 3, available on the *Arthritis & Rheumatology* web site at <http://onlinelibrary.wiley.com/doi/10.1002/art.40810/abstract>) were identified in nonresponders that had not been seen in pretreatment samples from the consensus group of good responders and nonresponders (i.e., labeled in grey [i.e., unassigned] in the consensus network; see Supplementary Figure 3).

In samples at 4 weeks following initiation of treatment with MTX, 4 modules (arbitrarily labeled in salmon, light cyan, grey60, and yellow colors in Supplementary Figure 4, available on the

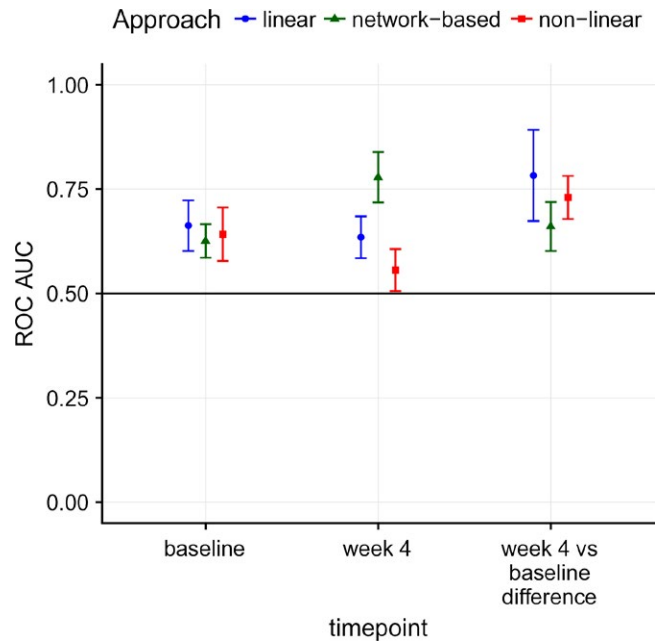


Figure 1. Performance of statistical machine learning models to distinguish therapeutic nonresponders from responders (assessed at 6 months) using gene expression data at pretreatment and 4 weeks after treatment initiation, and using the ratio of gene expression (i.e., the difference in log₂-transformed transcript expression intensity between 4 weeks of treatment and pretreatment). Area under the receiver operating characteristic (ROC) curves (AUCs) were calculated for estimating the predicted performance of a linear method (regularized logistic regression), a nonlinear method (random forest), and a network-based approach to evaluating methotrexate nonresponse in patients with rheumatoid arthritis. Results are the mean ± SEM.

Arthritis & Rheumatology web site at <http://onlinelibrary.wiley.com/doi/10.1002/art.40810/abstract>) were identified in nonresponders that were unassigned (i.e., labeled in grey) in the consensus samples.

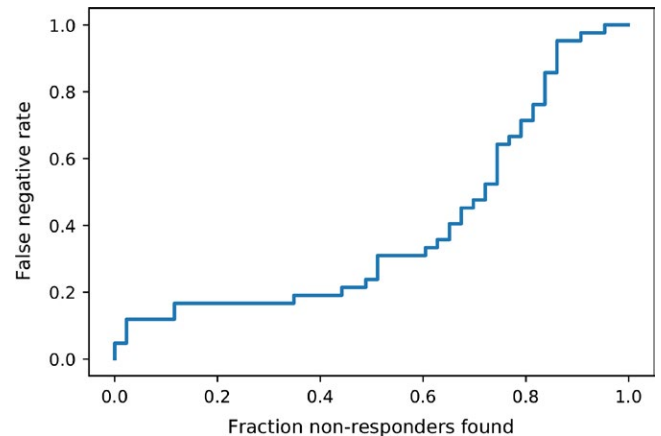


Figure 2. L2-regularized logistic regression model performance using the gene expression ratio between 4 weeks and pretreatment. Results are the fraction of true nonresponders found versus false negative rate.

Pathway analysis. Functional analysis of the gene lists derived from the identified modules (as described above) revealed a number of biologic processes relevant to inflammatory processes, such as genes involved in the response to type I interferon ($P = 2.8 \times 10^{-25}$) at pretreatment, and the type I interferon signaling pathway ($P = 4.9 \times 10^{-28}$) at 4 weeks (labeled in light green and light cyan, respectively; see Supplementary Tables 1, 2, and 3, available on the *Arthritis & Rheumatology* web site at <http://onlinelibrary.wiley.com/doi/10.1002/art.40810/abstract>). Using data from the Gene Expression Omnibus database, we found that >90% of hub genes from within these modules had prior evidence of coexpression, thus validating the gene network approach (see Supplementary Figures 5 and 6, available on the *Arthritis & Rheumatology* web site at <http://onlinelibrary.wiley.com/doi/10.1002/art.40810/abstract>).

We tested the interferon pathway transcripts for their predictive accuracy as a classifier of MTX nonresponse. Although we observed nonrandom performance (e.g., with the linear method at baseline, balanced accuracy 0.52 ± 0.04 , ROC AUC 0.64 ± 0.06), this classifier performed less well than the model that included all transcripts present on the array (see Supplementary Figure 7, available on the *Arthritis & Rheumatology* web site at <http://onlinelibrary.wiley.com/doi/10.1002/art.40810/abstract>).

DISCUSSION

In this study, we performed gene expression profiling in samples of whole blood collected at pretreatment and 4 weeks following the initiation of MTX therapy from patients with RA who had been started on MTX for the first time. By assessing a number of cutting edge model-building approaches, we developed a gene expression classifier that could potentially provide an early-response biomarker of MTX inefficacy. The classifier was found to be stable in cross-validation (SEM of 0.11 for the ROC AUC) and performed better than models that included the clinical covariates alone.

Pathway analysis revealed that genes involved in the response to type I interferon ($P = 2.8 \times 10^{-25}$) and the type I interferon signaling pathway ($P = 4.9 \times 10^{-28}$) were enriched in coexpressed gene modules identified in nonresponsive patients at pretreatment and at 4 weeks post-treatment initiation, respectively. Importantly, type I IFN signaling activates the JAK/STAT pathway and influences the development of innate and adaptive immune responses (27). Type I interferon gene responses are known to be increased in RA, to be correlated with autoantibody production (28), and to potentially be correlated with the response to tumor necrosis factor inhibitor therapy (28–34). It is important to note that the coexpressed genes were not differentially expressed between responder groups or between time points (data not shown).

The results of this study highlight the potential of early treatment biomarker monitoring in RA, and raise important questions regarding acceptable levels of performance for complementary diagnostic testing. To address this, decisions by key stakeholders (e.g., patient groups, clinicians) need to be made. Acceptable classifier performance must also be viewed in context, since ~46% of RA patients started on MTX therapy will discontinue the treatment by 3 years, due to intolerance/safety and inefficacy (35). Therefore, we believe that high recall (correctly identifying nonresponders) is preferable even at the expense of misclassifying a fraction of good responders. For example, the current model was able to detect ~50% of nonresponders at the expense of a false negative rate of ~20% (Figure 2).

The strengths of the current study include a large sample size, the availability of genome-wide transcript data at pretreatment and also during early treatment, rigorous internal model validation, and a focus on one drug (i.e., MTX). Furthermore, a comparison with external data confirmed that the gene expression networks identified in the current data have previous evidence of coexpression, providing external validity.

A limitation in investigating MTX nonresponse is the semi-quantitative nature of the methods used to approximate disease activity, for example, the DAS28 (36) and related EULAR response classification. The DAS28 score is composed of both objective (e.g., swollen joint count) and subjective (e.g., tender joint count) measures. As a result of it being made up of several components, it can be difficult to interpret, particularly because the subjective measures receive more weighting in the score calculation, and tend to correlate more strongly with psychological variables, such as anxiety (37) and fibromyalgia tender points (38). Improved classifier performance might therefore be achieved if a biologic measure of disease activity, particularly one that might be more strongly reflective of synovitis levels, were to be used to assess the treatment response, as opposed to the DAS28 or its components.

Another potential limitation to the current study is the use of whole blood for transcript profiling. While the purpose of the study was not to resolve mechanisms of nonresponse, model performance may have been improved by targeting enriched cell subsets within the blood.

The utility of a gene expression classifier of MTX nonresponse will now require validation, not only in independent samples but also using independent technology. For example, more mileage may be gained from RNA sequencing, as opposed to array-based data sets. If the predictive utility of gene expression data can be confirmed, this could pave the way for a paradigm shift in treatment outcomes from clinically based treat-to-target approaches to biologically driven precision medicine.

In conclusion, these data reveal a potential role for early treatment biomarker monitoring in RA patients started on MTX, and highlight the utility of machine learning and network-based

approaches in investigations of treatment response in inflammatory diseases.

ACKNOWLEDGMENTS

We thank Pfizer I-CRP, the Medical Research Council, and Arthritis Research UK, which jointly funded the MATURA (Maximizing Therapeutic Utility in RA) collaboration and the National Institute for Health Research Manchester Biomedical Research Centre.

AUTHOR CONTRIBUTIONS

All authors were involved in drafting the article or revising it critically for important intellectual content, and all authors approved the final version to be published. Dr. Barton had full access to all of the data in the study and takes responsibility for the integrity of the data and the accuracy of the data analysis.

Study conception and design. Plant, Maciejewski, Hyrich, Ziemek, Barton, Verstappen.

Acquisition of data. Smith, Nair, Barton, Verstappen.

Analysis and interpretation of data. Plant, Maciejewski, Hyrich, Ziemek, Barton, Verstappen.

ROLE OF THE STUDY SPONSOR

Pfizer provided support for the study but had no role in the study design or in the collection, analysis, or interpretation of the data, the writing of the manuscript, or the decision to submit the manuscript for publication. Publication of this article was not contingent upon approval by Pfizer.

REFERENCES

- Salliot C, van der Heijde D. Long-term safety of methotrexate monotherapy in patients with rheumatoid arthritis: a systematic literature research. *Ann Rheum Dis* 2009;68:1100–4.
- National Institute for Health and Care Excellence. Rheumatoid arthritis in adults: management. URL: <https://www.nice.org.uk/guidance/cg79>.
- Farragher TM, Lunt M, Fu B, Bunn D, Symmons DP. Early treatment with, and time receiving, first disease-modifying antirheumatic drug predicts long-term function in patients with inflammatory polyarthritis. *Ann Rheum Dis* 2010;69:689–95.
- Bluett J, Sergeant J, MacGregor AJ, Symmons D, Verstappen S. Predictors of oral methotrexate failure in patients with early inflammatory arthritis: a competing risks analysis. *Rheumatology (Oxford)* 2015;54 Suppl 1:i71.
- Wessels JA, van der Kooij SM, le Cessie S, Kievit W, Barerra P, Allaart CF, et al. A clinical pharmacogenetic model to predict the efficacy of methotrexate monotherapy in recent-onset rheumatoid arthritis. *Arthritis Rheum* 2007;56:1765–75.
- Rheumatoid Arthritis Clinical Trial Archive Group. The effect of age and renal function on the efficacy and toxicity of methotrexate in rheumatoid arthritis. *J Rheumatol* 1995;22:218–23.
- Hoekstra M, van Ede AE, Haagsma CJ, van de Laar MA, Huizinga TW, Kruijsen MW, et al. Factors associated with toxicity, final dose, and efficacy of methotrexate in patients with rheumatoid arthritis. *Ann Rheum Dis* 2003;62:423–6.
- Lie E, van der Heijde D, Uhlig T, Heiberg MS, Koldingsnes W, Rødevand E, et al. Effectiveness and retention rates of methotrexate in psoriatic arthritis in comparison with methotrexate-treated patients with rheumatoid arthritis. *Ann Rheum Dis* 2010;69:671–6.
- Plant D, Wilson AG, Barton A. Genetic and epigenetic predictors of responsiveness to treatment in RA. *Nat Rev Rheumatol* 2014;10:329–37.
- Smith SL, Plant D, Eyre S, Barton A. The potential use of expression profiling: implications for predicting treatment response in rheumatoid arthritis. *Ann Rheum Dis* 2013;72:1118–24.
- Hobl EL, Mader RM, Erlacher L, Duhm B, Mustak M, Bröll H, et al. The influence of methotrexate on the gene expression of the pro-inflammatory cytokine IL-12A in the therapy of rheumatoid arthritis. *Clin Exp Rheumatol* 2011;29:963–9.
- Parker A, Izmailova ES, Narang J, Badola S, Le T, Roubenoff R, et al. Peripheral blood expression of nuclear factor- κ B-regulated genes is associated with rheumatoid arthritis disease activity and responds differentially to anti-tumor necrosis factor- α versus methotrexate. *J Rheumatol* 2007;34:1817–22.
- Dowsett M, Smith IE, Ebbs SR, Dixon JM, Skene A, A'Hern R, et al. Prognostic value of Ki67 expression after short-term presurgical endocrine therapy for primary breast cancer. *J Natl Cancer Inst* 2007;99:167–70.
- Dowsett M, Allred C, Knox J, Quinn E, Salter J, Wale C, et al. Relationship between quantitative estrogen and progesterone receptor expression and human epidermal growth factor receptor 2 (HER-2) status with recurrence in the arimidex, tamoxifen, alone or in combination trial. *J Clin Oncol* 2008;26:1059–65.
- Harvey JM, Clark GM, Osborne CK, Allred DC. Estrogen receptor status by immunohistochemistry is superior to the ligand-binding assay for predicting response to adjuvant endocrine therapy in breast cancer. *J Clin Oncol* 1999;17:1474–81.
- Houston SJ, Plunkett TA, Barnes DM, Smith P, Rubens RD, Miles DW. Overexpression of c-erbB2 is an independent marker of resistance to endocrine therapy in advanced breast cancer. *Br J Cancer* 1999;79:1220–6.
- McGuire WL. Steroid receptors in human breast cancer. *Cancer Res* 1978;38:4289–91.
- Fries JF, Spitz PW, Young DY. The dimensions of health outcomes: the health assessment questionnaire, disability and pain scales. *J Rheumatol* 1982;9:789–93.
- DAS28. EULAR response criteria. URL: <https://www.das-score.nl/das28/en/difference-between-the-das-and-das28/importance-of-das28-and-tight-control/eular-response-criteria.html>.
- Ritchie ME, Phipson B, Wu D, Hu Y, Law CW, Shi W, et al. Limma powers differential expression analyses for RNA-sequencing and microarray studies. *Nucleic Acids Res* 2015;43:e47.
- Zarringhalam K, Degras D, Brockel C, Ziemek D. Robust phenotype prediction from gene expression data using differential shrinkage of co-regulated genes. *Sci Rep* 2018;8:1237.
- Langfelder P, Horvath S. WGCNA: an R package for weighted correlation network analysis. *BMC Bioinformatics* 2008;9:559.
- Van Dam S, Vösa U, van der Graaf A, Franke L, de Magalhães JP. Gene co-expression analysis for functional classification and gene-disease predictions. *Brief Bioinform* 2018;19:575–92.
- Falcon S, Gentleman R. Using GOstats to test gene lists for GO term association. *Bioinformatics* 2007;23:257–8.
- Barrett T, Troup DB, Wilhite SE, Ledoux P, Rudnev D, Evangelista C, et al. NCBI GEO: archive for high-throughput functional genomic data. *Nucleic Acids Res* 2009;37:D885–90.
- Warde-Farley D, Donaldson SL, Comes O, Zuberi K, Badrawi R, Chao P, et al. The GeneMANIA prediction server: biological network integration for gene prioritization and predicting gene function. *Nucleic Acids Res* 2010;38:W214–20.

27. Ivashkiv LB, Donlin LT. Regulation of type I interferon responses. *Nat Rev Immunol* 2014;14:36–49.
28. Castañeda-Delgado JE, Bastián-Hernandez Y, Macias-Segura N, Santiago-Algarra D, Castillo-Ortiz JD, Alemán-Navarro AL, et al. Type I interferon gene response is increased in early and established rheumatoid arthritis and correlates with autoantibody production. *Front Immunol* 2017;8:285.
29. Wright HL, Thomas HB, Moots RJ, Edwards SW. Interferon gene expression signature in rheumatoid arthritis neutrophils correlates with a good response to TNFi therapy. *Rheumatology (Oxford)* 2015;54:188–93.
30. Vosslamber S, Raterman HG, van der Pouw Kraan TC, Schreurs MW, von Blomberg BM, Nurmohamed MT, et al. Pharmacological induction of interferon type I activity following treatment with rituximab determines clinical response in rheumatoid arthritis. *Ann Rheum Dis* 2011;70:1153–9.
31. Sellam J, Marion-Thore S, Dumont F, Jacques S, Garchon HJ, Rouanet S, et al. Use of whole-blood transcriptomic profiling to highlight several pathophysiologic pathways associated with response to rituximab in patients with rheumatoid arthritis: data from a randomized, controlled, open-label trial. *Arthritis Rheumatol* 2014;66:2015–25.
32. Sanayama Y, Ikeda K, Saito Y, Kagami S, Yamagata M, Furuta S, et al. Prediction of therapeutic responses to tocilizumab in patients with rheumatoid arthritis: biomarkers identified by analysis of gene expression in peripheral blood mononuclear cells using genome-wide DNA microarray. *Arthritis Rheumatol* 2014;66:1421–31.
33. Raterman HG, Vosslamber S, de Ridder S, Nurmohamed MT, Lems WF, Boers M, et al. Interferon type I signature may predict non response upon rituximab in rheumatoid arthritis patients. *Arthritis Res Ther* 2012;14:R95.
34. Mesko B, Poliska S, Váncsa A, Szekanecz Z, Palatka K, Hollo Z, et al. Peripheral blood derived gene panels predict response to infliximab in rheumatoid arthritis and Crohn's disease. *Genome Med* 2013;5:59.
35. Curtis JR, Wallenstein G, Takiya L, Gruben D, Chen C, Shan Y, et al. Patterns of methotrexate use and discontinuation in a U.S. rheumatoid arthritis registry [abstract]. *Arthritis Rheumatol* 2017; 69 Suppl 10. URL: <http://acrabstracts.org/abstract/patterns-of-methotrexate-use-and-discontinuation-in-a-u-s-rheumatoid-arthritis-registry/>.
36. Prevoo ML, van't Hof MA, Kuper HH, van Leeuwen MA, van de Putte LB, van Riel PL. Modified disease activity scores that include twenty-eight-joint counts: development and validation in a prospective longitudinal study of patients with rheumatoid arthritis. *Arthritis Rheum* 1995;38:44–8.
37. Cordingley L, Prajapati R, Plant D, Maskell D, Morgan C, Ali FR, et al. Impact of psychological factors on subjective disease activity assessments in patients with severe rheumatoid arthritis. *Arthritis Care Res (Hoboken)* 2014;66:861–8.
38. Ton E, Bakker MF, Verstappen SM, Ter Borg EJ, van Albada-Kuipers IA, Schenk Y, et al. Look beyond the Disease Activity Score of 28 Joints (DAS28): tender points influence the DAS28 in patients with rheumatoid arthritis. *J Rheumatol* 2012;39:22–7.

Evaluation of the Short-, Mid-, and Long-Term Effects of Tofacitinib on Lymphocytes in Patients With Rheumatoid Arthritis

Ronald van Vollenhoven,¹ Eun Bong Lee,² Sander Strengholt,³ Christopher Mojciak,³ Hernan Valdez,³ Sriram Krishnaswami,⁴ Pinaki Biswas,³ Irina Lazariciu,⁵ Anasuya Hazra,⁴ James D. Clark,⁶ Jennifer Hodge,³ Lisy Wang,⁴ and Ernest Choy⁷

Objective. Tofacitinib is an oral JAK inhibitor for the treatment of rheumatoid arthritis (RA). Altered lymphocyte cell counts and a potential association with increased infection rates have been reported in RA patients treated with JAK inhibitors. This analysis was undertaken to evaluate the short-, mid-, and long-term effects of tofacitinib on lymphocytes and infection rates in patients with RA.

Methods. In this post hoc analysis, absolute lymphocyte counts (ALCs) were obtained from phase III studies (12–24 months; n = 717–958) and phase I/II/III/long-term extension studies of tofacitinib (≤ 117 months) (All RA population; n = 7,061); lymphocyte subset counts (LSCs) were from phase II studies (1.5–6 months' exposure; n = 236–486), an ORAL Sequel vaccine substudy (~22 months; n = 198), and an ORAL Sequel lymphocyte substudy (~50 months; n = 55–1,035) of tofacitinib. The reversibility of ALC/LSC changes was evaluated. The relationship of ALC and LSC to infections was analyzed in the All RA population. The value of monitoring ALC alone was assessed by examining correlations between ALCs and LSCs.

Results. Tofacitinib treatment resulted in an initial increase in ALC versus pretreatment baseline, which gradually declined to steady state by ~48 months. CD4+ and CD8+ T cell counts decreased over long-term treatment, and ALC and LSC changes were reversible upon treatment cessation. Patients with ALCs of < 500 cells/mm³ had an increased risk of serious infections. There was no strong association between CD4+ T cell, CD8+ T cell, B cell, or natural killer cell counts and serious infection incidence rates. ALC and CD4+ or CD8+ T cell counts correlated well (R = 0.65–0.86).

Conclusion. Our findings indicate that monitoring of ALC alone appears to be adequate to assess infection risk in tofacitinib-treated patients with RA.

INTRODUCTION

Tofacitinib is an oral JAK inhibitor for the treatment of rheumatoid arthritis (RA). The efficacy and safety of tofacitinib 5 mg and 10 mg twice daily, administered as mon-

otherapy or in combination with conventional synthetic disease-modifying antirheumatic drugs (DMARDs) (mainly methotrexate [MTX]), in patients with moderately to severely active RA, have been demonstrated in phase II (1–5) and phase III (6–11) studies of up to 24 months' duration and in

Supported by Pfizer Inc.

¹Ronald van Vollenhoven, MD, PhD: Amsterdam Rheumatology and Immunology Center, Amsterdam, The Netherlands; ²Eun Bong Lee, MD, PhD: Seoul National University, Seoul, Republic of Korea; ³Sander Strengholt, MSc, Christopher Mojciak, MD, PhD, Hernan Valdez, MD, Pinaki Biswas, PhD, Jennifer Hodge, PhD: Pfizer Inc, New York, New York; ⁴Sriram Krishnaswami, PhD, Anasuya Hazra, PhD, Lisy Wang, MD: Pfizer Inc, Groton, Connecticut; ⁵Irina Lazariciu, MSc: IQVIA Canada, Montreal, Quebec, Canada; ⁶James D. Clark, PhD: Pfizer Inc, Cambridge, Massachusetts; ⁷Ernest Choy, MD, FRCP: CREATE Center, Division of Infection and Immunity, Cardiff University School of Medicine, Cardiff, UK.

Dr. van Vollenhoven has received consulting fees, speaking fees, and/or honoraria from AbbVie, AstraZeneca, Biotest, Bristol-Myers Squibb, Celgene, GlaxoSmithKline, Janssen, Lilly, Novartis, Pfizer Inc, and UCB (less than \$10,000 each) and research support from AbbVie, Bristol-Myers Squibb, GlaxoSmithKline, Pfizer Inc, and UCB. Dr. Lee has received

consulting fees from Pfizer Inc (less than \$10,000) and research support from Green Cross Co. and Hanmi Pharmaceutical. Mr. Strengholt and Drs. Valdez, Krishnaswami, Biswas, Hodge, and Wang own stock or stock options in Pfizer Inc. Drs. Mojciak, Hazra, and Clark owned stock in Pfizer Inc at the time of the analysis. Ms Lazariciu is a consultant for Pfizer Inc through her employment with IQVIA Canada. Dr. Choy has received consulting fees, speaking fees, and/or honoraria from Amgen, Biogen, Chugai Pharma, Eli Lilly, Janssen, Novartis, Pfizer Inc, Regeneron, Roche, R-Pharm, Sanofi-Aventis, Bristol-Myers Squibb, Boehringer Ingelheim, Hospira, MSD, and UCB (less than \$10,000 each) and research support from BioCancer, Pfizer Inc, Roche, and UCB.

Address correspondence to Lisy Wang, MD, Inflammation and Immunology, Global Product Development, Pfizer Inc, 445 Eastern Point Road, Groton, CT 06340. E-mail: lisy.wang@pfizer.com.

Submitted for publication May 11, 2018; accepted in revised form November 8, 2018.

long-term extension (LTE) studies with up to 114 months of observation (12–14).

Tofacitinib partially and reversibly inhibits signaling of multiple cytokines via the JAK/STAT pathway (15,16). Members of the common γ -chain family of cytokines, including interleukin-2 (IL-2), IL-4, IL-7, IL-9, IL-15, and IL-21, signal through JAK1/JAK3 and are important for the development and proliferation of T cells, natural killer (NK) cells, and B cells (17–19); therefore, the modulation of cytokine signaling by tofacitinib might be expected to change immune cell counts and function over time, resulting in immune response suppression. Several studies within the tofacitinib development program have evaluated cell-mediated immunity and humoral-mediated immunity (20–23).

Treatment with tofacitinib is associated with increased infections, likely related to immunomodulation, relative to findings in patients treated with placebo. In a meta-analysis of interventional studies, rates of serious infections associated with tofacitinib in patients with moderately to severely active RA were similar to those reported with biologic DMARDs (24). A recent report noted a trend toward increasing risk of serious infection with lower lymphocyte counts (25). Confirmed decreases in absolute lymphocyte counts (ALCs) to <500 cells/mm³ occur during the first 3 months of exposure in $\sim 0.04\%$ of patients receiving tofacitinib at 5 mg or 10 mg twice daily; recommendations state that these patients should discontinue treatment if this threshold is reached, due to an increased risk of serious infection (26,27).

Here, we evaluate the effects of tofacitinib on ALCs, lymphocyte subset counts (LSCs), and infection rates in patients with RA. The data are discussed in the context of immune function. Our primary objective was to characterize the short-, mid-, and long-term effects of tofacitinib treatment on ALCs and LSCs in patients with RA. Additional objectives were 1) to assess whether ALC and LSC changes observed with long-term tofacitinib treatment are reversible upon treatment cessation, 2) to evaluate the association of infection rates in patients receiving tofacitinib with ALCs or LSCs, and 3) to assess the value of monitoring LSCs in addition to ALCs to mitigate the risk of infection.

PATIENTS AND METHODS

Patient populations. Patient data were derived from relevant phase I, II, and III and LTE studies from the tofacitinib development program. Patients were age ≥ 18 years and fulfilled the American College of Rheumatology 1987 revised criteria for classification of RA (28). Patients in LTE studies had previously participated in a qualifying phase I, II, or III index study of tofacitinib (12). An overview of the patient populations evaluated in this study is presented in Figure 1.

ALC assessments. ALCs were recorded as part of safety monitoring procedures throughout the tofacitinib RA clinical program.

Short-term changes. Short-term changes in ALCs were assessed in 2 phase III studies: ORAL Standard (NCT00853385) and ORAL Start (NCT01039688). ORAL Standard was a study to evaluate tofacitinib plus MTX versus adalimumab plus MTX over 12 months in 717 patients with RA and prior inadequate response to MTX (MTX-IR) (11). ORAL Start (NCT01039688) evaluated tofacitinib versus MTX over 24 months in 958 MTX-naive patients with RA (9).

Long-term changes. Long-term changes in ALCs were evaluated using pooled data from studies of tofacitinib, across the entire duration of tofacitinib exposure (phases I, II, and III and LTE “All RA” population [$n = 7,061$], up to 117 months of treatment [median ~ 36 months] overall; ORAL Sequel lymphocyte substudy database lock March 02, 2017). A detailed study list is provided in Figure 1.

LSC assessments. **Short-term changes.** Short-term changes in LSCs were assessed using data from 3 phase II studies (NCT00147498, NCT00413660, and NCT00550446) of 1.5–6 months’ duration ($n = 236$ –486 contributing to each LSC subtype at baseline). LSCs were not collected within any of the phase III or IIIb/IV studies.

Mid-term changes. Mid-term changes in LSCs were assessed using data from a vaccine substudy of ORAL Sequel (NCT00413699) in patients who had received tofacitinib 10 mg twice daily for a median of 22 months (up to 1,632 days) before enrollment into the vaccine substudy ($n = 198$).

Long-term changes. Long-term changes in LSCs were assessed using data from a lymphocyte substudy of ORAL Sequel (NCT00413699) in patients who had previously received tofacitinib 5 mg or 10 mg twice daily for a median of ~ 50 months before enrollment into the lymphocyte substudy. The lymphocyte substudy comprised 3 cohorts (Figure 1). Cohort 1 was investigated to ascertain the effects of long-term treatment with tofacitinib for a further 2 years in 1,035 patients (~ 50 months prior tofacitinib exposure). Cohort 2 evaluated whether the effects of tofacitinib on LSC were reversible upon temporary withdrawal (for 4 weeks) after long-term treatment in 55 patients (~ 50 months’ prior exposure). In cohort 3, the long-term effects of tofacitinib in patients enrolling only from the qualifying zoster vaccine study (A3921237) were evaluated (~ 4 months’ prior exposure; $n = 71$) (NCT02147587).

Analyses. ALCs and LSCs were ascertained and described by dose and visit over time, via descriptive statistics, line graphs, and box plots. For evaluations of LSC stability during long-term treatment, reference ranges were derived from pretreatment baseline values (5th–95th percentile) in the tofacitinib development program in RA, and verified against values reported in literature (see Supplementary Table 1, on the *Arthritis & Rheumatology* web site at <http://onlinelibrary.wiley.com/doi/10.1002/art.40780/abstract>). Lymphocyte subsets were evaluated by flow cytometric analysis at a central

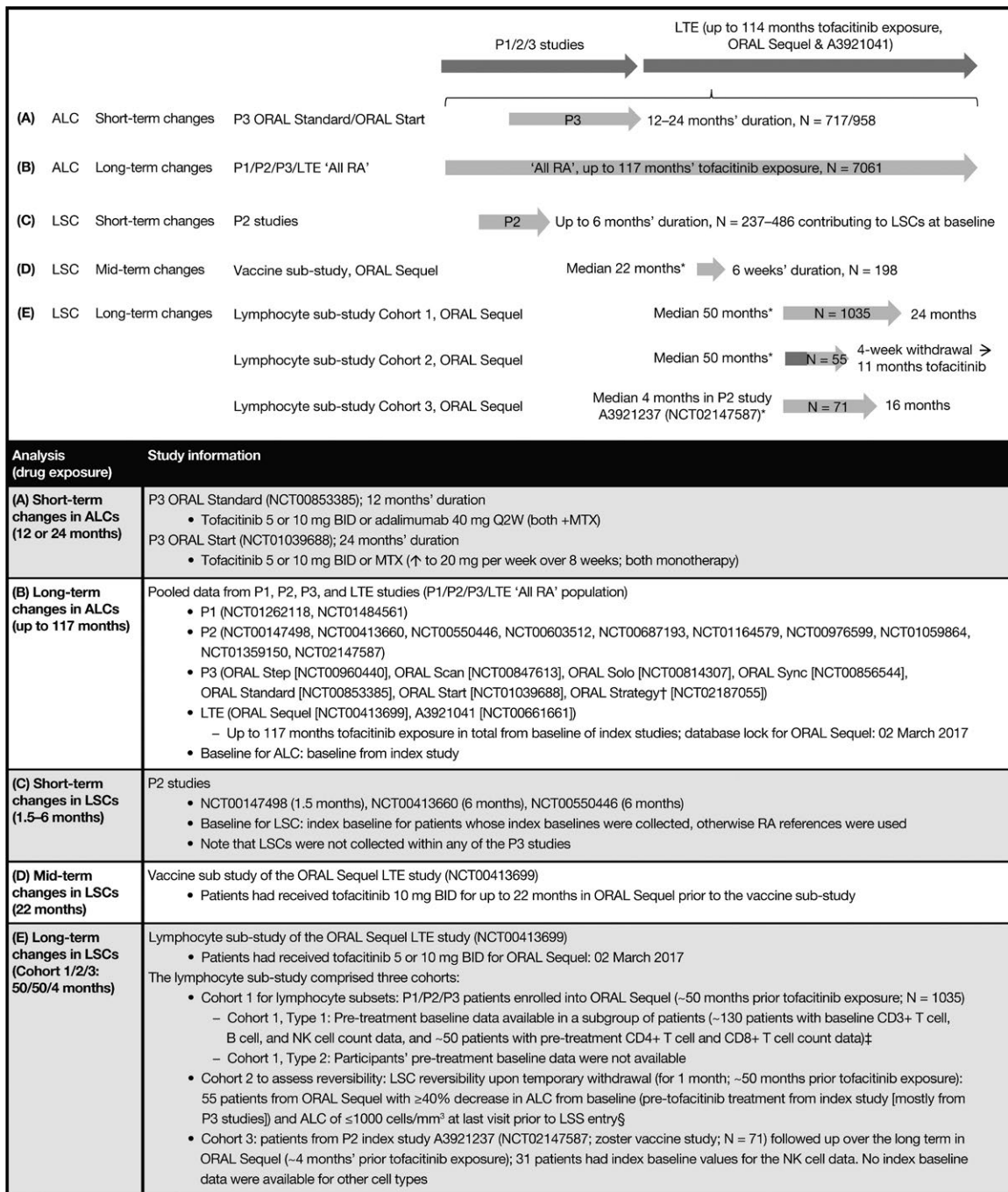


Figure 1. Overview of the study and analysis populations. * = Prior tofacitinib exposure. † = ORAL Strategy is a phase IIIb/IV study. ‡ = Power calculations indicated that these sample sizes (patients with available pretreatment baseline data) were adequate to detect long-term changes of ≥20% in each of the lymphocyte subset counts (LSCs) with at least 80% probability. § = Nearly all patients were originally participants in phase III studies and thus did not have pretreatment baseline LSC data. P = phase; LTE = long-term extension; ALC = absolute lymphocyte count; RA = rheumatoid arthritis; BID = twice daily; Q2W = every 2 weeks; MTX = methotrexate; NK = natural killer; LSS = lymphocyte sub-study.

laboratory, and included the following: total T cells (CD3+), CD4+ T helper cells (CD3+CD4+), CD8+ cytotoxic T cells (CD3+CD8+), NK cells (CD3–CD16+CD56+), and B cells (CD3–CD19+).

The reversibility of long-term changes in ALC was investigated during follow-up of patients in the All RA population who permanently discontinued tofacitinib treatment due to

confirmed ALC of <500 cells/mm³. The reversibility of short-term changes in LSC was evaluated using data from phase II study NCT00147498, in which patients received tofacitinib for 6 weeks, followed by treatment withdrawal for 6 weeks. The reversibility of long-term changes in LSCs was evaluated in cohort 2 of the lymphocyte sub-study through a 4-week tempo-

rary withdrawal phase in patients previously treated with tofacitinib for a median of ~50 months. Patients in cohort 2 had a $\geq 40\%$ reduction in ALC from the index study baseline and an ALC of $\leq 1,000$ cells/mm³ at the last visit prior to entry into the lymphocyte substudy.

The clinical effect of changes in ALC and LSC on risk of infections was analyzed using the All RA population. To ascertain whether modifications to current monitoring and discontinuation recommendations (ALC < 500 cells/mm³) are warranted, incidence rates of infections were calculated by ALC categories and by patient groups, defined by quartiles of nadir LSC values for each patient.

To evaluate the value of monitoring LSCs in addition to ALC to minimize risk of infection, the relationship between LSCs and ALC was assessed by examining their correlation before and after tofacitinib treatment. The maintenance of a correlation between ALC and LSC at low cell counts

was also evaluated. Scatterplots for each pair of observations (ALC, LSC) and estimated Pearson correlation coefficients were generated at pretreatment baseline and after tofacitinib exposure.

A Cox regression model was used to identify and assess factors associated with time to confirmed lymphopenia (ALC < 500 cells/mm³). Each factor was assessed individually, and a multivariable model was developed using an automated, backward elimination procedure.

RESULTS

Changes in ALC over time. *Short-term changes in ALC: data from ORAL Standard and ORAL Start.* In the ORAL Standard study (MTX-IR), increases in ALC were observed at month 1 in both tofacitinib plus MTX treatment groups and the adalimumab plus MTX treatment group, but these did not persist in the tofaci-

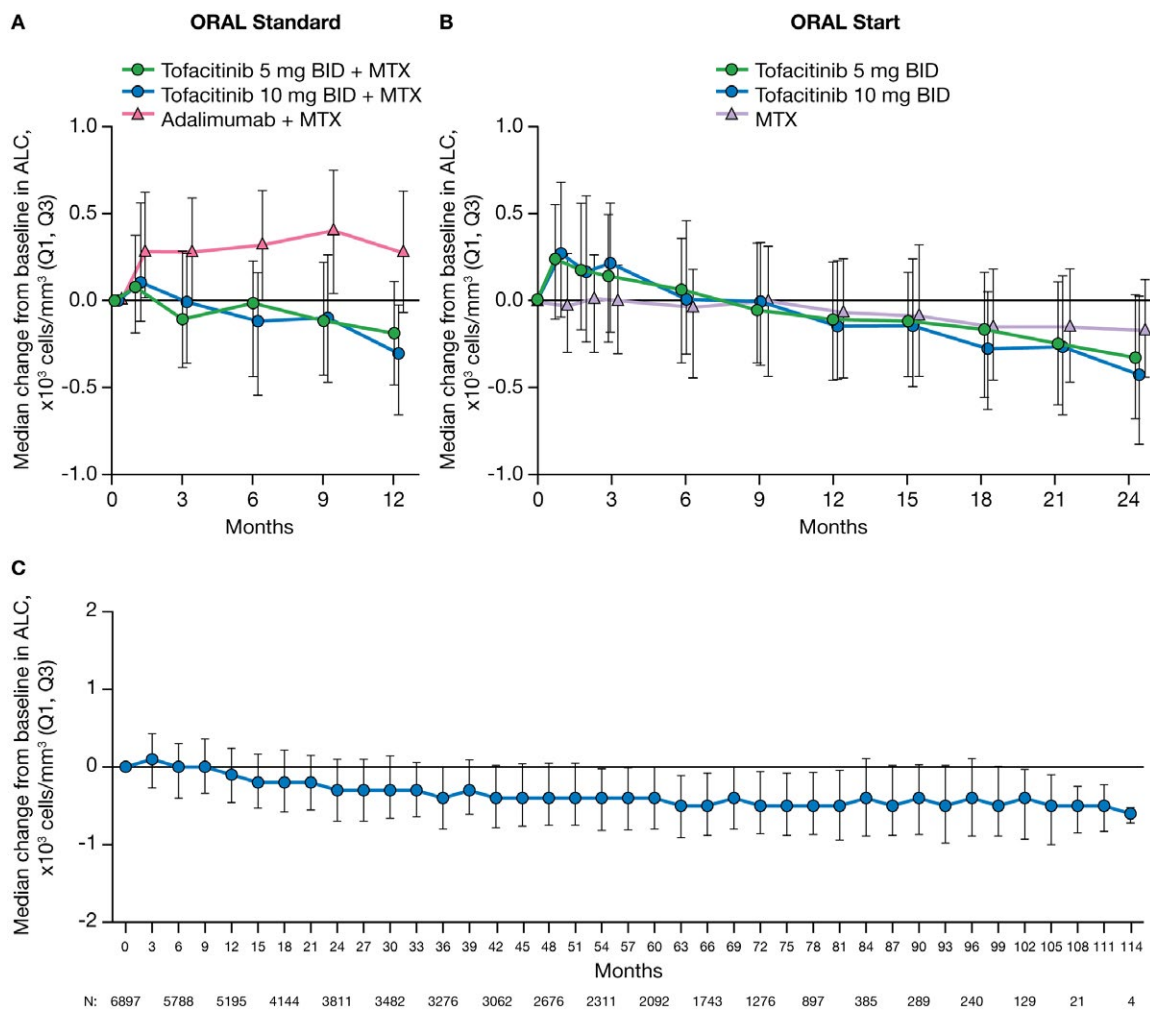


Figure 2. Median change from baseline in absolute lymphocyte counts (ALCs) in rheumatoid arthritis (RA) patients from the phase III ORAL Standard study (0–12 months) (A), the phase III ORAL Start study (0–24 months) (B), and the phase I/phase II/phase III/long-term extension All RA population (0–114 months) (C). Data reported here for the All RA population include patients experiencing up to 114 months of exposure to tofacitinib; however, due to limited numbers of patients with data after month 102, interpretations should be made with caution. Only 1 patient had data at month 117, and that data point was therefore removed. Q1, Q3 = first through third quartiles; BID = twice daily; MTX = methotrexate.

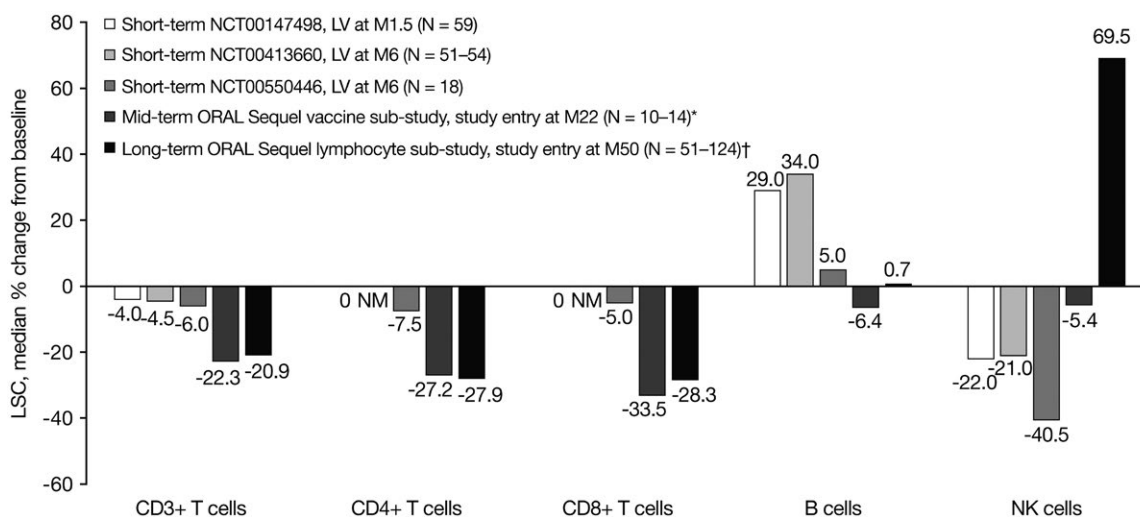


Figure 3. Median percentage change from baseline in lymphocyte subset counts (LSCs) in rheumatoid arthritis patients from phase II studies of tofacitinib 5 mg twice daily (short-term), from the ORAL Sequel vaccine substudy of tofacitinib 10 mg twice daily (mid-term), and at entry into the ORAL Sequel lymphocyte substudy (tofacitinib 5 mg or 10 mg twice daily) (long-term). * = Includes only the subgroup of patients with pretreatment baseline LSC data (for CD3+ T cells, B cells, and natural killer [NK] cells, $n = 14$; for CD4+ and CD8+ T cells, $n = 10$). † = Cohort 1 type 1, i.e., the subgroup of patients in cohort 1 who originally participated in the phase II program and had pretreatment baseline data (for CD3+ T cells and B cells, $n = 124$; for CD4+ and CD8+ T cells, $n = 51$; for NK cells, $n = 121$). LV = last visit; M = month; NM = not measured.

tinib plus MTX groups (Figure 2A). At month 12, median decreases in ALC from baseline were -190 cells/ mm^3 with tofacitinib 5 mg twice daily plus MTX and -310 cells/ mm^3 with tofacitinib 10 mg twice daily plus MTX. In ORAL Start (MTX-naive), increases in ALC from baseline were observed from month 1 to month 3, followed by decreases to month 24; at month 12, the median change in ALC was -110 cells/ mm^3 with tofacitinib 5 mg twice daily and -150 cells/ mm^3 with tofacitinib 10 mg twice daily; at month 24, decreases were numerically greater with tofacitinib 5 mg twice daily (-330 cells/ mm^3) and tofacitinib 10 mg twice daily (-430 cells/ mm^3) as monotherapy compared to MTX monotherapy (-170 cells/ mm^3) (Figure 2B).

Long-term changes in ALC: data from the All RA population. In the All RA population, the median ALC in tofacitinib-treated patients declined by $\sim 24\%$ from pretreatment baseline to 48 months, stabilizing at approximately -400 cells/ mm^3 (Figure 2C). Despite stable median ALC values after 48 months, 80 patients (1.2%; 25 of 2,983 patients in the tofacitinib 5 mg twice daily group and 55 of 3,914 patients in the tofacitinib 10 mg twice daily group) experienced a confirmed (2 sequential measurements) ALC of <500 cells/ mm^3 . Fifty-eight of these 80 patients were from the LTE studies. At the time of the event, 64 of the 80 patients were receiving combination therapy (tofacitinib plus background treatment) and 16 patients were receiving tofacitinib monotherapy.

Changes in LSCs over time. Short-term, mid-term, and long-term changes in LSCs are shown in Figure 3. In the phase II studies of tofacitinib in RA, treatment with tofacitinib 5 mg twice daily for up to 6 months (short-term) was associated with a min-

imal decrease from baseline in CD3+, CD4+, and CD8+ T cell counts; B cell counts increased from baseline, while NK cell counts decreased. At study entry in the ORAL Sequel vaccine substudy, treatment with tofacitinib for a median of 22 months (mid-term) was associated with a decrease from baseline in CD3+, CD4+, and CD8+ T cell counts and a slight decrease in B cell and NK cell counts. Treatment with tofacitinib for ~ 50 months from index study baseline to entry into the ORAL Sequel lymphocyte substudy (long-term) was associated with a decrease in CD3+, CD4+, and CD8+ T cell counts, a minimal change in B cell counts, and a large increase in NK cell counts in the subset of patients with available pretreatment baseline data. Short-, mid-, and long-term changes in CD4+ T cell counts and in CD8+ T cell counts were observed to be similar.

Stability of LSCs during extended long-term treatment. Patients in cohort 1 entered the lymphocyte substudy after a median of ~ 50 months of treatment in ORAL Sequel. During the next 27 months, there was no change in CD3+ T cell counts (Supplementary Figure 1A, on the *Arthritis & Rheumatology* web site at <http://onlinelibrary.wiley.com/doi/10.1002/art.40780/abstract>), CD4+ or CD8+ T cell counts (data not shown; results similar to CD3+ T cell results), NK cell counts (Supplementary Figure 1B), or B cell counts (Supplementary Figure 1C), and the long-term effects of tofacitinib in this study were reflective of steady state.

The proportion of patients with LSC values below RA reference ranges for T cells and NK cells, and above the RA reference range for B cells in the lymphocyte substudy (cohort 1) is shown in Supplementary Table 2 (<http://onlinelibrary.wiley.com/doi/10.1002/art.40780/abstract>). Across all visits, despite stable

mean changes over time, CD3+, CD4+, and CD8+ T cell counts were below the RA reference range in ~13–18%, 17–21%, and 12–19% of the patients, respectively, after long-term tofacitinib treatment. B cell counts above the RA reference range were recorded in ~2–6% of the patients, and NK cell counts were below the RA reference range in ≤0.9% of the patients. These proportions were consistent across visits.

Reversibility of changes in ALC and LSC values over time.

Reversibility of changes in ALCs after long-term treatment. Of 80 patients in the All RA population with a confirmed ALC of <500 cells/mm³ during treatment with tofacitinib, 88% (n = 70) had ALCs in the lymphopenic range (<1,500 cells/mm³) prior to tofacitinib initiation (Table 1). In 70 of 75 patients (93%) with follow-up ALC data after the confirmed ALC of <500 cells/mm³ during tofacitinib treatment, the ALC increased to ≥500 cells/mm³ (median 3–6 weeks following tofacitinib discontinuation) (Table 1). In the remaining 5 patients, the ALC of <500 cells/mm³ persisted for the entire duration of their follow-up (0.5–6 months). One patient had a diagnosis of lymphoma, and another had a diagnosis of acute promyelocytic leukemia, when low ALCs occurred. The remaining 3 patients discontinued from

the study due to lymphopenia, per protocol requirement. Of the 5 patients who had no follow-up ALC data after the confirmed ALC of <500 cells/mm³, 4 either discontinued or were hospitalized for a serious adverse event, and 1 completed the study with no occurrence of an adverse event associated with the lymphopenia event.

Reversibility of changes in LSCs after short-term treatment.

The reversibility of LSCs (toward baseline values) was evaluated in a 6-week withdrawal phase following a 6-week treatment phase in the phase II study A3921019/NCT00147498. Observed changes in T cell counts in patients treated with tofacitinib 5 mg twice daily were small and similar to changes with placebo treatment. This resulted in similar distributions of T cell counts during tofacitinib treatment and following treatment withdrawal, compared to placebo (data not shown). At week 6 of treatment, a 29% median increase from baseline in B cell counts was observed with tofacitinib 5 mg twice daily; after the treatment withdrawal phase, B cell counts decreased toward baseline levels and were similar to those in the placebo group. A 22% median decrease in NK cells was observed at week 6 of treatment with tofacitinib 5 mg twice daily; after the treatment withdrawal phase, NK cell counts increased toward baseline levels and were similar to those in patients who received placebo. For both NK cells and B cells, the median percentage change from pretreatment baseline at week 12 was close to 0 with tofacitinib 5 mg twice daily, indicating complete reversibility of the observed changes.

Reversibility of changes in LSCs after long-term treatment.

The lymphocyte substudy (cohort 2) assessed reversibility of changes in LSCs after temporary withdrawal of tofacitinib treatment for 4 weeks, following treatment for ~50 months. In 12 of 22 patients (54.5%), 11 of 26 patients (42.3%), and 12 of 17 patients (70.6%) who had low CD3+, CD4+, or CD8+ T cell counts, respectively, values returned to within the RA reference range after the 4-week withdrawal (for LSC cutoff values, see Supplementary Table 1, <http://onlinelibrary.wiley.com/doi/10.1002/art.40780/abstract>).

After the 4-week withdrawal, B cell and NK cell counts remained within the RA reference range in the majority of patients; no patient had an NK cell value below the reference range or a B cell value above the reference range. Of 2 patients who had high NK cell values, the level returned to within the RA reference range in 1 but remained above the reference range in the other. Three patients had low B cell values prior to tofacitinib withdrawal; the level had returned to within the RA reference range at week 4 in 1 but remained below the reference range in the other 2.

Association of ALC and LSC with infection rates following long-term treatment. Incidence rates of serious infections and herpes zoster in the All RA safety population (n = 7,061) are presented in Table 2. The incidence rates of serious infections following a confirmed ALC of <500 cells/mm³ were higher versus ALC categories ≥500 cells/mm³, and herpes

Table 1. Baseline ALC categories patients in the All RA population who developed an ALC of <500 cells/mm³ during tofacitinib treatment, and time to first ALC of ≥500 cells/mm³ in patients in the All RA population who had a confirmed ALC of <500 cells/mm³ during tofacitinib treatment and discontinued treatment at any time during the study*

	No. (%) of patients/median time to first observation
Baseline ALC, cells/mm ³	
<500	4 (5.0)
≥500 to <750	22 (27.5)
≥750 to <1,000	19 (23.8)
≥1,000 to <1,500	25 (31.3)
≥1,500	8 (10.0)
Missing data	2 (2.5)
Total	80 (100)
First ALC of ≥500 cells/mm ³ after tofacitinib discontinuation, cells/mm ³	
≥500 to <1,000	61 (87.1)/6.0 weeks
≥1,000 to <1,500	8 (11.4)/4.4 weeks
≥1,500	1 (1.4)/2.9 weeks
Total	70 (100)†

* Baseline data on absolute lymphocyte counts (ALCs) were obtained from the index study. All RA = rheumatoid arthritis patients from the tofacitinib phases I, II, and III and long-term extension studies.

† Five patients whose ALC never reached ≥500 cells/mm³ after confirmed ALC <500 cells/mm³ during tofacitinib treatment, as well as 5 patients without available follow-up ALC data, were not included.

Table 2. Incidence rates of serious infections and herpes zoster by confirmed ALC category in the All RA population*

Confirmed ALC, cells/mm ³	Serious infection			Herpes zoster		
	n	No. (%) of patients with event	IR (95% CI) following confirmed ALC†	n	No. (%) of patients with event	IR (95% CI) following confirmed ALC†
Missing data	35	0 (0)		35	1 (2.9)	
≥2,000	6,092	94 (1.5)	2.4 (1.9–2.9)	6,092	113 (1.9)	2.9 (2.4–3.5)
≥1,500 to <2,000	4,477	130 (2.9)	2.3 (2.0–2.8)	4,427	177 (4.0)	3.3 (2.9–3.9)
≥1,000 to <1,500	4,271	215 (5.0)	2.4 (2.1–2.7)	4,154	311 (7.5)	3.7 (3.3–4.2)
≥750 to <1,000	1,706	83 (4.9)	2.6 (2.0–3.2)	1,589	122 (7.7)	4.3 (3.6–5.1)
≥500 to <750	614	48 (7.8)	4.0 (2.9–5.3)	568	55 (9.7)	5.3 (4.0–6.9)
<500	76	6 (7.9)	7.1 (2.6–15.5)	67	3 (4.5)	4.2 (0.9–12.2)
Overall	7,061	576 (8.2)	2.5 (2.3–2.7)	7,061	782 (11.1)	3.6 (3.4–3.9)

* Only patients with at least 2 visits at which absolute lymphocyte counts (ALCs) were obtained after the tofacitinib start date were included in the analysis. ALC was monitored independently of infection events. Patients with an ALC of <500 cells/mm³ discontinued tofacitinib treatment and continued to be followed up to resolution or until the ALC was determined by the investigator to be stabilized. All RA = rheumatoid arthritis patients from the tofacitinib phases I, II, and III and long-term extension (LTE) studies; 95% CI = 95% confidence interval.

† Incidence rates (IRs) are the number of patients with events per 100 patient-years and are based on events occurring after the confirmed ALC value was reached, i.e., an event is counted in a category if the event occurred only after the patient reached that category and did not occur while the patient was in any of the previous categories. For patient-years, the total follow-up time was calculated up to the day of the first event, subject to a risk period of 28 days beyond the last dose or to the data cutoff date. Gaps in dosing between index and LTE studies are included up to 28 days or to the data cutoff date.

zoster generally showed an increasing risk with lower ALC values. The rate of opportunistic infections also exhibited a trend toward an increase with decreasing ALC (data not shown), but there were too few cases to draw meaningful conclusions.

Table 3 shows the relationship between LSCs and the risk of serious infections and herpes zoster. Overall, there were generally no strong associations between LSCs (CD3+ T cells, CD4+ T cells, CD8+ T cells, NK cells, and B cells) and serious infections or herpes zoster.

A Cox regression analysis was performed to identify and assess potential risk factors for lymphopenia (i.e., ALC <500 cells/mm³). The results showed that patients with lower ALCs at baseline ($P < 0.0001$), older age ($P = 0.0012$), higher tofacitinib dose ($P = 0.0071$), and those receiving background MTX ($P = 0.0068$) were at increased risk.

Correlation between ALCs and LSCs: utility of LSC monitoring. LSCs did not appear to be strongly associated with infection events; hence, if subset counts correlate well with ALCs, additional measurement of LSCs would not add value over and above the ALC to minimize risk of infection. The relationship between CD3+ T cell counts and ALCs was evaluated by estimating Pearson correlation coefficients (R) at pretreatment baseline (phase II baseline) and after short-term (phase II post-baseline), mid-term (ORAL Sequel vaccine substudy entry), and long-term (ORAL Sequel lymphocyte substudy entry) treatment with tofacitinib. A high degree of correlation was seen at baseline ($R = 0.79$), which increased with long-term tofacitinib treatment ($R = 0.89$), indicating that changes in ALCs reflect changes in

CD3+ T cell counts. This correlation was also observed at low values, i.e., low ALCs were associated with low CD3+ T cell counts (data not shown). Comparable results were observed for CD4+ T cell counts and ALCs ($R = 0.82$ – 0.86 ; Supplementary Figure 2A, <http://onlinelibrary.wiley.com/doi/10.1002/art.40780/abstract>), likely because CD4+ T cells constituted ~50% of the ALC at baseline. The correlation between CD8+ T cell counts and ALCs was only slightly lower at baseline and after tofacitinib treatment ($R = 0.65$ – 0.70) versus that observed with CD4+ T cells (Supplementary Figure 2B).

In contrast to CD4+ and CD8+ T cell counts, a poor correlation between ALC and NK cell counts was noted at baseline ($R = 0.27$), which improved with long-term tofacitinib treatment ($R = 0.47$). B cell counts and ALCs were moderately correlated at baseline ($R = 0.61$), with the correlation slightly decreasing following long-term tofacitinib treatment ($R = 0.55$).

DISCUSSION

This post hoc pooled analysis of tofacitinib therapy in patients with RA evaluated the short-, mid-, and long-term effects of tofacitinib on ALCs and LSCs, the reversibility of changes in ALCs or LSCs, the association between ALCs/LSCs and infections, and the value of monitoring LSCs in addition to ALCs. A summary of the effects of tofacitinib on immune cells is presented in Supplementary Table 3, on the *Arthritis & Rheumatology* web site at <http://onlinelibrary.wiley.com/doi/10.1002/art.40780/abstract>.

Tofacitinib treatment initially resulted in a transient increase in ALC, followed by a gradual decline to steady state by ~48 months.

Table 3. Incidence rates (95% CI) of serious infections and herpes zoster by quartile of nadir CD3+ T cell, CD4+ T cell, CD8+ T cell, and NK cell counts, and zenith B cell counts, in the All RA population*

LSC, quartile, ×1,000 cells/mm ³	Serious infection		Herpes zoster	
	n/no. with event	IR (95% CI)	n/no. with event	IR (95% CI)
CD3+ T cells				
Q1, <0.62	531/25	0.85 (0.55–1.26)	533/109	4.17 (3.42–5.03)
Q2, 0.62 to <0.90	533/28	1.07 (0.71–1.55)	534/82	3.42 (2.72–4.25)
Q3, 0.90 to <1.26	533/30	1.37 (0.92–1.96)	539/73	3.54 (2.78–4.45)
Q4, ≥1.26	534/40	2.04 (1.46–2.78)	536/61	3.31 (2.53–4.25)
CD3+CD4+ T cells				
Q1, <0.39	353/11	0.53 (0.26–0.95)	355/76	4.12 (3.25–5.16)
Q2, 0.39 to <0.55	354/11	0.58 (0.29–1.04)	356/53	3.05 (2.28–3.99)
Q3, 0.55 to <0.76	353/12	0.71 (0.37–1.24)	357/45	2.83 (2.07–3.79)
Q4, ≥0.76	354/15	1.15 (0.64–1.90)	357/28	2.26 (1.50–3.27)
CD3+CD8+ T cells				
Q1, <0.13	351/12	0.60 (0.31–1.04)	353/75	4.25 (3.35–5.33)
Q2, 0.13 to <0.21	356/9	0.50 (0.23–0.94)	359/49	2.90 (2.14–3.83)
Q3, 0.21 to <0.31	353/13	0.75 (0.40–1.28)	356/43	2.64 (1.91–3.56)
Q4, ≥0.31	354/15	1.07 (0.60–1.77)	357/35	2.64 (1.84–3.68)
B cells (CD3–CD19+)				
Q1, <0.14	532/46	2.01 (1.47–2.68)	535/101	4.87 (3.97–5.92)
Q2, 0.14 to <0.22	534/27	1.09 (0.72–1.58)	536/83	3.65 (2.90–4.52)
Q3, 0.22 to <0.33	539/26	1.05 (0.69–1.54)	541/74	3.23 (2.54–4.05)
Q4, ≥0.33	536/24	0.97 (0.62–1.45)	540/67	2.92 (2.26–3.71)
NK cells (CD3–CD16+CD56+)				
Q1, <0.07	427/34	1.70 (1.18–2.37)	429/58	3.16 (2.40–4.08)
Q2, 0.07 to <0.12	426/14	0.69 (0.38–1.17)	429/61	3.27 (2.50–4.20)
Q3, 0.12 to <0.18	429/18	0.85 (0.50–1.34)	432/62	3.19 (2.44–4.08)
Q4, ≥0.18	428/15	0.71 (0.40–1.17)	431/55	2.78 (2.10–3.62)

* Incidence rates (IRs) are the number of patients with events per 100 patient-years. Events are counted up to 28 days beyond the last dose or to the data cutoff date. 95% CI = 95% confidence interval; NK = natural killer; All RA = rheumatoid arthritis patients from the tofacitinib phases I, II, and III and long-term extension studies; LSC = lymphocyte subset count; Q = quartile.

In contrast, adalimumab-treated patients in the ORAL Standard trial experienced a sustained increase in ALC over 12 months, and MTX-treated patients in ORAL Start showed smaller decreases compared to tofacitinib-treated patients over 24 months. The different populations evaluated in these studies (MTX-naive versus MTX-IR) should, however, be acknowledged. Approximately 1% of patients in the All RA population experienced a confirmed ALC of <500 cells/mm³, and 80% of these patients were receiving tofacitinib plus background therapy at the time of the event. In most patients who permanently discontinued tofacitinib treatment due to an ALC of <500 cells/mm³, the ALC reverted to ≥500 cells/mm³ between 3 and 6 weeks after discontinuation. Patients receiving tofacitinib with a confirmed nadir ALC of <500 cells/mm³ had an increased risk of serious infection, while herpes zoster showed a trend toward an increasing risk with lower ALC values.

The rate of opportunistic infections also showed a trend toward increases with decreasing ALC, but there were too few cases to draw meaningful conclusions. Given that lymphopenia is associated with an increased risk of serious infections during tofacitinib treatment (29), ALC evaluation at baseline and monitoring every 3 months is recommended.

Initiation of tofacitinib is not recommended in patients with an ALC of <500 cells/mm³, and therapy should be discontinued in those developing a confirmed ALC of <500 cells/mm³ during treatment (26). Patients receiving tofacitinib with a confirmed nadir ALC of between 500 and <750 cells/mm³ showed a trend toward increased risk of serious infection and herpes zoster, which is relevant to the recommendation in the European Union label to interrupt dosing within this range until ALC returns to >750 cells/mm³, due to increased risk of infection (27). A higher

threshold has the potential to avoid more infections, but may also disproportionately exclude patients who could benefit from tofacitinib and not experience a serious infection (30).

Regarding LSCs, tofacitinib treatment resulted in 1) a slight initial decrease in T cell counts compared to pretreatment baseline, which decreased further with mid- to long-term treatment, 2) an initial decrease in NK cell counts, followed by a shift to increased NK cell counts with mid- to long-term treatment, and 3) an initial increase in B cell counts, which returned to baseline with long-term treatment. Reversible decreases in NK cells and increases in B cells with tofacitinib have been reported previously (20). For all cell types evaluated, no further progressive decline in LSCs occurred in the lymphocyte substudy. Withdrawal of tofacitinib for 4 weeks in patients previously treated with tofacitinib for ~50 months demonstrated that changes in T cell and B cell levels are reversible, although the increase in NK cells upon treatment withdrawal is somewhat counterintuitive given the observed increases in NK cell counts over long-term tofacitinib treatment. Potential mechanisms for this phenomenon are discussed below. Also, there were no strong associations between LSCs and serious infections. ALCs correlated well with CD4+ T cell/CD8+ T cell counts; hence, specific CD4+ T cell or CD8+ T cell monitoring would be unlikely to further minimize infection risk. CD4+ and CD8+ T cells together constitute ~70% of ALCs (31,32), and changes in these subtypes therefore should be reflected in ALCs.

Similar early effects on NK, B, and T cells have been reported with other JAK inhibitors. In a 12-week study of upadacitinib in RA, a dose-dependent reduction in NK cell counts was reported, with a mean decrease of 18.3% and 28.0% with upadacitinib at 6 mg and 12 mg twice daily, respectively (33); the safety profiles were found to be comparable to those reported in a phase III study of upadacitinib in daily doses of 15 mg or 30 mg (34). The European Public Assessment Report for baricitinib describes a 20% decrease in NK cells, with recovery to near-baseline levels at week 52 (35). Also, early increases in B cell counts that were sustained through ≥ 24 weeks were reported for baricitinib (36). An early increase in lymphocyte counts followed by a gradual decrease to baseline by ~1 year has been reported for baricitinib as well (37); however, the effects beyond 1 year have not been published, and it is unclear whether the lymphocytes reached steady state.

The initial increase in ALC with both adalimumab and tofacitinib treatment in this study may be due to the initial amelioration of disease or, alternatively, to a direct/indirect effect of JAK inhibition on lymphocyte trafficking and margination. In the absence of foreign antigens, cytokines such as IL-7/IL-15 provide survival and/or proliferation signals to maintain the population of CD4+ and CD8+ T cells (38–40). IL-15 is also the dominant cytokine for prolonging NK cell survival (40,41). Therefore, long-term modulation of cytokine signaling by tofacitinib, but not adalimumab or MTX, could impact the setpoint for steady-state populations of CD4+ T, CD8+ T, and NK cells, which compete for a limited pool of IL-7/IL-15. With decreased IL-7/IL-15 signaling, a reduction in

NK cell numbers may be observed earlier than CD4+ and CD8+ T cells, due to the relatively shorter half-life of NK cells. With continued tofacitinib dosing, CD4+ and CD8+ T cell numbers decrease slowly to a new setpoint, reducing the competition for IL-15. The increased availability of IL-15, coupled with >10-fold higher expression of the IL-15 receptor (CD122, IL-2/IL-15R β) on NK cells, may lead to a compensatory increase in IL-15 signaling, resulting in a higher NK cell number setpoint after long-term dosing (40,42). Upon treatment discontinuation, CD4+, CD8+, and NK cells all increase in response to increased cytokine signaling. The physiologic implications of the observed increase in circulating B cell numbers in response to JAK inhibition, followed by an eventual normalization after 4 years, are unclear. Overall, there is a lack of information concerning the mechanism of action for the effect of tofacitinib on ALC/LSC; hence, discussions can only be considered in hypothesis-generating terms.

The impact of immunotherapy on the immune system cannot be understood without considering both numerical and functional changes in immune cells, and several studies have been conducted to characterize the potential effect of tofacitinib on immune function, i.e., cell-mediated immunity (T cell and NK cell function) and humoral-mediated immunity (B cell and vaccination responses). Cell-mediated immunity data suggest that tofacitinib does not significantly impair T cell function assessed via non-antigen-specific stimulation, nor does it affect the generation and maintenance of responses using antigens as varied as tetanus toxoid (study A3921061/NCT01163253) (ref. 21 and Supplementary Figure 3, on the *Arthritis & Rheumatology* web site at <http://onlinelibrary.wiley.com/doi/10.1002/art.40780/abstract>) and herpesviruses (23). A modest decrease in NK cell cytotoxic activity was observed in tofacitinib-treated patients with RA (study A3921237/NCT02147587) (Supplementary Figure 4, <http://onlinelibrary.wiley.com/doi/10.1002/art.40780/abstract>); the clinical significance of these data is unclear, although the possibility of an impact on herpes zoster risk cannot be excluded. Similarly, studies measuring serum Ig levels and vaccination responses in tofacitinib-treated patients with RA and psoriasis suggest that tofacitinib may not impair humoral-mediated immunity (21–23).

This analysis had several limitations. Multiple patient populations (some small), from several different studies, were evaluated. Also, most patients did not have baseline index study values for LSCs. Data on the All RA population were not evaluated continuously, and the LTE population is a selected population of patients tolerant to treatment, potentially limiting the generalizability of results. Protocol amendments prevented the inclusion of patients with lymphopenia (ALC <500 cells/mm³) and patients who developed confirmed lymphopenia were withdrawn from the studies, making it difficult to capture information on serious infections after the occurrence of confirmed lymphopenia. Finally, no direct investigation of the relationship between the level and function of ALCs/LSCs was performed.

In conclusion, tofacitinib treatment results in a transient increase in ALC, followed by a gradual decline to reach steady state by ~48 months. Changes in both ALC and LSC are reversible upon treatment cessation. Although the overall effects of tofacitinib on cell-mediated and humoral-mediated immunity appear to be modest, risks of serious infections and herpes zoster were generally increased in the setting of confirmed low ALCs (<500 cells/mm³). From a clinical perspective, evaluation of ALC at baseline and monitoring every 3 months during tofacitinib treatment is recommended. Initiation of tofacitinib is not recommended in patients with an ALC of <500 cells/mm³, and if this develops, tofacitinib therapy should be discontinued (26). ALC and CD4+/CD8+ T cell counts correlated well, and there was no strong correlation between CD4+/CD8+ T cell counts and serious infections, suggesting that monitoring of these lymphocyte subsets may not provide any additional information. Thus, ALC monitoring alone appears to be adequate to minimize risk. Laboratory and safety outcomes related to immune function continue to be evaluated within the tofacitinib development program.

ACKNOWLEDGMENTS

The authors would like to acknowledge the support of all the study patients and investigators.

AUTHOR CONTRIBUTIONS

All authors were involved in drafting the article or revising it critically for important intellectual content, and all authors approved the final version to be published. Dr. van Vollenhoven had full access to all of the data in the study and takes responsibility for the integrity of the data and the accuracy of the data analysis.

Study concept and design. Valdez, Krishnaswami, Biswas, Lazariciu, Hodge, Wang, Choy.

Acquisition of data. Van Vollenhoven, Lee, Biswas, Lazariciu, Hodge, Wang.

Analysis and interpretation of data. Van Vollenhoven, Lee, Strengholt, Mojciak, Valdez, Krishnaswami, Biswas, Lazariciu, Hazra, Clark, Hodge, Wang, Choy.

ROLE OF THE STUDY SPONSOR

Medical writing support, under the guidance of the authors, was provided by Paul Scutt, PhD, at CMC Connect, a division of McCann Health Medical Communications Ltd, Manchester, UK, and was funded by Pfizer Inc, New York, NY, in accordance with Good Publication Practice (GPP3) guidelines (Ann Intern Med 2015;163:461–4). The authors had the final decision to submit the manuscript for publication.

REFERENCES

- Fleischmann R, Cutolo M, Genovese MC, Lee EB, Kanik KS, Sadis S, et al. Phase IIb dose-ranging study of the oral JAK inhibitor tofacitinib (CP-690,550) or adalimumab monotherapy versus placebo in patients with active rheumatoid arthritis with an inadequate response to disease-modifying antirheumatic drugs. *Arthritis Rheum* 2012;64:617–29.
- Kremer JM, Bloom BJ, Breedveld FC, Coombs JH, Fletcher MP, Gruben D, et al. The safety and efficacy of a JAK inhibitor in patients with active rheumatoid arthritis: results of a double-blind, placebo-controlled phase IIa trial of three dosage levels of CP-690,550 versus placebo. *Arthritis Rheum* 2009;60:1895–905.
- Kremer JM, Cohen S, Wilkinson BE, Connell CA, French JL, Gomez-Reino J, et al. A phase IIb dose-ranging study of the oral JAK inhibitor tofacitinib (CP-690,550) versus placebo in combination with background methotrexate in patients with active rheumatoid arthritis and an inadequate response to methotrexate alone. *Arthritis Rheum* 2012;64:970–81.
- Tanaka Y, Suzuki M, Nakamura H, Toyozumi S, Zwillich SH, Tofacitinib Study Investigators. Phase II study of tofacitinib (CP-690,550) combined with methotrexate in patients with rheumatoid arthritis and an inadequate response to methotrexate. *Arthritis Care Res (Hoboken)* 2011;63:1150–8.
- Tanaka Y, Takeuchi T, Yamanaka H, Nakamura H, Toyozumi S, Zwillich S. Efficacy and safety of tofacitinib as monotherapy in Japanese patients with active rheumatoid arthritis: a 12-week, randomized, phase 2 study. *Mod Rheumatol* 2015;25:514–21.
- Burmester GR, Blanco R, Charles-Schoeman C, Wollenhaupt J, Zerbini C, Benda B, et al. Tofacitinib (CP-690,550) in combination with methotrexate in patients with active rheumatoid arthritis with an inadequate response to tumour necrosis factor inhibitors: a randomized phase 3 trial. *Lancet* 2013;381:451–60.
- Fleischmann R, Kremer J, Cush J, Schulze-Koops H, Connell CA, Bradley JD, et al. Placebo-controlled trial of tofacitinib monotherapy in rheumatoid arthritis. *N Engl J Med* 2012;367:495–507.
- Kremer J, Li ZG, Hall S, Fleischmann R, Genovese M, Martin-Mola E, et al. Tofacitinib in combination with nonbiologic disease-modifying antirheumatic drugs in patients with active rheumatoid arthritis: a randomized trial. *Ann Intern Med* 2013;159:253–61.
- Lee EB, Fleischmann R, Hall S, Wilkinson B, Bradley J, Gruben D, et al. Tofacitinib versus methotrexate in rheumatoid arthritis. *N Engl J Med* 2014;370:2377–86.
- Van der Heijde D, Tanaka Y, Fleischmann R, Keystone E, Kremer J, Zerbini C, et al. Tofacitinib (CP-690,550) in patients with rheumatoid arthritis receiving methotrexate: twelve-month data from a twenty-four-month phase III randomized radiographic study. *Arthritis Rheum* 2013;65:559–70.
- Van Vollenhoven RF, Fleischmann R, Cohen S, Lee EB, García Mejjide JA, Wagner S, et al. Tofacitinib or adalimumab versus placebo in rheumatoid arthritis. *N Engl J Med* 2012;367:508–19.
- Wollenhaupt J, Silverfield J, Lee EB, Curtis JR, Wood SP, Soma K, et al. Safety and efficacy of tofacitinib, an oral Janus kinase inhibitor, for the treatment of rheumatoid arthritis in open-label, long-term extension studies. *J Rheumatol* 2014;41:837–52.
- Wollenhaupt J, Silverfield J, Lee EB, Terry K, Kwok K, Strengholt S, et al. Tofacitinib, an oral Janus kinase inhibitor, in the treatment of rheumatoid arthritis: safety and efficacy in open-label, long-term extension studies over 9 years [abstract]. *Arthritis Rheumatol* 2017;69 Suppl 10. URL: <https://acrabstracts.org/abstract/tofacitinib-an-oral-janus-kinase-inhibitor-in-the-treatment-of-rheumatoid-arthritis-safety-and-efficacy-in-open-label-long-term-extension-studies-over-9-years/>.
- Yamanaka H, Tanaka Y, Takeuchi T, Sugiyama N, Yuasa H, Toyozumi S, et al. Tofacitinib, an oral Janus kinase inhibitor, as monotherapy or with background methotrexate, in Japanese patients with rheumatoid arthritis: an open-label, long-term extension study. *Arthritis Res Ther* 2016;18:34.
- Boyle DL, Wei N, Singhal AK, Rosengren S, Kaplan I, Soma K, et al. The JAK inhibitor tofacitinib suppresses synovial JAK1-STAT1 signaling in rheumatoid arthritis [abstract]. *Ann Rheum Dis* 2013;72 Suppl 3. URL: <http://scientific.sparx-ip.net/archiveular/?c=a&view=4&searchfor=Boyle&item=2013OPO253>.

16. Cutolo M. The kinase inhibitor tofacitinib in patients with rheumatoid arthritis: latest findings and clinical potential. *Ther Adv Musculoskelet Dis* 2013;5:3–11.
17. Arend WP. Physiology of cytokine pathways in rheumatoid arthritis [review]. *Arthritis Rheum* 2001;45:101–6.
18. Ghoreschi K, Jesson MI, Li X, Lee JL, Ghosh S, Alsup JW, et al. Modulation of innate and adaptive immune responses by tofacitinib (CP-690,550). *J Immunol* 2011;186:4234–43.
19. Rochman Y, Spolski R, Leonard WJ. New insights into the regulation of T cells by γ_c family cytokines. *Nat Rev Immunol* 2009;9:480–90.
20. Hodge JA, Kawabata TT, Krishnaswami S, Clark JD, Telliez JB, Dowty ME, et al. The mechanism of action of tofacitinib: an oral Janus kinase inhibitor for the treatment of rheumatoid arthritis. *Clin Exp Rheumatol* 2016;34:318–28.
21. Winthrop K, Korman N, Abramovits W, Rottinghaus ST, Tan H, Gardner A, et al. T-cell-mediated immune response to pneumococcal conjugate vaccine (PCV-13) and tetanus toxoid vaccine in patients with moderate-to-severe psoriasis during tofacitinib treatment. *J Am Acad Dermatol* 2018;78:1149–55.
22. Winthrop KL, Silverfield J, Racewicz A, Neal J, Lee EB, Hrycaj P, et al. The effect of tofacitinib on pneumococcal and influenza vaccine responses in rheumatoid arthritis. *Ann Rheum Dis* 2016;75:687–95.
23. Winthrop KL, Wouters AG, Choy EH, Soma K, Hodge JA, Nduaka CI, et al. The safety and immunogenicity of live zoster vaccination in patients with rheumatoid arthritis before starting tofacitinib: a randomized phase II trial. *Arthritis Rheumatol* 2017;69:1969–77.
24. Strand V, Ahadiet S, French J, Geier J, Krishnaswami S, Menon S, et al. Systematic review and meta-analysis of serious infections with tofacitinib and biologic disease-modifying antirheumatic drug treatment in rheumatoid arthritis clinical trials. *Arthritis Res Ther* 2015;17:362.
25. Cohen SB, Tanaka Y, Mariette X, Curtis JR, Lee EB, Nash P, et al. Long-term safety of tofacitinib for the treatment of rheumatoid arthritis up to 8.5 years: integrated analysis of data from the global clinical trials. *Ann Rheum Dis* 2017;76:1253–62.
26. Xeljanz (tofacitinib) prescribing information. New York (NY): Pfizer Inc; 2017. URL: <http://labeling.pfizer.com/ShowLabeling.aspx?id=959>.
27. Xeljanz (tofacitinib citrate) prescribing information. Sandwich (UK): Pfizer Ltd; 2017. URL: <https://www.medicines.org.uk/emc/medicine/33167>.
28. Arnett FC, Edworthy SM, Bloch DA, McShane DJ, Fries JF, Cooper NS, et al. The American Rheumatism Association 1987 revised criteria for the classification of rheumatoid arthritis. *Arthritis Rheum* 1988;31:315–24.
29. Van Vollenhoven RF, Riese R, Krishnaswami S, Kawabata T, Fossier C, Rottinghaus S, et al. Relationship between lymphocyte count and risk of infection in rheumatoid arthritis patients treated with tofacitinib [abstract]. *Arthritis Rheum* 2013;65 Suppl 10. URL: <https://acrabstracts.org/abstract/relationship-between-lymphocyte-count-and-risk-of-infection-in-rheumatoid-arthritis-patients-treated-with-tofacitinib/>.
30. Burmester GR, Szekanecz Z, Biswas P, Krishnaswami S, Mojcik CF, Valdez H, et al. Monitoring of absolute lymphocyte count in patients with rheumatoid arthritis treated with tofacitinib [abstract]. *Arthritis Rheumatol* 2017;69 Suppl 10. URL: <https://acrabstracts.org/abstract/monitoring-of-absolute-lymphocyte-count-in-patients-with-rheumatoid-arthritis-treated-with-tofacitinib/>.
31. Bisset LR, Lung TL, Kaelin M, Ludwig E, Dubs RW. Reference values for peripheral blood lymphocyte phenotypes applicable to the healthy adult population in Switzerland. *Eur J Haematol* 2004;72:203–12.
32. Jentsch-Ullrich K, Koenigsmann M, Mohren M, Franke A. Lymphocyte subsets' reference ranges in an age- and gender-balanced population of 100 healthy adults: a monocentric German study. *Clin Immunol* 2005;116:192–7.
33. Kremer JM, Emery P, Camp HS, Friedman A, Wang L, Othman AA, et al. A phase IIb study of ABT-494, a selective JAK-1 inhibitor, in patients with rheumatoid arthritis and an inadequate response to anti-tumor necrosis factor therapy. *Arthritis Rheumatol* 2016;68:2867–77.
34. Burmester GR, Kremer J, van Den Bosch F, Li Y, Zhou Y, Othman AA, et al. A phase 3 randomized, placebo-controlled, double-blind study of upadacitinib (ABT-494), a selective JAK-1 inhibitor, in patients with active rheumatoid arthritis with inadequate response to conventional synthetic DMARDs [abstract]. *Arthritis Rheumatol* 2017;69 Suppl 10. URL: <https://acrabstracts.org/abstract/a-phase-3-randomized-placebo-controlled-double-blind-study-of-upadacitinib-abt-494-a-selective-jak-1-inhibitor-in-patients-with-active-rheumatoid-arthritis-with-inadequate-response-to-convention/>.
35. European Medicines Agency. European Public Assessment Report for Olumiant—international non-proprietary name: baricitinib. 2016. URL: https://www.ema.europa.eu/documents/assessment-report/olumiant-epar-public-assessment-report_en.pdf.
36. Emery P, McInnes I, Genovese MC, Smolen JS, Kremer J, Dougados M, et al. Characterization of changes in lymphocyte subsets in baricitinib-treated patients with rheumatoid arthritis in two phase 3 studies [abstract]. *Arthritis Rheumatol* 2015;67 Suppl 10. URL: <https://acrabstracts.org/abstract/characterization-of-changes-in-lymphocyte-subsets-in-baricitinib-treated-patients-with-rheumatoid-arthritis-in-two-phase-3-studies/>.
37. Kremer J, Huizinga TW, Chen L, Saifan CG, Issa M, Witt SL, et al. Analysis of neutrophils, lymphocytes, and platelets in pooled phase 2 and phase 3 studies of baricitinib for rheumatoid arthritis [abstract]. *Ann Rheum Dis* 2017;76 Suppl 2. URL: <http://scientific.sparx-ip.net/archiveeular/?searchfor=Kremer&c=a&view=4&item=2017FRI0090>.
38. Boyman O, Letourneau S, Krieg C, Sprent J. Homeostatic proliferation and survival of naive and memory T cells. *Eur J Immunol* 2009;39:2088–94.
39. Boyman O, Krieg C, Homann D, Sprent J. Homeostatic maintenance of T cells and natural killer cells. *Cell Mol Life Sci* 2012;69:1597–608.
40. Ma A, Koka R, Burkett P. Diverse functions of IL-2, IL-15, and IL-7 in lymphoid homeostasis. *Annu Rev Immunol* 2006;24:657–79.
41. Ali AK, Nandagopal N, Lee SH. IL-15-PI3K-AKT-mTOR: a critical pathway in the life journey of natural killer cells. *Front Immunol* 2015;6:355.
42. Bielekova B, Catalfamo M, Reichert-Scriver S, Packer A, Cerna M, Waldmann TA, et al. Regulatory CD56(bright) natural killer cells mediate immunomodulatory effects of IL-2R α -targeted therapy (daclizumab) in multiple sclerosis. *Proc Natl Acad Sci U S A* 2006;103:5941–6.

BRIEF REPORT

Association of Baseline Peptidylarginine Deiminase 4 Autoantibodies With Favorable Response to Treatment Escalation in Rheumatoid Arthritis

Erika Darrah,¹  Fang Yu,² Laura C. Cappelli,¹ Antony Rosen,¹ James R. O'Dell,³ and Ted R. Mikuls³

Objective. To determine if the baseline presence of autoantibodies to peptidylarginine deiminase 4 (PAD4) predicts therapeutic response to biologic and conventional disease-modifying antirheumatic drugs (DMARDs) in patients with rheumatoid arthritis (RA) in whom methotrexate (MTX) monotherapy was unsuccessful.

Methods. Baseline serum from 282 RA patients in whom MTX monotherapy was unsuccessful was screened for the presence of anti-PAD4 antibodies by immunoprecipitation. Clinical response to either triple DMARD (MTX, sulfasalazine, and hydroxychloroquine) or MTX/etanercept combination therapy was determined at 24 and 48 weeks post-treatment initiation. Disease activity was measured using the Disease Activity Score 28-joint assessment (DAS28), and erosive disease was quantified using the Sharp/van der Heijde scoring method. Generalized estimating equations (GEEs) were used to model the clinical responses to treatment in patients with and those without baseline anti-PAD4 antibodies.

Results. Anti-PAD4 antibody positivity was associated with male sex, a history of never smoking, and anti-citrullinated protein antibodies. At baseline, patients with anti-PAD4 antibodies had longer disease duration and significantly more radiographic joint damage than anti-PAD4-negative patients, but did not differ in disease activity according to the DAS28. In unadjusted analyses and multivariable GEE models, patients with anti-PAD4 antibodies exhibited greater improvements in DAS28 (adjusted $P = 0.02$ and $P = 0.008$, respectively) and less radiographic progression (adjusted $P = 0.01$ and $P = 0.002$, respectively) compared to anti-PAD antibody-negative patients, independent of treatment received.

Conclusion. Although anti-PAD4 antibodies were associated with worse baseline radiographic joint damage, suggesting a history of active or undiagnosed disease, treatment escalation therapy was more effective in reducing disease activity and slowing the progression of joint damage in this patient subset.

INTRODUCTION

Disease-modifying antirheumatic drugs (DMARDs) have greatly improved clinical outcomes for patients with rheumatoid arthritis (RA). Among these treatments, methotrexate (MTX) is the most commonly prescribed first-line DMARD, but is often insuffi-

cient for long-term disease control when used as oral monotherapy (1). Following suboptimal responses to MTX monotherapy, the addition of other DMARDs, including tumor necrosis factor (TNF) inhibitors, has been shown to be an effective therapeutic strategy and is the current standard of care (2,3). While these treatment algorithms have greatly improved disease prognosis,

The content of this paper is solely the responsibility of the authors and does not represent the official views of the NIH.

Drs. Darrah and Cappelli's work was supported by the Jerome L. Greene Foundation and the NIH (National Institute of Arthritis and Musculoskeletal and Skin Diseases grants P30-AR-053503 and P30-AR-070254). Dr. O'Dell's work was supported by the VA Cooperative Studies Program. Dr. Mikuls' work was supported by a VA Merit Award (CX000896) and the NIH (National Institute of General Medical Sciences grant U54GM115458).

¹Erika Darrah, PhD, Laura C. Cappelli, MD, MHS, Antony Rosen, MD: Johns Hopkins University School of Medicine, Baltimore, Maryland; ²Fang Yu, PhD: University of Nebraska Medical Center, Omaha; ³James R. O'Dell, MD, Ted R. Mikuls, MD, MSPH: VA Nebraska-Western Iowa Health Care System and University of Nebraska Medical Center, Omaha.

Dr. Darrah has received research support from Pfizer. Drs. Darrah and Rosen are coinventors on a patent relating to the use of anti-PAD3 human autoantibodies and their benefit in the diagnosis and treatment of rheumatoid arthritis and related diseases. Dr. Cappelli has received consulting fees from Regeneron/Sanofi (less than \$10,000) and research support from Bristol-Myers Squibb. Dr. Rosen has received research support from Siemens Healthineers. Dr. Mikuls has received consulting fees from Pfizer (less than \$10,000) and research support from Bristol-Myers Squibb. No other disclosures relevant to this article were reported.

Address correspondence to Erika Darrah, PhD, 5200 Eastern Avenue, MFL Center Tower, Suite 5300, Baltimore, MD 21224. E-mail: edarrah1@jhmi.edu.

Submitted for publication June 1, 2018; accepted in revised form November 27, 2018.

this stepwise approach and variable treatment response between patients suggest the need to personalize the early selection of effective therapeutics. Initiation of effective therapy early in the disease course can prevent the accumulation of joint damage and disability in RA (4). Interestingly, differential treatment responses among patients with the RA-associated autoantibodies, rheumatoid factor (RF) and anti-citrullinated protein antibodies (ACPAs), have been shown in some studies, suggesting that baseline autoantibody status may be associated with clinical responses to specific DMARDs (5).

Antibodies to peptidylarginine deiminase 4 (PAD4), a key enzyme in RA pathogenesis, have been identified in the serum of 23–45% of patients with established disease and have been associated with severe erosive joint disease in several RA cohorts (6–8). Radiographic joint damage was greater in a subset of RA patients who were positive for anti-PAD4 antibodies that cross-reacted with the related enzyme PAD3 (9,10). Antibodies that recognize PAD3 alone have not been described. In a small, open-label TNF inhibitor study, the baseline presence of anti-PAD4 antibodies was associated with persistent disease activity and progression of erosive disease despite 12 months of treatment (11). In an observational study of patients with longstanding RA, anti-PAD3/4 cross-reactive antibodies were associated with increased progression of erosive joint disease (9), but this trend was not observed in a similar study of patients with early RA (10).

The prevalence and association of anti-PAD4 antibodies with severe erosive joint disease in patients with RA suggests that they may be informative predictors of poor clinical response to DMARD therapy; however, data from a large patient cohort receiving standardized treatment with rigorous pre- and posttreatment clinical assessments are lacking. To address this, the association of baseline anti-PAD4 antibodies with clinical response to triple DMARD (MTX, sulfasalazine, and hydroxychloroquine) or MTX/etanercept combination therapy in patients with active RA despite MTX monotherapy was explored.

PATIENTS AND METHODS

Study subjects. Sera from 282 patients in the Veterans Affairs Cooperative Study Program 551: RA Comparison of Active Therapies in Patients With Active Disease Despite Methotrexate Therapy (RACAT) trial were retrospectively screened for anti-PAD4 and anti-PAD3/4 antibodies (3). Patients provided written informed consent. RACAT was a double-blind, noninferiority trial comprising patients with active RA despite MTX monotherapy who were randomized to receive triple DMARD (MTX, sulfasalazine, and hydroxychloroquine) or combination therapy (MTX and etanercept). Baseline data on demographic, clinical, and serologic features were collected. Anti-cyclic citrullinated peptide (anti-CCP) antibodies were measured by enzyme-linked immunosorbent assay (Axis-Shield Diagnostics) and RF was measured by nephelometry (Siemens), using banked serum from baseline. Disease

Activity Score 28-joint counts (12), calculated using the erythrocyte sedimentation rate (DAS28-ESR), and radiographic burden of erosive disease, as calculated by the Sharp/van der Heijde scoring method (13), were determined at baseline, as well as at 24 and 48 weeks post-treatment initiation. At 24 weeks, patients whose DAS28 had not improved by at least 1.2 points were switched to the other treatment arm under blinded conditions.

PAD autoantibody detection. Anti-PAD4 and anti-PAD3/4 cross-reactive antibodies were detected in patient serum by immunoprecipitation of ³⁵S-labeled in vitro-transcribed and translated (Promega) PAD4 or PAD3 protein (6,9). Immunoprecipitated proteins were separated by sodium dodecyl sulfate–polyacrylamide gel electrophoresis, visualized by radiography, and quantified by densitometry. A densitometry value greater than 0.02 was considered positive. Baseline serum from patients in the RACAT cohort was first screened for autoantibodies to PAD4, then anti-PAD4-positive serum was further screened for cross-reactivity with PAD3. Patients who were positive for both PAD4 and PAD3 reactivity were designated as having anti-PAD3/4 cross-reactive antibodies “(XR),” as described in previous studies (9,10). Subjects with reactivity to PAD4, but not PAD3 were determined to have anti-PAD4 monospecific antibodies “(P4),” and patients who did not have reactivity to either PAD were designated as anti-PAD antibody negative “(P0).”

Statistical analysis. Patients were grouped by their baseline anti-PAD antibody status, and demographic, clinical, and serologic variables were compared using SAS 9.4 software (SAS Institute Inc.). Baseline treatment assignments, the number of patients whose treatment was switched, and treatment following switching were also compared between groups. The total anti-PAD4 antibody-positive group (P4 and XR patients combined) was also compared to P0 patients for these parameters. Normally distributed variables were compared using Student’s *t*-tests, non-normally distributed variables were compared using the Kruskal-Wallis test, and categorical variables were compared using the chi-square test or Fisher’s 2-sided exact test, as appropriate.

Generalized estimating equations (GEEs) were used to model the clinical responses in patients with and those without anti-PAD4 antibodies with regard to DAS28 and the Sharp/van der Heijde score. P4 and XR patients were combined in these analyses, given similar changes observed in DAS28 and Sharp/van der Heijde scores in these groups over follow-up. A GEE model with an identity link and a compound symmetry correlation between repeated measures was used to replicate the DAS28 scores over time, while a GEE log link model for count data and compound symmetry correlation between repeated measures was used to model the Sharp/van der Heijde scores over time. Both GEE models included baseline anti-PAD4 antibody status, follow-up time, and interaction between anti-PAD4 status and follow-up time to assess the association of anti-PAD4 with

the change in the DAS28 score or Sharp/van der Heijde score. The GEE models also included other covariates such as age, sex, race, body mass index (BMI), disease duration, anti-CCP status, treatment arm, treatment switching, and smoking status. Changes in the DAS28 score and relative changes in the Sharp/van der Heijde score were estimated and compared between treatment groups at each follow-up visit. Similar models were created using baseline anti-CCP status and its interaction with

follow-up time as the primary covariates. The Quasi-Akaike's information criterion (QIC) was used to identify the optimal model when modeling the DAS28 score or Sharp/van der Heijde score over time, as is appropriate for GEE, a non-likelihood-based model (14). To ensure a fair comparison using the same data set, the models under comparison were restricted to patients with non-missing values for both anti-PAD4 and anti-CCP status at baseline. The QIC scores between the anti-CCP model and

Table 1. Baseline characteristics of RACAT patients by anti-PAD antibody status*

	Anti-PAD4 negative (P0) (n = 208)	Anti-PAD4 positive		P			
		P4 (n = 43)	XR (n = 31)	P0 vs. P4 + XR	P0 vs. P4	P0 vs. XR	P4 vs. XR
Age, mean \pm SD years	58.2 \pm 12.0	57.7 \pm 13.1	56.9 \pm 14.2	0.61	0.79	0.59	0.80
Sex, male	113 (54)	29 (67)	21 (68)	0.048	0.11	0.16	0.98
Caucasian†	184 (88)	35 (81)	30 (97)	0.89	0.21	0.22	0.071
Ever smoking	152 (73)	25 (58)	20 (65)	0.048	0.051	0.32	0.58
RA duration, median (IQR) years‡	1 (1–3)	1 (1–6)	5 (1–10)	0.010	0.23	0.004	0.12
RF positive	140 (67.3)	34 (79.1)	21 (67.7)	0.26	0.13	0.96	0.27
Anti-CCP positive†	133 (63.9)	34 (79.1)	27 (87.1)	0.004	0.075	0.013	0.54
Anti-CCP titer, median (IQR)‡	54.3 (1.5–209.2)	130.4 (13.7–225.5)	91.4 (24.5–245.2)	0.027	0.10	0.082	0.84
Sharp/van der Heijde score, median (IQR)‡	5 (2–12)	13 (5–25)	15 (2–29)	0.0002	0.002	0.012	0.72
DAS28, median (IQR)‡	5.8 (5.2–6.4)	5.6 (5.2–6.7)	5.7 (5.1–6.6)	0.91	0.94	0.93	0.99
Tender joint count, median (IQR)‡	13 (9–18)	13 (9–18)	13 (9–16)	1.00	0.95	0.94	0.88
Swollen joint count, median (IQR)‡	11 (8–14.5)	11 (9–15)	9 (6–13)	0.89	0.19	0.17	0.047
ESR, mm/hour‡	23.5 (11.5–40)	20 (10–42)	18 (11–31)	0.45	0.55	0.57	0.87
Treatment at baseline							
Triple DMARD	110 (53)	19 (44)	13 (42)	0.15	0.30	0.26	0.85
MTX/etanercept	98 (47)	24 (56)	18 (58)				
Treatment switched at 24 weeks†	61 (29)	12 (28)	3 (10)	0.13	0.85	0.028	0.079
Treatment after switching							
Triple DMARD	103 (50)	23 (53)	16 (52)	0.64	0.64	0.83	0.87
MTX/etanercept	105 (50)	20 (47)	15 (48)				

* Except where indicated otherwise, values are the number (%) of patients. RACAT = RA Comparison of Active Therapies in Patients With Active Disease Despite Methotrexate Therapy; P4 = anti-peptidylarginine deiminase 4 (anti-PAD4) monospecific antibodies; XR = anti-PAD3/4 cross-reactive antibodies; RA = rheumatoid arthritis; IQR = interquartile range; RF = rheumatoid factor; anti-CCP = anti-cyclic citrullinated peptide; DAS28 = Disease Activity Score 28-joint count; ESR = erythrocyte sedimentation rate; DMARD = disease-modifying antirheumatic drug; MTX = methotrexate.

† P values were determined by Fisher's exact test.

‡ P values were determined by nonparametric Wilcoxon rank sum test.

anti-PAD4 model were compared, and the model with the lower QIC score was determined to be the best fit.

RESULTS

Association of anti-PAD4 antibodies with radiographic joint disease at baseline. Anti-PAD4 antibodies were present in 26% of patients at baseline (74 of 282). Demographic, clinical, and serologic characteristics of patients grouped by anti-PAD4 antibody status are shown in Table 1. Compared to anti-PAD4-negative subjects, patients with anti-PAD4 antibodies were more often male and less likely to have ever smoked. They also had longer RA duration and were more likely to be anti-CCP positive, with a 98% higher median anti-CCP titer than anti-PAD4 antibody-negative patients. While there were no significant differences in baseline measures of disease activity or inflammation between the groups, including DAS28, ESR, and number of tender or swollen joints, patients with anti-PAD4 antibodies had more radiographic joint damage, as reflected by a 190% higher median baseline Sharp/van der Heijde score compared to anti-PAD4-negative patients.

Among the anti-PAD4 antibody-positive patients, 58% had anti-PAD4 monospecific antibodies (P4), and 42% had anti-PAD3/4 cross-reactive antibodies (XR). Subanalysis of anti-PAD4-positive patients according to P4 or XR status did not reveal any significant demographic or clinical differences, other than a slightly higher mean swollen joint count in P4 individuals (Table 1). Despite similar randomization to triple DMARD or MTX/etanercept combination therapy in P0, P4, and XR patients, XR patients were 2.9 times less likely to be switched to the alternative treatment arm at 24 weeks, compared to P0 individuals. Since treatment switching was blinded and driven by a lack of clinical response to treatment at 24 weeks, this suggested a more favorable early treatment response in XR-positive individuals.

More favorable treatment response among anti-PAD4-positive patients. To determine if the clinical response to treatment escalation differed based on the anti-PAD4 autoantibody subtype present at baseline, the mean change in DAS28 score or Sharp/van der Heijde score in P0, P4, and XR patients at 24 and 48 weeks posttreatment was calculated, as shown in Supplementary Table 1 (available on *Arthritis & Rheumatology* web site at <http://onlinelibrary.wiley.com/doi/10.1002/art.40791/abstract>). In unadjusted analyses, patients in all antibody groups exhibited a decrease in the DAS28 at 24 and 48 weeks posttreatment, indicating a reduction in disease activity, but with progression of their erosive joint disease, as measured by an increase in the Sharp/van der Heijde score. At 48 weeks, the magnitude of DAS28 improvement was similar in P4 and XR patients (−2.36 and −2.56 DAS28 points, respectively) and greater than that in P0 patients (−2.08 DAS28 points). Similarly, less progression of radiographic joint damage was observed in P4 and XR patients (33% and 29% higher Sharp/van der Heijde score at 48 weeks posttreatment versus baseline) compared to patients with no anti-PAD4 antibodies (69% higher Sharp/van der Heijde score at 48 weeks posttreatment versus baseline). Similar trends in DAS28 score and Sharp/van der Heijde score according to anti-PAD4 antibody subtype were observed in patients irrespective of treatment with triple DMARD or MTX/etanercept combination therapy, as shown in Supplementary Table 2 (available on *Arthritis & Rheumatology* web site at <http://onlinelibrary.wiley.com/doi/10.1002/art.40791/abstract>).

Multivariable GEE models were then created to estimate the mean change in DAS28 score or relative change in Sharp/van der Heijde scores by anti-PAD4 antibody status following treatment. Due to similar baseline characteristics and clinical outcomes observed in P4 and XR patients in both treatment arms (Supplementary Tables 1 and 2), clinical responses in anti-PAD4 antibody-positive patients (P4 and XR groups combined) were compared to responses in anti-PAD4-negative patients.

Table 2. Estimated change in DAS28 with treatment according to anti-PAD4 antibody status

GEE model, weeks posttreatment	Estimated change in DAS28 (95% confidence interval)		P*
	Anti-PAD4 negative	Anti-PAD4 positive	
Unadjusted			
24	−1.83 (−2.02 to −1.65)	−2.25 (−2.58 to −1.92)	0.03
48	−2.09 (−2.26 to −1.92)	−2.50 (−2.81 to −2.20)	0.02
Adjusted†			
24	−1.84 (−2.02 to −1.65)	−2.27 (−2.60 to −1.94)	0.02
48	−2.09 (−2.26 to −1.92)	−2.55 (−2.84 to −2.26)	0.008

* P values were based on testing the interaction between time and anti-peptidylarginine deiminase 4 (anti-PAD4) status, or equivalently comparing the difference in the Disease Activity Score in 28 joints (DAS28) changes between the anti-PAD4-negative and anti-PAD4-positive groups.

† Generalized estimating equation (GEE) model adjusted for age, sex, race, body mass index, disease duration, anti-cyclic citrullinated peptide status, treatment arm, treatment switching, and smoking status.

Table 3. Estimated change in Sharp/van der Heijde score with treatment according to anti-PAD4 antibody status

GEE model, weeks posttreatment	Estimated relative change in Sharp/van der Heijde score (95% confidence interval)		<i>P</i> *
	Anti-PAD4 negative	Anti-PAD4 positive	
Unadjusted			
24	0.21 (0.12 to 0.31)	0.03 (−0.05 to 0.12)	0.006
48	0.24 (0.15 to 0.34)	0.03 (−0.06 to 0.12)	0.001
Adjusted†			
24	0.24 (0.15 to 0.33)	0.08 (0.00 to 0.16)	0.01
48	0.27 (0.18 to 0.37)	0.07 (−0.02 to 0.16)	0.002

* *P* values were based on testing the interaction between time and anti-peptidylarginine deiminase 4 (anti-PAD4) status, or equivalently comparing the difference in the relative Sharp/van der Heijde score changes from baseline between the anti-PAD4-negative and anti-PAD4-positive groups.

† Generalized estimating equation (GEE) model adjusted for age, sex, race, body mass index, disease duration, anti-cyclic citrullinated peptide status, treatment arm, treatment switching, and smoking status.

Although anti-PAD4-positive patients who did not respond to MTX monotherapy had significantly higher Sharp/van der Heijde scores at baseline compared to anti-PAD4-negative patients (Table 1), they had more favorable clinical outcomes in response to treatment, even after adjusting for age, sex, race, BMI, disease duration, anti-CCP status, treatment switching, and smoking status (Tables 2 and 3). While both patient groups had a reduction in disease activity following treatment, anti-PAD4 antibody-positive patients had a 22–23% greater decrease in DAS28 compared to anti-PAD4 antibody-negative patients (Table 2). This equated to a 2.27-point versus 1.84-point decrease in DAS28 score at 24 weeks ($P = 0.02$) and a 2.55-point versus 2.09-point decrease at 48 weeks ($P = 0.008$) in patients with anti-PAD4 antibodies compared to those without anti-PAD4 antibodies.

Despite the observed improvement in disease activity with treatment, patients in both groups demonstrated modest radiographic disease progression, as indicated by slightly increasing Sharp/van der Heijde scores at 24 and 48 weeks (Table 3). However, anti-PAD4 antibody-positive patients demonstrated less relative progression of joint disease compared to anti-PAD4 antibody-negative patients (8% versus 24% increase in the Sharp/van der Heijde score at 24 weeks [$P = 0.01$], and 7% versus 27% increase at 48 weeks [$P = 0.002$]).

The QIC was calculated for each model to compare how models containing anti-CCP or anti-PAD4 as a covariate performed in relation to changes in the DAS28 score or Sharp/van der Heijde score. When the DAS28 was modeled, models including anti-PAD4 and those including anti-CCP antibodies performed similarly, with a QIC of 824.4 and 823.2, respectively. In contrast, when the Sharp/van der Heijde score was modeled, the multivariable model including anti-CCP performed better than the model including anti-PAD4 antibodies (QIC −46,535.1 versus −44,522.4, respectively). However, in contrast to the results from the model containing anti-PAD4 antibodies, baseline anti-

CCP antibodies were associated with more radiographic disease progression (23% versus 7% increase in Sharp/van der Heijde score at 24 weeks [$P = 0.02$], and 26% versus 7% increase at 48 weeks [$P = 0.006$]).

DISCUSSION

This study explored the utility of baseline anti-PAD4 antibodies in predicting future treatment response in RA patients with active disease despite MTX monotherapy. Baseline clinical characteristics associated with anti-PAD4 antibodies in the RACAT cohort were consistent with those in previous studies, including a longer disease duration, less frequent smoking history, association with anti-CCP antibodies, and higher Sharp/van der Heijde scores (6–8,15). Although anti-PAD4 antibody-positive patients had the most radiographic joint damage at baseline, importantly, they had better clinical outcomes following triple DMARD or MTX/etanercept combination therapy than anti-PAD4 antibody-negative patients. This more favorable response was indicated by a greater decrease in disease activity according to the DAS28 and less progression of radiographic joint damage, as measured by the Sharp/van der Heijde score. These data suggest that although patients with anti-PAD4 antibodies in whom MTX monotherapy was unsuccessful have a higher burden of erosive disease at baseline, they respond favorably to treatment escalation therapy, as measured by traditional markers of disease activity.

These results are both surprising and intriguing, given the significant radiographic joint disease burden found in anti-PAD4-positive patients at baseline in this and other cohorts (6–8). In the only published treatment study exploring the predictive value of anti-PAD4 antibodies it was concluded that patients with baseline anti-PAD4 antibodies had persistent disease activity and progressive erosive disease, despite 12 months of treatment with TNF inhibitor therapy (11). Important differences in study design may have

contributed to the discrepant conclusions in that study and our current study. The study by Halvorsen et al was a small, open-label analysis of 40 patients who started TNF inhibitor therapy (i.e., adalimumab, infliximab, or etanercept) as part of routine clinical care. Information on inclusion criteria as well as past and concomitant DMARD use was not provided, and baseline erosive disease or DAS28 was not controlled for in the statistical modeling, due to the small sample size (11). Our larger cohort study provided increased statistical power, focused exclusively on patients who had suboptimal responses to MTX monotherapy, and contained 2 treatment escalation arms, both of which included concomitant MTX therapy, providing a well-characterized patient population for studying the effect of baseline anti-PAD4 antibodies on treatment response. In addition, our use of GEE models for longitudinal data analysis allowed for the estimated change in radiographic joint damage and DAS28 following treatment to be determined at the individual patient level, as a function of baseline anti-PAD4 antibody status.

We previously explored the association of anti-PAD3/4 cross-reactive antibodies with radiographic joint disease progression in 2 observational cohorts of patients with RA. In a study of patients with established disease (9), patients with anti-PAD3/4 antibodies were significantly more likely to experience radiographic joint disease progression compared to anti-PAD antibody-negative patients over a mean follow-up period of 39 months. In a smaller study of patients with early RA (disease duration <2 years), baseline Sharp/van der Heijde score, rather than anti-PAD3/4 antibodies, was associated with erosive disease progression over a 36-month period (10). There are crucial differences between these observational studies and our current RACAT substudy that are worth noting. In contrast to the RACAT cohort, patients in these 2 previous studies received treatment with diverse therapeutics as part of routine clinical care and had a much longer time between radiographic assessments (36 and 39 months versus 6 and 12 months in the RACAT). This raises important questions about the durability of the favorable treatment response observed in anti-PAD4 antibody-positive RACAT patients beyond the 12-month time point, as well as the persistence of subclinical disease that may drive progression over the longer term. In addition, our focus on patients whose disease was not adequately controlled by MTX monotherapy precludes us from determining the effect of baseline anti-PAD4 antibodies on the clinical response to MTX monotherapy alone. Additional double-blind treatment studies, and those with a longer follow-up period, are therefore necessary to determine the generalizability of these findings in other RA patient populations.

Although disease activity improved and radiographic joint damage slowed more significantly in patients with anti-PAD4 antibodies once effective therapy was initiated, the extensive joint damage observed in these patients at baseline suggests a history of inadequate disease control. This could reflect the accumulation of joint damage early in disease prior to diagnosis, a longer disease duration before diagnosis, suboptimal

disease management prior to study enrollment, or an accumulation of occult joint damage in the absence of classic disease activity markers, as has been described in the general RA population (4). Anti-PAD4 antibodies are present in 18% of patients prior to disease diagnosis and are found in 21% of patients with early RA (10,16). This suggests that future treatment studies of early RA cohorts are needed to identify the therapeutic window for this unique patient subset and expedite disease diagnosis. It may be that clinical indicators, other than traditional disease activity measures, are needed to detect and prevent the accumulation of joint damage in patients with anti-PAD4 antibodies. Our finding that patients with anti-PAD4 antibodies have a high burden of joint damage at baseline, but respond favorably to treatment escalation therapy once initiated, highlights the importance of understanding the early events that drive joint damage in this unique patient subset.

ACKNOWLEDGMENT

We would like to thank David Hines (Rheumatic Disease Research Core Center, Johns Hopkins University School of Medicine) for technical support.

AUTHOR CONTRIBUTIONS

All authors were involved in drafting the article or revising it critically for important intellectual content, and all authors approved the final version to be published. Dr. Darrah had full access to all of the data in the study and takes responsibility for the integrity of the data and the accuracy of the data analysis.

Study conception and design. Darrah, Rosen, Mikuls.

Acquisition of data. Darrah, O'Dell, Mikuls.

Analysis and interpretation of data. Darrah, Yu, Cappelli, Mikuls.

REFERENCES

1. Favalli EG, Biggoggero M, Meroni PL. Methotrexate for the treatment of rheumatoid arthritis in the biologic era: still an "anchor" drug? *Autoimmun Rev* 2014;13:1102–8.
2. Singh JA, Furst DE, Bharat A, Curtis JR, Kavanaugh AF, Kremer JM, et al. 2012 update of the 2008 American College of Rheumatology recommendations for the use of disease-modifying antirheumatic drugs and biologic agents in the treatment of rheumatoid arthritis. *Arthritis Care Res (Hoboken)* 2012;64:625–39.
3. O'Dell JR, Mikuls TR, Taylor TH, Ahluwalia V, Brophy M, Warren SR, et al. Therapies for active rheumatoid arthritis after methotrexate failure. *N Engl J Med* 2013;369:307–18.
4. Plant MJ, Williams AL, O'Sullivan MM, Lewis PA, Coles EC, Jessop JD. Relationship between time-integrated C-reactive protein levels and radiologic progression in patients with rheumatoid arthritis. *Arthritis Rheum* 2000;43:1473–7.
5. Pratt AG, Isaacs JD. Seronegative rheumatoid arthritis: pathogenic and therapeutic aspects. *Best Pract Res Clin Rheumatol* 2014;28:651–9.
6. Harris ML, Darrah E, Lam GK, Bartlett SJ, Giles JT, Grant AV, et al. Association of autoimmunity to peptidylarginine deiminase type 4 with genotype and disease severity in rheumatoid arthritis. *Arthritis Rheum* 2008;58:1958–67.

7. Zhao J, Zhao Y, He J, Jia R, Li Z. Prevalence and significance of anti-peptidylarginine deiminase 4 antibodies in rheumatoid arthritis. *J Rheumatol* 2008;35:969–74.
8. Halvorsen EH, Pollmann S, Gilboe IM, van der Heijde D, Landewe R, Odegard S, et al. Serum IgG antibodies to peptidylarginine deiminase 4 in rheumatoid arthritis and associations with disease severity. *Ann Rheum Dis* 2008;67:414–7.
9. Darrah E, Giles JT, Ols ML, Bull HG, Andrade F, Rosen A. Erosive rheumatoid arthritis is associated with antibodies that activate PAD4 by increasing calcium sensitivity. *Sci Transl Med* 2013;5:186ra65.
10. Navarro-Millán I, Darrah E, Westfall AO, Mikuls TR, Reynolds RJ, Danila MI, et al. Association of anti-peptidyl arginine deiminase antibodies with radiographic severity of rheumatoid arthritis in African Americans. *Arthritis Res Ther* 2016;18:241.
11. Halvorsen EH, Haavardsholm EA, Pollmann S, Boonen A, van der Heijde D, Kvien TK, et al. Serum IgG antibodies to peptidylarginine deiminase 4 predict radiographic progression in patients with rheumatoid arthritis treated with tumour necrosis factor- α blocking agents. *Ann Rheum Dis* 2009;68:249–52.
12. Prevoo ML, van 't Hof MA, Kuper HH, van Leeuwen MA, van de Putte LB, van Riel PL. Modified disease activity scores that include twenty-eight-joint counts: development and validation in a prospective longitudinal study of patients with rheumatoid arthritis. *Arthritis Rheum* 1995;38:44–8.
13. Van der Heijde DM, van Riel PL, Gribnau FW, Nuver-Zwart IH, van de Putte LB. Effects of hydroxychloroquine and sulphasalazine on progression of joint damage in rheumatoid arthritis. *Lancet* 1989;1:1036–8.
14. Pan W. Akaike's information criterion in generalized estimating equations. *Biometrics* 2001;57:120–5.
15. Cappelli LC, Konig MF, Gelber AC, Bingham CO III, Darrah E. Smoking is not linked to the development of anti-peptidylarginine deiminase 4 autoantibodies in rheumatoid arthritis. *Arthritis Res Ther* 2018;20:59.
16. Kolfenbach JR, Deane KD, Derber LA, O'Donnell CI, Gilliland WR, Edison JD, et al. Autoimmunity to peptidylarginine deiminase type 4 precedes clinical onset of rheumatoid arthritis. *Arthritis Rheum* 2010;62:2633–9.

Ibudilast Inhibits Chemokine Expression in Rheumatoid Arthritis Synovial Fibroblasts and Exhibits Immunomodulatory Activity in Experimental Arthritis

Felix I. L. Clanchy and Richard O. Williams

Objective. Ibudilast is a well-tolerated, orally available phosphodiesterase 4 (PDE4) inhibitor used to treat asthma and stroke. Since PDE4 inhibition suppresses inflammatory mediator production and cell proliferation in leukocytes, ibudilast may be a valuable therapy for the treatment of inflammatory autoimmune diseases such as rheumatoid arthritis (RA). This study was undertaken to assess the therapeutic potential of ibudilast by measuring its capacity to modulate inflammation in human leukocytes and RA synovial fibroblasts (RASFs) and in experimental arthritis.

Methods. Using standard curve quantitative polymerase chain reaction, the effect of ibudilast on gene expression in activated human leukocytes and RASFs was measured. Ibudilast was used to treat DBA/1 mice with collagen-induced arthritis, and an adoptive transfer model was used to assess its tolerogenic capacity.

Results. Ibudilast inhibited the expression of *TNF*, *IL12A*, and *IL12B* and the secretion of tumor necrosis factor (TNF) and interleukin-12 (IL-12)/23p40 from leukocytes, and reduced the expression of *CCL5* and *CCL3* in activated RASFs. Treatment of experimental arthritis with ibudilast resulted in a reduction in IL-17–producing cells and inhibition of disease progression. When combined with a TNF inhibitor, ibudilast caused marked suppression of active disease. Exposure of leukocytes from type II collagen–immunized DBA/1 mice to ibudilast *in vitro* attenuated their ability to adoptively transfer arthritis to DBA/1J-*Prkdc*^{SCID} mice, providing evidence of an immunomodulatory effect.

Conclusion. Our findings indicate that ibudilast reduces the expression and/or secretion of inflammatory mediators from activated human leukocytes and RASFs, inhibits Th17 cell responses *in vivo*, and improves established arthritis. Given the established safety profile of ibudilast in humans, its clinical evaluation in RA, either alone or in combination with a TNF inhibitor, should be considered.

INTRODUCTION

Rheumatoid arthritis (RA) is a disease that primarily affects the joints and is in many cases amenable to biologic therapies that target inflammatory mediators, particularly tumor necrosis factor (TNF), but also interleukin-1 β (IL-1 β) or IL-6 (1). However, high cost, the need for repeated parenteral administration, and a significant nonresponder rate are major disadvantages of these therapies and there continues to be an unmet need for new orally active drugs for RA.

Phosphodiesterase 4 (PDE4) is an attractive therapeutic target in inflammatory disease. Of the 11 subtypes of PDE, PDE4 is most commonly expressed in leukocytes (2), and its inhibition leads to an increase in intracellular cAMP which promotes signaling via the protein kinase A pathway, resulting in the suppres-

sion of key elements of the immune response (3). Several PDE4 inhibitors have recently been demonstrated to have therapeutic efficacy without the gastrointestinal side effects that are associated with older PDE4 inhibitors such as rolipram. For example, roflumilast is effective in severe chronic obstructive pulmonary disease and chronic bronchitis (4), and apremilast has been approved for the treatment of psoriatic arthritis (5).

Ibudilast (2-methyl-1-[2-(propan-2-yl)pyrazolo[1,5-a]pyridin-3-yl]propan-1-one) is a PDE4 inhibitor but also inhibits other PDE subtypes to varying degrees (6). It has been suggested that ibudilast can also block the actions of macrophage migration inhibitory factor by inhibiting the catalytic activity of its tautomerase domain (7). Ibudilast has recently been tested as a potential treatment for multiple sclerosis (MS) (8) and neuropathic pain (9) but is better known as a treatment for stroke and asthma (10). Ibudilast is an

Felix I. L. Clanchy, PhD, LLB, Richard O. Williams, PhD: Kennedy Institute of Rheumatology, University of Oxford, Oxford, UK.

Drs. Clanchy and Williams have submitted a patent application for the use of ibudilast in rheumatoid arthritis for therapeutic benefit.

Address correspondence to Felix I. L. Clanchy, PhD, LLB, Kennedy Institute of Rheumatology, University of Oxford, Roosevelt Drive, Oxford OX3 7FY, UK. E-mail: felix.clanchy@kennedy.ox.ac.uk.

Submitted for publication November 2, 2017; accepted in revised form November 20, 2018.

orally available and well-tolerated drug with an excellent safety profile that has been used for more than 20 years, particularly in Japan. Since ibudilast is known to suppress TNF production (11), an investigation of its antiarthritic potential was undertaken.

MATERIALS AND METHODS

Animals and reagents. Human synovial explants were obtained from RA patients and cultured for 2–3 passages to deplete leukocytes, leaving only RA synovial fibroblasts (RASFs). Peripheral blood mononuclear cells (PBMCs) were obtained from apheresis cones from the NHS Blood Service. DBA/1 mice were acquired from Harlan UK. DBA/1J-*Prkdc*^{SCID} mice were bred in house. TaqMan probes were purchased from Life Technologies. All mice were housed in pathogen-free conditions with food and water available ad libitum. All procedures were undertaken in accordance with project and personal licenses issued by the UK Home Office.

The enzyme-linked immunosorbent assay (ELISA) antibodies TNF capture antibody (MAb1), TNF detection antibody (MAb11), IL-6 capture antibody (MQ2-13A5), IL-6 detection antibody (MQ2-39C3), IL-10 capture antibody (JES3-19F1), IL-10 detection antibody (JES3-12G8), anti-mouse IgG1 (X56), and anti-mouse IgG2a (R19-15) were obtained from Becton Dickinson and used according to the manufacturer's instructions. Human IL-12/23p40 level was measured using a Legend Max ELISA kit (BioLegend). Serum cytokine levels were measured using a Th1/Th2 9-plex assay ultra-sensitive kit (Meso Scale Discovery). Fluorescence-activated cell sorting antibodies were as follows: fluorescein isothiocyanate (FITC)-conjugated CD4 (GK1.5; Becton Dickinson), phycoerythrin (PE)-conjugated CD4 (GK1.5; eBioscience), allophycocyanin-Cy7-conjugated CD8 (53-6.7; Becton Dickinson), eFluor 450-conjugated FoxP3 (FJK-16s; eBioscience), Alexa Fluor 647-conjugated interferon- γ (IFN γ) (XMG1.2; Becton Dickinson), PE-conjugated IL-17 (TC11-18H10; Becton Dickinson), and FITC-conjugated bromodeoxyuridine (BrdU) (B44; Becton Dickinson). RASFs were cultured in DMEM supplemented with 5% FBS/1% penicillin/streptomycin. PBMCs were cultured in RPMI supplemented with 10% FBS/1% penicillin/streptomycin. Ibudilast was obtained from TCI Europe.

RASF cultures. Human RASFs were expanded over 3 passages. Each experiment was performed in duplicate wells of 6-well plates. The cells were pretreated for 1 hour with ibudilast or vehicle or left untreated, and then stimulated with lipopolysaccharide (LPS; 10 ng/ml) (Sigma) for 2, 4, or 8 hours.

PBMC cultures. For gene expression studies, PBMCs were cultured at 2×10^7 cells/2 ml medium/well in a 6-well plate and pretreated for 1 hour with ibudilast (100 μ M) or vehicle (DMSO; final concentration 0.025%) or left untreated. Cells were then stimulated with LPS (10 ng/ml) for 4 hours and then

harvested. To determine the effect of ibudilast on secreted cytokines, PBMCs were pretreated with differing concentrations of ibudilast or vehicle (DMSO; 0.025% equivalent to 100 μ M ibudilast) or left untreated. Cells were then stimulated with LPS (10 ng/ml) for 18 hours, and medium was then harvested. To demonstrate the effect of ibudilast on anti-CD3-stimulated PBMCs, cells were treated with differing concentrations of ibudilast for 72 hours. The cells were pulsed for the final 18 hours with an equimolar concentration of BrdU and cytidine to give a final concentration of 50 μ M.

Collagen-induced arthritis (CIA). Briefly, mice were injected subcutaneously with bovine type II collagen (200 μ g) in Freund's complete adjuvant (CFA) at the base of the tail, as previously described (12). At disease onset mice were treated daily with an intraperitoneal (IP) injection of ibudilast (10 mg/kg) (11) or vehicle alone (10% PEG 200 in phosphate buffered saline [PBS]); etanercept (3 mg/kg) was injected IP every other day (13). Disease activity in each paw was scored on a scale of 0–2, where 0 = normal/unaffected, 1 = moderate swelling/erythema, and 2 = severe swelling. The maximum possible score was 8. The thickness of all paws of the affected mice was also measured every day with calipers. On day 10 after disease onset, the mice were euthanized, paws were removed for histologic assessment, and blood was obtained via cardiac puncture for preparation of serum. Mouse joints were processed and assessed for histologic severity as previously described (14).

Adoptive transfer model. The tolerogenic capacity of ibudilast was evaluated using a modification of an adoptive transfer model described previously (15). Briefly, CIA was induced in 10 DBA/1 mice, and 10 days later cells from the spleens and lymph nodes were harvested and combined. The cells were cultured for 18 hours in RPMI supplemented with 10% FBS/1% penicillin/streptomycin containing ibudilast (100 μ M) or vehicle (DMSO 0.025%). The cells were then harvested, washed with PBS, and injected IP (10^7 cells/mouse) into DBA/1 mice carrying the SCID mutation (DBA/1J-*Prkdc*^{SCID}). Arthritis was induced by coadministration of 100 μ g of bovine type II collagen. The experimental period began on the day that the first mouse displayed clinical signs of arthritis and ended 10 days later, at which point all animals were euthanized. Paws were collected for histologic analysis and blood was obtained for measurement of serum murine Ig.

Pre-onset T cell responses. DBA/1 mice were immunized with type II collagen in CFA 10 days before the beginning of treatment with ibudilast (10 mg/kg) or vehicle alone (10% PEG200 in PBS). Mice were treated daily for 10 days. Mouse spleens and inguinal lymph nodes were then removed for T cell subset analyses. The mice were injected IP with BrdU (1 mg/mouse in 100 μ l of PBS) 4 hours prior to harvest for assessment of proliferation.

Flow cytometric analysis. Mouse spleens and inguinal lymph nodes were processed by passing through a 70- μ cell strainer. Splenocytes were washed and then resuspended in red cell lysis buffer to remove erythrocytes. After washing, lymph node cells and splenocytes were counted and cultured. Intracellular cytokines were detected after stimulation with 20 ng/ml 12-O-tetradecanoylphorbol-13-acetate and 1 μ M ionomy-

cin in the presence of 12.5 μ g/ml brefeldin A. After 4 hours the cells were washed, stained with extracellular surface marker antibodies (CD4 and CD8) for 30 minutes on ice in the dark, and then fixed and permeabilized with a FoxP3 staining buffer kit (eBioscience). Intracellular cytokine staining for FoxP3, IFN γ , and IL-17 was performed. Cells were then washed and analyzed using a FACSCanto II flow cytometer. BrdU-pulsed cell fixation,

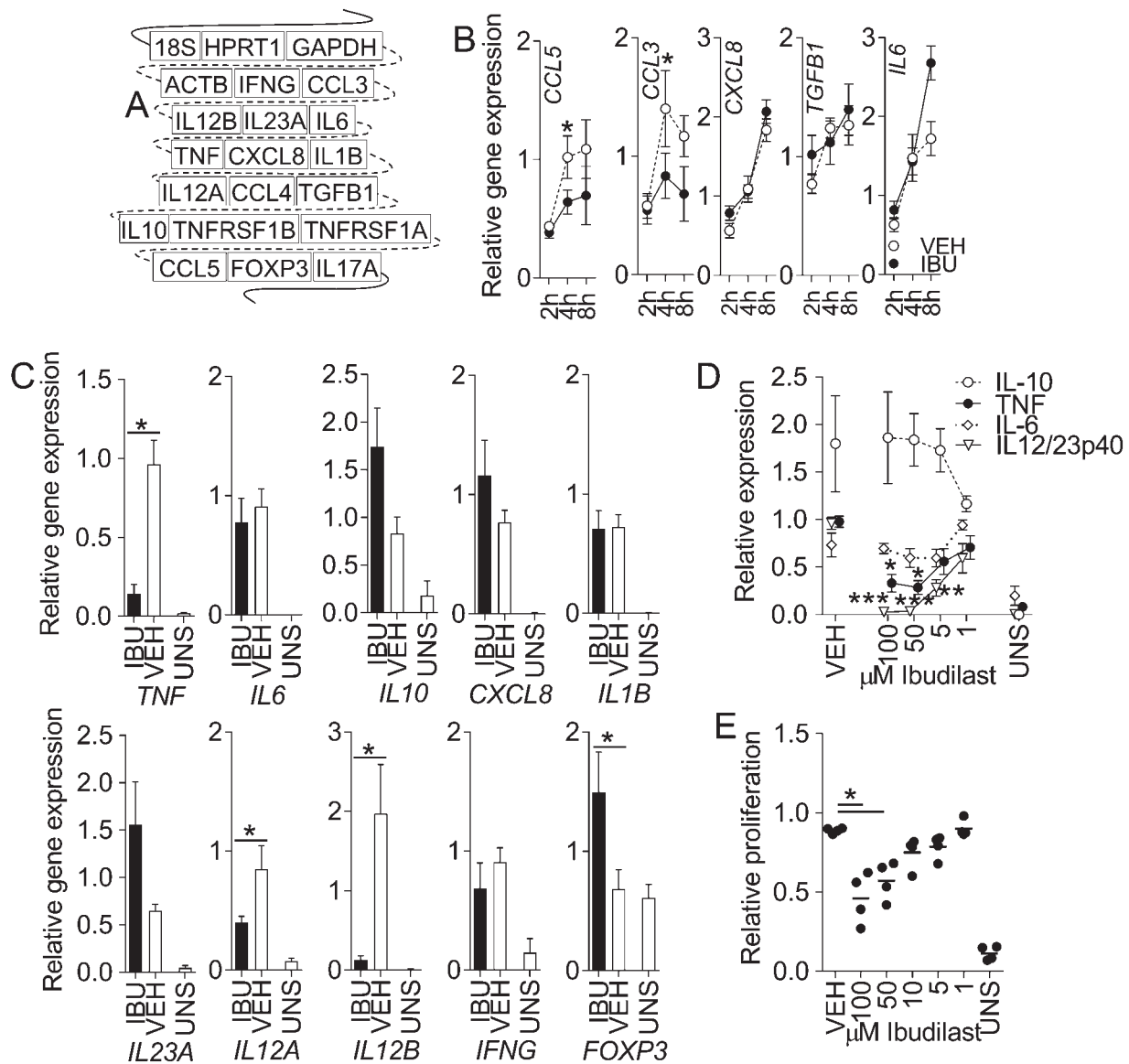


Figure 1. Modulation of the expression of inflammatory mediators in rheumatoid arthritis synovial fibroblasts (RASFs) and peripheral blood mononuclear cells (PBMCs) by ibudilast (IBU). **A**, Map of the linearized quantitative polymerase chain reaction standard. **B**, Expression of the indicated genes in vehicle (VEH)-treated and ibudilast-treated RASFs in response to lipopolysaccharide (LPS). * = $P < 0.05$ versus ibudilast-treated cells, by analysis of variance (ANOVA). **C**, Expression of the indicated genes in ibudilast-treated, vehicle-treated, and unstimulated (UNS) PBMCs in response to LPS. * = $P < 0.05$ by Student's *t*-test. **D**, Expression of interleukin-10 (IL-10), tumor necrosis factor (TNF), IL-6, and IL-12/23p40 proteins in PBMCs pretreated with differing concentrations of ibudilast (0–100 μ M) for 1 hour and then stimulated with LPS, as measured by enzyme-linked immunosorbent assay. * = $P < 0.05$; ** = $P < 0.01$; *** = $P < 0.001$ versus vehicle-treated cells, by ANOVA. **E**, Proliferation in PBMCs left unstimulated or stimulated with anti-CD3 and treated with vehicle or differing concentrations of ibudilast (0–100 μ M). * = $P < 0.05$ by ANOVA. Values in **B–D** are the mean \pm SEM expressed relative to stimulated cells not treated with ibudilast or vehicle ($n = 3$ donors in **B**, 7 donors in **C**, and 6 donors in **D**). In **E**, symbols represent individual samples; horizontal lines show the mean ($n = 4$ donors).

permeabilization, and intracellular staining were performed as previously described (16).

Gene expression. Messenger RNA was extracted from RASFs and PBMCs using RNeasy RNA extraction columns (Qiagen) and converted to complementary DNA (High-Capacity Reverse Transcription kit; Applied Biosystems). TaqMan gene expression assays were performed using standard curve quantitative polymerase chain reaction (qPCR). Standard curves were created using a linearized plasmid containing all sequences detected by TaqMan probes, and data were calibrated with *GAPDH*.

Antibody responses. Serum levels of anti-type II bovine collagen IgG1 and IgG2a were measured as previously described (17). All samples were expressed relative to an internal titrated standard composed of pooled serum from vehicle-treated mice.

Statistical analysis. Comparisons between groups were conducted using analysis of variance, *t*-tests, Fisher's exact test, and Pearson's correlation coefficient, as indicated. Data were analyzed using GraphPad Prism software.

RESULTS

Inhibition of human RASF chemokine expression by ibudilast. We first set out to assess the effect of ibudilast on RASF expression of key inflammatory mediators. In order to conveniently measure gene expression with TaqMan probes using the standard curve method, the relevant sequences were cloned and concatenated into one plasmid, which was linearized by restriction enzyme digestion (Figure 1A). RASFs were stimulated with LPS for 2, 4, or 8 hours after being left untreated or pretreated for 1 hour with ibudilast or vehicle. There was decreased expression of 2 key chemokines, *CCL5* and *CCL3*, in the presence of ibudilast compared to vehicle but no statistically significant difference in *CXCL8*, *TGFB1*, or *IL6* expression (Figure 1B).

Inhibition of human PBMC expression of TNF and IL-12/23 p40 by ibudilast. Human PBMCs were left untreated or pretreated with ibudilast or vehicle for 1 hour and then stimulated with LPS for 4 hours. The expression of inflammatory mediators was measured by standard curve qPCR (Figure 1C). *TNF*, *IL12A*, and *IL12B* levels were significantly reduced by ibudilast treatment. However, levels of *IL6*, *CXCL8*, and *IL1B* were not significantly different compared to untreated cells. *IL10* expression was moderately, but not significantly, increased by ibudilast treatment ($P = 0.11$ by Student's *t*-test). A similar difference was observed with *IL23A*, although the effect of this difference would be comparatively minor since the other component of the IL-23 heterodimer (*IL12B*) was significantly reduced, and IL-10 is a homodimer. Interestingly, *FOXP3* expression was significantly increased by ibudilast treatment.

To determine the effect of ibudilast on cytokine secretion, PBMCs were pretreated with differing concentrations of ibudilast (0–100 μM) for 1 hour and then stimulated with LPS for 18 hours. Medium was collected, and the concentration of cytokines was determined by ELISA (Figure 1D). The most remarkable finding to emerge was that IL-12/23p40 secretion was potently suppressed by ibudilast. TNF levels were also significantly reduced at concentrations of 100 μM and 50 μM . IL-6 levels were not significantly modulated by ibudilast concentration, and IL-10 expression was variable but tended to rise with increasing doses of ibudilast. Ibudilast also significantly inhibited proliferation by anti-CD3–stimulated PBMCs at concentrations of 50 μM and 100 μM (Figure 1E).

Inhibition of Th17 cell responses in vivo by ibudilast. Since ibudilast inhibited the expression of IL-12/23 p40 and other inflammatory mediators in vitro, we hypothesized that it would influence T helper cell subset differentiation in vivo. To test this hypothesis, mice were immunized with type II collagen and, beginning 10 days after immunization, injected daily with ibudilast or vehicle. After 10 days of treatment, the numbers of CD4+ and CD8+ lymphocytes in the mouse spleen and lymph nodes were determined. The mice were injected with BrdU 4 hours prior to harvest to measure the degree of in vivo proliferation.

Numbers of CD4+IL-17+ (Th17) and CD8+IL-17+ (Tc17) lymph node cells were significantly reduced in mice treated with ibudilast, but the trend toward reduced numbers of CD4+IFN γ + and CD8+IFN γ + cells in ibudilast-treated mice did not reach statistical significance. There was no significant difference in FoxP3+ cells between ibudilast-treated mice and control mice (data not shown). Lymph nodes from ibudilast-treated mice had fewer cells, and across the subsets measured there were consequently fewer cells compared to vehicle-treated mice (Figure 2A). There was no significant difference in T cell proliferation, as judged by the prevalence of CD4+ and CD8+ cells entering the S phase, in either the spleen or lymph nodes (Figure 2B).

Tolerogenic capacity of ibudilast. The effect of transient exposure of leukocytes to ibudilast and subsequently on experimental arthritis was determined using a SCID adoptive transfer model. DBA/1 mice were immunized with bovine type II collagen in CFA, and 10 days later lymph node and spleen cells were harvested and processed to a single-cell suspension. After 18 hours of culture in medium containing ibudilast or vehicle, the cells were injected IP into DBA/1J-*Prkdc*^{SCID} mice. The incidence of disease was reduced and delayed in animals receiving ibudilast-treated cells compared to those receiving control cells (Figure 3A). Similarly, the average number of affected paws was greater in vehicle-treated mice (Figure 3B), and the clinical score was lower in mice receiving ibudilast-treated cells compared to those receiving control cells (Figure 3C).

The histologic score was determined in the affected and unaffected paws of all mice (Figure 3D); there were significantly

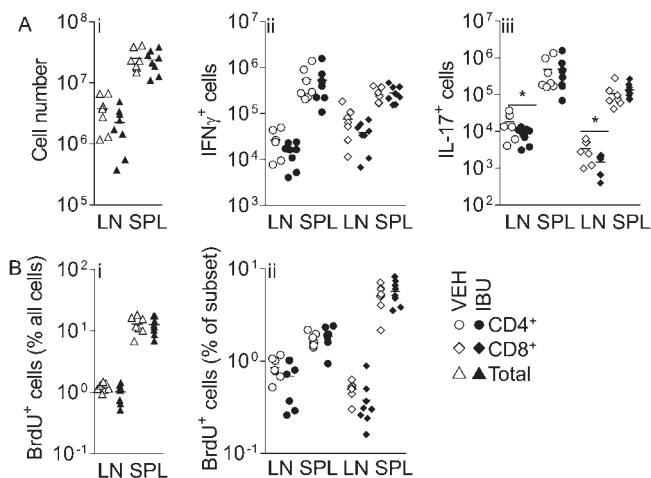


Figure 2. Reduction in the number of Th17 cells in mice treated with ibudilast (IBU) after the induction but before the onset of arthritis. **A**, Total number of CD4⁺ and CD8⁺ cells (i), number of interferon- γ (IFN γ)⁺ CD4⁺ and CD8⁺ cells (ii), and number of interleukin-17 (IL-17)⁺ CD4⁺ and CD8⁺ cells (iii) in the lymph nodes (LNs) and spleen (SPL) of mice treated with vehicle (VEH) or ibudilast after the induction but before the onset of arthritis. **B**, In vivo proliferation of all cells (i) and CD4⁺ cells and CD8⁺ cells (ii) from the lymph nodes and spleen of mice treated with vehicle or ibudilast after the induction but before the onset of arthritis. Symbols represent individual mice (n = 7–8 per group); horizontal lines show the mean. * = $P < 0.05$ by Student's t -test.

more disease-affected paws in mice receiving vehicle-treated cells (Figure 3D). The histologic difference between affected and unaffected paws was most apparent in mice receiving ibudilast-treated cells (Figure 3D). There was a significant positive correlation between the clinical and histologic scores for the DBA/1J-*Prkdc*^{SCID}-transfer mice (data not shown) (Pearson's correlation coefficient $r = 0.3642$, $P = 0.0058$; n = 56 paws). Serum obtained from DBA/1J-*Prkdc*^{SCID}-transfer mice was assayed by dot-blot for the presence of murine Ig, which was found in higher levels than the extremely low levels found in serum from normal DBA/1J-*Prkdc*^{SCID} mice (data not shown). We concluded that ibudilast has tolerogenic potential.

Attenuation of experimental arthritis by ibudilast.

In view of the inhibitory effect of ibudilast on the expression of proinflammatory mediators, we tested its effect in CIA. To ensure clinical relevance, a protocol was used in which mice were treated after the onset of clinical arthritis. The effect of ibudilast on mice with CIA was evaluated as monotherapy and in combination with etanercept. Ibudilast alone significantly reduced the total clinical score compared to the vehicle control (Figure 4A). There was also a significant reduction in the number of paws affected in ibudilast-treated mice (Figure 4B) and reduced paw swelling in ibudilast-treated mice (Figures 4C and D) compared to control-treated mice.

Consistent with the reduced number of paws affected in mice treated with ibudilast (Figure 4B), there was a significant delay in

the progression of disease from the first to subsequent paws (Figure 5A). When mice were treated with ibudilast, there was an average delay of 4 days prior to the disease becoming clinically apparent in the second paw, compared to 2 days for vehicle-treated mice.

The relative amount of IgG1 and IgG2a anticollagen antibodies did not significantly differ in serum obtained on day 10. However, the ratio of IgG2a to IgG1 was higher in vehicle-treated mice (Figure 5B). There was a slight but nonsignificant decrease in the histologic score of the first affected paw in ibudilast-treated mice (Figure 5C). The levels of TNF and IL-12p70 were reduced in the serum in ibudilast-treated mice, and there was strong trend toward reduced IL-1 β levels in ibudilast-treated mice (Figure 5D). In combination with etanercept, ibudilast produced profound suppression of arthritis (Figure 4), and it was concluded that there was an additive effect between the 2 drugs at the doses used.

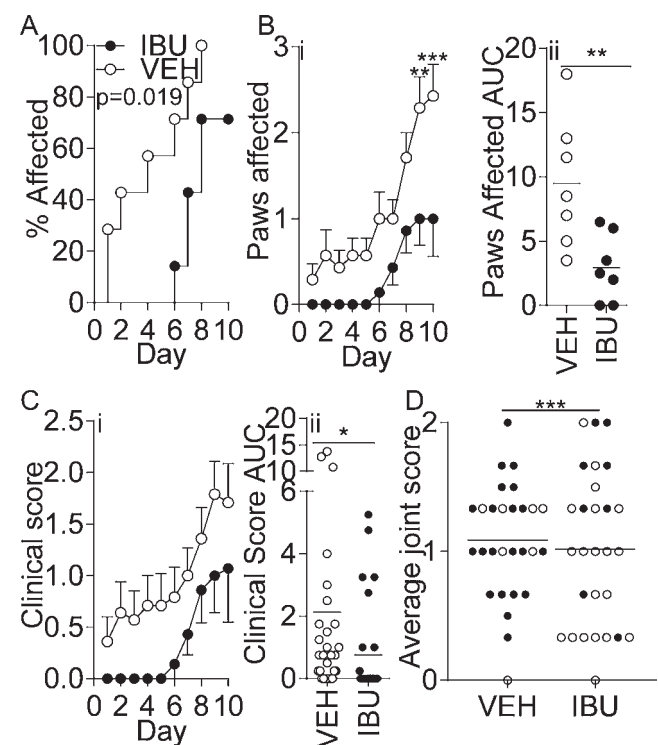


Figure 3. The action of ibudilast (IBU) on leukocytes reduces adoptive transfer arthritis. **A**, Survival curve of DBA/1J-*Prkdc*^{SCID} transfer for ibudilast-treated and vehicle (VEH)-treated mice ($P = 0.019$ by log rank Mantel-Cox test). **B**, Number of paws affected (i) and area under the curve (AUC) (ii) for each mouse. ** = $P < 0.01$; *** = $P < 0.001$, by analysis of variance in i and by Student's t -test in ii. **C**, Clinical score (i) and area under the curve (AUC) (ii) for each mouse. * = $P < 0.05$ by Student's t -test. **D**, Histologic scores of the paws of vehicle-treated and ibudilast-treated mice. Solid circles represent affected paws (clinical score >0); open circles represent unaffected paws (clinical score 0). *** = $P = 0.001$ by Fisher's exact test. Values in **Bi** and **Ci** are the mean \pm SEM. In **Bii**, and **Cii**, symbols represent individual mice; horizontal lines show the mean. In **D**, symbols represent individual mouse paws; horizontal lines show the mean.

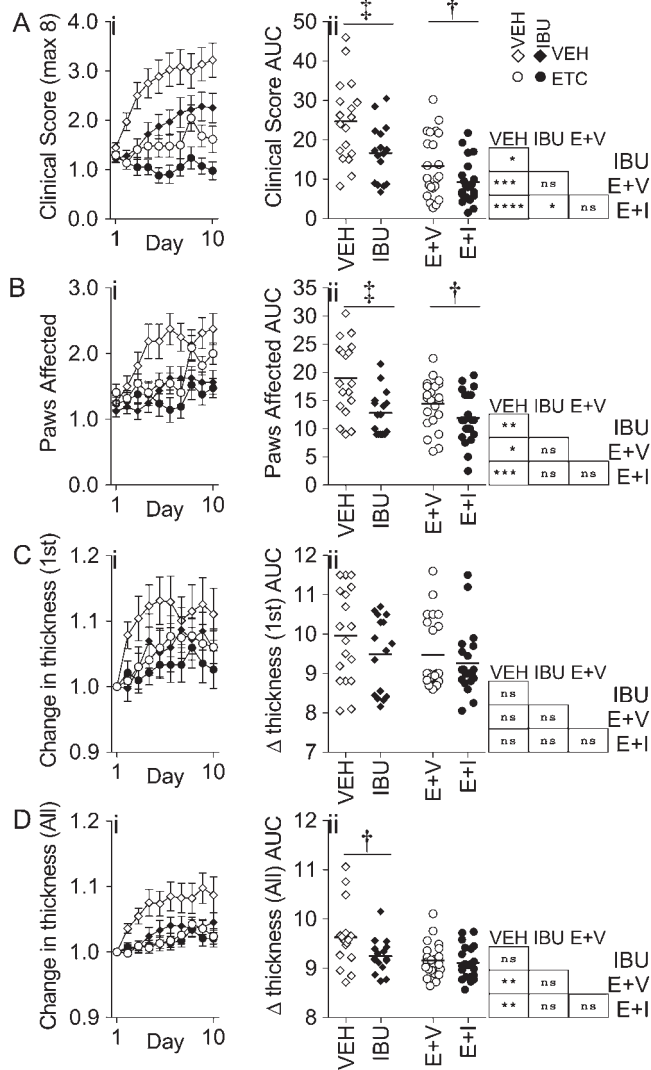


Figure 4. Attenuation of experimental arthritis by ibudilast (IBU) in combination with etanercept (ETC). The clinical score (A), number of paws affected (B), change in thickness of the first paw affected (C), and change in thickness of all paws (D) were determined in mice treated with vehicle (VEH) alone, mice treated with ibudilast alone, mice treated with etanercept and vehicle (E+V), and mice treated with etanercept and ibudilast (E+I). Values in the left panels are the mean \pm SEM. Right panels show the area under the curve (AUC). In the right panels, symbols represent individual mice; horizontal lines show the mean. Data were pooled from 3 experiments ($n = 16$ or more mice per group). * = $P < 0.05$; ** = $P < 0.01$; *** = $P < 0.005$; **** = $P < 0.001$, by analysis of variance; † = $P < 0.05$; ‡ = $P < 0.01$, by Student's *t*-test.

Reduction in the TNF blockade-induced increase in Th17 cells by ibudilast. Several studies have reported a perturbation in the number of IL-17-producing cells in the blood of RA patients, and in the lymph nodes of arthritic mice, treated with TNF-blocking therapies (18,19). The increase in Th17 cells is associated with higher levels of circulating IL-23 (18). In etanercept-treated mice that were coadministered ibudilast or

vehicle, the proportions of relevant T cell subsets were measured (Figure 6). There was a statistically significant decrease in the proportion of Th17 cells in the lymph nodes and spleens of mice treated with etanercept and ibudilast compared to those treated with etanercept and vehicle (Figure 6B). When the total numbers of each T cell subset were calculated for each tissue, the ratio of Th1 and Treg cells to Th17 cells was greater in mice receiving ibudilast. The ratio of Th1 cells to Th17 cells in ibudilast-treated mice was significantly greater in the lymph nodes, and the ratio of Treg cells to Th17 cells was significantly greater in the spleen and the blood, with a similar trend which did not reach statistical significance ($P = 0.093$) in the lymph nodes. Although the differences in T cell subsets between treatment groups were moderate and observed at one point in time, their association

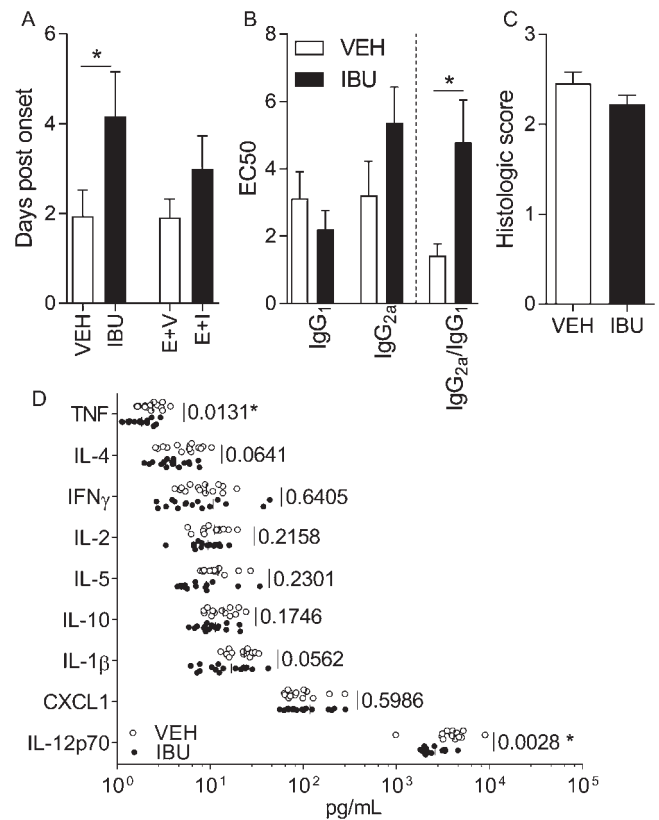


Figure 5. Inhibition of disease progression in experimental arthritis by ibudilast (IBU). **A**, Number of days after disease onset the second paw became clinically affected in arthritic mice treated with vehicle (VEH) alone, arthritic mice treated with ibudilast alone, arthritic mice treated with etanercept and vehicle (E+V), and arthritic mice treated with etanercept and ibudilast (E+I). * = $P < 0.05$ by Student's *t*-test. **B**, Serum levels of anti-type II collagen IgG1 and IgG2a antibodies (50% maximum response concentration [EC₅₀] of the serum titration curve) on day 10 after onset and the ratio of IgG2a to IgG1. * = $P < 0.05$ by Student's *t*-test. **C**, Total histologic score for the first affected paw in vehicle-treated mice and ibudilast-treated mice. In **A-C**, bars show the mean \pm SEM. **D**, Serum cytokine concentrations in arthritic mice 10 days after onset. Values are *P* values determined by Student's *t*-test. Asterisk indicates significance ($P < 0.05$). TNF = tumor necrosis factor; IL-4 = interleukin-4; IFN γ = interferon- γ .

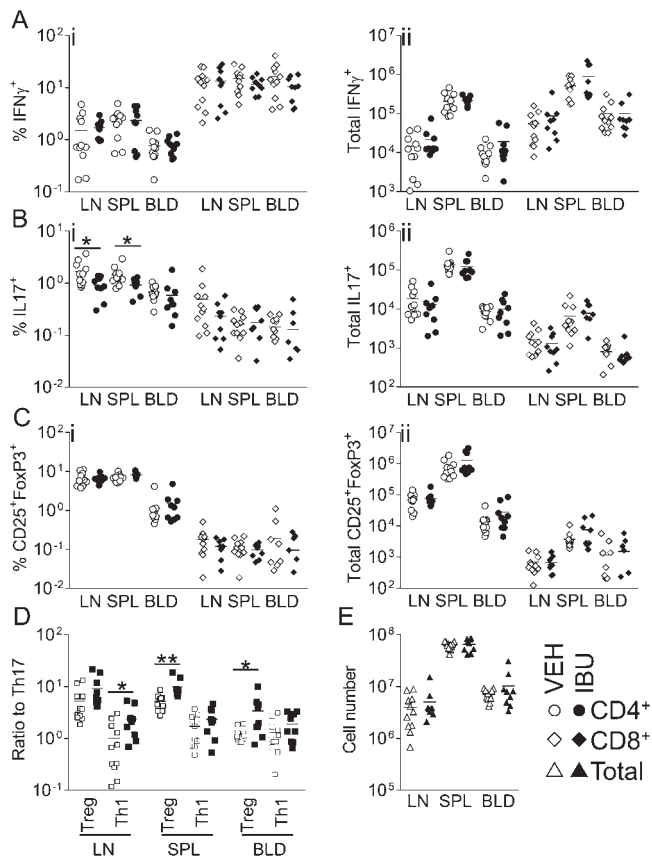


Figure 6. Ibudilast (IBU) reduces the tumor necrosis factor blockade-induced increase in Th17 cells. The prevalence of Th cell subsets was measured after arthritis onset in the draining lymph nodes (LNs), spleen (SPL), and erythrocyte-lysed blood (BLD) of mice treated with etanercept and vehicle (VEH) and mice treated with etanercept and ibudilast. **A–C**, Interferon- γ (IFN γ)⁺ (**A**) interleukin-17 (IL-17)⁺ (**B**), and CD25⁺FoxP3⁺ (**C**) subsets of CD4⁺ and CD8⁺ cells. Left panels show the proportion of CD4 or CD8 cells. Right panels show the total number of the indicated cells harvested from each tissue. * = $P < 0.05$ by Student's t -test. **D**, Ratio of total CD4+IL17⁺ (Th17) cells to CD4+IFN γ ⁺ (Th1) cells or CD4+CD25⁺FoxP3⁺ (Treg) cells. * = $P < 0.05$; ** = $P < 0.005$, by Student's t -test. **E**, Total number of cells harvested from each tissue. Symbols represent individual mice; horizontal lines show the mean.

with the reduction in disease activity is potentially indicative of a mechanistic role.

DISCUSSION

This study has confirmed the therapeutic potential for RA of ibudilast, a safe and well-tolerated drug used for over 20 years for the treatment of asthma and stroke. First, we demonstrated that ibudilast inhibits expression of 2 major chemokines, *CCL5* and *CCL3*, by RASFs. Next, we showed that ibudilast inhibits the expression of IL-12/23 p40 and TNF and also reduces proliferation in cultures of human PBMCs. Last, we demonstrated the therapeutic potential of ibudilast in experimental arthritis.

IL-12 and IL-23 are important for the differentiation and survival of Th1 and Th17 cells, respectively, and the inhibitory effect of ibudilast on IL-12/23 p40 expression led us to test its immunomodulatory potential in vivo. Ibudilast was found to reduce the numbers of Th17 and Tc17 cells in draining lymph nodes, even when given to mice 10 days after immunization with type II collagen in CFA. This is a particularly notable finding, given the potent Th17-inducing action of CFA. Ibudilast also caused a significant reduction in the numbers of lymph node cells, but this reduction in cell number does not appear to be solely due to differences in proliferation, since in vivo BrdU incorporation was similar between the ibudilast-treated and vehicle-treated groups.

The reduction in the number of Th17 cells, which are associated with inflammation and tissue injury in RA, by ibudilast would be predicted to lead to a reduction in disease. We therefore assessed the effect of ibudilast in established CIA. We report for the first time that it significantly reduces the severity of disease principally by attenuating the progression of disease rather than by affecting ongoing inflammatory lesions. Thus, ibudilast treatment reduced the overall disease and attenuated the rate of disease progression. There was little or no difference in the swelling or histologic score of the first affected paw. The relative reduction in swelling in all paws (Figure 4D) may be in part due to the known effects of PDE4 inhibition on edema (20,21).

There was, however, a significant difference in the time taken for subsequent paws to become affected. In addition, combination therapy with etanercept was highly efficacious. The ratio of the titers of IgG2a to IgG1 anticollagen antibodies was lower in ibudilast-treated mice, indicating relatively lower levels of collagen-specific IgG2a. This reduction is indicative of a switch toward a more predominant Th2 response, which is an effect that has previously been observed with ibudilast in a murine model of MS (8).

Previous work by our group has shown that one of the unexpected consequences of the use of TNF inhibitors is an increase in the number of Th17 cells, a finding that has been confirmed in at least 4 independent studies (18,22–24). We have also shown that at least one of the mechanisms involved in the expansion of Th17 cells is increased expression of IL-12/23 p40 expression after anti-TNF treatment. Hence, it is anticipated that ibudilast would act synergistically with a TNF inhibitor and this would need to be demonstrated over several doses. In this study, we showed a cumulative effect between ibudilast and etanercept, but it must be emphasized that etanercept alone is highly effective in CIA and was administered at an optimal dose. Therefore, we were unlikely to observe synergy under these conditions. We also observed that ibudilast reduced the Th17-inducing effect of etanercept, as there was a reduction in the proportion of Th17 cells and a higher ratio of Th1 and Treg cells to Th17 cells in mice treated with the combination of etanercept and ibudilast.

This study also demonstrated, using an adoptive transfer model, that leukocytes from collagen-immunized mice treated

transiently with ibudilast had a reduced capacity to transfer disease to naive DBA/1J-*Prkdc^{SCID}* mice, compared to vehicle-treated leukocytes. The treatment of leukocytes with ibudilast significantly delayed the onset of clinical symptoms, and there was a significant difference in the number of paws affected. The histologic score is a composite of scores for infiltration, bone erosion, and loss of architecture, and while there was a good correlation between the clinical score and the histologic score, there was an ~50% reduction in clinical score compared to mice with classic CIA, which resulted in less significant differences between ibudilast-treated mice and vehicle-treated mice at the histologic level. Nevertheless, this finding clearly provides further evidence of an immunomodulatory effect of ibudilast, which raises the question of whether the drug has the capacity to induce long-term disease remission, perhaps in combination with a TNF inhibitor.

PDE4 inhibitors have long been considered potential anti-inflammatory and immunomodulatory drugs, but their clinical development has been hampered largely due to side effects, particularly emesis. Ibudilast is a well-tolerated, orally available drug with a long period of safe use that generally lacks side effects such as nausea. Recently, our group demonstrated the antiarthritic potential of another PDE4 inhibitor, apremilast (14), which has subsequently been approved for use in psoriatic arthritis as well as psoriasis. Although we have not tested apremilast alongside ibudilast in CIA, our data show that both drugs have similar levels of efficacy. The potential for ibudilast to treat other inflammatory diseases has also been demonstrated. An observation that ibudilast reduced microglial gene expression of IL-12B (25) has culminated in a recent phase II clinical trial for progressive MS (26). In the latter study, patients who were treated with ibudilast at up to 100 mg/day for 96 days experienced slower rates of brain atrophy compared to those treated with placebo, but had more gastrointestinal side effects compared to the control group (26). We have provided data on the efficacy of ibudilast as a potential treatment for RA based on its capacity to inhibit *CCL5*, *CCL3*, and TNF and reduce the numbers of Th17 cells, all of which are known to contribute to the pathogenesis of RA.

ACKNOWLEDGMENTS

We would like to acknowledge animal house staff for the general care of animals, Dany Perocheau for maintenance of DBA/1J-*Prkdc^{SCID}* mice, and Dr. Lynn Williams for assistance with RASFs. We thank Geethanjali Bahal and Angela Seedhar for performing histologic analysis.

AUTHOR CONTRIBUTIONS

All authors were involved in drafting the article or revising it critically for important intellectual content, and all authors approved the final version to be published. Dr. Clanchy had full access to all of the data in the study and takes responsibility for the integrity of the data and the accuracy of the data analysis.

Study conception and design. Clanchy, Williams.

Acquisition of data. Clanchy.



Analysis and interpretation of data. Clanchy.

REFERENCES

1. Feldmann M, Maini RN. TNF defined as a therapeutic target for rheumatoid arthritis and other autoimmune diseases. *Nat Med* 2003;9:1245–50.
2. Souness JE, Aldous D, Sargent S. Immunosuppressive and anti-inflammatory effects of cyclic AMP phosphodiesterase (PDE) type 4 inhibitors. *Immunopharmacology* 2000;47:127–62.
3. Castro A, Jerez MJ, Gil C, Martinez A. Cyclic nucleotide phosphodiesterases and their role in immunomodulatory responses: advances in the development of specific phosphodiesterase inhibitors. *Med Res Rev* 2005;25:229–44.
4. Milara J, Lluch J, Almudever P, Freire J, Xiaozhong Q, Cortijo J. Roflumilast N-oxide reverses corticosteroid resistance in neutrophils from patients with chronic obstructive pulmonary disease. *J Allergy Clin Immunol* 2014;134:314–22.
5. Poole RM, Ballantyne AD. Apremilast: first global approval. *Drugs* 2014;74:825–37.
6. Gibson LC, Hastings SF, McPhee I, Clayton RA, Darroch CE, Mackenzie A, et al. The inhibitory profile of ibudilast against the human phosphodiesterase enzyme family. *Eur J Pharmacol* 2006;538:39–42.
7. Cho Y, Crichlow GV, Vermeire JJ, Leng L, Du X, Hodsdon ME, et al. Allosteric inhibition of macrophage migration inhibitory factor revealed by ibudilast. *Proc Natl Acad Sci U S A* 2010;107:11313–8.
8. Feng J, Misu T, Fujihara K, Sakoda S, Nakatsuji Y, Fukaura H, et al. Ibudilast, a nonselective phosphodiesterase inhibitor, regulates Th1/Th2 balance and NKT cell subset in multiple sclerosis. *Mult Scler* 2004;10:494–8.
9. Ledeboer A, Hutchinson MR, Watkins LR, Johnson KW. Ibudilast (AV-411): a new class therapeutic candidate for neuropathic pain and opioid withdrawal syndromes. *Expert Opin Investig Drugs* 2007;16:935–50.
10. Rolan P, Hutchinson M, Johnson K. Ibudilast: a review of its pharmacology, efficacy and safety in respiratory and neurological disease. *Expert Opin Pharmacother* 2009;10:2897–904.
11. Kagitani-Shimono K, Mohri I, Fujitani Y, Suzuki K, Ozono K, Urade Y, et al. Anti-inflammatory therapy by ibudilast, a phosphodiesterase inhibitor, in demyelination of twitcher, a genetic demyelination model. *J Neuroinflammation* 2005;2:10.
12. Williams RO. Collagen-induced arthritis in mice: a major role for tumor necrosis factor- α . *Methods Mol Biol* 2007;361:265–84.
13. Hsu YH, Chang MS. Interleukin-20 antibody is a potential therapeutic agent for experimental arthritis. *Arthritis Rheum* 2010;62:3311–21.
14. McCann FE, Palfreman AC, Andrews M, Perocheau DP, Inglis JJ, Schafer P, et al. Apremilast, a novel PDE4 inhibitor, inhibits spontaneous production of tumour necrosis factor- α from human rheumatoid synovial cells and ameliorates experimental arthritis. *Arthritis Res Ther* 2010;12:R107.
15. Williams RO, Plater-Zyberk C, Williams DG, Maini RN. Successful transfer of collagen-induced arthritis to severe combined immunodeficient (SCID) mice. *Clin Exp Immunol* 1992;88:455–60.
16. Clanchy FI, Hamilton JA. Proliferative monocyte frequency is associated with circulating monocyte prevalence. *Leuk Res* 2012;36:e175–7.
17. Campbell IK, Rich MJ, Bischof RJ, Dunn AR, Grail D, Hamilton JA. Protection from collagen-induced arthritis in granulocyte-macrophage colony-stimulating factor-deficient mice. *J Immunol* 1998;161:3639–44.

18. Alzabin S, Abraham SM, Taher TE, Palfreeman A, Hull D, McNamee K, et al. Incomplete response of inflammatory arthritis to TNF α blockade is associated with the Th17 pathway. *Ann Rheum Dis* 2012;71:1741–8.
19. Notley CA, Inglis JJ, Alzabin S, McCann FE, McNamee KE, Williams RO. Blockade of tumor necrosis factor in collagen-induced arthritis reveals a novel immunoregulatory pathway for Th1 and Th17 cells. *J Exp Med* 2008;205:2491–7.
20. Flemming S, Schlegel N, Wunder C, Meir M, Baar W, Wollborn J, et al. Phosphodiesterase 4 inhibition dose dependently stabilizes microvascular barrier functions and microcirculation in a rodent model of polymicrobial sepsis. *Shock* 2014;41:537–45.
21. Lee JY, Cho E, Ko YE, Kim I, Lee KJ, Kwon SU, et al. Ibudilast, a phosphodiesterase inhibitor with anti-inflammatory activity, protects against ischemic brain injury in rats. *Brain Res* 2012;1431:97–106.
22. Aerts NE, De Knop KJ, Leysen J, Ebo DG, Bridts CH, Weyler JJ, et al. Increased IL-17 production by peripheral T helper cells after tumour necrosis factor blockade in rheumatoid arthritis is accompanied by inhibition of migration-associated chemokine receptor expression. *Rheumatology (Oxford)* 2010;49:2264–72.
23. Chen DY, Chen YM, Chen HH, Hsieh CW, Lin CC, Lan JL. Increasing levels of circulating Th17 cells and interleukin-17 in rheumatoid arthritis patients with an inadequate response to anti-TNF- α therapy. *Arthritis Res Ther* 2011;13:R126.
24. Hull DN, Williams RO, Pathan E, Alzabin S, Abraham S, Taylor PC. Anti-tumour necrosis factor treatment increases circulating T helper type 17 cells similarly in different types of inflammatory arthritis. *Clin Exp Immunol* 2015;181:401–6.
25. Suzumura A, Ito A, Mizuno T. Phosphodiesterase inhibitors suppress IL-12 production with microglia and T helper 1 development. *Mult Scler* 2003;9:574–8.
26. Fox RJ, Coffey CS, Conwit R, Cudkowicz ME, Gleason T, Goodman A, et al. Phase 2 trial of ibudilast in progressive multiple sclerosis. *N Engl J Med* 2018;379:846–55.

Association of Geography and Access to Health Care Providers With Long-Term Prescription Opioid Use in Medicare Patients With Severe Osteoarthritis: A Cohort Study

Rishi J. Desai,¹ Yinzhu Jin,¹ Patricia D. Franklin,² Yvonne C. Lee,³  Brian T. Bateman,¹ Joyce Lii,¹ Daniel H. Solomon,¹ Jeffrey N. Katz,¹ and Seouyoung C. Kim¹ 

Objective. To evaluate the variation in long-term opioid use in osteoarthritis (OA) patients according to geography and health care access.

Methods. We designed an observational cohort study among OA patients undergoing total joint replacement (TJR) in the Medicare program (2010 through 2014). The independent variables of interest were the state of residence and health care access, which was quantified at the primary care service area (PCSA) level as categories of number of practicing primary care providers (PCPs) and categories of rheumatologists per 1,000 Medicare beneficiaries. The percentage of OA patients taking long-term opioids (≥ 90 days in the 360-day period immediately preceding TJR) within each PCSA was the outcome variable in a multilevel, generalized linear regression model, adjusting for case-mix at the PCSA level and for policies, including rigor of prescription drug monitoring programs and legalized medical marijuana, at the state level.

Results. A total of 358,121 patients with advanced OA, with a mean age of 74 years, were included from 4,080 PCSAs. The unadjusted mean percentage of long-term opioid users varied widely across states, ranging from 8.9% (Minnesota) to 26.4% (Alabama), and this variation persisted in the adjusted models. Access to PCPs was only modestly associated with rates of long-term opioid use between PCSAs with highest (>8.6) versus lowest (<3.6) concentration of PCPs (adjusted mean difference 1.4% [95% confidence interval 0.8%, 2.0%]), while access to rheumatologists was not associated with long-term opioid use.

Conclusion. We note a substantial statewide variation in rates of long-term treatment with opioids in OA, which is not fully explained by the differences in access to health care providers, varying case-mix, or state-level policies.

INTRODUCTION

Long-term use of prescription opioids to treat chronic non-cancer pain has received intense scrutiny due to the accumulating evidence of uncertain clinical benefit and well-recognized risks associated with their use (1). A comprehensive systematic review summarizing evidence from 40 studies concluded that evidence demonstrating the effectiveness of long-term opioid therapy for

improving chronic pain and functioning was insufficient, and the available evidence supported potentially dose-dependent risk for serious harms, including overdose, abuse, fractures, and cardiac events (2). Recently, a large randomized trial demonstrated equivalent outcomes between prescription opioids and nonopioid treatments at 12 months in patients with chronic back pain or hip or knee osteoarthritis (OA) pain (3). In light of all available evidence, the Centers for Disease Control and Prevention (CDC) has

Supported by the NIH/National Institute of Arthritis and Musculoskeletal and Skin Diseases (grant R01-AR-069557).

¹Rishi J. Desai, MS, PhD, Yinzhu Jin, MPH, Brian T. Bateman, MD, MPH, Joyce Lii, MS, Daniel H. Solomon, MD, MPH, Jeffrey N. Katz, MD, MS, Seouyoung C. Kim, MD, ScD: Brigham and Women's Hospital, Harvard Medical School, Boston, Massachusetts; ²Patricia D. Franklin, MD, MPH: University of Massachusetts Medical School, Worcester; ³Yvonne C. Lee, MD, MMSc: Northwestern University Feinberg School of Medicine, Chicago, Illinois.

Dr. Desai has received research support from Merck and Vertex for Brigham and Women's Hospital. Dr. Solomon has received research support

from Lilly, Pfizer, AstraZeneca, Genentech, Amgen, and Corrona for Brigham and Women's Hospital. Dr. Kim has received research support from Roche/Genentech, Pfizer, Bristol-Myers Squibb, Merck, and AstraZeneca for Brigham and Women's Hospital. No other disclosures relevant to this article were reported.

Address correspondence to Rishi J. Desai, MS, PhD, Division of Pharmacoepidemiology and Pharmacoeconomics, Department of Medicine, Brigham and Women's Hospital and Harvard Medical School, 1620 Tremont Street, Suite 3030-R, Boston, MA 02120. E-mail: rdesai@bwh.harvard.edu.

Submitted for publication July 24, 2018; accepted in revised form January 3, 2019.

recommended that in patients with chronic pain, clinicians should assess the risk–benefit tradeoffs of long-term opioid therapy every 3 months or more frequently and gradually taper or discontinue treatment when harms outweigh benefits (4).

OA of the hip or knee is one of the most common causes of chronic pain in the US and affects nearly 30 million US adults, and the prevalence is expected to rise as the population ages (5). Moderate-to-severe pain in patients with OA is often managed with nonsteroidal antiinflammatory drugs, steroids, and opioid analgesics (6), and in patients with severe pain that is inadequately controlled with medications, total joint replacement (TJR) is considered to improve quality of life (7,8). Although 2 previous studies have investigated the cross-sectional prevalence of prescription opioid use in OA patients, neither of these studies investigated long-term use (9,10).

Studies conducted to describe patterns and predictors of opioid use on a societal level, without focusing on patients with chronic pain, have noted that geographic variation in opioid-prescribing practices and health care access are important determinants of prescription opioid use (11,12). However, patients with chronic pain comprise a population of special interest for studying prescription opioid use, as the need for effective pain management in these patients can lead to long-term opioid use. Careful examination of long-term opioid use patterns in routine care patient populations affected by chronic pain is urgently needed to effectively disseminate opioid-prescribing guidelines and target policy interventions to minimize harm. Therefore, we conducted an observational cohort study in a nationwide sample of Medicare enrollees with severe OA to describe long-term opioid use and to evaluate the role of geography and health care access in determining long-term opioid use. We restricted the study sample to TJR recipients and evaluated opioid use in the year leading up to TJR in order to include a homogeneous patient population with advanced OA and a clinical indication for pain control.

PATIENTS AND METHODS

Data sources. Medicare claims from Parts A (inpatient services), B (outpatient services), and D (pharmacy claims) from 2010 through 2014 were used in this study. These data sources contain longitudinally traceable information for the enrollees' medical diagnoses, recorded with the International Classification of Diseases, Ninth Revision, Clinical Modification (ICD-9-CM) codes; medical procedures recorded as Current Procedural Terminology or ICD-9-CM procedure codes; and medication dispensing recorded using National Drug Code numbers. In addition, we retrieved information regarding patient demographics, including race, sex, age, and geography of their residence at ZIP code level from Medicare enrollment files.

We also used Primary Care Service Area (PCSA) data files (2010) available from the Health Resources and Services Admin-

istration (HRSA) data warehouse to quantify access to primary care providers (PCPs) (13). The PCSA is a discrete service area defined for Medicare beneficiaries based on the receipt of primary care services and contains ≥ 1 contiguous ZIP code tabulation area (14). PCSA data files include information on the total number of Medicare enrollees in each PCSA, along with a wide range of information related to health care services, e.g., the number of clinically active PCPs, physician assistants, or federally qualified health centers, as well as socioeconomic status indicators derived from the American Community Survey conducted by the US Census Bureau (13). PCSA data files do not contain information on the number of practitioners by specialty. Therefore, we obtained a comprehensive de-identified list of all practicing US-based rheumatologists as of 2010 and their corresponding business addresses from the American College of Rheumatology (ACR). Medicare files were linked with PCSA files and the list of rheumatologists using ZIP codes to assign a PCSA to each patient in this study. The Brigham & Women's Hospital Institutional Review Board approved the protocol for this study.

Study population. We randomly sampled 1 million Medicare beneficiaries who underwent TJR (identified using ICD-9-CM procedure codes 81.51 for total hip replacement or 81.54 for total knee replacement) from 2010 through 2014 with no record of TJR in the prior year. Of these, we excluded patients who were age < 65 years, who did not have continuous enrollment in Medicare Parts A, B, and D for a 12-month baseline period immediately preceding TJR, who had both hip and knee replacement performed on the same date, or who had a diagnosis of cancer during the baseline period. We further restricted the study population to OA patients by excluding patients with hip fracture (which could be the reason for total hip replacement), as well as patients without diagnosis codes for OA during the baseline period. For patients undergoing multiple TJR procedures in the study period, we only included the first procedure. Patients meeting all our inclusion criteria were grouped by their PCSA, and the data were analyzed with the PCSA as the unit of analysis. To reliably estimate the outcome, which was measured as the percentage of patients in each PCSA taking long-term opioids, we excluded from the analysis PCSAs with ≤ 25 patients.

Outcome variable. We defined long-term opioid use for each patient in a 360-day period immediately preceding TJR based on prescription dispensing for any opioid with the day supply totaling ≥ 90 days, in accordance with the long-term opioid use definition outlined by the CDC (4). The opioids considered in our analysis included hydrocodone, dihydrocodeine, oxycodone, propoxyphene, tramadol, meperidine, hydromorphone, morphine, fentanyl, methadone, pentazocine, tapentadol, levorphanol, and oxymorphone. The percentage of patients receiving long-term opioid therapy within each PCSA was the main outcome variable of interest.

Independent variables of interest. *PCP access.* We quantified PCP access on the PCSA level based on the total number of clinically active PCPs per 1,000 Medicare beneficiaries. This variable was categorized into 4 quartiles as follows: Q1 = 0–3.6, Q2 = >3.6–5.5, Q3 = >5.5–8.6, and Q4 = >8.6 PCPs.

Rheumatologist access. The total number of rheumatologists in each PCSA was determined based on the ZIP codes recorded in the business addresses in the list received from the ACR. We quantified rheumatologist access on the PCSA level based on the total number of practicing rheumatologists per 1,000 Medicare beneficiaries as a categorical variable. As >70% of the included PCSAs did not have any practicing rheumatologists, we created a category of “no rheumatologist access” and created 3 additional categories from PCSAs with at least 1 practicing rheumatologist based on tertiles (<0.15, 0.15–0.29, and >0.29).

Geographic region. We identified states for each PCSA from the PCSA data files and used state as an independent variable of interest. New York was selected as the reference state because of a large sample size and consistently low opioid use reported in previous investigations (12,15).

Covariates. *PCSA-level case-mix adjustment.* To account for the varying case-mix from one PCSA to another, we aggregated patient demographics at the PCSA level, including age, race (white or nonwhite), and sex; dual enrollment in Medicare and Medicaid; type of joint replacement surgery (total knee or hip replacement); and prevalence of other pain-related and comorbid condition diagnoses that may influence prescription opioid use, including back pain, neuropathic pain, migraine, rheumatoid arthritis, fractures, falls, depression, anxiety, bipolar disorder, drug abuse, and alcohol abuse. As a marker for the patients’ general health, we accounted for a comorbidity score that combines 20 chronic conditions from the Charlson and Elixhauser systems, including metastatic cancer, congestive heart failure, dementia, renal failure, weight loss, hemiplegia, alcohol abuse, any tumor, cardiac arrhythmias, chronic pulmonary disease, coagulopathy, complicated diabetes mellitus, deficiency anemias, fluid and electrolyte disorders, liver disease, peripheral vascular disorders, psychosis, pulmonary circulation disorders, HIV, and hypertension (16). Additionally, to account for the aggregate poverty and literacy levels in PCSAs, we included 2 indicators for socioeconomic status in each PCSA, the percentage of the population living under the federal poverty limit and the percentage of the population age >25 years with less than a high-school education.

State-level policy interventions. It is important to consider various state-level policies in the analysis in order to isolate the unexplained variation in long-term opioid use by state from the effect of these policies. Therefore, we accounted for the rigor of prescription drug–monitoring programs (PDMPs) and the presence of medical marijuana policies in a state, both of which could have an impact on long-term prescription opioid use. Op-

erationally, we identified the dates of implementation of these policies within each state. Additionally, for PDMPs, we identified program rigor and classified state programs into 3 categories as follows: 1) high rigor: included states that required prescribers to check PDMP database each time prior to prescribing opioids to all patients or to chronic pain patients, 2) low rigor: included states where an operational PDMP was available, but no requirement for checking PDMPs was implemented or checking PDMP was only required prior to prescribing opioids for the first time, and 3) no operational PDMP.

For medical marijuana, we created a binary variable indicating presence or absence of state laws for legally obtaining medical marijuana. To account for implementation of these policies during our study period (2010 through 2014), we first identified whether the policy concerned had been implemented by the time we started measuring each patient’s long-term opioid use to define policy-exposed patients. We then aggregated this information at the PCSA level by assigning each PCSA to a specific level of policy exposure when a majority of the patients (>50%) within that PCSA were exposed to that specific level of the policy. Policy implementation dates and details regarding the rigor of PDMPs were derived from the Prescription Drug Abuse Policy System web portal (17), which is a National Institute on Drug Abuse–supported initiative to track key state laws related to prescription drug abuse.

Statistical analysis. Patient characteristics were reported using descriptive statistics among opioid non-users, short-term users (<90 days), and long-term users (≥90 days) in the year leading up to TJR. Characteristics of opioid use, including total day supply, average daily dose in morphine milligram equivalents (MME), total number of different agents used, and incidence of the most frequently used agents, were described for short-term and long-term opioid users. The average daily dose was also reported in categories of <50, 50–90, and ≥90 MME. These categories were selected based on the CDC guidelines, which define average daily dose of 50–90 MME as the range where a careful assessment of risk–benefit is suggested and ≥90 MME as the range that should be avoided (4). We also described the case-mix across 4,080 PCSAs using descriptive statistics.

The proportion of long-term opioid users and density of clinically active PCPs and rheumatologists within each PCSA were plotted on a map of the US to visually demonstrate the geographic variation in opioid use and health care access. To quantify the impact of access and geography on long-term opioid use rates, a generalized linear regression model with identity link was constructed with the PCSA as the unit of analysis and the percentage of long-term opioid users in each PCSA as the dependent variable. To account for the hierarchical structure of the data where PCSAs are clustered within states, we used a multilevel model. Level 1 variables included PCSA-level variables to adjust for the case-mix and were modeled as fixed effects.

Level 2 variables included state effects, which were modeled as random effects, and policy interventions, which were modeled as fixed effects. The statistical analysis was conducted in SAS with PROC GLIMMIX, version 9.4.

RESULTS

Study population. A total of 358,121 OA patients with an average age of 74 years who underwent TJR met all our inclusion criteria and contributed to this analysis (Figure 1). The majority of the patients (91.9%) were white and 67.8% were women. A total of 59,387 patients (16.5%) were identified as long-term opioid users (≥ 90 days) and 152,308 (42.3%) were identified as short-term users (< 90 days). Over the study years from 2011 through 2014, the proportion of TJR patients taking opioids long-term remained relatively stable (16.8% in 2011, 16.8% in 2012, 16.6% in 2013, and 16.3% in 2014). Table 1 summarizes the patient characteristics across non-users, short-term users, and long-term users. The prevalence of pain-related conditions, as well as the comorbidity burden, were substantially higher among long-term opioid users compared to short-term and non-users.

Table 1 further provides details regarding opioid use characteristics in long-term and short-term opioid users. The median day supply for prescription opioids was 218 (interquartile range 142–307) among long-term users and 15 (interquartile range

6–34) among short-term users. Nineteen percent of the long-term users and 15.9% of the short-term users consumed an average daily dose of ≥ 50 MME. Compared to short-term opioid users, a notably higher use of tramadol (45.8% versus 36.8%), oxycodone (32.2% versus 21.7%), and fentanyl (6.2% versus 0.5%) was noted among long-term users.

A total of 4,080 PCSAs or 57.1% of the 7,144 total PCSAs defined in the US by the HRSA were represented in our analysis. The average number of patients in each PCSA was 87.7 (range 26–1,038). The case-mix across the included PCSAs was heterogeneous, with varying proportions of pain-related diagnoses and a wide range of socioeconomic statuses and access to health care providers (Table 2). Across the 4,080 included PCSAs, the mean \pm SD percentage of long-term opioid users was $17.2\% \pm 7.8\%$, ranging from a low of 0% to a high of 60%. Supplementary Figure 1 (available on the *Arthritis & Rheumatology* web site at <http://onlinelibrary.wiley.com/doi/10.1002/art.40834/abstract>) shows the distribution of the percentage of long-term opioid users across the included PCSAs.

Association of long-term opioid use with geographic region and access to health care providers.

Figure 2 summarizes long-term opioid use by PCSAs in our study population across the US. PCSAs with a higher proportion of long-term opioid users were generally in the South, and PCSAs with a lower proportion of long-term opioid users

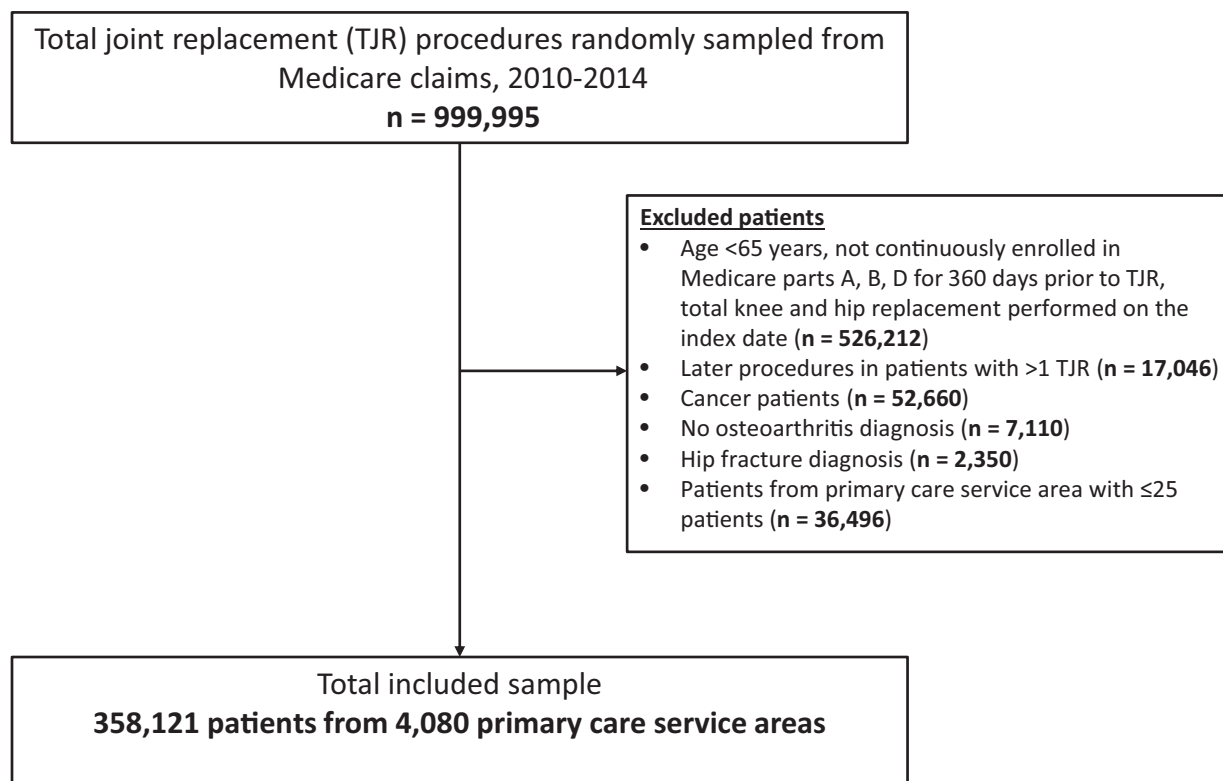


Figure 1. Cohort selection flow chart.

Table 1. Patient-level descriptive statistics and opioid use characteristics in the year leading up to total joint replacement in a cohort of patients with severe osteoarthritis, Medicare data, 2010–2014*

	Non-users	Short-term users (<90 days)	Long-term users (≥90 days)
Total patients, no.	146,426	152,308	59,387
Patient characteristics			
Age, mean ± SD years	74.3 ± 5.9	73.9 ± 5.9	73.5 ± 6.1
Male sex, no. (%)	52,480 (35.8)	48,661 (31.9)	14,421 (24.3)
White race, no. (%)	136,213 (93.0)	139,730 (91.7)	53,119 (89.4)
Medicare/Medicaid dual eligibility, no. (%)	12,089 (8.3)	17,929 (11.8)	15,017 (25.3)
Type of total joint replacement surgery, no. (%)			
Total knee replacement	105,188 (71.8)	101,159 (66.4)	37,827 (63.7)
Total hip replacement	41,238 (28.2)	51,149 (33.6)	21,560 (36.3)
Pain-related diagnoses and other comorbid conditions, no. (%)			
Rheumatoid arthritis	4,603 (3.1)	7,374 (4.8)	5,862 (9.9)
Neuropathic pain	29,244 (20.0)	49,911 (32.8)	27,106 (45.6)
Back pain	57,840 (39.5)	84,146 (55.2)	42,393 (71.4)
Migraine	8,911 (6.1)	14,375 (9.4)	8,062 (13.6)
Falls	4,809 (3.3)	9,664 (6.3)	6,071 (10.2)
Fractures	7,209 (4.9)	14,549 (9.6)	7,799 (13.1)
Anxiety	10,980 (7.5)	17,579 (11.5)	12,027 (20.3)
Depression	14,165 (9.7)	23,163 (15.2)	16,212 (27.3)
Drug abuse	67 (0)	192 (0.1)	506 (0.9)
Bipolar disorder	988 (0.7)	1,505 (1)	1,268 (2.1)
Alcohol abuse	919 (0.6)	1,468 (1)	1,003 (1.7)
Comorbidity score, mean ± SD	0.6 ± 1.6	0.8 ± 1.8	1.3 ± 2.1
Opioid use characteristics			
Day supply of prescription opioids, median (IQR) days	–	15 (6–34)	218 (142–307)
Average daily dose of opioids, median (IQR) MME	–	30 (20–42.9)	27.3 (17.8–41.7)
Average daily dose categories, no. (%)			
<50 MME	–	128,145 (84.1)	48,106 (81.0)
50–90 MME	–	19,911 (13.1)	6,836 (11.5)
≥90 MME	–	4,252 (2.8)	4,445 (7.5)
Total number of different agents used, median (IQR)	–	1 (1–2)	2 (1–2)
Five most commonly used agents, no. (%)			
Tramadol	–	55,968 (36.8)	27,224 (45.8)
Hydrocodone	–	58,134 (38.2)	17,793 (30.0)
Oxycodone	–	32,998 (21.7)	19,154 (32.2)
Propoxyphene	–	3,018 (2.0)	1,953 (3.3)
Fentanyl	–	731 (0.5)	3,671 (6.2)

* IQR = interquartile range; MME = morphine milligram equivalent.

were typically from the Northeast and the Midwest. Supplementary Figure 2 (available at <http://onlinelibrary.wiley.com/doi/10.1002/art.40834/abstract>) summarizes health care provider access by PCSAs in our study population across the US. The distribution of PCPs and rheumatologists was noted to be more concentrated in the Northeast and the Midwest.

The unadjusted mean percentage of long-term opioid users increased monotonically from the PCSA categories representing highest to lowest concentration of PCPs (16.0% to 18.3%) and rheumatologists (15.4% to 17.6%) (Table 3). Variation in the unadjusted mean percentage of long-term opioid users was substantial across states, ranging from a low of 8.9% in Minnesota to a

Table 2. PCSA-level descriptive statistics for the case-mix across 4,080 PCSAs in a cohort of patients with severe osteoarthritis, Medicare data, 2010–2014*

Population characteristic within each PCSA	Mean ± SD	Minimum	Maximum
Sample size, no.	87.7 ± 84.5	26.0	1,038.0
Demographic			
Age, years	74 ± 1.1	69.5	78.4
White, %	92 ± 11.9	0.0	100.0
Male, %	32.4 ± 7.4	3.4	63.0
Medicare-Medicaid dual eligibility, %	13.6 ± 12.2	0.0	92.2
Type of joint replacement surgery, %			
Total knee replacement	68.7 ± 8.1	38.5	96.3
Total hip replacement	31.3 ± 8.1	3.7	61.5
Pain-related diagnoses and other comorbid conditions, %			
Rheumatoid arthritis	5 ± 3.4	0.0	36.8
Neuropathic pain	29.3 ± 7.5	7.1	68.5
Back pain	51.3 ± 8.1	20.5	85.6
Migraine	8.7 ± 4.2	0.0	30.2
Falls	5.8 ± 3.5	0.0	28.6
Fracture	8.2 ± 3.9	0.0	31.3
Anxiety	11.4 ± 5	0.0	38.5
Depression	14.9 ± 5.7	0.0	41.9
Bipolar disorder	1 ± 1.4	0.0	10.3
Drug abuse	0.2 ± 0.7	0.0	10.7
Alcohol abuse	0.9 ± 1.3	0.0	11.5
Average combined comorbidity score	0.8 ± 0.4	−0.3	3.2
Socioeconomic status variables, %			
Below the poverty level	9.5 ± 5.6	0.0	41.6
Below high-school education	5.6 ± 4.3	0.0	39.7
Provider access			
PCPs per 1,000 Medicare beneficiaries, no.	7 ± 6.1	0.0	116.6
Rheumatologists per 1,000 Medicare beneficiaries, no.	0.1 ± 0.3	0.0	7.0

* PCSA = primary care service area; PCPs = primary care providers.

high of 26.4% in Alabama. Supplementary Table 1, available at <http://onlinelibrary.wiley.com/doi/10.1002/art.40834/abstract>, provides this information for all states and Washington, DC.

In the regression model adjusted for case-mix, the variation across states in long-term opioid use rates persisted. Compared to the reference state (New York), the mean difference in long-term opioid users in percentage points was >10 for West Virginia and Alabama (Table 3 shows the mean difference for 10 states with the highest mean differences). A total of 31 states had statistically significantly higher rates of long-term opioid users compared to New York, and in 19 states, the rates were similar (see Supplementary Table 2, available at <http://onlinelibrary.wiley.com/doi/10.1002/art.40834/abstract>, for results from the full regression model). The adjusted mean difference in long-term opioid users between PCSAs with the highest (>8.6) versus low-

est (<3.6) concentration of PCPs per 1,000 beneficiaries was 1.4% (95% confidence interval 0.8%, 2.0%), and the adjusted mean difference between PCSAs with the highest (>0.29) versus lowest (0.00) concentration of rheumatologists was 0.6% (95% confidence interval −0.1%, 1.3%) (Table 3).

DISCUSSION

In this large observational cohort study of Medicare enrollees with OA undergoing TJR, we noted that 1 in 6 patients took long-term prescription opioids (≥90 days) for pain management in the year leading up to TJR, with an average treatment duration of approximately 7 months. Nearly 20% of the long-term users consumed an average daily dose of ≥50 MME, a range that is identified by the recent CDC guidelines as potentially imparting a

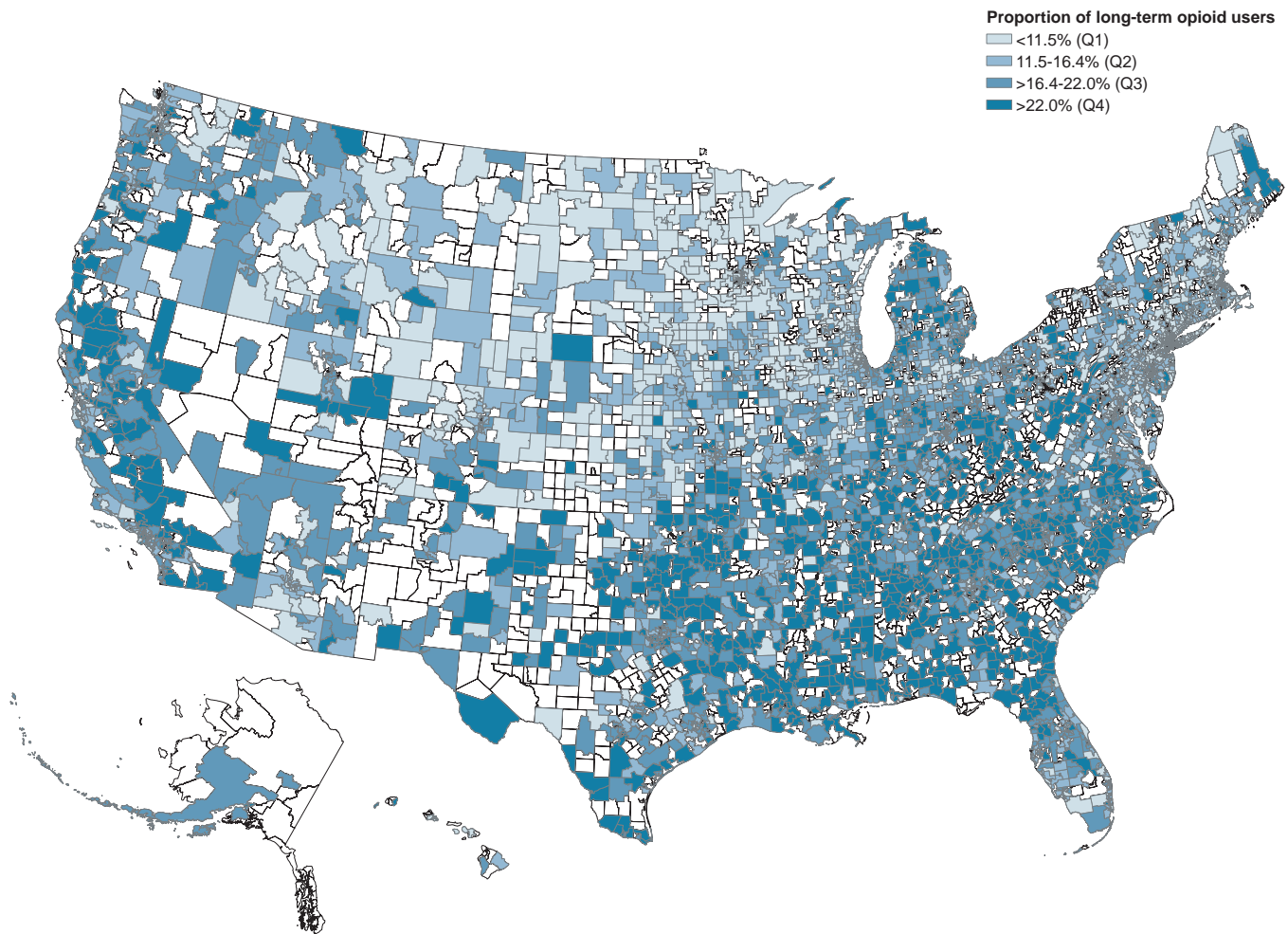


Figure 2. Long-term opioid use rates prior to total joint replacement in primary care service areas (PCSAs) across the US, Medicare data, 2010–2014. PCSAs shown as white did not contribute patients to this analysis.

high risk of opioid-related harms (4). Long-term opioid use varied substantially by state and had only a modest association with low access to PCPs.

Although OA is one of the most common reasons for chronic pain in the US, long-term prescription opioid use is not well-studied in this population. One previous study using self-reported medication use data from the Medicare Current Beneficiary Surveys showed that 40% of OA patients interviewed in 2009 took opioids at least once, but this study did not investigate the length of opioid use in these patients (9). Among all Medicare Part D enrollees, the prevalence of long-term prescription opioid use was reported to be 7.3% in 2012 (18). The estimates for long-term opioid use observed in this study of Medicare patients with severe OA from 2010 through 2014 are more than 2-fold higher than this previously reported estimate. Thus, our study identifies patients with advanced OA as a population with substantially high rates of long-term prescription opioid use compared to the overall Medicare population. We also noted that 1 in 5 long-term users consumed an average daily dose of ≥ 50 MME and the average length of treatment with opioids was approxi-

mately 7 months in the year prior to TJR among long-term users. These observations are important to consider in light of results from a recent randomized controlled trial suggesting questionable effectiveness of long-term prescription opioids in treatment of chronic pain (3). In patients with severe OA, a special emphasis on periodically monitoring prescription opioid use is required to ensure benefits outweigh risks at the prescribed doses.

We noted a substantial geographic variation in use of long-term prescription opioids in this study. This finding is in accordance with the results of earlier studies that also demonstrated wide geographic variation in prescribing of opioids, with lower rates on average in the Northeast and Midwest and generally higher rates in the South (12,15,18–20). Using a comprehensive risk-adjustment approach, we further evaluated whether this geographic variation could be explained by differences in access to health care providers, in patient populations, in socioeconomic characteristics, or in policy interventions across states.

After adjusting for these differences, we observed that state of residence had an independent association with rates of long-term opioid use, suggesting that regional prescribing practices

Table 3. Association of health care access and geographic region with long-term preoperative opioid use rates in a cohort of patients with severe osteoarthritis, Medicare data, 2010–2014*

Independent variable of interest	PCSA, no. (%) (n = 4,080)	Percentage of long-term opioid users, unadjusted mean \pm SD	Adjusted mean difference in proportion (percentage points) of long-term opioid users (95% CI) [†]
State [‡]			
New York	181 (4.4)	12.3 \pm 6.1	Reference
West Virginia	26 (0.6)	24.9 \pm 8.6	10.3 (7.9, 12.6)
Alabama	69 (1.7)	26.4 \pm 7.0	10.2 (7.3, 13.2)
Georgia	111 (2.7)	22.9 \pm 8.2	9.4 (6.8, 12)
Kentucky	81 (2)	24 \pm 9.6	8.8 (7.2, 10.4)
Louisiana	53 (1.3)	25 \pm 8.6	8.3 (6.5, 10.1)
Oklahoma	77 (1.9)	22.3 \pm 6.1	8.2 (6.6, 9.8)
North Carolina	135 (3.3)	22.6 \pm 8.1	7.9 (5.5, 10.3)
Virginia	123 (3)	17 \pm 6.3	7.2 (5.8, 8.7)
Indiana	128 (3.1)	19.1 \pm 6.1	7.2 (5.8, 8.6)
Mississippi	67 (1.6)	25 \pm 7.7	7.1 (4.5, 9.7)
PCPs per 1,000 Medicare beneficiaries in the PCSA, no.			
>8.6 (Q4)	1,020 (25)	16.0 \pm 7.2	Reference
>5.5–8.6 (Q3)	1,020 (25)	16.4 \pm 7.2	0.9 (0.4, 1.4)
3.6–5.5 (Q2)	1,020 (25)	18.3 \pm 8.0	1.7 (1.1, 2.2)
<3.6 (Q1)	1,020 (25)	18.3 \pm 8.5	1.4 (0.8, 2.0)
Rheumatologists per 1,000 Medicare beneficiaries in the PCSA, no.			
>0.29 (T3)	381 (9.4)	15.4 \pm 7.2	Reference
0.15–0.29 (T2)	381 (9.4)	16.3 \pm 6.4	0.4 (–0.4, 1.2)
<0.15 (T1)	381 (9.3)	17.5 \pm 6.0	0.1 (–0.8, 0.9)
None	2,938 (72)	17.6 \pm 8.2	0.6 (–0.1, 1.3)

* 95% CI = 95% confidence interval; PCPs = primary care providers.

[†] Adjusted for case-mix, including age, race, sex, dual Medicare-Medicaid enrollment, pain-related diagnoses, comorbid conditions, type of joint replacement surgery, and socioeconomic characteristics in each primary care service area (PCSA) as well as state-level policies, including rigor of prescription drug-monitoring programs and legal availability of medical marijuana.

[‡] Based on the highest adjusted estimates, the top 10 states are presented in descending order of the adjusted mean difference compared to New York. New York was selected as the reference state based on the low proportion of long-term opioid users and a large sample size. Estimates for the rest of the states are provided in Supplementary Table 1, available on the *Arthritis & Rheumatology* web site at <http://onlinelibrary.wiley.com/doi/10.1002/art.40834/abstract>.

play a key role in determining rates of long-term opioid use in this population. This finding suggests that geographically targeted interventions to ensure widespread dissemination and implementation of safe opioid prescribing guidelines are necessary to make a meaningful impact on prescribing practices. While our study did not identify an association between state-level policies, including PDMPs and legal medical marijuana, and rates of long-term prescription opioid use (see Supplementary Table 2, available on the *Arthritis & Rheumatology* web site at <http://onlinelibrary.wiley.com/doi/10.1002/art.40834/abstract>), this finding should not be interpreted as causal. Evidence regarding the impact of these policies on overall opioid prescribing is mixed, with some studies indicating a modest reduction in opioid prescribing rates

(21,22) and some suggesting no consistent reduction as a result of implementation of these policies (23,24). However, it must be noted that our study was not designed to evaluate the direct impact of these policies on rates of long-term prescription opioid use. Instead, our focus was on ruling out variation in these policies as a potential explanation for state-to-state variation in long-term prescription opioid rates. Future research employing more suitable methods for policy evaluations, such as a controlled interrupted time-series design (25), should be considered to evaluate the impact of the introduction of specific policies on long-term prescription opioid use in patients with severe OA.

Our study also adds information to the literature regarding the complex association between health care access and

use of prescription opioids in patients with chronic pain. Some previous studies have demonstrated a positive correlation between the number of clinically active practitioners in a geographic area and the amount of opioids prescribed (11,12), suggesting that higher access to multiple providers may make it easier for patients to seek opioid prescriptions from more than 1 provider or to find a provider readily willing to prescribe opioids. In contrast, we noted a modestly negative association between the number of active PCPs in a PCSA and long-term opioid use rates, as well as no association between the number of rheumatologists and long-term opioid use rates in this patient population of elderly individuals with severe OA. Although the effect size for the association between higher PCP concentration and lower long-term opioid use was small, the contrast from previous studies suggests that factors driving long-term opioid use in patients with chronic pain may be unique, and easier access may not be a risk factor for higher opioid use in these patients.

There are some important strengths of this study. First, it describes rates of long-term opioid use in a nationally representative population of Medicare enrollees with severe OA. We conducted comprehensive risk adjustment based on patient demographics, comorbid conditions, and variation in state-level policies. Second, since all patients included in this study had full pharmacy and medical benefits under the fee-for-service Medicare program during the study period, confounding by patient-level financial factors, such as differential health plan coverage of medications or differences in copays, is likely to be limited.

There are also some limitations that deserve mention. First, we did not have data on pain severity or pain-related functioning for patients in this cohort, which makes residual confounding possible. However, restricting the study population to TJR recipients may have limited such confounding by ensuring the inclusion of a somewhat homogeneous population seeking pain relief for knee and hip OA. Second, the data used in this study are not recent due to the time it takes the Centers for Medicare & Medicaid Services to release Medicare claims. Therefore, our study may not have captured more recent shifts (after 2014) in prescription opioid use patterns in this population in response to the growing awareness about the opioid epidemic in the US. A third limitation of the current study is that we did not evaluate whether undergoing TJR changes opioid use patterns in these patients. Future research should address the impact of pre-TJR opioid use on postsurgical functional outcomes as well as the impact of TJR on postsurgical opioid use. Another limitation is that we did not have complete information on access to other health care services, such as physical therapy, which precluded evaluation of the impact of access to these services on long-term opioid use in this population. An additional limitation is that we did not focus on variation in prescribing practices across individual providers, which may be important to consider when designing interventions. Finally, by including a population of TJR

recipients and evaluating the opioid use prior to TJR, our study may underestimate the extent of prescription opioid use in this population due to exclusion of patients with severe OA who may die without ever undergoing TJR. Further, there exists a substantial racial disparity in the use of TJR, with rates among blacks approximately 40% lower compared to whites (26); therefore, the restriction of the study population to TJR recipients also limits the generalizability of our estimates.

In conclusion, we observed frequent use of long-term opioids in elderly patients with severe knee or hip OA prior to TJR. Importantly, substantial statewide variation in rates of treatment with long-term opioids was noted in this population, which was not fully explained by the differences in access to PCPs or rheumatologists, variation in patient characteristics, or state-level policies including PDMPs and legalized medical marijuana. These findings suggest that geographically targeted dissemination strategies for safe opioid prescribing guidelines may be required to address the high use observed in certain states.

AUTHOR CONTRIBUTIONS

All authors were involved in drafting the article or revising it critically for important intellectual content, and all authors approved the final version to be submitted for publication. Dr. Desai had full access to all of the data in the study and takes responsibility for the integrity of the data and the accuracy of the data analysis.

Study conception and design. Desai, Franklin, Lee, Bateman, Solomon, Katz, Kim.

Acquisition of data. Desai, Kim.


Analysis and interpretation of data. Desai, Jin, Lii, Kim.

REFERENCES

1. Volkow N, Benveniste H, McLellan AT. Use and misuse of opioids in chronic pain. *Annu Rev Med* 2018;69:451–65.
2. Chou R, Turner JA, Devine EB, Hansen RN, Sullivan SD, Blazina I, et al. The effectiveness and risks of long-term opioid therapy for chronic pain: a systematic review for a National Institutes of Health Pathways to Prevention Workshop. *Ann Intern Med* 2015;162:276–86.
3. Krebs EE, Gravelly A, Nugent S, Jensen AC, DeRonne B, Goldsmith ES, et al. Effect of opioid vs nonopioid medications on pain-related function in patients with chronic back pain or hip or knee osteoarthritis pain: the SPACE Randomized Clinical Trial. *JAMA* 2018;319:872–82.
4. Dowell D, Haegerich TM, Chou R. CDC guideline for prescribing opioids for chronic pain: United States, 2016. *JAMA* 2016;315:1624–45.
5. Centers for Disease Control. Osteoarthritis. URL: <http://www.cdc.gov/arthritis/basics/osteoarthritis.htm>.
6. Hochberg MC, Altman RD, April KT, Benkhalti M, Guyatt G, McGowan J, et al. American College of Rheumatology 2012 recommendations for the use of nonpharmacologic and pharmacologic therapies in osteoarthritis of the hand, hip, and knee. *Arthritis Care Res (Hoboken)* 2012;64:465–74.
7. Losina E, Thornhill TS, Rome BN, Wright J, Katz JN. The dramatic increase in total knee replacement utilization rates in the United States cannot be fully explained by growth in population size and the obesity epidemic. *J Bone Joint Surg Am* 2012;94:201–7.

8. Harris WH, Sledge CB. Total hip and total knee replacement. *N Engl J Med* 1990;323:725–31.
9. Wright EA, Katz JN, Abrams S, Solomon DH, Losina E. Trends in prescription of opioids from 2003–2009 in persons with knee osteoarthritis. *Arthritis Care Res (Hoboken)* 2014;66:1489–95.
10. DeMik DE, Bedard NA, Dowdle SB, Burnett RA, McHugh MA, Callaghan JJ. Are we still prescribing opioids for osteoarthritis? *J Arthroplasty* 2017;32:3578–82.
11. Guy GP Jr, Zhang K, Bohm MK, Losby J, Lewis B, Young R, et al. Vital signs: changes in opioid prescribing in the United States, 2006–2015. *MMWR Morb Mortal Wkly Rep* 2017;66:697–704.
12. McDonald DC, Carlson K, Izrael D. Geographic variation in opioid prescribing in the US. *J Pain* 2012;13:988–96.
13. Health Resources & Services Administration. Primary care service area data download 2010 (census tract basis). URL: <https://datawarehouse.hrsa.gov/data/datadownload/pcs2010download.aspx>.
14. Goodman DC, Mick SS, Bott D, Stukel T, Chang CH, Marth N, et al. Primary care service areas: a new tool for the evaluation of primary care services. *Health Serv Res* 2003;38:287–309.
15. Desai RJ, Hernandez-Diaz S, Bateman BT, Huybrechts KF. Increase in prescription opioid use during pregnancy among Medicaid-enrolled women. *Obstet Gynecol* 2014;123:997–1002.
16. Gagne JJ, Glynn RJ, Avorn J, Levin R, Schneeweiss S. A combined comorbidity score predicted mortality in elderly patients better than existing scores. *J Clin Epidemiol* 2011;64:749–59.
17. Prescription drug abuse policy system (PDAPS). 2018. URL: <http://pdaps.org/>.
18. Kuo YF, Raji MA, Chen NW, Hasan H, Goodwin JS. Trends in opioid prescriptions among part D Medicare recipients from 2007 to 2012. *Am J Med* 2016;129:221.
19. Zerzan JT, Morden NE, Soumerai S, Ross-Degnan D, Roughead E, Zhang F, et al. Trends and geographic variation of opiate medication use in state Medicaid fee-for-service programs, 1996 to 2002. *Med Care* 2006;44:1005–10.
20. Paulozzi LJ, Mack KA, Hockenberry JM. Vital signs: variation among states in prescribing of opioid pain relievers and benzodiazepines: United States, 2012. *MMWR Morb Mortal Wkly Rep* 2014;63:563–8.
21. Bao Y, Pan Y, Taylor A, Radakrishnan S, Luo F, Pincus HA, et al. Prescription drug monitoring programs are associated with sustained reductions in opioid prescribing by physicians. *Health Aff (Millwood)* 2016;35:1045–51.
22. Wen H, Hockenberry JM. Association of medical and adult-use marijuana laws with opioid prescribing for Medicaid enrollees. *JAMA Intern Med* 2018;178:673–9.
23. Brady JE, Wunsch H, DiMaggio C, Lang BH, Giglio J, Li G. Prescription drug monitoring and dispensing of prescription opioids. *Public Health Rep* 2014;129:139–47.
24. Finley EP, Garcia A, Rosen K, McGearry D, Pugh MJ, Potter JS. Evaluating the impact of prescription drug monitoring program implementation: a scoping review. *BMC Health Serv Res* 2017;17:420.
25. Lopez Bernal J, Cummins S, Gasparini A. The use of controls in interrupted time series studies of public health interventions. *Int J Epidemiol* 2018;47:2082–93.
26. Singh JA, Lu X, Rosenthal GE, Ibrahim S, Cram P. Racial disparities in knee and hip total joint arthroplasty: an 18-year analysis of national Medicare data. *Ann Rheum Dis* 2014;73:2107–15.

Progression of Structural Damage in the Sacroiliac Joints in Patients With Early Axial Spondyloarthritis During Long-Term Anti-Tumor Necrosis Factor Treatment: Six-Year Results of Continuous Treatment With Etanercept

Valeria Rios Rodriguez,¹ Kay-Geert Hermann,¹ Anja Weiß,² Joachim Listing,² Hiltrun Haibel,¹ Christian Althoff,¹ Fabian Proft,¹ Olaf Behmer,³ Joachim Sieper,¹ and Denis Poddubnyy⁴ 

Objective. To evaluate radiographic progression in the sacroiliac (SI) joints and to identify its predictors during long-term treatment (up to 6 years) with the tumor necrosis factor (TNF) inhibitor etanercept in patients with early axial spondyloarthritis (SpA).

Methods. Patients with early axial SpA who were treated with etanercept for up to 6 years in the Etanercept versus Sulfasalazine in Early Axial Spondyloarthritis (ESTHER) trial were selected based on the availability of radiographs of the SI joints. Two readers who were blinded with regard to clinical data scored the radiographs according to the modified New York criteria (range 0–4 per SI joint). A sacroiliitis sum score (total range 0–8) was calculated as the mean of the scores of the 2 readers. Active and chronic inflammatory changes in the SI joints on magnetic resonance imaging (MRI) performed at baseline, year 2, and year 4 were assessed according to the Berlin MRI scoring system.

Results. Of the 76 patients originally included in the study, 42 had radiographs of the SI joints available at baseline and at least 1 follow-up time point (year 2, 4, or 6). The mean \pm SD change in the sacroiliitis sum score was 0.13 ± 0.73 , -0.27 ± 0.76 , and -0.09 ± 0.68 , in the time intervals baseline to year 2, year 2 to year 4, and year 4 to year 6, respectively. In the longitudinal mixed model analysis, elevated C-reactive protein level ($\beta = 0.58$ [95% confidence interval 0.24, 0.91]) and MRI SI joint osteitis score ($\beta = 0.06$ [95% confidence interval 0.03, 0.10]) were independently associated with progression of the sacroiliitis sum score.

Conclusion. Our findings indicate that long-term anti-TNF therapy decelerates the progression of structural damage in the SI joints. Elevated CRP level and presence of osteitis on MRI were independently associated with radiographic sacroiliitis progression.

INTRODUCTION

For years researchers have undertaken a detailed investigation of the progression of structural damage in the spine in patients with axial spondyloarthritis (SpA). Recent insights have

heightened interest in the investigation of the progression of structural damage in the sacroiliac (SI) joints. First, the emerging concept of axial SpA as one disease with two stages (1,2), nonradiographic axial SpA and radiographic axial SpA, depending on the absence or presence of definite radiographic sacroiliitis according

The Etanercept versus Sulfasalazine in Early Axial Spondyloarthritis (ESTHER) study was supported by Pfizer.

¹Valeria Rios Rodriguez, MD, Kay-Geert Hermann, MD, Hiltrun Haibel, MD, Christian Althoff, MD, Fabian Proft, MD, Joachim Sieper, MD: Charité Universitätsmedizin Berlin, Berlin, Germany; ²Anja Weiß, MSc, Joachim Listing, PhD: German Rheumatism Research Centre, Berlin, Germany; ³Olaf Behmer: Pfizer Pharma, Berlin, Germany; ⁴Denis Poddubnyy, MD, MSc: Charité Universitätsmedizin Berlin and German Rheumatism Research Centre, Berlin, Germany.

Dr. Rios Rodriguez has received consulting fees, speaking fees, and/or honoraria from AbbVie, MSD, and Novartis (less than \$10,000 each). Dr. Hermann has received consulting fees, speaking fees, and/or honoraria from AbbVie, MSD, Novartis, Pfizer, and UCB (less than \$10,000 each). Dr. Haibel has received consulting fees, speaking fees, and/or honoraria from AbbVie, Janssen,

MSD, and Novartis (less than \$10,000 each). Dr. Proft has received consulting fees, speaking fees, and/or honoraria from AbbVie, BMS, MSD, Novartis, Pfizer, Roche, and UCB (less than \$10,000 each). Dr. Sieper has received consulting fees, speaking fees, and/or honoraria from AbbVie, Janssen, Lilly, MSD, Novartis, Pfizer, Roche, and UCB (less than \$10,000 each). Dr. Poddubnyy has received consulting fees, speaking fees, and/or honoraria from AbbVie, BMS, Boehringer, Janssen, MSD, Novartis, Pfizer, Roche, and UCB (less than \$10,000 each). No other disclosures relevant to this article were reported.

Address correspondence to Valeria Rios Rodriguez, MD, Department of Gastroenterology, Infectiology, and Rheumatology, Campus Benjamin Franklin, Charité Universitätsmedizin Berlin, Hindenburgdamm 30, 12203 Berlin, Germany. E-mail: valeria.rios-rodriguez@charite.de.

Submitted for publication May 3, 2018; accepted in revised form November 15, 2018.

to the modified New York criteria for ankylosing spondylitis (AS) (3), requires more data about progression from one stage to the other. Second, with improvement in the early diagnosis of axial SpA, there is increased interest in the natural course of the disease at an early stage. Third, recent data suggest that structural damage in the SI joint might have functional relevance in patients with axial SpA independently of structural damage in the spine (4). Finally, biologic therapy retards spinal progression, raising the question of whether it also has such an effect on the SI joint. Until now, observational studies have suggested a natural low, but still detectable, level of progression of radiographic sacroiliitis over a period of 2–5 years (5–7).

So far, only one study has shown some deceleration of radiographic sacroiliitis progression over 2 years of treatment with the tumor necrosis factor (TNF) inhibitor etanercept in patients with nonradiographic axial SpA as compared to a historical control group (8). No long-term studies have addressed this question to date, although it has been shown that in the case of the spine the progression rate might decrease over time in patients receiving long-term anti-TNF therapy (9). The aim of the present study was to investigate the long-term course (up to 6 years) of radiographic progression in the SI joint in patients with early active axial SpA treated with the TNF inhibitor etanercept and to explore factors associated with such progression.

PATIENTS AND METHODS

Study design and patient selection. The design of the Etanercept versus Sulfasalazine in Early Axial Spondyloarthritis (ESTHER) trial (ClinicalTrials.gov identifier: NCT00844142), including detailed clinical and magnetic resonance imaging (MRI) outcome data, has been reported elsewhere (10–13). Briefly, a total of 76 patients with early axial SpA (with a disease duration of ≤ 5 years) who had active inflammatory lesions (osteitis) on MRI in either the SI joint or the spine were randomized to receive treatment with etanercept ($n = 40$) or sulfasalazine ($n = 36$) for 1 year. At the end of year 1, all patients who were not in remission continued with or (for those receiving sulfasalazine therapy) switched to etanercept until the end of year 6. Patients in remission discontinued therapy and were followed up until the end of year 2. If a patient experienced a disease flare, etanercept was introduced or re-introduced and continued until the end of year 6. Patients were selected for the present analysis based on the availability of radiographs of the SI joints, which were obtained at baseline and every 2 years thereafter.

Radiographic assessment. Two trained readers (VRR and DP), who had good interreader reliability (were well calibrated) and were blinded with regard to all clinical data and time points, independently scored the SI joint radiographs (obtained at up to 4 time points per patient: baseline, year 2, year 4, and year 6). Radiographs were scored according to the grading system of the

modified New York criteria for AS (3), where 0 = normal, 1 = suspicious changes, 2 = minimal abnormality (small localized areas with erosion or sclerosis, without alteration in the joint width), 3 = unequivocal abnormality (moderate or advanced sacroiliitis with erosions, evidence of sclerosis, widening, narrowing, or partial ankylosis), and 4 = severe abnormality (total ankylosis). Patients were classified as having radiographic axial SpA if both readers recorded the presence of definite radiographic sacroiliitis of at least grade 2 bilaterally or at least grade 3 unilaterally. Otherwise, patients were classified as having nonradiographic axial SpA.

MRI assessment. MRIs of the SI joints, as part of whole-body MRIs, were obtained at baseline, year 2, and year 4 in all patients. Two trained and calibrated readers (K-GH and CA), who were blinded with regard to all clinical data and time points, evaluated the images according to the Berlin MRI scoring system (14) with minor modifications concerning the fatty deposition subscore (13). Briefly, osteitis and fatty deposition in the bone marrow were scored per SI joint quadrant from 0 (no lesion) to 3 ($\geq 66\%$ of the quadrant involved), resulting in an entire score range for every lesion type of 0–24. Erosions were graded on a scale of 0–3 per joint, ankylosis on a scale of 0–2 per joint, and subchondral sclerosis on a scale of 0–1 per joint. The mean of the 2 readers' scores was calculated.

Ethics committee approval. The study was approved by the central ethics committee of the federal state of Berlin (Landesamt für Gesundheit und Soziales, Ethikkommission Berlin; approval number ZS EK 14 EA4/100/05). Written consent was obtained from all patients.

Statistical analysis. The sacroiliitis sum score was calculated as the sum of the grades for the left and right SI joints (ranging from 0 [no signs of radiographic sacroiliitis in either SI joint] to 8 [total ankylosis of both SI joints]). The mean of 2 readers' sacroiliitis sum scores was used in the subsequent analysis. The following definitions of radiographic sacroiliitis progression were used: 1) absolute change in the sacroiliitis sum score, 2) progression of at least 1 grade in the absolute sacroiliitis sum score, 3) progression of at least 1 grade in at least 1 SI joint in the opinion of both readers, and 4) progression from nonradiographic axial SpA to radiographic axial SpA in the opinion of both readers. For definitions 2, 3, and 4, corresponding rates of "regression" were calculated.

To determine the interreader reliability of the radiographic sacroiliitis assessment, we calculated the intraclass correlation coefficients (ICCs) for the sacroiliitis sum score. To identify factors associated with radiographic sacroiliitis progression over time, a longitudinal linear mixed model analysis was performed. The change in the sacroiliitis sum score over a 2-year interval (with up to 3 such intervals per patient) was used as an outcome variable. Possible predictors of progression assessed at the

beginning of each 2-year interval were explored in the univariable and multivariable analyses. Predictor candidates included age, sex, HLA-B27 status, treatment with sulfasalazine in the first study year, duration of treatment with etanercept, intake of non-steroidal antiinflammatory drugs (NSAIDs), symptom duration, C-reactive protein (CRP) level, active and chronic inflammatory changes on MRI of the SI joints, and radiographic sacroiliitis sum score. Parameter estimates (β) with corresponding 95% confidence intervals (95% CIs) were calculated. Statistical analysis was performed using SPSS version 25 (IBM) and SAS version 9.4 (SAS Institute).

RESULTS

Patient characteristics. Of the 76 patients enrolled in the ESTHER study, a total of 55 patients had radiography of the SI joints performed at baseline. For 42 patients, at least 1 follow-up radiograph was available to assess progression of radiographic sacroiliitis. Radiographs were available to assess progression for 42 patients between baseline and year 2, for 32 patients between year 2 and year 4, and for 27 patients between year 4 and year 6. Fifteen patients (35.7%) were classified as having radiographic axial SpA and 27 patients (64.3%) were classified as having non-radiographic axial SpA at baseline based on radiographs of the SI joints. The characteristics of the patients included in this analysis were similar to those of the 76 patients in the ESTHER study (10). Table 1 summarizes the baseline characteristics of the patients.

Agreement between readers. There was good to excellent agreement between the 2 readers regarding the sacroiliitis sum score at all time points: baseline (ICC 0.83 [95% CI 0.71,

0.90]), year 2 (ICC 0.82 [95% CI 0.67, 0.90]), year 4 (ICC 0.72 [95% CI 0.45, 0.86]), and year 6 (ICC 0.76 [95% CI 0.49, 0.89]).

Radiographic sacroiliitis progression. The distribution of sacroiliitis sum scores at baseline is shown in Figure 1. The majority of the patients had low-level sacroiliitis and none of the patients had a complete ankylosis of SI joints (sacroiliitis sum score of 8), reflecting an early stage of the disease in the patients included in this analysis. The mean \pm SD change in sacroiliitis sum score was 0.13 ± 0.73 , -0.27 ± 0.76 , and -0.09 ± 0.68 from baseline to year 2, year 2 to year 4, and year 4 to year 6, respectively. The highest level of progression was observed in the period from baseline to year 2 and was clearly lower in the following years according to all 4 definitions of progression (Table 2). Similar results were obtained when progression was analyzed only in those patients for whom radiographs for all time points were available ($n = 27$) (change in sacroiliitis sum score 0.20 ± 0.72 between baseline and year 2, -0.22 ± 0.8 between year 2 and year 4, and -0.09 ± 0.68 between year 4 and year 6).

The change in the sacroiliitis sum score was higher over the first 2 years in patients who received etanercept during this period ($n = 24$) than in patients who were treated with sulfasalazine in the first year and then switched to etanercept in the second year ($n = 18$) (0.31 ± 0.62 versus -0.11 ± 0.82 ; $P = 0.04$). In the following years, no impact of sulfasalazine treatment in the initial study phase on radiographic sacroiliitis progression was observed.

Predictors of radiographic sacroiliitis progression.

A longitudinal mixed model analysis was performed in the entire group of patients with data on 2-year intervals from baseline till year

Table 1. Baseline characteristics of the patients with axial SpA in the ESTHER study who were included in the present analysis*

	All patients (n = 42)	Patients with nonradiographic axial SpA (n = 27)	Patients with radiographic axial SpA (n = 15)
Sex, no. (%) male	26 (62)	17 (63)	9 (60)
Age, mean \pm SD years	34.1 \pm 7.9	34.3 \pm 7.8	33.7 \pm 8.2
Symptom duration, mean \pm SD years	3.1 \pm 1.6	2.6 \pm 1.6	4.0 \pm 1.1†
No. (%) HLA-B27 positive	34 (81)	19 (70.4)	15 (100)‡
CRP, mean \pm SD mg/liter	11.2 \pm 15.4	10.2 \pm 15.5	13.0 \pm 15.7
Elevated CRP (>5 mg/liter), no. (%)	22 (52)	12 (44.4)	10 (66.6)
BASDAI, mean \pm SD (range 0–10)	5.6 \pm 1.2	5.6 \pm 1.2	5.5 \pm 1.2
ASDAS, mean \pm SD	3.3 \pm 0.8	3.3 \pm 0.8	3.4 \pm 0.6
No. treated with etanercept/no. treated with sulfasalazine during the first year	24/18	17/10	7/8

* The Mann-Whitney U test was used for statistical analysis of continuous variables, and Fisher's exact test was used for categorical variables. ESTHER = Etanercept versus Sulfasalazine in Early Axial Spondyloarthritis; CRP = C-reactive protein; BASDAI = Bath Ankylosing Spondylitis Disease Activity Index; ASDAS = Ankylosing Spondylitis Disease Activity Score.

† $P = 0.01$ versus patients with nonradiographic axial spondyloarthritis (SpA).

‡ $P = 0.04$ versus patients with nonradiographic axial SpA.

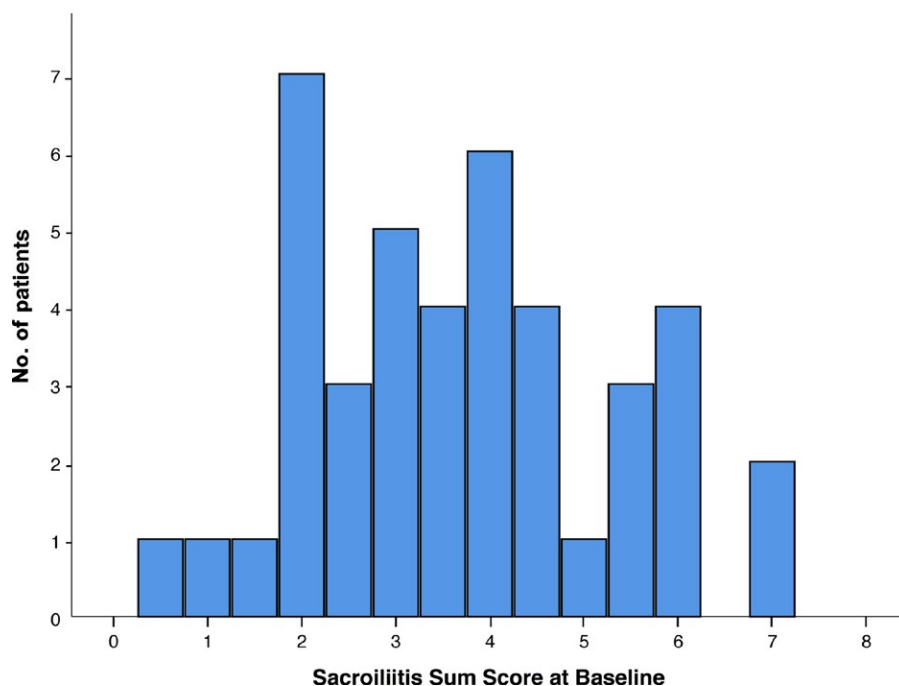


Figure 1. Distribution of the sacroiliitis sum score at baseline in patients with early axial spondyloarthritis from the Etanercept versus Sulfasalazine in Early Axial Spondyloarthritis trial (n = 42). Values are the mean of the scores from 2 readers.

6 to determine possible factors associated with a change in the total sacroiliitis sum score. In the univariable analysis, elevated CRP level ($\beta = 0.45$ [95% CI 0.14, 0.75]) and the SI joint osteitis score on MRI ($\beta = 0.05$ [95% CI 0.02, 0.08]) were significantly associated with an increase in the sacroiliitis sum score after 2 years.

For the multivariable analysis, we created 2 models; each one included one of the parameters reflecting inflammatory activity (CRP level or osteitis on MRI) that showed a significant association in the univariable analysis. Both models were adjusted for age, sex, HLA-B27 positivity, symptom duration, duration

of treatment with etanercept, NSAID intake, and the sacroiliitis sum score. The strength of the association for elevated CRP level and SI joint osteitis score on MRI was even greater than in the univariable analysis, with $\beta = 0.58$ (95% CI 0.24, 0.91) and $\beta = 0.06$ (95% CI 0.03, 0.10), respectively (Table 3).

DISCUSSION

This is the first study to analyze the long-term (up to 6 years) progression of radiographic sacroiliitis in patients with axial SpA

Table 2. Progression of radiographic sacroiliitis in patients with early axial SpA treated with etanercept for up to 6 years*

Definition of progression	Baseline to year 2 (n = 42)	Year 2 to year 4 (n = 32)	Year 4 to year 6 (n = 27)
Change in the sacroiliitis sum score, mean \pm SD	0.13 \pm 0.73	-0.27 \pm 0.76	-0.09 \pm 0.68
Progression \geq 1 grade in the sacroiliitis sum score			
Progression	9/42 (21.4)	2/32 (6.3)	3/27 (11.1)
Regression	4/42 (9.5)	7/32 (21.9)	5/27 (18.5)
Progression \geq 1 grade in at least 1 SI joint in the opinion of both readers			
Progression	5/42 (11.9)	1/32 (3.1)	0/27 (0)
Regression	1/42 (2.4)	4/32 (12.5)	1/27 (3.7)
Progression from nonradiographic axial SpA to radiographic axial SpA			
Progression	5/27 (18.5)	1/24 (4.1)	0/19 (0)
Regression	2/15 (13)	1/8 (12.5)	1/8 (12.5)

* Except where indicated otherwise, values are the number of patients/number for whom data were available (%). SpA = spondyloarthritis; SI = sacroiliac.

Table 3. Longitudinal mixed model analysis of the association between progression of radiographic sacroiliitis (change in the sacroiliitis sum score) and disease-related parameters in patients with early axial SpA treated with etanercept for up to 6 years*

Parameter	Univariable analysis, β (95% CI)	Multivariable analysis model 1, β (95% CI)	Multivariable analysis model 2, β (95% CI)
Age, years	0.00 (-0.02, 0.02)	-0.01 (-0.03, 0.01)	-0.01 (-0.03, 0.01)
Male sex	-0.04 (-0.35, 0.27)	-0.25 (-0.59, 0.09)	-0.05 (-0.37, 0.28)
Symptom duration, years	-0.01 (-0.08, 0.06)	0.06 (-0.04, 0.15)	0.06 (-0.03, 0.15)
HLA-B27 positivity	-0.08 (-0.47, 0.32)	-0.26 (-0.72, 0.20)	-0.33 (-0.78, 0.13)
CRP, mg/liter	0.01 (0.00, 0.03)	-	-
Elevated CRP (>5 mg/liter)	0.45 (0.14, 0.75)	-	0.58 (0.24, 0.91)
SI joint osteitis score on MRI (range 0–24)	0.05 (0.02, 0.08)	0.06 (0.03, 0.10)	-
SI joint fatty deposition score on MRI (range 0–24)	0.00 (-0.03, 0.02)	-	-
SI joint erosion score on MRI (range 0–6)	-0.01 (-0.09, 0.07)	-	-
SI joint sclerosis score on MRI (range 0–2)	-0.04 (-0.29, 0.22)	-	-
Treatment with sulfasalazine in the first study year	-0.15 (-0.46, 0.16)	-	-
Duration of etanercept treatment, years	-0.04 (-0.13, 0.04)	-0.06 (-0.20, 0.09)	-0.06 (-0.19, 0.06)
NSAID intake (yes versus no)	0.21 (-0.08, 0.51)	-0.03 (-0.41, 0.36)	-0.01 (-0.35, 0.34)
Sacroiliitis sum score (range 0–8)	-0.08 (-0.17, 0.01)	-0.17 (-0.28, -0.06)	-0.17 (-0.28, -0.06)

* Sacroiliac (SI) joint ankylosis score on magnetic resonance imaging (MRI) was not included in the analysis because ankylosis was not recorded in any of the cases. SpA = spondyloarthritis; 95% CI = 95% confidence interval; CRP = C-reactive protein; NSAID = nonsteroidal antiinflammatory drug.

treated with an anti-TNF agent, in this case with etanercept. Our results suggest that long-term treatment with a potent antiinflammatory drug like a TNF inhibitor may influence the evolution of the disease by decelerating radiographic progression in the SI joints in patients with early axial SpA.

In our analysis, progression of radiographic sacroiliitis occurred mostly in the first years of anti-TNF treatment; these results were consistent among all 4 definitions of progression used. For instance, progression from nonradiographic axial SpA to radiographic axial SpA occurred only in the first years of anti-TNF treatment. In 5 of 27 patients with nonradiographic axial SpA, the disease evolved into radiographic axial SpA in the first 2 years of the study, while in 2 of 15 patients radiographic axial SpA regressed to nonradiographic axial SpA over the same time period, giving a net progression (calculated according to the methodology of the Devenir des Spondylarthropathies Indifférenciées Récentes [DESIR] cohort) (7) of 7.1% $([5 - 2]/[27 + 15])$. In the following time intervals (year 2 to year 4 and year 4 to year 6), the progression rate did not exceed the measurement error.

The net progression rate of 7.1% within the first 2 years of the ESTHER study was higher than the 3.8% net progression

over 2 years in the German Spondyloarthritis Inception Cohort (GESPIC) and the 5.1% net progression over 5 years in the DESIR cohort (5,7). This might be related to 1) a higher degree of inflammation in the SI joints in the present study (the presence of active osteitis on MRI of the SI joint or spine was an inclusion criterion of the ESTHER study), and 2) treatment with a TNF inhibitor (which was not the case in the GESPIC and DESIR cohorts) that might have triggered a faster bone repair visible on radiographs as progression of structural damage. Our data also indicate a faster progression of radiographic sacroiliitis over 2 years in patients who received etanercept for 2 years compared to patients who received etanercept for 1 year following a 1-year treatment with sulfasalazine.

In another analysis of the 2-year progression rate from nonradiographic axial SpA to AS in patients treated with etanercept, the Study Comparing Etanercept Against a Placebo for Etanercept on a Background Nonsteroidal Antiinflammatory Drug in the Treatment of Early Spondyloarthritis Patients Who Do Not Have X-ray Structural Changes (EMBARK), almost no progression was reported over 2 years (8). This might again be related to a lower proportion of patients with active inflammation or a lower extent of inflammation on MRI of the SI joints, a known risk factor for pro-

gression of radiographic sacroiliitis (8,15), in the EMBARK study (16) as compared to the ESTHER population. The evidence of a deceleration of structural damage progression in the SI joint with increasing duration of anti-TNF therapy shown here seems congruent with the retardation of the spine progression seen in AS patients treated long-term with TNF inhibitors (9,17,18).

There is some evidence of the effect of NSAIDs on radiographic progression of the spine (19,20); however, its role is still a subject of debate (21). Currently, there are no data on its effect on radiographic progression in the SI joints; therefore, further studies are needed. In the ESTHER study, NSAID intake was recorded at every study visit for 1 previous week only. Thus, we could not quantify the NSAID intake using the Assessment of SpondyloArthritis international Society NSAIDs index (22), but we could include the NSAID intake itself (yes/no) recorded at each study visit in the longitudinal analysis. As a result, no association with radiographic progression in the SI joint was observed.

Our data from the longitudinal analysis, consistent with the findings of previous studies (5,8,15), showed a positive and independent association between elevated CRP level, the presence of osteitis on MRI, and progression of radiographic sacroiliitis in patients with early axial SpA. The level of osteitis on MRI could be reduced in these patients after 3 years of continuous treatment with etanercept, as previously described (23). Thus, these findings support the hypothesis that long-term treatment with TNF inhibitors could reduce new bone formation by preventing the development of new inflammatory lesions resulting in structural damage (24,25). The negative association between the baseline sacroiliitis sum score and its subsequent progression can be explained by a higher probability of progression within a given timeframe in patients with low-grade sacroiliitis (grade 0–1) compared to those with high-grade sacroiliitis (grade 2 and especially grade 3).

The clinical relevance of our results is related to the fact that evidence of inhibition of progression of structural damage in the SI joints (i.e., progression of radiographic sacroiliitis, progression from nonradiographic axial SpA to radiographic axial SpA) would mean disease modification in axial SpA. This is important in light of recent data suggesting that structural damage in the SI joint might have an impact on functional status and spinal mobility in patients with axial SpA, independent of structural damage to the spine (4).

The strength of our study is mainly related to the longitudinal analysis of data collected from a homogeneous group of patients with definite early axial SpA treated with a TNF inhibitor etanercept for up to 6 years; this aspect of the study is, to date, unique.

The major limitation of any analysis of radiographic progression in the SI joints, including ours, is the low reliability of radiographic assessment even in the case of well-trained and calibrated readers (26). Another limitation of our study is the small number of patients included in the analysis, due to the requirement of availability of radiographs from baseline and at least year 2, and the number of dropouts during the study. Nonetheless, 42 patients were assessed at up to 4 time points (3 two-year time

intervals), allowing a robust modeling of radiographic sacroiliitis progression and the identification of strong predictors. A further limitation of our study is related to the absence of a control group. Our data can only be indirectly compared to historical data from the GESPIC or DESIR cohorts, for instance. Patients enrolled in the ESTHER study had high disease activity and active inflammation confirmed by MRI despite the use of NSAIDs, which would have made a control group not treated with TNF inhibitors for years almost impossible.

In conclusion, the results presented here could indicate a reduction in radiographic progression in the SI joints over time in patients who received long-term anti-TNF treatment (for up to 6 years). An elevated CRP level and the presence of osteitis on MRI were the strongest predictors of radiographic sacroiliitis progression.

ACKNOWLEDGMENTS

We would like to thank ESTHER investigators Dr. R. Alten, Dr. M. Bohl-Bühler, Professor G-R. Burmester, Dr. T. Klopsch, Professor A. Krause, Dr. F. Mielke, Dr. U. Prothmann, and Dr. S. Zinke, former study physician Dr. In-Ho Song who did essential practical work in establishing the trial, and all of the patients who participated in the study for their contribution. We also thank Dr. A. Weiß and Dr. J. Listing for support in data management and statistical analysis. We are deeply thankful to B. Buß and P. Tietz for support monitoring and coordinating the study. We thank K. Ireland for editorial support.

AUTHOR CONTRIBUTIONS

All authors were involved in drafting the article or revising it critically for important intellectual content, and all authors approved the final version to be published. Dr. Rios Rodriguez had full access to all of the data in the study and takes responsibility for the integrity of the data and the accuracy of the data analysis.

Study conception and design. Rios Rodriguez, Sieper, Poddubnyy.

Acquisition of data. Rios Rodriguez, Hermann, Haibel, Althoff, Poddubnyy.

Analysis and interpretation of data. Rios Rodriguez, Weiß, Listing, Proft, Behmer, Poddubnyy.

ROLE OF THE STUDY SPONSOR

Pfizer had no role in the study design or in the collection, analysis, or interpretation of the data, the writing of the manuscript, or the decision to submit the manuscript for publication. Pfizer provided the study drug etanercept. Publication of this article was not contingent upon approval by Pfizer.

REFERENCES

1. Rudwaleit M, Landewe R, van der Heijde D, Listing J, Brandt J, Braun J, et al. The development of Assessment of SpondyloArthritis international Society classification criteria for axial spondyloarthritis (part I): classification of paper patients by expert opinion including uncertainty appraisal. *Ann Rheum Dis* 2009;68:770–6.
2. Rudwaleit M, van der Heijde D, Landewe R, Listing J, Akkoc N, Brandt J, et al. The development of Assessment of SpondyloArthritis interna-

- tional Society classification criteria for axial spondyloarthritis (part II): validation and final selection. *Ann Rheum Dis* 2009;68:777–83.
3. Van der Linden S, Valkenburg HA, Cats A. Evaluation of diagnostic criteria for ankylosing spondylitis: a proposal for modification of the New York criteria. *Arthritis Rheum* 1984;27:361–8.
 4. Protopopov M, Sieper J, Haibel H, Listing J, Rudwaleit M, Poddubnyy D. Relevance of structural damage in the sacroiliac joints for the functional status and spinal mobility in patients with axial spondyloarthritis: results from the German Spondyloarthritis Inception Cohort. *Arthritis Res Ther* 2017;19:240.
 5. Poddubnyy D, Rudwaleit M, Haibel H, Listing J, Marker-Hermann E, Zeidler H, et al. Rates and predictors of radiographic sacroiliitis progression over 2 years in patients with axial spondyloarthritis. *Ann Rheum Dis* 2011;70:1369–74.
 6. Dougados M, Demattei C, van den Berg R, Vo Hoang V, Thevenin F, Reijnierse M, et al. Rate and predisposing factors for sacroiliac joint radiographic progression after a two-year follow-up period in recent-onset spondyloarthritis. *Arthritis Rheumatol* 2016;68:1904–13.
 7. Dougados M, Sepriano A, Molto A, van Lunteren M, Ramiro S, de Hooge M, et al. Sacroiliac radiographic progression in recent onset axial spondyloarthritis: the 5-year data of the DESIR cohort. *Ann Rheum Dis* 2017;76:1823–8.
 8. Dougados M, Maksymowych WP, Landewe RB, Molto A, Claudepierre P, de Hooge M, et al. Evaluation of the change in structural radiographic sacroiliac joint damage after 2 years of etanercept therapy (EMBARK trial) in comparison to a contemporary control cohort (DESIR cohort) in recent onset axial spondyloarthritis. *Ann Rheum Dis* 2018;77:221–7.
 9. Baraliakos X, Haibel H, Listing J, Sieper J, Braun J. Continuous long-term anti-TNF therapy does not lead to an increase in the rate of new bone formation over 8 years in patients with ankylosing spondylitis. *Ann Rheum Dis* 2014;73:710–5.
 10. Song IH, Hermann K, Haibel H, Althoff CE, Listing J, Burmester G, et al. Effects of etanercept versus sulfasalazine in early axial spondyloarthritis on active inflammatory lesions as detected by whole-body MRI (ESTHER): a 48-week randomised controlled trial. *Ann Rheum Dis* 2011;70:590–6.
 11. Song IH, Althoff CE, Haibel H, Hermann KG, Poddubnyy D, Listing J, et al. Frequency and duration of drug-free remission after 1 year of treatment with etanercept versus sulfasalazine in early axial spondyloarthritis: 2 year data of the ESTHER trial. *Ann Rheum Dis* 2012;71:1212–5.
 12. Song IH, Hermann KG, Haibel H, Althoff CE, Poddubnyy D, Listing J, et al. Consistently good clinical response in patients with early axial spondyloarthritis after 3 years of continuous treatment with etanercept: longterm data of the ESTHER trial. *J Rheumatol* 2014;41:2034–40.
 13. Song IH, Hermann KG, Haibel H, Althoff CE, Poddubnyy D, Listing J, et al. Inflammatory and fatty lesions in the spine and sacroiliac joints on whole-body MRI in early axial spondyloarthritis: 3-year data of the ESTHER trial. *Semin Arthritis Rheum* 2016;45:404–10.
 14. Althoff CE, Sieper J, Song IH, Haibel H, Weiss A, Diekhoff T, et al. Active inflammation and structural change in early active axial spondyloarthritis as detected by whole-body MRI. *Ann Rheum Dis* 2013;72:967–73.
 15. Barkham N, Keen HI, Coates LC, O'Connor P, Hensor E, Fraser AD, et al. Clinical and imaging efficacy of infliximab in HLA-B27-positive patients with magnetic resonance imaging-determined early sacroiliitis. *Arthritis Rheum* 2009;60:946–54.
 16. Maksymowych WP, Dougados M, van der Heijde D, Sieper J, Braun J, Citera G, et al. Clinical and MRI responses to etanercept in early non-radiographic axial spondyloarthritis: 48-week results from the EMBARK study. *Ann Rheum Dis* 2016;75:1328–35.
 17. Maas F, Arends S, Wink FR, Bos R, Bootsma H, Brouwer E, et al. Ankylosing spondylitis patients at risk of poor radiographic outcome show diminishing spinal radiographic progression during long-term treatment with TNF- α inhibitors. *PLoS One* 2017;12:e0177231.
 18. Molnar C, Scherer A, Baraliakos X, de Hooge M, Micheroli R, Exer P, et al. TNF blockers inhibit spinal radiographic progression in ankylosing spondylitis by reducing disease activity: results from the Swiss Clinical Quality Management cohort. *Ann Rheum Dis* 2018;77:63–9.
 19. Wanders A, van der Heijde D, Landewe R, Behier JM, Calin A, Olivier I, et al. Nonsteroidal antiinflammatory drugs reduce radiographic progression in patients with ankylosing spondylitis: a randomized clinical trial. *Arthritis Rheum* 2005;52:1756–65.
 20. Poddubnyy D, Rudwaleit M, Haibel H, Listing J, Marker-Hermann E, Zeidler H, et al. Effect of non-steroidal anti-inflammatory drugs on radiographic spinal progression in patients with axial spondyloarthritis: results from the German Spondyloarthritis Inception Cohort. *Ann Rheum Dis* 2012;71:1616–22.
 21. Sieper J, Listing J, Poddubnyy D, Song IH, Hermann KG, Callhoff J, et al. Effect of continuous versus on-demand treatment of ankylosing spondylitis with diclofenac over 2 years on radiographic progression of the spine: results from a randomised multicentre trial (ENRADAS). *Ann Rheum Dis* 2016;75:1438–43.
 22. Dougados M, Simon P, Braun J, Burgos-Vargas R, Maksymowych WP, Sieper J, et al. ASAS recommendations for collecting, analysing and reporting NSAID intake in clinical trials/epidemiological studies in axial spondyloarthritis. *Ann Rheum Dis* 2011;70:249–51.
 23. Song IH, Hermann KG, Haibel H, Althoff CE, Poddubnyy D, Listing J, et al. Prevention of new osteitis on magnetic resonance imaging in patients with early axial spondyloarthritis during 3 years of continuous treatment with etanercept: data of the ESTHER trial. *Rheumatology (Oxford)* 2015;54:257–61.
 24. Maksymowych WP, Morency N, Conner-Spady B, Lambert RG. Suppression of inflammation and effects on new bone formation in ankylosing spondylitis: evidence for a window of opportunity in disease modification. *Ann Rheum Dis* 2013;72:23–8.
 25. Sieper J, Appel H, Braun J, Rudwaleit M. Critical appraisal of assessment of structural damage in ankylosing spondylitis: implications for treatment outcomes. *Arthritis Rheum* 2008;58:649–56.
 26. Van den Berg R, Lenczner G, Feydy A, van der Heijde D, Reijnierse M, Saraux A, et al. Agreement between clinical practice and trained central reading in reading of sacroiliac joints on plain pelvic radiographs: results from the DESIR cohort. *Arthritis Rheumatol* 2014;66:2403–11.

Sensitivity and Specificity of Autoantibodies Against CD74 in Nonradiographic Axial Spondyloarthritis

Elke Riechers,¹ Niklas Baerlecken,¹ Xenofon Baraliakos,² Katrin Achilles-Mehr Bakhsh,³ Peer Aries,⁴ Bettina Bannert,⁵ Klaus Becker,⁶ Jan Brandt-Jürgens,⁷ Jürgen Braun,² Boris Ehrenstein,⁸ Hans-Hartwig Euler,⁹ Martin Fleck,⁸ Reinhard Hein,¹⁰ Kirsten Karberg,⁷ Lars Köhler,³ Torsten Matthias,¹¹ Regina Max,¹² Adelheid Melzer,¹³ Dirk Meyer-Olson,¹⁴ Jürgen Rech,¹⁵ Karin Rockwitz,¹⁶ Martin Rudwaleit,¹⁷ Reinhold E. Schmidt,¹ Eva Schweikhard,¹¹ Joachim Sieper,¹⁸ Carsten Stille,³ Ulrich von Hinüber,¹⁹ Peter Wagener,¹⁰ Heike-Franziska Weidemann,³ Silke Zinke,⁷ and Torsten Witte¹

Objective. Autoantibodies against CD74 (anti-CD74) are associated with ankylosing spondylitis (AS). The present multicenter study, the International Spondyloarthritis Autoantibody (InterSpA) trial, was undertaken to compare the sensitivity and specificity of anti-CD74 and HLA-B27 in identifying patients with nonradiographic axial spondyloarthritis (axSpA).

Methods. Patients ages 18–45 years with inflammatory back pain of ≤ 2 years' duration and a clinical suspicion of axSpA were recruited. HLA-B27 genotyping and magnetic resonance imaging of sacroiliac joints were performed in all patients. One hundred forty-nine patients with chronic inflammatory back pain (IBP) not caused by axSpA served as controls, and additional controls included 50 AS patients and 100 blood donors whose specimens were analyzed.

Results. One hundred patients with inflammatory back pain received a diagnosis of nonradiographic axSpA from the investigators and fulfilled the Assessment of SpondyloArthritis international Society (ASAS) criteria. The mean age was 29 years, and the mean symptom duration was 12.5 months. The sensitivity of IgA anti-CD74 and IgG anti-CD74 for identifying the 100 axSpA patients was 47% and 17%, respectively. The specificity of both IgA anti-CD74 and IgG anti-CD74 was 95.3%. The sensitivity of HLA-B27 was 81%. The positive likelihood ratios were 10.0 (IgA anti-CD74), 3.6 (IgG anti-CD74), and 8.1 (HLA-B27). Assuming a 5% pretest probability of axSpA in chronic back pain patients, the posttest probability, after consideration of the respective positive test results, was 33.3% for IgA anti-CD74, 15.3% for IgG anti-CD74, and 28.8% for HLA-B27. A combination of IgA anti-CD74 and HLA-B27 results in a posttest probability of 80.2%.

Conclusion. IgA anti-CD74 may be a useful tool for identifying axSpA. The diagnostic value of the test in daily practice requires further confirmation.

INTRODUCTION

Axial spondyloarthritis (axSpA) is one of the most common inflammatory disorders, comprising ankylosing spondylitis (AS)

and nonradiographic axSpA, with a prevalence of 0.5–1.9% in the US and Europe (1). Classification of the disease relies mainly on imaging of the sacroiliac (SI) joints or on the presence of HLA-B27 (2). However, HLA-B27 may be present in up to 10% of healthy

Supported in part by AbbVie Deutschland GmbH.

¹Elke Riechers, MD, Niklas Baerlecken, MD, Reinhold E. Schmidt, MD, Torsten Witte, MD: Hannover Medical School, Hannover, Germany; ²Xenofon Baraliakos, MD, Jürgen Braun, MD: Ruhr University Bochum, Rheumazentrum Ruhrgebiet, Herne, Germany; ³Katrin Achilles-Mehr Bakhsh, MD, Lars Köhler, MD, Carsten Stille, MD, Heike-Franziska Weidemann, MD: Hannover, Germany; ⁴Peer Aries, MD: Rheumatologie Struensee-Haus, Hamburg, Germany; ⁵Bettina Bannert, MD: University Medical Center Freiburg, Freiburg, Germany; ⁶Klaus Becker, MD: Kreiskrankenhaus Blaubeuren, Blaubeuren, Germany; ⁷Jan Brandt-Jürgens, MD, Kirsten Karberg, MD, Silke Zinke, MD: Berlin, Germany; ⁸Boris Ehrenstein, MD, Martin Fleck, MD: University Hospital Regensburg, Asklepios Klinikum Bad Abbach, Bad Abbach, Germany; ⁹Hans-Hartwig Euler, MD: Hamburg, Germany; ¹⁰Reinhard Hein, MD, Peter Wagener, MD: Nienburg, Germany; ¹¹Torsten Matthias, PhD, Eva Schweikhard, PhD: Aesku Diagnostics GmbH, Wendelsheim, Germany; ¹²Regina Max, MD: University Hospital Heidelberg,

Heidelberg, Germany; ¹³Adelheid Melzer, MD: Seesen, Germany; ¹⁴Dirk Meyer-Olson, MD: Fachklinik Bad Pyrmont, Bad Pyrmont, Germany; ¹⁵Jürgen Rech, MD: Universitätsklinikum Erlangen, Erlangen, Germany; ¹⁶Karin Rockwitz, MD: Goslar, Germany; ¹⁷Martin Rudwaleit, MD: Klinikum Bielefeld Rosenhöhe, Bielefeld, Germany; ¹⁸Joachim Sieper, MD: Charité Universitätsmedizin Berlin, Berlin, Germany; ¹⁹Ulrich von Hinüber, MD: Hildesheim, Germany.

Drs. Baerlecken and Witte share a patent on the commercial use of antibodies against CD74. Drs. Matthias and Schweikhard own stock or stock options in Aesku Diagnostics. No other disclosures relevant to this article were reported.

Address correspondence to Torsten Witte, MD, Clinic for Immunology and Rheumatology, Medical University Hannover, Carl-Neuberg Street 1, 30625 Hannover, Germany. E-mail: Witte.torsten@mh-hannover.de.

Submitted for publication June 19, 2017; accepted in revised form November 6, 2018.

individuals in Central Europe and the US (3–5). In addition, the prevalence of HLA–B27 is low in many other populations, even in patients diagnosed as having axSpA (5,6). Magnetic resonance imaging (MRI) allows the early detection of inflammatory changes in the SI joints and is therefore frequently used for early identification of axSpA (7). Use of the current diagnostic algorithms has been associated with a delay of 5–10 years between the onset of inflammatory back pain (IBP) and the diagnosis of axSpA (8,9). Recent awareness campaigns about the condition may have shortened this interval (10).

We previously identified autoantibodies against CD74 as highly prevalent markers in patients with established AS (11). CD74 plays a role in the assembly of major histocompatibility complex (MHC) class II and in preventing premature binding of peptides to MHC class II. In addition, CD74 has an impact on B cell differentiation (11,12). Cell surface–expressed CD74 is the receptor of the macrophage migration inhibitory factor (MIF). Binding of MIF to CD74 leads to activation of NF- κ B, elevated Bcl-x_L expression, and cell proliferation. In order to examine whether anti-CD74 is a suitable diagnostic marker of nonradiographic axSpA, we conducted the International Spondyloarthritis Autoantibody (InterSpA) trial with patients who had IBP (lasting for ≤ 2 years) and in whom there was a high clinical suspicion of axSpA.

PATIENTS AND METHODS

Patients. Recruitment for the InterSpA trial occurred from February 2013 to August 2015. The study was approved by the local ethics committee of the Medical University of Hannover (project number 6330), and patients provided informed written consent for participation in the trial. Overall, 204 patients who had IBP were prospectively recruited by 22 rheumatology providers in Germany. For each patient, a single visit was conducted, at which time demographics, medical history, and clinical and laboratory data were collected. MRI of the SI joints had to be performed within 6 months prior to (or up until the day of) the study visit.

Inclusion criteria were an age of 18–45 years at the time of study visit and the presence of IBP (according to the Assessment of SpondyloArthritis international Society [ASAS] Berlin criteria) (12,13), with a duration of 3–25 months. Exclusion criteria were other inflammatory rheumatic diseases, prior treatments with biologic drugs, treatment with oral glucocorticoids (prednisolone > 10 mg per day) in the previous 4 weeks, contraindications to MRI (e.g., claustrophobia, gadolinium intolerance), pregnancy and lactation, and the presence of radiographic axSpA. The conventional radiographs of the SI joints were evaluated locally.

One hundred patients fulfilled the ASAS criteria and were regarded as having nonradiographic axSpA by the recruiting rheumatologists (see Results for full details). Twenty-four patients did not meet these axSpA prerequisites and served as part of the control population. After the InterSpA study was concluded, further sera were obtained from 125 patients with chronic IBP

lasting for ≤ 2 years, who did not fulfil the ASAS criteria. These patients and the 24 patients from the InterSpA trial formed the control group. Sera from 100 blood donors were also collected as controls. The mean age of blood donors was 38.9 years, 56% were male, and the presence of back pain was unknown among this population. Potential blood donors were asked about medication use, and those who had taken nonsteroidal antiinflammatory drugs (NSAIDs) or analgesics within 7 days were excluded from blood donation. In addition, sera from 50 AS patients (with a disease duration of ≥ 10 years) were collected as further controls. The mean age of these patients was 52.3 years, and 82% were male.

Clinical assessments. Demographic and clinical information collected included patient age, sex, ethnicity, date of onset and location of IBP, history of diseases possibly associated with sacroiliitis (e.g., psoriasis, peripheral arthritis, enthesitis, uveitis, dactylitis, ulcerative colitis, or Crohn's disease), current infections, family history of SpA, current treatment with NSAIDs, and response to medication (NSAIDs, analgesics, or glucocorticoids). The physical examination included recording of IBP symptoms, examination for number of tender joints (of 62) and swollen joints (of 64), and assessment of enthesitis at the sternoclavicular joints, seventh sternocostal joints, and proximal insertion of the Achilles tendons. Furthermore, spinal mobility was assessed by the Bath Ankylosing Spondylitis Metrology Index (BASMI) (14). Diagnosis of axSpA by a rheumatologist, which was made after the patient was examined (when the results of HLA–B27 testing and the MRI evaluation by a local radiologist became available), was recorded as a binary variable (axSpA, yes/no). Disease activity was measured by the Bath Ankylosing Spondylitis Disease Activity Index (BASDAI) (15) and by the Bath Ankylosing Spondylitis Patient Global Score (BAS-G) (16), both of which rely on patient-reported measures.

Laboratory assessments. Erythrocyte sedimentation rate, C-reactive protein (CRP) level, and HLA–B27 were assessed and documented in all patients locally. For detection of HLA–B27 in the blood donors, we used GenoQuick HLA–B27 (catalog no. 31196, version 2.0; Hain Lifescience). For the examination of antibodies against CD74, serum from all patients was frozen within 30 minutes after blood withdrawal and was stored at -20°C . Serum IgA was measured centrally on a BN ProSpec System (Siemens Healthineers) (normal reference range 0.7–4.0 gm/liter).

Imaging. MRI was performed, and images were evaluated for positive results according to the ASAS definition (17). T1-weighted and STIR sequences were available. All images were read by a central reader and a local reader. The central reader was blinded with regard to clinical data, laboratory data, and other patient data, including the presence of CD74 antibodies. Only images on which the central reader and the local reader were in agreement were included in the final group for analysis.

Laboratory methods for measuring CD74 antibodies. For the measurement of IgA antibodies against CD74, a commercially available AESKULISA SpA Detect kit (RAF 3190; Aesku Diagnostics) was used. This kit uses recombinant human CD74 as antigen. A total of 10 μ l of the serum was diluted in 1 ml of sample buffer (Aesku Diagnostics), and 100 μ l of the diluted serum was added to the well for 30-minute incubation at room temperature. The sample was then skipped and the wells were washed 3 times with Aesku washing solution. Thereafter, 100 μ l of horseradish peroxidase (HRP)-conjugated anti-human IgA was added to each well for 30 minutes, the conjugate was skipped, and the wells were washed 3 times with Aesku washing solution. Tetramethylbenzidine (TMB) solution was added for 30 minutes. After addition of stop solution, an enzyme-linked immunosorbent assay (ELISA) reader was used to measure optical density (OD). An OD standard of 0–3.0 was applied to the measured ODs.

To measure IgG antibodies against CD74, the AESKULISA SpA Detect kits were also used. However, instead of using a conjugate binding to human IgA, 100 μ l of HRP-conjugated goat anti-human IgG (heavy and light chain) secondary antibody (Jackson ImmunoResearch) was added in a dilution of 0.5 μ l IgG per 20 ml 1% bovine serum albumin.

In order to measure immune complexes of soluble CD74 and IgG antibodies against CD74, rabbit anti-human CD74 serum (Sino Biological) was bound to Maxisorb ELISA plates overnight at a 1:1,000 dilution (100 μ l/well). The plates were blocked with 300 μ l phosphate buffered saline (PBS)/well with 10% rabbit serum. After thorough washing, 100 μ l of the sera diluted 1:20 in PBS and 1% rabbit serum was incubated on the plates for 30 minutes. After a further washing, a purified peroxidase-labeled rabbit anti-human IgG serum (Jackson ImmunoResearch) was added at a 1:1,000 dilution in PBS for 30 minutes. Following an additional washing, the plates were developed with TMB solution and the ODs were measured.

For the measurement of immune complexes containing IgA antibodies against CD74 and soluble CD74, a similar protocol was used. However, a purified peroxidase-labeled rabbit serum against human IgA (Jackson ImmunoResearch), instead of against IgG, was used.

Statistical analysis. The upper limit of the normal range in the ELISA measuring IgA anti-CD74 and IgG anti-CD74 antibodies was defined as the OD value that was observed in <5% of the 149 controls with back pain but without axSpA. The significance of the difference in IgA and IgG antibody levels in axSpA patients and the IBP controls was calculated using the Mann-Whitney 2-tailed U test, and the significance of the difference in HLA-B27 status between the 2 groups was calculated using Fisher's exact test. We calculated the association between IgA antibodies against CD74 and axSpA, and between total IgA and axSpA, by univariate and multivariate logistic regression with both forward selection and backward elimination.

The positive and negative likelihood ratios (LRs) of HLA-B27, IgA antibodies against CD74, and IgG antibodies against CD74 were calculated. Posttest probabilities were calculated from the positive LR and the assumption that the prevalence of axSpA in IBP controls is 5%, using a method described by Rudwaleit et al (18).

RESULTS

A total of 204 patients with IBP were recruited. Eighty of these patients could not be evaluated due to the following reasons: they did not fulfill the inclusion criteria (or did fulfill the exclusion criteria) (39 of 204 patients), they had no evaluable MRI (10 of 204 patients), or they had divergent MRI results (31 of 204 patients). The remaining 124 patients had an evaluable MRI with consistent SI joint MRI assessments by the local reader and the trained specialist (XB). These patients were included in the evaluation of the study results. Patient characteristics are presented in Table 1.

Table 1. Patient characteristics*

	axSpA patients (n = 100)	IBP controls (n = 149)
Age, mean years	28.8	42.7
Male sex	56	23
Duration of IBP, mean months	12.5	18.9
IBP duration \leq 12 months	55	22
History of uveitis, peripheral arthritis, psoriasis, dactylitis, inflammatory bowel disease, and/or enthesitis	31	8
Family history of SpA	19	6
TJC \geq 1/SJC \geq 1†	25/8	20/0
BASDAI score, mean \pm SD	4.2 \pm 1.7	6.1 \pm 1.5
Good response to NSAIDs‡	81	23
Normal CRP level	64	87
HLA-B27 positive	81	10
Positive sacroiliitis MRI§	81	3

* Except where indicated otherwise, values are the % of patients. axSpA = axial spondyloarthritis; IBP = inflammatory back pain; BASDAI = Bath Ankylosing Spondylitis Disease Activity Index; CRP = C-reactive protein.

† Tender joint count (TJC) out of 62 joints, swollen joint count (SJC) out of 64 joints.

‡ Only patients treated with nonsteroidal antiinflammatory drugs (NSAIDs) were considered for this metric.

§ Three consistent positive magnetic resonance imaging (MRI) assessments of sacroiliac joints from a local reader and trained specialist.

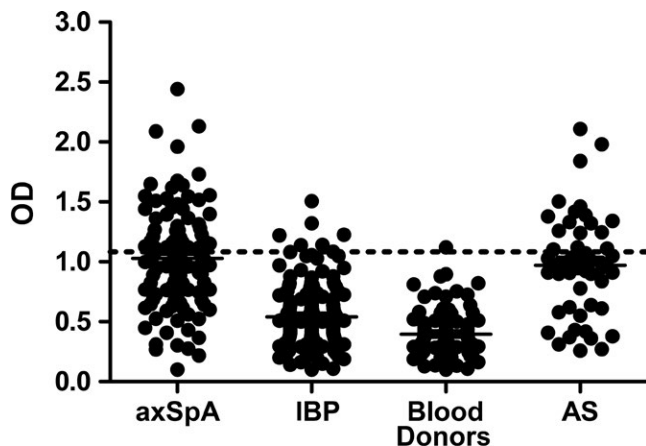


Figure 1. IgA anti-CD74 antibodies detected in 100 nonradiographic axial spondyloarthritis (axSpA) patients (diagnosed by a rheumatologist and fulfilling the Assessment of SpondyloArthritis international Society criteria), in 149 controls with inflammatory back pain (IBP), in 100 blood donors, and in 50 ankylosing spondylitis (AS) patients. The mean ODs in the axSpA patients were significantly higher than those in the IBP controls ($P < 0.0001$). Symbols represent individual subjects; bars show the mean \pm SD. Broken line represents the upper reference limit.

Of the 124 patients with IBP, 100 (80.6%) had been diagnosed as having nonradiographic axSpA by the investigators and fulfilled the ASAS criteria. Fifty-eight of these 100 patients fulfilled both the imaging and the clinical elements of the ASAS criteria, 23 fulfilled only the imaging element, and 19 fulfilled only the clinical element. Sixty-four of these 100 patients had normal CRP levels. The 24 patients who did not fulfill the ASAS criteria for axSpA and/or were not regarded as having axSpA by the investigators, in addition to 125 patients with chronic IBP not caused by axSpA who were recruited later, served as the IBP control group (Table 1).

Next, we calculated the frequency of IgA anti-CD74 antibodies, IgG anti-CD74 antibodies, and HLA-B27 in all patients with nonradiographic axSpA (according to investigator diagnosis and fulfillment of ASAS criteria; $n = 100$), as well as in the subgroups of patients fulfilling both the imaging and clinical elements of the ASAS criteria ($n = 58$), those fulfilling only the imaging element ($n = 23$), and those fulfilling only the clinical element ($n = 19$), and in the control groups (149 IBP patients without axSpA, 100 blood donors, and 50 AS patients). Cutoffs were defined as values higher than the 95th percentile of the OD values in the 149 IBP controls without axSpA. Results are presented in Figures 1 and 2.

OD values of IgA antibodies against CD74 were significantly higher in axSpA patients than in IBP controls ($P < 0.0001$). IgA antibodies against CD74 were present in 47% of all patients with nonradiographic axSpA, in 41.4% of patients fulfilling both the imaging and clinical elements of the ASAS criteria, in 52.2% of patients fulfilling only the imaging element, and in 57.9% of the patients fulfilling only the clinical element.

IgA antibodies against CD74 were present in 4.7% of the IBP controls, in 1% of the blood donors, and in 36% of the AS patients.

OD values of IgG antibodies against CD74 were higher in the axSpA group compared to the IBP controls ($P = 0.02$) (Figure 2). IgG antibodies against CD74 were present in 17% of all patients with nonradiographic axSpA, in 17.2% of patients fulfilling both the imaging and the clinical elements of the ASAS criteria, in 21.7% of patients fulfilling only the imaging element, and in 10.5% of the patients fulfilling only the clinical element. IgG antibodies against CD74 were present in 4.7% of the IBP controls, in 2% of the blood donors, and in 40% of the AS patients.

HLA-B27 was found in 81% of all patients with nonradiographic axSpA, in 100% of patients fulfilling both the imaging and the clinical elements of the ASAS criteria, in 17.4% of patients fulfilling only the imaging element, and in 100% of the patients fulfilling only the clinical element. HLA-B27 was detected in 10% of the IBP controls, in 8% of the blood donors, and in 90% of the AS patients.

From the results observed in our IBP control group, the specificity for identifying nonradiographic axSpA was 95.3% for IgA anti-CD74 antibodies, 95.3% for IgG anti-CD74 antibodies, and 90% for HLA-B27. IgA anti-CD74 and IgG anti-CD74 antibodies were not associated with HLA-B27. We calculated a positive LR for IgA anti-CD74 antibodies of 10.0 in all 100 nonradiographic axSpA patients, of 8.8 in patients fulfilling both imaging and clinical elements of the ASAS criteria, of 11.1 in patients fulfilling only the imaging element, and of 12.3 in patients fulfilling only the clinical element. The negative LRs for IgA anti-CD74 antibodies in each of these groups were 0.56, 0.61, 0.50, and 0.44, respectively.

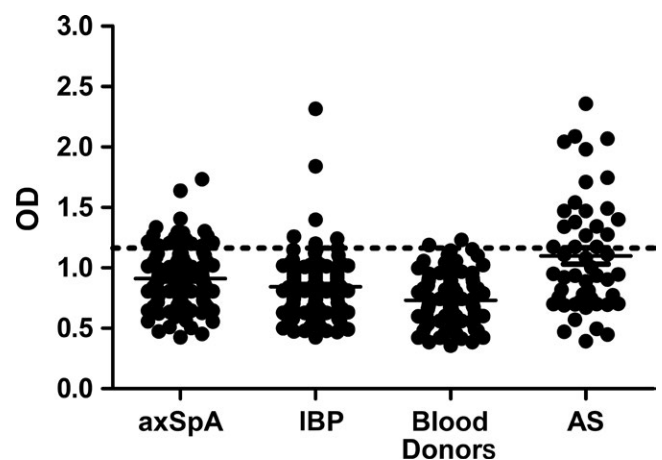


Figure 2. IgG anti-CD74 antibodies detected in 100 axSpA patients (diagnosed by a rheumatologist and fulfilling the Assessment of SpondyloArthritis international Society criteria), in 149 IBP controls, in 100 blood donors, and in 50 AS patients. Symbols represent individual subjects; bars show the mean \pm SD. Broken line represents the upper reference limit. See Figure 1 for definitions.

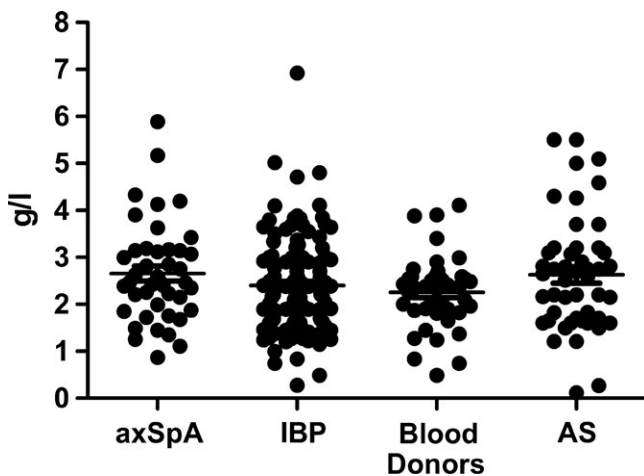


Figure 3. Serum IgA concentration detected in 44 axSpA patients (diagnosed by a rheumatologist and fulfilling the Assessment of SpondyloArthritis international Society criteria), in 145 IBP controls, in 44 blood donors, and in 50 AS patients. The mean IgA serum concentration was significantly higher in the axSpA patients than in the IBP controls. Symbols represent individual subjects; bars show the mean \pm SD. Broken line represents the upper reference limit. See Figure 1 for definitions.

The positive LR for IgG anti-CD74 antibodies was 3.6 in all 100 nonradiographic axSpA patients, 3.7 in patients fulfilling both imaging and clinical elements of the ASAS criteria, 4.6 in patients fulfilling only the imaging element, and 2.2 in patients fulfilling only the clinical element. The negative LRs for IgG anti-CD74 antibodies in each of these groups were 0.87, 0.87, 0.82, and 0.94, respectively.

The calculated positive LR for HLA-B27 was 8.1 in all 100 nonradiographic axSpA patients, 10.0 in patients fulfilling both imaging and clinical elements of the ASAS criteria, 1.7 in patients fulfilling only the imaging element, and 10.0 in patients fulfilling only the clinical element. The negative LRs for HLA-B27 in each of these groups were 0.21, 0, 0.92, and 0, respectively.

Assuming that the pretest probability of a diagnosis of axSpA in a group of patients with chronic back pain is 5%, the posttest probability after consideration of the respective positive test results would be 33.3% (IgA anti-CD74 antibodies), 15.3% (IgG anti-CD74 antibodies), and 28.8% (HLA-B27). Combination of the detected laboratory markers provided posttest probabilities of axSpA of 80.2% (IgA anti-CD74 antibodies and HLA-B27), 64.3% (IgA anti-CD74 antibodies and IgG anti-CD74 antibodies), 59.4% (IgG anti-CD74 antibodies and HLA-B27), and 93.6% (IgA anti-CD74 antibodies, IgG anti-CD74 antibodies, and HLA-B27).

IgA concentrations were measured in frozen samples after the evaluation of the study (nonradiographic axSpA, $n = 44$; IBP controls, $n = 145$; blood donors, $n = 44$; and AS patients, $n = 50$). The IgA concentrations were higher in axSpA patients than in IBP controls ($P < 0.05$) (Figure 3), even though only 11% of the

axSpA patients had IgA concentrations above the upper reference limit of 4.0 gm/liter. Furthermore, the OD values of IgA anti-CD74 antibodies correlated with the IgA concentrations in serum (not shown). After logistic regression that took into account both parameters, only IgA anti-CD74 antibodies remained significantly associated with axSpA.

DISCUSSION

Results from the InterSpA trial show that IgA anti-CD74 may be a useful diagnostic tool to identify axSpA in early stages of the disease. The sensitivity of 47% and the good LR of IgA anti-CD74, which is comparable to the LR of HLA-B27, suggest a diagnostic benefit. The combination of positive test results for both IgA anti-CD74 and HLA-B27, which we found in 34% of axSpA patients, yields a posttest probability of $>80\%$ and appears to be a fast and easy way to make a diagnosis of axSpA.

IgG antibodies against CD74 did not clearly distinguish axSpA from other causes of chronic IBP, and the sensitivity of IgG antibodies against CD74 was lower than expected based on results from an earlier study in which we used sera that had been frozen (most samples for 10 years) (12). Subsequently, we have been able to show that in freshly obtained sera, a large proportion of anti-CD74 antibodies are bound to soluble CD74 (see Supplementary Figures 1 and 2, on the *Arthritis & Rheumatology* web site at <http://onlinelibrary.wiley.com/doi/10.1002/art.40777/abstract>) and therefore are not detectable by the ELISA measuring only free antibodies against CD74 described here. The immune complexes of anti-CD74 and soluble CD74 may be broken by the long freezing procedure, so that free antibodies against CD74 are released and detectable by conventional ELISAs. In order to measure the presumably low amounts of free antibodies against CD74, we modified the original ELISA and used complete recombinant CD74 instead of only a peptide, in order to increase the number of epitopes available for antibody binding. The rather low proportion of nonradiographic axSpA patients with IgG antibodies in this study may suggest that IgA antibodies are formed ahead of IgG antibodies, but it could also be reflective of a technical problem due to the low concentration of antibodies in the sera.

The average OD values of IgA anti-CD74 were higher in the IBP control group than in the blood donors. At our institution, blood donors were not accepted if they had taken anti-inflammatory or analgesic drugs within 7 days, which suggests that they may have been negatively selected with regard to the presence of back pain, compared to the general population. It remains unclear whether antibodies against CD74 are associated with back pain generally or with axSpA specifically. Therefore, further studies should be performed to investigate the prevalence of IgA anti-CD74 in subsets of back pain patients with prospective follow-up to assess possible development of axSpA.

The average serum IgA level was also higher in the axSpA group than in IBP controls, but IgA anti-CD74 was still associated with axSpA after correction for the serum IgA concentration. This finding is inconsistent with results from a recent study on Dutch patients with chronic back pain (19). In that study, the rate of HLA-B27 positivity was ~2–3 times higher in the back pain control group than in the general Dutch population. This suggests that the distinction between axSpA and non-axSpA patients from the pool of back pain patients may not have been perfect and may partially account for the finding of a higher proportion of back pain patients with antibodies against CD74. The fact that total serum IgA levels were also elevated in axSpA in both studies suggests that the formation of antibodies against CD74 is part of a wave of other IgA antibodies forming. It will be interesting to analyze the specificity of the other IgA antibodies by protein array technology and to assess whether other antibodies that may participate in the pathogenesis of axSpA are produced.

Another open question is whether antibodies against CD74 are involved in the pathogenesis of axSpA. CD74 is the receptor of the chemokine macrophage migration inhibitory factor (MIF) (20). MIF concentrations have been found to be higher in the sera of axSpA patients compared to healthy controls (21,22). MIF stimulates osteoblasts (23) and therefore may be involved in the increased ossification observed in axSpA. Indeed, elevated MIF concentrations in the sera of patients with axSpA predict faster structural disease progression (22). Provided that antibodies against CD74 stimulate the same pathways as MIF, they may be involved in the progression of axSpA. In this regard, we have found an association of the presence of IgA anti-CD74 with the sacroiliitis grade and with the number of syndesmophytes in AS patients (24).

The trigger for the production of IgA anti-CD74 remains unclear. IgA antibodies are frequently produced in the gut. Thus, a dysbiosis of the gut microbiome may be responsible for IgA anti-CD74 production. It is possible that IgA antibodies against CD74 (and elevated concentrations of serum IgA) are markers of subsets of axSpA, for which the triggering factors differ. A study in which we compare the stool microbiomes of axSpA patients with and those without IgA anti-CD74 is currently being conducted.

In summary, IgA anti-CD74 may help to improve the value of HLA-B27 in diagnosing axSpA. Identification of IgA anti-CD74 antibodies without and, particularly, with, the simultaneous presence of HLA-B27 is a potentially useful diagnostic tool for practicing rheumatologists.

ACKNOWLEDGMENT

We are grateful to the Deutsche Forschungsgemeinschaft Klinische Forschergruppe (KFO 250; grant TP03) for supporting our biobank.

AUTHOR CONTRIBUTIONS

All authors were involved in drafting the article or revising it critically for important intellectual content, and all authors approved the final version to be published. Dr. Witte had full access to all of the data in the study and takes responsibility for the integrity of the data and the accuracy of the data analysis.

Study conception and design. Riechers, Baerlecken, Baraliakos, Braun, Rudwaleit, Sieper, Witte.

Acquisition of data. Riechers, Baerlecken, Baraliakos, Achilles-Mehr Bakhsh, Aries, Bannert, Becker, Brandt-Jürgens, Braun, Ehrenstein, Euler, Fleck, Hein, Karberg, Köhler, Matthias, Max, Melzer, Meyer-Olson, Rech, Rockwitz, Rudwaleit, Schmidt, Schweikhard, Sieper, Stille, von Hinüber, Wagener, Weidemann, Zinke, Witte.

Analysis and interpretation of data. Riechers, Baerlecken, Baraliakos, Braun, Rudwaleit, Sieper, Witte.

ROLE OF THE STUDY SPONSOR

AbbVie Deutschland GmbH & Co contributed to the study logistics and site management. The authors independently determined study design, conduct of the study, and the content of the publication. No payments were made to the authors for writing and presenting this contribution. Publication of this article was not contingent upon approval by AbbVie.

ADDITIONAL DISCLOSURES

Drs. Torsten Matthias and Eva Schweikhard are employees of Aesku Diagnostics GmbH.

REFERENCES

- Braun J, Bollow M, Remlinger G, Eggens U, Rudwaleit M, Distler A, et al. Prevalence of spondylarthropathies in HLA-B27 positive and negative blood donors. *Arthritis Rheum* 1998;41:58–67.
- Sieper J, van der Heijde D, Landewe R, Brandt J, Burgos-Vagas R, Collantes-Estevez E, et al. New criteria for inflammatory back pain in patients with chronic back pain: a real patient exercise by experts from the Assessment of SpondyloArthritis international Society (ASAS). *Ann Rheum Dis* 2009;68:784–8.
- Barkham N, Marzo-Ortega H, McGonagle D, Emery P. How to diagnose axial spondyloarthritis early. *Ann Rheum Dis* 2004;63:471–2.
- Trontzas P, Andrianakos A, Miyakis S, Pantelidou K, Vafiadou E, Garantziotou V, et al. Seronegative spondyloarthropathies in Greece: a population-based study of prevalence, clinical pattern, and management: the ESORDIG study. *Clin Rheumatol* 2005;24:583–9.
- De Angelis R, Salaffi F, Grassi W. Prevalence of spondyloarthropathies in an Italian population sample: a regional community-based study. *Scand J Rheumatol* 2007;36:14–21.
- Bakland G, Alsing R, Singh K, Nossent JC. Assessment of SpondyloArthritis International Society criteria for axial spondyloarthritis in chronic back pain patients with a high prevalence of HLA-B27. *Arthritis Care Res (Hoboken)* 2013;65:448–53.
- Blachier M, Coutanceau B, Dougados M, Saraux A, Bastuji-Garin S, Ferkal S, et al. Does the site of magnetic resonance imaging abnormalities match the site of recent-onset inflammatory back pain? The DESIR cohort. *Ann Rheum Dis* 2013;72:979–85.
- Braun J, Sieper J. Ankylosing spondylitis. *Lancet* 2007;369:1379–90.
- Dougados M, Baeten D. Spondyloarthritis. *Lancet* 2011;377:2127–37.
- Masson Behar V, Dougados M, Etcheto A, Kreis S, Fabre S, Hudry C, et al. Diagnostic delay in axial spondyloarthritis: a cross-sectional study of 432 patients. *Joint Bone Spine* 2017;84:467–71.

11. Baerlecken NT, Nothdorff S, Stummvoll GH, Sieper J, Rudwaleit M, Reuter S, et al. Autoantibodies against CD74 in spondyloarthritis. *Ann Rheum Dis* 2014;73:1211–4.
12. Baraliakos X, Baerlecken N, Witte T, Heldmann F, Braun J. High prevalence of anti-CD74 antibodies specific for the HLA class II-associated invariant chain peptide (CLIP) in patients with axial spondyloarthritis. *Ann Rheum Dis* 2014;73:1079–82.
13. Rudwaleit M, Metter A, Listing J, Sieper J, Braun J. Inflammatory back pain in ankylosing spondylitis: a reassessment of the clinical history for application as classification and diagnostic criteria. *Arthritis Rheum* 2006;54:569–78.
14. Jones SD, Porter J, Garrett SL, Kennedy LG, Whitelock H, Calin A. A new scoring system for the Bath Ankylosing Spondylitis Metrology Index (BASMI). *J Rheumatol* 1995;22:1609.
15. Garrett S, Jenkinson T, Kennedy LG, Whitelock H, Gaisford P, Calin A. A new approach to defining disease status in ankylosing spondylitis: the Bath Ankylosing Spondylitis Disease Activity Index (BASDAI). *J Rheumatol* 1994;21:2286–91.
16. Jones SD, Steiner A, Garrett SL, Calin A. The Bath Ankylosing Spondylitis Patient Global Score (BAS-G). *Br J Rheumatol* 1996;35:66–71.
17. Lambert RG, Bakker PA, van der Heijde D, Weber U, Rudwaleit M, Hermann KG, et al. Defining active sacroiliitis on MRI for classification of axial spondyloarthritis: update by the ASAS MRI working group. *Ann Rheum Dis* 2016;75:1958–63.
18. Rudwaleit M, Khan MA, Sieper J. The challenge of diagnosis and classification in early ankylosing spondylitis: do we need new criteria? *Arthritis Rheum* 2005;52:1000–8.
19. De Winter JJ, van de Sande MG, Baerlecken N, Berg I, Ramonda R, van der Heijde D, et al. Anti-CD74 antibodies have no diagnostic value in early axial spondyloarthritis: data from the spondyloarthritis caught early (SPACE) cohort. *Arthritis Res Ther* 2018;20:38.
20. Leng L, Metz CN, Fang Y, Xu J, Donnelly S, Baugh J, et al. MIF signal transduction initiated by binding to CD74. *J Exp Med* 2003;197:1467–76.
21. Kozaci LD, Sari I, Alacacioglu A, Akar S, Akkoc N. Evaluation of inflammation and oxidative stress in ankylosing spondylitis: a role for macrophage migration inhibitory factor. *Mod Rheumatol* 2010;20:34–9.
22. Ranganathan V, Ciccio F, Zeng F, Sari I, Guggino G, Muralitharan J, et al. Macrophage migration inhibitory factor induces inflammation and predicts spinal progression in ankylosing spondylitis. *Arthritis Rheumatol* 2017;69:1796–806.
23. Onodera S, Nishihira J, Iwabuchi K, Koyama Y, Yoshida K, Tanaka S, et al. Macrophage migration inhibitory factor up-regulates matrix metalloproteinase-9 and -13 in rat osteoblasts: relevance to intracellular signaling pathways. *J Biol Chem* 2002;277:7865–74.
24. Matthias T, Schweikhard E, Reuter S, Köhler M, Georgi J, Baerlecken NT, et al. Autoantibodies against CD74: a new diagnostic marker for spondyloarthritis (SpA) [abstract]. *Arthritis Rheumatol* 2016;68 Suppl 10. URL: <https://acrabstracts.org/abstract/autoantibodies-against-cd74-a-new-diagnostic-marker-for-spondyloarthritis-spa-2/>.

Comprehensive Longitudinal Surveillance of the IgG Autoantibody Repertoire in Established Systemic Lupus Erythematosus

Stefan Vordenbäumen,¹ Ralph Brinks,¹ Annika Hoyer,² Rebecca Fischer-Betz,¹ Georg Pongratz,¹ Torsten Lowin,¹ Hans-Dieter Zucht,³ Petra Budde,³ Ellen Bleck,¹ Peter Schulz-Knappe,³ and Matthias Schneider¹

Objective. To investigate the role of epitope spreading in established systemic lupus erythematosus (SLE).

Methods. IgG autoantibody reactivity with 398 distinct recombinant proteins was measured over a period of 6 years in 69 SLE patients and compared to that in 45 controls. Changes in mean fluorescence intensity (MFI), number of autoantibodies to distinct antigens, and reactivity with distinct clones of established antigenic targets (e.g., U1 RNP, Sm, and ribosomal P) representing epitope fine mapping were assessed. Linear mixed modeling, adjusted with Bonferroni correction for age and sex, was applied.

Results. The total number of autoantibodies, mean MFI, and number of autoantibodies in epitope fine mapping were higher in SLE patients compared to controls ($P < 0.0001$). The total number of antibodies to distinct autoantigens remained stable over time, while the mean MFI decreased over time in SLE ($P < 0.021$). SLE patients showed variable recognition of epitopes in fine mapping over time. In particular, in SLE patients, more clones of the U1 RNP complex were recognized at the time of new organ involvement (+0.65) ($P = 0.007$). Mean MFI was higher in patients with lupus nephritis ($P = 0.047$). The time-averaged MFIs of 22 individual autoantibodies (including double-stranded DNA [dsDNA]) were higher, after Bonferroni correction, in SLE ($P < 0.0001$). The MFIs of dsDNA and histone cluster 2 H3c were associated with scores on the Systemic Lupus Activity Measure ($P < 0.0001$).

Conclusion. Longitudinal surveillance of the IgG autoantibody repertoire in established SLE reveals evidence of sustained breadth of autoantibody repertoire without significant expansion. Associations of disease activity with dsDNA and with histone H3 autoantibodies were confirmed.

INTRODUCTION

Epitope spreading is a process by which the immune system increasingly targets previously tolerated or unrecognized epitopes of the same or different antigens (also known as intramolecular or intermolecular spreading, respectively) (1,2). Tissue damage following infections, immunoreactions, or autoimmune processes is thought to constitute a crucial event that incites an immune response against previously unrecognized or hidden antigenic targets (3). Systemic lupus erythematosus (SLE) is an autoimmune disease that features tissue damage caused by autoreactive T cells and B cells, in addition to a vast repertoire of autoantibodies. There is considerable evidence from animal studies that the breakdown of self toler-

ance to crucial antigens (particularly epitopes of small nuclear RNPs) results in epitope spreading and initiation of overt SLE (4–9). Similar mechanisms are likely to apply to human SLE as well, since autoantibodies to a few specific autoantigens are present in a preclinical state with significantly diversified autoantigenic targets at disease onset (2,10). However, genetic background and other potential triggers are important to consider, as epitope spreading in experimental or human SLE does not necessarily result in overt disease (2,11,12).

Unlike SLE initiation, little is known about how epitope spreading contributes to disease activity or disease course, once SLE is established. This is especially true for human SLE, and it has been suggested that the extent to which B cells contribute to epitope spreading and disease progression

Supported by the Hiller Research Foundation.

¹Stefan Vordenbäumen, MD, Ralph Brinks, PhD, Rebecca Fischer-Betz, MD, Georg Pongratz, MD, Torsten Lowin, PhD, Ellen Bleck, Matthias Schneider, MD: University Hospital Düsseldorf and Heinrich-Heine University Düsseldorf, Medical Faculty, Düsseldorf, Germany; ²Annika Hoyer, PhD: Heinrich-Heine University Düsseldorf, Düsseldorf, Germany; ³Hans-Dieter Zucht, PhD, Petra Budde, PhD, Peter Schulz-Knappe, MD: Protagen AG, Dortmund, Germany.

Drs. Zucht, Budde, and Schulz-Knappe own stock or stock options in Protagen AG. No other disclosures relevant to this article were reported.

Address correspondence to Stefan Vordenbäumen, MD, Hiller Research Center Rheumatology, Merowingerplatz 1a, 40225 Düsseldorf, Germany. E-mail: stefan.vordenbaeumen@med.uni-duesseldorf.de.

Submitted for publication March 1, 2018; accepted in revised form November 20, 2018.

should be further assessed (1). Therefore, in the present study, we performed high-content profiling of IgG autoantibodies in SLE patients over a period of 6 years and compared findings to those from healthy controls, and assessed associations of overall autoantibody reactivity and the number of distinct autoantibodies with the disease course.

PATIENTS AND METHODS

Samples. Two hundred consecutive patients with SLE were prospectively enrolled in an observational long-term study at the outpatient department of Heinrich-Heine University Düsseldorf. All patients fulfilled the American College of Rheumatology (ACR) 1997 revised criteria for SLE (13). For 69 patients, a complete data set comprising 4 standardized clinical visits and routine laboratory assessments over the course of 6 years was available. These cases were further analyzed. Samples from 45 healthy blood donors over the course of 4 years were available and served as controls (Table 1). Serum from patients and controls was obtained at enrollment and at 2-year intervals (at 2 years, at 4 years, and, for SLE patients only, at 6 years). A flare was defined as an increase in the Systemic Lupus Activity Measure (SLAM) (14) of >3 . New major organ involvement was defined as the onset of a new organ involvement with subsequent initiation of cyclophosphamide or mycophenolate mofetil. All serum samples were obtained by standard procedures and stored at -80°C until use. Informed patient consent was obtained, and the study was approved by the Ethics Committee of the Medical Faculty of Heinrich-Heine University Düsseldorf (study no. 2850).

Multiplex bead-based autoantibody detection.

Bead-based antigen arrays were used for the multiplex analysis of IgG autoantibody reactivity against 398 antigens representing 354 unique genes. In addition to well-described SLE-specific autoantigens, diagnostic antigens from other autoimmune diseases were selected based on literature data and autoantibody reactivity data identified in previous high-content profiling studies in rheumatoid arthritis and SLE (15,16). The full list of antigens is provided in Supplementary Table 1, available on the *Arthritis & Rheumatology* web site at <http://onlinelibrary.wiley.com/doi/10.1002/art.40788/abstract>. For some established SLE antigenic complexes, multiple clones were available (U1 RNP, $n = 6$; Sm, $n = 10$; ribosomal P, $n = 5$), representing different antigens within the target protein complex (Supplementary Table 1). Protocols for the expression, purification, and bead-coupling of proteins were applied as previously described (15,16). Briefly, antigens were produced in *Escherichia coli*, purified, and covalently coupled with magnetic carboxylated color-coded beads (MagPlex microspheres; Luminex). Antigen-coupled beads were combined, incubated with sera from probands, and after

Table 1. Baseline characteristics of the SLE patients ($n = 69$)*

General	
Age, mean \pm SD years	36.97 \pm 11.65†
Female	55 (79.7)‡
Disease duration, mean \pm SD years	14.74 \pm 23.04
Organ involvement	
Lupus nephritis	31 (47)
APS	13 (20)
Anemia	9 (14)
Cutaneous lupus	9 (14)
Arthritis	7 (11)
CNS lupus	7 (11)
Serositis	3 (5)
Medication	
Glucocorticoid use	41 (61)
Glucocorticoid dosage, mean \pm SD mg/day	7.3 \pm 13
Antimalarials	35 (52)
Azathioprine	16 (24)
Mycophenolate	4 (6)
Cyclophosphamide	5 (7)
Activity/damage parameters	
SLAM (range 0–81), mean \pm SD score	7.3 \pm 4.8
SDI (range 0–48), mean \pm SD score	1.7 \pm 2.2
dsDNA RIA, mean \pm SD units/ml	87.7 \pm 196.6

* Except where indicated otherwise, values are the number (%) of patients. SLE = systemic lupus erythematosus; APS = antiphospholipid syndrome; CNS = central nervous system; SLAM = Systemic Lupus Activity Measure; SDI = Systemic Lupus International Collaborating Clinics/American College of Rheumatology Damage Index; dsDNA RIA = double-stranded DNA radioimmunoassay.

† Mean \pm SD age of the healthy controls ($n = 45$) was 43 \pm 15 years.

‡ The number (%) of female healthy controls was 37 (82).

appropriate washing procedures, incubated with a secondary phycoerythrin-labeled anti-human IgG antibody. The beads were washed again and then analyzed in a FlexMap3D instrument (Luminex).

Statistical analysis. An antibody to a specific antigen was considered to be positive if the mean fluorescence intensity (MFI) was at least 2 SDs above the mean observed in healthy controls at baseline. Antibody reactivity as a measure of the immunoreaction intensity was obtained by calculating the number of positive antigenic targets, as well as the mean MFI of all positive targets, in SLE patients and healthy controls. Linear mixed modeling or generalized linear modeling was used for longitudinal comparison of patients and controls, including a random intercept to account for interindividual differences. The significance of group differences in categorical variables was determined by chi-square tests. Correlation of disease activity parameters with

longitudinal autoantibody measurements was assessed with a bivariate linear mixed model, and 95% confidence intervals (95% CIs) were calculated. The statistical software R (version 3.1; R Foundation) and SAS (SAS Institute) were used for analyses.

RESULTS

Patient characteristics. The SLE patient group ($n = 69$) was predominantly female (79.7%), with a mean \pm SD age of 37 ± 12 years at baseline. The mean \pm SD disease activity SLAM score was 7.3 ± 4.8 , and the mean \pm SD Systemic Lupus International Collaborating Clinics/ACR Damage Index (SDI) (17) was 1.7 ± 2.2 . The main organ involvement was lupus nephritis (47%). Patients were treated with antimalarials (52%), glucocorticoids (61%), and other immunosuppressants (at smaller rates) (Table 1). Over the course of the study, 8 patients (11.6%) showed an increase in the SDI by ≥ 2 points (mean increase \pm SD 2.6 ± 1.2), and 22 flares were observed.

New major organ involvement was observed in 13 patients: lupus nephritis ($n = 10$), central nervous system involvement ($n = 1$), severe myositis ($n = 1$), and severe pancytopenia ($n = 1$).

Autoepitope numbers over time. The number of distinct epitopes recognized by autoantibodies was assessed over time in SLE patients and healthy controls, in order to appraise changes in the total IgG autoantibody repertoire. Linear mixed models revealed that, on average, reactivity with 16.6 antigens was observed in controls, while reactivity with 68.5 distinct autoantigens was observed in SLE patients ($P < 0.0001$) (Figure 1A). This association remained significant after adjusting for age and/or sex (data not shown). Over time, controls lost reactivity with 0.44 antigens per year ($P = 0.77$), while SLE patients lost reactivity with 0.78 antigens per year ($P = 0.26$). Notably, the change in the number of autoepitopes recognized over time in both groups was not statistically significant. In order to explore the clinical significance of changes in the overall count of dis-

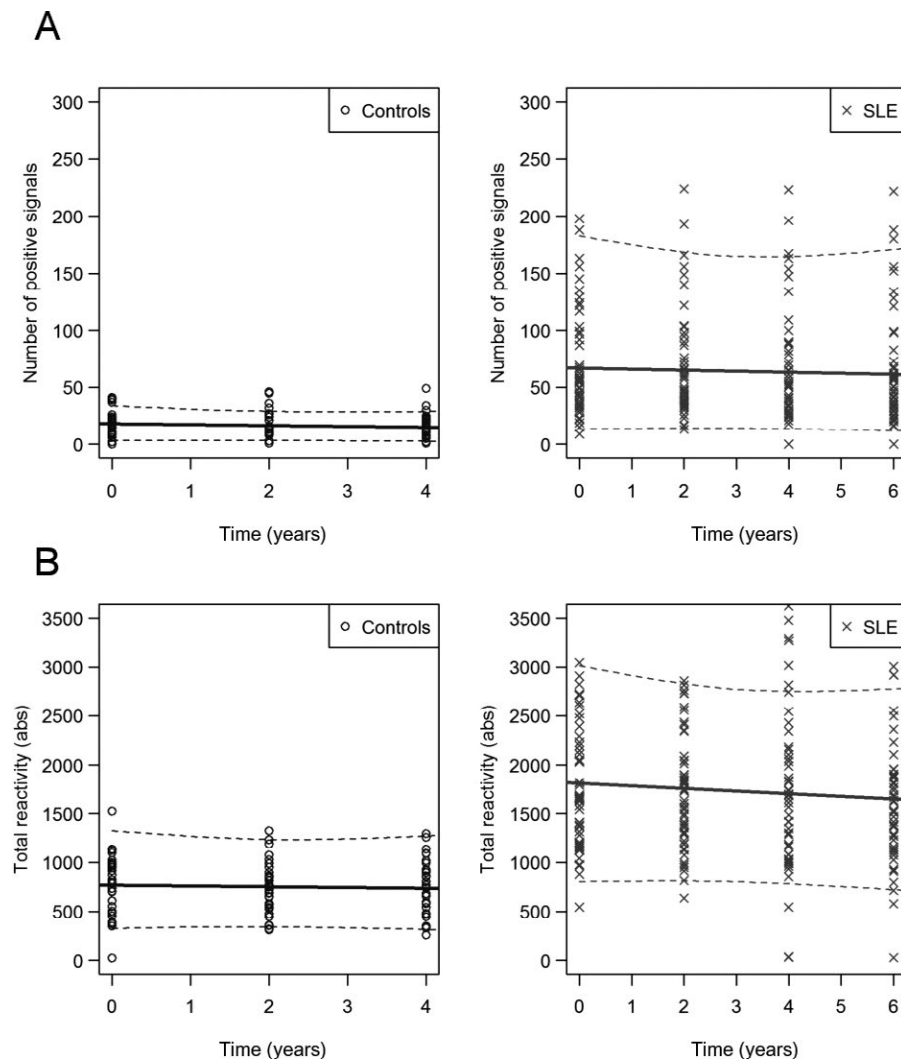


Figure 1. Number of positive autoantibodies (abs) (A) and mean fluorescence intensity of all positive autoantibodies (B) in individual healthy controls and systemic lupus erythematosus (SLE) patients over time. Solid and broken lines show the mean and 95% confidence intervals.

Table 2. Mean reactivity of IgG antibodies in SLE patients and healthy controls*

	Estimate	SE	<i>P</i>
Mean MFI at baseline			
Healthy controls	751.60	109.30	<0.0001
SLE patients	1,846.21	78.94	<0.0001
Change in mean MFI, time/group interaction			
Healthy controls	-1.82	24.92	0.94
SLE patients	-26.63	11.58	0.021

* Data were derived from linear mixed modeling. *P* values are for the comparison across groups over time. SLE = systemic lupus erythematosus; MFI = mean fluorescence intensity.

tinct epitopes recognized by autoantibodies, this parameter was compared to disease activity measures, such as dsDNA antibodies measured by radioimmunoassay, C3 and C4 complement levels, SLAM scores, and new major organ involvement in SLE patients. No significant correlation between the overall number of autoepitopes recognized and the above-mentioned disease activity parameters was found.

Additionally, we investigated (using bivariate linear mixed models) whether patients with a history of proliferative lupus nephritis at baseline ($n = 31$) showed different numbers of distinct

autoepitopes recognized over time, compared to SLE patients without nephritis ($n = 37$). The mean number of distinct autoantibodies measured was 61.5 in patients without nephritis and 74.9 in patients with nephritis ($P = 0.13$). There was no change over time ($P = 0.33$), and there were no differences between groups ($P = 0.41$).

Furthermore, we investigated whether gains or losses in the number of distinct epitopes recognized by autoantibodies differed between SLE patients and controls. Participants were assigned the following categories for each autoantibody based on the presence of the antibody over time: loss, gain, and stable. After Bonferroni correction, there were no significant differences regarding gains or losses between SLE patients and controls. Next, we explored whether gains or losses were associated with disease activity according to the SLAM or with the presence of lupus nephritis. The number of signals in each category (gain, loss, etc.) were compared between SLE patient groups (e.g., lupus nephritis versus no lupus nephritis, or SLAM above the median versus SLAM below the median) for each autoantibody. No significant differences were noted.

Overall autoantibody reactivity over time. The mean MFI across all autoantigens was calculated for each study participant as a measure of overall autoantibody reactivity. Subsequently, mean reactivities across groups were obtained. Bivariate linear mixed modeling (adjusted for age and sex) was

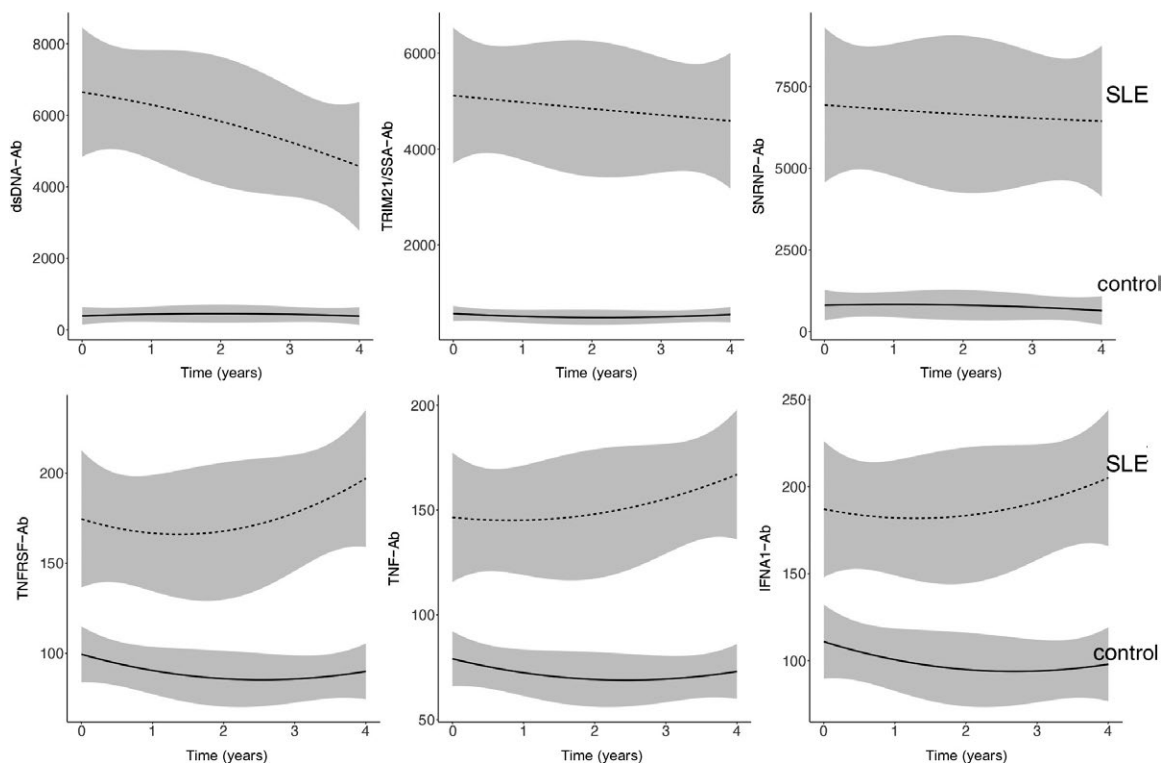


Figure 2. Autoantibody fluorescence over time. Mean trajectories of antibodies (Ab) against double-stranded DNA (dsDNA), SSA (TRIM21), small nuclear RNP U1 subunit 70 (SNRNP70), tumor necrosis factor (TNF) receptor superfamily member 1B (TNFRSF1B), TNF, and interferon- α 1 (INF-A1), in healthy controls and systemic lupus erythematosus (SLE) patients, are shown. Shaded areas represent 95% confidence intervals.

used to calculate regressions accounting for intraindividual correlations. As illustrated in Table 2 and Figure 1B, mean MFI was substantially higher in SLE patients than in healthy controls (1,846.2 versus 751.6, respectively; $P < 0.0001$). The decrease in mean MFI over time was significant in SLE patients (average decrease 26.63 per year; $P = 0.021$), but not in controls (average decrease 1.82 per year; $P = 0.94$).

Next, the number of autoantibodies to distinct antigens with increased reactivity over time was compared across groups. Increased reactivity was observed for 207 autoantibodies (52%) in SLE patients, but only 150 autoantibodies (37.7%) in controls ($P < 0.0001$ by chi-square test). In order to explore the clinical significance of changes in the overall autoantibody reactivity, this parameter was compared to disease activity measures (adjusted for total IgG). Trends toward associations with changes in autoantibody reactivity were noted for C3 (Pearson correlation coefficient -0.24 [95% CI $-0.49, -0.01$]) and C4 (-0.22 [$-0.48, -0.01$]), but not for SLAM

scores (0.2 [$-0.07, -0.48$]), dsDNA levels (0.13 [$-0.17, -0.42$]), or the SDI (0.11 [$-0.17, -0.39$]). Finally, we investigated whether patients with proliferative lupus nephritis ($n = 31$) at any time point showed different overall antibody reactivity compared to SLE patients without nephritis ($n = 37$), using linear mixed modeling. Lupus nephritis patients showed significantly more antibody reactivity ($2,072.5$ versus $1,715.5$; $P = 0.047$), with no significant change in reactivity over time.

Reactivity with distinct autoantigens over time.

We wished to determine if the reactivity of certain distinct autoantibodies over time in SLE patients differed significantly from that in healthy controls. Figure 2 illustrates differences in the antibody trajectories for selected antigenic targets. We noted a trend toward increased reactivity with cytokines such as tumor necrosis factor or the respective receptor, and a decline in antibodies targeting nuclear antigens such as dsDNA or SSA (Figure 2). The slope of individual autoan-

Table 3. Significant differences in time-averaged autoantigen reactivity between SLE patients and healthy controls*

Gene ID	Antigen	Fold change	<i>P</i>
<i>HNRNPA1</i>	Heterogeneous nuclear RNP A1	9.0	7.1×10^{-6}
<i>HNRNPA2B1</i>	Heterogeneous nuclear RNP A2/B1	8.8	1.4×10^{-5}
<i>SNRPB</i>	snRNP polypeptides B/B1	4.9	2.2×10^{-6}
<i>SNRPC</i>	snRNP polypeptides C	3.9	1.0×10^{-5}
<i>SNRPA</i>	snRNP polypeptides A	4.9	6.3×10^{-6}
<i>SNRNP70</i>	snRNP U1 subunit 70	12.3	7.5×10^{-5}
<i>NRBF2</i>	Nuclear receptor binding factor 2	5.0	9.7×10^{-6}
<i>HIST1H2AC</i>	Histone cluster 1 H2A family member C	2.9	1.4×10^{-5}
<i>HIST1H2BD</i>	Histone cluster 1 H2B family member D	2.6	4.5×10^{-5}
<i>HIST2H2BE</i>	Histone cluster 1 H2B family member E	2.6	4.3×10^{-6}
<i>TRIM21</i>	Ro52/SSA	8.6	5.2×10^{-6}
-†	dsDNA antibody	7.9	1.3×10^{-6}
-†	Cyclic citrullinated peptide	1.5	1.1×10^{-4}
<i>TNF</i>	TNF	2.2	1.8×10^{-5}
<i>TNFRSF1B</i>	TNF receptor superfamily member 1B	2.0	5.5×10^{-5}
<i>IFNA1</i>	IFN α 1	2.0	6.6×10^{-5}
<i>HSP90B1</i>	Heat-shock protein 90 beta family member 1	2.4	4.4×10^{-6}
<i>KDM6B</i>	Lysine demethylase 6B	7.0	3.4×10^{-6}
<i>NONO</i>	Non-POU domain containing octamer binding	3.7	6.8×10^{-5}
<i>SSX2</i>	SSX family member 2	8.4	6.7×10^{-6}
<i>GAD2</i>	Glutamate decarboxylase 2	2.3	9.8×10^{-6}
<i>LYZ</i>	Lysozyme	2.0	5.0×10^{-5}

* Values were calculated using linear mixed modeling, with adjustment for age and sex and Bonferroni correction for multiple testing. In instances in which reactivities with DNA clones targeted the same antigen, the best *P* value is given. Magnitude of difference is represented by fold change reactivity among systemic lupus erythematosus (SLE) patients compared to that among controls. snRNP = small nuclear RNP; TNF = tumor necrosis factor; IFN α 1 = interferon- α 1.

† Double-stranded DNA (dsDNA) and cyclic citrullinated peptides were acquired commercially and used as antigenic targets.

tibody reactivities was calculated by linear mixed regression and used to compare SLE patients to controls (with adjustment for age and sex). Overall, the slopes representing SLE patients and controls were significantly different ($P < 0.0001$ by Welch's modified 2-sample t -test). After Bonferroni correction, no significant differences for any distinct autoantibody remained. However, trends were noted for dsDNA (-415.7 in SLE patients versus 47.1 in controls; unadjusted $P = 0.039$). Notably, the time course of the antibody changes and the slope were not adjusted for disease activity at this point. We then compared time-averaged individual autoantibody reactivities between SLE and healthy controls, adjusting for age and sex by linear mixed modeling. A total of 22 distinct autoantigens were significantly different after Bonferroni correction (Table 3).

In order to explore whether the reactivity with distinct antigens over time relates to SLAM levels, SLE flares, new major organ involvement, or damage, linear mixed modeling was carried out for antibody levels against the above-mentioned 22 autoantigens (Table 3), with Bonferroni correction. SLAM scores were significantly associated with dsDNA antibodies (estimate 0.00017 ; $P < 0.0001$). Increased damage was significantly associated with lower nuclear receptor binding factor 2 (*NRBF2*) antibodies (estimate -0.000035 ; $P = 0.0009$). When all 398 antigenic targets were used for linear mixed modeling with the above-mentioned clinical activity parameters, associations were observed between SLAM and antibodies to dsDNA (estimate 0.00017 ; $P < 0.0001$), and between SLAM and histone cluster 2 H3c (*HIST2H3C*) (estimate 0.0011 ; $P < 0.0001$).

Epitope fine mapping. In order to investigate epitope spreading to distinct peptides within the same protein complex or subcellular localization, we selected proteins based on gene ontology molecular function terms. For certain established SLE antigenic complexes, multiple clones were available (e.g., U1 RNP, Sm, ribosomal P) (see Supplementary Table 1, <http://onlinelibrary.wiley.com/doi/10.1002/art.40788/abstract>). These clones represent slightly different antigenic targets within the target protein complex, and changes in the reactivity with these targets therefore represent intra-protein complex extensions of the patient's antibody repertoire (known as epitope fine mapping). The number of positive autoantibodies to the antigens produced with different clones was compared between SLE patients and healthy controls. SLE patients had significantly more autoantibodies to different antigenic targets of U1 RNP (estimate 0.77 ; $P < 0.0005$), Sm (estimate 1.69 ; $P < 0.0005$), and ribosomal P complexes (estimate 0.61 ; $P = 0.0031$), compared to healthy controls (Figure 3). Over time, the number of antibodies to the clones of certain complexes increased in SLE patients and decreased in controls but with no statistically significant differences: U1 RNP ($+0.02$ per year versus -0.04 per year, respectively; $P = 0.068$), Sm ($+0.02$ per year versus -0.02

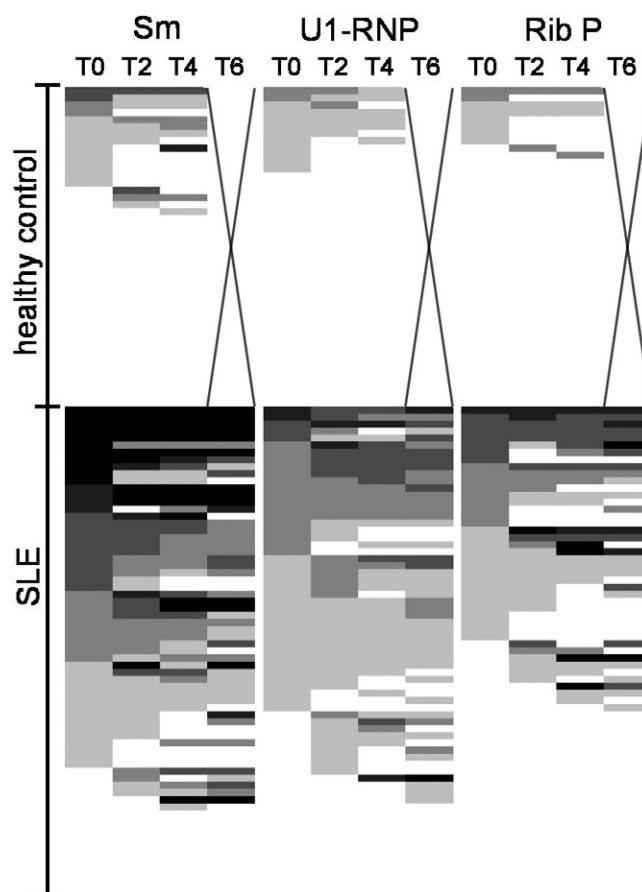


Figure 3. Results of epitope fine mapping in healthy controls and systemic lupus erythematosus (SLE) patients. The heatmap shows the number of IgG autoantibodies to distinct clones of Sm ($n = 10$), U1 RNP ($n = 6$), and ribosomal P (Rib P) ($n = 5$) in healthy controls and SLE patients over time (T0 = baseline, T2 = 2 years, T4 = 4 years, T6 = 6 years), ordered by respective reactivities. The range is represented by white blocks (no reactivity) and black blocks (maximum reactivity), with gradual gray shading in between. No samples were available for controls at T6.

per year; $P = 0.6$), and ribosomal P ($+0.02$ per year versus -0.02 per year; $P = 0.3$).

Within the SLE group, we investigated a potential association between the number of positive autoantibodies to the antigens produced with different clones and disease activity parameters such as SLAM, flare, and new major organ involvement (adjusted for age and sex). An increase in antibodies to the U1 RNP epitopes at the time of new organ involvement was observed ($+0.65$ [$P = 0.0068$] and $+0.39$ [$P = 0.066$] by multivariable and univariable analysis, respectively). The association did not reach significance for either Sm or ribosomal P.

DISCUSSION

Epitope spreading is considered to be a highly important aspect of the development of systemic autoimmune diseases. It is

conceivable that consecutive breakdowns of self tolerance to an increasing number of autoantigens following tissue damage result in a vicious circle (e.g., an unrestrained, autoreactive amplification loop) (18). Although there is ample evidence that supports this hypothesis for the initiation of systemic autoimmunity, there is considerably less information on how and to what extent epitope spreading contributes to long-term perpetuation of or deterioration in autoimmune diseases (1). Moreover, there may be differences in how epitope spreading contributes to ongoing disease activity among distinct autoimmune diseases; for example, studies on experimental encephalomyelitis showed that the recognition of new epitopes can be observed prior to disease relapses (3). Circumstantial evidence suggests that this may also be true for human autoimmune encephalomyelitis, as children with central demyelinating disease that evolved to chronic disease had an observable increase in their autoantigen repertoire, but there was a contraction if the event was monophasic (19). Similarly, previously detectable autoantibodies were shown to be lost in patients with mixed connective tissue disease in remission (20). In summary, findings from these studies suggest a connection between epitope spreading and disease activity.

In our study, no general increase in the number of autoantigens was observed in patients with established SLE, over a period of 6 years, and the total number of recognized autoepitopes did not correlate with disease activity. This seems to dispute the theory that an autoreactive amplification loop remains unrestrained in established disease. These findings are in line with an earlier observation made by Arbuckle et al, who conducted a study in which exclusively SLE-specific (routine) autoantibodies were tested in serum samples from 118 SLE patients prior to disease onset and up to 5 years after (10). Once a diagnosis was made, no significant increase in the number of autoantibodies was noted (10). Findings from a subsequent multiplex study of 65 antigens in 5 SLE patients over a period of 10–18 months, in which IgG autoantibody clustering remained stable (12), suggest that Arbuckle and colleagues' findings may extend to a larger panel of autoantigens. This is directly supported by a study by Yurasov et al, where it was shown that, in SLE, many self-reacting antibodies persist, even though the number of B cells expressing these autoantibodies is lower during remission than in active disease (21).

Most of the cited studies, and our findings that focus on a considerably larger IgG autoantibody repertoire, pertain to broad intermolecular epitope spreading. In contrast, in the present study, we observed in SLE patients a numerical increase over time in autoantibodies to very distinct epitopes within the selected antigenic complexes (i.e., U1 RNP, Sm, and ribosomal P), for which multiple clones were available. Moreover, new major organ damage coincided with an increase of U1 RNP peptide recognition.

In general, the level of a distinct autoantibody to an antigen or the more general antinuclear antibody titer is not thought to correlate with disease activity. An important exception to this has been observed with dsDNA antibodies, which demonstrate a clin-

ically useful association with more active SLE disease states (22). Despite a large number of tested antigens and no strict optimization of the assay specifically for dsDNA, our findings confirm that these antibodies can be used as measures of disease activity and flares. *HIST2H3C* showed similar properties and should be further assessed. Interestingly, we recently reported on the diagnostic potential of IgG antibodies to defined histone core components, including *HIST2H3C* in SLE (23). Furthermore, higher levels of antibodies to *NRBF2* (which was unphosphorylated in our experimental setting) were related to less damage over time. *NRBF2* is a regulator of autophagy, a cellular process for disassembly of dysfunctional cytosolic components (24). In its phosphorylated form, *NRBF2* inhibits autophagy, while promoting it in its unphosphorylated form (25). Intact autophagy, in turn, was recently reported to confer protection against autoimmune disorders such as lupus nephritis (26,27). Thus, one could speculate that *NRBF2* autoantibodies may have a protective role against damage acquisition by inhibiting *NRBF2* phosphorylation and thereby promoting autophagy.

Our study confirms that the level of dsDNA antibodies is a highly robust disease activity parameter, even when compared to a range of antibodies against almost 400 distinct autoantigens, and confirms that the total number of autoantibodies to distinct antigens remains stable in established disease. Additionally, our findings suggest that differences in fine specificity to selected autoantigens (e.g., intramolecular epitope spreading) may be a more sensitive correlate of disease activity in established SLE, as evidenced by increased epitope recognition of U1 RNP before new major organ involvement. Furthermore, they suggest that *HISTH3C* and *NRBF2* autoantibodies are associated with disease activity and with inhibition of damage acquisition, respectively, and should be further assessed.

This study has some limitations, including heterogeneity in the treatment of included SLE patients. For ethical reasons, restrictions on the treatment of individual patients with this heterogeneous disorder could not be applied over a period of 6 years. Major strengths of our study include the long-term surveillance of a considerable number of antigens, and the attempt to identify broad intermolecular epitope spreading and epitope fine mapping of selected pathogenetically relevant antigenic complexes. However, our methodologic approach of enzyme-linked immunosorbent assay-based detection of antibodies using different clones did not contain specific information regarding the epitope (e.g., protein folding), as would be available using x-ray crystallographic approaches, for example (28). Furthermore, we related the IgG autoantibody measurements for disease activity and damage as assessed by the SLAM or the SDI respectively. However, a rather stable clinical course was observed in our patients. Thus, we cannot exclude the possibility that expansion of the autoantibody repertoire may be observable in SLE patient cohorts with higher levels of disease activity. Our statistical approach using linear mixed modeling was chosen to overcome this drawback, at

least partially, by modeling individual disease activity changes in relation to concurrent autoantibody status. Finally, we did not control for potential cross-reactivities between the antigens assessed.

In conclusion, longitudinal surveillance of the IgG autoantibody repertoire in established SLE reveals evidence of sustained breadth of autoantibody repertoire without significant expansion. Epitope fine mapping shows continuous variability in the number of recognized epitopes to distinct antigenic complexes in SLE patients. U1 RNP epitope recognition relates to organ involvement. Associations of disease activity with dsDNA and histone H3 autoantibodies are confirmed.

AUTHOR CONTRIBUTIONS

All authors were involved in drafting the article or revising it critically for important intellectual content, and all authors approved the final version to be published. Dr. Vordenbäumen had full access to all of the data in the study and takes responsibility for the integrity of the data and the accuracy of the data analysis.

Study conception and design. Vordenbäumen, Brinks, Schneider.

Acquisition of data. Vordenbäumen, Fischer-Betz, Budde, Bleck, Schulz-Knappe.

Analysis and interpretation of data. Vordenbäumen, Brinks, Hoyer, Pongratz, Lowin, Zucht, Budde, Schulz-Knappe, Schneider.

ADDITIONAL DISCLOSURES

Drs. Zucht, Budde, and Schulz-Knappe are employees of Protagen AG.

REFERENCES

- Cornaby C, Gibbons L, Mayhew V, Sloan CS, Welling A, Poole BD. B cell epitope spreading: mechanisms and contribution to autoimmune diseases. *Immunol Lett* 2015;163:56–68.
- Greidinger EL, Hoffman RW. The appearance of U1 RNP antibody specificities in sequential autoimmune human antisera follows a characteristic order that implicates the U1–70 kd and B'/B proteins as predominant U1 RNP immunogens. *Arthritis Rheum* 2001;44:368–75.
- Vanderlugt CL, Miller SD. Epitope spreading in immune-mediated diseases: implications for immunotherapy. *Nat Rev Immunol* 2002;2:85–95.
- Craft J, Fatenejad S. Self antigens and epitope spreading in systemic autoimmunity. *Arthritis Rheum* 1997;40:1374–82.
- Deshmukh US, Gaskin F, Lewis JE, Kannapell CC, Fu SM. Mechanisms of autoantibody diversification to SLE-related autoantigens. *Ann N Y Acad Sci* 2003;987:91–8.
- James JA, Harley JB. B-cell epitope spreading in autoimmunity. *Immunol Rev* 1998;164:185–200.
- Monneaux F, Muller S. Epitope spreading in systemic lupus erythematosus: identification of triggering peptide sequences [review]. *Arthritis Rheum* 2002;46:1430–8.
- Vanderlugt CJ, Miller SD. Epitope spreading. *Curr Opin Immunol* 1996;8:831–6.
- Powell AM, Black MM. Epitope spreading: protection from pathogens, but propagation of autoimmunity? *Clin Exp Dermatol* 2001;26:427–33.
- Arbuckle MR, McClain MT, Rubertone MV, Scofield RH, Dennis GJ, James JA, et al. Development of autoantibodies before the clinical onset of systemic lupus erythematosus. *N Engl J Med* 2003;349:1526–33.
- Deshmukh US, Bagavant H, Lewis J, Gaskin F, Fu SM. Epitope spreading within lupus-associated ribonucleoprotein antigens. *Clin Immunol* 2005;117:112–20.
- Silverman GJ, Srikrishnan R, Germar K, Goodyear CS, Andrews KA, Ginzler EM, et al. Genetic imprinting of autoantibody repertoires in systemic lupus erythematosus patients. *Clin Exp Immunol* 2008;153:102–16.
- Hochberg MC. Updating the American College of Rheumatology revised criteria for the classification of systemic lupus erythematosus [letter]. *Arthritis Rheum* 1997;40:1725.
- Liang MH, Socher SA, Larson MG, Schur PH. Reliability and validity of six systems for the clinical assessment of disease activity in systemic lupus erythematosus. *Arthritis Rheum* 1989;32:1107–18.
- Vordenbäumen S, Lueking A, Budde P, Zucht HD, Goehler H, Brinks R, et al. Sequential high-content profiling of the IgG-autoantibody repertoire reveals novel antigens in rheumatoid arthritis. *Arthritis Res Ther* 2016;18:235.
- Budde P, Zucht HD, Vordenbäumen S, Goehler H, Fischer-Betz R, Gamer M, et al. Multiparametric detection of autoantibodies in systemic lupus erythematosus. *Lupus* 2016;25:812–22.
- Gladman D, Ginzler E, Goldsmith C, Fortin P, Liang M, Urowitz M, et al. The development and initial validation of the Systemic Lupus International Collaborating Clinics/American College of Rheumatology Damage Index for systemic lupus erythematosus. *Arthritis Rheum* 1996;39:363–9.
- Bolland S, Garcia-Sastre A. Vicious circle: systemic autoreactivity in Ro52/TRIM21-deficient mice: figure 1. *J Exp Med* 2009;206:1647–51.
- Quintana FJ, Patel B, Yeste A, Nyirenda M, Kenison J, Rahbari R, et al. Epitope spreading as an early pathogenic event in pediatric multiple sclerosis. *Neurology* 2014;83:2219–26.
- Burd MA, Hoffman RW, Deutscher SL, Wang GS, Johnson JC, Sharp GC. Long-term outcome in mixed connective tissue disease: longitudinal clinical and serologic findings. *Arthritis Rheum* 1999;42:899–909.
- Yurasov S, Tiller T, Tsujii M, Velinzon K, Pascual V, Wardemann H, et al. Persistent expression of autoantibodies in SLE patients in remission. *J Exp Med* 2006;203:2255–61.
- Floris A, Piga M, Cauli A, Mathieu A. Predictors of flares in systemic lupus erythematosus: preventive therapeutic intervention based on serial anti-dsDNA antibodies assessment—analysis of a monocentric cohort and literature review. *Autoimmun Rev* 2016;15:656–63.
- Vordenbäumen S, Böhmer P, Brinks R, Fischer-Betz R, Richter J, Bleck E, et al. High diagnostic accuracy of histone H4-IgG autoantibodies in systemic lupus erythematosus. *Rheumatology (Oxford)* 2018;57:533–7.
- Klionsky DJ. Autophagy revisited: a conversation with Christian de Duve. *Autophagy* 2008;4:740–3.
- Ma X, Zhang S, He L, Rong Y, Brier LW, Sun Q, et al. Mtorc1-mediated NRBF2 phosphorylation functions as a switch for the class III PtdIns3K and autophagy. *Autophagy* 2017;13:592–607.
- Qi YY, Zhou XJ, Cheng FJ, Hou P, Ren YL, Wang SX, et al. Increased autophagy is cytoprotective against podocyte injury induced by antibody and interferon- α in lupus nephritis. *Ann Rheum Dis* 2018;77:1799–809.
- Yin H, Wu H, Chen Y, Zhang J, Zheng M, Chen G, et al. The therapeutic and pathogenic role of autophagy in autoimmune diseases. *Front Immunol* 2018;9:1512.
- Abbott WM, Damschroder MM, Lowe DC. Current approaches to fine mapping of antigen-antibody interactions. *Immunology* 2014;142:526–35.

Identification of Low-Abundance Urinary Biomarkers in Lupus Nephritis Using Electrochemiluminescence Immunoassays

Samantha Stanley,¹ Chi Chiu Mok,² Kamala Vanarsa,¹ Deena Habazi,¹ Jennifer Li,¹ Claudia Pedroza,^{*3} Ramesh Saxena,⁴ and Chandra Mohan¹

Objective. To investigate the utility of a sensitive platform using electrochemiluminescence (ECL) for the identification of low-abundance urinary protein biomarkers in lupus nephritis (LN).

Methods. Forty-eight urine samples were obtained from subjects in 2 independent cohorts, each consisting of 3 groups (matched for age, sex, and race) of 8 patients with active LN (renal Systemic Lupus Erythematosus Disease Activity Index [SLEDAI] >0), 8 patients with inactive SLE (renal SLEDAI 0), and 8 healthy controls. Samples were tested using a preexisting 40-plex ECL panel. A custom 5-plex ECL panel was then developed for further validation studies and used to test 140 urine samples (from 44 patients with active LN, 41 patients with inactive SLE, 28 healthy controls, and 27 patients with other kidney diseases).

Results. Levels of 17 urinary proteins were elevated ($P < 0.05$ by 2-tailed Mann-Whitney U test) in samples from patients with active LN compared to samples from patients with inactive SLE and healthy controls in cohort 1, while 9 were similarly elevated in cohort 2. Of these, interleukin-7 (IL-7), IL-12p40, IL-15, interferon- γ -inducible protein 10 (IP-10), and thymus and activation-regulated chemokine (TARC) were chosen for further validation. These 5 proteins were undetectable by enzyme-linked immunosorbent assay (ELISA). Hence, a custom 5-plex ECL panel was developed and used to validate the results from the initial 40-plex screening panel. Urinary IL-7, IL-12p40, IL-15, IP-10, and TARC levels were again significantly elevated in patients with active LN compared to those with inactive SLE and healthy controls, and correlated well with the renal SLEDAI and physician's global assessment of disease activity ($R > 0.67$, $P < 0.05$). All 5 urinary proteins were more frequently elevated in LN compared to controls with other chronic kidney diseases, although overall group differences attained significance only for urinary IL-7 and IL-15.

Conclusion. Urinary levels of IL-7, IL-12p40, IL-15, IP-10, and TARC are potentially useful diagnostic tools in LN. The use of ECL assays may allow detection of urinary biomarkers that are below ELISA detection limits.

INTRODUCTION

Systemic lupus erythematosus (SLE) is a chronic autoimmune disorder, in which the body produces anti-double-stranded DNA and antinuclear antibodies, that leads to multisystem inflammation and tissue damage. One of the leading causes of mortality and morbidity in SLE is lupus nephritis (LN) (1); it has been estimated that more than half of all SLE patients will develop LN and 10–15% of these patients will experience end-stage renal disease (2). Early diagnosis of the disease could allow for earlier treatment, which has been shown to be effective (3). The current

gold standard of care for the evaluation of renal involvement in SLE is a renal biopsy. While renal biopsies are highly informative, they cannot be performed repeatedly, and come with attendant risks to the patient. Moreover, there is the possibility of sampling error, since the biopsy specimen taken is not representative of the entire kidney. The need for earlier diagnostic tools for LN has sparked research interests in urinary proteins to identify a noninvasive biomarker for LN.

There have been many advances made in the field of biomarker screening. New proteomic screening technologies such as aptamer-based assays (4), antibody-based microarrays (5),

Supported in part by the Lupus Research Alliance.

¹Samantha Stanley, PhD, Kamala Vanarsa, MS, Deena Habazi, BS, Jennifer Li, Chandra Mohan, MD, PhD: University of Houston, Houston, Texas; ²Chi Chiu Mok, MD, FRCP: Tuen Mun Hospital, Hong Kong, China; ³Claudia Pedroza*, PhD: University of Texas Health Science Center, Houston; ⁴Ramesh Saxena, MD, PhD: University of Texas Southwestern Medical Center, Dallas.

No potential conflicts of interest relevant to this article were reported.

Address correspondence to Chandra Mohan, MD, PhD, Department of Biomedical Engineering, University of Houston, 3605 Cullen Boulevard, Houston, TX 77204. E-mail: cmohan@central.uh.edu.

Submitted for publication February 26, 2018; accepted in revised form December 4, 2018.

*Correction added 20 April 2019 after online publication: the author surname Pedroza has been corrected throughout.

and others (6) are revolutionizing biomarker discovery, allowing researchers to screen for new biomarkers in an unbiased manner. These new technologies vary in sensitivity and cannot handle the high-volume sample throughput needed for subsequent biomarker validation studies or routine clinical diagnostics.

Newer technologies have attempted to reduce the levels of background noise seen in a traditional enzyme-linked immunosorbent assay (ELISA) or antibody-based arrays by replacing an enzymatic-based detection signal with an alternative signal. One of the most promising techniques is the use of an electrode-coupled immunoassay with an electrochemiluminescent (ECL) signal. In this arrangement, the capture antibody is coupled to an electrode, and the detection antibody is labeled with a tag that emits a chemiluminescent signal once a voltage is applied across the electrode (7,8). This new platform allows the input signal (the voltage) to be independent of the output signal (the chemiluminescent signal) and allows for multiplexing where each individual electrode can act as an independent assay to detect a unique protein. Compared to traditional ELISAs, such ECL-based assays have lower background noise, and hence a low limit of detection of analytes (9). To our knowledge, no other study using this technology to interrogate urinary biomarkers in LN has been published to date. Therefore, the goal of this study was to evaluate the use of ECL-based multiplex panels to identify potential urinary biomarkers of LN that may have escaped detection using earlier, less sensitive screening platforms.

PATIENTS AND METHODS

Patients and samples. Patients with LN and patients with other chronic kidney diseases were enlisted from either the University of Texas Southwestern Medical Center's Renal Clinic or Tuen Mun Renal Clinic. Informed consent was obtained from all patients, and all procedures were approved by the institutional review boards of University of Texas Southwestern Medical Center, Tuen Mun Hospital, and the University of Houston. Patients with a known history of LN were included in the study in addition to patients with SLE but no history of LN. The 27 control patients with chronic kidney disease included 10 with focal segmental glomerulosclerosis (FSGS), 10 with diabetic nephropathy, and 7 with other causes of chronic kidney disease (including IgA nephropathy, membranous nephropathy, and antineutrophil cytoplasmic antibody-associated glomerulopathy).

Clean-catch midstream urine samples were collected in sterile containers and chilled (at 4°C) or frozen (at -20°C) within 1 hour of sample collection. These samples were then aliquoted and stored at -80°C until they were tested. No protease inhibitors were added. Each patient was assessed by an attending physician at each sample collection appointment, and the following data were obtained: Systemic Lupus Erythematosus Disease Activity Index (SLEDAI) (10), renal SLEDAI (or SLEDAI specific to renal function) (10), physician's global assessment of disease activity, complement C3 and C4 levels, and anti-DNA antibody levels.

Commercial V-PLEX ECL screening. For the initial protein screening phase, 48 human urine samples were tested for 40 proteins using a Meso Scale Discovery V-PLEX Human Biomarker 40-Plex kit, and the levels of urinary creatinine were measured using an R&D Systems Creatinine Parameter Assay Kit according to the respective manufacturer's instructions. The protein concentrations from the V-PLEX assay results were then multiplied by their respective dilution factors and divided by the levels of urinary creatinine to obtain the normalized concentration of biomarkers.

The technology behind Meso Scale Discovery's multiplex assays is based on a combination of a traditional sandwich ELISA and ECL. In this platform, the bottom portion of a 96-well plate is coated with up to 10 electrodes, and each electrode has a unique monolayer of linker molecules that allow for selective coating of capture antibodies; from here, each individual electrode can act as its own independent "ELISA". Once the capture antibodies are attached to the electrodes, the samples containing the biomarker of interest are added, followed by a detection antibody. This detection antibody is labeled with Meso Scale Discovery's unique SULFO-TAG, which emits a chemiluminescent signal when a voltage is applied across the electrode. Without a voltage or electrical current present, this tag emits no signal (11). This arrangement reduces the level of background noise in the platform, and thus increases the sensitivity and detection ranges.

Construction and use of custom U-PLEX ECL assays.

Once the proteins were selected for a custom multiplex assay, their relative concentrations and optimal sample dilutions were determined using the data obtained from the initial 40-plex assay. Custom plexing assays for interleukin-7 (IL-7), IL-12p40, IL-15, interferon- γ -inducible protein 10 (IP-10), and thymus and activation-regulated chemokine (TARC) were purchased from Meso Scale Discovery, and a multiplex panel was developed by coating the capture antibodies onto the 96-well electrode plates. Next, the sample dilution for the custom panel and the compatibility of the respective antibody pairs were optimized to ensure that there was no cross-reactivity or interference.

ELISA. All ELISAs were performed using commercially available ELISA kits (DY207, DY1240, DY247, DY266, DY364, DY720, and DY622; R&D Systems). All manufacturer's instructions and recommendations were followed for each assay kit.

Statistical analysis. All statistical analyses involving disease state comparisons were conducted in GraphPad Prism software using a 2-tailed Mann-Whitney U test. For the screening platform, a *P* value less than 0.10 and a fold change greater than 1 were used as cutoffs for follow-up, whereas *P* values less than 0.05 were considered significant in the validation study. The custom U-PLEX panel was analyzed using Spearman's correlation analysis and a linear regression model; *P* values less than 0.05 were considered significant. In addition to the 2-tailed

Mann-Whitney U test, receiver operating characteristic curve analysis was conducted within the validation cohort to assess the effectiveness of these biomarkers as a diagnostic tool for active LN. Linear regression and Spearman's correlation analysis were performed in GraphPad Prism to analyze the relationship between the urinary biomarkers and various clinical parameters, including renal SLEDAI and physician's global assessment of disease activity. Multivariate linear regression analysis was also conducted to compare the contribution of individual biomarkers to the overall panel; a LASSO regression was initially conducted as a feature selection method to identify optimized panels of 2, 3, and 4 biomarkers. A second linear regression containing only these optimized panels was constructed; the panels that contained the greatest increase in area under the curve (AUC) values compared to the individual biomarkers were selected as the optimal model. These panels were then also corrected for demographic characteristics and medication dosage. Analysis of variance (ANOVA) was conducted in GraphPad Prism 6, while multivariate regression analyses and LASSO regression analysis were conducted using MATLAB (MathWorks) or SAS.

RESULTS

Initial screening. Urine samples from 48 subjects were initially screened for 40 unique proteins using a prebuilt multiplex panel. The protein concentrations determined were then normalized to urinary creatinine levels. Next, to display the respective fold changes and *P* values, a volcano plot outlining all protein levels from the screening assay after creatinine normalization was constructed, as shown in Figure 1. Table 1 outlines the screening assay results for 39 of these 40 proteins in greater detail. (No data were recorded for vascular endothelial growth factor receptor 1 [VEGFR-1].) The data are shown separately for cohort 1 (comprising 24 African American or Hispanic SLE subjects) and cohort 2 (comprising 24 Chinese SLE subjects). In this screening assay, levels of 17 proteins were found to be elevated in samples from patients with active LN compared to either samples from patients with inactive SLE or samples from healthy controls ($P < 0.05$ by 2-tailed Mann-Whitney U test) in cohort 1, while levels of 9 proteins were similarly elevated in cohort 2.

Taken together, the following 14 proteins were significantly elevated in at least 3 of the previously mentioned comparison groups

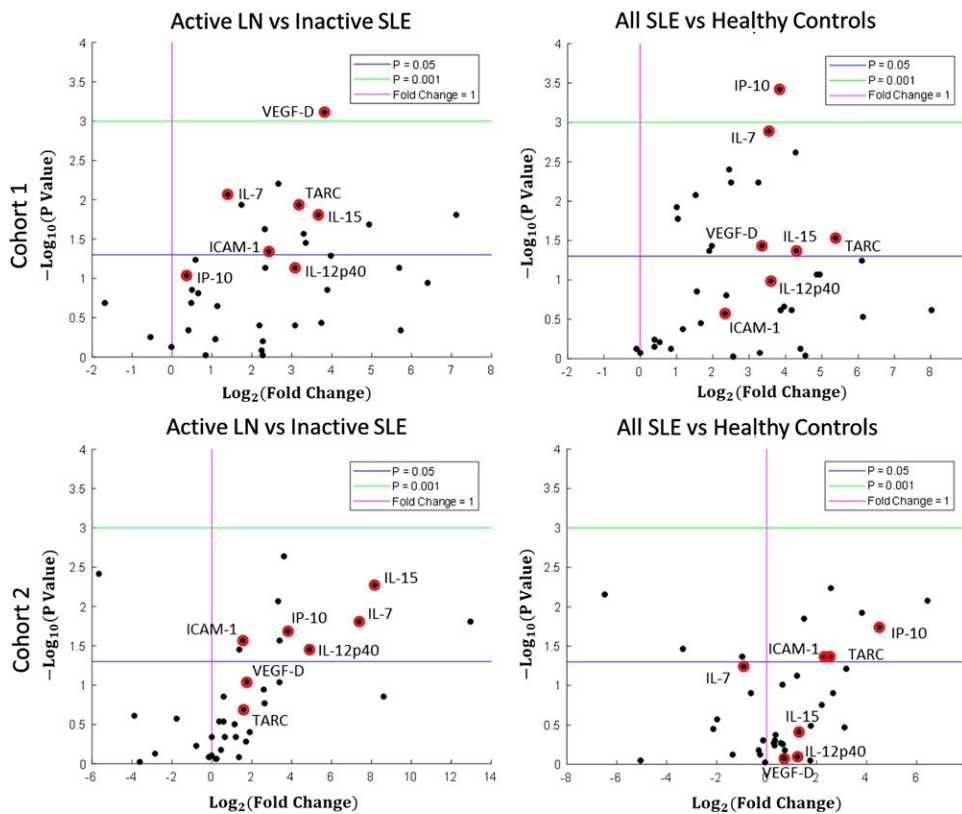


Figure 1. Volcano plots of the results of a 40-marker electrochemiluminescence (ECL) assay of urine samples from 2 cohorts of patients with lupus nephritis (LN). Results for patients with active LN ($n = 8$ in each cohort) versus patients with inactive systemic lupus erythematosus (SLE; $n = 8$ in each cohort) and for all patients with SLE ($n = 16$ in each cohort) versus healthy controls ($n = 8$ in each cohort) are shown. Protein concentrations were normalized to urinary creatinine levels. Each plot shows the *P* values and fold change for all 40 proteins screened in the assay, with the following top 7 proteins selected for further validation: soluble intercellular adhesion molecule 1 (sICAM-1), interleukin-7 (IL-7), IL-12p40, IL-15, interferon- γ -inducible 10-kd protein (IP-10), thymus and activation-regulated chemokine (TARC), and vascular endothelial growth factor D (VEGF-D). The x-axis shows the log-transformed ratio between the disease group and controls; the y-axis shows negative log-transformed *P* values determined by 2-tailed Mann-Whitney U test.

Table 1. ECL-based 40-plex screening assay results*

Protein	Cohort 1					Cohort 2						
	Healthy controls (n = 8)	Inactive SLE (n = 8)	Active LN (n = 8)	All SLE (n = 16)	Fold change, active LN vs. inactive SLE	Fold change, active LN vs. all SLE vs. healthy controls	Healthy controls (n = 8)	Inactive SLE (n = 8)	Active LN (n = 8)	All SLE (n = 16)	Fold change, active LN vs. inactive SLE	Fold change, active LN vs. all SLE vs. healthy controls
bFGF	0.1 (0)	0.5 (0)	8.2 (0.9)	4.4 (0)	14.9	70.7	0.31 (0)	0.46 (0.1)	0.47 (0)	0.47 (0.1)	1	1.5
CRP	217 (92.6)	108.2 (9)	9,201.2 (138.1)	4,654.7 (17.6)	85	21.5	50 (29.9)	86.9 (46.9)	551.2 (89.8)	319 (78.4)	6.3	6.4
Eotaxin	7 (1.7)	30.8 (21.8)	48.8 (40.4)	39.8 (28.6)	1.6	5.7†	15.57 (11)	57.71 (41.8)	129.1 (99)	93.4 (43.9)	2.2	6†
Eotaxin 3	1.3 (0)	6.3 (3.8)	2 (0)	4.2 (1.5)	0.3	3.2	9.23 (3.7)	6 (2.1)	9.55 (11.4)	7.77 (5.3)	1.6	0.8
GM-CSF‡	0.1 (0)	0.1 (0)	2.9 (1.3)	1.5 (0)	30.8§	14.7	0.81 (0.3)	0 (0)	2 (0.8)	1 (0)	NA§	1.2
IFN γ	0.1 (0)	0.1 (0)	0.1 (0)	0.1 (0)	1	1	1.07 (1)	0.21 (0)	0 (0)	0.11 (0)	0	0.1§
IL-10	0 (0)	0 (0)	0 (0)	0 (0)	1.8	1.3	0.21 (0.1)	0.21 (0.1)	0.13 (0)	0.17 (0.1)	0.6	0.8
IL-12p40†	0.4 (0.3)	0.9 (0.5)	7.8 (4.3)	4.4 (1.5)	8.5¶	12.2	1.66 (0.9)	0.25 (0)	7.64 (5.8)	3.94 (0.2)	30.2§	2.4
IL-12p70	0 (0)	0 (0)	0.2 (0)	0.1 (0)	4.9	5.9	0.19 (0)	0.25 (0)	0.23 (0)	0.24 (0)	0.9	1.3
IL-13	0.4 (0.3)	0.2 (0)	1 (0)	0.6 (0)	4.9	1.3	1.91 (1.4)	2.45 (2.4)	0.05 (0)	1.25 (0.2)	0†	0.7
IL-15†	0.4 (0.3)	1.1 (0.7)	13.7 (7.6)	7.4 (2.4)	12.8§	19.9§	3.32 (1.9)	0.06 (0)	16.39 (6.6)	8.22 (0)	288.1†	2.5
IL-16	0.2 (0)	0.7 (0)	101.9 (13.5)	51.3 (0)	139.7§	261.7	23.56 (0.4)	0.03 (0)	10.8 (1.1)	5.41 (0)	395.6	0.2
IL-17	0.1 (0)	0.1 (0)	5.6 (0)	2.8 (0)	53.3	23.6	6.37 (0)	0.18 (0)	0.21 (0)	0.19 (0)	1.2	0
IL-1 α	25.8 (2.7)	24 (3.9)	51.2 (11)	37.6 (4.6)	2.1	1.5	45.97 (23.8)	0 (0)	1.04 (0.5)	0.52 (0)	NA¶	0†
IL-1 β	0.2 (0)	0.5 (0.1)	4.6 (1.4)	2.6 (0.1)	8.5	15.7	8.92 (4.5)	24.41 (3.7)	3.44 (3.2)	13.93 (3.2)	0.1	1.6
IL-2	0 (0)	0.1 (0)	0.2 (0.1)	0.1 (0)	4.6	29.3¶	0.24 (0)	0.07 (0)	0.11 (0.1)	0.09 (0.1)	1.5	0.4
IL-4	0 (0)	0 (0)	0 (0)	0 (0)	NA	2.3	0.03 (0)	0 (0)	0.01 (0)	0.01 (0)	2.6	0.3
IL-5	0.5 (0.4)	1.2 (0.8)	1.7 (1.6)	1.5 (1)	1.3	2.9†	2.16 (2.3)	1.81 (1.6)	2.36 (2.5)	2.09 (2.2)	1.3	1
IL-6†	0.2 (0.1)	0.5 (0.5)	24.9 (2.6)	12.7 (0.8)	51.9¶	69.3¶	0.61 (0.3)	0.92 (0.2)	9.82 (3)	5.37 (0.6)	10.6¶	8.8
IL-7†	0.2 (0)	1.3 (1.3)	3.4 (3.6)	2.3 (2.3)	2.6†	11.7†	2.38 (1)	0.01 (0)	2.53 (2.1)	1.27 (0)	170§	0.5¶
IL-8	102 (12.7)	99.6 (46.9)	506.2 (147.8)	302.9 (83.1)	5.1¶	3	282.17 (94.4)	683.13 (125.1)	46.84 (55.8)	364.98 (62.5)	0.1	1.3
IP-10†	4.5 (0.3)	56.2 (18.6)	72.7 (78.4)	64.5 (50)	1.3¶	14.4†	4.55 (1.9)	13.71 (4.2)	195.65 (89.5)	104.68 (31.4)	14.3§	23§
MCP-1†	129.6 (114)	337.7 (236.3)	2,152.7 (1,838.8)	1,245.2 (409.7)	6.4†	9.6†	75.45 (52.7)	192.43 (119.8)	1,952 (1603)	1,072 (308)	10.1†	14.2§
MCP-4	4.2 (1.1)	25.7 (12.1)	17.8 (16.2)	21.7 (12.8)	0.7	5.2	7.05 (0)	13.72 (7.8)	51.93 (18.1)	32.83 (14.9)	3.8	4.7
MDC	0.7 (0)	1.5 (0)	24.2 (26.3)	12.9 (0)	15.9¶	18.1	6.9 (0)	2.42 (0)	14.91 (9.9)	8.67 (0)	6.2	1.3
MIP-1 α	0 (0)	1.7 (0)	22.8 (0)	12.2 (0)	13.5	NA	2.62 (0)	8.34 (0)	9.68 (0)	9.01 (0)	1.2	3.4

(continued)

Table 1. (Cont'd)

Protein	Cohort 1				Cohort 2							
	Healthy controls (n = 8)	Inactive SLE (n = 8)	Active LN (n = 8)	All SLE (n = 16)	Fold change, active LN vs. inactive SLE	Fold change, active LN vs. all SLE vs. healthy controls	Healthy controls (n = 8)	Inactive SLE (n = 8)	Active LN (n = 8)	All SLE (n = 16)	Fold change, active LN vs. inactive SLE	Fold change, active LN vs. all SLE vs. healthy controls
MIP-1β†	4.9 (3.1)	6.1 (6.3)	30.6 (15.6)	18.4 (8.6)	5§	3.8§	9.46 (4.6)	12.48 (12.3)	41.45 (12.1)	26.96 (12.3)	3.3	2.9§
PIGF	38.8 (31.3)	29 (28.5)	43.8 (39.3)	36.4 (30.6)	1.5¶	0.9	45.99 (46.8)	57.02 (57.7)	87.07 (83.2)	72.05 (66.9)	1.5	1.6*
SAA†	13.4 (7.8)	48.2 (50.5)	475.9 (219.2)	262 (73.5)	9.9§	19.6†	38.29 (6)	60.44 (29.3)	644.46 (259.2)	352.45 (131.5)	10.7§	9.2¶
sFlt-1	1.7 (0.2)	4.1 (1.3)	9 (7.9)	6.5 (4.3)	2.2	4§	4.98 (4.1)	4.69 (4.7)	10.94 (5.1)	7.81 (4.8)	2.3	1.6
sICAM-1†	3.5 × 10 ³ (1.3 × 10 ³)	5.8 × 10 ³ (6.2 × 10 ³)	3.0 × 10 ⁴ (2.3 × 10 ⁴)	1.8 × 10 ⁴ (9.8 × 10 ³)	5.4§	5.1	2.1 × 10 ³ (1.8 × 10 ³)	5.3 × 10 ³ (2.1 × 10 ³)	1.6 × 10 ⁴ (1.6 × 10 ⁴)	1.0 × 10 ⁴ (5.9 × 10 ³)	3§	5§
sVCAM-1†	1.4 × 10 ⁴ (1.3 × 10 ³)	3.5 × 10 ⁴ (3.2 × 10 ⁴)	1.2 × 10 ⁵ (9.6 × 10 ⁴)	7.5 × 10 ⁴ (5.6 × 10 ⁴)	3.4§	5.5†	1.4 × 10 ³ (1.2 × 10 ³)	1.9 × 10 ⁴ (5.5 × 10 ³)	2.3 × 10 ⁵ (2.2 × 10 ⁵)	1.3 × 10 ⁵ (6.2 × 10 ⁴)	12.4†	87.6†
TARC†	0.2 (0)	1.7 (0.4)	15.8 (15.3)	8.8 (1.8)	9.1§	42§	0.37 (0)	1.06 (0.6)	3.22 (2.8)	2.14 (0.7)	3.1	5.9§
Tie-2	2.1 (0)	11.5 (0)	117.7 (91.3)	64.6 (15.3)	10.3§	31¶	23.22 (19.4)	36.56 (12.5)	36.94 (0)	36.75 (5.7)	1	1.6
TNF	0.1 (0)	0 (0)	1.3 (0)	0.6 (0)	NA	9.9	0.12 (0)	0.33 (0)	0.46 (0)	0.39 (0)	1.4	3.4
Lymphotoxin	0 (0)	0 (0)	0 (0)	0 (0)	NA	NA	0.01 (0)	0.03 (0)	0 (0)	0.01 (0)	0	0.9
VEGF†	99.2 (103.3)	169.3 (178.7)	240.8 (262.3)	205.1 (179.1)	1.4	2§	401.36 (254.2)	0.05 (0)	411.39 (307.5)	205.72 (0)	2.6§	2.3¶
VEGF-C	0 (0)	0 (0)	6.4 (0)	3.2 (0)	NA	NA	0 (0)	5.85 (0)	0.48 (0)	3.17 (0)	0.1	NA
VEGF-D†	1 (1.1)	1.3 (1)	18.6 (7.5)	10 (3.5)	14.2†	10.3§	10.01 (7.3)	7.51 (3.2)	25.59 (11.1)	16.55 (8.6)	3.4¶	1.7

* No data were recorded for vascular endothelial growth factor receptor 1 (VEGFR-1). Values are the mean (median) picograms of urinary protein per milligram of urinary creatinine. ECL = enhanced chemiluminescence; SLE = systemic lupus erythematosus; LN = lupus nephritis; bFGF = basic fibroblast growth factor; CRP = C-reactive protein; GM-CSF = granulocyte-macrophage colony-stimulating factor; NA = not applicable; IFNγ = interferon-γ; IL-10 = interleukin-10; MCP-1 = monocyte chemoattractant protein 1; MDC = macrophage-derived chemokine; MIP-1α = macrophage inflammatory protein 1α; PIGF = phosphatidylinositol-glycan biosynthesis class F protein; SAA = serum amyloid A; sFlt-1 = soluble Flt-1; sICAM-1 = soluble intercellular adhesion molecule 1; sVCAM-1 = soluble vascular cell adhesion molecule 1; TARC = thymus and activation-regulated chemokine; TNF = tumor necrosis factor.

† P < 0.01.

‡ Significantly elevated in at least 3 comparison groups.

§ P < 0.05.

¶ P < 0.1.

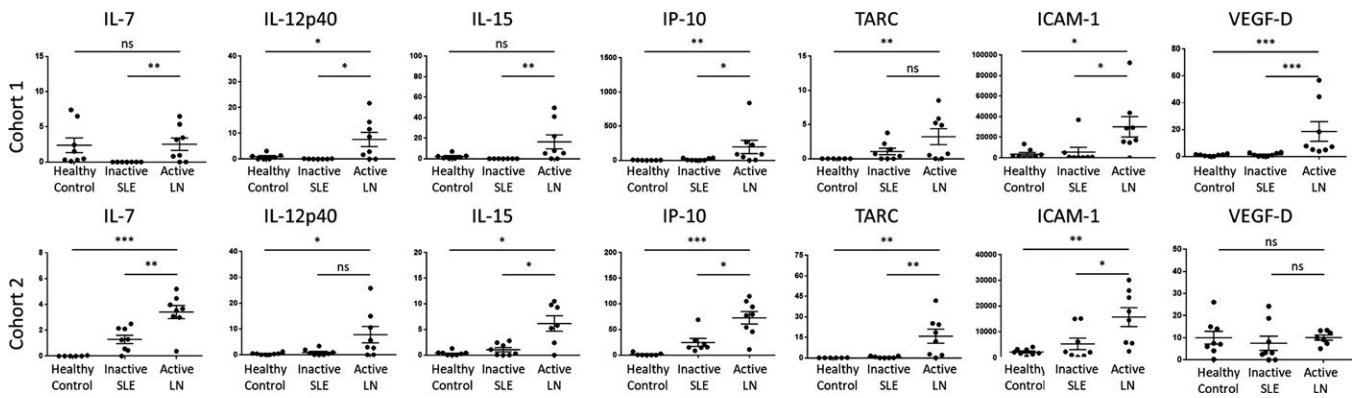


Figure 2. Electrochemiluminescence (ECL) assay screening results for urinary interleukin-7 (IL-7), IL-12p40, IL-15, interferon- γ -inducible 10-kd protein (IP-10), thymus and activation-regulated chemokine (TARC), intercellular adhesion molecule 1 (ICAM-1), and vascular endothelial growth factor D (VEGF-D) in 2 cohorts of healthy controls, patients with inactive systemic lupus erythematosus (SLE), and patients with active lupus nephritis (LN). Urine samples were tested for 40 proteins using an ECL assay. Protein concentrations were normalized to urinary creatinine levels. Symbols represent individual samples (n = 8 per group in each cohort); horizontal lines and error bars show the mean \pm SD picogram of urinary protein per milligram of urinary creatinine. * = $P < 0.05$; ** = $P < 0.01$; *** = $P < 0.001$, by 2-tailed Mann-Whitney U test. ns = not significant.

(active LN versus inactive SLE in cohort 1, all SLE versus healthy controls in cohort 1, active LN versus inactive SLE in cohort 2, all SLE versus healthy controls in cohort 2): granulocyte-macrophage colony-stimulating factor, IL-12p40, IL-15, IL-6, IL-7, IP-10, monocyte chemoattractant protein 1 (MCP-1), macrophage inflammatory protein 1 β , serum amyloid A, soluble intercellular adhesion molecule 1 (sICAM-1), soluble vascular cell adhesion molecule 1, TARC, VEGF, and VEGF-D. Of these proteins, the following 7 were selected for further validation: IL-7, IL-12p40, IL-15, IP-10, sICAM-1, TARC, and VEGF-D. The remaining 7 proteins were not examined further in this study because they have already been studied extensively as potential urinary biomarkers of LN, since they are present in sufficient concentrations to permit ELISA validation. In contrast, IL-7, IL-12p40, IL-15, IP-10, sICAM-1, TARC, and VEGF-D have not been examined in LN urine samples, possibly because their lower concentrations precluded ELISA validation. Figure 2 shows the screening results for the 7 proteins selected for validation.

Initial validation of IL-7, IL-12p40, IL-15, IP-10, sICAM-1, TARC, and VEGF-D by ELISA. ELISA kits for these 7 proteins were purchased, and 6 urine samples (2 from patients with active LN, 2 from patients with inactive SLE, and 2 from healthy controls, each with the highest concentrations of the selected protein per group) from the screening assay were used to analyze the kit detection sensitivity and compatibility with urine. None of the 7 urinary proteins tested could be detected by ELISA.

Custom multiplex panel development and validation. After the initial ELISA testing, the concentrations from the screening assay were analyzed and compared to the detection limits of the custom plexing assays to determine which proteins would be compatible for the development of a new panel in terms of their optimal dilutions. Of the 7 proteins initially selected, sICAM-1 and VEGF-D were not compatible with the remaining 5 because of differences in dilution needed. Hence, a custom 5-plex panel was constructed for assaying IL-7, IL-12p40, IL-15, IL-10, and TARC.

Table 2. Comparison between ECL-based protein detection platforms and traditional sandwich ELISA*

Protein, pg/ml	Prebuilt ECL panel			Custom-built ECL panel			ELISA		
	Healthy controls (n = 16)	Inactive SLE (n = 16)	Active LN (n = 16)	Healthy controls (n = 16)	Inactive SLE (n = 16)	Active LN (n = 16)	Healthy controls (n = 2)	Inactive SLE (n = 2)	Active LN (n = 2)
IL-7	2.38 \pm 1.04	0.10 \pm 0.01	2.53 \pm 0.88	0.26 \pm 0.13	0.83 \pm 0.26	3.66 \pm 0.69	ND	ND	ND
IL-12p40	1.66 \pm 0.84	0.25 \pm 0.2	7.64 \pm 2.79	ND	0.62 \pm 0.49	11.09 \pm 3.42	ND	ND	ND
IL-15	3.32 \pm 1.47	0.60 \pm 0.06	16.39 \pm 6.81	0.11 \pm 0.07	4.58 \pm 2.6	30.43 \pm 9.68	ND	ND	ND
IP-10	4.55 \pm 2.67	13.71 \pm 5.75	195.65 \pm 98.02	7.1 \pm 2.99	22.04 \pm 8.21	217.67 \pm 82.82	ND	ND	ND
TARC	0.37 \pm 0.32	1.06 \pm 0.48	3.22 \pm 1.17	0.42 \pm 0.19	0.39 \pm 0.11	1.1 \pm 0.22	ND	ND	ND

* Values are the mean \pm SEM. ECL = electrochemiluminescence; ELISA = enzyme-linked immunosorbent assay; SLE = systemic lupus erythematosus; LN = lupus nephritis; IL-7 = interleukin-7; ND = not detected; IP-10 = interferon- γ -inducible protein 10; TARC = thymus and activation-regulated chemokine.

A comparison between the concentrations detected with the prebuilt V-PLEX ECL panel, the custom-built U-PLEX ECL panel, and ELISA is shown in Table 2. Once this custom panel was constructed, the 48 human urine samples from the screening assay were used to validate the panel. The validation results are shown in Figure 3A, with a comparison between the pre-built V-PLEX and

custom 5-plex panel. For all 5 molecules, the custom 5-plex results correlated significantly with the V-PLEX screening results, with correlation coefficients ranging from 0.3 to 0.89. Fold changes and *P* values for the initial 48 screening samples are listed in Supplementary Table 1 (available on the *Arthritis & Rheumatology* web site at <http://onlinelibrary.wiley.com/doi/10.1002/art.40813/abstract>).

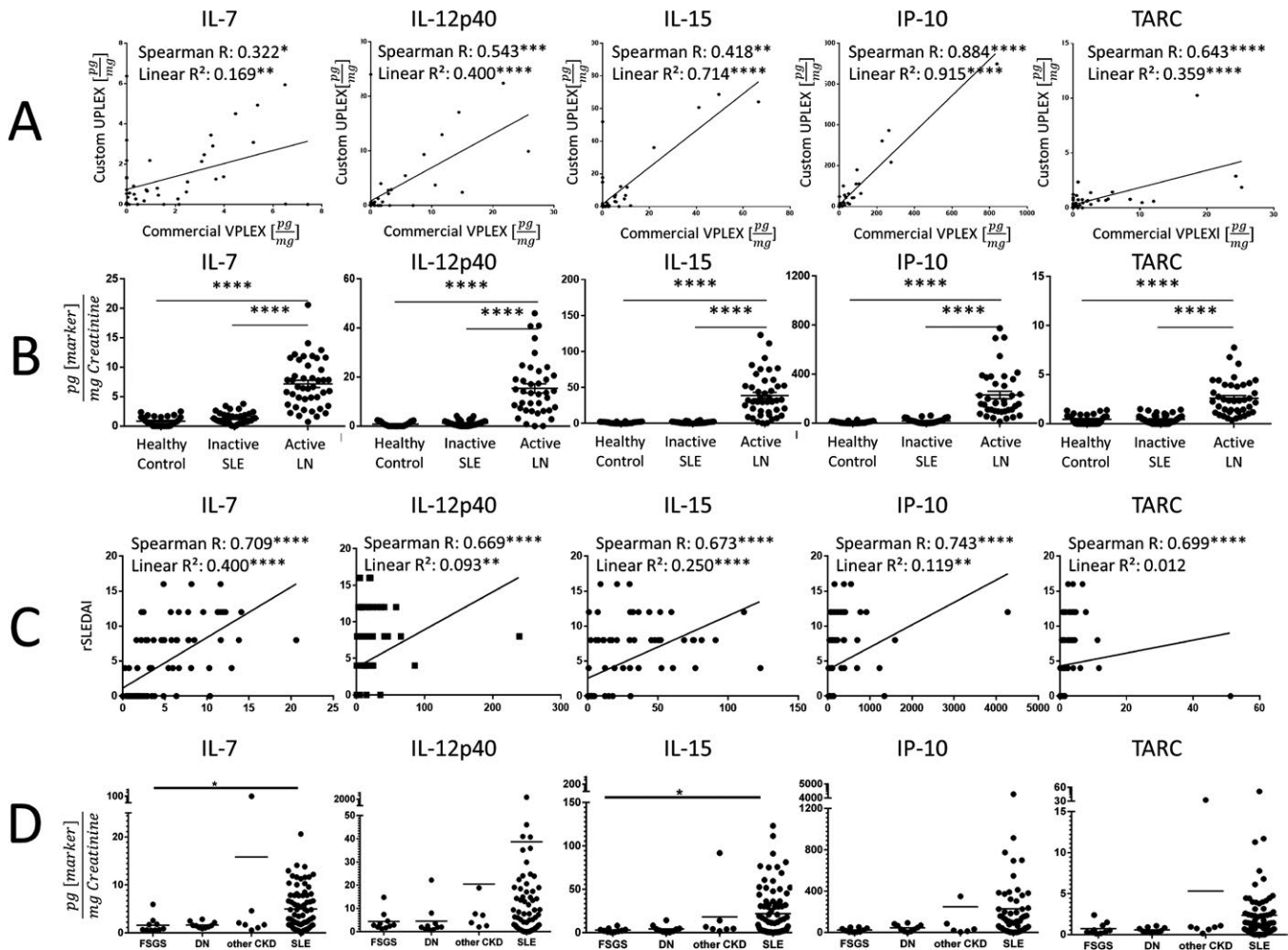


Figure 3. **A**, Correlation between the results of a prebuilt ECL panel and the results of a custom-built ECL panel. Urine samples from 2 cohorts of patients with active LN, patients with inactive SLE, and healthy controls ($n = 8$ per group in each cohort) were analyzed for IL-7, IL-12p40, IL-15, IP-10, and TARC using both the prebuilt 40-plex panel and a custom-built 5-plex panel to validate the custom-built ECL panel. All protein concentrations within each sample were multiplied by their respective dilution factors. Correlation coefficients were calculated using Spearman's method, and linear regression analysis was conducted to determine the R^2 value for each protein. **B**, ECL assay of the indicated urinary proteins using the custom 5-plex panel in samples from healthy controls ($n = 28$), patients with inactive SLE ($n = 41$), and patients with active LN ($n = 44$). Protein concentrations were normalized to urinary creatinine levels. **C**, Correlation between creatinine-normalized urinary biomarker level and the renal Systemic Lupus Erythematosus Disease Activity Index (rSLEDAI) score in 2 cohorts of patients with active LN, patients with inactive SLE, and healthy controls ($n = 8$ per group in each cohort) analyzed for the indicated urinary proteins using the custom 5-plex panel. Correlation coefficients were calculated using Spearman's method, and linear regression analysis was conducted to determine the R^2 value for each protein. Units for the x-axis are picogram of urinary protein per milligram of urinary creatinine. **D**, ECL assay of the indicated urinary proteins using the custom 5-plex panel in samples from patients with focal segmental glomerulosclerosis (FSGS; $n = 10$), patients with diabetic nephropathy (DN; $n = 10$), patients with other chronic kidney diseases (CKD; $n = 7$), and patients with SLE (pooled data from patients with inactive SLE and patients with active LN; $n = 85$). Protein concentrations were normalized to urinary creatinine levels. See Results and Supplementary Table 3 for results of post hoc analyses and chi-square tests. In **B** and **D**, symbols represent individual samples; horizontal lines with error bars show the mean \pm SD. * = $P < 0.05$; ** = $P < 0.01$; *** = $P < 0.001$; **** = $P < 0.0001$, by 2-tailed Mann-Whitney U-test in **B** and by one-way analysis of variance in **D**. See Figure 2 for other definitions.

Biomarker validation using a custom multiplex panel. Having successfully validated the custom 5-plex panel, we next used this custom panel to test 113 additional human urine samples from subjects from the same center as cohort 2, consisting of 44 samples from patients with active LN, 41 samples from patients with inactive SLE, and 28 samples from healthy controls. Creatinine-normalized urinary levels of IL-7, IL-12p40, IL-15, IP-10, and TARC were all significantly elevated in patients with active LN compared to either patients with inactive SLE or healthy controls ($P < 0.05$ by 2-tailed Mann-Whitney U test), as shown in Figure 3B. Linear regression and Spearman's correlation analysis were performed to analyze the association between the urinary biomarker levels and renal SLEDAI (Figure 3C). All 5 urinary proteins analyzed were significantly correlated with renal SLEDAI ($P < 0.05$), with correlation coefficients ranging from 0.67 to 0.74. Table 3 lists a summary of the extended cross-sectional study results, the diagnostic capabilities of these biomarkers, and a direct comparison of these newly identified protein markers to that of serum C3 and C4 and anti-DNA antibodies. In this study, all 5 of the validated urinary biomarkers (IL-7, IL-12p40, IL-15, IP-10, and TARC) exhibited good diagnostic potential ($P < 0.0001$ for active LN compared to either inactive SLE or healthy controls, AUC >0.91 for active LN compared to inactive SLE). In addition, each protein displayed improved sensitivity when compared to traditional clinical measurements of SLE disease activity, leading to an overall increase in diagnostic accuracy (Table 3 and Supplementary Figure 1).

A multivariate linear regression analysis was also conducted to investigate the predictive power of the biomarkers in relation to renal disease activity, renal pathology activity index, and renal pathology chronicity index (Supplementary Table 2, available on the *Arthritis & Rheumatology* web site at <http://onlinelibrary.wiley.com/doi/10.1002/art.40813/abstract>). A 4-plex panel consisting of IL-7, IL-15, IP-10, and TARC was the most powerful discriminator of active LN (AUC 0.943), while a panel comprising all 5 proteins best predicted renal pathology activity index scores of ≥ 7 (AUC 0.736), and a panel of IL-12p40 and IL-15 was optimal for predicting renal pathology chronicity index scores of ≥ 4 (AUC 0.800). A comprehensive breakdown of this analysis can be found in Supplementary Table 2.

Assessment of the specificity of urinary IL-7, IL-12p40, IL-15, IP-10, and TARC for LN. In order to examine the diagnostic specificity of the newly described panel of urinary proteins for LN, these biomarkers were examined in urine samples from 27 patients with other chronic kidney diseases, using the custom 5-plex panel, after urinary creatinine normalization. These patients included 10 with FSGS, 10 with diabetic nephropathy, and 7 with other causes of chronic kidney disease. In general,

most patients with other chronic kidney diseases exhibited basal levels of these 5 urinary molecules, similar to the levels noted in healthy controls, with the exception of a couple of outliers, notably in the group with other chronic kidney diseases (Figure 3D). One-way ANOVA was performed to test whether levels of any of the 5 urinary biomarkers (IL-7, IL-12p40, IL-15, IP-10, and TARC) were different among the different disease groups. Overall group differences were significant for IL-7 and IL-15 but not for IL-12p40, IP-10, or TARC, as indicated in Figure 3D. In post hoc analyses comparing patients with SLE to those with FSGS, IL-15 levels were significantly elevated in SLE ($P = 0.029$). IL-15 levels were also significantly elevated in patients with SLE compared to those with diabetic nephropathy ($P = 0.041$). Specifically, the IL-15 concentration was 18 pg/mg and 19 pg/mg higher in patients with SLE compared to those with diabetic nephropathy and those with FSGS, respectively.

Group differences were also examined by comparing the percentage of subjects who tested positive for each biomarker, setting the cutoff at a value that was 2 SD above the mean in healthy controls. As detailed in Supplementary Table 3 (available on the *Arthritis & Rheumatology* web site at <http://onlinelibrary.wiley.com/doi/10.1002/art.40813/abstract>), all 5 urinary biomarkers were more frequently expressed in the urine of patients with active LN, compared to the different chronic kidney disease groups tested, with these differences being most notable and/or significant for urinary IL-7, IL-12, and IP-10, as assessed by chi-square tests. For example, 88.6% of the patients with active LN tested positive for IL-12, compared to 12.2% of the patients with inactive SLE, 25% of those with FSGS ($P < 0.001$), 16.7% of those with diabetic nephropathy, and 44.4% of controls with other chronic kidney diseases ($P < 0.0001$ for all).

DISCUSSION

In this study, we used a multiplex ECL immunoassay panel to screen for potentially novel urinary biomarkers of LN, the hits from which were used to develop a custom multiplex immunoassay to validate 5 selected urinary proteins in a cohort consisting of 113 subjects (44 with active LN, 41 with inactive SLE, and 28 healthy controls). All 5 of the validated biomarkers (IL-7, IL-12p40, IL-15, IP-10, and TARC) exhibited sound diagnostic capabilities ($P < 0.0001$ for active LN compared to either inactive SLE or healthy controls, AUC > 0.91 for active LN compared to inactive SLE). In addition, all 5 biomarkers outperformed serum C3 or C4 and anti-DNA antibodies as diagnostic tools for LN in this cohort. The urinary biomarkers presented in this study match the high sensitivity of conventional serum tests while increasing the specificity, hence reducing the number of false-positive results.

In this study, urinary levels of IL-7, IL-12p40, IL-15, IP-10, and TARC could only be validated with our custom 5-plex ECL panel. None of these biomarkers were detectable with a conven-

Table 3. Summary of extended cross-sectional validation study of urinary levels of IL-7, IL-12p40, IL-15, IP-10, and TARC*

Protein/bio-marker	Urinary marker, mean (median) pg/mg†			SLE vs. healthy controls				Active LN vs. inactive SLE							
	Healthy controls (n = 28)	Inactive SLE (n = 41)	Active LN (n = 44)	Fold change	AUC	Cutoff value, pg/mg	Sensitivity/specificity, %	NPV/PPV, %	Accuracy, %	Fold change	AUC	Cutoff value, pg/mg	Sensitivity/specificity, %	NPV/PPV, %	Accuracy, %
IL-7	0.9 (0.7)	1.8 (1.3)	6.7 (6.2)	4.8‡	0.798‡	1.897	61.45/92.86	44.83/96.23	69.37	3.7§	0.921§	2.926	83.72/94.74	83.72/94.74	88.89
IL-12p40	0.6 (0.0)	3.2 (0.5)	22.2 (17.2)	21.5‡	0.771‡	2.539	54.05/100	44.26/100	66.34	6.9‡	0.911§	4.660	86.84/100	88.37/100	93.42
IL-15	1.2 (1.5)	4.3 (1.5)	32.1 (30.0)	15.4‡	0.789‡	3.380	56.79/100	44.44/100	67.89	7.5§	0.933§	5.274	93.02/100	92.31/100	96.20
IP-10	22.0 (10.4)	82.5 (11.9)	357.0 (179.3)	10.1¶	0.741¶	22.73	63.38/95.83	46.94/97.83	71.58	4.3§	0.940§	62.62	87.18/100	88.37/100	93.51
TARC	0.5 (0.7)	2.8 (0.2)	2.5 (2.0)	5.2#	0.6457	0.06572	82.61/46.43	52.00/79.17	72.16	0.9§	0.913§	1.183	78.05/92.50	80.43/91.43	85.19
Low C3 or C4	NA	53.49	95	NA	NA	NA	NA	NA	NA	NA	NA	NA	NA	90.48/64.62	70.93
Anti-DNA	NA	48.78	86.36	NA	NA	NA	NA	NA	NA	NA	NA	NA	86.36/51.22	77.78/65.52	69.41

* IL-17 = interleukin-17; IP-10 = interferon- γ -inducible protein 10; TARC = thymus and activation-regulated chemokine; SLE = systemic lupus erythematosus; LN = lupus nephritis; AUC = area under the curve; NPV = negative predictive value; PPV = positive predictive value; NA = not applicable.

† Values for low C3 or C4 and anti-DNA are the percent of patients.

‡ $P < 0.001$.

§ $P < 0.0001$.

¶ $P < 0.01$.

$P < 0.05$.

tional sandwich ELISA. A sandwich ELISA has an estimated lower limit of detection of 10–20 pg/ml (9). In comparison, the estimated lower limit of detection for the ECL-based assays used in this study is <1 pg/ml (9). The urinary levels of all 5 proteins presented in this study were estimated to be as low as 0.05 pg/ml before creatinine normalization, which is too low for a traditional ELISA to detect.

The largest obstacle to the lower limits of detection in any platform is the level of background noise in the assay. The main source of background noise in a traditional ELISA is the coupling of the input and output signals for the detection mechanism. If the detection antibody is directly labeled with a fluorescent or other signal-emitting probe, the lower limit of detection will increase because there is no mechanism for signal amplification. In order to incorporate a system of signal amplification, the detection antibody can be labeled with an enzyme that can catalyze a reaction that emits a detectable signal. This coupling of the input signal (enzyme plus reactive solution) and output signal (fluorescent or colorimetric signal) also generates background noise. In contrast, the use of ECL in the multiplexed ECL immunoassays described in this study eliminates this coupled relationship. The user is able to control the chemiluminescent output signal by adjusting the input signal or the voltage applied across each electrode. This decoupling is responsible for the increase in sensitivity and lower detection limits observed in ECL-based assays; in addition, this mechanism can increase the dynamic range of the overall assay. A traditional ELISA has a dynamic range of ~2 or 3 logs (9), whereas an ECL-based immunoassay has a dynamic range of 4–5 logs (9), allowing it to accurately measure across a larger spectrum of protein concentrations.

This study is not the first to investigate chemokines and cytokines as potential urinary biomarkers of LN. Several other studies have examined MCP-1 (12,13), TWEAK (14,15), CXCL16 (16,17), IL-6 (18), and IL-8 (18) as potential biomarkers of LN. Many of these molecules have incredibly short half-lives (19,20), which contributes to their overall low concentrations in urine, making it difficult to conduct validation studies reliably using an ELISA platform. Cytokines such as tumor necrosis factor, IL-6, and interferon- γ (IFN γ) all have half-lives of less than 24 hours when stored at room temperature (20). Storing biologic samples at lower temperatures and treating them with protease inhibitors and preservatives can improve proteomic preservation (21). Even then, a large decrease in cytokines has still been observed over a 24-hour time period (20). This rapid degradation rate can quickly lead to cytokine levels falling below the typical limits of detection of an ELISA, but newer ECL-based platforms such as those used in this study offer an alternative detection method. The ECL assay presented in this study mirrors an ELISA in workflow and principle, but offers an increase in sensitivity with reduced background noise, thus allowing researchers to evaluate biomarkers at much lower concentrations.

IL-7 is a cytokine that is known to influence lymphocyte differentiation, dimerize with hepatocyte growth factor to form a B cell growth-stimulating factor, and play a major role in B cell maturation and lymphoid cell survival (22). It has previously been studied as a potential biomarker for graft-versus-host disease (23), and potentially Graves' disease (24). IL-7 has also been shown to be dysregulated in SLE patients at the messenger RNA level (25) and has been studied as a potential treatment option to correct dysregulated apoptosis in SLE B cells (26). IL-7 is also a critical cytokine for T cell development, survival, and homeostasis, including T cell memory homeostasis (24). To date, no other studies have explored the use of IL-7 as a serum or urinary biomarker for SLE or LN.

IL-12p40 is a subunit of the IL-12 cytokine that is expressed by activated macrophages and enhances the activity of T cells and natural killer (NK) cells (27). IL-12p40 has been implicated in other inflammatory diseases (28,29) and extensively studied in the context of SLE (30–33), with conflicting results. Some studies have indicated that IL-12 and its subunits are up-regulated in SLE, while others have demonstrated a decrease in expression levels. However, the finding that IL-12p40 levels are elevated in SLE has ramifications beyond IL-12, since the p40 subunit is shared with IL-23, which is very important in driving Th17 cell formation. Hence, the elevated IL-12p40 levels seen in urine samples from patients with LN may correlate with increased Th1 and Th17 cell activity that has been extensively documented in patients with SLE and LN (34). No other studies have examined IL-12p40 as a potential biomarker for LN.

IL-15 is a cytokine that induces the proliferation of NK cells and is up-regulated in the presence of a viral infection. It is also known to reduce disease activity in celiac disease (35) and has been implicated as a potential biomarker for Alzheimer's disease (36). Serum levels of IL-15 in SLE patients have been examined previously (37–39), but the sample sizes of those studies were too limited for findings to be considered conclusive. Interestingly, those investigators note that IL-15 was difficult to reliably detect in human serum samples. Given the importance of IL-15 in memory T cell function and follicular dendritic cell proliferation, IL-15 could contribute to lupus through several avenues. There are no published studies on urinary levels of IL-15 in the context of SLE or LN.

IP-10, or CXCL10, is an IFN-driven chemokine secreted by multiple cell types and acts as a regulator for T cell movement (40). Serum IP-10 has previously been studied in the context of SLE (41–43) and shown to be associated with disease activity, but studies on urinary levels of IP-10 are limited.

TARC, also known as CCL17, is a chemokine that mediates chemoattraction of T cells (44). It has been extensively studied in the context of atopic dermatitis and other skin diseases (45) and implicated as a biomarker for systemic sclerosis (46). Serum levels of TARC have previously been reported to be elevated in SLE patients (47,48), but correlations between TARC levels and SLE

disease activity have been inconclusive. It has also been noted that CCR4, the receptor that binds TARC/CCL17, is up-regulated in T cells in multiple autoimmune disorders, including SLE, rheumatoid arthritis, and ankylosing spondylitis (49). It is interesting to note that 2 of the 5 biomarkers examined here are heavily involved in T cell migration or recruitment patterns. It is possible that IP-10 and TARC are both involved in disease pathology of LN by determining the extent of T cell migration into the end organs to initiate or propagate inflammation.

While the data presented in this study suggest that IL-7, IL-12p40, IL-15, IP-10 and TARC are all promising diagnostic biomarkers, further studies are warranted to validate these findings. A longitudinal study monitoring the change in these proteins relative to disease activity is needed to determine if these biomarkers are specific for lupus renal disease activity and to assess their ability to monitor disease activity over time. Further cross-sectional studies that include patients with different demographic characteristics are also needed.

Although the urinary molecules assayed showed fairly good specificity for LN, these differences were not always significant, owing partly to outliers in the group with other chronic kidney diseases. In particular, relatively high levels of urinary IL-7, IL-15, IP-10, and TARC were noted in one subject with IgA nephropathy. Hence, it is important to expand these groups of chronic kidney disease controls in future analyses in order to get a better read of the specificity of the molecules assayed for LN, as well as IgA nephropathy.

In conclusion, custom ECL-based multiplex immunoassay panels are a promising technology for the identification and validation of potential urinary biomarkers of LN. This method is an effective hybrid that combines the sensitivity of the ECL proteomic screening platform with the sample throughput of a traditional 96-well-based assay, in order to detect novel low-abundance biomarkers in body fluids. The use of this new platform has identified IL-7, IL-12p40, IL-15, IP-10, and TARC as novel low-abundance urinary biomarkers of LN, with reasonable specificity.

AUTHOR CONTRIBUTIONS

All authors were involved in drafting the article or revising it critically for important intellectual content, and all authors approved the final version to be published. Dr. Mohan had full access to all of the data in the study and takes responsibility for the integrity of the data and the accuracy of the data analysis.

Study conception and design. Stanley, Mohan.

Acquisition of data. Stanley, Mok, Vanarsa, Habazi, Li, Saxena.





Analysis and interpretation of data. Stanley, Pedroza*, Mohan.

REFERENCES

- Belendiuk KA, Trinh H, Cascino MD, Dragone L, Keebler D, Garg J. Lupus nephritis is associated with increased rates of hospitalization and in-hospital mortality compared with non-renal lupus and matched controls: an analysis of insurance claims data. *Ann Rheum Dis* 2017;76:593–4.
- Cameron JS. Lupus nephritis. *J Am Soc Nephrol* 1999;10:413–24.
- Esdaile JM, Joseph L, MacKenzie T, Kashgarian M, Hayslett JP. The benefit of early treatment with immunosuppressive agents in lupus nephritis. *J Rheumatol* 1994;21:2046–51.
- SomaLogic. SOMAscan proteomic assay technical white paper. 2015. p. 1–14.
- Jones VS, Tang H, Huang RP. Exploring protein phosphorylation with RayBio antibody arrays and ELISAs. URL: https://www.raybiotech.com/files/Tech-Support/App-Notes/Protein-Phosphorylation_appnote.pdf.
- Pan S, Aebersold R, Chen R, Rush J, Goodlett DR, McIntosh MW, et al. Mass spectrometry based targeted protein quantification: methods and applications. *J Proteome Res* 2008;8:787–97.
- Bard AJ, Debad JD, Leland JK, Sigal GB, Wilbur JL, Wohlstadter JN. Chemiluminescence: electrogenerated. In: Meyers RA, editor. *Encyclopedia of analytical chemistry: applications, theory and instrumentation*. New York: John Wiley & Sons; 2000. p. 9842–9.
- Debad JD, Glezer EN, Wohlstadter JN, Sigal GB, Leland JK. Clinical and biological applications of ECL. In: Bard AJ, editor. *Electrogenerated chemiluminescence*. New York: Marcel Dekker; 2004. p. 43–78.
- Richter MM. Electrochemiluminescence. *Chemical Rev* 2004;104:3003–36.
- Scussel Lonzetti L, Joyal F, Raynauld JP, Roussin A, Goulet JR, Rich E, et al. Updating the American College of Rheumatology preliminary classification criteria for systemic sclerosis: addition of severe nailfold capillaroscopy abnormalities markedly increases the sensitivity for limited scleroderma [letter]. *Arthritis Rheum* 2001;44:735–6.
- Nepomnyashchii AB, Bard AJ, Leland JK, Debad JD, Sigal GB, Wilbur JL, et al. Chemiluminescence, electrogenerated. In: *Encyclopedia of analytical chemistry: applications, theory, and instrumentation*. New York: John Wiley & Sons; 2014. p. 1–12.
- El-Shehaby A, Darweesh H, El-Khatib M, Momtaz M, Marzouk S, El-Shaarawy N, et al. Correlations of urinary biomarkers, TNF-like weak inducer of apoptosis (TWEAK), osteoprotegerin (OPG), monocyte chemoattractant protein-1 (MCP-1), and IL-8 with lupus nephritis. *J Clin Immunol* 2011;31:848–56.
- Singh RG, Usha, Rathore SS, Behura SK, Singh NK. Urinary MCP-1 as diagnostic and prognostic marker in patients with lupus nephritis flare. *Lupus* 2012;21:1214–8.
- Korbet SM, Schwartz MM, Evans J, Lewis EJ, for the Collaborative Study Group. Severe lupus nephritis: racial differences in presentation and outcome. *J Am Soc Nephrol* 2007;18:244–54.
- Zhao Z, Burkly LC, Campbell S, Schwartz N, Molano A, Choudhury A, et al. TWEAK/Fn14 interactions are instrumental in the pathogenesis of nephritis in the chronic graft-versus-host model of systemic lupus erythematosus. *J Immunol* 2007;179:7949–58.
- Wu T, Xie C, Wang HW, Zhou XJ, Schwartz N, Calixto S, et al. Elevated urinary VCAM-1, P-selectin, soluble TNF receptor-1, and CXC chemokine ligand 16 in multiple murine lupus strains and human lupus nephritis. *J Immunol* 2007;179:7166–75.
- Mok CC. Biomarkers for lupus nephritis: a critical appraisal. *J Biomed Biotechnol* 2010;2010:638413.
- Tsai CY, Wu TH, Yu CL, Lu JY, Tsai YY. Increased excretions of β 2-microglobulin, IL-6, and IL-8 and decreased excretion of Tamm-Horsfall glycoprotein in urine of patients with active lupus nephritis. *Nephron* 2000;85:207–14.
- Oliver JC, Bland LA, Oettinger CW, Arduino MJ, McAllister SK, Aguero SM, et al. Cytokine kinetics in an in vitro whole blood model following an endotoxin challenge. *Lymphokine Cytokine Res* 1993;12:115–20.
- Thavasu PW, Longhurst S, Joel SP, Slevin ML, Balkwill FR. Measuring cytokine levels in blood: importance of anticoagulants, processing, and storage conditions. *J Immunol Methods* 1992;153:115–24.

21. Panicker G, Meadows KS, Lee DR, Nisenbaum R, Unger ER. Effect of storage temperatures on the stability of cytokines in cervical mucous. *Cytokine* 2007;37:176–9.
22. National Center for Biotechnology Information. IL7 interleukin 7 [homo sapiens (human)]. URL: <https://www.ncbi.nlm.nih.gov/gene/3574>.
23. Thiant S, Yakoub-Agha I, Magro L, Trauet J, Coiteux V, Jouet JP, et al. Plasma levels of IL-7 and IL-15 in the first month after myeloablative BMT are predictive biomarkers of both acute GVHD and relapse. *Bone Marrow Transplant* 2010;45:1546–52.
24. Motylewska E, Niec M, Siejka A, Komorowski J, Lawnicka H, Swietoslawki, et al. Decreased serum level of IL-7 in patients with active Graves' disease. *Cytokine* 2015;75:373–9.
25. Sun LY, Zhang HY, Feng XB, Hou YY, Lu LW, Fan LM. Abnormality of bone marrow-derived mesenchymal stem cells in patients with systemic lupus erythematosus. *Lupus* 2007;16:121–8.
26. Graninger WB, Steiner CW, Graninger MT, Aringer M, Smolen JS. Cytokine regulation of apoptosis and Bcl-2 expression in lymphocytes of patients with systemic lupus erythematosus. *Cell Death Differ* 2000;7:966–72.
27. UniProt. UniProtKB: P29460 (IL12B_HUMAN). URL: <https://www.uniprot.org/uniprot/P29460>.
28. Lee SY, Jung YO, Kim DJ, Kang CM, Moon YM, Heo YJ, et al. IL-12p40 homodimer ameliorates experimental autoimmune arthritis. *J Immunol* 2015;195:3001–10.
29. Bielekova B, Komori M, Xu Q, Reich DS, Wu T. Cerebrospinal fluid IL-12p40, CXCL13 and IL-8 as a combinatorial biomarker of active intrathecal inflammation. *PLoS One* 2012;7:e48370.
30. Lauwerys BR, Garot N, Renaud JC, Houssiau FA. Interleukin-10 blockade corrects impaired in vitro cellular immune responses of systemic lupus erythematosus patients. *Arthritis Rheum* 2000;43:1976–81.
31. Koenig KF, Groeschl I, Pesickova SS, Tesar V, Eisenberger U, Trendelenburg M. Serum cytokine profile in patients with active lupus nephritis. *Cytokine* 2012;60:410–6.
32. Liu TF, Jones BM, Wong RW, Srivastava G. Impaired production of IL-12 in systemic lupus erythematosus. III: deficient IL-12 p40 gene expression and cross-regulation of IL-12, IL-10 and IFN- γ gene expression. *Cytokine* 1999;11:805–11.
33. Huang X, Hua J, Shen N, Chen S. Dysregulated expression of interleukin-23 and interleukin-12 subunits in systemic lupus erythematosus patients. *Mod Rheumatol* 2007;17:220–3.
34. Yang J, Chu Y, Yang X, Gao D, Zhu L, Yang X, et al. Th17 and natural Treg cell population dynamics in systemic lupus erythematosus. *Arthritis Rheum* 2009;60:1472–83.
35. Yokoyama S, Watanabe N, Sato N, Perera PY, Filkoski L, Tanaka T, et al. Antibody-mediated blockade of IL-15 reverses the autoimmune intestinal damage in transgenic mice that overexpress IL-15 in enterocytes. *Proc Natl Acad Sci U S A* 2009;106:15849–54.
36. Bishnoi RJ, Palmer RF, Royall DR. Serum interleukin (IL)-15 as a biomarker of Alzheimer's disease. *PLoS One* 2015;10:e0117282.
37. Aringer M, Stummvoll GH, Steiner G, Köller M, Steiner CW, Höfler E, et al. Serum interleukin-15 is elevated in systemic lupus erythematosus. *Rheumatology (Oxford)* 2001;40:876–81.
38. Baranda L, de la Fuente H, Layseca-Espinosa E, Portales-Pérez D, Niño-Moreno P, Valencia-Pacheco G, et al. IL-15 and IL-15R in leukocytes from patients with systemic lupus erythematosus. *Rheumatology (Oxford)* 2005;44:1507–13.
39. Robak E, Robak T, Wozniacka A, Zak-Prelich M, Sysa-Jedrzejowska A, Stepień H. Proinflammatory interferon- γ -inducing monokines (interleukin-12, interleukin-18, interleukin-15): serum profile in patients with systemic lupus erythematosus. *Eur Cytokine Netw* 2002;13:364–8.
40. UniProt. UniProtKB: P02778 (CXL10_HUMAN). URL: <https://www.uniprot.org/uniprot/P02778>.
41. Narumi S, Takeuchi T, Kobayashi Y, Konishi K. Serum levels of IFN-inducible protein-10 relating to the activity of systemic lupus erythematosus. *Cytokine* 2000;12:1561–5.
42. Rose T, Grützkau A, Hirseland H, Huscher D, Dähnrich C, Dzionek A, et al. IFN α and its response proteins, IP-10 and SIGLEC-1, are biomarkers of disease activity in systemic lupus erythematosus. *Ann Rheum Dis* 2013;72:1639–45.
43. Abujam B, Cheekatla SS, Aggarwal A. Urinary CXCL-10/IP-10 and MCP-1 as markers to assess activity of lupus nephritis. *Lupus* 2013;22:614–23.
44. Imai T, Baba M, Nishimura M, Kakizaki M, Takagi S, Yoshie O. The T cell-directed CC chemokine TARC is a highly specific biological ligand for CC chemokine receptor 4. *J Biol Chem* 1997;272:15036–42.
45. Tamaki K, Kakinuma T, Saeki H, Horikawa T, Kataoka Y, Fujisawa T, et al. Serum levels of CCL17/TARC in various skin diseases. *J Dermatol* 2006;33:300–2.
46. Fujii H, Shimada Y, Hasegawa M, Takehara K, Sato S. Serum levels of a Th1 chemoattractant IP-10 and Th2 chemoattractants, TARC and MDC, are elevated in patients with systemic sclerosis. *J Dermatol Sci* 2004;35:43–51.
47. Okamoto H, Koizumi K, Yamanaka H, Saito T, Kamatani N. A role for TARC/CCL17, a CC chemokine, in systemic lupus erythematosus. *J Rheumatol* 2003;30:2369–73.
48. Lit LC, Wong CK, Tam LS, Li EK, Lam CW. Raised plasma concentration and ex vivo production of inflammatory chemokines in patients with systemic lupus erythematosus. *Ann Rheum Dis* 2006;65:209–15.
49. Yang PT, Kasai H, Zhao LJ, Xiao WG, Tanabe F, Ito M. Increased CCR4 expression on circulating CD4+ T cells in ankylosing spondylitis, rheumatoid arthritis and systemic lupus erythematosus. *Clin Exp Immunol* 2004;138:342–7.

Monitoring Disease Activity in Systemic Lupus Erythematosus With Single-Molecule Array Digital Enzyme-Linked Immunosorbent Assay Quantification of Serum Interferon- α

Alexis Mathian,¹  Suzanne Mouries-Martin,² Karim Dorgham,³  Hervé Devilliers,⁴ Laura Barnabei,⁵ Elyès Ben Salah,³ Fleur Cohen-Aubart,¹  Laura Garrido Castillo,³ Julien Haroche,¹ Miguel Hie,⁶ Marc Pineton de Chambrun,⁶ Makoto Miyara,³ Delphine Sterlin,³ Micheline Pha,⁶ Du Lê Thi Huong,⁶ Frédéric Rieux-Laucat,⁵ Flore Rozenberg,⁷ Guy Gorochov,³  and Zahir Amoura¹

Objective. No simple or standardized assay is available to quantify interferon- α (IFN α) in routine clinical practice. Single-molecule array (Simoa) digital enzyme-linked immunosorbent assay (ELISA) technology enables direct IFN α quantification at attomolar (femtogram per milliliter [fg/ml]) concentrations. This study was undertaken to assess IFN α digital ELISA diagnostic performances to monitor systemic lupus erythematosus (SLE) activity.

Methods. IFN α concentrations in serum samples from 150 consecutive SLE patients in a cross-sectional study were determined with digital ELISA and a functional biologic activity assay (bioassay). According to their Safety of Estrogens in Lupus Erythematosus National Assessment version of the Systemic Lupus Erythematosus Disease Activity Index (SLEDAI) flare composite scores, patients were divided into groups with inactive SLE (SLEDAI score of <4 or clinical SLEDAI score of 0) or active SLE (SLEDAI score of \geq 4 or clinical SLEDAI score of >0), and into groups with no flare or mild/moderate flare or severe flare.

Results. Based on serum samples from healthy blood donors, the abnormal serum IFN α level threshold value was 136 fg/ml. Next, using receiver operating characteristic curves for an SLE patient series that was widely heterogeneous in terms of disease activity and organ involvement, the threshold IFN α value associated with active disease was determined to be 266 fg/ml. The digital ELISA–assessed serum IFN α level was a better biomarker of disease activity than the Farr assay because its specificity, likelihood ratio for positive results, and positive predictive value better discerned active SLE or flare from inactive disease. The digital ELISA was more sensitive than the bioassay for detecting low-abnormal serum IFN α concentrations and identifying patients with low disease activity.

Conclusion. Direct serum IFN α determination with a highly sensitive assay might improve monitoring of clinical SLE activity and selection of the best candidates for anti-IFN α treatment.

INTRODUCTION

Systemic lupus erythematosus (SLE) is a chronic autoimmune disease of unknown etiology characterized by the presence

of antinuclear autoantibodies and inflammation in a wide spectrum of organs (1,2). The survival of SLE patients has plateaued since the middle 1990s (3). To date, anti–double-stranded DNA (anti-dsDNA) antibody titration, best achieved with the standard

Supported by the AP-HP (Centre d'Investigations Biomédicales Pitié-Salpêtrière), INSERM, Sorbonne Université, the French Arthritis Foundation, the Société Nationale Française de Médecine Interne, and the Fondation pour la Recherche Médicale. Ms Barnabei is a fellow of the ImaginePhD international program supported by the Fondation Bettencourt Schueller.

¹Alexis Mathian, MD, PhD, Fleur Cohen-Aubart, MD, PhD, Julien Haroche, MD, PhD, Zahir Amoura, MD, MSc: Sorbonne Université, Assistance Publique-Hôpitaux de Paris, Groupement Hospitalier Pitié-Salpêtrière, French National Referral Center for Systemic Lupus Erythematosus, Antiphospholipid Antibody Syndrome and Other Autoimmune Disorders, Service de Médecine Interne 2, Institut E3M, INSERM UMRS, Centre d'Immunologie et des Maladies Infectieuses (CIMI-Paris), Paris, France; ²Suzanne Mouries-Martin, MD, MSc: Centre Hospitalier Universitaire de Dijon, Hôpital François-Mitterrand, service de médecine interne et maladies systémiques (médecine

interne 2), Dijon, France; ³Karim Dorgham, PhD, Elyès Ben Salah, PharmD, Laura Garrido Castillo, MSc, Makoto Miyara, MD, PhD, Delphine Sterlin, PharmD, PhD, Guy Gorochov, MD, PhD: Sorbonne Université, INSERM UMRS, Centre d'Immunologie et des Maladies Infectieuses (CIMI-Paris), Assistance Publique-Hôpitaux de Paris, Groupement Hospitalier Pitié-Salpêtrière, Paris, France; ⁴Hervé Devilliers, MD, PhD: Centre Hospitalier Universitaire de Dijon, Hôpital François-Mitterrand, service de médecine interne et maladies systémiques (médecine interne 2) and Centre d'Investigation Clinique, INSERM CIC 1432, Dijon, France; ⁵Laura Barnabei, MSc, Frédéric Rieux-Laucat, PhD: Laboratory of Immunogenetics of Pediatric Autoimmune Diseases, INSERM UMR-Institut Imagine, Sorbonne Paris Cité, Paris, France; ⁶Miguel Hie, MD, MSc, Marc Pineton de Chambrun, MD, MSc, Micheline Pha, MD, MSc, Du Lê Thi Huong, MD, PhD: Assistance Publique-Hôpitaux de Paris, Groupement Hospitalier Pitié-Salpêtrière, French National Referral Center

Farr assay, has been used to monitor global disease activity and SLE renal involvement (4–7). However, because associations with disease characteristics are at best modest, clinicians and researchers still lack reliable biomarkers of SLE activity (4–7). At present, many authors consider the dysregulation of interferons (IFNs) to be a central cause of the immunologic abnormalities observed in SLE (8–14).

Early studies showed elevated serum IFN α levels in SLE patients to be associated with disease activity and severity (15–17). More recently, transcriptome analysis using microarray technology revealed up-regulation of numerous IFN-stimulated genes (ISGs) in the peripheral blood mononuclear cells of patients with SLE, constituting an overall “IFN signature” (18,19). That signature is found in almost all pediatric patients and 50–80% of adults with SLE (20). Thus, the close association between IFN α overexpression and SLE activity suggests that monitoring this cytokine might help physicians better evaluate disease activity (21–25). Knowing the IFN α concentration might also help select the best candidates for anti-IFN α treatment (26,27). Unfortunately, no reliable, simple, or standardized assays to quantify IFN α in routine clinical practice are available; notably, enzyme-linked immunosorbent assays (ELISAs) to detect IFN α in human sera have been hindered by low sensitivity and low specificity (28), and assays based on detecting IFN α biologic activity are difficult to standardize (15–17). Alternatively, quantification of the expression of different ISGs as “IFN scores” can be used as a surrogate to monitor IFN activity in SLE (29–31). Not surprisingly, IFN scores have been associated with SLE activity (29,32–34). However, the low availability and high complexity of transcriptome–microarray technology means that the IFN scores, as well, are not standardized and cannot be used in routine practice.

The new single-molecule array (Simoa) assay, also called digital ELISA, based on counting individual enzyme-labeled immunocomplexes of proteins captured on beads in single-molecule arrays, enables direct IFN α quantification at attomolar (femtogram per milliliter [fg/ml] or 5×10^{-15} moles/ml) concentrations (35–37), corresponding to a 5,000-fold increased sensitivity over commercial ELISAs. We hypothesized that serum IFN α levels determined with this new standardized assay would represent a better biomarker of SLE activity than the Farr assay. Therefore, the primary objective of this study was to characterize the relationship between digital ELISA–determined serum IFN α concentrations and clinically assessed SLE activity. We also compared

that assay to a functional sensitive biologic assay (bioassay), based on IFN α antiviral properties, that has been used routinely in our institution for 30 years (38–40).

PATIENTS AND METHODS

Study design, patients, and controls. Serum samples were obtained from 150 consecutive patients (139 women, 11 men) diagnosed as having SLE according to the 1997 updated American College of Rheumatology criteria for SLE classification (41). SLE patients were referred to our National Referral Center for SLE. SLE clinical characteristics, the Safety of Estrogens in Lupus Erythematosus National Assessment (SELENA) version of the Systemic Lupus Erythematosus Disease Activity Index (SLEDAI) (42–44), and the therapeutic regimen were recorded on the day blood was drawn (day 0). The class of lupus nephritis, according to the International Society of Nephrology/Renal Pathology Society 2003 classification (45), was recorded, and the serum sample was obtained within 3 days before or after the renal biopsy. Routine testing to determine anti-dsDNA antibody titers using the Farr assay (cutoff value 9.0 IU/ml) (Trinity Biotech) and anti-RNP antibody levels (anti-Sm, anti-SSA/Ro60, anti-Ro 52/TRIM21, and anti-SSB) (Luminex FIDIS; Theradiag) was conducted, and laboratory analyses to determine C3 and C4 levels (Optilite; The Binding Site), complete blood cell counts, serum creatinine levels, and presence of proteinuria and hematuria were performed.

According to their SELENA–SLEDAI scores, patients were divided into groups of inactive SLE (SLEDAI score <4; $n = 68$) or active SLE (SLEDAI score ≥ 4 ; $n = 82$). The presence of a severe or mild/moderate lupus flare was recorded according to the SELENA–SLEDAI flare instrument (see Supplementary Methods, available on the *Arthritis & Rheumatology* web site at <http://onlinelibrary.wiley.com/doi/10.1002/art.40792/abstract>) (43,44). For logistic regression analyses, the domains of activity were assigned by the SELENA–SLEDAI scores in those domains. Serum samples from 68 age- and sex-matched healthy donors (Établissement Français du Sang, Île-de-France, Pitié–Salpêtrière Hospital) were collected during the same time period.

The primary objective of the study was to assess the diagnostic performance of the IFN α digital ELISA to monitor SLE activity. The secondary goal was to compare the performances of the digital ELISA and the bioassay. Exclusion criteria were 1) known or suspected infection on day 0, or 2) increased hydroxychloroquine, prednisone, and/or immunosuppressant dose(s)

for Systemic Lupus Erythematosus, Antiphospholipid Antibody Syndrome and Other Autoimmune Disorders, Service de Médecine Interne 2, Institut E3M, Paris, France; ⁷Flore Rozenberg, MD, PhD: Sorbonne Paris Cité, Assistance Publique–Hôpitaux de Paris, Hôpital Cochin, Service de Virologie, Paris, France.

Drs. Mathian, Mouries-Martin, and Dorgham contributed equally to this work. Drs. Gorochov and Amoura contributed equally to this work.

No potential conflicts of interest relevant to this article were reported.

Address correspondence to Alexis Mathian, MD, PhD, Service de Médecine Interne 2, Institut E3M, Hôpital de la Pitié–Salpêtrière, 47–83, Boulevard de l’Hôpital, 75651 Paris Cedex 13, France. E-mail: alexis.mathian@aphp.fr.

Submitted for publication December 18, 2017; accepted in revised form November 18, 2018.

during the 4 weeks preceding day 0. The study was approved by the local ethics committee (no. 30052012), and informed consent was provided by all participants. The research was carried out in compliance with the Helsinki Declaration.

IFN α bioassay. Serum IFN α biologic activity (in IU/ml) was determined by assessing the protection afforded by each patient's serum to cultured Madin-Darby bovine kidney cells infected with vesicular stomatitis virus, as described previously (38,46–48) (see Supplementary Methods, available on the *Arthritis & Rheumatology* web site at <http://onlinelibrary.wiley.com/doi/10.1002/art.40792/abstract>). Bioassay sensitivity (the lower limit of detection) was 2 IU/ml. Serum IFN α activity in healthy individuals is undetectable at a level of <2 IU/ml (39,49).

IFN α digital ELISA. Serum IFN α concentrations (in fg/ml) were determined with an IFN α digital ELISA technology reagent kit (Simoa; Quanterix), which is based on a 3-step protocol using an HD-1 Analyzer (Quanterix) (35) (see Supplementary Methods, available at <http://onlinelibrary.wiley.com/doi/10.1002/art.40792/abstract>).

Statistical analysis. Qualitative variables are expressed as the number (percentage), and quantitative parameters as the mean \pm SD or median (range), as appropriate. Differences between patient groups were tested with the Mann-Whitney U test or Student's *t*-test for continuous data, and Fisher's exact test or chi-square test for categorical data. Spearman's correlation coefficients were computed for quantitative values. The diagnostic performances of the Farr assay, IFN α digital ELISA, and the bioassay to detect SLE disease activity were investigated by analyzing receiver operating characteristic (ROC) curves, with the SELENA-SLEDAI-assessed clinical activity as the gold standard for those analyses. Because the SELENA-SLEDAI measure includes the Farr assay among the domains scored, we used for this analysis the clinical SELENA-SLEDAI that refers to symptoms, signs, and routine laboratory testing, disregarding the points that can be given for the presence of anti-DNA antibodies and/or low complement levels (50). The areas under the ROC curves (AUCs) to differentiate active versus inactive SLE and an SLE flare versus no flare according to the digital ELISA, bioassay, and Farr assay were compared using a nonparametric approach (51). The optimal thresholds were determined using a compromise among the maximum correct classification rate, the minimum distance to the upper left corner of the ROC curve, the minimum sensitivity – specificity difference, and the Youden index. Sensitivities, specificities, likelihood ratios, positive predictive values, and negative predictive values were calculated. McNemar's test for paired proportions was used to compare sensitivities and specificities. No statistical analyses were performed on likelihood ratios and predictive values.

To identify SLE parameters independently associated with the absence of detectable serum IFN α in patients with

active disease, variables significantly associated with the false-negative rate in bivariable analyses were entered into a multivariable logistic regression model with stepwise selection of variables ($P = 0.30$ for entry and $P = 0.10$ for exit). Alternatively, to identify SLE parameters independently associated with bioassay- or digital ELISA-detected abnormal IFN α levels, univariable and multivariable logistic regression analyses using backward stepwise variable elimination were performed (with the variable exit threshold set at $P > 0.10$). All potential explanatory variables included in the multivariable analyses were subjected to collinearity analysis with a correlation matrix. None of these variables were associated with each other. Model goodness-of-fit was assessed with the determination coefficient (R^2). All tests were 2-sided, and P values less than 0.05 were considered significant. Statistical analyses were performed using GraphPad Prism (version 5.0), IBM SPSS Statistics (version 22.0), and SAS 9.4 software.

RESULTS

Patient characteristics. The baseline characteristics of the patients are described in Table 1. Approximately half of the patients had SELENA-SLEDAI-defined active SLE (score ≥ 4) or a SELENA-defined flare. Immunosuppressant therapy was mycophenolate mofetil for 18 patients, methotrexate for 13 patients, and azathioprine for 6 patients.

Serum IFN α concentrations in SLE patients. Digital ELISA-determined serum IFN α concentrations in patients with active SLE (median 1,396 fg/ml [range 0–53,000]) were significantly higher than those in patients with inactive SLE (median 14 fg/ml [range 0–4,328]) ($P < 0.0001$) and healthy controls (median 0 fg/ml [range 0–269]) ($P < 0.0001$). Concentrations also differed significantly between patients with inactive SLE and healthy controls ($P < 0.0001$) (Figure 1).

The IFN α digital ELISA positivity threshold was 136 fg/ml, which is 3 SD above the mean serum IFN α concentration calculated from the serum samples from the 68 healthy blood donors. Using that cutoff value, the digital ELISA was able to detect abnormal serum IFN α concentrations (>136 fg/ml) in 78 SLE patients (52%).

Bioassay-determined serum IFN α levels were significantly higher in patients with active SLE (median 5 IU/ml [range 0–200]) than those with inactive disease (median 0 IU/ml [range 0–12]) ($P < 0.0001$) (Figure 1). The bioassay was able to detect abnormal serum IFN α levels (≥ 2 IU/ml) in 56 SLE patients (37%).

Sensitivity of digital ELISA versus the bioassay to detect abnormal serum IFN α levels. Although the digital ELISA- and bioassay-determined serum IFN α levels were significantly correlated (Spearman's rank $r = 0.77$ [95% confidence

Table 1. Baseline characteristics and disease parameters in SLE patients (n = 150)*

Women	139 (92.7)
Age, mean \pm SD years	36.2 \pm 12.5
Disease duration, mean \pm SD years	9.8 \pm 9.1
SELENA-SLEDAI score, median (range)	4 (0–36)
SELENA-SLEDAI score \geq 4	82 (54.7)
Mild/moderate flare \dagger	21 (14)
Severe flare \dagger	53 (35.3)
Fever	31 (20.7)
Weight loss or anorexia	18 (12)
Lymphadenopathy	21 (14)
Active cutaneous lupus	37 (24.7)
Active lupus serositis	17 (11.3)
Active lupus arthritis	44 (29.3)
Active lupus nephropathy	20 (13.3)
Active neuropsychiatric lupus	6 (4)
Hydroxychloroquine use	124 (82.7)
Prednisone use	90 (60)
Prednisone \geq 10 mg/day	38 (25.3)
Immunosuppressive agent use \ddagger	37 (24.7)
Positive Farr assay	87 (58)
Positive for anti-RNP antibodies	53 (35.3)
Positive for anti-Sm antibodies	28 (18.7)
Positive for anti-Ro/SSA 52 antibodies	48 (32)
Positive for anti-Ro/SSA 60 antibodies	64 (42.7)
Positive for anti-La/SSB antibodies	20 (13.3)
Low C3 level	54/147 (36.7) \S

* Except where indicated otherwise, values are the number (%). SLE = systemic lupus erythematosus; SELENA-SLEDAI = Safety of Estrogens in Lupus Erythematosus National Assessment version of the Systemic Lupus Erythematosus Disease Activity Index.

\dagger Defined using the SELENA flare instrument.

\ddagger Excluding antimalarials and prednisone.

\S Value shown is the number of positive assay results/number of patients assessed (%).

interval 0.69–0.83]) ($P < 0.0001$), the digital ELISA was able to identify 29 SLE patients with a serum IFN α concentration of >136 fg/ml (Figure 2) and negative biologic activity (data not shown), thereby indicating the digital ELISA's higher sensitivity than the bioassay to detect abnormal serum IFN α concentrations. We also compared digital ELISA IFN α measurements with the ISG score of samples from 22 SLE patients (see Supplementary Figure 2, available on the *Arthritis & Rheumatology* web site at <http://onlinelibrary.wiley.com/doi/10.1002/art.40792/abstract>). We used an ISG score, described previously by Rice et al, based on quantitative polymerase chain reaction assessment of 6 ISGs (52,53). In this test, the median fold change of the ISGs when compared with the median in healthy controls is used to create an IFN score. Serum IFN α levels were highly positively correlated with the ISG scores ($r = 0.74$, $P < 10^{-4}$). Only 2 patients showed

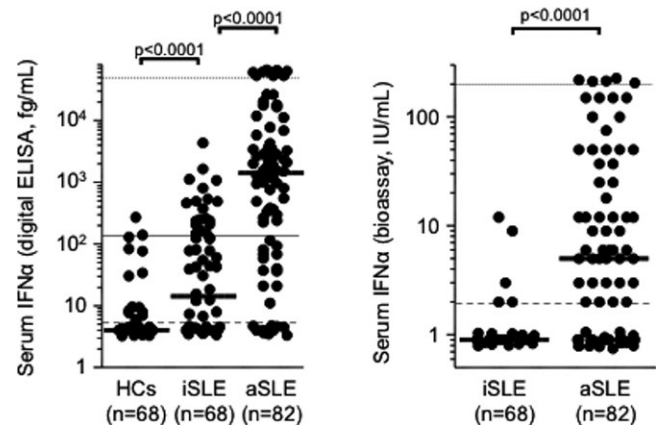


Figure 1. Serum interferon- α (IFN α) concentrations according to systemic lupus erythematosus (SLE) activity assessed with digital enzyme-linked immunosorbent assay (ELISA) (left) or functional bioassay (right). Patients were divided into groups with inactive SLE (iSLE; Systemic Lupus Erythematosus Disease Activity Index [SLEDAI] score of <4) or active SLE (aSLE; SLEDAI score of ≥ 4). The IFN α digital ELISA positivity threshold (solid lines) was 3 SD above the mean of the 68 serum samples from healthy control (HC) blood donors, i.e., 136 fg/ml. The lower limits (broken lines) and upper limits (dotted lines) of quantification were 5–52,200 fg/ml for the digital ELISA and 2–200 IU/ml for the functional bioassay. Symbols represent individual subjects; bars show the median. Statistical analyses were conducted using the Mann-Whitney U test.

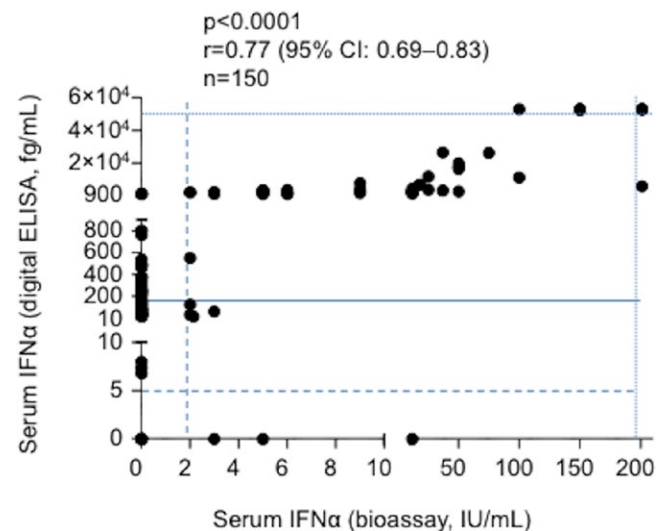


Figure 2. Correlation between the interferon- α (IFN α) digital enzyme-linked immunosorbent assay (ELISA)– and bioassay-determined concentrations. The IFN α digital ELISA positivity threshold (solid line), the upper limit of quantification (dotted line), and the lower limit of detection (broken lines) are shown. The IFN α cutoff concentration of 1,130 fg/ml gave the best agreement between the digital ELISA and the bioassay (see Supplementary Figure 1 and Supplementary Table 1, available on the *Arthritis & Rheumatology* web site at <http://onlinelibrary.wiley.com/doi/10.1002/art.40792/abstract>). Symbols represent individual patients. Statistical analyses were conducted using Spearman's rank correlation coefficient. 95% CI = 95% confidence interval.

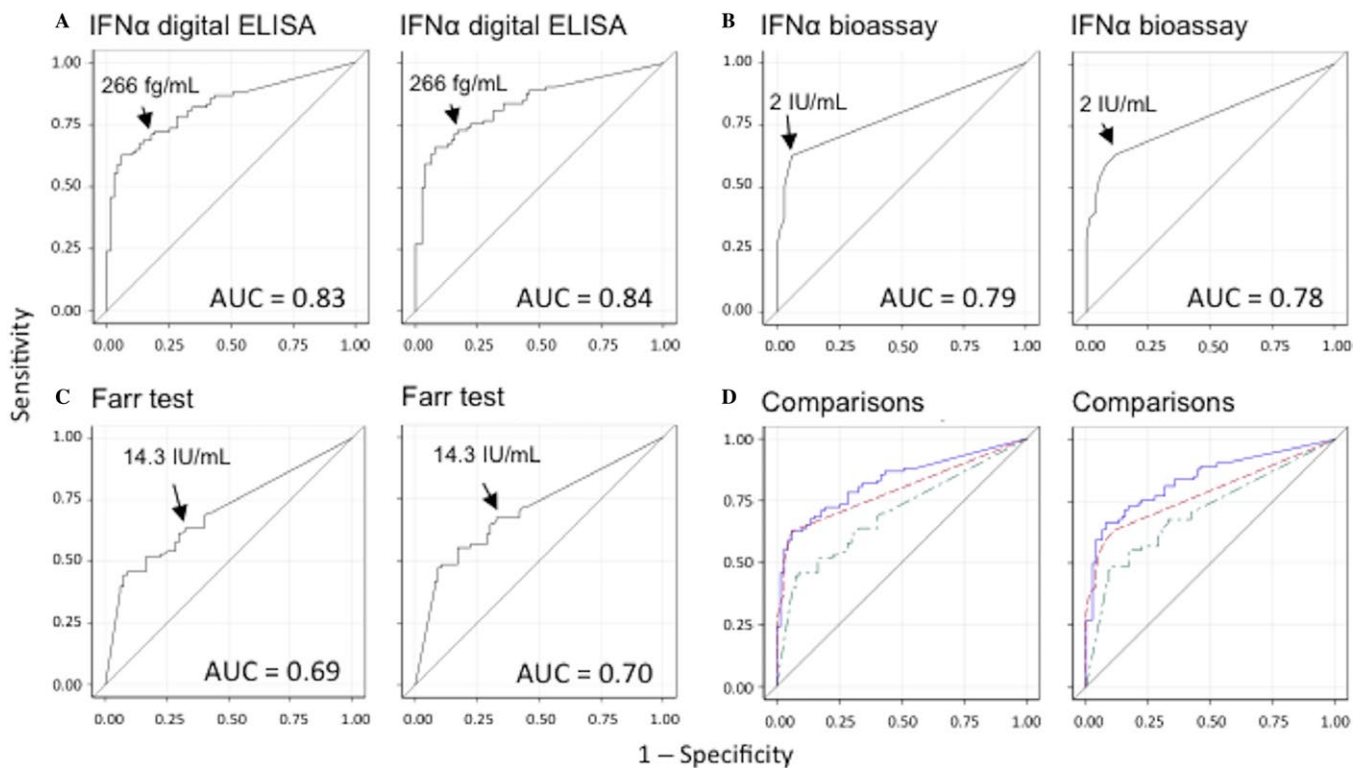


Figure 3. Receiver operating characteristic (ROC) curves of interferon- α (IFN α) concentrations to discern active systemic lupus erythematosus (SLE). **A–C**, The diagnostic performances of the serum IFN α digital enzyme-linked immunosorbent assay (ELISA) (**A**), bioassay (**B**), and Farr assay (**C**) to detect SLE activity (active versus inactive) were investigated by analyzing ROC curves, with the Safety of Estrogens in Lupus Erythematosus National Assessment (SELENA) version of the Systemic Lupus Erythematosus Disease Activity Index (SLEDAI)-assessed clinical activity score serving as the gold standard. **D**, The area under each ROC curve (AUC) is given for the digital ELISA (blue), the Farr test (green), and the bioassay (red). The optimal cutoff point represented for each ROC curve was determined using the maximum correct classification rate, the minimum distance to the upper left corner of the curve, the minimum sensitivity – specificity difference, and Youden's index score. In **A–D** (left), patients were divided into groups with inactive (clinical SLEDAI score of 0) or active SLE (clinical SLEDAI score of >0). In **A–D** (right), using the SELENA flare identifier, patients were divided into groups with no flare or experiencing a flare.

a positive ISG score and a serum IFN α level below the positivity threshold for the digital ELISA (<136 fg/ml).

Digital ELISA and bioassay diagnostic performances to discriminate active SLE. The ROC AUC for the IFN α digital ELISA to differentiate between active and inactive SLE was 0.83, better than that of the Farr assay (0.69; $P = 0.007$) (Figure 3). The ROC AUC for the IFN α digital ELISA to differentiate between an SLE flare and no flare was 0.84, better than that of the Farr assay (0.70; $P = 0.006$). The ROC AUC for the IFN α bioassay was 0.79 to differentiate between active and inactive SLE ($P = 0.04$ versus the Farr assay) and 0.78 to differentiate between an SLE flare and no flare ($P = 0.09$ versus the Farr assay).

The optimal thresholds to distinguish between patients with active SLE and those with inactive SLE or between patients with a flare and those without a flare were identical, equal to 266 fg/ml for the digital ELISA, 2 IU/ml for the bioassay, and 14.3 IU/ml for the Farr assay. Using ROC curve-defined thresholds, the IFN α digital ELISA and the IFN α bioassay had significantly better specificity than the Farr assay to differentiate between active and inactive

SLE and between a flare and no flare (Table 2). The IFN α digital ELISA and the IFN α bioassay also had a better likelihood ratio for positive results and positive predictive value to identify active disease and flare than the Farr assay.

Sensitivity of IFN α digital ELISA versus IFN α bioassay to identify patients with active SLE.

The IFN α digital ELISA had significantly better sensitivity than the IFN α bioassay to differentiate between an SLE flare and no flare. Supplementary Table 2 (available on the *Arthritis & Rheumatology* web site at <http://onlinelibrary.wiley.com/doi/10.1002/art.40792/abstract>) reports positivity rates of the IFN α digital ELISA, bioassay, and Farr test according to SLE activity. The digital ELISA was able to identify a subset of 20 SLE patients with serum IFN α levels between 266 fg/ml (the cutoff associated with active SLE) and 1,130 fg/ml (the cutoff associated with the best agreement between the digital ELISA and the bioassay). In this subset of patients the median SLEDAI score was slightly, but significantly, higher than that in the subset of patients with serum IFN α levels below normal (4 versus 2; $P = 0.01$) (see Supplementary Figure 3, at <http://onlinelibrary>.

Table 2. Sensitivity and specificity of the IFN α digital ELISA, bioassay, and Farr assays to detect active SLE or flare*

	Sensitivity, % (95% CI)	Specificity, % (95% CI)	PLR	NLR	PPV, %	NPV, %
Active SLE†						
Digital ELISA‡	68.7 (57.6–78.4)	85.1 (74.3–92.6)§	4.6	0.37	85.1	68.7
Bioassay¶	62.7 (51.3–73.0)	94.0 (85.4–98.4)#	10.5	0.40	92.9	67.0
Farr assay**	63.9 (52.6–74.1)	67.2 (54.6–78.2)	1.9	0.54	70.7	60.0
SLE flare††						
Digital ELISA‡	73.0 (61.4–82.7)‡‡	82.9 (72.5–90.6)§	4.3	0.32	80.6	75.9
Bioassay¶	63.5 (51.5–74.4)	88.2 (78.7–94.4)§§	5.4	0.41	83.9	71.3
Farr assay**	67.6 (55.7–78.0)	67.1 (55.4–77.5)	2.0	0.48	66.7	68.0

* No statistical analyses were performed on likelihood ratios and predictive values. IFN α = interferon- α ; ELISA = enzyme-linked immunosorbent assay; 95% CI = 95% confidence interval; PLR = positive likelihood ratio; NLR = negative likelihood ratio; PPV = positive predictive value; NPV = negative predictive value.

† Safety of Estrogens in Lupus Erythematosus National Assessment (SELENA) version of the Systemic Lupus Erythematosus Disease Activity Index (SLEDAI)-defined groups were classified as having inactive systemic lupus erythematosus (SLE; clinical SLEDAI score of 0) or active SLE (clinical SLEDAI score of >0).

‡ The chosen positivity threshold for this assay was 266 fg/ml.

§ $P < 0.05$ versus Farr assay.

¶ The chosen positivity threshold for this assay was 2 IU/ml.

$P < 0.001$ versus Farr assay.

** The chosen positivity threshold for this assay was 14.3 IU/ml.

†† Defined using the SELENA flare instrument.

‡‡ $P < 0.05$ versus bioassay.

§§ $P < 0.01$ versus Farr assay.

wiley.com/doi/10.1002/art.40792/abstract). The vast majority of the subset of patients with serum IFN α levels of 266–1,130 fg/ml (17 of 20) had negative results on the bioassay. Thus, the digital ELISA was more sensitive than the bioassay to detect low-abnormal serum IFN α concentrations and patients with low disease activity.

Characteristics of digital ELISA false-negatives.

Patients with a digital ELISA false-negative result (active SLE but with a serum IFN α concentration of <266 fg/ml), as compared to patients with a true-positive result (active SLE and a serum IFN α concentration of \geq 266 fg/ml), were more likely to be treated with hydroxychloroquine, have more frequent arthritis without other organ involvement, lower anti-RNP antibody rates, and lower SELENA–SLEDAI activity scores (Table 3).

Patient characteristics associated with abnormal serum IFN α levels.

According to multivariable analyses, abnormal digital ELISA–determined IFN α concentrations were significantly associated with SLE-specific fever, active mucocutaneous lupus, active lupus nephritis, and anti-Sm antibodies, but no other anti-RNP antibodies (anti-Ro/SSA 52, anti-Ro/SSA 60, anti-La/SSB, and anti-RNP) (see Supplementary Table 3, at <http://onlinelibrary.wiley.com/doi/10.1002/art.40792/abstract>). Similar results were obtained with the bioassay except that abnormal IFN α levels were significantly associated with the presence of anti-RNP antibodies, while anti-Ro/SSA 52, anti-Ro/SSA 60, anti-La/SSB

and anti-Sm antibodies were not (see Supplementary Table 4, at <http://onlinelibrary.wiley.com/doi/10.1002/art.40792/abstract>).

DISCUSSION

The contribution of IFN α as a biomarker of SLE activity has been limited so far by the absence of a simple and standardized sensitive assay to quantify this cytokine routinely. The new ultrasensitive digital ELISA Simoa technology enabled direct IFN α quantification, with a 5,000-fold increased sensitivity over commercial ELISAs (35,36). Recent findings described by Rodero et al suggested that this assay would enhance our understanding of IFN α biology and potentially improve the diagnosis and stratification of pathologies associated with IFN α dysregulation (37). Based on a large series of SLE patients, we confirmed that routine, highly sensitive IFN α quantification is feasible and of interest for monitoring SLE activity. First, using serum samples from healthy blood donors, we calculated that the threshold for abnormal serum IFN α levels was 136 fg/ml. Next, by studying a series of patients with widely ranging SLE activity and organ involvement, we determined that the threshold associated with active disease in the patients was 266 fg/ml. Finally, according to ROC curve analysis, we demonstrated that the digital ELISA–determined serum IFN α concentration was a better biomarker of SLE activity than concentrations measured with the Farr assay.

To date, anti-dsDNA antibody titration, better achieved with the Farr assay, has been used to monitor global disease

Table 3. Baseline characteristics of and SLE features in patients with active disease according to detection of IFN α with digital ELISA*

	IFN α detectable, true-positive (n = 57)	IFN α not detectable, false-negative (n = 25)	P†	P‡	OR (95% CI)‡
Age, mean \pm SD years	30.1 \pm 9.7	36.1 \pm 12.2	0.021	NS	–
Disease duration, mean \pm SD years	6.4 \pm 6.3	8.5 \pm 7.4	0.19	–	–
Hydroxychloroquine use	35 (61.4)	24 (96)	0.001	0.04	13.0 (1.1–148.3)
Prednisone use	42 (73.6)	15 (60)	0.22	–	–
Immunosuppressive agent use§	20 (35.1)	8 (32)	0.79	–	–
Positive Farr assay	43 (75.4)	17 (68)	0.48	–	–
Positive for anti-RNP antibodies	38 (66.7)	5 (20)	<0.001	0.008	0.2 (0.1–0.6)
Positive for anti-Sm antibodies	21 (36.8)	2 (8)	0.007	NS	–
Low C3 level	40/56 (71.4)¶	9 (36)	0.003	ND	–
SELENA–SLEDAI score, median (range)#	10 (4–36)	6 (4–20)	<0.001	ND	–
SELENA–SLEDAI score \geq 8#	43 (75.4)	7 (28)	<0.001	0.046	0.3 (0.1–0.9)
Flare#	54 (94.7)	19 (76)	0.012	ND	–
Active cutaneous lupus	30 (52.6)	6 (24)	0.016	NS	–
Active serositis	13 (22.8)	4 (16)	0.48	–	–
Active arthritis	29 (50.8)	15 (60)	0.45	–	–
Active arthritis (no other organ involvement)	7 (12.2)	10 (40)	0.004	0.034	5.5 (1.1–26.4)
Active nephropathy	16 (28.1)	4 (16)	0.24	–	–
Active neuropsychiatric lupus	5 (8.8)	1 (4)	0.44	–	–

* Except where indicated otherwise, values are the number (%). Systemic lupus erythematosus (SLE) was defined as active based on a Safety of Estrogens in Lupus Erythematosus National Assessment (SELENA) version of the Systemic Lupus Erythematosus Disease Activity Index (SLEDAI) score of \geq 4. ELISA = enzyme-linked immunosorbent assay; OR = odds ratio; 95% CI = 95% confidence interval; NS = not significant; ND = not done.

† Bivariable analysis (Mann-Whitney U test for continuous variables and chi-square test for categorical variables).

‡ Multivariable analysis (stepwise logistic regression model with *P* for entry = 0.3 and *P* for exit = 0.1). Using bivariable analysis, low C3 level, SELENA–SLEDAI score, SELENA–SLEDAI score of \geq 8, and flare were associated with the detection of IFN α . These 4 items were clearly linked and interdependent. We therefore chose to include in the multivariable analysis only the items that seemed the most relevant and the most significant in bivariable analysis (i.e., SELENA–SLEDAI score \geq 8).

§ Excluding antimalarials and prednisone.

¶ Value shown is the number of positive assay results/number of patients assessed (%).

Defined using the SELENA flare instrument.

activity in SLE (4–7). Indeed, anti-DNA antibody positivity is associated with overall SLE activity and can be useful in monitoring that activity. However, the sensitivity and specificity of that association are relatively low, both ~66% (6), which is in good accordance with our results. Clearly, some SLE populations have persistently elevated anti-DNA antibody titers but not active disease (54,55). The latter observation implies that positivity for anti-DNA antibodies will have limited impact on the pretest likelihood of active disease for a given SLE patient (6). That discordance might be overcome by using the IFN α digital ELISA, which has better specificity, likelihood ratio for positive results, and positive predictive value to identify active disease and a flare than the Farr assay. Importantly, the bioassay-assessed serum IFN α level, already used routinely in

our institution, was also a better biomarker of disease activity than the Farr assay. However, the ability of the digital ELISA to detect low-abnormal serum IFN α concentrations and low disease activity was more sensitive than the bioassay. Furthermore, it is important to note that bioassays based on IFN α antiviral properties are difficult to standardize, which could limit the generalization of the data presented in this study.

Considering the unprecedented number of new agents being developed to treat SLE via targeting of IFN signaling, having an ultrasensitive, valid, easy-to-use, and standardized assay to directly assess IFN α expression in SLE patients will certainly help guide physicians' treatment choices. Whether the direct IFN α determination can be used to predict an SLE flare in the ensuing weeks after assessment remains to be tested. IFN scores have been dis-

appointing for that purpose, with several studies showing a lack of association between the IFN signature and longitudinal disease activity changes or risk of SLE flare (34,56). Despite that lack of association, the possibility that IFN α -related biomarkers could predict future flares was highlighted by the monitoring of IFN-regulated chemokine levels in SLE patients (24). In that study, serum levels of CXCL10, CCL2, and CCL19 chemokines were linked with SLE activity and performed better as biomarkers than the currently available laboratory tests to predict a flare over the following year (24). However, monitoring of those 3 chemokines remains difficult in routine practice. We are currently studying the abilities of the IFN α digital ELISA and bioassay to predict a lupus flare.

Using an ultrasensitive assay may also contribute to improving our understanding of SLE pathogenesis. Indeed, with the digital ELISA, abnormal IFN α levels were significantly associated with the presence of anti-Sm antibodies, but not with other anti-RNP antibodies tested. That finding contrasts with the bioassay analysis and other previous studies that used different cytokine dosage methods and showed abnormal IFN α levels to be associated with other anti-RNP antibodies, such as anti-RNP or anti-Ro/SSA antibodies (29,32–34,57,58). Whether this new information is important in SLE pathogenesis remains to be elucidated.

Our study has certain limitations. We compared the IFN α digital ELISA measurements with the ISG score and found a highly positive correlation between the 2 parameters, suggesting that the digital assay may be used in assignment of patients to anti-IFN drugs (26). According to a recent study, for some patients an ISG score could be more sensitive than a digital assay to detect low IFN α concentrations (<5 fg/ml) (37). However, because our calculated threshold associated with active disease was 266 fg/ml, which is far above the lower limit of detection of the digital ELISA, a very low IFN α concentration might not contribute to identifying patients with clinically active SLE. Furthermore, unless the digital ELISA results are compared directly to ISG scores in a larger panel of patients, it will not be possible to determine their clinical value in patient assignment to anti-IFN treatment. Moreover, these results must be validated in other independent cohorts.

In conclusion, our data support the notion that direct serum IFN α determination with a highly sensitive, easy-to-standardize assay might be useful for clinical monitoring of SLE activity and the selection of the best candidates for anti-IFN α treatment.

ACKNOWLEDGMENTS

We thank the patients, the healthy donors, the nurses, and the Department of Internal Medicine 2 staff who participated in this study.

AUTHOR CONTRIBUTIONS

All authors were involved in drafting the article or revising it critically for important intellectual content, and all authors approved the final ver-

sion to be submitted for publication. Dr. Mathian had full access to all of the data in the study and takes responsibility for the integrity of the data and the accuracy of the data analysis.

Study conception and design. Mathian, Mouries-Martin, Dorgham, Barnabei, Rozenberg, Gorochov, Amoura.

Acquisition of data. Mathian, Mouries-Martin, Dorgham, Barnabei, Ben Salah, Cohen-Aubart, Garrido Castillo, Haroche, Hie, Pineton de Chambrun, Miyara, Sterlin, Pha, Lê Thi Huong, Rieux-Laucat, Rozenberg.

Analysis and interpretation of data. Mathian, Mouries-Martin, Dorgham, Devilliers, Barnabei, Pineton de Chambrun, Rozenberg, Gorochov, Amoura.

REFERENCES


1. Tsokos GC. Systemic lupus erythematosus. *N Engl J Med* 2011;365:2110–21.
2. Lisnevskaja L, Murphy G, Isenberg D. Systemic lupus erythematosus. *Lancet* 2014;384:1878–88.
3. Tektonidou MG, Lewandowski LB, Hu J, Dasgupta A, Ward MM. Survival in adults and children with systemic lupus erythematosus: a systematic review and Bayesian meta-analysis of studies from 1950 to 2016. *Ann Rheum Dis* 2017;76:2009–16.
4. Agmon-Levin N, Damoiseaux J, Kallenberg C, Sack U, Witte T, Herold M, et al. International recommendations for the assessment of autoantibodies to cellular antigens referred to as anti-nuclear antibodies. *Ann Rheum Dis* 2014;73:17–23.
5. Neogi T, Gladman DD, Ibanez D, Urowitz M. Anti-dsDNA antibody testing by Farr and ELISA techniques is not equivalent. *J Rheumatol* 2006;33:1785–8.
6. Kavanaugh AF, Solomon DH. Guidelines for immunologic laboratory testing in the rheumatic diseases: anti-DNA antibody tests. *Arthritis Rheum* 2002;47:546–55.
7. Sherer Y, Gorstein A, Fritzler MJ, Shoenfeld Y. Autoantibody explosion in systemic lupus erythematosus: more than 100 different antibodies found in SLE patients. *Semin Arthritis Rheum* 2004;34:501–37.
8. Theofilopoulos AN, Baccala R, Beutler B, Kono DH. Type I interferons (α/β) in immunity and autoimmunity. *Annu Rev Immunol* 2005;23:307–36.
9. Obermoser G, Pascual V. The interferon- α signature of systemic lupus erythematosus. *Lupus* 2010;19:1012–9.
10. Ronnblom L, Elkon KB. Cytokines as therapeutic targets in SLE. *Nat Rev Rheumatol* 2010;6:339–47.
11. Niewold TB. Interferon α as a primary pathogenic factor in human lupus. *J Interferon Cytokine Res* 2011;31:887–92.
12. Ronnblom L, Alm GV, Eloranta ML. The type I interferon system in the development of lupus. *Semin Immunol* 2011;23:113–21.
13. Lauwerys BR, Ducreux J, Houssiau FA. Type I interferon blockade in systemic lupus erythematosus: where do we stand? *Rheumatology (Oxford)* 2014;53:1369–76.
14. Kirou KA, Gkrouzman E. Anti-interferon α treatment in SLE. *Clin Immunol* 2013;148:303–12.
15. Hooks JJ, Moutsopoulos HM, Geis SA, Stahl NI, Decker JL, Notkins AL, et al. Immune interferon in the circulation of patients with autoimmune disease. *N Engl J Med* 1979;301:5–8.
16. Preble OT, Black RJ, Friedman RM, Klippel JH, Vilcek J. Systemic lupus erythematosus: presence in human serum of an unusual acid-labile leukocyte interferon. *Science* 1982;216:429–31.
17. Ytterberg SR, Schnitzer TJ. Serum interferon levels in patients with systemic lupus erythematosus. *Arthritis Rheum* 1982;25:401–6.
18. Bennett L, Palucka AK, Arce E, Cantrell V, Borvak J, Banchereau J, et al. Interferon and granulopoiesis signatures in systemic lupus erythematosus blood. *J Exp Med* 2003;197:711–23.

19. Baechler EC, Batliwalla FM, Karypis G, Gaffney PM, Ortmann WA, Espe KJ, et al. Interferon-inducible gene expression signature in peripheral blood cells of patients with severe lupus. *Proc Natl Acad Sci U S A* 2003;100:2610–5.
20. Chiche L, Jourde-Chiche N, Whalen E, Presnell S, Gersuk V, Dang K, et al. Modular transcriptional repertoire analyses of adults with systemic lupus erythematosus reveal distinct type I and type II interferon signatures. *Arthritis Rheumatol* 2014;66:1583–95.
21. Kanayama Y, Kim T, Inariba H, Negoro N, Okamura M, Takeda T, et al. Possible involvement of interferon α in the pathogenesis of fever in systemic lupus erythematosus. *Ann Rheum Dis* 1989;48:861–3.
22. Bengtsson AA, Sturfelt G, Truedsson L, Blomberg J, Alm G, Vallin H, et al. Activation of type I interferon system in systemic lupus erythematosus correlates with disease activity but not with antiretroviral antibodies. *Lupus* 2000;9:664–71.
23. Dall'Era MC, Cardarelli PM, Preston BT, Witte A, Davis JC Jr. Type I interferon correlates with serological and clinical manifestations of SLE. *Ann Rheum Dis* 2005;64:1692–7.
24. Bauer JW, Petri M, Batliwalla FM, Koeuth T, Wilson J, Slattery C, et al. Interferon-regulated chemokines as biomarkers of systemic lupus erythematosus disease activity: a validation study. *Arthritis Rheum* 2009;60:3098–107.
25. Rose T, Grutzkau A, Klotsche J, Enghard P, Flechsig A, Keller J, et al. Are interferon-related biomarkers advantageous for monitoring disease activity in systemic lupus erythematosus? A longitudinal benchmark study. *Rheumatology (Oxford)* 2017;56:1618–26.
26. Khamashta M, Merrill JT, Werth VP, Furie R, Kalunian K, Illei GG, et al. Sifalimumab, an anti-interferon- α monoclonal antibody, in moderate to severe systemic lupus erythematosus: a randomized, double-blind, placebo-controlled study. *Ann Rheum Dis* 2016;75:1909–16.
27. Furie R, Khamashta M, Merrill JT, Werth VP, Kalunian K, Brohawn P, et al. Anifrolumab, an anti-interferon- α receptor monoclonal antibody, in moderate-to-severe systemic lupus erythematosus. *Arthritis Rheumatol* 2017;69:376–86.
28. Jabs WJ, Hennig C, Zawatzky R, Kirchner H. Failure to detect antiviral activity in serum and plasma of healthy individuals displaying high activity in ELISA for IFN- α and IFN- β . *J Interferon Cytokine Res* 1999;19:463–9.
29. Feng X, Wu H, Grossman JM, Hanvivadhanakul P, FitzGerald JD, Park GS, et al. Association of increased interferon-inducible gene expression with disease activity and lupus nephritis in patients with systemic lupus erythematosus. *Arthritis Rheum* 2006;54:2951–62.
30. Yao Y, Higgs BW, Morehouse C, de Los Reyes M, Trigona W, Brohawn P, et al. Development of potential pharmacodynamic and diagnostic markers for anti-IFN- α monoclonal antibody trials in systemic lupus erythematosus. *Hum Genomics Proteomics* 2009;2009:374312.
31. Yao Y, Higgs BW, Richman L, White B, Jallal B. Use of type I interferon-inducible mRNAs as pharmacodynamic markers and potential diagnostic markers in trials with sifalimumab, an anti-IFN α antibody, in systemic lupus erythematosus. *Arthritis Res Ther* 2010;12 Suppl 1:S6.
32. Kirou KA, Lee C, George S, Louca K, Papagiannis IG, Peterson MG, et al. Coordinate overexpression of interferon- α -induced genes in systemic lupus erythematosus. *Arthritis Rheum* 2004;50:3958–67.
33. Kirou KA, Lee C, George S, Louca K, Peterson MG, Crow MK. Activation of the interferon- α pathway identifies a subgroup of systemic lupus erythematosus patients with distinct serologic features and active disease. *Arthritis Rheum* 2005;52:1491–503.
34. Petri M, Singh S, Tesfayone H, Dedrick R, Fry K, Lal P, et al. Longitudinal expression of type I interferon responsive genes in systemic lupus erythematosus. *Lupus* 2009;18:980–9.
35. Rissin DM, Kan CW, Campbell TG, Howes SC, Fournier DR, Song L, et al. Single-molecule enzyme-linked immunosorbent assay detects serum proteins at subfemtomolar concentrations. *Nat Biotechnol* 2010;28:595–9.
36. Wilson DH, Rissin DM, Kan CW, Fournier DR, Piech T, Campbell TG, et al. The simoa HD-1 analyzer: a novel fully automated digital immunoassay analyzer with single-molecule sensitivity and multiplexing. *J Lab Autom* 2016;21:533–47.
37. Rodero MP, Decalf J, Bondet V, Hunt D, Rice GI, Werneke S, et al. Detection of interferon α protein reveals differential levels and cellular sources in disease. *J Exp Med* 2017;214:1547–55.
38. Lebon P, Ponsot G, Aicardi J, Goutieres F, Arthuis M. Early intrathecal synthesis of interferon in herpes encephalitis. *Biomedicine* 1979;31:267–71.
39. Lebon P, Badoual J, Ponsot G, Goutieres F, Hemeury-Cukier F, Aicardi J. Intrathecal synthesis of interferon- α in infants with progressive familial encephalopathy. *J Neurol Sci* 1988;84:201–8.
40. Hausfater P, Fillet AM, Rozenberg F, Arthaud M, Trystram D, Huraux JM, et al. Prevalence of viral infection markers by polymerase chain reaction amplification and interferon- α measurements among patients undergoing lumbar puncture in an emergency department. *J Med Virol* 2004;73:137–46.
41. Hochberg MC. Updating the American College of Rheumatology revised criteria for the classification of systemic lupus erythematosus [letter]. *Arthritis Rheum* 1997;40:1725.
42. Bombardier C, Gladman DD, Urowitz MB, Caron D, Chang CH, the Committee on Prognosis Studies in SLE. Derivation of the SLEDAI: a disease activity index for lupus patients. *Arthritis Rheum* 1992;35:630–40.
43. Buyon JP, Petri MA, Kim MY, Kalunian KC, Grossman J, Hahn BH, et al. The effect of combined estrogen and progesterone hormone replacement therapy on disease activity in systemic lupus erythematosus: a randomized trial. *Ann Intern Med* 2005;142:953–62.
44. Petri M, Kim MY, Kalunian KC, Grossman J, Hahn BH, Sammaritano LR, et al. Combined oral contraceptives in women with systemic lupus erythematosus. *N Engl J Med* 2005;353:2550–8.
45. Weening JJ, D'Agati VD, Schwartz MM, Seshan SV, Alpers CE, Appel GB, et al. The classification of glomerulonephritis in systemic lupus erythematosus revisited. *Kidney Int* 2004;65:521–30.
46. Gresser I, Bandu MT, Brouty-Boye D, Tovey M. Pronounced antiviral activity of human interferon on bovine and porcine cells. *Nature* 1974;251:543–5.
47. Lebon P, Commoy-Chevalier MJ, Robert-Galliot B, Morin A, Chany C. Production of human type I interferon by lymphocytes in contact with cells infected by herpes virus and fixed with glutaraldehyde. *C R Seances Acad Sci D* 1980;290:37–40.
48. Batteux F, Palmer P, Daeron M, Weill B, Lebon P. FCyRII (CD32)-dependent induction of interferon- α by serum from patients with lupus erythematosus. *Eur Cytokine Netw* 1999;10:509–14.
49. Vezinet F, Lebon P, Amoudry C, Gibert C. Herpes encephalitis in adults and interferon. *Nouv Presse Med* 1981;10:1135–8.
50. Van Vollenhoven R, Voskuyl A, Bertsias G, Aranow C, Aringer M, Arnaud L, et al. A framework for remission in SLE: consensus findings from a large international task force on definitions of remission in SLE (DORIS). *Ann Rheum Dis* 2017;76:554–61.
51. DeLong ER, DeLong DM, Clarke-Pearson DL. Comparing the areas under two or more correlated receiver operating characteristic curves: a nonparametric approach. *Biometrics* 1988;44:837–45.

52. Rice GI, Forte GM, Szykiewicz M, Chase DS, Aeby A, Abdel-Hamid MS, et al. Assessment of interferon-related biomarkers in Aicardi-Goutieres syndrome associated with mutations in TREX1, RNASEH2A, RNASEH2B, RNASEH2C, SAMHD1, and ADAR: a case-control study. *Lancet Neurol* 2013;12:1159–69.
53. Rice GI, Melki I, Fremont ML, Briggs TA, Rodero MP, Kitabayashi N, et al. Assessment of type I interferon signaling in pediatric inflammatory disease. *J Clin Immunol* 2017;37:123–32.
54. Gladman DD, Urowitz MB, Keystone EC. Serologically active clinically quiescent systemic lupus erythematosus: a discordance between clinical and serologic features. *Am J Med* 1979;66:210–5.
55. Walz LeBlanc BA, Gladman DD, Urowitz MB. Serologically active clinically quiescent systemic lupus erythematosus—predictors of clinical flares. *J Rheumatol* 1994;21:2239–41.
56. Landolt-Marticorena C, Bonventi G, Lubovich A, Ferguson C, Unnithan T, Su J, et al. Lack of association between the interferon- α signature and longitudinal changes in disease activity in systemic lupus erythematosus. *Ann Rheum Dis* 2009;68:1440–6.
57. Weckerle CE, Franek BS, Kelly JA, Kumabe M, Mikolaitis RA, Green SL, et al. Network analysis of associations between serum interferon- α activity, autoantibodies, and clinical features in systemic lupus erythematosus. *Arthritis Rheum* 2011;63:1044–53.
58. Ko K, Franek BS, Marion M, Kaufman KM, Langefeld CD, Harley JB, et al. Genetic ancestry, serum interferon- α activity, and autoantibodies in systemic lupus erythematosus. *J Rheumatol* 2012;39:1238–40.

BRIEF REPORT

Promotion of Calcium/Calmodulin-Dependent Protein Kinase 4 by GLUT1-Dependent Glycolysis in Systemic Lupus Erythematosus

Tomohiro Koga,¹ Tomohito Sato,¹ Kaori Furukawa,¹ Shimpei Morimoto,¹ Yushiro Endo,¹ Masataka Umeda,² Remi Sumiyoshi,¹ Shoichi Fukui,¹ Shin-ya Kawashiri,¹ Naoki Iwamoto,¹ Kunihiro Ichinose,¹  Mami Tamai,¹ Tomoki Origuchi,¹ Hideki Nakamura,¹ and Atsushi Kawakami¹

Objective. To clarify the significance of immunometabolism in systemic lupus erythematosus (SLE), and to determine the effect of calcium/calmodulin-dependent protein kinase 4 (CaMK4) on T cell metabolism.

Methods. Metabolomic profiling was performed using capillary electrophoresis mass spectrometry in naive T cells from MRL/lpr mice treated with anti-CD3/CD28 antibodies in the absence or presence of a CaMK4 inhibitor (KN-93). The expression of GLUT1 and CaMK4 in CD4+ T cells from healthy controls (n = 16), patients with inactive SLE (n = 13), and patients with active SLE (n = 14) was examined by flow cytometry and quantitative polymerase chain reaction. In vitro experiments were performed to determine the effect of KN-93 on the expression of GLUT1 during Th17 cell differentiation in T cells from patients with SLE.

Results. CaMK4 inhibition significantly decreased the levels of glycolytic intermediates such as glucose-6-phosphate, fructose-6-phosphate, fructose-1,6-diphosphate, pyruvate, and lactate ($P < 0.05$), whereas it did not affect the levels of the pentose phosphate pathway intermediates such as 6-phospho-D-gluconate, ribulose-5-phosphate, ribose-5-phosphate, and phosphoribosyl pyrophosphate. The expression levels of GLUT1 and CaMK4 in effector memory CD4+ T cells were significantly higher in patients with active SLE compared to healthy controls ($P < 0.01$ and $P < 0.05$, respectively) and patients with inactive SLE ($P < 0.05$ and $P < 0.01$, respectively). A functional analysis revealed that CaMK4 inhibition decreased the expression of GLUT1 during Th17 cell differentiation ($P < 0.01$), followed by a reduction of interleukin-17 (IL-17) production ($P < 0.05$).

Conclusion. The results of the study indicate that the activity of CaMK4 could be responsible for glycolysis, which contributes to the production of IL-17, and CaMK4 may contribute to aberrant expression of GLUT1 in T cells from patients with active SLE.

INTRODUCTION

Systemic lupus erythematosus (SLE) is a heterogeneous disease with various immunologic abnormalities and different types of organ involvement. It has been demonstrated that aberrant expression of type I interferon, involving innate immunity and

functional abnormalities of T cells and B cells involved in adaptive immunity, contributes to the pathogenesis of SLE (1).

Among these immune cells, T cells play a central role in the process of autoantibody production, immune complex formation, and immune dysregulation, resulting in multiple organ damage. Importantly, the balance between interleukin-17 (IL-17)-producing Th17 cells and FoxP3+ Treg cells is crucially involved in SLE

Supported by the Leading Initiative for Excellent Young Researchers of the Ministry of Education, Culture, Sports, Science, and Technology (grant 16810055 to Dr. Koga) and the Japan Society for the Promotion of Science (KAKENHI grants 16K19604 and 24790999 to Drs. Umeda and Ichinose, respectively).

¹Tomohiro Koga, MD, PhD, Tomohito Sato, Kaori Furukawa, PhD, Shimpei Morimoto, PhD, Yushiro Endo, MD, Remi Sumiyoshi, MD, Shoichi Fukui, MD, PhD, Shin-ya Kawashiri, MD, PhD, Kaoki Iwamoto, MD, PhD, Kunihiro Ichinose, MD, PhD, Mami Tamai, MD, PhD, Tomoki Origuchi, MD, PhD, Hideki Nakamura, MD, PhD, Atsushi Kawakami, MD, PhD: Nagasaki University

Graduate School of Biomedical Sciences, Nagasaki, Japan; ²Masataka Umeda, MD, PhD: Nagasaki University Graduate School of Biomedical Sciences and Nagasaki University Hospital, Nagasaki, Japan.

No potential conflicts of interest relevant to this article were reported.

Address correspondence to Tomohiro Koga, MD, PhD, Center for Bioinformatics and Molecular Medicine, Nagasaki University Graduate School of Biomedical Sciences, 1-12-4 Sakamoto, Nagasaki 852-8523, Japan. E-mail: tkoga@nagasaki-u.ac.jp.

Submitted for publication May 10, 2018; accepted in revised form November 15, 2018.

pathogenesis. Limited Treg cell numbers and impaired function have been observed in subjects with SLE, and these defects have been associated with increased lupus disease activity (2).

The transition from quiescence to rapid proliferation requires energy and cellular biosynthetic activities. Over the past decade, important findings regarding cellular metabolism in T cell activation, proliferation, and differentiation have been obtained. Glycolysis is critical for T cell effector functions, and increased glycolysis leads to autoimmunity (3). ATP production by effector T cells is dependent on the mitochondria-independent glycolysis system. In addition, expression of GLUT1, a major glucose transporter, is enhanced when T cells are activated.

Increased expression of GLUT1 is also involved in the pathogenesis of autoimmune diseases. Autoantibody production and immune complex deposition in glomeruli are observed in mice that overexpress Glut1 (4). Consistent with a role of GLUT1 in immune activation and inflammation, CD4⁺ T cell-specific Glut1 conditional knockout mice showed diminished effector CD4⁺ T cell differentiation and survival, and Glut1-deficient effector T cells were unable to induce either graft-versus-host disease or colitis (5). In addition, naive CD4⁺ T cells from lupus-prone mice showed higher glycolytic rates than those of age-matched control cells (6).

Experiments performed using lupus-prone mice showed that the administration of 2-deoxy-D-glucose and metformin inhibited the expression of GLUT1 and the activation of mechanistic target of rapamycin complex 1 (mTORC1), and suppressed the activity of nephritis and the production of antinuclear antibodies (7). However, the mechanisms underlying GLUT1 expression that affect the pathologic condition in CD4⁺ T cells from SLE patients have not been identified. We investigated the effect of pharmacologic calcium/calmodulin-dependent protein kinase 4 (CaMK4) inhibition on T cell metabolism and the clinical significance of the expression of GLUT1 in SLE patients.

MATERIALS AND METHODS

Mice. Female MRL/MpJ-*Tnfrsf6*^{pr} (MRL/*lpr*) mice were purchased from The Jackson Laboratory and killed at 6 or 16 weeks of age. Prior to being killed, the mice were maintained in a specific pathogen-free animal facility at Nagasaki University, and the experiments were approved by the Institutional Animal Care Committee of Nagasaki University (approval no. 1412261190-6).

Metabolite measurements. Spleens were removed from the mice, and single-cell suspensions were obtained by gently pressing the organs through a nylon mesh. Naive CD4⁺ T cells from the spleens were then purified by magnetic cell sorting using a CD4⁺CD62L⁺ T Cell Isolation Kit II (Miltenyi Biotec). Twenty-four hours after stimulation with anti-CD3/CD28 antibodies in the presence or absence of the CaMK4 inhibitor KN-93 (3 μ M for 24 hours; Calbiochem), we prepared extracts from 4–6 \times 10⁶ CD4⁺ T cells from MRL/*lpr* mice with Internal Stand-

ard Solution contained methanol (Human Metabolome Technologies). The amounts of intermediate metabolites were analyzed with the use of a capillary electrophoresis-connected electrospray ionization time-of-flight mass spectrometry system.

Flow cytometry. We isolated peripheral blood mononuclear cells (PBMCs) from the blood of SLE patients and healthy controls using density-gradient centrifugation with a RosetteSep system (Stemcell Technologies). Isolated PBMCs were stained for flow cytometry with antibodies against CD3 (SK7; BD Biosciences), CD4 (SK3; BD Biosciences), CD45RA (HI100; BioLegend), CCR6 (G034E3, BioLegend), CCR7 (GO43H7; BioLegend), GLUT1 (202915; R&D Systems), or CaMK4 (EP2526AY; Abcam) for 30 minutes at 4°C. Dead cells were excluded by using 7-aminoactinomycin D viability staining solution (BioLegend). All samples were run on a BD-FACSVerse (BD Biosciences), and the data were analyzed using FlowJo version X.0.5 software (Tree Star).

RNA isolation and real-time polymerase chain reaction analysis. We isolated total messenger RNA (mRNA) from human CD4⁺ T cells using RNeasy Mini Kit (Qiagen), and we then synthesized complementary DNA using cDNA EcoDry Premix (Clontech) for polymerase chain reaction (PCR) amplification. The following primers and probes were from Applied Biosystems: CAMK4 (Hs00174318_m1), GLUT1 (Hs00892681_m1), hexokinase 1 (Hs00175976_m1), hexokinase 2 (Hs00606086_m1), and GAPDH (Hs02758991_g1). Gene expression was assessed by C_t method.

Human SLE T cells. Forty-two patients fulfilling the American College of Rheumatology revised criteria for the classification of SLE were enrolled in this study (8). Disease activity was assessed using the SLE Disease Activity Index (SLEDAI) (9). The patients' peripheral venous blood was collected in heparin-lithium tubes, and CD4⁺ T cells from the blood were purified with a RosetteSep human CD4⁺ T cell enrichment cocktail. Naive CD4⁺ T cells were isolated using a T Cell Isolation Kit II. All patients provided written informed consent, and the study protocol was approved by the Institutional Review Board of Nagasaki University (approval no. 12012397-5).

In vitro T cell differentiation. Freshly isolated naive CD4⁺ T cells were stimulated in complete RPMI medium with anti-CD3 and anti-CD28-bearing beads (Dynabeads Human T-Activator CD3/CD28; Veritas) in the presence of IL-1 β (25 ng/ml), IL-6 (50 ng/ml), or IL-23 (50 ng/ml) (all from BioLegend) for 4 days. Samples were analyzed by flow cytometry and Western blotting.

Western blotting. CD4⁺ T cells from SLE patients were lysed in radioimmunoprecipitation assay (RIPA) buffer at 4°C for 30 minutes. After centrifugation (16,400g, 30 minutes at 4°C), the supernatants were collected and an identical amount of protein from each lysate (100 ng/well) was separated on NuPAGE 4–12% Bis-Tris Gel (Life Technologies).

Proteins were transferred to a nitrocellulose membrane using an iBlot 2 Dry transfer system (Thermo Fisher Scientific). Membranes were probed using the following primary antibodies: rabbit anti-HK1 (Cell Signaling Technology) and rabbit anti-actin (Sigma-Aldrich), and with horseradish peroxidase-conjugated goat anti-rabbit IgG (Jackson ImmunoResearch) as secondary antibody. Blocking, staining, and washing were done overnight using an iBind Flex Western device and reagents according to the protocol recommended by the manufacturer (Thermo Fisher Scientific). An ECL Select Western Blotting Detection Reagent (Amersham) was used for detection. Bands on blots corresponding to proteins of interest were quantified with ImageJ software (National Institutes of Health).

Multiplex cytokine assay. We measured inflammatory cytokines in the supernatant from Th17-polarized CD4⁺ T cells from SLE patients by performing a multiplex cytokine bead assay. In parallel and under blinded conditions, we used a Milliplex MAP human cytokine/chemokine panel 1 kit, according to the instructions of the manufacturer (Millipore).

Statistical analysis. We used Student's 2-tailed *t*-test and the Mann-Whitney test to analyze the significance of dif-

ferences between pairs of groups. Differences between 3 data sets were analyzed by one-way analysis of variance followed by Tukey's multiple comparison test. A linear mixed-effects model was utilized to analyze the differences between treatment groups (phosphate buffered saline versus KN-93) in the concentrations of metabolites from the glycolysis pathway and the pentose phosphate pathway. Under the model, metabolites' molecular species were assumed to be a random slope, results in the individual mice as a random intercept, and the treatment groups as a fixed effect. All statistical analyses were performed with JMP Pro 13, GraphPad Prism 7.0 software, or the nlme R package (10). *P* values less than 0.05 were considered significant.

RESULTS

Down-regulation of the glycolysis pathway, but not the pentose phosphate pathway, by CaMK4 inhibition.

To evaluate the relevance of CaMK4 in metabolic pathways during T cell activation, we isolated naive CD4⁺ T cells from MRL/*lpr* mice at 6 weeks of age (prior to the onset of disease) and at 16 weeks of age (established disease), and stimulated the cells with anti-CD3/CD28 antibodies in the absence or presence of KN-93 (3 μ M). In the presence of KN-93, the concentration of all metabolites

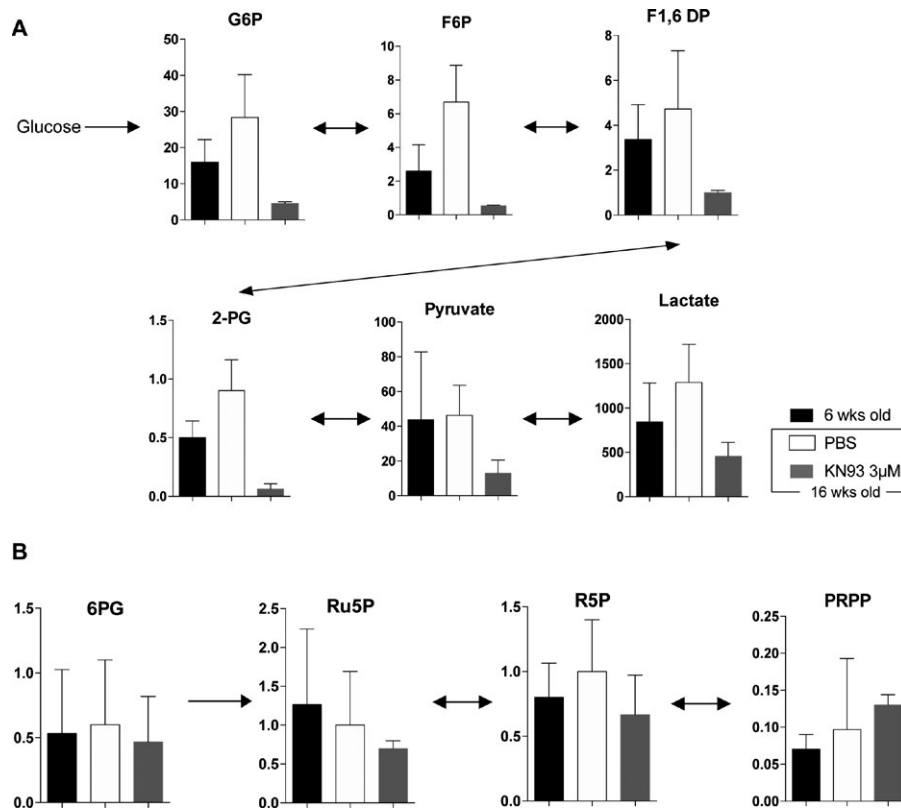


Figure 1. Calcium/calmodulin-dependent protein kinase 4 (CaMK4) inhibition down-regulates the glycolysis pathway, but not the pentose phosphate pathway. Levels of metabolites involved in the glycolysis pathway (A) and the pentose phosphate pathway (B) were measured in CD4⁺ T cells from MRL/*lpr* mice after administration of the CaMK4 inhibitor KN-93 or phosphate buffered saline (PBS). Values are the mean \pm SD pmoles/ 10^6 cells ($n = 4$ mice per group). G6P = glucose 6-phosphate; F6P = fructose 6-phosphate; F1,6DP = fructose-1,6-diphosphate; 2-PG = 2-phosphoglycerate; 6PG = 6-phospho-D-gluconate; Ru5P = ribulose-5-phosphate; R5P = ribose-5-phosphate; PRPP = phosphoribosyl pyrophosphate.

involved in the glycolysis pathway (including glucose-6-phosphate, fructose-6-phosphate, fructose-1,6-diphosphate, 2-phosphoglycerate, pyruvate, and lactate) decreased significantly ($P < 0.05$) in T cells from 16-week-old MRL/lpr mice (Figure 1A). In contrast, CaMK4 inhibition by KN-93 did not affect the pentose phosphate pathway ($P = 0.45$) (Figure 1B). Collectively, these data suggest that CaMK4 inhibition results in decreased levels of glycolysis-related proteins during CD4+ T cell activation in lupus-prone mice.

Correlation of CaMK4 and GLUT1 expression with SLE disease activity. Since we observed that the inhibition of CaMK4 altered the glycolysis pathway in MRL/lpr mice, we wished to investigate whether the expression levels of CaMK4 and GLUT1 are associated with disease activity in SLE patients. We examined the expression of GLUT1 and CaMK4 in CD4+ T cells from 16 healthy controls (mean age 37.0 years, 75% female), 13 patients with inactive SLE, and 14 patients with active SLE by flow cytometry and quantitative PCR (qPCR). For all patients, the mean age was 38.1 years and the number of female subjects was 89%. There were no significant differences between the inactive SLE and active SLE groups regarding age, sex, or concomitant treatments. The characteristics of the patients studied are shown

in Supplementary Table 1 (available on *Arthritis & Rheumatology* web site at <http://onlinelibrary.wiley.com/doi/10.1002/art.40785/abstract>).

As shown in Figure 2A, the expression of CaMK4 mRNA in CD4+ T cells was significantly higher in patients with active SLE (SLEDAI ≥ 8), compared to healthy controls and patients with inactive SLE (SLEDAI < 8). Similarly, we found that the mean fluorescence intensity of CaMK4 in effector memory CD4+ T cells (CD3+CD4+CD45RA-CCR7-) was significantly higher in patients with active SLE compared to healthy controls and patients with inactive SLE (Figure 2B). Although there was no significant difference in gene expression of GLUT1 among these 3 groups (Figure 2C), surface expression of GLUT1 in effector memory CD4+ T cells detected by flow cytometry was higher in SLE patients with SLEDAI scores of ≥ 8 than in healthy controls or patients with SLE with SLEDAI scores of < 8 (Figures 2D and E). Collectively, our observations indicate that aberrant expression of CaMK4 and GLUT1 contributes to the progression of SLE.

CaMK4 inhibition alters the expression of glycolysis-related genes in T cells from SLE patients under Th17-polarizing conditions. To determine whether the pharmacologic inhibition of CaMK4 could affect glycolysis-related genes, including

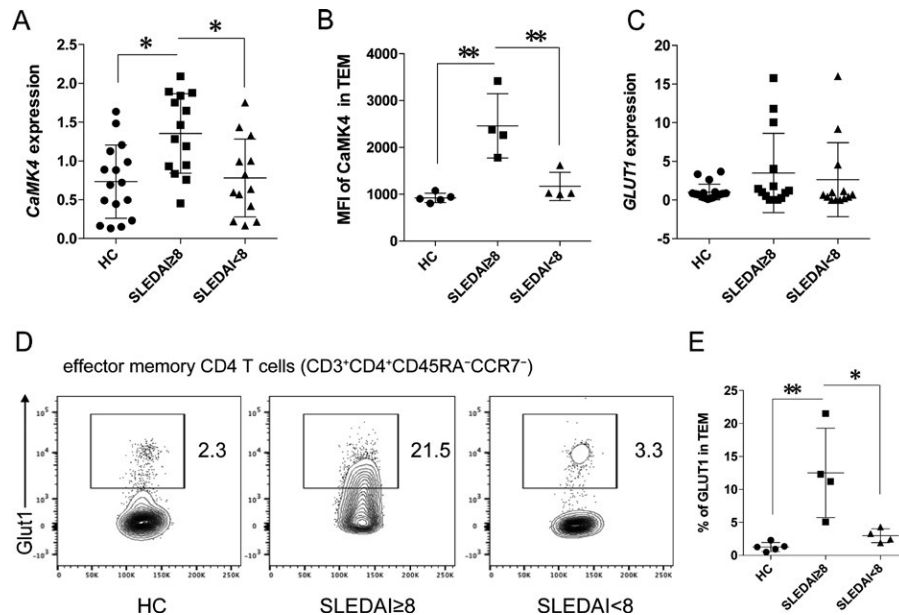


Figure 2. Expression levels of calcium/calmodulin-dependent protein kinase 4 (CaMK4) and GLUT1 correlate with systemic lupus erythematosus (SLE) disease activity. **A**, Expression levels of CaMK4 in CD4+ T cells from healthy controls (HCs) ($n = 16$), patients with active SLE (SLE Disease Activity Index [SLEDAI] ≥ 8) ($n = 14$), and patients with inactive SLE (SLEDAI < 8) ($n = 13$) were determined by quantitative polymerase chain reaction (qPCR). **B**, The mean fluorescence intensity (MFI) of CaMK4 in effector memory T cells (TEM) (CD3+CD4+CD45RA-CCR7-) was measured by flow cytometry in healthy controls, patients with active SLE, and patients with inactive SLE ($n = 4$ –5 per group). **C**, Expression levels of GLUT1 in CD4+ cells from healthy controls ($n = 16$), patients with active SLE ($n = 14$), and patients with inactive SLE ($n = 13$) were determined by qPCR. **D**, Flow cytometric staining for GLUT1 expression was performed in effector memory T cells from healthy controls, patients with active SLE, and patients with inactive SLE. Representative staining profiles are shown. **E**, The percentage of GLUT1 in effector memory T cells was measured in healthy controls, patients with active SLE, and patients with inactive SLE ($n = 4$ –5 per group). In **A**, **B**, **C**, and **E**, each symbol represents an individual subject; bars show the mean \pm SD. * = $P < 0.05$; ** = $P < 0.01$.

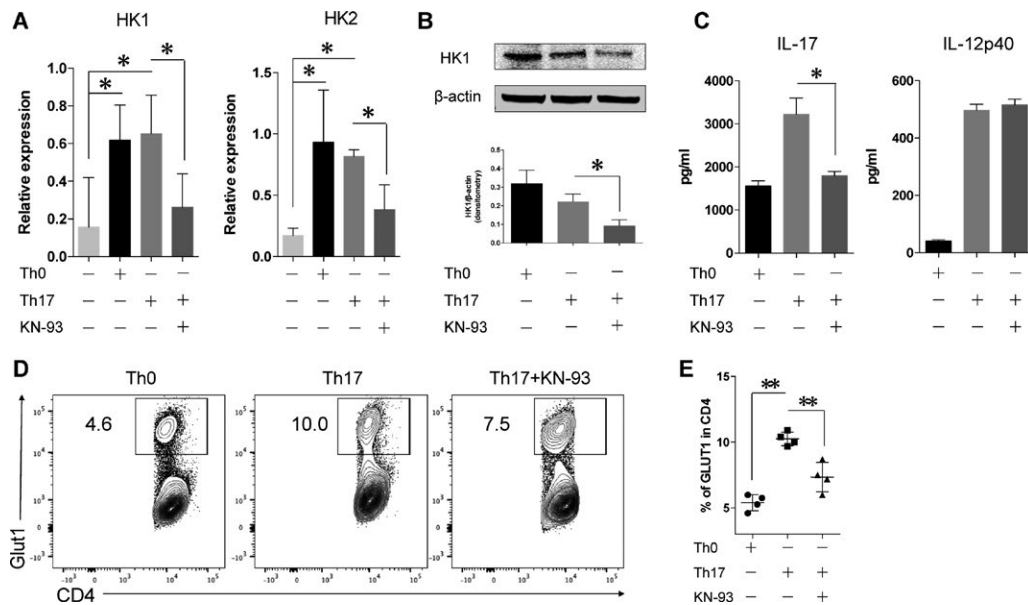


Figure 3. CaMK4 inhibition alters the expression of glycolysis-related genes in T cells from SLE patients under Th17-polarizing conditions. **A**, Expression levels of HK1 and HK2 in CD4⁺ T cells from patients with active SLE ($n = 6$ per group) that were left unstimulated, Th0-polarized, Th17-polarized, or Th17-polarized with or without addition of KN-93 were determined by qPCR. Values are the mean \pm SEM. **B**, Western blot analysis of HK1 in CD4⁺ T cells from patients with active SLE ($n = 3$ per group) that were Th0-polarized, Th17-polarized, or Th17-polarized with or without addition of KN-93 was performed. Graph shows cumulative densitometry data. Values are the mean \pm SEM. **C**, The production of interleukin-17 (IL-17) and IL-12p40 in CD4⁺ T cells from patients with active SLE ($n = 6$ per group) that were Th0-polarized, Th17-polarized, or Th17-polarized with or without addition of KN-93 was determined by qPCR. Values are the mean \pm SD. **D**, Flow cytometric staining for GLUT1 expression in CD4⁺ T cells from patients with active SLE that were Th0-polarized, Th17-polarized, or Th17-polarized with or without addition of KN-93 was performed. Representative staining profiles are shown. **E**, The percentage of GLUT1 expression in CD4⁺ T cells from patients with active SLE ($n = 4$ per group) that were Th0-polarized, Th17-polarized, or Th17-polarized with or without addition of KN-93 was determined. Data are cumulative results from 2 independent experiments, including a total of 4 patients. Each symbol represents an individual subject; bars show the mean \pm SD. * = $P < 0.05$ (after Bonferroni correction in **C**); ** = $P < 0.01$. See Figure 2 for other definitions.

HK1 and HK2, in T cells from SLE patients under Th17-polarizing conditions, we isolated naive T cells from patients with active SLE. The cells were then stimulated under Th17-polarizing conditions, and gene expression of HK1 and HK2 was quantified by qPCR (Figure 3A). As expected, the inhibition of CaMK4 resulted in less expression of glycolysis-related genes under Th17-polarizing conditions. Similarly, we found that the protein level of HK1 in T cells from SLE patients under Th17-polarizing conditions was significantly lower in the presence of KN-93 (Figure 3B). These results were accompanied by a reduction in IL-17 production, but not IL-12p40 production (Figure 3C). We also observed that KN-93 inhibited the expression of GLUT1 under Th17-polarizing conditions (Figures 3D and E). Collectively, these data suggest that CaMK4 is a necessary element in GLUT1-dependent glycolysis, which promotes Th17 cell differentiation and IL-17 production that can be modulated by a pharmacologic inhibitor of CaMK4.

DISCUSSION

Metabolic pathways must be tightly regulated to allow normal proliferation and T cell effector function. Altered metabolic regulation may contribute to impaired T cell function in

autoimmune diseases. While resting T cells utilize catabolic metabolism, effector T cells up-regulate anabolic metabolism by inducing glycolysis-related proteins such as GLUT1 and hexokinase (11). In this study, we identified a novel role of CaMK4 in anabolic metabolism: CaMK4 facilitated the glycolysis pathway, but not the pentose phosphate pathway, during T cell activation. Of note, GLUT1 and CaMK4 expression levels in CD4⁺ T cells from SLE patients were positively correlated with disease activity.

The pentose phosphate pathway supplies ribose-5-phosphate (R5P) for the production of nucleic acids in support of cell proliferation, and supplies NADPH for lipid biosynthesis, maintenance of a reducing environment, and protection against oxidative stress (12). Previous studies on metabolic changes in SLE indicate that the pentose phosphate pathway, including R5P and sedoheptulose 7-phosphate, is activated in the peripheral blood of SLE patients (6,13). In this study, the effect of CaMK4 inhibition on the pentose phosphate pathway was not significant, at least at the activation stage of CD4⁺ T cells. Further studies are needed to clarify the association between CaMK4 and the pentose phosphate pathway in the development of SLE.

Reactive oxygen species (ROS) are produced in the mitochondria during the process of oxygen being taken into the cell, and the accumulation of ROS impairs DNA and proteins in mitochondria, resulting in dysfunction of oxidative phosphorylation (OXPHOS). Though ATP production in naive T cells is dependent on OXPHOS, ATP production by effector T cells is dependent on the mitochondria-independent glycolytic pathway. It has been proposed that the Akt/mTOR pathway plays a pivotal role in regulating cellular metabolic pathways, including glycolysis. Since mTOR has a central role in T cell differentiation, including the development of Treg cells, and since activation of the mTOR pathway underlies the pathogenesis of SLE (14), mTOR has become a therapeutic target in this disease. A recent single-arm, open-label, phase I/II trial of the mTOR inhibitor sirolimus showed its efficacy in patients with active SLE (15). Our present data show that CaMK4 inhibition results in decreased levels of glycolysis-related proteins during CD4+ T cell activation, suggesting that CaMK4 is involved in metabolic regulation including T cell glycolysis. Since CaMK4 can promote Akt/mTORC1 signaling (16), we speculate that the CaMK4 inhibitor suppresses glycolysis via inhibition of the Akt/mTORC1 pathway caused by T cell activation.

Although previous experiments using mice suggested that aberrant expression of GLUT1 is important in the development of autoimmune diseases, it is not clear whether this observation is relevant to human SLE. This study is the first to show that the expression of CaMK4 and GLUT1 in CD4+ T cells correlates with SLE disease activity, suggesting that measuring the surface level of GLUT1 by flow cytometry may be a useful method to predict the amount of pathologic effector T cells in SLE patients. Further functional studies, including investigations of the mechanisms underlying aberrant levels of GLUT1 during the progression of SLE, are warranted.

CD4+ T cell differentiation is controlled differently at the metabolic level between T cell subsets. Importantly, Th17 cells have been found to express high surface levels of GLUT1 and were highly glycolytic (17). Th17 cells were also shown to require mTORC1 activity (17). We observed that expression of GLUT1 as well as that of glycolysis-related genes such as HK1 and HK2 during Th17 cell differentiation in SLE T cells was suppressed by a CaMK4 inhibitor.

In conclusion, the results of our study demonstrate that CD4+ T cells treated with a CaMK4 inhibitor display decreased levels of glycolytic intermediates. These effects are mediated by suppression of the CaMK4–GLUT1 axis during T cell activation and Th17 cell differentiation. Importantly, the expression levels of GLUT1 and CaMK4 in CD4+ T cells correlated with SLE disease activity, suggesting that CaMK4 may contribute to aberrant expression of GLUT1 in T cells from patients with active SLE. Further studies are needed to identify the precise mechanisms by which CaMK4 is involved in T cell metabolism in autoimmune diseases.

ACKNOWLEDGMENTS

We thank Megumi Matoba and Yuko Mizunoo (Nagasaki University Graduate School of Biomedical Sciences) for technical assistance.

AUTHOR CONTRIBUTIONS

All authors were involved in drafting the article or revising it critically for important intellectual content, and all authors approved the final version to be published. Dr. Koga had full access to all of the data in the study and takes responsibility for the integrity of the data and the accuracy of the data analysis.

Study conception and design. Koga.

Acquisition of data. Sato, Furukawa, Endo, Umeda, Sumiyoshi, Fukui, Kawashiri, Iwamoto, Ichinose, Tamai, Origuchi, Nakamura, Kawakami.

Analysis and interpretation of data. Morimoto.

REFERENCES

- Hahn BH, Ebling F, Singh RR, Singh RP, Karpouzas G, La Cava A. Cellular and molecular mechanisms of regulation of autoantibody production in lupus. *Ann N Y Acad Sci* 2005;1051:433–41.
- Valencia X, Yarboro C, Illei G, Lipsky PE. Deficient CD4+CD25high T regulatory cell function in patients with active systemic lupus erythematosus. *J Immunol* 2007;178:2579–88.
- Shi LZ, Wang R, Huang G, Vogel P, Neale G, Green DR, et al. HIF1 α -dependent glycolytic pathway orchestrates a metabolic checkpoint for the differentiation of Th17 and Treg cells. *J Exp Med* 2011;208:1367–76.
- Jacobs SR, Herman CE, Maciver NJ, Wofford JA, Wieman HL, Hammen JJ, et al. Glucose uptake is limiting in T cell activation and requires CD28-mediated Akt-dependent and independent pathways. *J Immunol* 2008;180:4476–86.
- Macintyre AN, Gerriets VA, Nichols AG, Michalek RD, Rudolph MC, Deoliveira D, et al. The glucose transporter Glut1 is selectively essential for CD4 T cell activation and effector function. *Cell Metab* 2014;20:61–72.
- Perl A, Hanczko R, Lai ZW, Oaks Z, Kelly R, Borsuk R, et al. Comprehensive metabolome analyses reveal N-acetylcysteine-responsive accumulation of kynurenine in systemic lupus erythematosus: implications for activation of the mechanistic target of rapamycin. *Metabolomics* 2015;11:1157–74.
- Yin Y, Choi SC, Xu Z, Perry DJ, Seay H, Croker BP, et al. Normalization of CD4+ T cell metabolism reverses lupus. *Sci Transl Med* 2015;7:274ra18.
- Hochberg MC, for the Diagnostic and Therapeutic Criteria Committee of the American College of Rheumatology. Updating the American College of Rheumatology revised criteria for the classification of systemic lupus erythematosus [letter]. *Arthritis Rheum* 1997;40:1725.
- Bombardier C, Gladman DD, Urowitz MB, Caron D, Chang CH, and the Committee on Prognosis Studies in SLE. Derivation of the SLEDAI: a disease activity index for lupus patients. *Arthritis Rheum* 1992;35:630–40.
- Team RC. R: a language and environment for statistical computing. Vienna: R Foundation for Statistical Computing; 2018.
- MacIver NJ, Michalek RD, Rathmell JC. Metabolic regulation of T lymphocytes. *Annu Rev Immunol* 2013;31:259–83.
- Perl A, Hanczko R, Telarico T, Oaks Z, Landas S. Oxidative stress, inflammation and carcinogenesis are controlled through the pentose phosphate pathway by transaldolase. *Trends Mol Med* 2011;17:395–403.
- Perl A. Metabolic control of immune system activation in rheumatic diseases [review]. *Arthritis Rheumatol* 2017;69:2259–70.

14. Kato H, Perl A. Blockade of Treg cell differentiation and function by the interleukin-21-mechanistic target of rapamycin axis via suppression of autophagy in patients with systemic lupus erythematosus. *Arthritis Rheumatol* 2018;70:427–38.
15. Lai ZW, Kelly R, Winans T, Marchena I, Shadakshari A, Yu J, et al. Sirolimus in patients with clinically active systemic lupus erythematosus resistant to, or intolerant of, conventional medications: a single-arm, open-label, phase 1/2 trial. *Lancet* 2018;391:1186–96.
16. Koga T, Hedrich CM, Mizui M, Yoshida N, Otomo K, Lieberman LA, et al. CaMK4-dependent activation of AKT/mTOR and CREM- α underlies autoimmunity-associated Th17 imbalance. *J Clin Invest* 2014;124:2234–45.
17. Michalek RD, Gerriets VA, Jacobs SR, Macintyre AN, MacIver NJ, Mason EF, et al. Cutting edge: distinct glycolytic and lipid oxidative metabolic programs are essential for effector and regulatory CD4⁺ T cell subsets. *J Immunol* 2011;186:3299–303.

Adenosine 2a Receptor Signal Blockade of Murine Autoimmune Arthritis via Inhibition of Pathogenic Germinal Center–Follicular Helper T Cells

Shirdi E. Schmiel, Lokesh A. Kalekar, Na Zhang, Thomas W. Blankespoor, Londyn J. Robinson,  and Daniel L. Mueller

Objective. CD4 germinal center (GC)–follicular helper T (Tfh) cells are important in the pathogenesis of autoimmune arthritis. Previous studies have shown that adenosine 2a receptor (A2aR; *Adora2a*) signaling can divert CD4 T cells away from the GC-Tfh cell lineage during the primary response to foreign antigens. This study was undertaken to examine the effects of A2aR signaling on CD4 T cells during the recognition of self antigen in a murine model of autoimmune arthritis.

Methods. Wild-type and *Adora2a*-deficient mouse KRN T cell receptor–transgenic CD4 T cells specific for glucose-6-phosphate isomerase (GPI)/I-A^{g7} were transferred into immunodeficient *Tcra*^{-/-} I-A^{g7}-expressing mice to induce arthritis. Recipients were then treated with either the selective A2aR agonist CGS-21680 (CGS) or phosphate buffered saline alone. Severity of disease, autoantibody titers, KRN T cell numbers and phenotype, and GPI-specific isotype class–switched plasmablasts were tracked.

Results. CGS treatment inhibited the development of arthritis and differentiation of KRN GC-Tfh cells, blocked the appearance of high-affinity GPI-specific and IgG1 isotype class–switched polyclonal plasmablasts, and led to a reduction in serum titers of anti-GPI IgG1. In addition, therapeutic administration of CGS after the onset of arthritis blocked further disease progression in association with reductions in the number of KRN GC-Tfh cells and anti-GPI IgG1 serum titers.

Conclusion. Strong A2aR signaling diverts autoreactive CD4 T cell differentiation away from the GC-Tfh cell lineage, thus reducing help for the differentiation of dangerous autoreactive B cells that promote arthritis. These data in a mouse model of autoimmune arthritis suggest that A2aR and its downstream signaling pathways in CD4 T cells may be promising therapeutic targets for interfering with potentially dangerous autoreactive GC-Tfh cell differentiation.

INTRODUCTION

Extracellular adenosine is an immunosuppressive purine nucleoside that reinforces immunologic tolerance (1). Numerous investigations in animal models have suggested that activation of adenosine receptors or biochemical pathways downstream of adenosine receptor signaling (e.g., cyclic adenosine monophosphate [cAMP] accumulation, protein kinase A [PKA] activation) can have ameliorative effects on autoimmune arthritis (2). Nevertheless, the translation of this information into successful therapies for human autoimmune diseases has been hampered by an insufficient knowledge regarding the adenosine receptors utilized for

this immunosuppressive effect, and a lack of understanding of the consequences of adenosine receptor engagement on immune cell differentiation and function.

Adenosine 2a receptors (A2aRs) have been observed to act as a barrier to autoimmunity by limiting inflammation and negatively regulating adaptive immune responses (3,4). A2aR signaling can maintain immune homeostasis by promoting the induction of CD4 T cell anergy and the differentiation of FoxP3⁺ regulatory T (Treg) cells, as well as by blocking the function of effector/memory CD4 T cells (3,5). A2aRs are expressed at high levels on human T cells during the course of autoimmune disease (6). The efficacy of the immunosuppressive agents methotrexate and sulfasalazine

Dr. Schmiel's work was supported by the NIH (training grant T32-AI-00731). Dr. Mueller's work was supported by the NIH (grant P01-AI-035296) and Lupus Link of Minnesota.

Shirdi E. Schmiel, PhD, Lokesh A. Kalekar, PhD, Na Zhang, MD, Thomas W. Blankespoor, Londyn J. Robinson, BS, Daniel L. Mueller, MD: University of Minnesota Medical School, Minneapolis.

No potential conflicts of interest relevant to this article were reported.

Address correspondence to Daniel L. Mueller, MD, Division of Rheumatic & Autoimmune Diseases, University of Minnesota Medical School, 3-186 Wallin Medical Biosciences Building, 2101 6th Street SE, Minneapolis, MN 55455. E-mail: muell002@umn.edu.

Submitted for publication April 26, 2018; accepted in revised form November 29, 2018.

has been demonstrated in autoimmune diseases such as rheumatoid arthritis (RA), acting through their ability to increase the expression and activation of A2aRs by extracellular adenosine (7). Consistent with these findings, the phosphodiesterase-4 inhibitor apremilast has been shown to control disease activity in patients with psoriatic arthritis, as a result of its ability to slow the turnover of the A2aR second-messenger cAMP (8).

Investigations in our laboratory and others have recently determined that A2aR signaling during the primary response to a foreign antigen in strong adjuvant has the ability to divert CD4 T cell differentiation away from the follicular helper T (Tfh) and germinal center (GC)-Tfh cell lineages, and consequently could reduce help for the differentiation of antigen-specific GC B cells and isotype class-switched plasmablasts (9,10). In RA, autoreactive B cells are thought to be induced by Tfh cells to undergo clonal expansion, isotype class-switch recombination, and somatic hypermutation within the GCs, and this ultimately leads to the differentiation of anti-citrullinated protein antibody-secreting plasma cells (11–13). In addition, the frequency of circulating Tfh cells is increased in the blood of patients with antibody-mediated autoimmune disorders (14–16), although this has not been universally observed (17). The nuclear factor Bcl-6 is responsible for the differentiation of CD4 T cells to the Tfh and GC-Tfh lineage fates by, in part, repressing other effector T cell lineage-specific transcription factors, such as T-bet and retinoic acid receptor-related orphan nuclear receptor γ t (ROR γ t) (18,19). Preclinical studies using a mouse model of autoimmune arthritis have indicated that Tfh and GC-Tfh cells contribute to the formation of GCs, production of high-affinity autoantibodies, and clinical manifestations of arthritis (20). Consistent with this, T cell-specific deficiencies in Tfh molecules, such as CXCR5, signaling lymphocytic activation molecule-associated protein, and interleukin-21 (IL-21), can protect against the development of severe arthritis in mice (21).

To determine whether strong A2aR signaling can preserve or restore immune homeostasis in autoreactive GC-Tfh cells during the recognition of self antigens, we utilized a mouse model of autoimmune arthritis in which KRN T cell receptor (TCR)-transgenic CD4 T cells specific for the self antigen glucose-6-phosphate isomerase (GPI)/I-A^{g7} differentiate into Tfh and GC-Tfh cells during the course of arthritis induction (22). Our data show that the activation of A2aRs on the KRN T cells using the selective agonist CGS-21680 (CGS) blocks the initial development of arthritis and also arrests disease progression. This therapeutic effect of A2aR signaling occurs in association with reductions in the differentiation of KRN Tfh and GC-Tfh cells and secondary anti-GPI humoral immunity. Therefore, the results of this study suggest that strong A2aR downstream signals within autoreactive CD4 T cells can raise the threshold for the differentiation of dangerous GC-Tfh effector cells, and could thus ultimately reduce the B cell-dependent immune responses that contribute to autoimmune arthritis.

MATERIAL AND METHODS

Mice. B6 mice were purchased from Charles River Breeding Laboratories under a contract from the National Cancer Institute. B6.g7 (H-2^{g7}-congenic) mice and KRN mice of the B6 strain expressing a TCR transgene specific for GPI/I-A^{g7} were gifts from Drs. Diane Mathis and Christophe Benoist (Harvard Medical School, Boston, MA) and the Institut de Génétique et de Biologie Moléculaire et Cellulaire (Strasbourg, France) (23). Wild-type and *Tcra*^{-/-} (B6 × B6.g7) F1 mice were bred as previously described (22). *Adora2a*^{fl/fl} mice containing *loxP* sites flanking exon 2 of the *Adora2a* gene (a gift from Joel Linden, La Jolla Institute for Allergy and Immunology, La Jolla, CA) (24) were crossed with CD4-Cre mice (a gift from Michael Farrar, University of Minnesota, Minneapolis, MN) to generate A2aR T cell conditional-knockout (*Adora2a*^{fl/fl}-KO) mice. The breeding of wild-type normal and *Adora2a*^{fl/fl}-KO CD45.1+ KRN mice as well as wild-type and *Tcra*^{-/-} F1 mice was carried out in our own animal colonies. All experimental protocols were performed in accordance with the guidelines of the University of Minnesota Institutional Animal Care and Use Committee and the National Institutes of Health.

Adoptive transfer and CGS treatment. Wild-type and *Tcra*^{-/-} F1 host mice were depleted of natural killer cells by the administration of anti-asialo GM1 antibody (Wako Chemicals) as previously described (22). Spleen and lymph node cells from donor wild-type and *Adora2a*-KO KRN mice were enriched for naive CD4 T cells using a Mouse CD4 T Cell Negative Isolation Kit (Stem Cell Technologies) in accordance with the manufacturer's instructions. Purified naive KRN T cells were then adoptively transferred (~10,000 cells per recipient) via tail vein injection into either wild-type or *Tcra*^{-/-} F1 host mice to initiate the recognition of the GPI/I-A^{g7} self antigen (Figures 1A–C). Beginning 1 day after adoptive transfer, host mice were given intraperitoneal injections of the selective A2aR agonist CGS twice daily, at a dose of 2.5 mg/kg (Tocris), or with vehicle alone (phosphate buffered saline [PBS]), as previously described (3,9).

Cell enrichment and flow cytometry. At the completion of all experiments, KRN CD4 T cells were analyzed by pooling the spleen and lymph node cells, and then staining with phycoerythrin (PE)-conjugated antibodies to CD45.1 (A20; eBioscience). KRN T cells were enriched using a PE positive selection kit (Stem Cell Technologies) in accordance with the manufacturer's instructions. Energy in KRN T cells was assessed as their ability to be stimulated, with the response characterized by intracellular cytokine accumulation, as previously described (9,22,25).

In addition, the differentiation of KRN T cells was assessed by flow cytometry for the expression of Bcl-6, T-bet, ROR γ t, and FoxP3, using a previously described protocol (9). KRN T cells were incubated in vitro for 3 hours at 37°C in RPMI 1640 medium

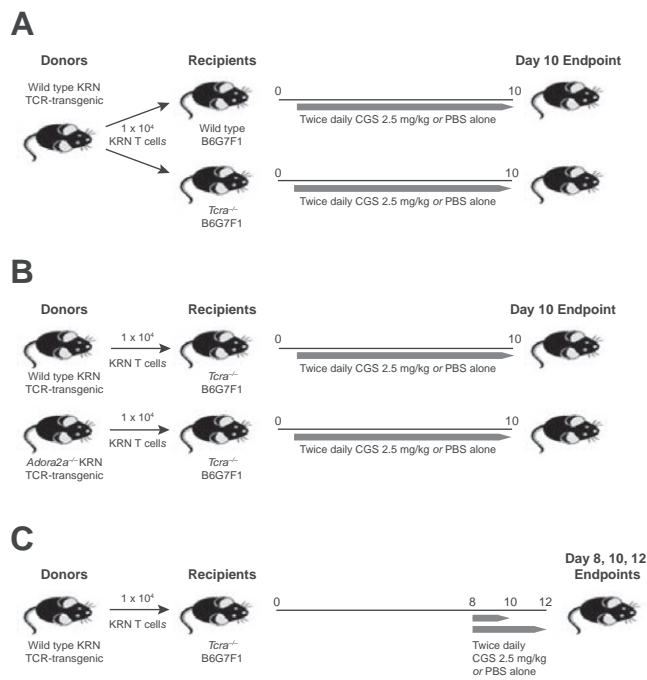


Figure 1. T cell adoptive transfer protocols for the assessment of murine autoimmune arthritis. **A**, Naive wild-type CD45.1+ KRN T cell receptor (TCR)-transgenic CD4 T cells specific for glucose-6-phosphate isomerase (GPI)/I-A^{g7} (10^4) were adoptively transferred into CD45.2+ wild-type F1 and *Tcr*^{-/-} (B6 × B6.g7) F1 host mice. After 24 hours, host mice were injected intraperitoneally twice daily with the selective adenosine 2a receptor (A2aR) agonist CGS-21680 (CGS) at 2.5 mg/kg or phosphate buffered saline (PBS) alone until the end point on day 10. **B**, Naive wild-type CD45.1+ KRN CD4 T cells were isolated from both CD4-Cre *Adora2a*^{fl/fl} conditional-knockout (*Adora2a*^{-/-}) and wild-type donor mice. The T cells (10^4) were then adoptively transferred into CD45.2+ *Tcr*^{-/-} F1 host mice to induce autoimmune arthritis. Mice were subsequently treated twice daily with either CGS or PBS alone for the duration of the experiment (10 days). **C**, Naive wild-type CD45.1+ KRN CD4 T cells were adoptively transferred into CD45.2+ *Tcr*^{-/-} F1 hosts to induce arthritis. Beginning on day 8, the mice were injected intraperitoneally twice daily with CGS at 2.5 mg/kg or PBS alone for the remainder of the experiment (with end points on days 8, 10, and 12).

and 10% fetal calf serum, in the presence of 50 ng/ml phorbol myristate acetate (Sigma-Aldrich) and 1 μ M ionomycin (EMD Chemicals), and in the final 2 hours, the KRN T cells were incubated with 10 mg/ml brefeldin A (Sigma-Aldrich). After incubation of the cells, cell surface and intracellular staining was performed as previously described (22,25).

To assess GPI-specific IgG1 plasmablasts, bulk polyclonal lymphocytes were stained with antibodies to B220 (RA3-6B2), GL7 (GL-7), CD38 (90), IgM (RMM-1), and IgD (11-26c.2a), with exclusion of irrelevant cells using antibodies to CD11c (N418), CD4 (GK1.5), CD8 (53-6.7), and F4/80 (BM8). Thereafter, the cells were treated with a fixation/permeabilization kit (eBioscience) and then subjected to intracellular staining with goat anti-mouse Ig (heavy and light chain) (A11068), biotin-conjugated recombinant

mouse GPI (kindly provided by Dr. Haochu Huang, University of Chicago, Chicago, IL), and anti-IgG1 (RMG1-1) (26). All cells were analyzed using a BD LSRII flow cytometer (BD Biosciences). Data were analyzed with FlowJo software (Tree Star). Examples of the flow cytometry gating strategy are provided in Supplementary Figure 1 (available on the *Arthritis & Rheumatology* web site at <http://onlinelibrary.wiley.com/doi/10.1002/art.40796/abstract>).

Arthritis scoring. Ankle swelling was measured using a Quick-Mini Series 700 comparator (Mitutoyo). Changes were reported as the percentage change in ankle thickness from day 0 or day 8, as indicated in the experiment. In addition, the arthritis clinical disease activity index was calculated by assigning a score of 0–3 for each paw based on the extent of erythema/swelling, and then summing the scores, as previously described (22).

Anti-GPI isotype-specific IgG antibody measurements. Serum was isolated from recipient mice on the specified days and measured for anti-GPI IgG1, IgG2b, IgG2c, IgG3, and total IgG antibodies by enzyme-linked immunosorbent assay, using recombinant mouse GPI together with isotype-specific anti-mouse Ig reagents, as previously described (22).

Serum transfer arthritis. Pooled serum from adult arthritic K/BxN mice was a kind gift from Dr. Bryce Binstadt (University of Minnesota). Age-matched wild-type F1 mice were injected twice, intraperitoneally, with 200 μ l pooled serum on days 0 and 2. Clinical disease activity and ankle thickness were measured daily. Treatments with CGS or PBS vehicle alone were initiated beginning on day 6 (Supplementary Figure 1 [<http://onlinelibrary.wiley.com/doi/10.1002/art.40796/abstract>]).

Joint histology. For analysis of histologic features, the ankles and feet of mice were dissected, frozen in OCT medium (Sakura Finetek USA), cryosectioned to a thickness of 10 μ m, and stained with hematoxylin and eosin.

Statistical analysis. Statistical tests were performed using GraphPad Prism software. *P* values (with 95% confidence intervals) were obtained using Student's unpaired one-tailed *t*-tests. The mean clinical arthritis disease activity scores were compared using Mann-Whitney U test.

RESULTS

A2aR signal response to CGS treatment characterized by reinforced immune self tolerance and prevention of autoimmune arthritis. To initially assess whether A2aR signals can act to maintain immune cell homeostasis during recognition of self antigen, we made use of an adoptive transfer of GPI-specific KRN TCR-transgenic CD4 T cells into mice that naturally express GPI/I-A^{g7} complexes (22) (see protocol in

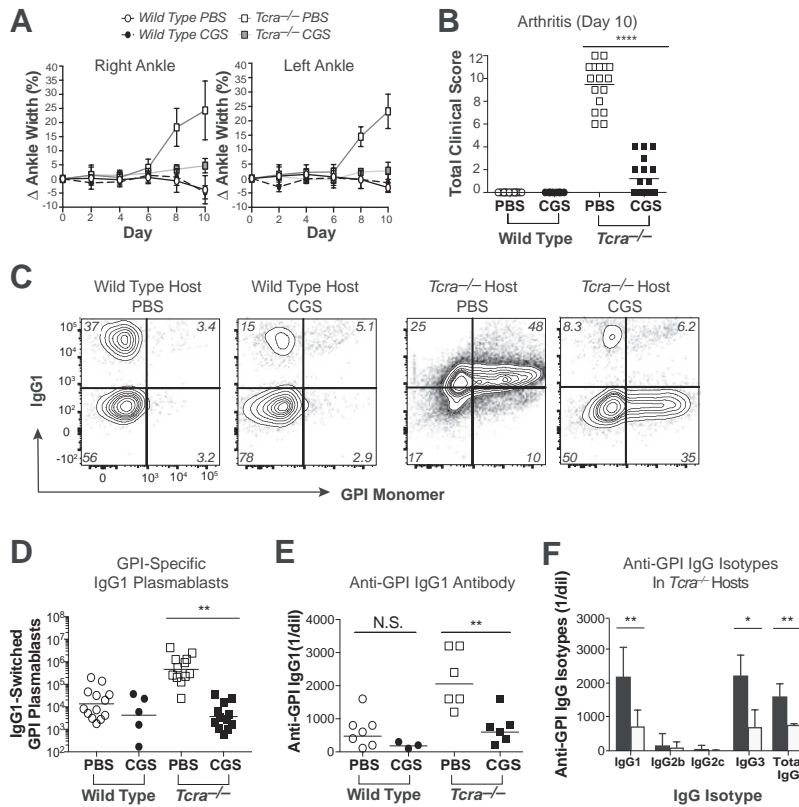


Figure 2. Treatment of mice with the A2aR agonist CGS blocks KRN T cell-dependent autoimmune arthritis. KRN CD4 T cells were adoptively transferred into wild-type and *Tcra*^{-/-} F1 host mice to initiate recognition of self antigen. **A**, Host mice were treated twice daily with CGS or PBS alone, and then assessed for change in ankle width (swelling) over the duration of the 10-day experiment. **B**, Aggregate clinical disease activity scores were determined on day 10. **C** and **D**, Frequencies (**C**) and numbers (**D**) of polyclonal, GPI-specific B220^{dim} intracellular Ig (H + L)^{high}GL7⁻IgG1+ plasmablasts in the spleens and pooled lymph nodes of host mice were determined on day 10. Note that weak IgG1 staining in the PBS-treated *Tcra*^{-/-} mice is typical of samples containing high numbers of class-switched IgG1-expressing plasmablasts. **E**, Serum titers of anti-GPI IgG1 antibodies were measured by enzyme-linked immunosorbent assay (ELISA) on day 10. **F**, Serum titers of individual anti-GPI IgG-isotype antibodies in *Tcra*^{-/-} host mice were determined by isotype-specific ELISA on day 10, either in the absence (solid bars) or presence (open bars) of CGS. In **A** and **F**, results are the mean \pm SEM of 3–17 mice per group. In **B**, **D**, and **E**, symbols represent individual mice; horizontal lines indicate the mean. Data are representative of 2–5 independent experiments. * = $P < 0.05$; ** = $P < 0.01$, by Student's *t*-test. **** = $P < 0.001$ by Mann-Whitney U test. NS = not significant (see Figure 1 for other definitions).

Figure 1A). As expected, PBS-treated *Tcra*^{-/-} F1 host mice that lacked a population of FoxP3+ Treg cells developed joint swelling and signs of severe arthritis by 8 days after transfer of the KRN T cells (Figures 2A and B). Signs of arthritis in the paws of these mice were accompanied by degradation of the articular cartilage, intense periarticular immune cell infiltration, and erosions of marginal cortical bone tissue (see Supplementary Figure 2, available on the *Arthritis & Rheumatology* web site at <http://onlinelibrary.wiley.com/doi/10.1002/art.40796/abstract>). In contrast, the adoptive transfer of KRN T cells into wild-type F1 host mice did not interfere with normal peripheral mechanisms of immune self tolerance, and no arthritis was observed.

Importantly, lymphopenic *Tcra*^{-/-} F1 host mice that were injected with KRN T cells and then immediately treated with the selective A2aR agonist CGS demonstrated essentially no ankle swelling, and their clinical disease activity scores were signifi-

cantly reduced as compared to that in PBS-treated *Tcra*^{-/-} F1 mice. Joint infiltration and damage were also reduced with this CGS treatment regimen in the *Tcra*^{-/-} F1 host mice.

GPI-specific autoantibody production is important to the pathogenesis of KRN T cell-dependent arthritis (23). IgG1 is the dominant autoantibody isotype found in these arthritic animals, and this is associated with the differentiation of GPI-specific IgG1 isotype class-switched polyclonal plasmablasts in the spleen and lymph nodes (20,23). Consistent with these previously reported findings, polyclonal IgG1 isotype class-switched GPI-specific plasmablasts were found at increased frequencies (mean \pm SEM 0.51 \pm 0.54% of total B cells) in the spleens and lymph nodes of PBS-treated *Tcra*^{-/-} F1 host mice with arthritis as compared to healthy wild-type F1 mice (a mean \pm SEM fold increase of 45.8 \pm 10.9). However, CGS treatment significantly reduced the number of GPI-specific IgG1+ plasmablasts present in the *Tcra*^{-/-} F1

host mice (Figures 2C and D). In contrast to IgG1+ plasmablasts, GPI-specific plasmablasts that were negative for IgG1 expression were only infrequently observed in *Tcra*^{-/-} host mice (mean ± SEM 0.08 ± 0.09% of total B cells), but these appeared resistant to the effects of the A2aR agonist (a mean ± SEM fold decrease of 1.1 ± 0.1) and represented the majority of GPI-binding plasmablasts remaining after the CGS treatment (Figure 2C and data not shown). Anti-GPI IgG1, IgG3, and total IgG serum antibody levels mirrored these differences in GPI-specific IgG1+ plasmablast differentiation (Figures 2E and F).

In contrast to lymphopenic *Tcra*^{-/-} F1 recipient mice, wild-type F1 host mice remained protected from a KRN T cell-mediated

breakdown of immune tolerance in the polyclonal B cell compartment, regardless of treatment group, and demonstrated persistently low levels of autoreactive plasmablasts and autoantibodies (Figures 2C–E and data not shown). Thus, A2aR-mediated suppression of autoimmune arthritis occurs in association with inhibition of the pathogenic anti-GPI IgG1 isotype class switch.

Lack of effect of A2aR signals on KRN CD4 T cell anergy or Treg cell induction. A2aR signals are thought to inhibit CD4 T cell reactivity in part through the induction of anergy and the differentiation of FoxP3+ Treg cells (3). However, KRN CD4 T cells recovered from *Tcra*^{-/-} F1 adoptive transfer recipient

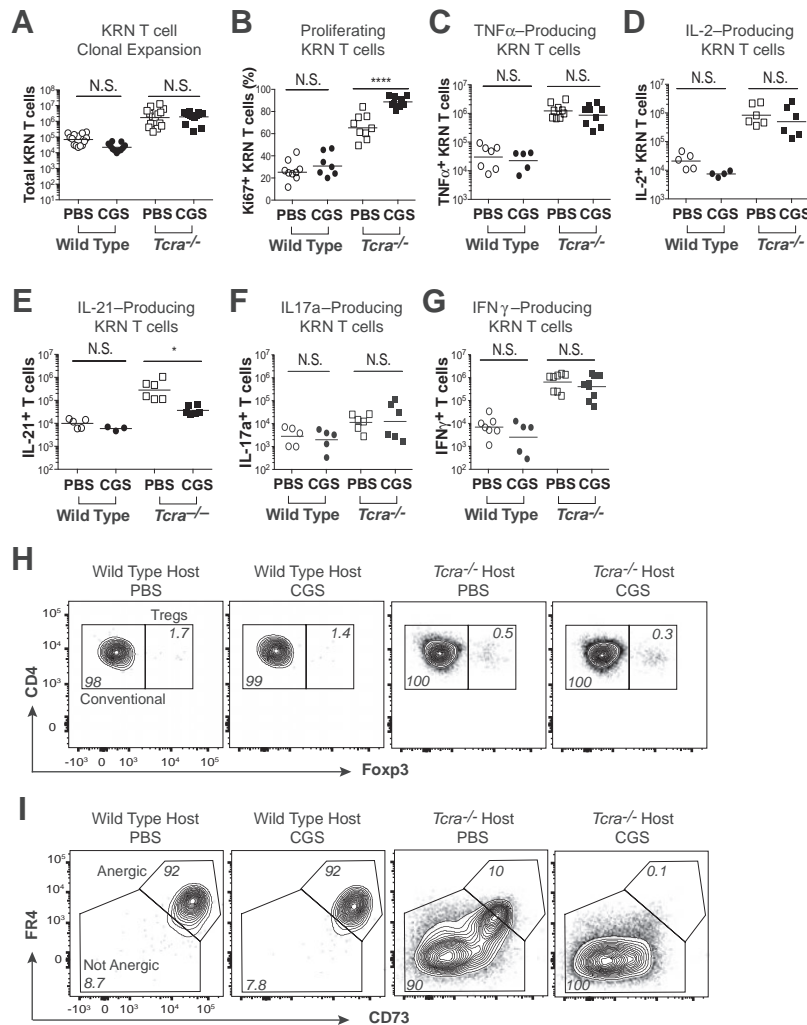


Figure 3. A2aR activation does not promote KRN T cell anergy or FoxP3+ regulatory T (Treg) cell differentiation in either normal or T cell-lymphopenic host mice. Naive KRN CD4 T cells were adoptively transferred into wild-type and *Tcra*^{-/-} F1 host mice. The mice were then injected twice daily with CGS or PBS alone for the duration of the experiment (10 days). **A** and **B**, Total numbers of KRN T cells (**A**) and percentages of Ki-67-expressing conventional FoxP3- KRN T cells (**B**) were determined. **C–G**, Production of tumor necrosis factor (TNF) (**C**), interleukin-2 (IL-2) (**D**), IL-21 (**E**), IL-17a (**F**), and interferon-γ (IFNγ) (**G**) by KRN T cells was determined following 3 hours of in vitro stimulation with ionomycin and phorbol myristate acetate. **H** and **I**, Frequencies of KRN FoxP3+ Treg cells (**H**) and conventional FoxP3-FR4+CD73+ (anergic phenotype) KRN T cells (**I**) were determined. Flow cytometry data are representative of at least 3 independent experiments in 5–10 mice per group. In **A–G**, symbols represent individual mice; horizontal lines indicate the mean. * = *P* < 0.05; **** = *P* < 0.001, by Student's *t*-test. NS = not significant (see Figure 1 for other definitions).

mice on day 10 demonstrated a robust clonal expansion relative to that in healthy wild-type F1 host mice, regardless of whether they were treated with CGS (Figure 3A). In fact, proliferation of KRN T cells in *Tcra*^{-/-} F1 host mice appeared to be enhanced by CGS, based on the expression of the proliferation marker Ki-67 (Figure 3B).

To formally test the effects of CGS on the functional responsiveness of the KRN T cells, cells from day 10 were stimulated in vitro with phorbol myristate acetate plus ionomycin, and intracellular cytokine accumulation was then measured. The synthesis of tumor necrosis factor (TNF) and IL-2 was similarly induced by stimulation of KRN T cells isolated from both CGS- and PBS-treated *Tcra*^{-/-} F1 host mice (Figures 3C and D); therefore, anergy induction in the presence of CGS appeared unlikely. Nonetheless,

the treatment of *Tcra*^{-/-} F1 mice with CGS did interfere with the differentiation of KRN effector/memory T cells, which were capable of secreting the T helper cytokine IL-21 (Figure 3E). This was an isolated defect, as KRN T cells treated with CGS continued to differentiate normally into IL-17a⁻ and interferon- γ (IFN γ)-producing effector T cells in the *Tcra*^{-/-} F1 mice (Figures 3F and G). Given that differentiation of GPI-specific GC B cells and isotype class switch to both IgG1 and IgG3 depend on T cell production of IL-21 (26,28), this reduced synthesis of IL-21 by KRN T cells in the setting of CGS treatment may have contributed to the observed reductions in GPI-specific IgG1⁺ plasmablasts and serum titers of anti-GPI IgG1 antibodies.

FoxP3⁺ Treg cells are indispensable for peripheral immune tolerance (4). We previously reported that a reconstitution of the

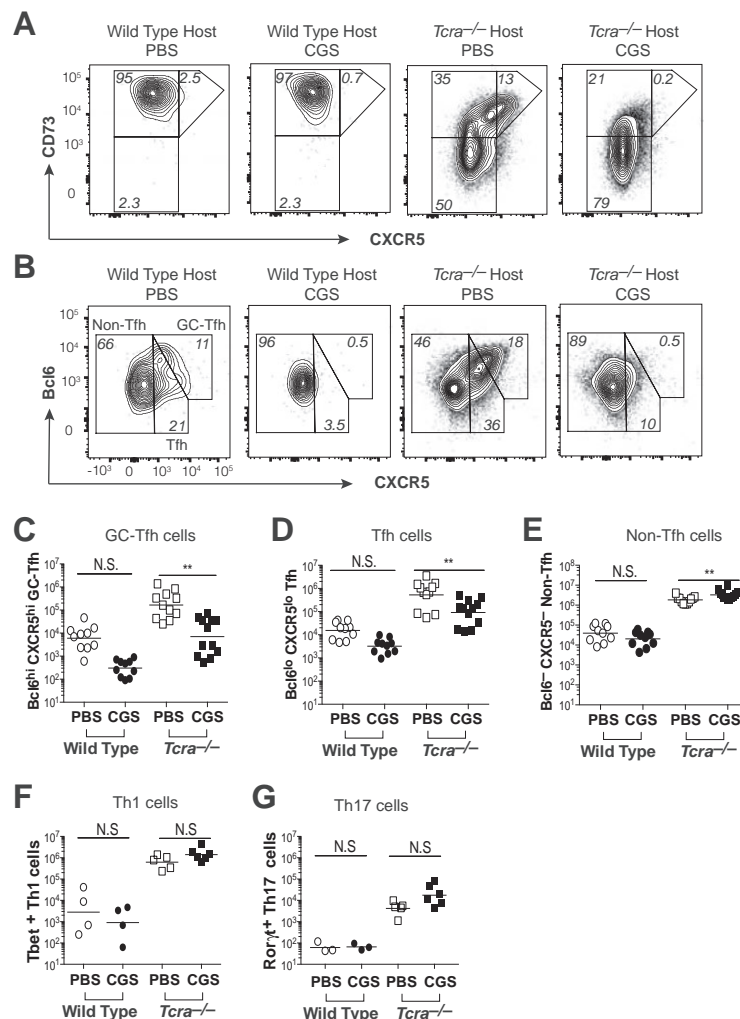


Figure 4. Treatment of mice with the A2AR agonist CGS blocks follicular helper T (Tfh) and germinal center (GC)-Tfh cell differentiation during recognition of self antigen. KRN CD4 T cells were transferred into wild-type and *Tcra*^{-/-} F1 host mice. The mice were then treated twice daily for 10 days with either CGS or PBS alone. **A** and **B**, Expression of CD73 and CXCR5 (**A**) and Bcl-6 and CXCR5 (**B**) on conventional FoxP3⁻ KRN T cells was determined. **C–E**, Aggregate numbers of Bcl-6^{high}CXCR5^{high} (GC-Tfh) (**C**), Bcl-6^{low}CXCR5^{low} (Tfh) (**D**), and Bcl-6⁻CXCR5⁻ (non-Tfh) (**E**) conventional FoxP3⁻ KRN T cells were determined. **F** and **G**, Th1 lineage (T-bet⁺) (**F**) and Th17 lineage (retinoic acid receptor-related orphan nuclear receptor γ t-positive [ROR γ t⁺]) (**G**) T cells within the non-Tfh (Bcl-6⁻CXCR5⁻) cell fraction of conventional FoxP3⁻ KRN T cells were determined. Data are representative of 3–4 independent experiments in 4–12 mice per group. Symbols represent individual mice; horizontal lines indicate the mean. ** = $P < 0.01$ by Student's *t*-test. NS = not significant (see Figure 1 for other definitions).

FoxP3+ Treg cell compartment in *Tcra*^{-/-} F1 mice restores immune homeostasis and suppresses KRN T cell-mediated adoptive transfer arthritis (22). To determine whether CGS treatment inhibits B cell-dependent arthritis development by promoting the differentiation of KRN FoxP3+ Treg cells, we investigated the expression of FoxP3 within the expanded KRN CD4 T cell population. We found that CGS treatment was not associated with the enhanced differentiation of KRN FoxP3+ Treg cells in either wild-type F1 or *Tcra*^{-/-} F1 mice (Figure 3H).

In *Tcra*^{-/-} F1 host mice, the expression of FR4 and CD73 on KRN T cells was typically only intermediate to low, consistent with the avoidance of anergy and successful differentiation of effector/memory T cells (22,25). This is in contrast to the findings in wild-type F1 host mice, in which anergic KRN T cells expressed high levels of FR4 and CD73. Perhaps surprisingly, treatment of the *Tcra*^{-/-} F1 host mice with CGS failed to induce anergy in the KRN T cells, and instead led to a loss of the subpopulation of effector/memory T cells that express intermediate levels of FR4 and CD73 (Figure 3I). These observations therefore reveal that A2aR signals promote neither anergy induction nor Treg cell differentiation in this arthritis model system, and instead can lead to alterations in the capacity of KRN effector/memory T cell populations to produce IL-21 and to express FR4 and CD73 at intermediate levels.

Role of A2aR signals in diverting KRN CD4 effector/memory T cells away from the Tfh and GC-Tfh lineage fates. CD4 GC-Tfh cells expressing the highest levels of Bcl-6 and CXCR5 are thought to provide cognate help in the form of production of CD40L and IL-21 by antigen-specific B cells within GCs (18,29,30). In addition, CXCR5+ Tfh cells have been reported to express FR4 and CD73 (31). We therefore reasoned that the ability of CGS to block both production of IL-21 by KRN T cells and differentiation of GPI-specific IgG1 class-switched plasmablasts might stem from its capacity to inhibit Tfh and GC-Tfh cell differentiation. In arthritic *Tcra*^{-/-} F1 mice, we observed increased levels of CXCR5 on the fraction of KRN effector/memory T cells that coexpressed low, but significant, amounts of FR4 and CD73 (Figure 4A and data not shown). In contrast to the findings in PBS-treated mice, KRN T cells in CGS-treated *Tcra*^{-/-} F1 host mice lacked this cell subpopulation altogether.

Given that strong A2aR signaling has been shown to directly antagonize the differentiation of Tfh and GC-Tfh cells during immunization with a foreign antigen in adjuvant (9), this result suggested the possibility of a similar loss of KRN Tfh and GC-Tfh cell differentiation during the recognition of self antigen in the presence of CGS. Consistent with this notion, PBS-treated *Tcra*^{-/-} F1 adoptive transfer recipient mice developed greatly expanded KRN T cell populations of Bcl-6^{low}CXCR5^{low} Tfh cells and Bcl-6^{high}CXCR5^{high} GC-Tfh cells, whereas differentiation of both Tfh cells and GC-Tfh cells was significantly

reduced in CGS-treated *Tcra*^{-/-} F1 mice (Figures 4B–D). KRN effector/memory T cells in CGS-treated *Tcra*^{-/-} F1 mice were instead more likely to display a non-Tfh cell phenotype (Bcl-6–CXCR5–); however, this difference was small and was not associated with any significant change in the numbers of Th1 or Th17 lineage cells (Figures 4B and E–G). Thus, the data suggest that strong A2aR signaling interferes specifically with the differentiation of KRN CD4 Tfh and GC-Tfh cells during recognition of self antigen.

CD4 T cell-intrinsic nature of the A2aR-mediated protection against development of autoimmune arthritis. A2aRs are expressed on CD4 T cells following TCR ligation; however, A2aRs can also be expressed on other cells of hematopoietic origin (6,24,27). Therefore, it was important to determine whether the effects of CGS on GC-Tfh cell differentiation and arthritis susceptibility were the result of direct engagement of A2aRs on KRN T cells, or instead represented an indirect effect of A2aR activation on some other cell type. To test this, we generated KRN T cell-transgenic CD4-Cre *Adora2a*^{fl/fl}-KO mice, which lack A2aRs only on their T cells. *Adora2a*-KO and wild-type mouse KRN T cells were then transferred into *Tcra*^{-/-} F1 recipient mice, which lacked their own T cells but appropriately expressed A2aRs on other cell types (see protocol in Figure 1B).

In the absence of KRN T cell-specific A2aRs, CGS treatment failed to inhibit the T cell expression of Bcl-6 and CXCR5, and the frequency of Tfh and GC-Tfh cells in *Tcra*^{-/-} F1 mice was unperturbed (Figures 5A and B). Likewise, CGS treatment failed to promote the expansion of non-Tfh cells in *Tcra*^{-/-} host mice when responder KRN T cells were A2aR-deficient.

A2aR-mediated inhibition of autoreactive IgG1 isotype class-switched plasmablast differentiation and of anti-GPI IgG1 autoantibody production in *Tcra*^{-/-} F1 mice was also lost when A2aRs were absent from the responding KRN T cells (Figures 5C and D and data not shown). Consistent with these findings, CGS treatment failed to protect *Tcra*^{-/-} F1 mice that received adoptive transfer of *Adora2a*-KO KRN T cells from the development of severe autoimmune arthritis (Figure 5E).

Blockade of ongoing progression of CD4 T cell-mediated autoimmune arthritis by CGS therapy. The abrogation of dangerous CD4 GC-Tfh cell differentiation using T cell-intrinsic strong A2aR signaling has potential therapeutic applications. Nevertheless, the most efficacious strategies for the treatment of autoimmune arthritis will require an ability to arrest clinical activity even after disease onset. Therefore, CGS was examined for its ability to interrupt KRN GC-Tfh cell differentiation and survival and to inhibit disease progression when administered after the onset of arthritis. Wild-type naive KRN CD4 T cells were adoptively transferred into *Tcra*^{-/-} F1 host mice to induce arthritis, and 8 days later, treatment with CGS

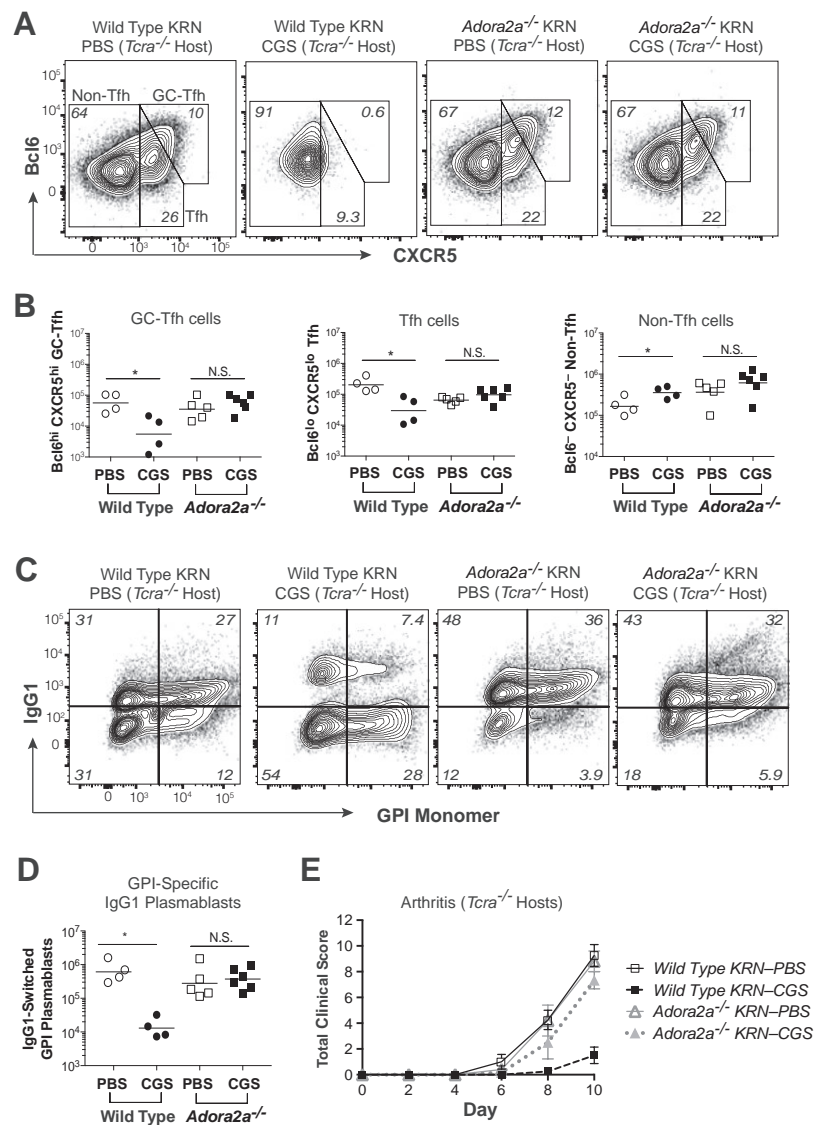


Figure 5. CGS-mediated blockade of germinal center–follicular helper T (GC-Tfh) cell differentiation and protection against autoimmune arthritis is intrinsic to T cells. KRN CD4 T cells (either wild-type or *Adora2a*^{-/-}) were adoptively transferred into *Tcra*^{-/-} F1 host mice. The mice were then injected twice daily with CGS or PBS alone for the duration of the experiment (10 days). **A**, Representative Bcl-6 and CXCR5 expression patterns on conventional FoxP3⁻ KRN T cells are shown. **B**, Absolute numbers of GC-Tfh (Bcl-6^{high}CXCR5^{high}), Tfh (Bcl-6^{low}CXCR5^{low}), and non-Tfh (Bcl-6⁻CXCR5⁻) conventional FoxP3⁻ KRN T cells were determined. **C** and **D**, Frequencies (**C**) and numbers (**D**) of polyclonal, GPI-specific B220^{dim} intracellular Ig (H + L)^{high}GL7–IgG1+ plasmablasts were determined in the same secondary lymphoid organs of host mice. **E**, Total clinical disease activity scores were determined over the duration of the experiment (10 days). In **B** and **D**, symbols represent individual mice; horizontal lines indicate the mean. In **E**, bars show the mean ± SEM of 4–12 mice per group. Data are representative of 3–4 independent experiments. * = *P* < 0.05 by Student's *t*-test. NS = not significant (see Figure 1 for other definitions).

(or PBS alone) was initiated (see protocol in Figure 1C). Mice were again monitored for signs of clinical disease activity, KRN effector/memory T cell differentiation, and polyclonal class-switched IgG1+ GPI-specific plasmablast differentiation within the spleens and lymph nodes between day 8 and day 12.

In PBS-treated control mice, clinical signs of arthritis worsened over time, as expected (Figures 6A and B, and Supplementary Figure 3, available on the *Arthritis & Rheumatology* web site at <http://onlinelibrary.wiley.com/doi/10.1002/art.40796/abstract>). However, activation of A2aRs significantly reduced the

clinical disease activity score and joint swelling on day 10, after just 4 twice-daily CGS treatments, and both of these parameters of arthritis severity remained low after 8 treatments with CGS (day 12).

Consistent with these findings, activation of A2aRs beginning on day 8 after adoptive transfer of KRN T cells led to a significant reduction in the frequency and number of Bcl-6^{high}CXCR5^{high} GC-Tfh cells by day 10, as compared to that in PBS-treated control animals (Figures 6C and D). The number of GC-Tfh cells remained low following CGS treatment

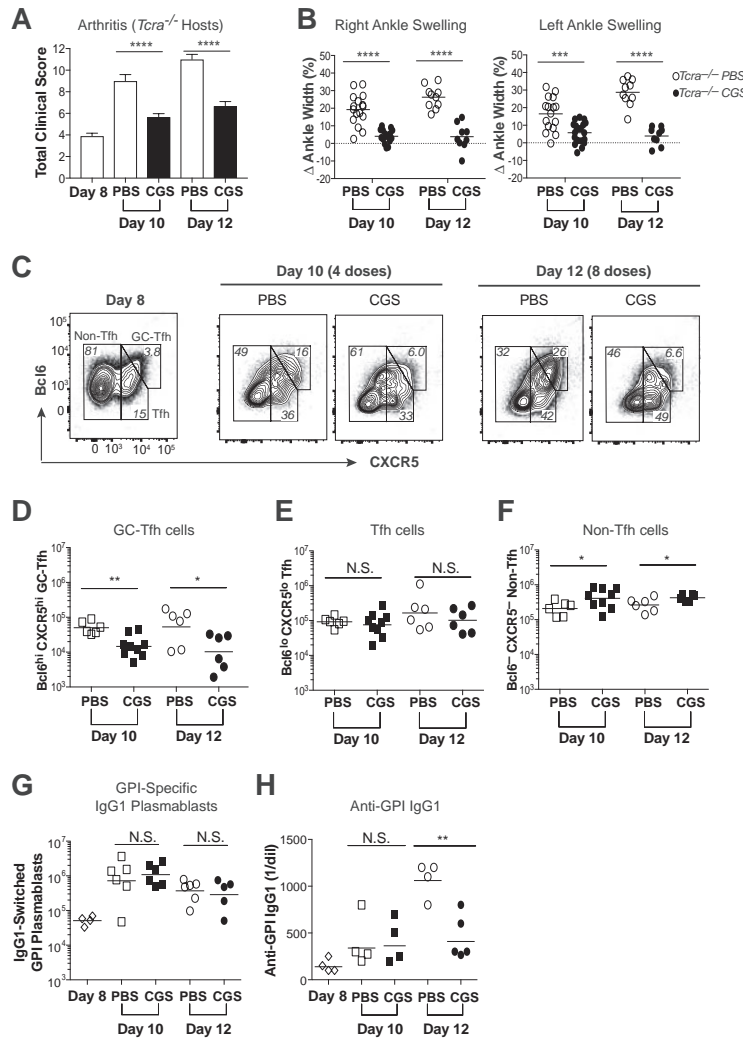


Figure 6. Treatment of mice with the A2aR agonist CGS arrests germinal center-follicular helper T (GC-Tfh) cell differentiation and blocks the progression of autoimmune arthritis. Wild-type KRN CD4 T cells were adoptively transferred into *Tcra*^{-/-} F1 host mice. Beginning on day 8, arthritic mice were injected twice daily with CGS or PBS alone. **A**, Total clinical disease activity scores were determined on days 8, 10, and 12. Results are the mean ± SEM of 4–9 mice per group. **B**, Change in ankle width (swelling) from day 8 to days 10 or 12 was determined. **** = *P* < 0.01; **** = *P* < 0.001, by Mann-Whitney U test. **C**, Representative Bcl-6 and CXCR5 expression patterns on conventional FoxP3⁻ KRN T cells on days 8, 10, and 12 are shown. Data are representative of at least 3 independent experiments. **D–F**, Absolute numbers of cells with the GC-Tfh (Bcl-6^{high}CXCR5^{high}) (**D**), Tfh (Bcl-6^{low}CXCR5^{low}) (**E**), and non-Tfh (Bcl-6–CXCR5⁻) (**F**) phenotype among conventional FoxP3⁻ KRN T cells were determined on days 10 and 12. **G** and **H**, Numbers of polyclonal, GPI-specific B220^{dim} intracellular Ig (H + L)^{high}GL7–IgG1+ plasmablasts (**G**) and anti-GPI IgG1 serum antibody titers (**H**) were determined in host mice on days 8, 10, and 12. Symbols represent individual mice; horizontal lines indicate the mean. Data are representative of at least 3 independent experiments. * = *P* < 0.05; ** = *P* < 0.01, by Student’s *t*-test. NS = not significant (see Figure 1 for other definitions).

through day 12. On the other hand, the percentage and number of Bcl-6^{low}CXCR5^{low} Tfh cells at these late time points were unchanged by exposure to CGS (Figures 6C and E). In contrast to GC-Tfh and Tfh cells, treatment with CGS resulted in a small, yet significant, increase in the percentages and numbers of KRN non-Tfh cells (Figures 6C and F).

As before, no alterations in KRN FoxP3⁺ Treg, Th1, or Th17 cell lineage differentiation events were observed in the presence of CGS (data not shown). Furthermore, the delay of CGS administration until day 8 resulted in a loss of its capacity to interfere

with IgG1+ GPI-specific plasmablast differentiation (Figure 6G). Nevertheless, administration of CGS at this later time point did blunt the rise in anti-GPI IgG1 serum antibody titers as measured on day 12 (Figure 6H). We previously noted that, unlike our findings in this KRN CD4 T cell-mediated autoimmune arthritis model, K/BxN serum transfer arthritis, with its anti-GPI IgG1 antibody-mediated inflammation, proved to be completely resistant to treatment with CGS (23,32,33) (see Supplementary Figure 4, available on the *Arthritis & Rheumatology* web site at <http://onlinelibrary.wiley.com/doi/10.1002/art.40796/abstract>).

DISCUSSION

Extracellular adenosine and its receptors have been previously demonstrated to suppress inflammatory arthritis in animal models (2). Nevertheless, the mechanisms responsible for their ameliorating effects have remained obscure. Activation of A2aRs can, in some circumstances, limit the secretion of proinflammatory cytokines and chemokines, including the production of IL-2 by T cells (5,6). A2aR agonists have also been reported to promote anergy induction and divert effector T cell differentiation toward a FoxP3+ Treg cell lineage (3). In this study, we confirmed that the A2aR agonist CGS blocks the development of autoimmune arthritis in mice, but only when the GPI-specific CD4 T cells express their own A2aRs. While this requirement for A2aRs on the KRN T cells does not exclude the possibility of important actions of CGS on additional immune cell types, the result is consistent with the key role that autoreactive CD4 T cells play in arthritis development, and suggests that therapies designed to increase A2aR downstream signaling specifically within CD4 T cells could be effective.

Following the adoptive transfer of normal naive KRN T cells to *Tcra*^{-/-} F1 host mice, arthritis development proved to be tightly associated with the expansion and differentiation of IL-21-producing, GPI-specific Tfh and GC-Tfh cells, as has been previously reported (27). Consistent with the observed role of IL-21-producing KRN Tfh and GC-Tfh cells in GPI/II-A⁹⁷-directed T cell/B cell collaboration in this murine model of autoimmune arthritis, polyclonal GPI-specific IgG1 isotype class-switched plasmablasts, as well as anti-GPI IgG1 (and IgG3) serum titers, were increased over the course of the arthritis response. Importantly, with CGS treatment, strong activation of A2aRs on the KRN CD4 T cells resulted in a selective blockade of both Tfh and GC-Tfh cell differentiation and the accompanying T cell-dependent B cell responses. This inhibition of CXCR5- and Bcl-6-expressing Tfh and GC-Tfh cells led to fewer KRN T cells that were capable of producing IL-21, although the secretion of IL-2, TNF, IFN γ , and IL-17a and the differentiation of FoxP3+ Treg cells were unchanged in this T cell population. Therefore, blunted expression of the *Bcl6* gene in KRN T cells in the setting of strong downstream activation of A2aR and resultant reductions in *CXCR5* and *Il21* gene expression represent a plausible mechanism for the inhibition of autoimmune arthritis by CGS. It should be noted that A2aR activation did not appear to influence the strength of the CD4 T cell clonal expansion or the general survival of KRN CD4 T cells, as the subpopulations of KRN non-Tfh cells remained stable or increased.

We found that neither the blocking of A2aR signaling with a selective A2aR antagonist nor the use of *Adora2a*-deficient KRN CD4 T cells for adoptive transfer reliably enhanced the differentiation of Tfh or GC-Tfh cells in our experimental model system, nor did either of these approaches provoke the development of arthritis in wild-type F1 host mice, even though both were sufficient to interfere with the effects of CGS (data

not shown). It is possible that compensatory mechanisms within autoreactive CD4 T cells make up for the loss of A2aR signaling, as adenosine 2b receptors can be expressed on some lymphocytes, are homologous to A2aRs, and share the same cAMP/PKA signaling pathways (6,27,34,35). Therefore, additional studies will be necessary to examine the relationship between endogenous extracellular adenosine and A2aRs to reveal their physiologic roles in the regulation of autoreactive Tfh/GC-Tfh cell differentiation and arthritis development.

The therapeutic benefits of increased adenosine receptor signaling in autoimmune disorders have previously been suggested in patients who were treated with methotrexate or sulfasalazine, both of which represent important disease-modifying antirheumatic drugs commonly prescribed to individuals with systemic rheumatic diseases such as RA (7,36). The antiinflammatory effects of methotrexate and sulfasalazine have been attributed to augmented levels of extracellular adenosine signaling (7,36). A recent study found that a combination therapy consisting of low-dose methotrexate and astilbin, a flavonoid compound that up-regulates A2aR expression, significantly alleviated collagen-induced arthritis in mice (36). Simultaneous treatment with the A2aR-specific antagonist ZM241385 blocked the therapeutic benefits of this combination regimen, suggesting that their synergistic efficacy was due to A2aR signaling (36). Therefore, identifying the molecular events downstream of A2aR signaling in CD4 T cells that interrupt *Bcl6* gene expression and GC-Tfh cell differentiation may offer a unique opportunity to develop more targeted and effective therapies for the management of autoimmune disorders.

AUTHOR CONTRIBUTIONS

All authors were involved in drafting the article or revising it critically for important intellectual content, and all authors approved the final version to be published. Dr. Mueller had full access to all of the data in the study and takes responsibility for the integrity of the data and the accuracy of the data analysis.

Study conception and design. Schmiel, Mueller.

Acquisition of data. Schmiel, Kalekar, Zhang, Blankespoor, Robinson, Mueller.


Analysis and interpretation of data. Schmiel, Kalekar, Mueller.

REFERENCES

1. Hasko G, Linden J, Cronstein B, Pacher P. Adenosine receptors: therapeutic aspects for inflammatory and immune diseases. *Nat Rev Drug Discov* 2008;7:759–70.
2. Cekic C, Linden J. Purinergic regulation of the immune system. *Nat Rev Immunol* 2016;16:177–92.
3. Zarek PE, Huang CT, Lutz ER, Kowalski J, Horton MR, Linden J, et al. A2A receptor signaling promotes peripheral tolerance by inducing T-cell anergy and the generation of adaptive regulatory T cells. *Blood* 2008;111:251–9.
4. Zarek PE, Powell JD. Adenosine and anergy. *Autoimmunity* 2007;40:425–32.

5. Naganuma M, Wiznerowicz EB, Lappas CM, Linden J, Worthington MT, Ernst PB. Cutting edge: critical role for A2A adenosine receptors in the T cell-mediated regulation of colitis. *J Immunol* 2006;177:2765–9.
6. Streitova D, Sefc L, Savvulidi F, Pospisil M, Hola J, Hofer M. Adenosine A(1), A(2a), A(2b), and A(3) receptors in hematopoiesis. 1. Expression of receptor mRNA in four mouse hematopoietic precursor cells. *Physiol Res* 2010;59:133–7.
7. Morabito L, Montesinos MC, Schreiber DM, Balter L, Thompson LF, Resta R, et al. Methotrexate and sulfasalazine promote adenosine release by a mechanism that requires ecto-5'-nucleotidase-mediated conversion of adenine nucleotides. *J Clin Invest* 1998;101:295–300.
8. Kavanaugh A, Mease PJ, Gomez-Reino JJ, Adebajo AO, Wollenhaupt J, Gladman DD, et al. Treatment of psoriatic arthritis in a phase 3 randomised, placebo-controlled trial with apremilast, an oral phosphodiesterase 4 inhibitor. *Ann Rheum Dis* 2014;73:1020–6.
9. Schmiel SE, Yang JA, Jenkins MK, Mueller DL. Cutting edge: adenosine A2a receptor signals inhibit germinal center T follicular helper cell differentiation during the primary response to vaccination. *J Immunol* 2017;198:623–8.
10. Abbott RK, Silva M, Labuda J, Thayer M, Cain DW, Philbrook P, et al. The GS protein-coupled A2a adenosine receptor controls T cell help in the germinal center. *J Biol Chem* 2017;292:1211–7.
11. Schroder AE, Greiner A, Seyfert C, Berek C. Differentiation of B cells in the nonlymphoid tissue of the synovial membrane of patients with rheumatoid arthritis. *Proc Natl Acad Sci U S A* 1996;93:221–5.
12. Kim HJ, Krenn V, Steinhauser G, Berek C. Plasma cell development in synovial germinal centers in patients with rheumatoid and reactive arthritis. *J Immunol* 1999;162:3053–62.
13. Titcombe PJ, Wigerblad G, Sippl N, Zhang N, Shmagel AK, Sahlström P, et al. Pathogenic citrulline-multispecific B cell receptor clades in rheumatoid arthritis. *Arthritis Rheumatol* 2018;70:1933–45.
14. Ma J, Zhu C, Ma B, Tian J, Baidoo SE, Mao C, et al. Increased frequency of circulating follicular helper T cells in patients with rheumatoid arthritis. *Clin Dev Immunol* 2012;2012:827480.
15. Wang J, Shan Y, Jiang Z, Feng J, Li C, Ma L, et al. High frequencies of activated B cells and T follicular helper cells are correlated with disease activity in patients with new-onset rheumatoid arthritis. *Clin Exp Immunol* 2013;174:212–20.
16. Simpson N, Gatenby PA, Wilson A, Malik S, Fulcher DA, Tangye SG, et al. Expansion of circulating T cells resembling follicular helper T cells is a fixed phenotype that identifies a subset of severe systemic lupus erythematosus. *Arthritis Rheum* 2010;62:234–44.
17. Chakera A, Bennett SC, Morteau O, Bowness P, Luqmani RA, Cornall RJ. The phenotype of circulating follicular-helper T cells in patients with rheumatoid arthritis defines CD200 as a potential therapeutic target. *Clin Dev Immunol* 2012;2012:948218.
18. Liu X, Nurieva RI, Dong C. Transcriptional regulation of follicular T-helper (Tfh) cells. *Immunol Rev* 2013;252:139–45.
19. Hatzi K, Nance JP, Kroenke MA, Bothwell M, Haddad EK, Melnick A, et al. BCL6 orchestrates Tfh cell differentiation via multiple distinct mechanisms. *J Exp Med* 2015;212:539–53.
20. Ditzel HJ. The K/BxN mouse: a model of human inflammatory arthritis. *Trends Mol Med* 2004;10:40–5.
21. Chevalier N, Macia L, Tan JK, Mason LJ, Robert R, Thorburn AN, et al. The role of follicular helper T cell molecules and environmental influences in autoantibody production and progression to inflammatory arthritis in mice. *Arthritis Rheumatol* 2016;68:1026–38.
22. Martinez RJ, Zhang N, Thomas SR, Nandiwada SL, Jenkins MK, Binstadt BA, et al. Arthritogenic self-reactive CD4+ T cells acquire an FR4hiCD73hi anergic state in the presence of Foxp3+ regulatory T cells. *J Immunol* 2012;188:170–81.
23. Matsumoto I, Staub A, Benoist C, Mathis D. Arthritis provoked by linked T and B cell recognition of a glycolytic enzyme. *Science* 1999;286:1732–5.
24. Cekic C, Sag D, Day YJ, Linden J. Extracellular adenosine regulates naive T cell development and peripheral maintenance. *J Exp Med* 2013;210:2693–706.
25. Kalekar LA, Schmiel SE, Nandiwada SL, Lam WY, Barsness LO, Zhang N, et al. CD4(+) T cell anergy prevents autoimmunity and generates regulatory T cell precursors. *Nat Immunol* 2016;17:304–14.
26. Block KE, Huang H. The cellular source and target of IL-21 in K/BxN autoimmune arthritis. *J Immunol* 2013;191:2948–55.
27. Koshiba M, Rosin DL, Hayashi N, Linden J, Sitkovsky MV. Patterns of A2A extracellular adenosine receptor expression in different functional subsets of human peripheral T cells: flow cytometry studies with anti-A2A receptor monoclonal antibodies. *Mol Pharmacol* 1999;55:614–24.
28. Ozaki K, Spolski R, Feng CG, Qi CF, Cheng J, Sher A, et al. A critical role for IL-21 in regulating immunoglobulin production. *Science* 2002;298:1630–4.
29. Ise W, Inoue T, McLachlan JB, Kometani K, Kubo M, Okada T, et al. Memory B cells contribute to rapid Bcl6 expression by memory follicular helper T cells. *Proc Natl Acad Sci U S A* 2014;111:11792–7.
30. Kitano M, Moriyama S, Ando Y, Hikida M, Mori Y, Kurosaki T, et al. Bcl6 protein expression shapes pre-germinal center B cell dynamics and follicular helper T cell heterogeneity. *Immunity* 2011;34:961–72.
31. Iyer SS, Latner DR, Zilliox MJ, McCausland M, Akondy RS, Penaloza-Macmaster P, et al. Identification of novel markers for mouse CD4(+) T follicular helper cells. *Eur J Immunol* 2013;43:3219–32.
32. Craft JE. Follicular helper T cells in immunity and systemic autoimmunity. *Nat Rev Rheumatol* 2012;8:337–47.
33. Mak A, Kow NY. The pathology of T cells in systemic lupus erythematosus. *J Immunol Res* 2014;2014:419029.
34. Mayr B, Montminy M. Transcriptional regulation by the phosphorylation-dependent factor CREB. *Nat Rev Mol Cell Biol* 2001;2:599–609.
35. Wen AY, Sakamoto KM, Miller LS. The role of the transcription factor CREB in immune function. *J Immunol* 2010;185:6413–9.
36. Ma Y, Gao Z, Xu F, Liu L, Luo Q, Shen Y, et al. A novel combination of astilbin and low-dose methotrexate respectively targeting A2AAR and its ligand adenosine for the treatment of collagen-induced arthritis. *Biochem Pharmacol* 2018;153:269–81.

Effect of Disease Activity at Three and Six Months After Diagnosis on Long-Term Outcomes in Antineutrophil Cytoplasmic Antibody–Associated Vasculitis

Seerapani Gopaluni,¹  Oliver Flossmann,² Mark A. Little,³ Paul O'Hara,³ Pirow Bekker,⁴ and David Jayne,¹ on behalf of the European Vasculitis Society

Objective. The treatment of antineutrophil cytoplasmic antibody (ANCA)–associated vasculitis (AAV) aims to suppress disease activity and prevent subsequent disease flare. This study sought to explore the association of early disease control with long-term outcomes to validate early disease control as an end point for future clinical trials in AAV.

Methods. Data from 4 European Vasculitis Society inception clinical trials in AAV (1995–2002) and subsequent data on long-term outcomes from the trial data registry were studied. Clinical parameters in patients with AAV at baseline and at 3 and 6 months after diagnosis were assessed to study the long-term risk of death and end-stage renal failure (ESRF). At 6 months, outcomes were defined based on a disease status of either sustained remission (remission by 3 months, sustained to 6 months), late remission (remission after 3 months and by 6 months), relapsing disease (remission by 3 months but relapse by 6 months), or refractory disease (no remission by 6 months).

Results. Of the 354 patients with AAV who were followed up for a median of 5.7 years, 46 (13%) developed ESRF, 66 (18.6%) died, and 89 (25.1%) had either died or developed ESRF. At 6 months, predictors of the composite end point of death or ESRF were as follows: age (hazard ratio [HR] 1.02, 95% confidence interval [95% CI] 1–1.05; $P = 0.012$), estimated glomerular filtration rate (HR 0.94, 95% CI 0.92–0.95; $P < 0.001$), and disease status at 6 months (late remission, HR 2.94, 95% CI 1.1–7.85 [$P = 0.031$]; relapsing disease, HR 8.21, 95% CI 2.73–24.65 [$P < 0.001$]; refractory disease, HR 4.89, 95% CI 1.96–12.18 [$P = 0.001$]). Similar results were observed when these analyses were performed separately for death and for ESRF.

Conclusion. The results of this study suggest that disease status at 3 and 6 months following the diagnosis of AAV may be predictive of the long-term risk of mortality and ESRF, and therefore these may be valid end points for induction trials in AAV. The current findings need to be validated in a larger data set.

INTRODUCTION

Antineutrophil cytoplasmic antibody (ANCA)–associated vasculitis (AAV) is an autoimmune condition associated with necrotizing inflammation of predominantly the small blood vessels, leading to organ damage and death if left untreated. ANCAs with pathogenic potential are directed against neutrophil proteinase 3 (PR3) and myeloperoxidase (MPO). Granulomatosis with polyangiitis (GPA) and microscopic polyangiitis (MPA), the 2 main subsets of AAV, share clinical and pathologic characteristics and are often studied together.

The European Vasculitis Society (EUVAS) conducted 4 clinical trials in AAV between 1995 and 2002, the results of which have informed the current management of patients with AAV (1–4). Subsequently, a registry was established to collate the longer-term outcome data from patients participating in these studies. Mortality rates associated with AAV at 2 years after diagnosis have declined to <20% over the last 20 years. However, mortality in patients with AAV remains higher than that in an age- and sex-matched general population (5). Severe renal involvement and higher disease activity at diagnosis are risk factors for death. Relapsing disease contributes to the accrual of

¹Seerapani Gopaluni, MBBS, MRCP, David Jayne, FMedSci: University of Cambridge, Cambridge, UK; ²Oliver Flossmann, MD (Res), FRCP: Royale Berkshire Hospitals NHS Trust, Reading, UK; ³Mark A. Little, MBCh, PhD, Paul O'Hara, BM, BS, MRCP: Trinity Health Kidney Center, Tallaght Hospital, Dublin, Ireland; ⁴Pirow Bekker, MB, ChB, PhD: ChemoCentryx, Mountain View, California.

Dr. Little has received consulting fees from ChemoCentryx (less than \$10,000). Dr. Bekker owns stock or stock options in ChemoCentryx and has received consulting fees from ChemoCentryx (less than \$10,000). Prof. Jayne

has received consulting fees from Aurinia, AstraZeneca, Boehringer, ChemoCentryx, GSK, and Takeda (less than \$10,000 each). No other disclosures relevant to this article were reported.

Address correspondence to Seerapani Gopaluni, MBBS, MRCP, Department of Medicine, University of Cambridge, Cambridge CB2 0QQ, UK. E-mail: sg743@cam.ac.uk.

Submitted for publication April 14, 2018; accepted in revised form November 6, 2018.

damage, cumulative drug toxicity, and the risk of end-stage renal failure (ESRF).

Clinical trials in AAV typically use disease remission or relapse as primary end points. The present study aimed to define the predictive value of early disease control at 3 and 6 months after the diagnosis of AAV in order to validate the use of early disease control as an end point for these trials. Our findings have the potential to improve the quality of clinical trials in patients with AAV and possibly shorten the duration of these trials.

PATIENTS AND METHODS

Methods. The 4 EUVAS trials (Table 1) aimed to establish evidence to support treatment strategies in the varying AAV disease severity subgroups as defined by the European League Against Rheumatism statement on conducting clinical studies and/or clinical trials in systemic vasculitis (6,7). Patients with a new diagnosis of AAV, according to the 1994 Chapel Hill Consensus Conference Criteria for Vasculitis (8), were included in the trials at the time of diagnosis. Patients were excluded if they had a coexistent multisystem autoimmune disease, active infection, pregnancy, or life-threatening pulmonary hemorrhage or were age <18 years or age >80 years. Long-term data were obtained from a substudy in which data on long-term outcomes were collected from the patients through the use of questionnaires that were sent to the participating doctors.

Baseline demographic and clinical data were obtained from the trial databases. Levels of disease activity and damage at 3 and 6 months after the diagnosis of AAV were quantified using the Birmingham Vasculitis Activity Score, (BVAS) version 2 and the Vasculitis Damage Index (VDI), which are 2 validated complementary scoring tools for documenting disease activity and damage, respectively, in AAV (9,10).

The BVAS comprises 65 items in 9 domains related to different organ systems, and each item is scored as actively involved or not. This produces a weighted summary score that reflects AAV disease activity.

The VDI is designed to capture “all cause” damage that occurs from the time of diagnosis. It incorporates 62 items in 10 domains, and the score is the summation of the checked items.

Disease remission in this study was defined as a BVAS of 0, reflecting absence of disease activity. A BVAS of >0 was considered to represent active disease.

Statistical analysis. Missing data were estimated by probability imputation techniques (11). At 6 months following the diagnosis of AAV, patients were divided into 4 disease status subgroups according to the BVAS scores obtained at 3 and 6 months. The disease status groups were as follows: 1) sustained remission, defined as those who achieved remission at 3 months (BVAS 0) and sustained remission to 6 months without relapse; 2) late remission, defined as those who achieved remission after 3 months and before 6 months; 3) relapsing disease, defined as those who achieved remission by 3 months (BVAS 0) but relapsed by 6 months (BVAS >0); and 4) refractory disease, those who had not achieved remission by 6 months.

Continuous variables were expressed as the median with interquartile range. Categorical variables were presented as percentages. The chi-square test was used for comparing categorical variables. The following predetermined parameters were included in Cox regression analyses: age at diagnosis (in years), sex, disease subtype (GPA or MPA), estimated glomerular filtration rate (eGFR) (in ml/minute) (determined using the Modification of Diet in Renal Disease Study equation), disease activity (categorized into the above-mentioned 4 disease status groups), damage index (categorized as a VDI of either ≤ 2 or > 2), ANCA specificity (PR3, MPO, or negative), trial, and year of enrollment; a minority of patients with double-positive and missing ANCA data were included in the MPO subgroup, as this disease phenotype was more consistent with the characteristics of MPA.

Multiple regression analyses were performed separately for mortality, ESRF, and for the composite end point of mor-

Table 1. Inception clinical trials in AAV*

Trial	Interventions	Inclusion criteria
NORAM (n = 95)	Induction therapy with MTX or CYC	Early systemic AAV (creatinine <150 μ moles/liter)
CYCAZAREM (n = 155)	Remission maintenance therapy with AZA or CYC	Generalized AAV (creatinine <500 μ moles/liter)
CYCLOPS (n = 148)	Induction therapy with IV pulsed CYC or oral CYC	Generalized AAV (creatinine between >150 and <500 μ moles/liter)
MEPEX (n = 137)	CYC induction therapy combined with plasma exchange or IV MP	Severe AAV (creatinine >500 μ moles/liter)

* NORAM = Nonrenal Wegener’s Granulomatosis Treated Alternatively with Methotrexate; MTX = methotrexate; CYC = cyclophosphamide; AAV = antineutrophil cytoplasmic antibody (ANCA)-associated systemic vasculitis; CYCAZAREM = Cyclophosphamide versus Azathioprine for Early Remission Phase of Vasculitis; AZA = azathioprine; CYCLOPS = Randomised Trial of Daily Oral versus Pulse Cyclophosphamide as Therapy for ANCA-associated Systemic Vasculitis; IV = intravenous; MEPEX = Randomized Trial of Plasma Exchange or High-Dosage Methylprednisolone as Adjunctive Therapy for Severe Renal Vasculitis; MP = methylprednisolone.

tality or ESRF. For ESRF analyses, the late remission group was not included, as there were no events in this group. The eGFR at the time of entry was not included in the regression models, due to multicollinearity with the eGFR at 6 months (Pearson's correlation coefficient 0.799, $P < 0.001$). All covariates in the multiple regression analyses were entered simultaneously.

The proportional hazards assumption for Cox regression models was tested using the weighted, scaled Schoenfeld residuals test and visual inspection of log-log plots. The hazard ratio (HR) of end point associations with age was expressed in relation to change in age by 1 year, while for analyses of associations with the eGFR, the HR was expressed in relation to change in the eGFR by 1 ml/minute.

Data were analyzed using SPSS software version 23 and R software version 3.1.2 (R Foundation for Statistical Computing). A 2-tailed P value less than or equal to 0.05 was considered significant.

RESULTS

Patient characteristics. In total, 535 patients with a new diagnosis of AAV from the 4 EUVAS inception clinical trials were studied. The demographic and clinical characteristics of the patients at the time of diagnosis and during follow-up are shown in Table 2. Of the 535 patients, data on disease status were available at both 3 months and 6 months in 354 patients. Complete data on all variables included in the regression analyses) were available from the following number of patients: for mortality, 329 patients; for ESRF, 325 patients; and for the composite end point of ESRF or death, 329 patients. It may sometimes be difficult to differentiate between ongoing disease activity and damage, especially in relation to renal items. Whereas 65% of the patients had at least 1 renal item scored at the time of entry, only 2.9% of the patients at 3 months and 3.5% at 6 months had at least 1 scored renal item. This suggests that the risk of misclassifying damage as disease activity was small.

Table 2. Characteristics of the trial participants at baseline and long-term outcomes*

	NORAM (n = 59)	CYCLOPS (n = 95)	CYCAZAREM (n = 118)	MEPEX (n = 82)	Total (n = 354)
Age, median (IQR) years	52.5 (40.8–62.4)	60.7 (48.5–68.5)	57.3 (46.2–67.7)	66.5 (57.9–71)	60.7 (48.2–69.1)
MPA, %	5.1	47.4	37.3	63.4	40.7
GPA, %	94.9	40	62.7	36.6	55.9
MPO, %	13.6	52.6	24.6	41.5	34.4
PR3, %	83.1	45.3	59.3	50	57.7
BVAS, median (IQR)					
At entry	12 (9–19)	21 (15–27)	18 (10–25)	20 (15–25)	18 (13–24)
At 3 months	0 (0–2)	0 (0–0)	0 (0–0)	0 (0–0)	0 (0–0)
At 6 months	0 (0–0)	0 (0–0)	0 (0–0)	0 (0–0)	0 (0–0)
Proportion achieving remission, %					
At 3 months	61	83.1	95.8	92.7	84.8
At 6 months	78	84.7	97.9	96.3	89.8
VDI, median (IQR)					
At 3 months	0 (0–1)	0 (0–1)	0 (0–0)	0 (0–1)	0 (0–1)
At 6 months	1 (0–2)	1 (0–3)	2 (1–3)	3 (2–3)	2 (1–3)
Mortality rate at median follow-up of 5 years, %	13.6	10.5	15.3	36.6	18.6
ESRF rate at 5 years, %	1.7	5.3	8.5	36.6	13
eGFR, median (IQR) ml/minute/1.73 m ²					
At entry	79.7 (71.7–98.3)	32.2 (19.5–53.7)	31.4 (19.7–63.7)	6.7 (4.5–8.4)	27.8 (10.3–64.7)
At 6 months	77.9 (64.8–88.5)	46.3 (31.7–63.7)	55.1 (40.2–72.3)	21.5 (5.8–32.1)	46.9 (29.4–66.9)
Follow-up, median (range) years	6.0 (3.2–7.3)	4.5 (3.5–5.5)	8.5 (4.9–9.3)	5.1 (1.0–7.3)	5.7 (3.32–8.33)
Enrollment period, years	1995–2000	1998–2002	1995–1997	1995–2001	1995–2002

* IQR = interquartile range; MPA = microscopic polyangiitis; GPA = granulomatosis with polyangiitis; MPO = myeloperoxidase; PR3 = neutrophil proteinase 3; BVAS = Birmingham Vasculitis Activity Score; VDI = Vasculitis Damage Index; ESRF = end-stage renal failure; eGFR = estimated glomerular filtration rate (see Table 1 for other definitions).

At 3 months and 6 months, 84.8% and 89.8% of patients, respectively, achieved remission. At 6 months, of the 354 patients with complete data, 283 (79.9%) were in sustained remission, 35 (10%) experienced late remission, 18 (5.1%) had relapsing disease, and 18 (5.1%) had refractory disease.

Patient survival. Over a median follow-up of 5.7 years, 66 (18.6%) of 354 patients died. Forty-eight (16.9%) of the 283 patients in the sustained remission group, 7 (20%) of 35 in the late remission group, 5 (27.8%) of 18 in the relapsed disease group, and 6 (33.3%) of 18 in the refractory disease group died. Of the 354 patients, complete data on all variables included in the regres-

sion analysis was available from 329 patients, in whom a total of 62 events occurred.

A Cox proportional hazards regression model using the above-mentioned predetermined parameters at 6 months was performed to identify predictors of mortality. Variables that were predictive of mortality at 6 months were as follows: age (HR 1.09, 95% confidence interval [95% CI] 1.05–1.13; $P < 0.001$), eGFR at 6 months (HR 0.96, 95% CI 0.94–0.98; $P < 0.001$), and disease status at 6 months, when comparing sustained remission to late remission (HR 3.31, 95% CI 1.28–8.57; $P = 0.013$), relapsing disease (HR 6.59, 95% CI 2.18–19.87; $P = 0.001$), and refractory disease (HR 6.15, 95%

Table 3. Cox proportional hazards regression models and competing risk analyses*

Covariate	Cox model for mortality (n = 329 patients; n = 62 events)		Cox model for ESRF (n = 282 patients; n = 35 events; n = 8 cases censored before the earliest event)		Competing risk model for ESRF (n = 290 patients; n = 35 events; n = 34 competing events)		Cox model for composite end point (mortality or ESRF) (n = 321 patients; n = 75 events)	
	HR (95% CI)	P†	HR (95% CI)	P†	Sub-HR	P†	HR (95% CI)	P†
Age (per year)	1.09 (1.05–1.13)	<0.001	0.98 (0.95–1)	0.141	0.98 (0.95–1)	0.17	1.02 (1–1.05)	0.012
ANCA specificity‡		0.694	0 (0–0)	0.469			0 (0–0)	0.907
PR3-ANCA	0.83 (0.42–1.63)	0.601	0.74 (0.33–1.64)	0.461	1.01 (0.49–2.07)	0.96	0.89 (0.5–1.56)	0.69
ANCA-negative	1.3 (0.46–3.72)	0.614	0.32 (0.05–2.13)	0.243	0.42 (0.1–1.71)	0.23	1.02 (0.39–2.67)	0.96
GPA	0.4 (0.19–0.8)	0.011	0.58 (0.23–1.46)	0.253	0.72 (0.32–1.59)	0.42	0.48 (0.26–0.89)	0.019
BVAS at entry (per unit rise)	1.03 (1–1.07)	0.036	1.04 (0.98–1.1)	0.175	1.02 (0.96–1.07)	0.44	1.03 (1–1.07)	0.03
eGFR at 6 months (per ml/minute increase)	0.96 (0.94–0.98)	<0.001	0.9 (0.87–0.93)	<0.001	0.9 (0.88–0.92)	<0.001	0.94 (0.92–0.95)	<0.001
Male	2.17 (1.18–3.99)	0.012	2.84 (1.12–7.21)	0.027	2.36 (0.93–5.95)	0.068	2.02 (1.17–3.47)	0.011
VDI >2 at 6 months	1.34 (0.74–2.44)	0.326	1.7 (0.8–3.6)	0.165	1.63 (0.76–3.49)	0.2	1.33 (0.81–2.2)	0.256
Disease status at 6 months§		<0.001	0 (0–0)				0 (0–0)	<0.001
Late remission	3.31(1.28–8.57)	0.013	–	–	–	–	2.94 (1.1–7.85)	0.031
Relapsing disease	6.59 (2.18–19.87)	0.001	34.22 (4.72–247.8)	<0.001	15.75 (2.53–97.92)	0.003	8.21 (2.73–24.65)	<0.001
Refractory disease	6.15 (2.26–16.73)	<0.001	9.64 (2.25–41.29)	0.002	5.98 (1.32–26.97)	0.02	4.89 (1.96–12.18)	0.001
Trial¶		0.003	0 (0–0)	0.384			0 (0–0)	0.011
CYCAZAREM	0.11 (0.03–0.39)	0.001	0.19 (0.01–2.71)	0.221	0.19 (0.01–3.25)	0.25	0.15 (0.04–0.49)	0.002
CYCLOPS	0.13 (0.04–0.45)	0.001	0.52 (0.04–5.9)	0.603	0.29 (0.02–3.31)	0.32	0.26 (0.09–0.77)	0.015
MEPEX	0.11 (0.03–0.41)	0.001	0.2 (0.01–2.77)	0.23	0.27 (0.01–5.58)	0.4	0.15 (0.04–0.51)	0.002
Year	1.01 (0.83–1.24)	0.858	1.46 (1.14–1.88)	0.003	–	–	1.17 (0.98–1.39)	0.079

* HR = hazard ratio; 95% CI = 95% confidence interval; ESRF = end-stage renal failure; PR3 = neutrophil proteinase 3; GPA = granulomatosis with polyangiitis; BVAS = Birmingham Vasculitis Activity Score; eGFR = estimated glomerular filtration rate; VDI = Vasculitis Damage Index (see Table 1 for other definitions).

† $P \leq 0.05$ was considered significant.

‡ Myeloperoxidase (MPO) antineutrophil cytoplasmic antibody (ANCA) positive is the referent group for ANCA specificity.

§ Complete remission is the referent group for the disease status at 6 months.

¶ NORAM is the referent group for the trials.

CI 2.26–16.73; $P < 0.001$). The specific trial in which each patient was enrolled (Table 1) was also predictive of mortality, but it was interesting to note that participants of trials that enrolled patients with severe disease had better survival rates. This may be due to the fact that our Cox proportional hazards models were adjusted for the eGFR. This analysis shows that patients in the sustained remission group had improved survival (large effect size) compared to patients in the other groups. Disease status subgroup at 6 months, sex, and BVAS at the time of entry were other significant predictors of mortality, as summarized in Table 3. The Cox regression curves are shown in Figure 1A.

ESRF. Of the 354 patients, 9 patients developed ESRF before 6 months and were therefore not included in the ESRF analyses. Of the 345 patients for whom disease status was available, 37 (10.4%) went on to develop late ESRF. Thirty-two (10.6%) of the 276 patients in the sustained remission group, no patients in the late remission group, 2 (11.1%) of the 18 patients in the relapsed disease group, and 3 (16.6%) of the 18 patients in the refractory disease group developed late ESRF. As there were no events

in the late remission group ($n = 35$ patients), this group was not included in the regression analysis.

Data on all variables for the Cox regression analysis of the ESRF were available from 290 patients, with 35 events. In this analysis, predictors of the ESRF at 6 months were the eGFR at 6 months (HR 0.9, 95% CI 0.87–0.93; $P < 0.001$), and disease status at 6 months (relapsing disease, HR 34.22, 95% CI 4.72–247.8 [$P < 0.001$]; refractory disease, HR 9.64, 95% CI 2.25–41.29 [$P = 0.002$]). Other significant variables included male sex and year of enrollment (Table 3). Those in the sustained remission group had a lower probability of ESRF at 6 months compared to those in the relapsing disease and refractory disease groups (Table 3). The Cox regression curves are shown in Figure 1B.

In a sensitivity analysis, we performed a competing risk regression subhazard (sub-HR) analysis, as proposed by Fine and Gray (12), for the estimation of the semiparametric proportional hazards of developing ESRF with death as a competing event. In this analysis, the eGFR at 6 months (sub-HR 0.9, 95% CI 0.88–0.92; $P < 0.001$) and disease status at 6 months (relapsing disease, sub-HR 15.75, 95% CI 2.53–97.92 [$P = 0.003$]; refrac-

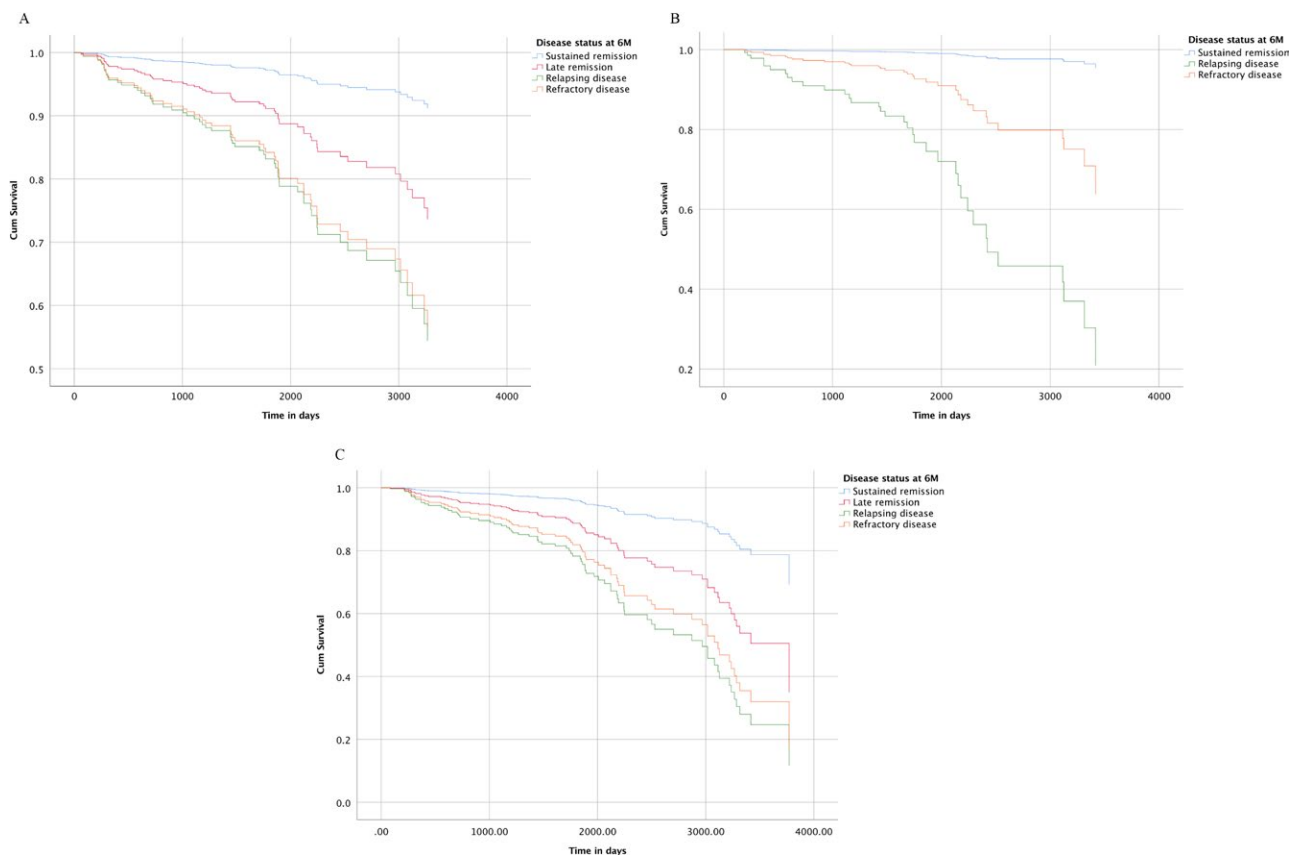


Figure 1. Cox proportional hazard curves based on the disease status at 6 months (6M) in relation to the risk of mortality (A), end-stage renal failure (ESRF) (B), and the composite end point of ESRF or death (C) in patients with antineutrophil cytoplasmic antibody-associated vasculitis. Disease status at 6 months was defined as either sustained remission, late remission, relapsing disease, or refractory disease. Cum = cumulative.

tory disease, sub-HR 5.98, 95% CI 1.32–26.97 [$P = 0.02$]) were covariates that independently predicted the development of ESRF by 6 months (Table 3).

Composite end point. We further analyzed the impact of these predictors on a composite end point of death or ESRF (whichever occurred earlier). Of the 345 patients who had not developed ESRF by 6 months, 80 (23.2%) went on to develop the composite end point. Sixty-two (22.4%) of 276 patients in the sustained remission group, 6 (18.2%) of 33 patients in the late remission group, 5 (27.7%) of 18 patients in the relapsed disease group, and 7 (38.8%) of 18 patients in the refractory disease group developed the composite end point.

Data on all variables included in the regression analysis were available from 321 patients, with 75 events. Results from the Cox proportional hazards model showed that age (HR 1.02, 95% CI 1–1.05; $P = 0.012$), eGFR (HR 0.94, 95% CI 0.92–0.95; $P < 0.001$), and disease status at 6 months (late remission, HR 2.94, 95% CI 1.1–7.85 [$P = 0.031$]; relapsing disease, HR 8.21, 95% CI 2.73–24.65 [$P < 0.001$]; refractory disease, HR 4.89, 95% CI 1.96–12.18 [$P = 0.001$]) were predictive of the composite end point (Table 3 and Figure 1C). Other predictors included disease subtype, male sex, and the trial in which the patient was enrolled (Table 3).

DISCUSSION

Improvements in the diagnosis and classification of vasculitis following the discovery of ANCA, as well as the development of several disease assessment tools, have permitted the implementation of large-scale multicenter randomized clinical trials in patients with AAV. However, long-term outcomes remain poor, and the treatment itself contributes to adverse outcomes. The existing treatments aim to control disease activity and prevent disease relapse, but there is no consensus as to the optimum end point for use in induction clinical trials. We sought to determine the value of early disease remission in an association study of patients recruited to inception clinical trials of AAV for whom long-term outcome data were available. In addition to contributing to an understanding of the current clinical epidemiology of vasculitis, the study aimed to validate disease remission at 3 and 6 months as end points for clinical trials. The principle observation was that disease remission present at 3 months and sustained to 6 months was the best predictor of a good outcome, based on the frequencies of death or ESRF, in patients with AAV.

Although there has been progressive improvement in the outcomes of AAV over the last decades, the mortality risk remains elevated. A systematic review has shown that patients with MPA are at increased risk of death as compared to patients with GPA (13), and also at increased risk of renal failure and cardiovascular events. In this study, we showed that achieving remission at 3

months sustained to 6 months was more important than other baseline variables, such as disease subtype or ANCA specificity. Advanced renal insufficiency and development of ESRF were previously shown to be risk factors for mortality in patients with AAV (13). However, even after correcting for renal function, disease status at 6 months remained an important predictor. It is evident from this analysis that those with any disease activity at or after 3 months will have a poor prognosis, possibly due to a combination of accrual of disease-related damage and drug toxicity.

In the Cox proportional hazards model, achieving remission reduced the risk of ESRF when compared to patients who did not achieve remission or developed early relapses. In this analysis, patients who died before the development of ESRF were censored. In the sensitivity analysis, this issue was addressed by competing risk regression modelling, and the results were not dissimilar to those of the initial analysis, supporting the primary contention that disease status is an important predictor of ESRF.

The response to therapy varies widely within disease severity subgroups in AAV, and therefore an evaluation of baseline characteristics does not have reliable prognostic value. On the other hand, using data from 3 and 6 months after diagnosis would give us an opportunity to assess the response to standard therapy, adding more weight to the prediction models. The results of the present study establish the fact that the data from 3 and 6 months can be used as surrogates for predicting the long-term risk of mortality or ESRF in AAV.

These findings emphasize the need for faster-acting therapies. For example, plasma exchange is currently being assessed in this context for severe AAV (14), while IVIG (15) and tumor necrosis factor blockade (16) were evaluated for this purpose. Furthermore, newer therapeutics, such as the complement inhibitor avacopan, have been shown, in a phase II study, to have a more rapid effect on disease activity than the current standard of care (17).

The present study is limited by the fact that it is a retrospective analysis of the data pooled from multiple clinical trials. There may be many confounders, such as the different immunosuppressive therapies used or the cumulative steroid dosage, that are likely to influence sustained remission and, consequently, long-term outcomes. The EUVAS clinical trials were designed to study patients with varying disease severity, and therefore pooling the trials offers the chance to study the whole spectrum of patients with AAV.

The steroid dosage has been reasonably consistent across the CYCAZAREM (Cyclophosphamide versus Azathioprine for Early Remission Phase of Vasculitis), CYCLOPS (Randomised Trial of Daily Oral versus Pulse Cyclophosphamide as Therapy for ANCA-associated Systemic Vasculitis), and MEPEX (Randomized Trial of Plasma Exchange or High-Dosage Methylprednisolone as Adjunctive Therapy for Severe Renal Vasculitis)

trials, while in the NORAM (Nonrenal Wegener's Granulomatosis Treated Alternatively with Methotrexate) trial, the steroid dosage was tapered by 12 months. However, similar analyses were shown to be helpful in drawing important conclusions in patients with AAV (18–20).

Moreover, as highlighted, the disease severity subtypes and treatment options differed across the studies. It is worth noting that none of the patients were treated with rituximab, which may change remission and relapse rates. The mortality in AAV patients is lower with the current treatment regimens compared to that in historical cohorts, and this study needs to be validated using prospective clinical trial data sets, such as the PEXIVAS (Plasma Exchange and Glucocorticoid Dosing in the Treatment of Anti-neutrophil Cytoplasm Antibody Associated Vasculitis) and MYCYC (Randomized Trial of Mycophenolate Mofetil versus Cyclophosphamide for Remission Induction of ANCA-associated Vasculitis) clinical trials (14,21), and in prospective registry cohorts.

A strength of this study lies in the fact that the threshold for disease activity was binary, defined as a BVAS of >0 versus a BVAS of 0, which should help with comparisons of studies using different versions of the BVAS. Another strength of this study is that the data were obtained from clinical trials in which assessments were standardized and treatments were defined by the protocol.

Thus, objective parameters obtained early in the course of the disease in patients with AAV may predict long-term outcomes, and early sustained remission may be an important goal of therapy. This study establishes early surrogate markers for long-term outcomes of value to future clinical trials with potentially shorter follow-up durations. However, these results should be viewed cautiously, as the toxicity associated with therapy can influence the long-term outcomes, and therefore the goal of achieving early remission by increased immunosuppression needs to be weighed carefully against the risk of drug toxicity.

ACKNOWLEDGMENTS

We thank Dr. James Wason, MRC (Biostatistician, University of Cambridge, UK) for his invaluable advice and guidance and for critically reviewing the manuscript. In addition, we thank the EUVAS clinical trial investigators.

AUTHOR CONTRIBUTIONS

All authors were involved in drafting the article or revising it critically for important intellectual content, and all authors approved the final version to be published. Dr. Gopaluni had full access to all of the data in the study and takes responsibility for the integrity of the data and the accuracy of the data analysis.

Study conception and design. Gopaluni, Bekker, Jayne.

Acquisition of data. Flossmann, Little, O'Hara.

Analysis and interpretation of data. Gopaluni, Flossmann, Little, O'Hara, Jayne.

ADDITIONAL DISCLOSURES

Author Bekker is an employee of ChemoCentryx.

REFERENCES

- Jayne D, Rasmussen N, Andrassy K, Bacon P, Tervaert JW, Dadoniené J, et al. A randomized trial of maintenance therapy for vasculitis associated with antineutrophil cytoplasmic autoantibodies. *N Engl J Med* 2003;349:36–44.
- De Groot K, Harper L, Jayne DR, Flores Suarez LF, Gregorini G, Gross WL, et al. Pulse versus daily oral cyclophosphamide for induction of remission in antineutrophil cytoplasmic antibody-associated vasculitis: a randomized trial. *Ann Intern Med* 2009;150:670–80.
- Jayne DR, Gaskin G, Rasmussen N, Abramowicz D, Ferrario F, Guillevin L, et al. Randomized trial of plasma exchange or high-dosage methylprednisolone as adjunctive therapy for severe renal vasculitis. *J Am Soc Nephrol* 2007;18:2180–8.
- De Groot K, Rasmussen N, Bacon PA, Tervaert JW, Feighery C, Gregorini G, et al. Randomized trial of cyclophosphamide versus methotrexate for induction of remission in early systemic antineutrophil cytoplasmic antibody-associated vasculitis. *Arthritis Rheum* 2005;52:2461–9.
- Flossmann O, Berden A, de Groot K, Hagen C, Harper L, Heijl C, et al. Long-term patient survival in ANCA-associated vasculitis. *Ann Rheum Dis* 2011;70:488–94.
- Jayne DR, Rasmussen N. Treatment of antineutrophil cytoplasm autoantibody-associated systemic vasculitis: initiatives of the European Community Systemic Vasculitis Clinical Trials Study Group. *Mayo Clin Proc* 1997;72:737–47.
- Hellmich B, Flossmann O, Gross WL, Bacon PA, Cohen-Tervaert JW, Guillevin L, et al. EULAR recommendations for conducting clinical studies and/or clinical trials in systemic vasculitis: focus on antineutrophil cytoplasm antibody-associated vasculitis. *Ann Rheum Dis* 2007;66:605–17.
- Jennette JC, Falk RJ, Andrassy K, Bacon PA, Churg J, Gross WL, et al. Nomenclature of systemic vasculitides: proposal of an international consensus conference. *Arthritis Rheum* 1994;37:187–92.
- Luqmani RA, Bacon PA, Moots RJ, Janssen BA, Pall A, Emery P, et al. Birmingham Vasculitis Activity Score (BVAS) in systemic necrotizing vasculitis. *QJM* 1994;87:671–8.
- Exley AR, Bacon PA, Luqmani RA, Kitas GD, Gordon C, Savage CO, et al. Development and initial validation of the Vasculitis Damage Index for the standardized clinical assessment of damage in the systemic vasculitides. *Arthritis Rheum* 1997;40:371–80.
- Schemper M, Smith TL. Efficient evaluation of treatment effects in the presence of missing covariate values. *Stat Med* 1990;9:777–84.
- Fine JP, Gray RJ. A proportional hazards model for the subdistribution of a competing risk. *J Am Stat Assoc* 1999;94:496–509.
- Mukhtyar C, Flossmann O, Hellmich B, Bacon PA, Cid M, Cohen-Tervaert JW, et al. Outcomes from studies of antineutrophil cytoplasm antibody associated vasculitis: a systematic review by the European League Against Rheumatism systemic vasculitis task force. *Ann Rheum Dis* 2008;67:1004–10.
- Walsh M, Merkel PA, Peh CA, Szpirt W, Guillevin L, Pusey CD, et al. Plasma exchange and glucocorticoid dosing in the treatment of anti-neutrophil cytoplasm antibody associated vasculitis (PEXIVAS): protocol for a randomized controlled trial. *Trials* 2013;14:73.
- Jayne DR, Chapel H, Adu D, Misbah S, O'Donoghue D, Scott D, et al. Intravenous immunoglobulin for ANCA-associated systemic vasculitis with persistent disease activity. *QJM* 2000;93:433–9.

16. Wegener's Granulomatosis Etanercept Trial (WGET) Research Group. Etanercept plus standard therapy for Wegener's granulomatosis. *N Engl J Med* 2005;352:351–61.
17. Jayne DR, Bruchfeld AN, Harper L, Schaier M, Venning MC, Hamilton P, et al. Randomized trial of C5a receptor inhibitor avacopan in ANCA-associated vasculitis. *J Am Soc Nephrol* 2017;28:2756–67.
18. Robson J, Doll H, Suppiah R, Flossmann O, Harper L, Hoggund P, et al. Damage in the ANCA-associated vasculitides: long-term data from the European Vasculitis Study Group (EUVAS) therapeutic trials. *Ann Rheum Dis* 2013;74:177–84.
19. Little MA, Nightingale P, Verburgh CA, Hauser T, De Groot K, Savage C, et al. Early mortality in systemic vasculitis: relative contribution of adverse events and active vasculitis. *Ann Rheum Dis* 2010;69:1036–43.
20. Westman K, Flossmann O, Gregorini G. The long-term outcomes of systemic vasculitis. *Nephrol Dial Transplant* 2015;30:i60–6.
21. Jones R, Harper L, Ballarin J, Blockmans D, Brogan P, Bruchfeld A, et al, on behalf of the European Vasculitis Study Group. A randomized trial of mycophenolate mofetil versus cyclophosphamide for remission induction of ANCA-associated vasculitis: "MYCYC." *Presse Med* 2013;42:678–9.

Monocyte-Derived Interleukin-1 β As the Driver of S100A12-Induced Sterile Inflammatory Activation of Human Coronary Artery Endothelial Cells: Implications for the Pathogenesis of Kawasaki Disease

Giulia Armaroli,¹ Emely Verweyen,¹ Carolin Pretzer,¹ Katharina Kessel,¹ Keiichi Hirono,² Fukiko Ichida,² Mako Okabe,² David A. Cabral,³ Dirk Foell,¹ Kelly L. Brown,³ and Christoph Kessel¹

Objective. Kawasaki disease (KD) is an acute vasculitis of childhood, predominantly affecting the coronary arteries. S100A12, a granulocyte-derived agonist of both the receptor for advanced glycation end products (RAGE) and Toll-like receptor 4 (TLR-4), is strongly up-regulated in KD. This study was undertaken to investigate the potential contributions of S100A12 to the pathogenesis of KD.

Methods. Serum samples from patients with KD ($n = 30$) at different stages pre- and post-intravenous immunoglobulin (IVIG) treatment were analyzed for the expression of S100A12, cytokines, chemokines, and soluble markers of endothelial cell activation. Primary human coronary artery endothelial cells (HCAECs) were analyzed for responsiveness to direct stimulation with S100A12 or lipopolysaccharide (LPS), as assessed by real-time quantitative reverse transcription–polymerase chain reaction analysis of cytokine and endothelial cell adhesion molecule messenger RNA expression. Alternatively, HCAECs were cultured in conditioned medium obtained from primary human monocytes that were stimulated with LPS or S100A12 in the absence or presence of IVIG or cytokine antagonists.

Results. In the serum of patients with KD, pretreatment S100A12 levels were associated with soluble vascular cell adhesion molecule 1 titers in the course of IVIG therapy ($r_s = -0.6$, $P = 0.0003$). Yet, HCAECs were not responsive to direct S100A12 stimulation, despite the presence of appropriate receptors (RAGE, TLR-4). HCAECs did, however, respond to supernatants obtained from S100A12-stimulated primary human monocytes, as evidenced by the gene expression of inflammatory cytokines and adhesion molecules. This response was strictly dependent on interleukin-1 β (IL-1 β) signaling ($P < 0.001$).

Conclusion. In its role as a highly expressed mediator of sterile inflammation in KD, S100A12 appears to activate HCAECs in an IL-1 β -dependent manner. These data provide new mechanistic insights into the contributions of S100A12 and IL-1 β to disease pathogenesis, and may therefore support current IL-1-targeting studies in the treatment of patients with KD.

INTRODUCTION

Kawasaki disease (KD) is an acute vasculitis of unknown etiology that affects small- and medium-sized coronary arteries in infants and children. It is the main cause of acquired heart dis-

ease during childhood in developed countries. A single infusion of 2 gm/kg of intravenous immunoglobulins (IVIGs), administered in conjunction with aspirin, has reduced the frequency of coronary artery aneurysms in patients with KD from 25% to 5%. However, 10–20% of patients are unresponsive to IVIG treatment, and

Drs. Brown and Christoph Kessel's work was supported by the Canadian Institutes of Health Research grant for the PedVas Initiative (TR2-119188 to Dr. Cabral). Dr. Brown's work was also supported by the Michael Smith Foundation for Health Research (Cassie and Friends Society Scholar Award).

¹Giulia Armaroli, MD, Emely Verweyen, MSc, Carolin Pretzer, MD, Katharina Kessel, PhD, Dirk Foell, MD, Christoph Kessel, PhD: University Children's Hospital, Munster, Germany; ²Keiichi Hirono, MD, Fukiko Ichida, MD, Mako Okabe, MD: University of Toyama, Toyama City, Japan; ³David A. Cabral, MD, Kelly L. Brown, PhD: University of British Columbia, British Columbia Children's Hospital, Vancouver, British Columbia, Canada.

Dr. Foell has served on the advisory boards of Chugai-Roche, Sobi, Novartis, and Pfizer (consulting fees less than \$10,000 each) and has received research support from Novartis and Pfizer. Drs. Foell and Christoph Kessel have submitted patent applications for the use of proinflammatory S100A12 homomultimers in the diagnosis and treatment of inflammatory disorders (WO 2016/178154 A1). No other disclosures relevant to this article were reported.

Address correspondence to Christoph Kessel, PhD, Department of Pediatric Rheumatology and Immunology, University Children's Hospital, Domagkstr. 3, 48149 Munster, Germany. E-mail: christoph.kessel@uni-muenster.de.

Submitted for publication January 19, 2018; accepted in revised form November 13, 2018.

thus present with persisting fever and inflammation and have an increased risk of cardiac complications and death (1,2).

Vasculitis in KD is characterized by proliferative granulomatous inflammation. Following an initial influx of neutrophils (3), the infiltration of monocytes and aberrant macrophage activation are thought to be involved in the formation of vascular lesions (4). Circulating neutrophils actively secrete S100A12 in the early stages of KD (5). Correspondingly, serum levels of S100A12 and the closely related molecules S100A8/A9 are elevated during the acute stage of KD, and their levels have been observed to decrease in the serum of patients who respond to IVIG treatment (6–8). This decrease in serum production of S100 proteins is not observed in patients who are not responsive to IVIG therapy (designated as nonresponders). Moreover, patients who develop coronary artery abnormalities in the course of the disease have higher serum titers of S100A12 prior to treatment (6,7).

Although there is clear evidence for an association between serum concentrations of S100A12 and KD activity, the pathomechanistic link between S100A12 and KD remains unclear. When released from human granulocytes, S100A12 can operate as a damage-associated molecular pattern (DAMP) molecule. In this role, it can mediate proinflammatory cellular responses via pattern-recognition receptors (PRRs), namely the receptor of glycation end products (RAGE) (9) or Toll-like receptor 4 (TLR-4) (10,11). The PRR that induces a cellular response to S100A12 may be dictated by cell type. For example, transgenic expression of S100A12 in murine vascular smooth muscle cells (VSMCs) promotes aortic wall remodeling and aortic aneurysms in a RAGE-dependent manner (12). Conversely, RAGE on human monocytes can engage S100A12, but cellular responsiveness is strictly TLR-4 dependent (10,11).

In KD, it is currently unknown whether S100A12 is functioning as a PRR ligand to actively trigger and/or perpetuate vascular inflammation or whether its functions merely reflect robust neutrophil activation. In giant cell arteritis, a chronic vasculitis found in adulthood, S100A12 serum levels are also elevated, and both neutrophils and S100A12 can be detected in close association with vascular endothelial cells (13). Both S100A8/A9 and S100A12 have been shown to stimulate microvascular endothelial cells (14,15), while in KD, an active contribution of endothelial cells to disease pathogenesis (16,17) and aneurysm formation (18) has been suggested. Observations in current animal models of KD, however, suggest that VSMCs, not vascular endothelial cells, are involved in disease development (19,20).

In this report, we are the first to describe a strong association between S100A12 and soluble vascular cell adhesion molecule 1 (sVCAM-1) as a marker of endothelial cell activation in the serum of patients with KD. We demonstrate that S100A12 can indirectly provoke a strong, sterile inflammatory response from human coronary artery endothelial cells (HCAECs) in a strictly interleukin-1 β (IL-1 β)-dependent manner. In contrast, infection-driven activation of endothelial cells, as mimicked by stimulation with lipopolysaccharide (LPS), is less dependent on the functions of monocytes and mediating influence of IL-1 β .

MATERIALS AND METHODS

Study subjects and samples. Serum samples from 30 patients with KD (Table 1) were collected at Toyama University Hospital and related facilities between July 2004 and June 2017. The study was approved by the ethics committee of the University of Toyama and performed in accordance with the Declaration

Table 1. Characteristics of the patients with KD and healthy controls*

	Healthy controls (n = 13)	Patients with KD	
		IVIG responders (n = 24)	IVIG nonresponders (n = 6)
Age, median (range) years	9 (5–11)	3.0 (0.9–10)	3.8 (1–8)
Sex, no. female/no. male	8/5	13/11	2/4
Days with fever, median (range)	NA	6 (4–10)	9 (8–12)
Maximum WBCs/ μ l, mean \pm SEM	NA	14,424 \pm 975	17,877 \pm 2,031
CALs, no. of patients	NA	1	1
CRP, mean \pm SEM mg/dl			
Maximum	<0.5	8.4 \pm 1.0	15.0 \pm 4.0
Initial pretreatment	NA	8.1 \pm 1.0	10.2 \pm 3.1
Post-IVIG treatment			
Initial	NA	3.6 \pm 0.6	9.7 \pm 2.0
2 weeks	NA	0.7 \pm 0.2	2.2 \pm 0.8
4 weeks	NA	0.1 \pm 0.0	0.5 \pm 0.2

* KD = Kawasaki disease; IVIG = intravenous immunoglobulin; NA = not applicable; WBCs = white blood cells; CALs = coronary artery lesions; CRP = C-reactive protein.

of Helsinki. Serum samples from healthy donors ($n = 13$) (Table 1) were collected to establish cutoff levels for each of the analyzed parameters. The healthy donor samples were obtained from pediatric subjects at Muenster University Children's Hospital between May 2016 and March 2017. All patients and healthy controls provided their informed consent to participate in the study.

The study was approved by the local ethics committee. Further details on the study subjects are provided in Supplementary Materials and Methods (available on the *Arthritis & Rheumatology* web site at <http://onlinelibrary.wiley.com/doi/10.1002/art.40784/abstract>).

Serum analysis by multiplex bead array. Serum cytokines and chemokines as well as S100A12 were measured using a multiplex immunoassay (ProcartaPlex; Thermo Fisher Scientific) in accordance with the manufacturer's instructions. A more detailed description of the multiplex bead array is provided in Supplementary Materials and Methods.

Cell isolation and cultures. Peripheral blood mononuclear cells (PBMCs) and primary human monocytes were isolated from fresh whole blood samples obtained from healthy donors. In addition, HCAECs were purchased and cultured in microvascular endothelial cell growth medium (both from PeloBiotech). Further details on the methods used for cell isolation and cultures are described in Supplementary Materials and Methods (<http://onlinelibrary.wiley.com/doi/10.1002/art.40784/abstract>).

IVIG in vitro assay. An IVIG in vitro assay was used to determine the S100A12-induced release of sVCAM-1 by IVIG-treated HCAECs, as described in more detail in Supplementary Materials and Methods.

Flow cytometry. HCAECs and primary human monocytes were treated with human Fc receptor block (Hu FcR binding inhibitor; eBioscience), and then stained with anti-TLR-4 (phycoerythrin [PE]-conjugated anti-human CD284 [TLR-4], clone HTA125; BioLegend) and anti-CD14 (allophycocyanin [APC]-conjugated anti-human CD14, clone 61D3; eBioscience) or their respective isotype controls (PE-conjugated mouse IgG2a [κ isotype control, clone MOPC-173; BioLegend] and APC-conjugated mouse IgG1 [κ isotype control, clone P3.6.2.8.1; eBioscience]). Cells were washed and samples were analyzed by flow cytometry on a BD FACSCanto (BD Biosciences), with results analyzed using FlowJo software, version 10.1r5 (Tree Star).

Transfection of HCAECs. To establish membrane expression of CD14, HCAECs were transfected with a vector specifically encoding for membrane CD14. The cells were then analyzed by flow cytometry as described in more detail in Supplementary Mate-

rials and Methods [<http://onlinelibrary.wiley.com/doi/10.1002/art.40784/abstract>]).

Direct and indirect stimulation of HCAECs. Direct stimulation of HCAECs by LPS or S100A12 as well as indirect stimulation of HCAECs with monocyte-conditioned medium are described in more detail in Supplementary Materials and Methods.

Real-time quantitative reverse transcription-polymerase chain reaction (qRT-PCR). Real-time qRT-PCR analyses were performed as described in Supplementary Materials and Methods (<http://onlinelibrary.wiley.com/doi/10.1002/art.40784/abstract>).

Statistical analysis. Data were analyzed using Graphpad Prism software (version 6.0 for Mac OS X). Spearman's correlation coefficients (r_s) were used for pairwise comparisons of serum analytes, and were plotted using the *corrplot* R package and Rstudio (RStudio Team 2015; <http://www.rstudio.com/>), with both circle size and color as output for the r_s calculations.

RESULTS

Rapid increase in sVCAM-1 levels in the serum of IVIG-responsive patients. We analyzed serum samples from healthy pediatric control subjects and pediatric patients with KD (Table 1) for the levels of S100A12, classic inflammatory cytokines and chemokines, and the vascular adhesion molecules soluble intercellular adhesion molecule 1 (sICAM-1) and sVCAM-1. Whereas both myeloid and endothelial cells produce ICAM-1 in response to inflammatory cytokines, expression of VCAM-1 is restricted mainly to endothelial cells, and thus can best reflect activation of these cells (21–23). Consistent with previous reports (6,7), our data demonstrated that the serum concentrations of S100A12 were elevated initially, prior to IVIG treatment, in patients with KD and declined with a positive response to therapy (Figures 1A and B). Clinically, this was indicated by diminishing duration of fever and declining levels of C-reactive protein in patients following the initial treatment with IVIG (Table 1). Similar observations were made with regard to the levels of cytokines such as IL-1 β and IL-6, as well as the chemokines CXCL9 and CXCL10 (see Supplementary Figure 1, available on the *Arthritis & Rheumatology* web site at <http://onlinelibrary.wiley.com/doi/10.1002/art.40784/abstract>). Conversely, the concentrations of sVCAM-1 increased in the serum of IVIG-responding patients after the first IVIG treatment (Figure 1C), whereas in patients who were nonresponders, the sVCAM-1 levels remained relatively unchanged (Figure 1D).

In all of the collected study samples, analytes whose concentrations significantly changed following IVIG treatment generally showed positive correlations with one another (Figure 1E

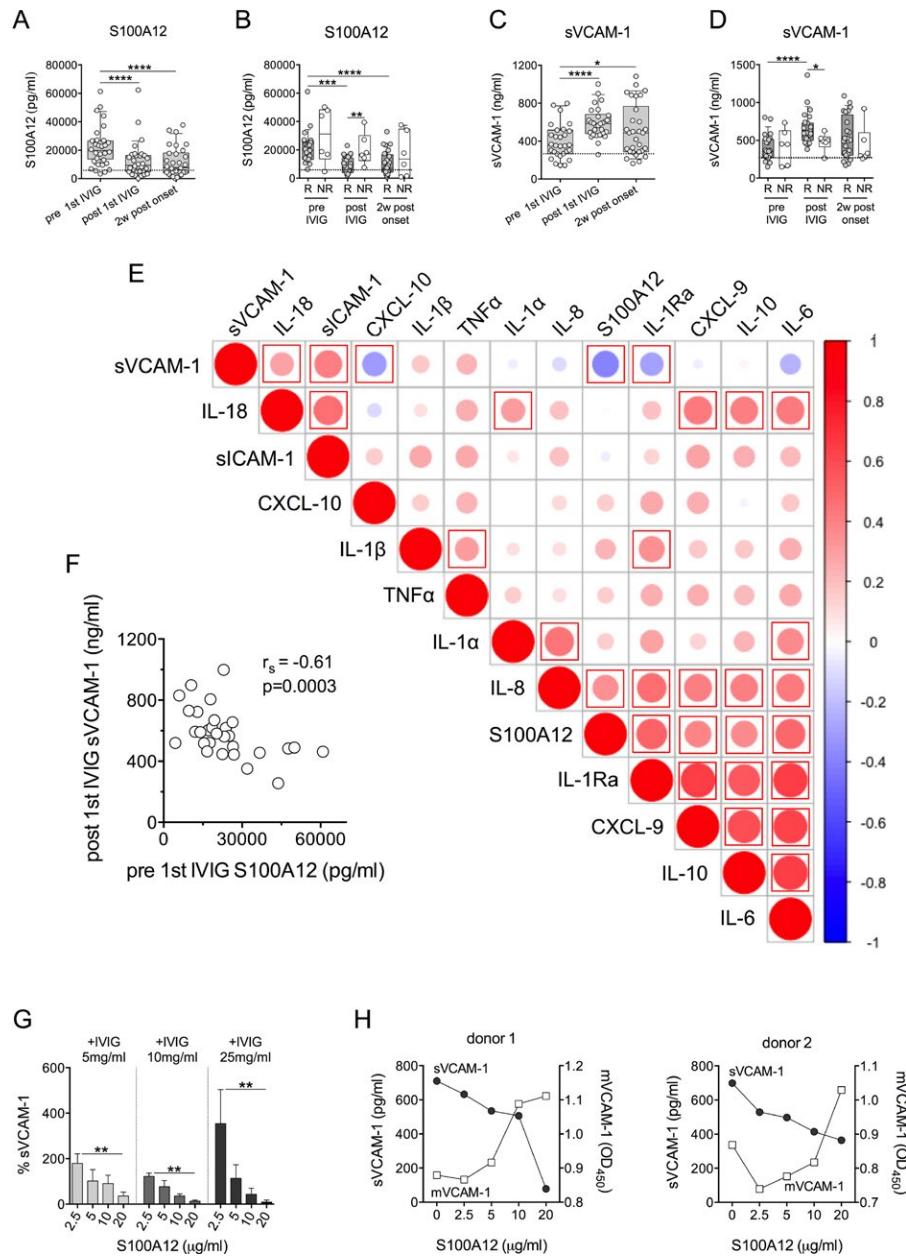


Figure 1. S100A12 and soluble vascular cell adhesion molecule 1 (sVCAM-1) levels fluctuate in the serum of patients with Kawasaki disease (KD) according to time point and response to intravenous immunoglobulin (IVIG) treatment. **A–D**, Serum from patients with KD ($n = 30$) before (pre 1st) and after (post 1st) initial IVIG treatment as well as 2 weeks after disease onset was analyzed for levels of S100A12 (**A** and **B**) and sVCAM-1 (**C** and **D**) by multiplexed bead array. In **B** and **D**, patients were separated into IVIG therapy responders (R) and nonresponders (NR). Data are presented as box plots, where the horizontal line inside the box shows the mean, the box shows the 10th and 90th percentiles, and bars outside the box show the interquartile range. Box plots are overlaid by scatterplots displaying the results per individual sample. The horizontal dashed line indicates the mean value in healthy controls. * = $P < 0.05$; ** = $P < 0.01$; *** = $P < 0.001$; **** = $P < 0.0001$, by Friedman's test followed by Dunn's test for multiple comparisons. **E**, Multiplexed parameters quantified in the patients' sera ($n = 90$ samples) were subjected to Spearman's correlation (r_s) analysis. The r_s correlation coefficients in the correlogram are visualized according to strength of association (circle size) and color range (blue indicating $r_s = -1$, red indicating $r_s = 1$). The red boxes indicate a significant association, as determined after Bonferroni's correction for multiple comparisons. **F**, Spearman's correlation analysis was used to assess correlations of serum S100A12 levels before initial IVIG treatment with serum sVCAM-1 levels post-first IVIG infusion. **G**, Healthy donor peripheral blood mononuclear cells ($n = 5$ donors) and primary human coronary artery endothelial cells were cocultured with S100A12 and intravenous IVIG preparations (5–25 mg/ml), and release of sVCAM-1 was determined in relation to that in untreated cells. **H**, The same cocultures as described in **G** ($n = 2$ donors) were stimulated with S100A12 and 25 mg/ml IVIG, and release of sVCAM-1 as well as relative VCAM-1 membrane expression (mVCAM-1) were quantified. sICAM-1 = intercellular adhesion molecule 1; IL-18 = interleukin-18; TNF α = tumor necrosis factor; IL-1Ra = IL-1 receptor antagonist.

and Supplementary Figures 2A and B [http://onlinelibrary.wiley.com/doi/10.1002/art.40784/abstract]). In contrast, serum levels of sVCAM-1 were negatively correlated with those of several cytokines and chemokines. This inverse correlation was most pronounced between sVCAM-1 and S100A12 or between sVCAM-1 and CXCL10 (interferon- γ -inducible protein 10) (Figure 1E and Supplementary Figures 2A and B).

To test for a possible relationship between the serum analyte concentrations prior to IVIG treatment and the elevated concentrations of sVCAM-1 in response to IVIG therapy, we analyzed correlations of the analytes at or between the different study time points (see Supplementary Figures 3A–D [http://onlinelibrary.wiley.com/doi/10.1002/art.40784/abstract]). In this analysis, we observed a pronounced negative correlation between the pretreatment serum concentrations of S100A12 and the serum levels of sVCAM-1 following the patients' first IVIG treatment (Figure 1F and Supplementary Figure 3D). In other words, the higher the S100A12 serum titers at the time of disease onset, the lower the sVCAM-1 serum titers following the initial IVIG infusion. This relationship was not observed with any of the other analyzed markers (Supplementary Figures 2 and 3). In particular, the levels of IL-6 correlated well with those of S100A12 in the patients' serum prior to treatment, and this correlation persisted over the course of IVIG therapy (Figure 1E and Supplementary Figure 2).

Contribution of increasing inflammatory activation of HCAECs to reduced sVCAM-1 shedding. Vasculitis in patients with KD affects the small- and medium-sized coro-

nary arteries. Correlation analyses of S100A12 and sVCAM-1 indicated that the higher the pretreatment S100A12 levels in the serum of patients with KD, the lower the serum levels of sVCAM-1 following IVIG therapy. Although membrane expression of VCAM-1, as has been observed on coronary artery endothelium, can facilitate extravasation of cells initially in the course of inflammation, the shedding of VCAM-1 and thus the increase in sVCAM-1 levels (for example, in the course of antiinflammatory treatment) is thought to indicate resolution of endothelial inflammation (24–26). As has been suggested in previous experiments investigating the antiinflammatory effects of statin treatments (26), our observation of an inverse correlation between high baseline serum S100A12 levels and low serum sVCAM-1 levels post-IVIG treatment could suggest a persisting contribution of S100A12 to inflammatory activation of endothelial cells and, thus, retention of VCAM-1 on the cell surface.

To test this hypothesis *in vitro*, we cocultured healthy donor PBMCs with HCAECs. Initially, we tested whether IVIG treatment, as the mainstay of KD therapy, would contribute to VCAM-1 shedding from HCAECs. We stimulated the cocultures with a fixed concentration of S100A12 (10 $\mu\text{g}/\text{ml}$), as well as different amounts of IVIGs (0–50 mg/ml). The results revealed a concentration-dependent contribution of IVIG treatment to sVCAM-1 release by HCAECs (see Supplementary Figure 4A [http://onlinelibrary.wiley.com/doi/10.1002/art.40784/abstract]).

We next tested whether increasing concentrations of S100A12 could reduce IVIG-induced VCAM-1 shedding by

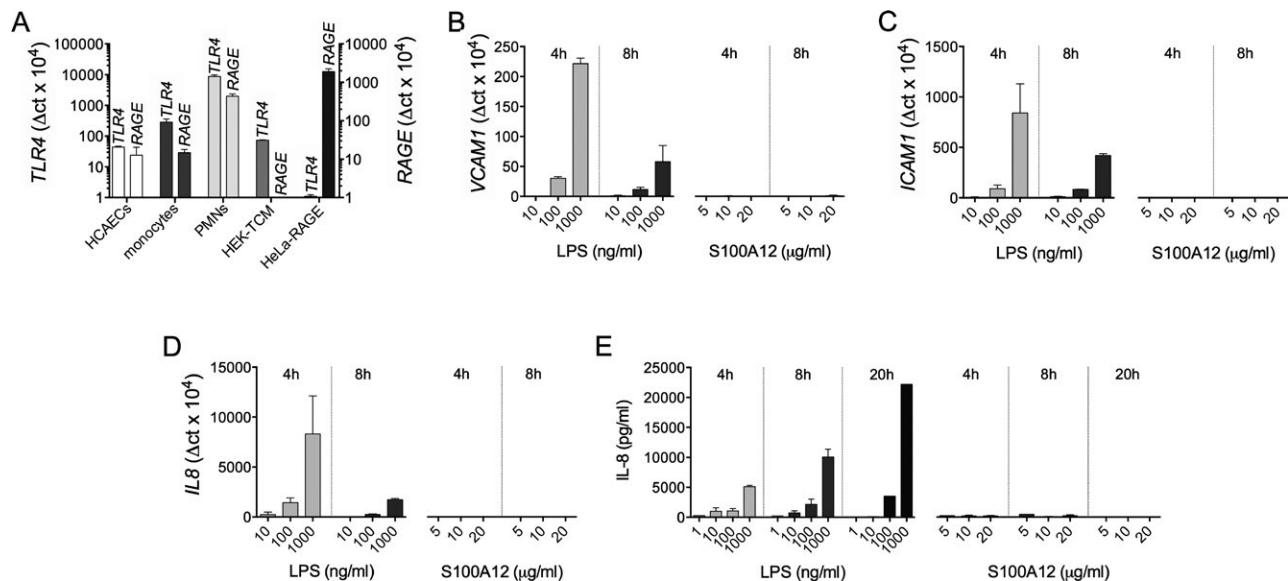


Figure 2. Human coronary artery endothelial cells (HCAECs) respond to lipopolysaccharide (LPS), but not to S100A12. **A**, Gene expression of *TLR4* and *RAGE* was quantified by real-time quantitative reverse transcription–polymerase chain reaction (qRT-PCR) in HCAECs compared to primary human monocytes and polymorphonuclear neutrophils (PMNs) as well as control cells expressing Toll-like receptor 4 (TLR-4) or receptor for advanced glycation end products (RAGE). **B–E**, HCAECs were stimulated with LPS or recombinant S100A12 at the indicated concentrations and time points, and analyzed by qRT-PCR for *VCAM1* (**B**), *ICAM1* (**C**), or *IL8* (**D**) gene expression as well as interleukin-8 (IL-8) protein secretion into the culture supernatants (**E**). Results are expressed as the increase over basal levels. Bars show the mean \pm SEM pooled data from 4 experiments.

increasing the retention of VCAM-1 on the cell membrane. Cocultures from healthy donor PBMCs and HCAECs were stimulated with S100A12 (0–20 μ g/ml) and IVIGs (5–25 mg/ml). In comparison to cocultures without IVIG treatment, we observed that increasing concentrations of S100A12 contributed to reduced sVCAM-1 release in the cocultures upon IVIG treatment (Figure 1G and Supplementary Figures 4B–D [<http://onlinelibrary.wiley.com/doi/10.1002/art.40784/abstract>]).

Furthermore, in analyses of both surface expression of VCAM-1 (membrane VCAM-1 [mVCAM-1]) as well as shedding of VCAM-1 (sVCAM-1), we studied cocultures of healthy donor PBMCs and HCAECs treated with 25 mg/ml IVIG. We noted that with increasing concentrations of S100A12, the concentrations of sVCAM-1 were reduced in the coculture supernatants, whereas the relative expression of mVCAM-1 was increased (Figure 1H).

Lack of direct activation of HCAECs by S100A12.

Our data from analyses of the serum of patients with KD as well as from in vitro experiments both supported the notion of a contribution of S100A12 to inflammatory activation of HCAECs. We therefore aimed to investigate whether S100A12 could directly activate inflammatory processes in these cells. Considering that S100A12 engagement of RAGE or TLR-4 may depend on the nature of the target cell (9,11), we evaluated *TLR4* and *RAGE* messenger RNA (mRNA) expression by HCAECs. Our results confirmed that HCAECs expressed both of these receptors, albeit at lower levels compared to that in primary human monocytes or neutrophils or cell lines that were engineered to overexpress either of these receptors (Figure 2A). However, despite their expression of appropriate receptors for S100A12, HCAECs were not responsive to direct stimulation with S100A12 (added at different concentrations and varying durations), as indicated by the lack of S100A12-induced expression of *VCAM1*, *ICAM1*, and *IL8* mRNA (Figures 2B–D) and IL-8 protein (Figure 2E). In contrast, all of these indicators were induced in HCAECs following stimulation with LPS (Figures 2B–E).

As a positive control for S100A12 activity, we stimulated primary human monocytes with S100A12 or LPS, and observed that these cells responded to both stimulants. Parallel stimulations of HCAECs with LPS revealed comparably lower levels of secreted IL-8, whereas, consistent with previous data, HCAECs did not respond to stimulation with S100A12 (Figure 3A).

To determine whether the muted response of HCAECs to LPS and S100A12 was attributable to lower expression of TLR-4 coreceptors, we measured the expression of CD14 both on primary human monocytes and on HCAECs, since detection of TLR-4 agonists can involve the interaction of TLR-4 with CD14 (10,27,28). As expected, our results showed that HCAECs expressed significantly lower levels of TLR-4 compared to that in human monocytes (Figure 3B). Furthermore, CD14 mRNA and protein levels in the HCAECs were below the levels of detection (Figures 3B and C).

In the absence of cell surface CD14, soluble CD14 (sCD14) can facilitate responses to LPS (29). To determine whether HCAECs could respond to S100A12 with the assistance of sCD14, we stimulated HCAECs with human serum, as a source of human sCD14, or with human recombinant sCD14. Our results demonstrated that none of these conditions improved the responsiveness of HCAECs to S100A12, as indicated by the lack of induced expression of *IL8*, *ICAM1*, and *VCAM1* mRNA (Figure 3D and Supplementary Figures 5A and B [<http://onlinelibrary.wiley.com/doi/10.1002/art.40784/abstract>]) and IL-8 protein release (Figure 3E).

However, transfection of HCAECs with a vector encoding for membrane CD14 established the cell surface expression of this molecule, when compared to that in naive or mock-transfected cells (Figures 3F and G and Supplementary Figure 5C [<http://onlinelibrary.wiley.com/doi/10.1002/art.40784/abstract>]). Treatment of the transfected HCAECs or control cells with LPS or S100A12 revealed surface expression of CD14 on HCAECs. The responsiveness of CD14-transfected HCAECs was increased following stimulation with LPS, and pronounced IL-8 release was observed in the cells upon S100A12 stimulation (Figure 3H).

Responsiveness of HCAECs to S100A12-activated monocytes.

In our assay systems, and counter to our hypothesis, S100A12 failed to directly activate HCAECs, since S100A12 signaling to the cells appeared strictly dependent on the expression of membrane CD14. However, in our initial experiments, we stimulated HCAECs by supernatant transfer or coculture with S100A12-stimulated PBMCs. It is known that human monocytes, as is present, for example, in PBMC preparations, respond well to S100A12 stimulation (10,11,30). Increased numbers of peripheral blood CD14+CD16+ monocytes have been observed in the serum of patients with KD (31), and monocytes have been found to be associated with endothelial cell dysfunction in patients with coronary artery disease (32). In patients with KD, both monocytes as well as monocyte-derived cytokines could interact with vascular endothelial cells.

To determine whether S100A12 mediates its effects through monocytes, we cultured HCAECs in conditioned medium obtained from LPS- and S100A12-stimulated primary human monocytes. As expected, LPS- and S100A12-stimulated monocyte supernatants contained proinflammatory cytokines (Figure 4B). In contrast to direct stimulation of HCAECs with S100A12, exposure of HCAECs to supernatants from S100A12-activated monocytes resulted in pronounced expression of *IL8*, *IL6*, *ICAM1*, and *VCAM1* mRNA by HCAECs (Figure 4A). However, when HCAEC stimulations were performed with monocyte supernatants obtained from S100A12- or LPS-treated cells, either with or without additional inflammasome activation by ATP, we observed that the presence of ATP during monocyte stimulation by S100A12 critically affected the down-

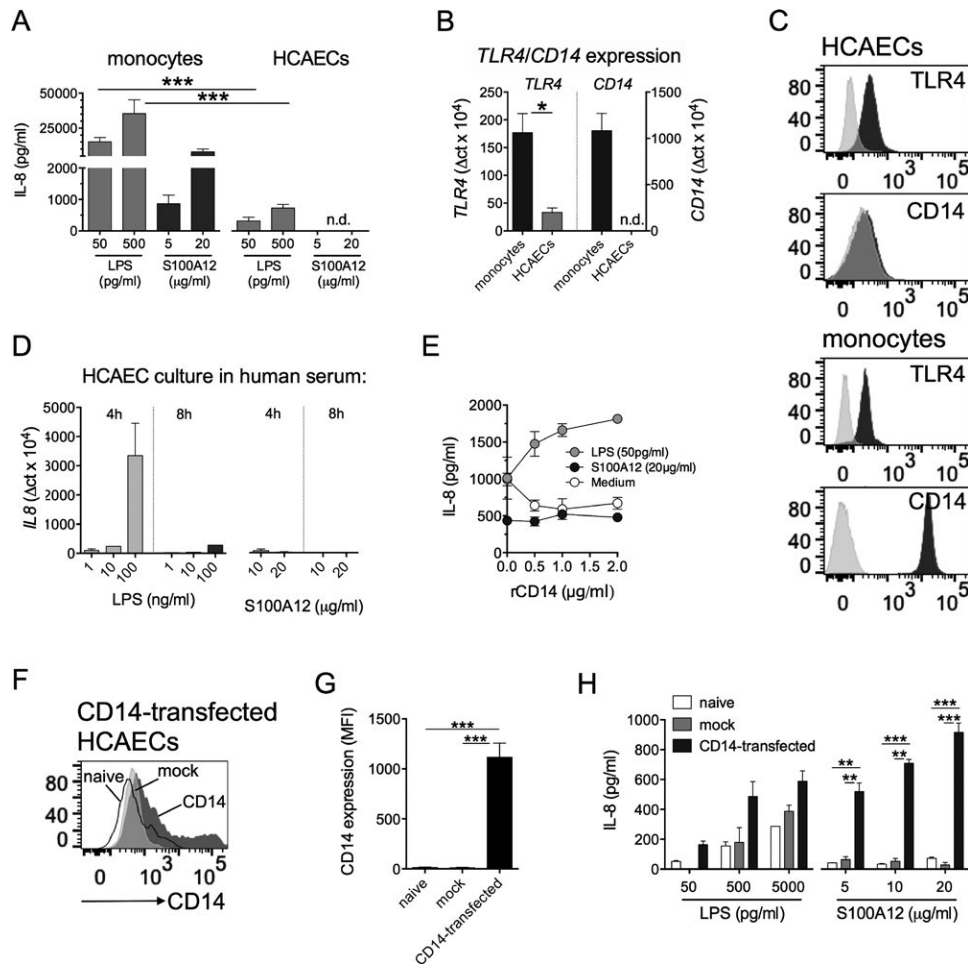


Figure 3. HCAECs lack surface CD14 expression. **A**, The response of primary human monocytes and HCAECs to either LPS or S100A12 stimulation (for 4 hours) was analyzed according to the secretion of IL-8. **B** and **C**, *Tlr4* and *Cd14* gene expression (**B**) and surface expression (**C**) by HCAECs or monocytes was quantified by qRT-PCR (**B**) or flow cytometry (**C**). In **C**, isotype controls are shown in light gray; the histogram plots are representative of 3 experiments. **D** and **E**, HCAECs cultured in medium supplemented with non-heat-inactivated human serum (10%) (pooled data from 4 experiments) (**D**) or in medium supplemented with human serum spiked with recombinant human soluble CD14 (rCD14) (pooled data from 2 experiments) (**E**) were analyzed for *il8* gene expression (**D**) or IL-8 protein release (**E**). Results are expressed as the increase over basal levels. **F**, HCAECs transfected with a membrane CD14-encoding vector, mock (no DNA)-transfected HCAECs, or HCAECs left untreated (naive) were analyzed for CD14 surface expression by flow cytometry. **G**, Surface expression of CD14 was analyzed using anti-CD14 staining. Results are presented as the mean fluorescence intensity (MFI). Bars show the mean \pm SEM pooled data from 3 experiments. **H**, Naive, mock-transfected, or CD14-transfected cells were stimulated with the indicated concentrations of LPS or S100A12, and IL-8 release into the culture supernatants was quantified. Results are the mean \pm SEM pooled data from 3 experiments. * = $P < 0.05$; ** = $P < 0.01$; *** = $P < 0.001$, by Mann-Whitney U test in **A** and **B** or by Kruskal-Wallis test followed by Dunn's test for multiple comparisons in **G** and **H**. See Figure 2 for other definitions.

stream endothelial expression of *IL8* mRNA (Figure 4C) as well as *IL6*, *ICAM1*, and *VCAM1* mRNA (Supplementary Figure 6A [http://onlinelibrary.wiley.com/doi/10.1002/art.40784/abstract]). In contrast, HCAECs responded to supernatants from LPS-activated monocytes regardless of whether or not ATP was present, while ATP enhanced endothelial expression of *IL8* mRNA (Figure 4C) as well as *il6*, *ICAM1*, and *VCAM1* mRNA (Supplementary Figure 6A).

We further tested whether, and to what extent, prominent inflammatory cytokines, such as IL-1, IL-6, or tumor necrosis factor (TNF), present in the monocyte supernatants may have contributed

to the activation of HCAECs in our experiments. For these experiments, monocyte supernatants obtained from S100A12 or LPS stimulations (S100A12 at 20 μ g/ml, LPS at 50 pg/ml), which had comparable cytokine expression levels (Figure 4C), were treated with cytokine (TNF)-blocking drugs or cytokine receptor (IL-1R, IL-6R)-blocking drugs before being transferred onto endothelial cells. Alternatively, supernatants were treated with IVIGs, as this is the mainstay of current KD therapy. As indicated by the expression of *IL8* mRNA (Figure 4D) and *IL6* mRNA (Supplementary Figure 6B [http://onlinelibrary.wiley.com/doi/10.1002/art.40784/abstract]), neither treatment with IVIG nor interference of TNF or IL-6 signaling

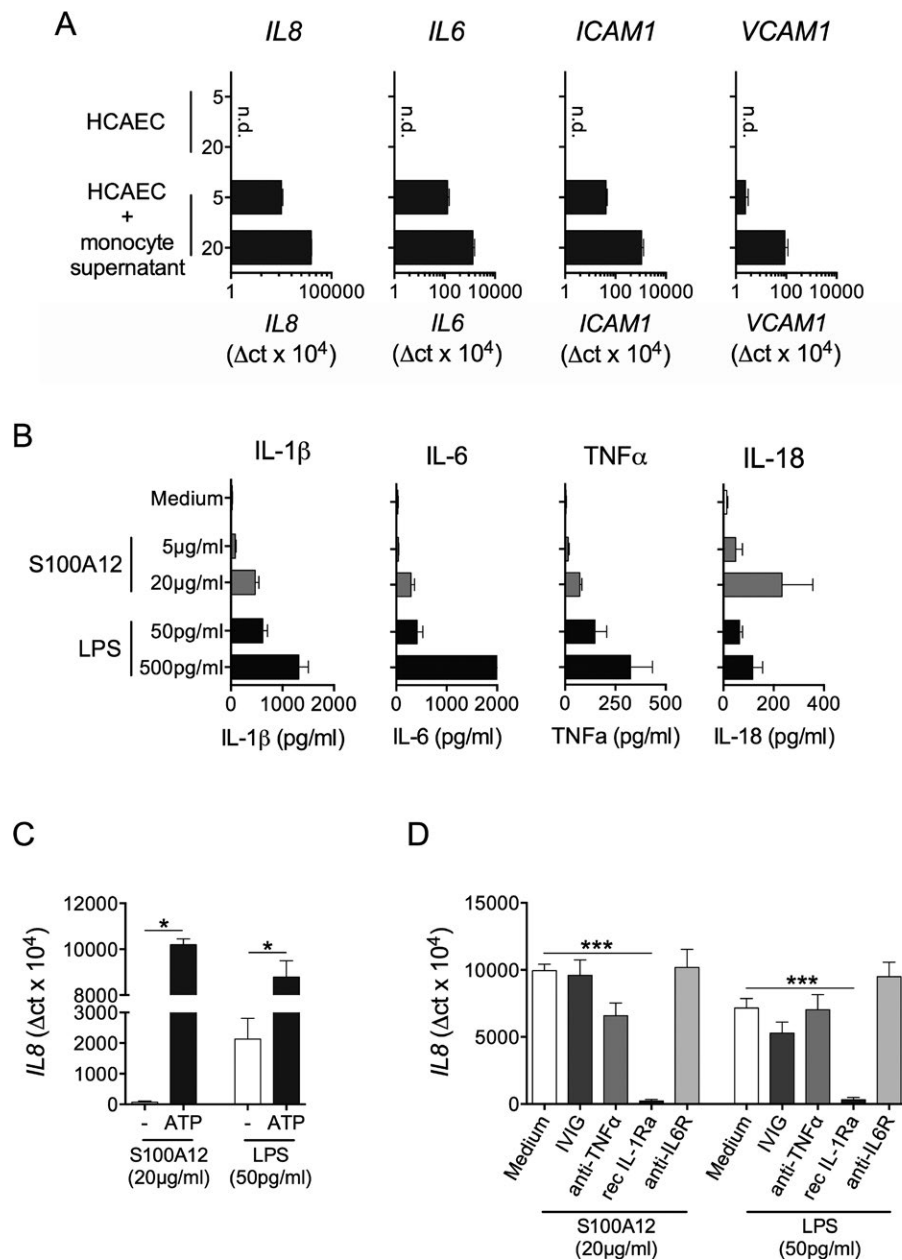


Figure 4. S100A12-stimulated monocytes trigger HCAEC activation via interleukin-1 β (IL-1 β). **A**, HCAECs cultured with or without supernatants obtained from human monocytes that were stimulated with S100A12 (at 5 or 20 μ g/ml for 4 hours) were analyzed for the expression of the indicated genes by real-time qRT-PCR. Monocyte stimulations included 5 mM ATP. **B**, Expression of inflammatory cytokines in monocyte supernatants prior to transfer onto HCAECs was quantified by multiplexed bead array. Bars show the mean \pm SEM pooled data from 4 experiments. **C**, HCAECs were cultured for 18 hours in supernatants obtained from monocytes that were stimulated for 4 hours with S100A12 (20 μ g/ml) or LPS (50 pg/ml) with or without 5 mM ATP, and *IL8* expression was analyzed by qRT-PCR. Results in **A** and **C** are the increase over basal expression. **D**, HCAECs were cultured for 18 hours in the presence of intravenous immunoglobulins (IVIGs) (25 mg/ml), anti-tumor necrosis factor (anti-TNF α) (adalimumab, 1 μ g/ml), IL-1 receptor antagonist (IL-1Ra) (anakinra, 250 ng/ml), or anti-IL-6 receptor (anti-IL-6R) (tocilizumab, 1 μ g/ml) in supernatants obtained from monocytes that were stimulated for 4 hours with S100A12 (20 μ g/ml) or LPS (50 pg/ml) and 5 mM ATP, and *IL8* expression was quantified by qRT-PCR. Results are the increase over basal expression. Bars show the mean \pm SEM pooled data from 3 experiments in **A** and **C** and 4 experiments in **B** and **D**. * = $P < 0.05$; *** = $P < 0.001$, by Wilcoxon's matched-pairs signed rank test in **C** or Friedman's test followed by Dunn's test for multiple comparisons in **D**. n.d. = not determined (see Figure 2 for other definitions).

in the monocyte supernatants significantly affected the stimulation of HCAECs. In contrast, interference of IL-1 α or IL-1 β signaling, via the blockade of IL-1R, abrogated endothelial cell activation.

As we have already demonstrated, endothelial cells also respond directly to LPS stimulation (Figures 2 and 3). In experiments using LPS for monocyte stimulation, some bystander activa-

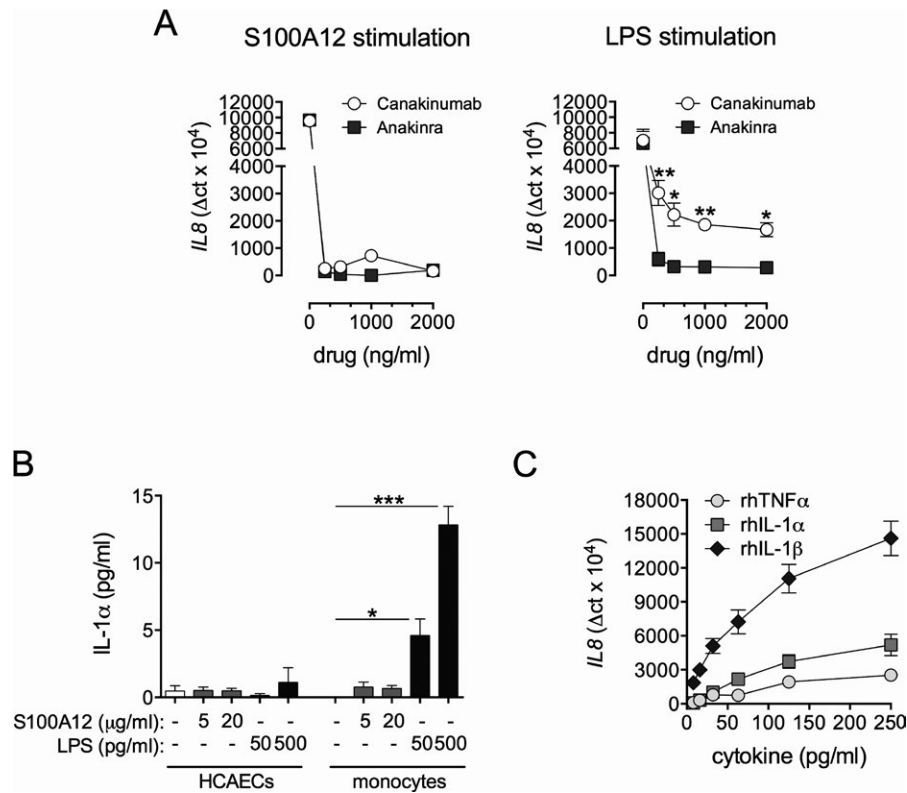


Figure 5. Stimulation of HCAECs by S100A12 depends strictly on interleukin-1 β (IL-1 β). **A**, HCAECs were cultured for 18 hours in the presence of either recombinant IL-1 receptor antagonist (IL-1Ra) (anakinra) or anti-IL-1 β antibody (canakinumab) at the indicated concentrations in supernatants obtained from monocytes that were stimulated for 4 hours with S100A12 (20 $\mu\text{g/ml}$) or LPS (50 $\mu\text{g/ml}$) and 5 mM ATP, and *IL8* expression was quantified by qRT-PCR. Results are the mean \pm SEM pooled data from 3 experiments. **B**, Culture supernatants of HCAECs or primary human monocytes were stimulated for 4 hours with the indicated concentrations of S100A12 or LPS as well as 5 mM ATP, and released IL-1 α levels were analyzed. Results are the mean \pm SEM pooled data from 4 experiments. **C**, HCAECs were stimulated with recombinant human tumor necrosis factor (rhTNF α), rhIL-1 α , or rhIL-1 β at the indicated concentrations, and *IL8* expression was quantified by qRT-PCR. Results are the mean \pm SEM pooled data from 2 experiments. * = $P < 0.05$; ** = $P < 0.01$; *** = $P < 0.001$, by Wilcoxon's matched-pairs signed rank test in **C** and **E** or Friedman's test followed by Dunn's test for multiple comparisons in **D**. See Figure 2 for other definitions.

tion of HCAECs may occur, due to remnant endotoxin in the transferred supernatants. To evaluate the extent of this phenomenon, we treated the monocyte supernatants, prior to transfer onto HCAECs, with polymyxin B (an endotoxin blocker) or anakinra (IL-1R blockade). The results suggested that activation of HCAECs following stimulation with low concentrations of LPS occurred predominantly via IL-1, while at higher concentrations of LPS, HCAECs could also respond directly to endotoxin (Supplementary Figure 6C [http://onlinelibrary.wiley.com/doi/10.1002/art.40784/abstract]).

HCAEC activation by S100A12 dependent on IL-1 β .

Our data assessing the importance of inflammasome activation by ATP (Figure 4C) as well as the effects of IL-1R blockade (Figure 4D) both point toward an integral role of IL-1 in activation of HCAECs by TLR-4-stimulated human monocytes. In contrast to IL-1 α , inflammasome activation is particularly relevant for the caspase-dependent generation of mature IL-1 β from its biologically inactive precursor (33). We therefore tested the efficacy of IL-1R blockade by an IL-1R antagonist (anakinra) compared to

an anti-IL-1 β neutralizing monoclonal antibody (canakinumab) for reducing the levels of S100A12 or LPS-mediated activation of HCAECs. In experiments in which endothelial cell activation was triggered by supernatants from S100A12-activated monocytes, both anakinra and canakinumab were effective at reducing (to baseline levels) the HCAEC expression of *IL8* mRNA (Figure 5A) or *IL6* mRNA (Supplementary Figure 7A [http://onlinelibrary.wiley.com/doi/10.1002/art.40784/abstract]). When HCAECs were cultured in supernatants from LPS-stimulated monocytes, IL-1R blockade with anakinra reduced the HCAEC expression of *IL8* mRNA (Figure 5A) and *IL6* mRNA (Supplementary Figure 7A) to a similar extent as that observed in the S100A12-stimulated monocytes. In contrast, IL-1 β neutralization with canakinumab was significantly less effective at reducing the *IL8* and *IL6* mRNA expression induced by LPS-stimulated monocytes as compared to that induced by S100A12-stimulated monocytes (Figure 5A and Supplementary Figure 7A).

These findings support the notion of a potentially important role of IL-1 α in assisting, in particular, with LPS-induced HCAEC

activation. IL-1 α can either be produced by stimulated monocytes (34) or arise directly from HCAECs (35). When we analyzed the supernatants of S100A12- or LPS-stimulated HCAECs or transferred monocyte supernatants obtained from either S100A12- or LPS-stimulated cells, we found that IL-1 α was released by LPS-stimulated primary human monocytes (Figure 5B).

To understand the proportion of IL-1 β , relative to IL-1 α , that was involved in the activation of HCAECs, we stimulated HCAECs with both of these cytokines or with TNF. We included TNF because, in the previous cytokine-blocking experiments, we observed some effect of TNF blockade on HCAEC activation (Figure 4D), albeit the effect was significantly weaker compared to interference of IL-1R signaling. Upon stimulation with the recombinant cytokines, we observed that stimulation of HCAECs with IL-1 β resulted in strong expression of *IL8* mRNA (Figure 5C) and *IL6* mRNA (Supplementary Figure 7B [<http://onlinelibrary.wiley.com/doi/10.1002/art.40784/abstract>]), whereas treatment of the cells with IL-1 α resulted in similar, but significantly lower, gene expression profiles. Stimulation of HCAECs upon treatment with TNF was comparably weak.

DISCUSSION

To our knowledge, this is the first study to demonstrate an association between shed VCAM levels and S100A12 in the context of responsiveness to IVIG therapy in patients with KD. In this context, we found that inflammatory activation of HCAECs by S100A12 depends strictly on IL-1 β .

Despite the fact that the serum samples from patients with KD enrolled in this study were, in part, kept in long-term storage, we were able to obtain conclusive data on serum levels of cytokines and chemokines, S100A12, and vascular adhesion molecules (sICAM-1, sVCAM-1). Correlation analyses of the KD patients' serum markers indicated that high pretreatment levels of S100A12 were associated with reduced VCAM-1 shedding post-IVIG infusion, thereby supporting the proposition that S100A12 may contribute to sustained inflammatory activation of endothelial cells in KD. However, HCAECs were not responsive to direct stimulation with S100A12, despite their expression of the S100A12 receptors RAGE and TLR-4, but were responsive to stimulation mediated by S100A12-activated monocytes. This response required the presence of ATP and was blocked by IL-1 β antagonism. In contrast, HCAECs were responsive to direct stimulation by LPS through TLR-4, as well as to LPS-stimulated monocytes by the concerted action of both monocyte-derived IL-1 α and IL-1 β .

Although the cell adhesion molecule VCAM-1 is highly expressed in the coronary lesions of patients with KD as well as in the neovasculature of coronary arteries, and elevated serum concentrations of sVCAM-1 have been associated with the disease (36–38), shedding of VCAM-1 from the cell surface is also thought to indicate resolution of endothelial inflammation (24). In

a previous study, treatment of healthy volunteers with 3 mg prednisolone increased the levels of sVCAM-1, but not sICAM-1, in LPS-treated serum as compared to that in untreated controls (25). In another study, statin treatment of endothelial cells reduced the TNF-induced up-regulation of VCAM-1 surface expression via increased protein shedding (26). Along similar lines, we observed an increase in sVCAM-1 levels in the serum of patients with KD who were responsive to IVIG treatment. In patients who were refractory to treatment, serum concentrations of sVCAM-1 remained relatively unchanged. Moreover, the inverse correlation between high serum concentrations of S100A12 pretreatment and low levels of sVCAM-1 posttreatment, as well as the experimental *in vitro* data obtained from HCAECs, suggest that circulating S100A12 suppresses VCAM-1 shedding as a function of persisting endothelial inflammation.

Although we observed activation of HCAECs on the level of VCAM-1 surface expression and shedding in S100A12-stimulated cocultures with PBMCs, our mechanistic discovery studies demonstrated that S100A12 was unable to directly stimulate HCAECs—the prime target in KD. This was somewhat surprising, given that these cells express the S100A12 putative receptors RAGE and TLR-4 (9,11). However, our data suggest that the unresponsiveness of HCAECs to S100A12 stimulation was the result of absent or extremely low surface CD14 expression, as has also been reported elsewhere (39). On the other hand, a study by Stoll et al also confirmed TLR-4 expression on coronary artery endothelial cells, both *in vitro* and by immunostaining of tissue (39). In a parallel study of human monocytes performed by us, we noted that CD14 serves as a coreceptor to TLR-4 with an integral role in S100A12 signaling (10). While the present data support these findings, they further suggest that S100A12 signaling in the absence of membrane CD14 cannot be bypassed by the soluble form of the receptor. In contrast to the unresponsiveness of HCAECs to S100A12, the cells responded well to direct LPS stimulation, which may, particularly at higher concentrations, have a reduced dependence on CD14 surface expression (40). Furthermore, LPS signaling can also be established through evaluation of sCD14 levels (29,39).

Instead, HCAECs were activated by supernatants obtained from S100A12-stimulated primary human monocytes. In these experiments, HCAEC responsiveness was predominantly dependent on IL-1 β , which was secreted by monocytes following stimulation with S100A12 and ATP. IL-1 α appears to play a lesser role, as blockade of IL-1R (which prevents both IL-1 α and IL-1 β signaling) and neutralization of IL-1 β were equally effective at abrogating the responsiveness of HCAECs. Intriguingly, neither IVIG treatment, as the mainstay of today's KD therapy (2), nor TNF neutralization or IL-6R blockade impacted HCAEC activation by monocyte-conditioned medium. It should be noted that both therapeutic TNF neutralization (41) and IL-6R blockade (42), either administered in addition to IVIG treatment (41) or tested in a prospective pilot study in IVIG-resistant cases (42), contributed to

improvement of some clinical and laboratory measures (41,42) but did not reduce treatment resistance (41). Pilot study data regarding IL-6R blockade have even suggested an association of therapy with formation of new-onset coronary artery aneurysms (42).

The apparently exclusive IL-1 β dependence of HCAEC activation by TLR-4-stimulated human monocytes is remarkable, as other studies have demonstrated that HCAECs were responsive to recombinant TNF (43) with overlapping profiles of induced gene expression in response to IL-1 β (44). However, an enhanced sensitivity of HCAECs toward IL-1 β , in terms of IL-6 release, has already been suggested (45).

Consistent with the IL-1 β dependence demonstrated in our in vitro experiments, disease development in a mouse model of *Lactobacillus casei* cell wall extract (LCWE)-induced KD was shown to require IL-1-producing macrophages as well as myeloid differentiation factor 88 (MyD88) signaling in hematopoietic cells (19). Moreover, a number of observations on both the gene and protein level have already suggested that IL-1 plays a crucial role in the pathologic processes of KD, and clinical trials aiming to evaluate the efficacy of IL-1-blocking therapies in KD are currently ongoing (46).

However, the relative contribution of IL-1 to vasculitis in KD is still insufficiently defined (19,46). Several studies have demonstrated that IL-1 β can drive proliferation of VSMCs as well as formation of myofibroblasts (46). Studies of endothelial MyD88 conditional-knockout mice revealed no protection from KD, which may suggest that nonendothelial stromal cells, such as murine VSMCs, are key IL-1 responder cells (19). In light of our reported findings, such species-specific differences in IL-1-responsive cells may be attributable to differences in pathologic features between the KD mouse model and the human disease (47) or to species-specific differential effects of IL-1 (48,49) or IL-1R signaling (48,50).

Intriguingly, our observations herein suggest that proinflammatory HCAEC activation by TLR-4-stimulated monocytes, particularly when mediated by S100A12, is strictly dependent on IL-1 β . Compared to experiments with S100A12, HCAECs cultured in supernatants from LPS-stimulated monocytes similarly up-regulated inflammatory cytokine and adhesion molecule expression, but dependence on IL-1 β was significantly less pronounced. We attribute these findings to the presence of IL-1 α , which we detected particularly in supernatants of LPS-stimulated human monocytes. Correspondingly, blocking the signaling of both IL-1 α and IL-1 β by IL-1R antagonism completely abrogated the stimulation of HCAECs. Similarly, mice subjected to LCWE-induced KD and receiving either IL-1 α - or IL-1 β -neutralizing antibodies were protected from KD, but protection was most evident when the treatments were combined (19,20).

Taken together, the results of these experiments illustrate an as yet-undescribed association between S100A12 expression and HCAEC activation in KD. We pinpoint IL-1 β as the key cytokine contributing to activation of HCAECs when mediated by TLR-4-stimulated human monocytes. Furthermore, we identify IL-

1 β signaling in coronary artery endothelium as particularly relevant in the course of sterile inflammation that is induced by DAMPs such as S100A12 and ATP (see Supplementary Figure 8 [<http://onlinelibrary.wiley.com/doi/10.1002/art.40784/abstract>]). Thus, our data highlight the concept that the coronary artery endothelium, which is critically involved in the early pathologic processes leading to the development of KD (16,17) and aneurysm formation (18), is particularly sensitive to IL-1 β blockade during DAMP-induced sterile inflammation in this disease.

Finally, although our observations may support further development of IL-1-targeting studies for the treatment of KD, IVIG treatment remains the gold standard of therapy. Although, in our short-term in vitro experiments constituted from monocytes and endothelial cells, IVIG treatment did not yield any effects comparable to those mediated by IL-1 blockade, IVIG therapy significantly reduced the circulating levels of S100A12, as well as IL-1 β or IL-6 levels, in the serum of patients with KD. Ex vivo, IVIG treatment of cells from patients with KD has been shown to reduce *S100a12* gene expression (51), and thus it may be speculated that IVIG treatment also affects circulating levels of this endogenous TLR-4 ligand (10,11), which can reduce inflammatory cytokine release as a downstream function.

ACKNOWLEDGMENTS

We thank Antje Hellige, Susanne Schleifenbaum, Melanie Saers, and Sabrina Fuehner for providing excellent technical assistance for the study. In addition, we acknowledge the medical faculty at the genomics core facility of Muenster University for providing technical support for all gene expression analyses.

AUTHOR CONTRIBUTIONS

All authors were involved in drafting the article or revising it critically for important intellectual content, and all authors approved the final version to be published. Dr. C. Kessel had full access to all of the data in the study and takes responsibility for the integrity of the data and the accuracy of the data analysis.

Study conception and design. Brown, C. Kessel.

Acquisition of data. Armaroli, Verweyen, Pretzer, K. Kessel, Hirono, Ichida, Okabe, C. Kessel.

Analysis and interpretation of data. Armaroli, K. Kessel, Hirono, Ichida, Okabe, Cabral, Foell, C. Kessel.

REFERENCES

1. Dusser P, Kone-Paut I. IL-1 inhibition may have an important role in treating refractory Kawasaki disease. *Front Pharmacol* 2017;8:163.
2. McCrindle BW, Rowley AH, Newburger JW, Burns JC, Bolger AF, Gewitz M, et al. Diagnosis, treatment, and long-term management of Kawasaki disease: a scientific statement for health professionals from the American Heart Association. *Circulation* 2017;135:e927–e99.
3. Takahashi K, Oharaseki T, Naoe S, Wakayama M, Yokouchi Y. Neurophilic involvement in the damage to coronary arteries in acute stage of Kawasaki disease. *Pediatr Int* 2005;47:305–10.

4. Naoe S, Takahashi K, Masuda H, Tanaka N. Kawasaki disease: with particular emphasis on arterial lesions. *Acta Pathol Jpn* 1991; 41:785–97.
5. Ye F, Foell D, Hirono KI, Vogl T, Rui C, Yu X, et al. Neutrophil-derived S100A12 is profoundly upregulated in the early stage of acute Kawasaki disease. *Am J Cardiol* 2004;94:840–4.
6. Foell D, Ichida F, Vogl T, Yu X, Chen R, Miyawaki T, et al. S100A12 (EN-RAGE) in monitoring Kawasaki disease. *Lancet* 2003;361:1270–2.
7. Wittkowski H, Hirono K, Ichida F, Vogl T, Ye F, Yanlin X, et al. Acute Kawasaki disease is associated with reverse regulation of soluble receptor for advance glycation end products and its proinflammatory ligand S100A12. *Arthritis Rheum* 2007;56:4174–81.
8. Hirono K, Foell D, Xing Y, Miyagawa-Tomita S, Ye F, Ahlmann M, et al. Expression of myeloid-related protein-8 and -14 in patients with acute Kawasaki disease. *J Am Coll Cardiol* 2006;48:1257–64.
9. Hofmann MA, Drury S, Fu C, Qu W, Taguchi A, Lu Y, et al. RAGE mediates a novel proinflammatory axis: a central cell surface receptor for S100/calgranulin polypeptides. *Cell* 1999;97:889–901.
10. Kessel C, Fuehner S, Zell J, Zimmermann B, Drewianka S, Brockmeyer S, et al. Calcium and zinc tune autoinflammatory Toll-like receptor 4 signaling by S100A12. *J Allergy Clin Immunol* 2018;142:1370–3.
11. Foell D, Wittkowski H, Kessel C, Luken A, Weinlage T, Varga G, et al. Proinflammatory S100A12 can activate human monocytes via Toll-like receptor 4. *Am J Respir Crit Care Med* 2013;187:1324–34.
12. Hofmann Bowman M, Wilk J, Heydemann A, Kim G, Rehman J, Lodato JA, et al. S100A12 mediates aortic wall remodeling and aortic aneurysm. *Circ Res* 2010;106:145–54.
13. Foell D, Hernandez-Rodriguez J, Sanchez M, Vogl T, Cid MC, Roth J. Early recruitment of phagocytes contributes to the vascular inflammation of giant cell arteritis. *J Pathol* 2004;204:311–6.
14. Viemann D, Strey A, Janning A, Jurk K, Klimmek K, Vogl T, et al. Myeloid-related proteins 8 and 14 induce a specific inflammatory response in human microvascular endothelial cells. *Blood* 2005;105:2955–62.
15. Wittkowski H, Sturrock A, van Zoelen MA, Viemann D, van der Poll T, Hoidal JR, et al. Neutrophil-derived S100A12 in acute lung injury and respiratory distress syndrome. *Crit Care Med* 2007;35:1369–75.
16. Leung DY, Cotran RS, Kurt-Jones E, Burns JC, Newburger JW, Pober JS. Endothelial cell activation and high interleukin-1 secretion in the pathogenesis of acute Kawasaki disease. *Lancet* 1989;2:1298–302.
17. Orenstein JM, Shulman ST, Fox LM, Baker SC, Takahashi M, Bhatti TR, et al. Three linked vasculopathic processes characterize Kawasaki disease: a light and transmission electron microscopic study. *PLoS One* 2012;7:e38998.
18. Senzaki H. The pathophysiology of coronary artery aneurysms in Kawasaki disease: role of matrix metalloproteinases. *Arch Dis Child* 2006;91:847–51.
19. Lee Y, Wakita D, Dagvadorj J, Shimada K, Chen S, Huang G, et al. IL-1 signaling is critically required in stromal cells in Kawasaki disease vasculitis mouse model: role of both IL-1 α and IL-1 β . *Arterioscler Thromb Vasc Biol* 2015;35:2605–16.
20. Wakita D, Kurashima Y, Crother TR, Noval Rivas M, Lee Y, Chen S, et al. Role of interleukin-1 signaling in a mouse model of Kawasaki disease-associated abdominal aortic aneurysm. *Arterioscler Thromb Vasc Biol* 2016;36:886–97.
21. Zhang J, Defelice AF, Hanig JP, Colatsky T. Biomarkers of endothelial cell activation serve as potential surrogate markers for drug-induced vascular injury. *Toxicol Pathol* 2010;38:856–71.
22. Blake GJ, Ridker PM. Novel clinical markers of vascular wall inflammation. *Circ Res* 2001;89:763–71.
23. Davies MJ, Gordon JL, Gearing AJ, Pigott R, Woolf N, Katz D, et al. The expression of the adhesion molecules ICAM-1, VCAM-1, PECAM, and E-selectin in human atherosclerosis. *J Pathol* 1993;171: 223–9.
24. Zonneveld R, Martinelli R, Shapiro NI, Kuijpers TW, Plotz FB, Carman CV. Soluble adhesion molecules as markers for sepsis and the potential pathophysiological discrepancy in neonates, children and adults. *Crit Care* 2014;18:204.
25. Lemaire LC, de Kruif MD, Giebelen IA, van Zoelen MA, van't Veer C, van der Poll T. Differential dose-dependent effects of prednisolone on shedding of endothelial adhesion molecules during human endotoxemia. *Immunol Lett* 2008;121:93–6.
26. Landsberger M, Wolff B, Jantzen F, Rosenstengel C, Vogelgesang D, Staudt A, et al. Cerivastatin reduces cytokine-induced surface expression of ICAM-1 via increased shedding in human endothelial cells. *Atherosclerosis* 2007;190:43–52.
27. Kim JI, Lee CJ, Jin MS, Lee CH, Paik SG, Lee H, et al. Crystal structure of CD14 and its implications for lipopolysaccharide signaling. *J Biol Chem* 2005;280:11347–51.
28. Yang H, Wang H, Ju Z, Ragab AA, Lundback P, Long W, et al. MD-2 is required for disulfide HMGB1-dependent TLR4 signaling. *J Exp Med* 2015;212:5–14.
29. Dziarski R, Viriyakosol S, Kirkland TN, Gupta D. Soluble CD14 enhances membrane CD14-mediated responses to peptidoglycan: structural requirements differ from those for responses to lipopolysaccharide. *Infect Immun* 2000;68:5254–60.
30. Kessel C, Lippitz K, Weinlage T, Hinze C, Wittkowski H, Holzinger D, et al. Proinflammatory cytokine environments can drive interleukin-17 overexpression by $\gamma\delta$ T cells in systemic juvenile idiopathic arthritis. *Arthritis Rheumatol* 2017;69:1480–94.
31. Katayama K, Matsubara T, Fujiwara M, Koga M, Furukawa S. CD14⁺CD16⁺ monocyte subpopulation in Kawasaki disease. *Clin Exp Immunol* 2000;121:566–70.
32. Urbanski K, Ludew D, Filip G, Filip M, Sagan A, Szczepaniak P, et al. CD14⁺CD16⁺⁺ “nonclassical” monocytes are associated with endothelial dysfunction in patients with coronary artery disease. *Thromb Haemost* 2017;117:971–80.
33. Rider P, Carmi Y, Guttman O, Braiman A, Cohen I, Voronov E, et al. IL-1 α and IL-1 β recruit different myeloid cells and promote different stages of sterile inflammation. *J Immunol* 2011;187:4835–43.
34. Fettelschoss A, Kistowska M, LeibundGut-Landmann S, Beer HD, Johansen P, Senti G, et al. Inflammation activation and IL-1 β target IL-1 α for secretion as opposed to surface expression. *Proc Natl Acad Sci U S A* 2011;108:18055–60.
35. Berda-Haddad Y, Robert S, Salers P, Zekraoui L, Farnarier C, Dinarello CA, et al. Sterile inflammation of endothelial cell-derived apoptotic bodies is mediated by interleukin-1 α . *Proc Natl Acad Sci U S A* 2011;108:20684–9.
36. Fukazawa R, Ikegami E, Watanabe M, Hajikano M, Kamisago M, Katsube Y, et al. Coronary artery aneurysm induced by Kawasaki disease in children show features typical senescence. *Circ J* 2007;71:709–15.
37. Miura M, Garcia FL, Crawford SE, Rowley AH. Cell adhesion molecule expression in coronary artery aneurysms in acute Kawasaki disease. *Pediatr Infect Dis J* 2004;23:931–6.
38. Nash MC, Shah V, Dillon MJ. Soluble cell adhesion molecules and von Willebrand factor in children with Kawasaki disease. *Clin Exp Immunol* 1995;101:13–7.
39. Stoll LL, Denning GM, Li WG, Rice JB, Harrelson AL, Romig SA, et al. Regulation of endotoxin-induced proinflammatory activation in human coronary artery cells: expression of functional membrane-bound CD14 by human coronary artery smooth muscle cells. *J Immunol* 2004;173:1336–43.

40. Borzecka K, Plociennikowska A, Bjorkelund H, Sobota A, Kwiatkowska K. CD14 mediates binding of high doses of LPS but is dispensable for TNF- α production. *Mediators Inflamm* 2013;2013:824919.
41. Tremoulet AH, Jain S, Jaggi P, Jimenez-Fernandez S, Pancheri JM, Sun X, et al. Infliximab for intensification of primary therapy for Kawasaki disease: a phase 3 randomised, double-blind, placebo-controlled trial. *Lancet* 2014;383:1731–8.
42. Nozawa T, Imagawa T, Ito S. Coronary-artery aneurysm in tocilizumab-treated children with Kawasaki's disease. *N Engl J Med* 2017;377:1894–6.
43. Matsuda A, Morita H, Unno H, Saito H, Matsumoto K, Hirao Y, et al. Anti-inflammatory effects of high-dose IgG on TNF- α -activated human coronary artery endothelial cells. *Eur J Immunol* 2012;42:2121–31.
44. Miura A, Honma R, Togashi T, Yanagisawa Y, Ito E, Imai J, et al. Differential responses of normal human coronary artery endothelial cells against multiple cytokines comparatively assessed by gene expression profiles. *FEBS Lett* 2006;580:6871–9.
45. Lakota K, Mrak-Poljsak K, Rozman B, Sodin-Semrl S. Increased responsiveness of human coronary artery endothelial cells in inflammation and coagulation. *Mediators Inflamm* 2009;2009:146872.
46. Burns JC, Kone-Paut I, Kuijpers T, Shimizu C, Tremoulet A, Arditi M. Found in translation: international initiatives pursuing interleukin-1 blockade for treatment of acute Kawasaki disease [review]. *Arthritis Rheumatol* 2017;69:268–76.
47. Orenstein JM, Rowley AH. An evaluation of the validity of the animal models of Kawasaki disease vasculopathy. *Ultrastructural Pathol* 2014;38:245–7.
48. Qin J, Jiang Z, Qian Y, Casanova JL, Li X. IRAK4 kinase activity is redundant for interleukin-1 (IL-1) receptor-associated kinase phosphorylation and IL-1 responsiveness. *J Biol Chem* 2004;279:26748–53.
49. Rader DJ. IL-1 and atherosclerosis: a murine twist to an evolving human story. *J Clin Invest* 2012;122:27–30.
50. Koziczak-Holbro M, Joyce C, Gluck A, Kinzel B, Muller M, Tschopp C, et al. IRAK-4 kinase activity is required for interleukin-1 (IL-1) receptor- and toll-like receptor 7-mediated signaling and gene expression. *J Biol Chem* 2007;282:13552–60.
51. Abe J, Jibiki T, Noma S, Nakajima T, Saito H, Terai M. Gene expression profiling of the effect of high-dose intravenous Ig in patients with Kawasaki disease. *J Immunol* 2005;174:5837–45.

Reduced Right Ventricular Output Reserve in Patients With Systemic Sclerosis and Mildly Elevated Pulmonary Artery Pressure

Christian Nagel,¹ Alberto M. Marra,² Nicola Benjamin,³ Norbert Blank,⁴ Antonio Cittadini,⁵ Gerry Coghlan,⁶ Oliver Distler,⁷ Christopher P. Denton,⁶ Benjamin Egenlauf,³ Christoph Fiehn,⁸ Christine Fischer,⁴ Satenik Harutyunova,³ Marius M. Hoeper,⁹ Hanns-Martin Lorenz,⁴ Panagiota Xanthouli,³ Eduardo Bossone,¹⁰ and Ekkehard Grünig³

Objective. This prospective study was undertaken to evaluate right ventricular function and pulmonary arterial compliance (PAC; ratio of stroke volume to pulse pressure) at rest and during exercise in patients with systemic sclerosis (SSc) with normal mean pulmonary artery pressure (PAP), patients with SSc with mildly elevated mean PAP, and patients with SSc with manifest pulmonary hypertension (PH).

Methods. Patients with SSc (n = 112) underwent clinical assessment and right-sided heart catheterization at rest and during exercise and were divided into 3 groups according to their resting mean PAP values: normal mean PAP (≤ 20 mm Hg), mildly elevated mean PAP (21–24 mm Hg), and PH (mean PAP ≥ 25 mm Hg). Results were compared between groups by analysis of variance followed by post hoc Student's *t*-test.

Results. Compared to patients with normal mean PAP, patients with mildly elevated mean PAP had a lower 6-minute walking distance ($P = 0.008$), lower cardiac index ($P = 0.027$) and higher pulmonary vascular resistance ($P = 0.0002$) during exercise, and lower PAC at rest ($P = 0.016$) and different stages of exercise ($P = 0.033$ for 25W and $P = 0.024$ for 75W).

Conclusion. The results of this study suggest that impaired 6-minute walking distance in SSc patients with mildly elevated mean PAP might be caused by reduced PAC during exercise and reduced right ventricular output reserve, presumably due to impaired coupling between the right ventricle and the pulmonary vasculature. These findings provide further evidence of the clinical relevance of mildly elevated mean PAP in patients with SSc.

INTRODUCTION

The natural course of systemic sclerosis (SSc) is often complicated by the occurrence of pulmonary arterial hyper-

tension (PAH) (1,2). Patients with SSc-associated PAH have a lower survival rate than patients with idiopathic PAH (3,4). The current hemodynamic definition of PAH is a resting mean pulmonary artery pressure (PAP) of ≥ 25 mm Hg with elevated

ClinicalTrials.gov identifier: NCT01387035.

Presented by Dr. Marra in partial fulfillment of the requirements for a PhD degree, SDN Scientific Institute for Research and Healthcare, Naples, Italy.

¹Christian Nagel, MD: Heidelberg University Hospital, German Center for Lung Research, Heidelberg, Germany, and Klinikum Mittelbaden Baden-Baden Balg, Baden-Baden, Germany; ²Alberto M. Marra, MD: SDN Scientific Institute for Research and Healthcare, Naples, Italy; ³Nicola Benjamin, MSc, Benjamin Egenlauf, MD, Satenik Harutyunova, MD, Panagiota Xanthouli, MD, Ekkehard Grünig, MD: Heidelberg University Hospital, German Center for Lung Research, Heidelberg, Germany; ⁴Norbert Blank, MD, Christine Fischer, Dr. sc. hum., Hanns-Martin Lorenz, MD: University Hospital Heidelberg, Heidelberg, Germany; ⁵Antonio Cittadini, MD, PhD: University Federico II of Naples, Naples, Italy; ⁶Gerry Coghlan, MD, Christopher P. Denton, MD: Royal Free Hospital, London, UK; ⁷Oliver Distler, MD: University Hospital, Zurich, Switzerland; ⁸Christoph Fiehn, MD: Baden-Baden, Germany; ⁹Marius M. Hoeper, MD: Hannover Medical School, Hannover, Germany; ¹⁰Eduardo Bossone, MD, PhD: A. Cardarelli Hospital, Naples, Italy.

Drs. Nagel and Marra contributed equally to this work.

Dr. Nagel has received consulting fees, speaking fees, and/or honoraria from Actelion, MSD, Boehringer, Novartis, Bayer, and AstraZeneca (less than \$10,000 each). Dr. Hoeper has received consulting fees, speaking fees, and/or honoraria from GlaxoSmithKline, MSD, and Pfizer (less than \$10,000 each) and from Actelion (more than \$10,000). Dr. Lorenz has received consulting fees, speaking fees, and/or honoraria from AbbVie, Bristol-Myers Squibb, Pfizer, Celgene, Medac, GlaxoSmithKline, Roche, Chugai, Novartis, UCB, Janssen-Cilag, AstraZeneca, and Lilly (less than \$10,000 each) and research support from AbbVie, MSD, Bristol-Myers Squibb, Cellgene, Medac, GlaxoSmithKline, Roche, Chugai, Novartis, UCB, Janssen-Cilag, AstraZeneca, Lilly, Baxter, SOBI, Biogen, Actelion, Bayer Vital, Shire, Octapharm, Sanofi, Hexal, Mundipharma, and ThermoFisher. Dr. Grünig has received consulting fees, speaking fees, and/or honoraria from Actelion, Bayer, GlaxoSmithKline, MSD, Novartis, Pfizer, and United Therapeutics (less than \$10,000 each). No other disclosures relevant to this article were reported.

Address correspondence to Ekkehard Grünig, MD, Centre for Pulmonary Hypertension, Thoraxklinik at Heidelberg University Hospital, Röntgenstrasse 1, D-69126 Heidelberg, Germany. E-mail: ekkehard.gruenig@med.uni-heidelberg.de.

Submitted for publication June 21, 2018; accepted in revised form December 13, 2018.

pulmonary vascular resistance (PVR) measured invasively by right-sided heart catheterization (RHC) (5,6). A post hoc analysis of the Detection of PAH in SSc (DETECT) study of SSc patients demonstrated that mildly elevated mean PAP between 21 and 24 mm Hg may represent an intermediate stage between normal mean PAP at rest (<21 mm Hg) and manifest pulmonary hypertension (PH) (7). Previous studies have shown that patients with mildly elevated mean PAP have reduced exercise capacity, higher World Health Organization (WHO) functional class (8,9), a high risk of developing manifest PH (10), and a poor prognosis (1). However, the pathophysiologic mechanisms underlying exercise intolerance in patients with a mean PAP of 21–24 mm Hg remain incompletely characterized.

In the present study we sought to evaluate the response of the right ventricle and pulmonary vasculature to exercise in 3 different groups of SSc patients: patients with a mean PAP of <21 mm Hg (normal resting mean PAP), patients with a mean PAP of 21–24 mm Hg (formerly called borderline mean PAP), and patients with a mean PAP of \geq 25 mm Hg (manifest PH). The question was whether these 3 groups show significant differences in right ventricular output reserve measured by an increase in cardiac index (CI) during exercise and by pulmonary arterial compliance (PAC) during exercise, as determined by Swan-Ganz RHC in routine clinical practice. Right ventricular output reserve is an emerging parameter which has been shown to be of prognostic importance in patients with PH (11,12). For estimation of PAC (or capacitance), the measurement of the ratio of stroke volume to pulse pressure (where stroke volume is defined as cardiac output [CO] divided by heart rate and pulse pressure is defined as systolic PAP minus diastolic PAP) by RHC has been shown to be the simplest and most practical method (13,14). Furthermore, right ventricular output reserve and PAC may add crucial information for the detection of pulmonary vascular disease in this at-risk population at an early stage (15,16), which may also assist in defining an indication for early targeted treatment.

PATIENTS AND METHODS

Study population and design. Patients with diffuse cutaneous SSc (dcSSc) and patients with limited cutaneous SSc (lcSSc) who were referred to our center for the purpose of PH screening were prospectively and consecutively enrolled in this study between October 2012 and August 2016. The referring specialists were rheumatologists, cardiologists, pulmonologists, and general practitioners. A definite diagnosis of SSc was confirmed by experienced rheumatologists (N. Blank, C. Fiehn, and H-ML) according to the standard criteria of the American College of Rheumatology (17). Exclusion criteria were inability to perform exercise RHC, manifest PH confirmed by RHC prior to enrollment, current PAH therapy, renal insufficiency, systemic arterial hypertension with pressure values >180/95 mm Hg at rest or >230/120

mm Hg during exercise despite optimized medical treatment, previous evidence of clinically relevant left-sided heart or lung disease, or pregnancy.

All patients who were referred to our center who did not fulfill the exclusion criteria were entered into the study even if baseline echocardiography did not suggest PH. All patients underwent a detailed clinical examination, including medical history, physical examination, electrocardiography, 2-dimensional echocardiography at rest, lung function test, measurement of arterial blood gases, chest radiography, functional class assessment, 6-minute walking distance test under standardized conditions (18), laboratory testing including N-terminal pro-brain natriuretic peptide levels, and RHC at rest and during exercise. All patients underwent a 12-lead electrocardiogram (Hellige EK 512 P). High-resolution computed tomography (CT), ventilation/perfusion single-photon-emission CT, and CT angiography of the lungs were performed in all patients to diagnose suspected chronic thromboembolic PH, interstitial lung disease, or other respiratory diseases. Patients diagnosed as having those diseases were excluded from the study. Left-sided heart catheterization was performed in all patients with suspected left-sided heart disease. Manifest PH/PAH was diagnosed according to the current European Society of Cardiology (ESC)/European Respiratory Society (ERS) guidelines (6).

Definitions of pulmonary hypertension and pulmonary arterial hypertension. PH and PAH were defined according to current ESC/ERS guidelines (6). The hemodynamic definition for PH is mean PAP \geq 25 mm Hg. The definition of PAH (group 1 according to the WHO classification) is mean PAP \geq 25 mm Hg and pulmonary artery wedge pressure (PAWP) \leq 15 mm Hg.

Right-sided heart catheterization. SSc patients were consecutively referred for RHC in order to screen this at-risk population for manifest PH. Patients were examined on a variable load supine bicycle ergometer (model 8420; KHL) by experienced investigators (CN and BE). The examination at rest was performed as previously described (1), in a supine position using the transjugular access with an 8F introducer set (MXI100; MEDEX Smiths Group). Catheterization was done using triple-lumen 7F Swan-Ganz thermodilution catheters (catalog no. 131F7; Edwards Lifesciences).

After measurement of hemodynamic parameters at rest, the supine position was changed to a 45° position. The zero reference point for pressure recordings was set at midchest at the insertion of the fourth rib to the sternum, consistent with current recommendations (19), at the left atrial level. Zero leveling at the 45° position was performed at the intersection of the frontal plane at the midthoracic level, the transverse plane at the level of the fourth anterior intercostal space, and the midsagittal plane at the left atrial level (20). The pulmonary vascular pressures (mean PAP and PAWP) were averaged throughout 3 respiratory cycles. CO

was measured at least in triplicate at rest and in duplicate at the end of each workload step during exercise by thermodilution, with a variation of <10% between the measured values. Exercise testing started at 25W and was increased 25W every 2 minutes until symptom-limited exercise capacity was reached. The pulmonary vascular pressures (mean PAP and PAWP), CO, heart rate, and systemic blood pressure were measured at the end of each workload step, consistent with current recommendations (20).

Transpulmonary pressure gradient (TPG) was defined as the difference between mean PAP and PAWP. PAC was calculated as the ratio of stroke volume to pulse pressure, where stroke volume was defined as CO divided by heart rate and pulse pressure was defined as systolic PAP minus diastolic PAP. Right ventricular output reserve was defined and measured by the increase in CI during incrementally increased exercise on the variable load supine bicycle ergometer compared to CI at rest. All examinations and measurements were performed by the same experienced team (CN, BE, and SH). There were no complications.

Transthoracic Doppler echocardiography at rest. A complete left- and right-sided echocardiographic examination was performed as previously described (16). Two-dimensional and color-flow guided continuous wave Doppler echocardiographic recordings at rest were obtained by experienced cardiac sonographers (CN, BE, SH, and EG) using 3.6–4 MHz Duplex probes and conventional equipment (Vivid 7; GE Healthcare) as previously described (16). Pulmonary artery systolic pressure was

estimated from peak tricuspid regurgitation jet velocities according to the equation $PASP = 4 (V)^2 + \text{right atrial pressure}$, where V is the peak velocity (in meters/second) of tricuspid regurgitation velocity (21). For all calculations the mean value of at least 3 tricuspid regurgitation velocity measurements was used. Right atrial pressure was estimated from characteristics of the inferior vena cava (22). If it was <20 mm in diameter and decreased during inspiration, 5 mm Hg were added. If it was ≥ 20 mm, 10 mm Hg were added.

Ethics statement. This study was conducted in accordance with Good Clinical Practice and the current version of the revised Declaration of Helsinki. The ethics committee of the University of Heidelberg approved the study (Internal Ethics No. S-360/2009). Written informed consent was obtained from each patient prior to enrollment.

Statistical analysis. Statistical analyses were conducted by 2 statisticians (N. Benjamin and C. Fischer). Data are presented as the mean \pm SD or number (%). Patients were divided into 3 groups according to their resting mean PAP values: normal mean PAP (≤ 20 mm Hg), mildly elevated mean PAP (21–24 mm Hg), and manifest PH (mean PAP ≥ 25 mm Hg) (Figure 1). Data for the 3 groups at rest were compared using analysis of variance (ANOVA) for quantitative variables and chi-square test or Fisher's exact test for categorical variables. The comparison of variables at rest and various levels of

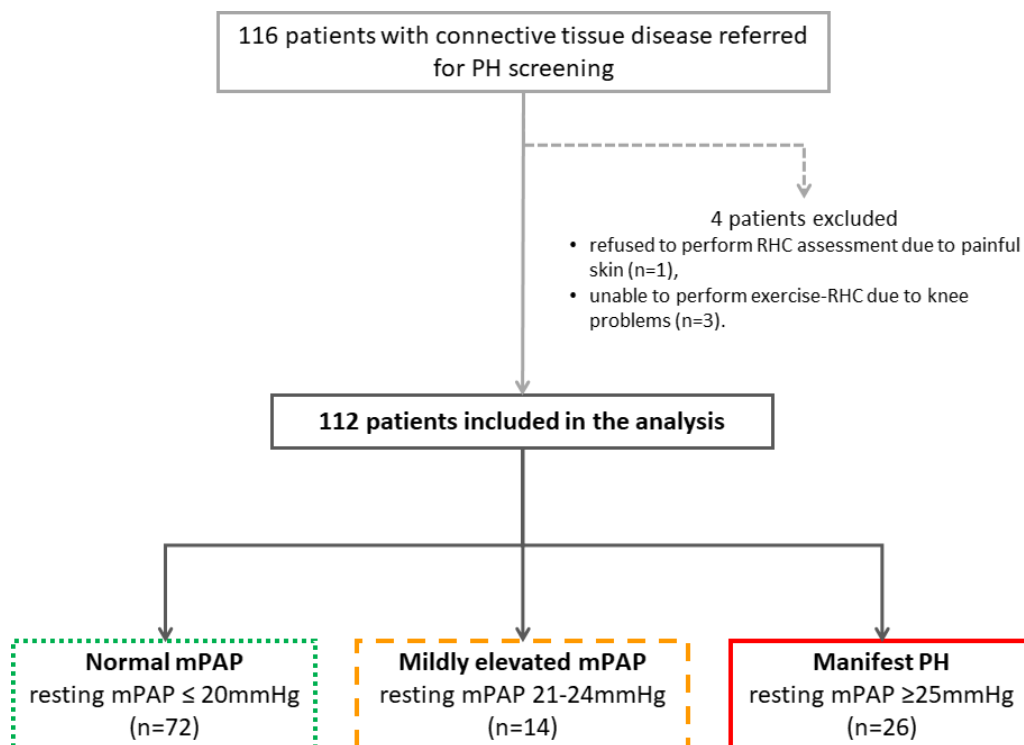


Figure 1. Disposition of the study patients. PH = pulmonary hypertension; RHC = right-sided heart catheterization; mPAP = mean pulmonary artery pressure.

Table 1. Clinical characteristics of the overall study population and the 3 groups of patients classified by hemodynamic findings*

	All patients (n = 112)†	Patients with normal mean PAP (n = 72)‡	Patients with mildly elevated mean PAP (n = 14)§	Patients with mani- fest PH (n = 26)¶	<i>P</i> among all groups (by ANOVA)	<i>P</i> , normal vs. mildly elevated mean PAP (by <i>t</i> -test)	<i>P</i> , mildly elevated mean PAP vs. manifest PH (by <i>t</i> -test)	<i>P</i> , normal vs. manifest PH (by <i>t</i> -test)
Sex, no. (%) female	88 (78.6)	55 (76.4)	12 (85.7)	21 (80.8)	NS	NT	NT	NT
Age, years	57.5 ± 13.0	54.1 ± 12.9	58.1 ± 11.0	66.7 ± 9.3	<0.0001	NS	0.014	<0.0001
Height, cm	165.4 ± 8.3	166.8 ± 7.7	163.5 ± 9.0	162.7 ± 8.9	NS	NT	NT	NT
Weight, kg	70.2 ± 15.1	71.8 ± 16.8	69.6 ± 12.0	66.2 ± 10.7	NS	NT	NT	NT
Systolic BP, mm Hg	124.6 ± 18.6	120.1 ± 15.1	138.6 ± 16.9	129.5 ± 23.4	0.001	0.001	NS	0.063
Diastolic BP, mm Hg	78.3 ± 11.1	77.1 ± 9.6	80.5 ± 13.6	80.3 ± 13.4	NS	NT	NT	NT
6-minute walking distance, m	436 ± 98	474 ± 79	396 ± 87	342 ± 87	<0.0001	0.008	NS	<0.0001
NT-proBNP, ng/ml	385 ± 580	201 ± 239	444 ± 677	977 ± 897	<0.001	NS	NS	0.005
SSc characteristics								
Type of SSc, no. (%)					NS	NT	NT	NT
dcSSc	76 (67.9)	46 (63.9)	11 (78.6)	15 (57.7)				
lcSSc (CREST syndrome)	36 (32.1)	26 (36.1)	3 (21.4)	11 (42.3)				
Disease duration, years	10.1 ± 9.1	8.6 ± 8.7	14.3 ± 9.8	11.7 ± 9.3	NS	NT	NT	NT
Digital ulcers, no. (%)	31 (27.7)	19 (26.4)	2 (14.3)	10 (38.5)	NS	NT	NT	NT
MRSS	14.8 ± 9.2	12.6 ± 7.5	20.3 ± 11.2	18.9 ± 11.1	0.019	NS	NS	0.029
Concomitant diseases, no. (%)								
Mild SSc-associated ILD	31 (27.7)	17 (23.6)	5 (35.7)	9 (34.6)	NS#	NT	NT	NS#
CAD	13 (11.6)	7 (9.7)	2 (14.3)	4 (15.4)	NS#	NT	NT	NS#
Arterial hypertension	34 (30.4)	16 (22.2)	5 (35.7)	13 (50.0)	<0.028#	NS#	NS#	<0.008#
Lung function								
Maximum VC, %	93.9 ± 23.2	98.3 ± 20.6	77.3 ± 18.1	90.4 ± 28.1	0.007	0.001	NS	NS
FEV ₁ , %	91.0 ± 23.3	96.7 ± 20.4	71.7 ± 18.5	85.3 ± 26.7	<0.001	<0.001	NS	0.028
TLC, %	93 ± 22	96 ± 22	85 ± 20	88 ± 25	NS	NT	NT	NT
Echocardiography								
Right ventricle free wall thickness, mm	6.7 ± 1.2	6.5 ± 1.2	6.5 ± 0.7	7.5 ± 1.3	0.007	NS	0.016	0.004
TAPSE, mm	23.6 ± 4.5	24.1 ± 3.8	24.1 ± 6.7	21.8 ± 4.7	NS	NT	NT	NS
Right atrium area, cm ²	12.5 ± 4.1	11.6 ± 3.2	11.0 ± 2.3	15.5 ± 5.3	<0.0001	NS	0.004	<0.0001
Right ventricle area, cm ²	15.4 ± 4.1	14.8 ± 3.8	13.8 ± 3.2	17.9 ± 4.2	0.001	NS	0.003	0.001
Estimated systolic PAP, mm Hg**	32.0 ± 14.5	26.1 ± 7.2	27.9 ± 4.6	50.2 ± 17.9	<0.0001	NS	<0.0001	<0.0001
Pericardial effusion, no. (%)	5 (4.5)	1 (1.4)	2 (14.3)	2 (2.7)	NS	NT	NT	NS

(Continued)

Table 1. (Cont'd)

WHO functional class, no. (%)	All patients (n = 112)†	Patients with normal mean PAP (n = 72)‡	Patients with mildly elevated mean PAP (n = 14)§	Patients with manifest PH (n = 26)¶	P among all groups (by ANOVA)	P, normal vs. mildly elevated mean PAP (by t-test)	P, mildly elevated mean PAP vs. manifest PH (by t-test)	P, normal vs. manifest PH (by t-test)
I	19 (17.0)	18 (25.0)	1 (7.1)	0 (0)	<0.0001#	NS#	0.030#	<0.0001#
II	62 (55.3)	45 (62.5)	9 (64.3)	8 (30.8)				
III	31 (27.7)	9 (12.5)	4 (28.6)	18 (69.2)				
IV	0 (0)	0 (0)	0 (0)	0 (0)				

* Except where indicated otherwise, values are the mean \pm SD. PH = pulmonary hypertension; ANOVA = analysis of variance; NS = not significant; NT = not tested; BP = blood pressure; NT-proBNP = N-terminal pro-brain natriuretic peptide; SSc = systemic sclerosis; dcSSc = diffuse cutaneous SSc; lcSSc = limited cutaneous SSc; CREST = calcinosis, Raynaud's phenomenon, esophageal dysmotility, sclerodactyly, telangiectasias; ILD = interstitial lung disease; CAD = coronary artery disease; VC = vital capacity; FEV₁ = forced expiratory volume in 1 second; TLC = total lung capacity; TAPSE = tricuspid annular plane systolic excursion; WHO = World Health Organization.

† Data were available for 105 patients for 6-minute walking distance, 70 patients for modified Rodnan skin thickness score (MRSS), 90 patients for right ventricle free wall thickness, and 111 patients for right atrium area and estimated systolic pulmonary artery pressure (PAP).

‡ Data were available for 69 patients for 6-minute walking distance, 47 patients for MRSS, 61 patients for right ventricle free wall thickness, and 71 patients for right atrium area and estimated systolic PAP.

§ Defined as mean PAP of 21–24 mm Hg. Data were available for 13 patients for 6-minute walking distance, 3 patients for MRSS, and 11 patients for right ventricle free wall thickness.

¶ Data were available for 23 patients for 6-minute walking distance, 20 patients for MRSS, and 18 patients for right ventricle free wall thickness.

By chi-square test.

** Measured by transthoracic echocardiography.

exercise or maximum level of exercise between the 3 groups were performed using ANOVA and mixed model ANOVA, respectively. If a significant difference was detected by ANOVA, post hoc tests were performed to compare patients with normal mean PAP and those with mildly elevated mean PAP. Post hoc analyses were conducted using Student's *t*-tests. All tests were 2-sided. *P* values of 0.05 were considered significant. For post hoc tests, statistical significance remained when *P* values were <0.016, <0.025, and <0.05 for the first, second, and third *P* value when ordered from lowest to highest (Bonferroni-Holm correction). Correlations of PAC at rest with 6-minute walking distance, Δ CO, and Δ CI were determined by Pearson's correlation analysis. All analyses were performed using IBM SPSS version 23.

RESULTS

Clinical characteristics of the patients. We prospectively included 116 patients diagnosed as having SSc. Four patients were excluded due to inability to perform RHC. One patient refused RHC assessment due to painful skin. Three patients were not able to perform exercise RHC due to knee or hip problems. There were no complications. Thus, the final study group consisted of 112 patients with SSc (88 women) with a mean \pm SD age of 57 \pm 13 years. Of these patients, 76 (67.9%)

had dcSSc and 36 (32.1%) had lcSSc (CREST syndrome [calcinosis, Raynaud's phenomenon, esophageal dysmotility, sclerodactyly, telangiectasias]) (Table 1). According to RHC measurements at rest, 72 patients (64.3%) presented with normal mean PAP (\leq 20 mm Hg), 14 (12.5%) with mildly elevated mean PAP (21–24 mm Hg), and 26 (23.2%) with manifest PH (mean PAP \geq 25 mm Hg) (Figure 1).

The patients with PH had been newly diagnosed during the study. Most of them had been diagnosed at a relatively early stage of disease, with a mean PAP of 32.5 \pm 7.2 mm Hg, a mean PVR of 326.2 \pm 188.3 dynes \cdot sec \cdot cm⁻⁵, and normal right ventricular function at rest but with impaired WHO functional class and exercise capacity (Table 1). Of the 26 patients with PH, 10 had PAH, 8 had PH due to left-sided heart disease, and 8 had PH due to lung disease. Of the 14 patients with mildly elevated mean PAP, 2 had concomitant coronary artery disease and 5 had concomitant interstitial lung disease.

Comparison of clinical parameters. The 3 groups (patients with normal mean PAP, patients with mildly elevated mean PAP, and patients with manifest PH) differed in age, with patients with manifest PH having the highest mean age (mean \pm SD 54.1 \pm 12.9 years for patients with normal mean PAP, 58.1 \pm 11.0 years for patients with mildly elevated mean PAP, and 66.7 \pm 9.3 years for patients with manifest PH; *P* < 0.0001 by

Table 2. Hemodynamic findings at rest and during exercise*

	Patients with normal mean PAP (n = 72)	Patients with mildly elevated mean PAP (n = 14)	Patients with manifest PH (n = 26)	P among all groups (by ANOVA)	P, normal vs. mildly elevated mean PAP (by t-test)	P, mildly elevated mean PAP vs. manifest PH (by t-test)	P, normal vs. manifest PH (by t-test)
Rest							
RAP, mm Hg	4.1 ± 2.8	4.5 ± 3.0	6.8 ± 4.5	0.003	NS	0.096	0.008
Systolic PAP, mm Hg	24.3 ± 4.6	33.5 ± 4.0	54.4 ± 15.1	<0.0001	<0.0001	<0.0001	<0.0001
Diastolic PAP, mm Hg	9.6 ± 2.5	12.8 ± 2.1	20.9 ± 5.7	<0.0001	<0.0001	<0.0001	<0.0001
Mean PAP, mm Hg	14.9 ± 3.0	22.0 ± 1.0	32.5 ± 7.2	<0.0001	<0.0001	<0.0001	<0.0001
PAWP, mm Hg	7.5 ± 3.0	9.3 ± 12.7	12.8 ± 19.7	<0.0001	0.039	0.013	<0.0001
TPG, mm Hg	7.5 ± 2.6	2.8 ± 3.0	5.7 ± 9.7	<0.0001	<0.0001	0.001	<0.0001
CO, liters/minute	5.3 ± 1.2	5.7 ± 1.0	5.1 ± 1.0	NS	NT	NT	NT
CI, liters/minute·m ⁻²	3.0 ± 0.6	3.3 ± 0.6	3.0 ± 0.5	NS	NT	NT	NT
PVR, dynes·seconds·cm ⁻⁵	117 ± 45	179 ± 32	326 ± 188	<0.0001	0.001	<0.0001	<0.0001
Peak workload							
Systolic PAP, mm Hg	48.8 ± 12.6	57.6 ± 10.2	84.4 ± 20.6	<0.0001	0.006	<0.0001	<0.0001
Diastolic PAP, mm Hg	21.7 ± 6.3	24.1 ± 5.7	30.4 ± 7.5	<0.0001	NS	0.098	<0.0001
Mean PAP, mm Hg	31.7 ± 7.5	37.4 ± 6.3	49.2 ± 10.0	<0.0001	<0.0001	<0.0001	<0.0001
PAWP, mm Hg	13.2 ± 6.7	13.4 ± 6.8	14.4 ± 7.0	NS	NT	NT	NT
TPG, mm Hg	18.4 ± 7.4	24.7 ± 7.4	34.8 ± 13.1	<0.0001	0.034	0.009	<0.0001
CO, liters/minute	11.1 ± 3.0	9.2 ± 2.3	8.5 ± 2.8	<0.0001	0.04	NS	<0.0001
CI, liters/minute·m ⁻²	6.3 ± 1.8	5.4 ± 0.9	4.9 ± 1.5	0.001	0.027	NS	0.001
PVR, dynes·seconds·cm ⁻⁵	140 ± 64	215 ± 77	377 ± 212	<0.0001	0.0002	0.001	<0.0001
Systolic BP, mm Hg	168 ± 27	157 ± 23	173 ± 22	NS	NT	NT	NT
Diastolic BP, mm Hg	90.7 ± 12.0	88.9 ± 14.1	93.9 ± 15.5	NS	NT	NT	NT
Workload, W	76.7 ± 21.9	62.5 ± 25.5	51.9 ± 19.9	<0.0001	0.033	NS	<0.0001
Δ systolic PAP, mm Hg	24.2 ± 11.0	23.6 ± 8.06	29.0 ± 12.4	NS	NT	NT	NT
Δ diastolic PAP, mm Hg	12.1 ± 6.3	11.2 ± 5.95	9.5 ± 5.5	NS	NT	NT	NT
Δ mean PAP, mm Hg	16.7 ± 7.1	15.4 ± 6.11	16.7 ± 7.1	NS	NT	NT	NT
Δ PAWP, mm Hg	5.8 ± 6.8	4.1 ± 6.42	1.6 ± 5.0	0.02	NS	NS	0.002
Δ TPG, mm Hg	18.4 ± 7.4	24.1 ± 7.38	34.8 ± 13.1	NS	NT	NT	NT
Δ CO, liters/minute	5.8 ± 2.6	3.5 ± 2.50	3.3 ± 2.2	<0.0001	0.003	NS	<0.0001
Δ CI, liters/minute·m ⁻²	3.3 ± 1.5	2.1 ± 1.18	1.9 ± 1.2	<0.0001	0.006	NS	<0.0001
Δ PVR, dynes·sec·cm ⁻⁵	24 ± 68	36 ± 92	51 ± 110	NS	NT	NT	NT
Δ systolic BP, mm Hg	47.4 ± 27.3	19.2 ± 22.1	43.5 ± 28.1	0.004	0.001	0.01	NS
Δ diastolic BP, mm Hg	13.3 ± 15.1	6.8 ± 16.7	13.7 ± 15.6	NS	NT	NT	NT
Δ heart rate, bpm	48.7 ± 20.7	41.9 ± 12.7	45.3 ± 25.1	NS	NT	NT	NT

* Values are the mean ± SD. PAP = pulmonary artery pressure; PH = pulmonary hypertension; ANOVA = analysis of variance; RAP = right atrial pressure; NS = not significant; PAWP = pulmonary artery wedge pressure; TPG = transpulmonary pressure gradient; CO = cardiac output; NT = not tested; CI = cardiac index; PVR = pulmonary vascular resistance; BP = blood pressure.

ANOVA) (Table 1). The modified Rodnan skin thickness score also differed between groups (12.6 ± 7.5 for patients with normal mean PAP, 20.3 ± 11.2 for patients with mildly elevated mean PAP, and 18.9 ± 11.1 for patients with manifest PH; $P = 0.019$ by ANOVA) (Table 1). There were no significant differences between

patients with normal mean PAP and those with mildly elevated mean PAP with regard to sex, body size, duration of SSc, or functional class (Table 1). A comparable prevalence of coronary artery disease and mild SSc-associated interstitial lung disease was found among the 3 different groups.

Although patients with mildly elevated mean PAP had higher values of resting systolic blood pressure than those with normal mean PAP (mean ± SD 138.6 ± 16.9 mm Hg versus 120.1 ± 15.1 mm Hg) (*P* = 0.001), their mean systolic blood pressure during maximum workload did not significantly differ from that in patients with normal mean PAP (156.9 ± 22.8 mm Hg versus 167.6 ± 26.8 mm Hg; *P* > 0.05) (Table 2). Furthermore, PAWP during exercise did not significantly differ between groups.

Exercise capacity. The mean 6-minute walking distance differed significantly between the 3 groups (*P* < 0.0001 by ANOVA), with the shortest walking distance in the manifest PH group (mean ± SD 342 ± 87 meters), followed by the group with mildly elevated mean PAP (396 ± 87 meters), and the longest walking distance in the group with normal mean PAP (474 ± 79 meters) (Table 1). Patients with mildly elevated mean PAP had a significantly lower mean 6-minute walking distance compared to the group with normal hemodynamic findings (*P* = 0.008) (Table 1).

The difference in exercise capacity was also seen in a difference in peak workload (*P* < 0.001 by ANOVA), with the highest peak workload in patients with normal mean PAP (76.7 ± 21.9W), and the lowest peak workload in patients with manifest PH (51.9 ± 19.9W). The peak workload in patients with mildly elevated mean PAP (62.5 ± 25.5W) was lower than that in patients with normal mean PAP (*P* = 0.033). Patients with mildly elevated mean PAP

did not significantly differ from those with manifest PH in peak workload.

Echocardiographic findings. The echocardiographic measurements showed no significant differences between patients with normal mean PAP and those with mildly elevated mean PAP with regard to the size of the right atrium and the right ventricle as well as systolic function measured by tricuspid annular plane systolic excursion and estimated pulmonary artery systolic pressure assessed by transthoracic Doppler echocardiography at rest. As expected, patients with manifest PH had a larger right atrium (15.5 ± 5.3 cm² versus 11.6 ± 3.2 cm²; *P* < 0.0001) and right ventricle area (17.9 ± 4.2 cm² versus 14.8 ± 3.8 cm²; *P* = 0.001) as well as a thicker right ventricle free wall (7.5 ± 1.3 mm versus 6.5 ± 1.2 mm; *P* = 0.004) than patients with normal hemodynamic findings (Table 1). Patients with mildly elevated mean PAP at rest differed significantly from patients with manifest PH in right atrium area (*P* = 0.004), right ventricle area (*P* = 0.003), systolic PAP (*P* < 0.0001), and right ventricle free wall (*P* = 0.016) (Table 1).

Pulmonary hemodynamic findings at rest. Patients with mildly elevated mean PAP showed significantly higher mean PVR at rest than patients with normal mean PAP (179 ± 32 versus 117 ± 45 dynes · sec · cm⁻⁵; *P* = 0.001) (Table 2) and higher TPG (12.7 ± 3 versus 7.5 ± 2.6 mm Hg; *P* < 0.0001) (Table 2). Values

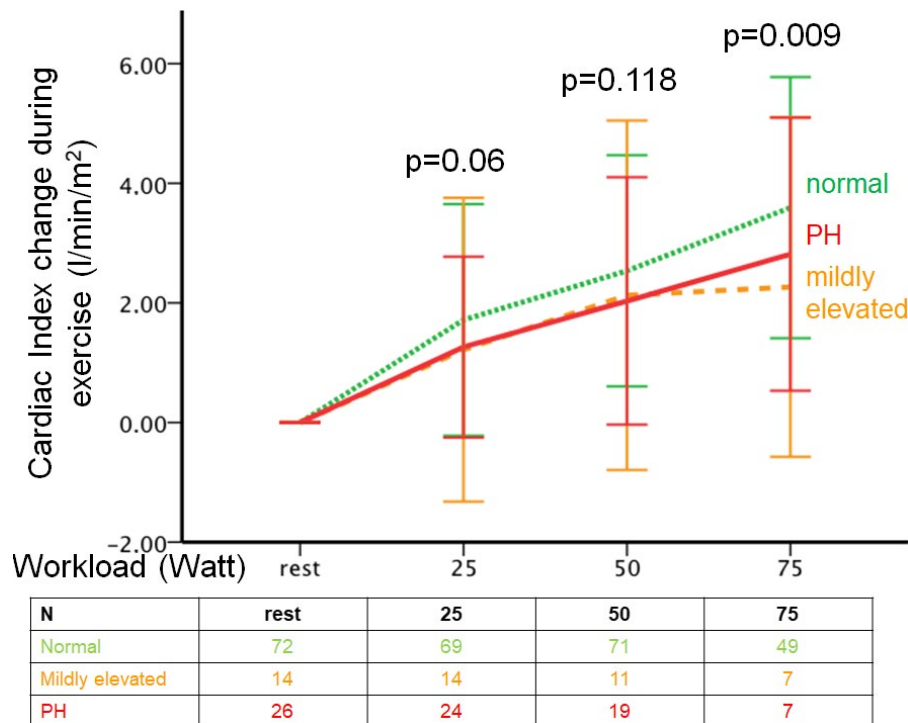


Figure 2. Increase in cardiac index (CI) during exercise in patients with normal mean pulmonary artery pressure (PAP), patients with mildly elevated mean PAP, and patients with manifest pulmonary hypertension (PH). Similar values were seen for patients with mildly elevated mean PAP and those with manifest PH. *P* values shown are for the differences between all 3 groups and were determined by analysis of variance. At a workload of 75W, patients with mildly elevated mean PAP had a significantly smaller increase in CI than patients with normal mean PAP (*P* = 0.005 by *t*-test). Error bars show ± 2 SD. Values are the number of patients in each group at each workload level. Color figure can be viewed in the online issue, which is available at <http://onlinelibrary.wiley.com/doi/10.1002/art.40814/abstract>.

for PVR and TPG were significantly lower in patients with mildly elevated mean PAP than in patients with manifest PH ($P < 0.0001$ and $P = 0.001$, respectively) (Table 2).

Mean PAWP was within normal range in patients with normal mean PAP, mildly elevated mean PAP, and manifest PH (Table 2). No differences were found among the 3 groups with regard to right ventricular function at rest (CO and CI at rest) (Table 2).

Pulmonary hemodynamic findings during exercise.

Patients with mildly elevated mean PAP at rest had significantly higher mean PAP and systolic pulmonary pressure at peak workload than patients with normal mean PAP at rest (mean PAP at peak workload 37.4 ± 6.3 mm Hg versus 31.7 ± 7.5 mm Hg; $P < 0.0001$). Patients with mildly elevated mean PAP had a significantly lower increase in CO and CI during exercise than patients with normal mean PAP (peak CI 5.4 ± 0.9 versus 6.3 ± 1.8 liters/minute/ m^2 ; $P = 0.027$ and Δ CI 2.1 ± 1.2 versus 3.3 ± 1.5 liters/minute/ m^2 ; $P = 0.006$) (Table 2) and did not significantly differ from patients with manifest PH.

Increases in CI during exercise showed an almost congruent course in patients with mildly elevated mean PAP and those with manifest PH up to the 50W level (Figure 2). At 75W, patients with mildly elevated mean PAP had a lower mean increase in CI than patients with manifest PH (for all 3 groups, $P = 0.009$ by ANOVA; for normal mean PAP versus mildly ele-

vated mean PAP, $P = 0.005$ by *t*-test). Two patients with mildly elevated mean PAP had a drop in CI during exercise, one at 25W and one at 50W.

Patients with mildly elevated mean PAP had a significantly higher TPG than patients with normal mean PAP at rest, 25W (both $P < 0.001$), and 75W ($P = 0.008$), and there was a trend toward a significant difference between these groups at 50W ($P = 0.059$). The slope of the increase in TPG during exercise was similar in patients with mildly elevated mean PAP and those with normal mean PAP.

PAC differed significantly between the 3 groups at rest and for each workload (each $P \leq 0.01$). Patients with mildly elevated mean PAP had a significantly lower PAC than patients with normal mean PAP at rest ($P = 0.016$), as well as at 25W ($P = 0.033$) and 75W ($P = 0.024$) (Figure 3). PAC at rest significantly correlated with 6-minute walking distance ($R = 0.448$, $P < 0.001$) (Figure 4) and Δ CO ($R = 0.227$, $P = 0.018$) and showed a trend toward significant correlation with Δ CI ($R = 0.178$; $P = 0.064$).

DISCUSSION

To the best of our knowledge, this is the first prospective study to assess and compare right ventricular output reserve and PAC in SSc patients with mildly elevated mean PAP, SSc patients

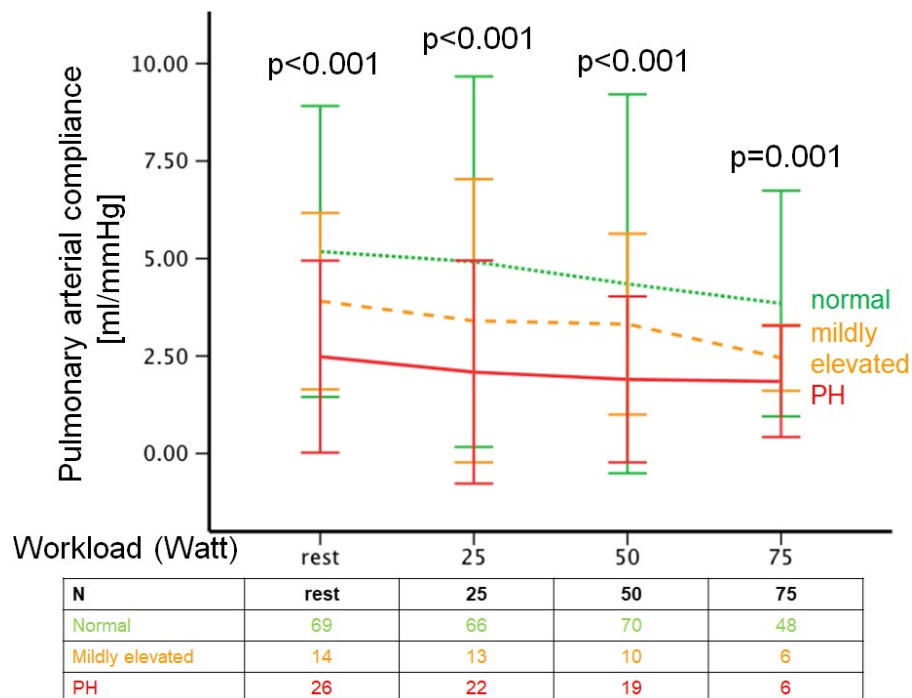


Figure 3. Pulmonary arterial compliance (PAC) during exercise in patients with normal mean pulmonary artery pressure (PAP), patients with mildly elevated mean PAP, and patients with manifest pulmonary hypertension (PH). PAC differed significantly between the 3 groups at each workload level ($P \leq 0.01$ for all, by analysis of variance). Patients with mildly elevated mean PAP had a significantly lower PAC than patients with normal mean PAP both at rest ($P = 0.016$) and during exercise at 25W ($P = 0.033$) and 75W ($P = 0.024$). Error bars show ± 2 SD. Values are the number of patients in each group at each workload level. Color figure can be viewed in the online issue, which is available at <http://onlinelibrary.wiley.com/doi/10.1002/art.40814/abstract>.

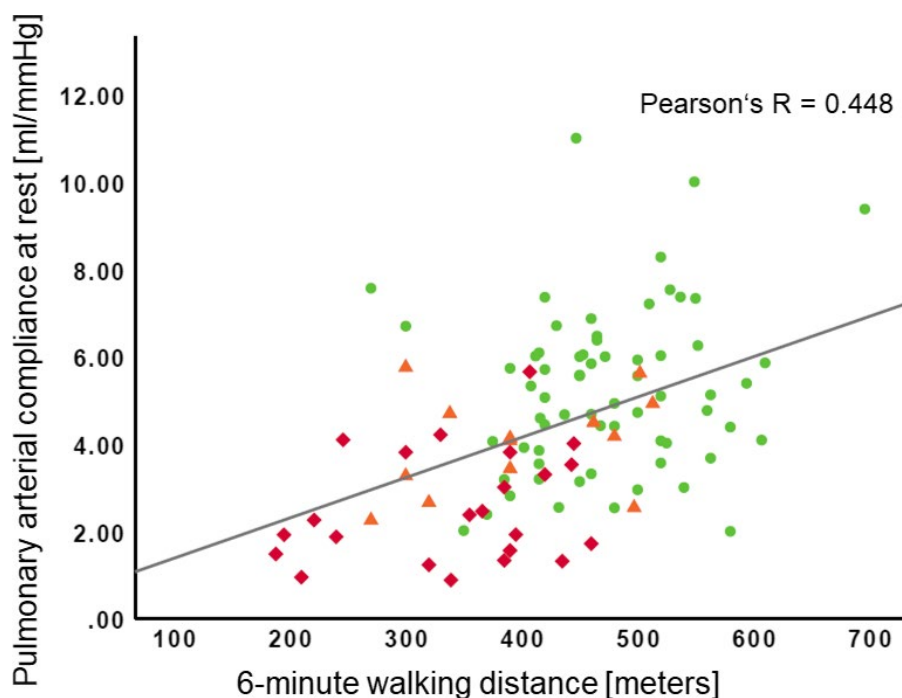


Figure 4. Significant correlation between pulmonary arterial compliance at rest and 6-minute walking distance, determined by Pearson's correlation analysis. Circles represent patients with mean pulmonary artery pressure (PAP) of ≤ 20 mm Hg, triangles represent patients with mean PAP of 21–24 mm Hg, and squares represent patients with mean PAP of ≥ 25 mm Hg. Color figure can be viewed in the online issue, which is available at <http://onlinelibrary.wiley.com/doi/10.1002/art.40814/abstract>.

with normal mean PAP, and SSc patients with manifest PH. The present study showed that SSc patients with mildly elevated mean PAP had normal CI values at rest but reduced right ventricular output reserve (defined as reduced CI during exercise) and reduced PAC compared to SSc patients with normal mean PAP at rest. Furthermore, SSc patients with mildly elevated mean PAP had higher PVR and TPG values than patients with normal mean PAP. The impairment in right ventricular function and pulmonary hemodynamic parameters in patients with mildly elevated mean PAP was associated with a shorter 6-minute walking distance and reduced peak exercise capacity compared to SSc patients with normal resting hemodynamic findings.

Right ventricular output reserve was reduced in SSc patients with mildly elevated mean PAP. Mean right ventricle CI at rest was normal in patients with mildly elevated mean PAP and did not differ from that in patients with normal mean PAP, as previously described (7,8,23). Even right-sided heart size (mean right atrial and ventricular areas) measured by echocardiography was comparable between groups. Thus, reduced right ventricular output reserve, reduced PAC, and higher PVR and TPG were the only hemodynamic parameters that characterized patients with mildly elevated mean PAP and might be the pathophysiologic underpinning of symptoms, reduced 6-minute walking distance, and reduced exercise capacity in these patients. These data suggest that hemodynamic findings during exercise might be more sensitive to early right ventricular dysfunction and vascular remodeling than hemodynamic findings at rest.

Right ventricular output reserve and contractile reserve in patients with PAH have previously been assessed using different methods and surrogate parameters, including invasive single-beat pressure-volume loop analysis (24–26), stress Doppler echocardiography assessing the capability of patients to increase right ventricular systolic pressure during low-level exercise (16), and echocardiographic strain during stress Doppler echocardiography (27). Although invasive single-beat pressure-volume loop analysis (27) is most likely the most sophisticated method to evaluate load-independent right ventricular contractile reserve, its application can be dangerous for patients (due to stiff catheters), is too costly and complex for routine clinical practice, and requires special equipment such as conductance catheters with special software for online pressure-volume signals (28,29) and transit-time ultrasonic flow probes (24). Therefore, RHC by Swan-Ganz catheters has previously been used to assess the increase in CI during exercise in PAH patients (11,12) and was performed in this study. It seems to be a simple and useful method of measuring right ventricular output reserve.

Reduced PAC in patients with mildly elevated mean PAP might indicate early vascular remodeling. Whereas right ventricular function was impaired during exercise only, PAC was significantly reduced at rest and during all exercise levels in patients with mildly elevated mean PAP and patients with PH compared to patients with normal mean PAP (Figure 3). Decreased PAC has been described in patients with idiopathic PAH (14) and was correlated with PH severity (30). In the present study, PAC was calculated

from RHC data, and it has been shown that PAC may be used to detect early vascular disease in patients at risk of developing PAH. This finding is consistent with the elevated PVR and TPG in SSc patients with mildly elevated mean PAP that was previously demonstrated in a retrospective study by Kovacs et al (8). Reduced PAC increases right ventricular pulsatile workload (31) and can lead to right ventricular dysfunction and failure (32,33). In patients with PAH, PAC was a stronger predictor of prognosis and response to therapy than PVR alone (34–37).

Right ventricle–pulmonary artery uncoupling requires pulmonary vascular disease, reduced right ventricular output reserve, or both. SSc patients show myocardial involvement even in the absence of PH. Hsu et al showed that patients with SSc who do not yet have resting PAH also exhibit abnormal sarcomere function due to reduced maximal calcium-activated tension and an abnormal increase in calcium sensitivity (38). This depressed right ventricular output reserve was also observed in manifest SSc-associated PAH compared to idiopathic PAH (26,39).

Besides a possible early pulmonary vascular disease indicated by reduced PAC, SSc patients with mildly elevated PAP might be affected by impaired myocardial contractility and therefore their exercise capacity, symptom load, and quality of life might be more affected.

We observed an overlap between the group of patients with a mean PAP of 21–24 mm Hg and those with exercise-induced PH. A resting mean PAP of 21–24 mm Hg is greater than the upper limit of normal but below the criteria for manifest PH. Exercise-induced PH is defined as a mean PAP of >30 mm Hg and total pulmonary resistance >3 Wood units (40). In a study by Lau et al, 86% of the patients with a mean PAP of 21–24 mm Hg had exercise-induced PH, nearly twice as many as in the group with a mean PAP of <21 mm Hg (41). The combination of a mean PAP of 21–24 mm Hg and exercise-induced PH in that population was associated with worse functional capacity (41), increased progression to resting PH (10), and worse survival (8,42). Oliveira et al found that exercise-induced PH was most frequently seen in patients with a mean PAP of 21–24 mm Hg, who have a reduction in exercise capacity similar to that in patients with resting PH (43). In the present study, 22 (30.6%) of 72 patients with a mean PAP of <21 mm Hg at rest fulfilled the criteria for exercise-induced PH versus 11 (78.6%) of 14 patients with a mean PAP of 21–24 mm Hg, consistent with the observations of Oliveira et al (43). However, in our study, regression and correlation analysis revealed a significant correlation of PAC at rest with 6-minute walking distance ($R = 0.448$, $P < 0.001$) (Figure 4) and ΔCO ($R = 0.227$, $P = 0.018$) and a trend toward correlation of PAC at rest with ΔCI ($R = 0.178$, $P = 0.064$). These findings support the hypothesis that PAC and right ventricular output reserve play another important role apart from exercise-induced PH in exercise limitation in SSc patients with a mean PAP of 21–24 mm Hg.

Early treatment may be a future strategy. The described changes in right ventricular function during exercise and pulmonary hemodynamic findings at rest and during exercise in patients with mildly elevated mean PAP raise the question of whether targeted PAH therapy could ameliorate these impairments and would be justified in these patients. In our study, those patients with reduced PAC may already be manifesting increased resting PVR, which supports the idea of an early targeted treatment. In a pilot study, bosentan was safe and effective in patients with SSc and mildly elevated mean PAP (44). Larger clinical trials with relevant outcome measures are needed to define the appropriate indication, safety, and tolerability of early treatment.

Our study had some limitations. The results may be influenced by the rather small sample size. Since not all patients reached high workloads, we only reported values up to 75W. Furthermore, the presentation of CI and TPG for each workload is an approximation and may be distorted, since different peak workload levels were reached. The method we used to calculate PAC may overestimate compliance since it does not account for blood flow from the pulmonary circulation into the capillary bed during systole (13). Thus, the true reduction of PAC in patients with mildly elevated mean PAP may be even greater.

Patients with mildly elevated mean PAP had higher resting systolic blood pressure than those with normal mean PAP. However, the systolic blood pressure at peak workload was not significantly higher than that in the group with normal mean PAP. Furthermore, PAWP during exercise did not significantly differ between groups. This indicates that the reduction in CI increase during exercise in patients with mildly elevated mean PAP was not due to systemic blood pressure. Data from a 2-dimensional echocardiogram obtained during exercise would have been helpful for interpretation of the results but were not part of the initial protocol.

The results of this study suggest that impaired 6-minute walking distance and exercise capacity in SSc patients with mildly elevated mean PAP (and normal right ventricular function at rest) might be caused by reduced PAC and reduced right ventricular output reserve (reduced right ventricular output during exercise). These findings are further evidence that mildly elevated mean PAP reflects an early stage of pulmonary vascular disease and right ventricular dysfunction. Screening of SSc patients by RHC at rest and during exercise may lead to an identification of early pulmonary vascular disease. Further studies are needed to evaluate if it is useful to start PAH-targeted medication in SSc patients with mildly elevated mean PAP.

ACKNOWLEDGMENTS

We would like to thank all patients who participated in the study.

AUTHOR CONTRIBUTIONS

All authors were involved in drafting the article or revising it critically for important intellectual content, and all authors approved the final version to be published. Dr. Nagel had full access to all of the data in the study and takes responsibility for the integrity of the data and the accuracy of the data analysis.

Study conception and design. Nagel, Benjamin, Blank, Coghlan, Distler, Denton, Fiehn, Hoepfer, Grünig.

Acquisition of data. Nagel, Benjamin, Blank, Coghlan, Distler, Denton, Egenlauf, Harutyunova, Hoepfer, Lorenz, Xanthouli, Grünig.

Analysis and interpretation of data. Nagel, Marra, Benjamin, Blank, Cittadini, Coghlan, Distler, Denton, Fiehn, Fischer, Hoepfer, Lorenz, Bossone, Grünig.

REFERENCES

- Condliffe R, Kiely DG, Peacock AJ, Corris PA, Gibbs JS, Vrapai F, et al. Connective tissue disease-associated pulmonary arterial hypertension in the modern treatment era. *Am J Respir Crit Care Med* 2009;179:151–7.
- Coghlan JG. Stress echocardiography and Cochin Risk Prediction Score for the prediction of pulmonary arterial hypertension in scleroderma: not yet ready for prime time [editorial]. *Arthritis Rheum* 2013;65:2236–9.
- Ngian GS, Stevens W, Prior D, Gabbay E, Roddy J, Tran A, et al. Predictors of mortality in connective tissue disease-associated pulmonary arterial hypertension: a cohort study. *Arthritis Res Ther* 2012;14:R213.
- Lefèvre G, Dauchet L, Hachulla E, Montani D, Sobanski V, Lambert M, et al. Survival and prognostic factors in systemic sclerosis-associated pulmonary hypertension: a systematic review and meta-analysis. *Arthritis Rheum* 2013;65:2412–23.
- Hoepfer MM, Bogaard HJ, Condliffe R, Frantz R, Khanna D, Kurzyrna M, et al. Definitions and diagnosis of pulmonary hypertension. *J Am Coll Cardiol* 2013;62:D42–50.
- Galiè N, Humbert M, Vachiery JL, Gibbs S, Lang I, Torbicki A, et al. 2015 ESC/ERS Guidelines for the diagnosis and treatment of pulmonary hypertension: the Joint Task Force for the Diagnosis and Treatment of Pulmonary Hypertension of the European Society of Cardiology (ESC) and the European Respiratory Society (ERS)—endorsed by the Association for European Paediatric and Congenital Cardiology (AEPC) and the International Society for Heart and Lung Transplantation (ISHLT). *Eur Heart J* 2016;37:67–119.
- Visovatti SH, Distler O, Coghlan JG, Denton CP, Grunig E, Bonderman D, et al. Borderline pulmonary arterial pressure in systemic sclerosis patients: a post-hoc analysis of the DETECT study. *Arthritis Res Ther* 2014;16:493.
- Kovacs G, Avian A, Tscherner M, Foris V, Bachmaier G, Olschewski A, et al. Characterization of patients with borderline pulmonary arterial pressure. *Chest* 2014;146:1486–93.
- Kovacs G, Berghold A, Scheidl S, Olschewski H. Pulmonary arterial pressure during rest and exercise in healthy subjects: a systematic review. *Eur Respir J* 2009;34:888–94.
- Valerio CJ, Schreiber BE, Handler CE, Denton CP, Coghlan JG. Borderline mean pulmonary artery pressure in patients with systemic sclerosis: transpulmonary gradient predicts risk of developing pulmonary hypertension. *Arthritis Rheum* 2013;65:1074–84.
- Blumberg FC, Arzt M, Lange T, Schroll S, Pfeifer M, Wensel R. Impact of right ventricular reserve on exercise capacity and survival in patients with pulmonary hypertension. *Eur J Heart Fail* 2013;15:771–5.
- Chaouat A, Sitbon O, Mercy M, Poncot-Mongars R, Provencher S, Guillaumot A, et al. Prognostic value of exercise pulmonary haemodynamics in pulmonary arterial hypertension. *Eur Respir J* 2014;44:704–13.
- Thenappan T, Prins KW, Pritzker MR, Scandurra J, Volmers K, Weir EK. The critical role of pulmonary arterial compliance in pulmonary hypertension. *Ann Am Thorac Soc* 2016;13:276–84.
- Jain P, Rao S, Macdonald P, Kotlyar E, Jabbour A, Hayward C, et al. Diagnostic performance of pulmonary capacitance at rest and during exercise in idiopathic pulmonary arterial hypertension. *Heart Lung Circ* 2019;28:289–94.
- Lewis GD, Bossone E, Naeije R, Grunig E, Saggarr R, Lancellotti P, et al. Pulmonary vascular hemodynamic response to exercise in cardiopulmonary diseases. *Circulation* 2013;128:1470–9.
- Grunig E, Tiede H, Enyimayew EO, Ehlken N, Seyfarth HJ, Bossone E, et al. Assessment and prognostic relevance of right ventricular contractile reserve in patients with severe pulmonary hypertension. *Circulation* 2013;128:2005–15.
- Subcommittee for Scleroderma Criteria of the American Rheumatism Association Diagnostic and Therapeutic Criteria Committee. Preliminary criteria for the classification of systemic sclerosis (scleroderma). *Arthritis Rheum* 1980;23:581–90.
- ATS Committee on Proficiency Standards for Clinical Pulmonary Function Laboratories. ATS statement: guidelines for the six-minute walk test [published erratum appears in *Am J Respir Crit Care Med* 2016;193:1185]. *Am J Respir Crit Care Med* 2002;166:111–7.
- Kovacs G, Avian A, Pienn M, Naeije R, Olschewski H. Reading pulmonary vascular pressure tracings: how to handle the problems of zero leveling and respiratory swings. *Am J Respir Crit Care Med* 2014;190:252–7.
- Kovacs G, Herve P, Barbera JA, Chaouat A, Chemla D, Condliffe R, et al. An official European Respiratory Society statement: pulmonary haemodynamics during exercise. *Eur Respir J* 2017;50:1700578.
- Yock PG, Popp RL. Noninvasive estimation of right ventricular systolic pressure by Doppler ultrasound in patients with tricuspid regurgitation. *Circulation* 1984;70:657–62.
- Ommen SR, Nishimura RA, Appleton CP, Miller FA, Oh JK, Redfield MM, et al. Clinical utility of Doppler echocardiography and tissue Doppler imaging in the estimation of left ventricular filling pressures: a comparative simultaneous Doppler-catheterization study. *Circulation* 2000;102:1788–94.
- Coghlan JG, Denton CP, Grunig E, Bonderman D, Distler O, Khanna D, et al. Evidence-based detection of pulmonary arterial hypertension in systemic sclerosis: the DETECT study. *Ann Rheum Dis* 2014;73:1340–9.
- Brimioulle S, Wauthy P, Ewalenko P, Rondelet B, Vermeulen F, Kerbaul F, et al. Single-beat estimation of right ventricular end-systolic pressure-volume relationship. *Am J Physiol Heart Circ Physiol* 2003;284:H1625–30.
- Spruijt OA, Bogaard HJ, Heijmans MW, Lely RJ, van de Veerdonk MC, de Man FS, et al. Predicting pulmonary hypertension with standard computed tomography pulmonary angiography. *Int J Cardiovasc Imaging* 2015;31:871–9.
- Hsu S, Houston BA, Tampakakis E, Bacher AC, Rhodes PS, Mathai SC, et al. Right ventricular functional reserve in pulmonary arterial hypertension. *Circulation* 2016;133:2413–22.
- Chia EM, Lau EM, Xuan W, Celermajer DS, Thomas L. Exercise testing can unmask right ventricular dysfunction in systemic sclerosis patients with normal resting pulmonary artery pressure. *Int J Cardiol* 2016;204:179–86.
- Latus H, Gummel K, Diederichs T, Bauer A, Rupp S, Kerst G, et al. Aortopulmonary collateral flow is related to pulmonary artery size and affects ventricular dimensions in patients after the fontan procedure. *PLoS One* 2013;8:e81684.

29. Wink J, de Wilde RB, Wouters PF, van Dorp EL, Veering BT, Versteegh MI, et al. Thoracic epidural anesthesia reduces right ventricular systolic function with maintained ventricular-pulmonary coupling. *Circulation* 2016;134:1163–75.
30. Sanz J, Kariisa M, Dellegrottaglie S, Prat-Gonzalez S, Garcia MJ, Fuster V, et al. Evaluation of pulmonary artery stiffness in pulmonary hypertension with cardiac magnetic resonance. *JACC Cardiovasc Imaging* 2009;2:286–95.
31. Vonk-Noordegraaf A, Haddad F, Chin KM, Forfia PR, Kawut SM, Lumens J, et al. Right heart adaptation to pulmonary arterial hypertension: physiology and pathobiology. *J Am Coll Cardiol* 2013;62:D22–33.
32. Rich S. Right ventricular adaptation and maladaptation in chronic pulmonary arterial hypertension. *Cardiol Clin* 2012;30:257–69.
33. Sutendra G, Michelakis ED. The metabolic basis of pulmonary arterial hypertension. *Cell Metab* 2014;19:558–73.
34. Chemla D, Lau EM, Papelier Y, Attal P, Herve P. Pulmonary vascular resistance and compliance relationship in pulmonary hypertension. *Eur Respir J* 2015;46:1178–89.
35. Mahapatra S, Nishimura RA, Oh JK, McGoon MD. The prognostic value of pulmonary vascular capacitance determined by Doppler echocardiography in patients with pulmonary arterial hypertension. *J Am Soc Echocardiogr* 2006;19:1045–50.
36. Medrek SK, Kloefkorn C, Nguyen DT, Graviss EA, Frost AE, Safdar Z. Longitudinal change in pulmonary arterial capacitance as an indicator of prognosis and response to therapy and in pulmonary arterial hypertension. *Pulm Circ* 2017;7:399–408.
37. Ghio S, D'Alto M, Badagliacca R, Vitulo P, Argiento P, Mule M, et al. Prognostic relevance of pulmonary arterial compliance after therapy initiation or escalation in patients with pulmonary arterial hypertension. *Int J Cardiol* 2017;230:53–8.
38. Hsu S, Kokkonen-Simon KM, Kirk JA, Kolb TM, Damico RL, Mathai SC, et al. Right ventricular myofilament functional differences in humans with systemic sclerosis-associated versus idiopathic pulmonary arterial hypertension. *Circulation* 2018;137:2360–70.
39. Tedford RJ, Mudd JO, Girgis RE, Mathai SC, Zaiman AL, Houston-Harris T, et al. Right ventricular dysfunction in systemic sclerosis-associated pulmonary arterial hypertension. *Circ Heart Fail* 2013;6:953–63.
40. Herve P, Lau EM, Sitbon O, Savale L, Montani D, Godinas L, et al. Criteria for diagnosis of exercise pulmonary hypertension. *Eur Respir J* 2015;46:728–37.
41. Lau EM, Godinas L, Sitbon O, Montani D, Savale L, Jaïs X, et al. Resting pulmonary artery pressure of 21–24 mmHg predicts abnormal exercise haemodynamics. *Eur Respir J* 2016;47:1436–44.
42. Heresi GA, Minai OA, Tonelli AR, Hammel JP, Farha S, Parambil JG, et al. Clinical characterization and survival of patients with borderline elevation in pulmonary artery pressure. *Pulm Circ* 2016;3:916–25.
43. Oliveira RK, Faria-Urbina M, Maron BA, Santos M, Waxman AB, Systrom DM. Functional impact of exercise pulmonary hypertension in patients with borderline resting pulmonary arterial pressure. *Pulm Circ* 2017;7:654–65.
44. Kovacs G, Maier R, Aberer E, Brodmann M, Graninger W, Kqjku X, et al. Pulmonary arterial hypertension therapy may be safe and effective in patients with systemic sclerosis and borderline pulmonary artery pressure. *Arthritis Rheum* 2012;64:1257–62.

Association of Dendritic Cell Signatures With Autoimmune Inflammation Revealed by Single-Cell Profiling

Michelle P. Ashton,¹ Anne Eugster,¹ Sevina Dietz,¹ Doreen Loebel,¹ Annett Lindner,¹ Denise Kuehn,¹ Anna E. Taranko,² Babett Heschel,¹ Anita Gavrisan,³ Anette-Gabriele Ziegler,⁴ Martin Aringer,¹ and Ezio Bonifacio⁵

Objective. To identify single-cell transcriptional signatures of dendritic cells (DCs) that are associated with autoimmunity, and determine whether those DC signatures are correlated with the clinical heterogeneity of autoimmune disease.

Methods. Blood-derived DCs were single-cell sorted from the peripheral blood of patients with rheumatoid arthritis, systemic lupus erythematosus, or type 1 diabetes as well as healthy individuals. DCs were analyzed using single-cell gene expression assays, performed immediately after isolation or after in vitro stimulation of the cells. In addition, protein expression was measured using fluorescence-activated cell sorting.

Results. CD1c+ conventional DCs and plasmacytoid DCs from healthy individuals exhibited diverse transcriptional signatures, while the DC transcriptional signatures in patients with autoimmune disease were altered. In particular, distinct DC clusters, characterized by up-regulation of *TAP1*, *IRF7*, and *IFNAR1*, were abundant in patients with systemic autoimmune disease, whereas DCs from patients with type 1 diabetes had decreased expression of the regulatory genes *PTPN6*, *TGFB*, and *TYROBP*. The frequency of CD1c+ conventional DCs that expressed a systemic autoimmune profile directly correlated with the extent of disease activity in patients with rheumatoid arthritis (Spearman's $r = 0.60$, $P = 0.03$).

Conclusion. DC transcriptional signatures are altered in patients with autoimmune disease and are associated with the level of disease activity, suggesting that immune cell transcriptional profiling could improve our ability to detect and understand the heterogeneity of these diseases, and could guide treatment choices in patients with a complex autoimmune disease.

INTRODUCTION

Autoimmunity occurs when the immune system mounts an unfavorable response toward a self antigen, which may lead to tissue damage and disease. The pathogenesis of autoimmune diseases is complex and the clinical manifestation of each disease varies between patients, which makes it difficult to predict the effectiveness of treatments or preventative strategies (1). For type 1 diabetes (T1D), a pancreas-specific autoimmune disease, immunotherapy has had limited success in reversing the disease or preventing progression to end-stage disease (2–4). In contrast, in many systemic autoimmune diseases, such as rheumatoid arthritis (RA) and systemic lupus erythematosus (SLE), treatment

with immunomodulatory and immunosuppressive agents has optimally achieved clinical remission. However, even with continued therapy, remission will often not last, and therefore regular, life-long reassessment of disease activity may be required. Moreover, the very same drug that yields measurable benefits in one patient with the disease may have no measurable effect in other patients with the same disease.

Dendritic cells (DCs) are important regulators of immunity that provide immunogenic and tolerogenic signals, which shape the adaptive immune response (5,6). In animal models, the absence of DCs or their abnormal function has been shown to induce autoimmunity, while alterations in the number of DCs, cytokine secretion, transcriptional signaling, and cell migration have been

Supported by the JDRF (17-2012-16) and by German Federal Ministry of Education and Research grants to the German Center for Diabetes Research (DZD). Dr. Bonifacio's work was supported by the DFG Research Center and the Cluster of Excellence (FZ 111).

¹Michelle P. Ashton, PhD, Anne Eugster, PhD, Sevina Dietz, BSc, Doreen Loebel, Annett Lindner, Denise Kuehn, Babett Heschel, Martin Aringer, MD: TU Dresden, Dresden, Germany; ²Anna E. Taranko, MSc: University of Potsdam, Potsdam, Germany; ³Anita Gavrisan: Forschergruppe Diabetes e.V., Neuherberg, Germany; ⁴Anette-Gabriele Ziegler, MD: Forschergruppe Diabetes e.V., Institute

of Diabetes Research, and DZD, Neuherberg, Germany, and Helmholtz Zentrum München, Munich, Germany; ⁵Ezio Bonifacio, PhD: TU Dresden, Dresden, Germany, and Forschergruppe Diabetes e.V. and DZD, Neuherberg, Germany.

No potential conflicts of interest relevant to this article were reported.

Address correspondence to Ezio Bonifacio, PhD, Center for Regenerative Therapies Dresden, Fetscherstrasse 105, 01307 Dresden, Germany. E-mail: ezio.bonifacio@tu-dresden.de.

Submitted for publication August 31, 2017; accepted in revised form November 29, 2018.

associated with development and progression of autoimmune diseases in humans (7–9). The DC compartment in mice and humans comprises several specialized subsets with different origins, localizations, morphologies, cytokine secretion patterns, and immunologic functions (5,6). Because these functionally distinct subsets have the potential to influence autoimmune responses in multiple ways, it has been proposed that diverse DC abnormalities could explain the broad spectrum of immunopathologic features and therapeutic responses in patients with autoimmune disease (7). Therefore, altered DC profiles may be associated with disease heterogeneity and could serve as a useful biomarker for monitoring disease pathogenesis or for predicting the response to treatment.

To explore this hypothesis, we used single-cell gene expression assays to analyze the diversity of blood-derived DCs, assess how the DC phenotype is altered in autoimmunity, and determine whether the alterations are correlated with the extent of disease activity. We profiled blood-derived CD1c⁺ conventional (or classical) DCs (cDCs) and plasmacytoid DCs (pDCs) from patients diagnosed as having either RA, SLE, or recent-onset T1D, using single-cell reverse transcription–polymerase chain reaction (RT-PCR) with a select panel of genes. The transcriptional profile of both of these DC subsets was altered in patients with systemic autoimmunity. Moreover, the frequency of CD1c⁺ cDCs that were characterized by a transcriptional signature associated with autoimmune disease varied among RA patients and was correlated with the extent of disease activity. Thus, our study shows a relationship between DC transcriptional profiles and autoimmune disease, and highlights the feasibility of profiling DCs or other immune cells to better understand the clinical heterogeneity of these diseases.

PATIENTS AND METHODS

Subjects. Samples of peripheral blood were collected from children with recent-onset T1D who were enrolled in the Diabetes Mellitus Incidence Cohort Registry (DiMelli) study (10), and from age-matched healthy children from the Prospective Evaluation of Risk Factors for the Development of Islet Autoimmunity and Type 1 Diabetes during Puberty (TEENDIAB) study (11). Protocols were approved by the Ethikkommission der Bayerischen Landesärztekammer (approval no. 08043) and the Ethikkommission der Fakultät für Medizin der Technischen Universität München (approval no. 2149/08). In addition, blood samples were collected from consenting patients with SLE or RA who fulfilled the respective American College of Rheumatology (ACR) (12) or ACR/European League Against Rheumatism (13) classification criteria, with approval provided by the ethics committee of TU Dresden (protocol no. EK 337122008). Routine clinical assessment parameters and C-reactive protein (CRP) values were obtained from the patients' charts.

Blood samples from healthy adults were provided by the Deutsches Rotes Kreuz Blutspendedienst Ost (Dresden, Ger-

many) after the subjects had given their informed consent and approval was provided by the ethics committee of TU Dresden (protocol no. EK 240062016). All research was performed in accordance with the Declaration of Helsinki.

Cell stimulation with Toll-like receptor 7 (TLR-7). Frozen peripheral blood mononuclear cells (PBMCs) were thawed and seeded into a 48-well tissue culture plate at 2.5×10^6 cells/ml in RPMI medium containing 10% fetal bovine serum, 1% streptomycin, 1% penicillin, and 1% L-glutamine with or without 2.5 µg/ml R848, a TLR-7 agonist (InvivoGen). Thereafter, the cells were incubated at 37°C in an atmosphere of 5% CO₂ for 3 hours, and then harvested, washed, and prepared for single-cell sorting of pDCs.

Intracellular staining. PBMCs were isolated by density centrifugation of sodium-heparinized peripheral venous blood samples over Ficoll-Hypaque. PBMCs were incubated with a Live/Dead Fixable Blue Dead Cell Stain Kit (ThermoFisher) for 20 minutes, and then washed, fixed, permeabilized, and incubated with a cocktail of anti-human monoclonal antibodies (mAb) (allophycocyanin [APC]–conjugated LIN, BV650-conjugated CD123, and V450-conjugated GZM mAb [BioLegend], phycoerythrin [PE]–Cy7-conjugated HLA–DR and BV785-conjugated CD303 mAb [BD Biosciences], AF700-conjugated IFNAR1 mAb [R&D Systems], PerCP–eF710-conjugated IRF8 mAb [eBioscience], and PE-conjugated IRF7 and PE–Vio770-conjugated IRF7[pS477/pS479] mAb [Miltenyi]) using the Foxp3/Transcription Factor Staining Buffer Set (eBioscience).

Cells were acquired and analyzed using a BD LSRII fluorescence-activated cell sorter, with the results analyzed using FACSDiva and FlowJo software (BD Biosciences). Aliquots of frozen PBMCs from a healthy donor were stained and analyzed concurrently with the study samples to control for interexperimental variation (see Statistical Analysis for more details). CST beads (BD Biosciences) were used to calibrate the instrument before each analysis.

Single-cell sorting of DC populations. PBMCs were isolated by density centrifugation of sodium-heparinized peripheral venous blood samples over Ficoll-Hypaque. Non-specific binding was blocked by incubating cells with a human Fc blocking reagent (Miltenyi) before adding a cocktail of anti-human mAb (APC-conjugated CD3, APC-conjugated CD19, PE–Cy7-conjugated CD14, PE–Cy7-conjugated CD56, and APC–Cy7-conjugated HLA–DR mAb [BD Biosciences], AF700-conjugated CD11c mAb [eBioscience], and BV650-conjugated CD123, BV605-conjugated CD15, BV421-conjugated CD141, and AF488-conjugated CD1c mAb [BioLegend]). Ten minutes before acquisition, 7-aminoactinomycin D (BD Biosciences) was added to the samples to enable discrimination of dead cells. Cells were acquired and sorted using

a BD FACSAria III, with results analyzed using FACSDiva software (BD Biosciences). Doublets and clumps were excluded using the side scatter–height versus side scatter–width plot. Two DC subsets, pDCs (CD3–CD19–CD56–CD14–CD16–HLA–DR+CD11c–CD123+) and CD1c+ cDCs (CD3–CD19–CD56–CD14–CD16–HLA–DR+CD11c+CD141–CD1c+), were single-cell sorted into 96-well PCR plates containing 5 μ l of EB elution buffer (Qiagen). The cells were then frozen at -80°C for RT-PCR analysis.

Gene expression analysis. Gene expression analysis of single-cell–sorted DCs was performed as previously described, with some modifications (14). Total complementary DNA was preamplified for 20 cycles (1 cycle at 95°C for 1 minute, 20 cycles at 95°C for 15 seconds, 60°C for 1 minute, and 72°C for 1.5 minutes, and 1 cycle at 72°C for 10 minutes) with TATAA GrandMaster Mix (TATAA Biocenter) and 29 primer pairs (see Supplementary Table 1, available on the *Arthritis & Rheumatology* web site at <http://onlinelibrary.wiley.com/doi/10.1002/art.40793/abstract>) at a final concentration of 25 nM in a total reaction volume of 35 μ l. Raw data were preprocessed as previously described (14) to regress out plate effects on each individual gene while controlling for group effects. Thus, all gene expression values are shown as regressed C_i values, where a value of 0 indicates no gene expression.

Statistical analysis. Gene and protein expression levels are reported as the mean with 95% confidence intervals (95% CIs) or mean \pm SEM. Various statistical tests were used (as described in the figure legends). To adjust for interexperimental variability, the fluorescence intensity values recorded during index sorting are displayed as the z-scores of data from each independent experiment. Single-cell gene expression correlation analyses were performed using corplot, with a significance threshold of 0.001 (15). To identify biologically meaningful transcriptional profiles, t-distributed stochastic neighbor embedding (t-SNE) dimensions were calculated with Rtsne (16,17), and unsupervised Ward hierarchical clustering was performed with hclust.

The significance of differential gene expression was determined using the Hurdle model (18), with correction for false-discovery rate and with a significance threshold of 0.001. Protein expression, as measured by the mean fluorescence intensity (MFI), was normalized for each fluorescence channel by dividing the MFI by the value for an internal control and then multiplying by the mean MFI value for all samples. All statistical analyses were performed using GraphPad Prism version 5 or RStudio software.

RESULTS

Single-cell expression analysis of DC populations. To investigate the transcriptional profile of DCs, CD1c+ cDCs and

pDCs were freshly isolated from PBMCs by single-cell sorting (Figure 1A) and then individually analyzed for gene expression using single-cell RT-PCR analysis, as previously described (14). We selected a panel of 29 genes involved in various aspects of DC function, including pathogen recognition, antigen uptake and processing, type I interferon (IFN) signaling and response, negative regulation, and cytokine/chemokine signaling.

The analysis of 327 CD1c+ cDCs and 325 pDCs isolated from 9 healthy adults (1 male, 8 female; median age 47 years [interquartile range (IQR) 30 to 59 years]) showed subset-specific expression of several genes, including *CD1C* in CD1c+ cDCs and *GZMB* in pDCs (Figure 1B). A common pDC marker at the protein level, *NRP1*, was included in the gene panel, but limited and variable expression of *NRP1* was observed in single cells, suggesting that the detection of this gene may be compromised in this single-cell assay. Furthermore, t-SNE analysis based on our gene panel showed that the gene signatures of the 2 DC subsets were distinct (Figure 1C).

The *CD1C* transcript was exclusively, but not universally, detected in CD1c+ cDCs (Figure 1B) and its abundance was correlated with CD1c protein expression, which was recorded as the fluorescence intensity (i.e., the MFI) by index sorting (for results, see Supplementary Figure 1, available on the *Arthritis & Rheumatology* web site at <http://onlinelibrary.wiley.com/doi/10.1002/art.40793/abstract>). CD1c protein expression was significantly lower in CD1c+ cDCs with undetectable *CD1C* transcript expression than in CD1c+ cDCs with *CD1C* transcript expression (MFI 4,486 [95% CI 3,629, 5,344] versus MFI 8,258 [95% CI 7,310, 9,206]; $P < 0.0001$) (Supplementary Figure 1A [<http://onlinelibrary.wiley.com/doi/10.1002/art.40793/abstract>]). In cells with detectable *CD1C* transcripts, the gene expression was positively correlated with CD1c protein expression (Spearman's $r = 0.26$, $P < 0.0001$) (Supplementary Figure 1B [<http://onlinelibrary.wiley.com/doi/10.1002/art.40793/abstract>]), indicating that the quantitative difference in transcript expression measured using this analytic method is likely to be a reflection of true biologic variation.

Heatmap analysis based on the restricted gene panel revealed genetic heterogeneity in both DC subsets (Figure 1B). For example, we observed a subpopulation of pDCs that expressed *CD86* but not *GZMB*. These *CD86*-expressing DCs within the pDC flow cytometry gate also displayed reduced CD123 protein expression and increased CD141 protein expression (Supplementary Figure 1C [<http://onlinelibrary.wiley.com/doi/10.1002/art.40793/abstract>]). This subset of cells may correspond to the newly identified pre-DC subset, which is functionally distinct from pDCs (19,20).

We examined the coexpression of genes at the single-cell level using Spearman's correlation analysis (Figure 1D). The regulatory genes *PTPN6*, *TYROBP*, *STAT3*, *IRF8*, and *TGFB* were significantly coexpressed in both DC subsets. Expression of *TGFB* and *TYROBP* in pDCs was also significantly correlated with the expression of other genes, including the type I IFN–related

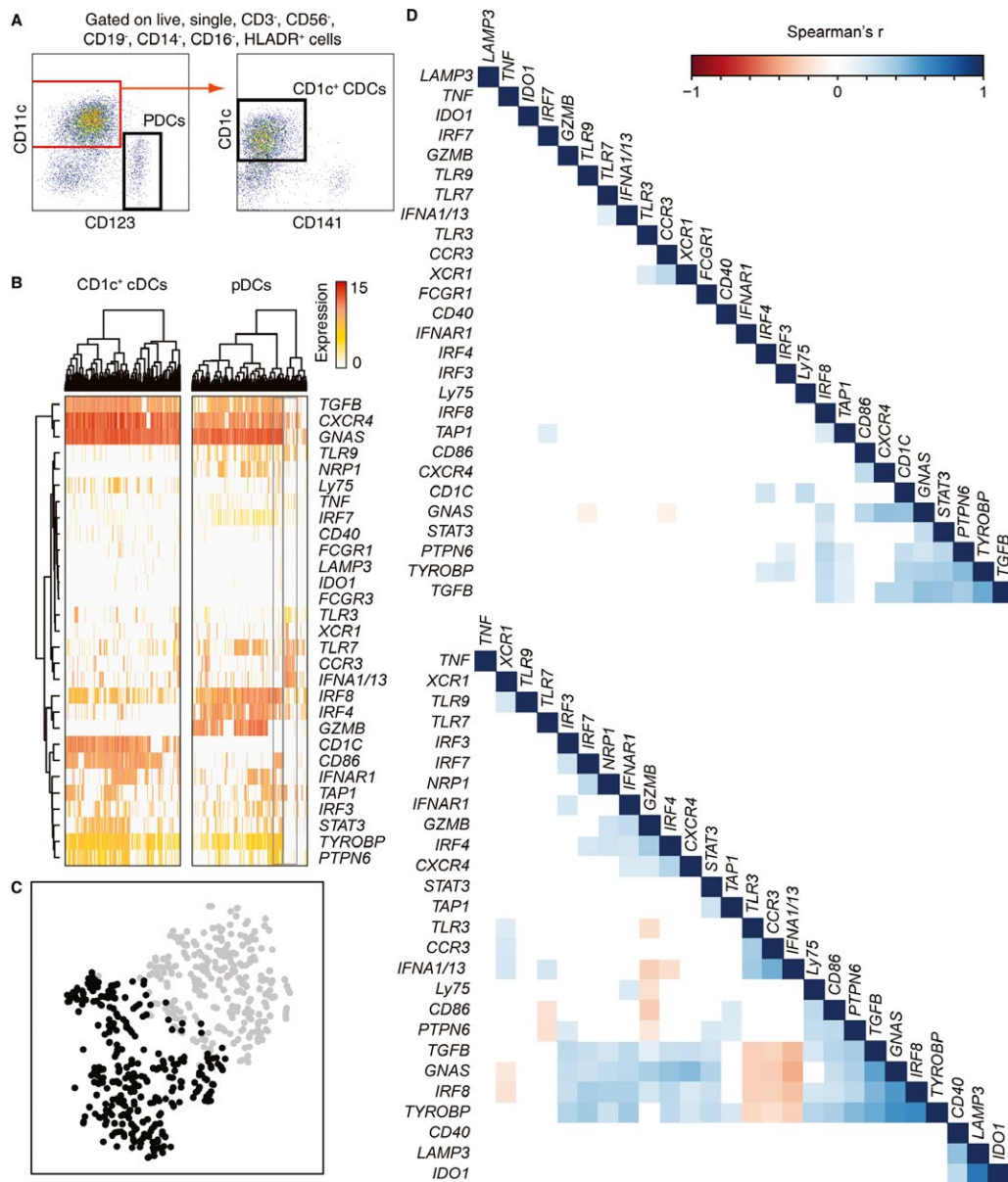


Figure 1. Transcriptional profiles of dendritic cell (DC) subsets isolated from the peripheral blood of healthy adults. **A**, Subsets of DCs were prepared by single-cell sorting of fresh peripheral blood mononuclear cells (PBMCs). After removing doublets, dead cells, and cells expressing CD3, CD56, CD19, CD14, and CD16, plasmacytoid DCs (pDCs) were identified as CD11c^{low}CD123⁺ cells, and CD1c⁺ conventional DCs (cDCs) were identified as CD11c^{high}CD141⁻CD1c⁺ cells. **B**, Heatmaps of single-cell gene expression data in CD1c⁺ cDCs and pDCs from the PBMCs of healthy adults are shown. Unsupervised Ward hierarchical clustering was applied to cells and genes. Clusters of gene coexpression are denoted by adjoining lines on the top and left. **C**, Analysis by t-distributed stochastic neighbor embedding shows gene expression data in CD1c⁺ cDCs (gray-shaded circles) and pDCs (black circles). Each circle represents a single cell. **D**, Correlation matrices of genes expressed by CD1c⁺ cDCs (top) and pDCs (bottom) from the PBMCs of 9 healthy adults are shown. Different colors represent the significance of the correlations ($P < 0.001$) by Spearman's correlation analysis.

genes *IFNAR1*, *IRF7*, and *IRF3*. The pDCs also significantly coexpressed *TLR3*, *CCR3*, and *IFNA1/13*, and this correlation appeared to arise from a distinct subpopulation of cells observed on the heatmap (Figure 1B).

These findings confirm that there is marked diversity within the CD1c⁺ cDC and pDC populations in peripheral blood. This diversity can be defined based on a relatively small number of

genes, and the quantitative differences in transcript expression are likely to be biologically relevant.

DC transcription phenotypes in systemic and organ-specific autoimmunity. To investigate the changes in DC transcriptional profiles in patients with autoimmune disease, we sorted fresh peripheral blood-derived pDCs and CD1c⁺ cDCs

from patients with systemic or organ-specific autoimmunity as well as age-matched healthy individuals. Our previous data set obtained from healthy adults was reanalyzed in combination with pDCs and cDCs from patients with RA (550 pDCs and 524 cDCs from 13 patients [2 male, 11 female]; median age 59 years [IQR 45 to 62 years]), patients with SLE (286 pDCs and 282 cDCs from 7 patients [2 male, 5 female]; median age 40 years [IQR 32 to 50.5 years]), patients with recent-onset T1D (248 pDCs and 245 cDCs from 7 patients [3 male, 4 female]; median age 13.7 years [IQR 11.2 to 15.8 years]), and a second group of healthy individuals comprising healthy children who were age-matched to the T1D

cohort (262 pDCs and 265 cDCs from 7 healthy children [4 male, 3 female]; median age 9.8 years [IQR 2.8 to 12.4 years]).

We identified 6 clusters of CD1c+ cDCs and 9 clusters of pDCs, based on unsupervised Ward hierarchical clustering of t-SNE dimensions generated from the single-cell gene expression data (Figures 2A–D and 3A–D). These clusters had distinct gene signatures. Within the CD1c+ cDC population, cluster 1 was defined by a lack of *CD1C* transcript and, along with cluster 2, exhibited reduced expression of *IRF3* relative to the other clusters. Clusters 2, 4, 5, and 6 were defined by increased expression of *CD86* transcript as compared to clusters 1 and 3. Clusters 4 and

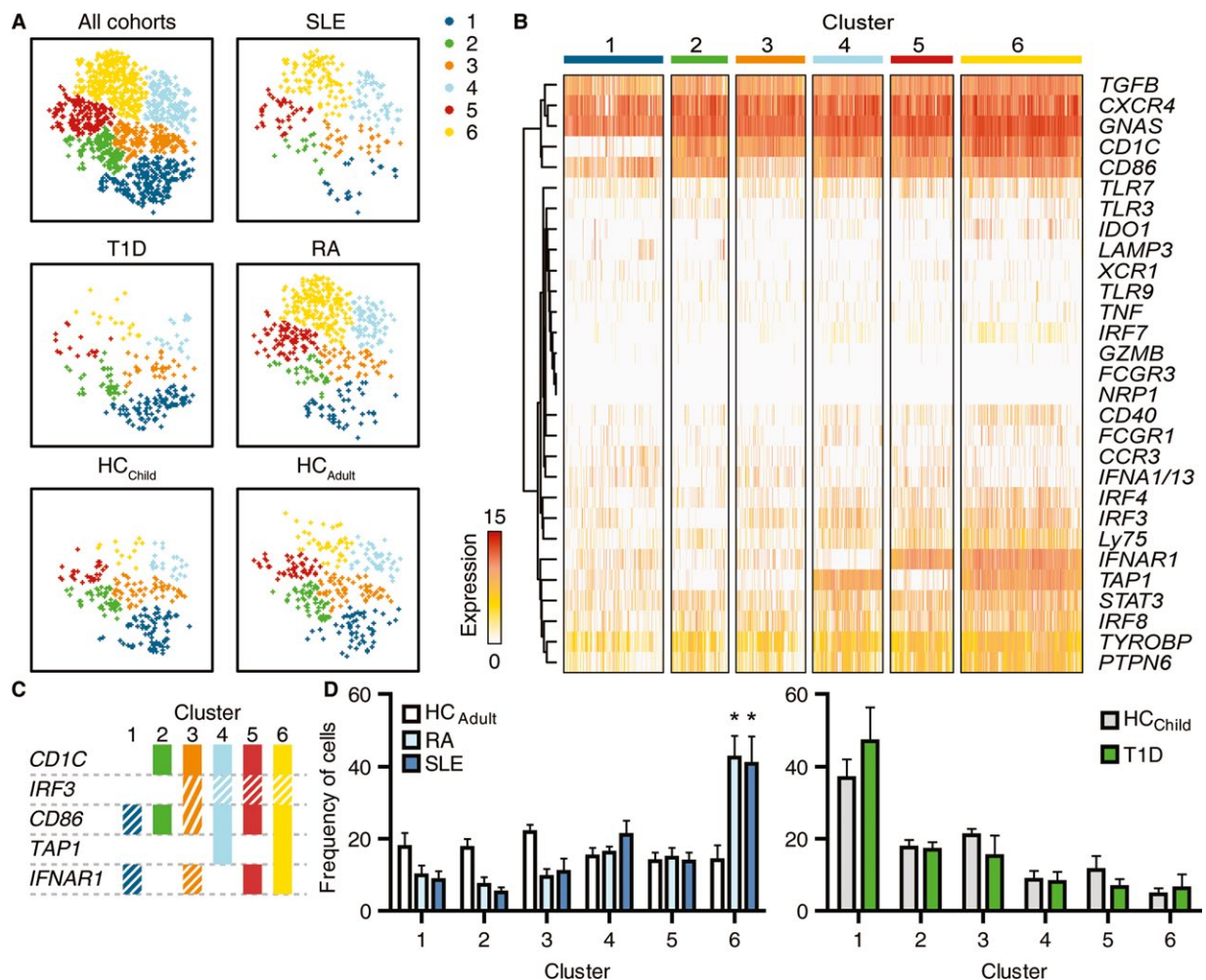


Figure 2. Distinct gene signatures of cDCs from patients with systemic autoimmune diseases. CD1c+ cDCs were single-cell sorted from freshly isolated PBMCs from a control cohort of healthy adults (HC_{Adult}), patients with rheumatoid arthritis (RA), patients with systemic lupus erythematosus (SLE), or patients with recent-onset type 1 diabetes (T1D) and a second healthy control cohort of children (HC_{Child}) age-matched to the T1D cohort. Sorted cells were subjected to single-cell reverse transcription–polymerase chain reaction analysis. **A**, Analysis by t-distributed stochastic neighbor embedding reveals CD1c+ cDC gene expression clusters (6 clusters, determined according to unsupervised Ward clustering analysis) in all cohorts and in each individual cohort. **B**, Heatmaps of single-cell gene expression data are sorted into the clusters defined in **A**. **C**, Transcriptional profiles of the clusters defined in **A** are shown. Colored bars represent the percentage of cells expressing the indicated gene (expression defined as a corrected $C_t > 0$). Solid bars = >75% of cells expressing the indicated gene in that cluster; hatched bars = 25–75% of cells expressing the indicated gene in that cluster. **D**, Frequency of CD1c+ cDCs in each cluster from PBMCs from each cohort is shown. Results are the mean \pm SEM of 7–13 individuals per cohort. * = $P < 0.05$ versus HC_{Adult}, by two-way analysis of variance. See Figure 1 for other definitions.

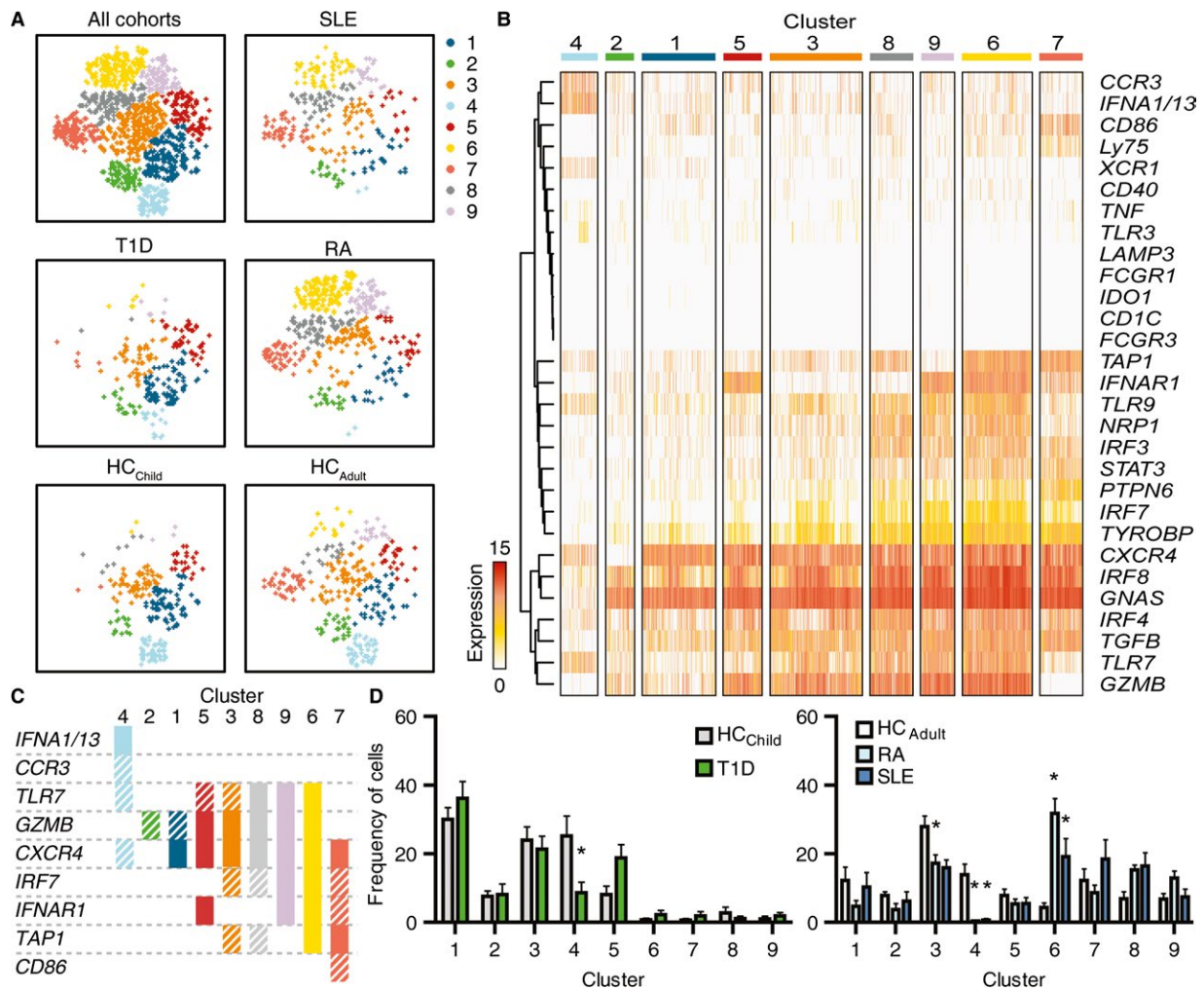


Figure 3. Distinct gene signatures of plasmacytoid dendritic cells (pDCs) from patients with systemic autoimmune disease. The pDCs were single-cell sorted from freshly isolated peripheral blood mononuclear cells (PBMCs) from a control cohort of healthy adults (HC_{Adult}), patients with rheumatoid arthritis (RA), patients with systemic lupus erythematosus (SLE), or patients with recent-onset type 1 diabetes (T1D) and a second healthy control cohort of children (HC_{Child}) age-matched to the T1D cohort. **A**, Analysis by t-distributed stochastic neighbor embedding reveals pDC gene expression clusters (9 clusters, determined according to unsupervised Ward clustering analysis) in all cohorts and in each individual cohort. **B**, Heatmaps of single-cell gene expression data are sorted into the clusters defined in **A**. **C**, Transcriptional profiles of the clusters defined in **A** are shown. Colored bars represent the percentage of cells expressing the indicated gene (expression defined as a corrected C_t > 0). Solid bars = >75% of cells expressing the indicated gene in that cluster; hatched bars = 25–75% of cells expressing the indicated gene in that cluster. **D**, Frequency of pDCs in each cluster from PBMCs is shown for each cohort. Results are the mean \pm SEM of 7–13 individuals per cohort. * = $P < 0.05$ versus HC_{Adult} by two-way analysis of variance.

6 were further defined by overexpression of *TAP1*, while clusters 5 and 6 were defined by overexpression of *IFNAR1*.

Within the pDC population, clusters 1, 2, and 4 were characterized by lower transcript expression of most of the genes analyzed, relative to that in clusters 3, 5, 6, 7, 8, and 9. The expression profiles of pDCs were similar between clusters 1 and 2, although cells in cluster 2 lacked *CXCR4* expression. Cluster 4 had a distinct profile characterized by expression of *CCR3* and *IFNA1/13*. Compared with clusters 3 and 5, clusters 6, 7, 8, and 9 were defined by increased expression of *IRF3*, *PTPN6*, and *STAT3*. Other distinguishing genes for these clusters included *IRF7* (absent from cluster 5), *IFNAR1* (absent from clusters 3 and 8),

and *TAP1* (up-regulated in clusters 6 and 7), while pDCs in cluster 7 were characterized by low expression of *TLR7* and *GZMB* as well as increased expression of *CD86*.

When we separated the t-SNE data (shown in Figures 2A and 3A) into the separate cohorts, we found that the profiles of $CD1c^+$ cDCs and pDCs were altered in patients with RA and patients with SLE relative to those in healthy adults. In particular, we found a higher proportion of $CD1c^+$ cDCs and pDCs in cluster 6 in samples from patients with RA ($CD1c^+$ cDCs, mean 42.5% [95% CI 29.5%, 55.4%], $P < 0.0001$; pDCs, mean 31.8% [95% CI 22.4%, 41.1%], $P < 0.0001$) and patients with SLE ($CD1c^+$ cDCs, mean 40.7% [95% CI 22.3%, 59.1%], $P < 0.0001$; pDCs, mean 19.2%

[95% CI 6.3%, 32.0%], $P < 0.01$) relative to that in healthy adults (CD1c+ cDCs, mean 14.1% [95% CI 5.7%, 23.5%]; pDCs, mean 4.4% [95% CI 1.4%, 7.3%]) (Figures 2D and 3D). For the pDCs, this was accompanied by a relative decrease in cells within clusters 3 and 4 in patients with RA (pDCs in cluster 3, mean 17.1% [95% CI 11.8%, 22.6%], $P < 0.05$; pDCs in cluster 4, mean 0.4% [95% CI -0.2%, 1.0%], $P < 0.01$) and a relative decrease in cells within cluster 4 in patients with SLE (mean 0.7% [95% CI -0.4%, 1.8%], $P < 0.05$) relative to that in healthy adults (pDCs in cluster 3, mean 27.9% [95% CI 20.8%, 35.0%]; pDCs in cluster 4, mean 13.9% [95% CI 7.0%, 20.8%]).

In contrast, the t-SNE profiles of both cell types were similar between patients with T1D and the corresponding healthy children (Figures 2A and 3A). A significant difference in the frequency of DC clusters between patients with T1D and healthy children was seen only for pDC cluster 4, which was decreased

in patients with T1D compared with healthy children (mean 25.2% [95% CI 11.0%, 39.3%] versus 8.6% [95% CI 1.0%, 16.2%], $P < 0.001$) (Figure 3D).

DC gene transcription in autoimmunity. In addition to analyzing the gene signatures, we compared expression levels of individual genes between the disease cohorts and healthy subjects by applying the Hurdle model, which accounts for the bimodal expression of single-cell populations (Table 1 and Supplementary Figures 2A and B, available on the *Arthritis & Rheumatology* web site at <http://onlinelibrary.wiley.com/doi/10.1002/art.40793/abstract>). The up-regulated genes in CD1c+ cDCs from patients with RA were *IFNAR1*, *CD1C*, and *IRF3*, which is consistent with the transcription profile observed for CD1c+ cDCs in cluster 6 (Figures 2B and C). *CXCR4* was down-regulated in CD1c+ cDCs from

Table 1. Differential gene expression in dendritic cells from patients versus age-matched healthy controls*

	CD1c+ cDCs			pDCs		
	RA	SLE	T1D	RA	SLE	T1D
<i>CD1C</i>	<0.0001†	0.132	0.7068	-	-	-
<i>IRF8</i>	<0.0001†	<0.0001†	<0.0001‡	<0.0001†	<0.0001†	0.2383
<i>IFNAR1</i>	<0.0001†	0.0497	0.0001†	0.0001†	0.1021	0.0024
<i>IRF3</i>	<0.0001†	0.0655	0.1584	0.0037	0.3604	0.6945
<i>IRF7</i>	0.0254	0.1255	0.6804	<0.0001†	<0.0001	0.4884
<i>IRF4</i>	0.0014	0.166	0.3764	<0.0001†	<0.0001‡	0.0015
<i>GZMB</i>	0.5951	0.3435	0.343	0.0006†	0.1829	0.6353
<i>TLR7</i>	0.0093	0.0073	0.0001†	0.0002†	0.6607	0.8875
<i>TAP1</i>	0.0014	0.0039	0.0142	0.0412	0.0008†	0.6353
<i>CD86</i>	0.0025	0.1206	<0.0001†	0.6789	0.1259	0.001†
<i>LAMP3</i>	0.1816	0.1055	<0.0001†	0.207	0.6494	0.6335
<i>CCR3</i>	0.0732	0.4197	<0.0001†	0.0004‡	0.5867	0.1565
<i>IFNA1/13</i>	0.0189	0.8275	0.0005†	0.0002‡	0.1591	0.6353
<i>TNF</i>	0.137	0.0206	0.3357	<0.0001‡	<0.0001‡	0.6353
<i>TLR3</i>	0.006	0.1055	0.4132	0.0007‡	0.0057	0.0002†
<i>XCR1</i>	0.0165	0.132	0.7921	0.0005‡	0.0128	0.1565
<i>CXCR4</i>	<0.0001‡	0.0001‡	0.0019	0.0048	0.6607	0.4884
<i>TYROBP</i>	0.0114	0.0039	<0.0001‡	0.0679	0.1591	<0.0001‡
<i>PTPN6</i>	0.0024	0.0206	<0.0001‡	0.8917	0.5867	0.4884
<i>TGFB</i>	0.3466	0.01	<0.0001‡	0.9009	0.2105	0.6353
<i>CD40</i>	0.0027	0.0039	0.013	0.9009	0.9518	0.9201
<i>FCGR1</i>	0.0016	0.0014	0.0688	-	0.6607	0.6353
<i>IDO1</i>	0.0025	0.0028	0.1135	0.2997	0.6607	-
<i>Ly75</i>	0.1061	0.4245	0.3349	0.3066	0.1114	0.6353
<i>NRP1</i>	-	-	-	0.1331	0.0738	0.6353
<i>STAT3</i>	0.0025	0.8054	0.1135	0.2153	0.498	0.641

* Values are P values from the Hurdle model for the significance of differential gene expression between patients with rheumatoid arthritis (RA), patients with systemic lupus erythematosus (SLE), and patients with type 1 diabetes (T1D) compared with age-matched healthy controls. cDCs = conventional dendritic cells; pDCs = plasmacytoid dendritic cells.

† Up-regulated genes.

‡ Down-regulated genes.

patients with RA and/or patients with SLE. Although we found no robust gene signature in patients with T1D, the transcripts *IFNAR1*, *CCR3*, *CD86*, *IFNA1/13*, *LAMP3*, and *TLR7* were up-regulated and *IRF8*, *PTPN6*, *TGFB*, and *TYROBP* were down-regulated in CD1c+ cDCs from patients with T1D relative to the expression levels in healthy children (Table 1 and Supplementary Figure 2A [<http://onlinelibrary.wiley.com/doi/10.1002/art.40793/abstract>]).

In pDCs, transcript levels of *IRF7* and *IRF8*, *TAP1*, *GZMB*, *IFNAR1*, and *TLR7* were up-regulated ($P < 0.0001$) in patients with SLE or patients with RA (Table 1 and Supplementary Figure 2B [<http://onlinelibrary.wiley.com/doi/10.1002/art.40793/abstract>]). Again, the up-regulated genes corresponded to those that were highly expressed in cluster 6 (Figures 3B and C). *IRF4* and *TNF* were down-regulated ($P < 0.0001$) in patients with RA and patients with SLE relative to healthy adults. Additionally, pDCs from patients with RA exhibited lower expression levels of *CCR3*, *IFNA1/13*, *XCR1*, and *TLR3* (Table 1 and Supplementary Figure 2B [<http://onlinelibrary.wiley.com/doi/10.1002/art.40793/abstract>]), all of which are genes that are characteristic of cluster 4. Similar to the findings in CD1c+ cDCs, *CD86* was up-regulated ($P = 0.001$) and *TYROBP* was down-regulated ($P < 0.0001$) in pDCs from patients with T1D relative to healthy children.

We subsequently analyzed the protein expression levels of IFN regulatory factor 7 (IRF-7; total protein or phosphorylated IRF-7 [pS477/pS479]), IRF-8, IFN- α -1/13 receptor 1 (IFNAR-1), and granzyme B by flow cytometry in pDCs from a second cohort of healthy adults ($n = 9$ [3 male, 6 female]; median age 49 years [IQR 30 to 59 years]), patients with RA ($n = 10$ [1 male, 9 female]; median age 60.5 years [IQR 57.3 to 67 years]), and patients with SLE ($n = 9$ [2 male, 7 female]; median age 43 years [IQR 36 to 48 years]) (see results in Supplementary Figures 3A–C, available on the *Arthritis & Rheumatology* web site at <http://onlinelibrary.wiley.com/doi/10.1002/art.40793/abstract>). Consistent with the gene expression data, protein expression levels of IRF-7 and IRF-8 were increased in pDCs from patients with RA (for IRF-7, MFI 347.4 [95% CI 326.9, 367.9], $P < 0.01$; for IRF-8, MFI 12,909 [95% CI 10,936, 14,882], $P < 0.05$) and pDCs from patients with SLE (for IRF-7, MFI 354.9 [95% CI 311.7, 398.2], $P < 0.01$; for IRF-8, MFI 13,002 [95% CI 10,710, 15,293], $P < 0.05$) relative to that in healthy adults (for IRF-7, MFI 288.9 [95% CI 262.3, 315.5]; for IRF-8, MFI 9,422 [95% CI 8,078, 10,768]).

Gene expression of *IFNAR1* and *GZMB* showed a trend toward up-regulated transcription in patients with SLE, and both were up-regulated at the protein level in pDCs from patients with SLE (for IFNAR-1, MFI 1,547 [95% CI 1,232, 1,861], $P < 0.05$; for granzyme B, MFI 793.2 [95% CI 623.3, 963.1], $P < 0.05$) relative to that in healthy adults (for IFNAR-1, MFI 1,124 [95% CI 835.7, 1,412]; for granzyme B, MFI 567.5 [95% CI 488.3, 646.7]). In patients with RA, both *IFNAR1* and *GZMB* were up-

regulated at the transcript level, but not at the protein level (for IFNAR-1, MFI 1,428 [95% CI 1,234, 1,621]; for granzyme B, MFI 662.2 [95% CI 552.1, 772.3]).

Taken together, these results indicate that the changes in gene expression for individual genes are reflected in the gene signatures characteristic of DCs from patients with RA and patients with SLE, and these gene signatures partially translated into protein signatures. DCs from patients with T1D exhibited altered expression of individual genes, but this did not yield an observable gene signature based on the gene panel studied herein.

Gene expression response of pDCs to stimulation with TLR-7 in patients with organ-specific autoimmunity.

The robust differences in DC gene signatures in healthy adults compared with that in patients with RA or patients with SLE, in whom a systemic inflammatory environment is present, were not unexpected. However, only subtle changes were observed in patients with T1D. Therefore, we investigated how DC stimulation with the TLR-7 agonist R848 could affect pDC transcripts, and whether stimulation elicited more robust differences in gene signatures in patients with T1D. We chose R848 because we expected it to affect the expression of several genes in our panel based on the results of a previous study (21), and we used pDCs, which have high TLR-7 expression (22).

We cultured previously frozen PBMCs from 4 patients with recent-onset T1D (2 male, 2 female; median age 14.5 years [IQR 13.2 to 15.7 years]) and 4 age-matched healthy individuals (2 male, 2 female; median age 14.5 years [IQR 13.3 to 15.6 years]) in the presence or absence of the TLR-7 agonist R848 for 3 hours, and then sorted pDCs (CD3–CD19–CD14–CD56–CD16–HLA–DR+CD11c^{low}CD123+CD303+) for single-cell gene expression analysis. Stimulation with R848 in pDCs from healthy children significantly altered the expression of 10 genes in our restricted panel (Figure 4A). As expected from the results of a prior study (21), *TNF*, *LAMP3*, and *CD40* were up-regulated and *CXCR4* was down-regulated by R848 stimulation.

Analysis with t-SNE and unsupervised Ward hierarchical clustering of R848-stimulated pDCs from healthy individuals and patients with T1D identified 5 pDC clusters, including cluster 1, that reflected the transcriptional changes induced by R848 stimulation (Figures 4B and C). The frequency of pDCs in each cluster was not significantly different between patients with T1D and healthy children (Figure 4D). It can also be noted that the expression profiles of the R848-stimulated pDCs differed from those of pDCs from patients with SLE, patients with RA, and patients with T1D (shown in Figure 3), indicating that the transcriptional profiles of patients are unlikely to reflect the response to a single stimulus or pathway.

Correlation of DC gene signatures with disease activity level in RA.

The frequency of pDCs or CD1c+ cDCs in cluster 6 was increased in patients with RA and patients with SLE. However, there was substantial variability between individual

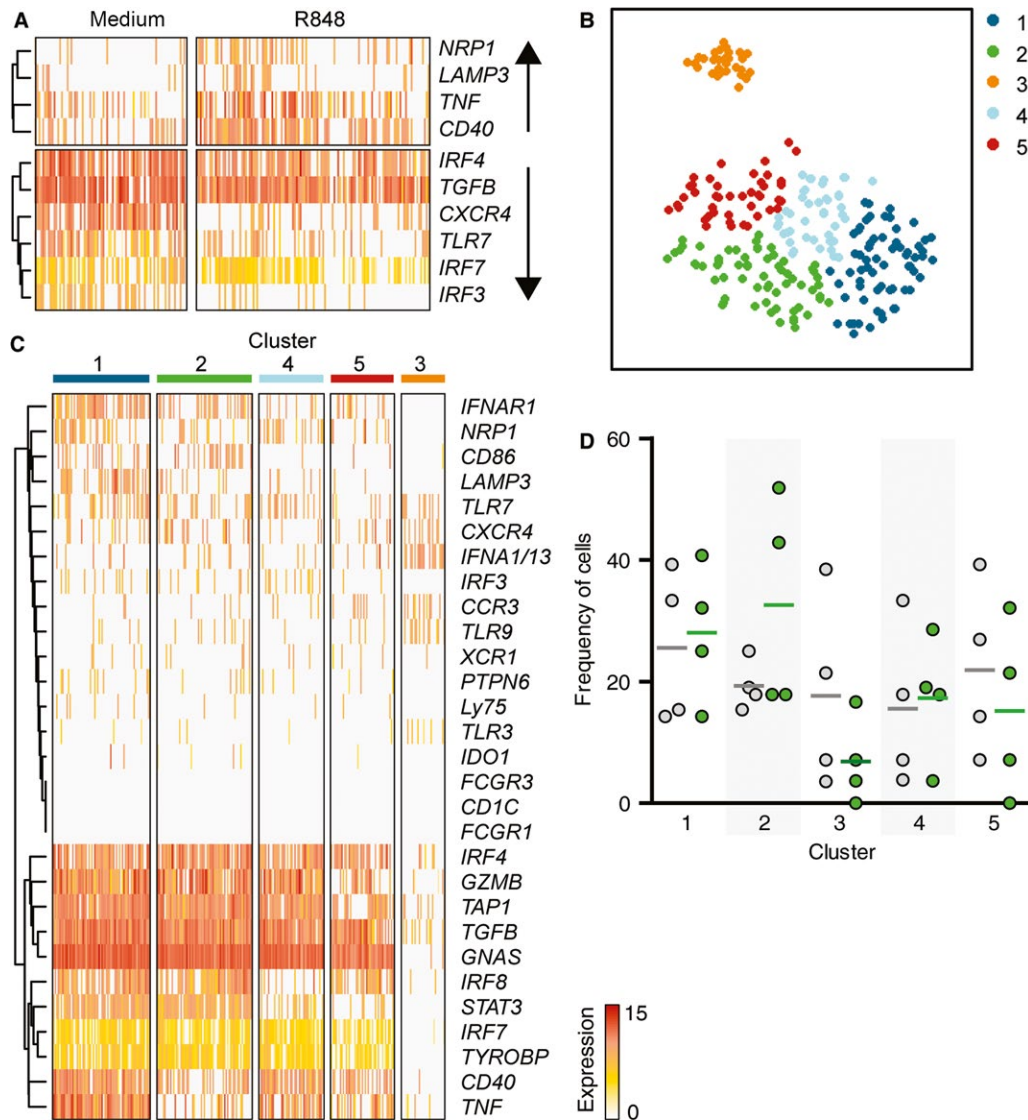


Figure 4. Single-cell analysis of R848-stimulated pDCs from patients with recent-onset type 1 diabetes (T1D) and healthy children. PBMCs from patients with recent-onset T1D and age-matched healthy children were cultured for 3 hours with a Toll-like receptor 7 agonist, R848. Single-cell-sorted pDCs were subjected to single-cell gene expression analysis. **A**, Heatmaps of gene expression in pDCs from healthy children are shown, separated according to the presence of stimulation with R848 or absence of stimulation (medium alone), with ordering according to unsupervised Ward hierarchical clustering analysis. Only genes that were significantly up-regulated (top) or down-regulated (bottom) after R848 stimulation are shown, based on the Hurdle model with correction for the false-discovery rate and a significance threshold of 0.001. **B**, Analysis by t-distributed stochastic neighbor embedding reveals gene expression clusters (5 clusters, determined according to unsupervised Ward hierarchical clustering analysis). **C**, Heatmaps of single-cell gene expression data are sorted into the clusters defined in **A**. **D**, Frequencies of cells in each cluster are shown for the healthy children (gray-shaded circles) and patients with T1D (green circles), where each circle represents an individual and the horizontal line represents the mean. There were no significant differences in the gene expression data, as determined by one-way analysis of variance. See Figure 3 for other definitions.

patients (Figure 5A). Therefore, we investigated whether this variability might be related to disease activity. Since disease activity in SLE is more difficult to measure, due to the multiorgan pattern of the disease, we focused on the larger cohort of patients with RA and used the Clinical Disease Activity Index (CDAI) as a measure of disease activity (23).

The frequency of CD1c+ cDCs in cluster 6 was positively correlated with the CDAI score in patients with RA (Spearman's $r =$

0.60, $P = 0.03$) (Figure 5B). Furthermore, in the group of patients with at least moderate disease activity (CDAI >10, $n = 5$) and a CRP concentration of >1 mg/liter, the frequency of CD1c+ cDCs in cluster 6 was higher (mean 65.6% [95% CI 57.5%, 73.7%]) than in the 8 patients with less severe inflammation (mean 28.0% [95% CI 18.1%, 38.0%], $P < 0.0001$) (Figure 5C). In contrast, the frequency of pDCs in cluster 6 was not correlated with the CDAI (Spearman's $r = 0.22$, $P = 0.47$) (Figure 5B), and segregation of

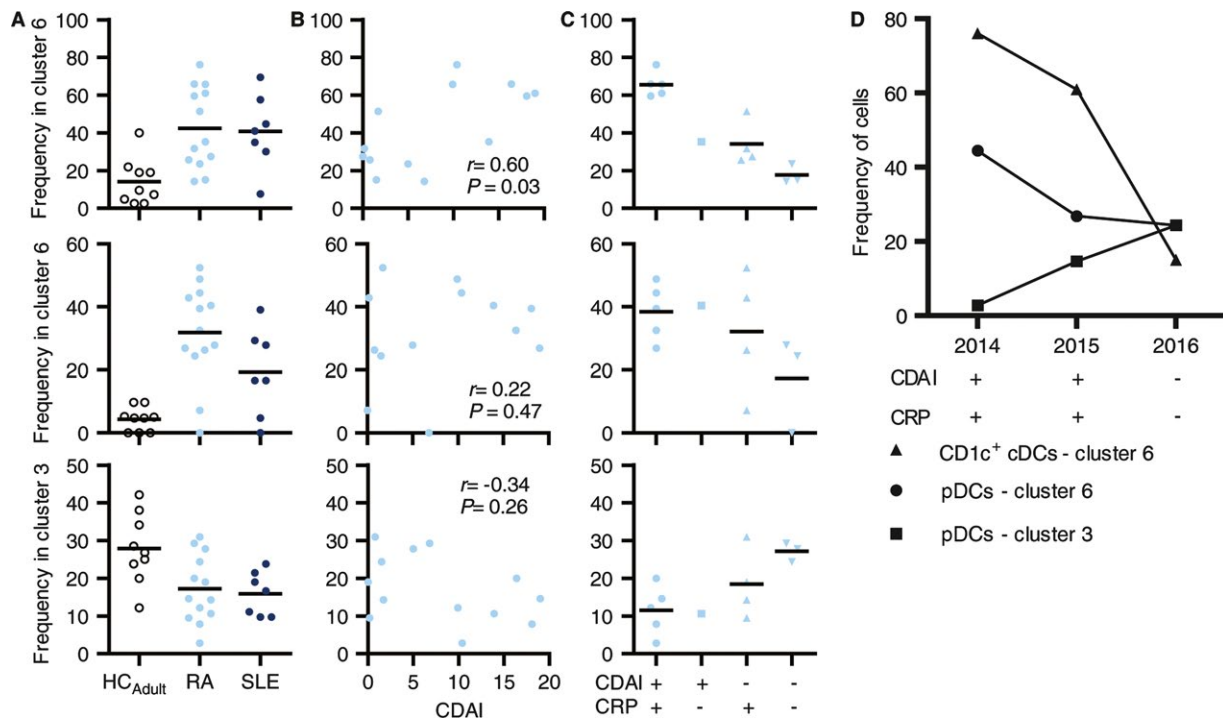


Figure 5. Correlation between cluster frequency and disease status. **A**, CD1c⁺ conventional dendritic cells (cDCs) and plasmacytoid DCs (pDCs) in cluster 6 (top and middle, respectively) and pDCs in cluster 3 (bottom) were examined for the frequency of enrichment in peripheral blood mononuclear cells (PBMCs) from healthy adults (HC_{Adult}), patients with rheumatoid arthritis (RA), and patients with systemic lupus erythematosus (SLE). Circles represent individual subjects, and the horizontal line represents the mean. **B**, Correlations between the frequency of CD1c⁺ cDCs and pDCs in cluster 6 and pDCs in cluster 3 and the Clinical Disease Activity Index (CDAI) in patients with RA were assessed by Spearman's correlation analysis. Circles represent individual subjects. *P* values are 2-tailed. **C**, Frequencies of CD1c⁺ cDCs and pDCs in cluster 6 and pDCs in cluster 3 were examined in patients with RA stratified according to CDAI score (+ = CDAI >10) and C-reactive protein (CRP) concentration in the blood (+ = >1 mg/liter). Symbols represent individual subjects, and the horizontal line represents the mean. **D**, Longitudinal changes in the frequencies of CD1c⁺ cDCs in cluster 6 and pDCs in clusters 3 and 6 in a single RA patient over 3 years are shown, including the patient's CDAI score (+ = CDAI >10) and CRP concentration in the blood (+ = >1 mg/liter) at each time point.

patients based on the CDAI and CRP level did not reveal a relationship between inflammation markers and cluster frequency (Figure 5C). However, the highest frequency of pDCs in cluster 3, which is characteristic of pDCs from healthy individuals (Figure 5A), was found in patients with RA who had low CDAI scores and a CRP concentration of <1 mg/liter (Figure 5C).

A relationship between increased disease activity and high frequency of CD1c⁺ cDCs in cluster 6 or a low frequency of pDCs in cluster 3 was observed in an individual patient over 3 consecutive years (Figure 5D). These findings suggest that the DC transcriptional profile is correlated with the severity of inflammation and disease.

DISCUSSION

In this study using single-cell gene expression analysis, we identified transcriptome heterogeneity of blood-derived DC subsets, and found transcriptional profiles of DC subsets that are associated with autoimmunity. We also found that the transcriptional profiles of the DC subsets are associated with disease activity in patients with RA.

We could identify distinct subpopulations of DCs using a restricted gene set, which was selected on the basis of DC markers and DC function. We observed transcriptionally distinct subpopulations within the pDC and CD1c⁺ cDC subsets. This included a population within the pDC subset with gene and protein expression patterns that corresponded to a T cell-activating DC population that has been newly identified by single-cell RNA sequencing (19,20). We also observed a unique pDC subpopulation characterized by increased expression of *IFNA1/13* and *CCR3*, which has not been previously described. Further studies are required to identify protein markers that may enable us to isolate these cells for functional characterization.

Our novel findings include identification of a DC gene expression signature with the potential to become a measure of disease activity in systemic autoimmune diseases such as RA and SLE, and a subtle alteration of DC gene expression in patients with T1D, an organ-specific autoimmune disease. We chose SLE and RA as systemic autoimmune disease models because these diseases, when active, often show systemic inflammation and immune complex-mediated IFN signatures (24–26). Consistent with this, patients with RA and those with SLE had a significantly greater

proportion of DCs with a transcriptional profile characterized by the concomitant up-regulation of multiple genes (cluster 6), such as *CD86* in CD1c+ cDCs, *TLR7* and *IRF7* in pDCs, and *TAP1* and *IFNAR1* in both subsets. Overexpression of these genes suggest that DCs with this cluster profile have an increased capacity to activate T cells, produce type I IFNs, and process antigens; these observations have previously been reported in RA and/or SLE (27–31). The profiles observed in patients could not be attributed to responses to a single stimulus, such as a TLR-7 agonist.

In contrast to that seen in patients with RA or SLE, the cluster profile of DCs isolated from patients with recent-onset T1D was not distinct from that of DCs from healthy children. Instead, we found changes in the expression of a small number of genes in CD1c+ cDCs and pDCs. As in patients with RA or SLE, *CD86* expression was increased in both DC subsets from patients with T1D. However, unlike in RA and SLE, we found decreased expression of *PTPN6* and *TGFB* in CD1c+ cDCs and decreased expression of *TYROBP* in both DC subsets from patients with T1D. These genes encode proteins with important roles in the negative regulation of the immune response, and their down-regulation or abnormal function can promote inflammatory or autoimmune responses (32–37). We speculate that the subtle changes in DCs from patients with T1D may occur downstream of genetic susceptibility, rather than being a reflection of generalized inflammation, and could therefore represent therapeutic targets.

Transcriptional profiles that can be used to monitor disease development or predict response to treatment would be valuable for developing personalized therapies for autoimmune diseases. Multiple studies have attempted to identify signatures that can clinically stratify patients for this purpose (38–41). A recent study, for example, showed that the IFN-stimulated genes associated with SLE were markedly different between populations of European ancestry and those of East Asian ancestry (42). Most of these studies used microarray or RNA sequencing to analyze bulk mixed-cell populations, but this approach can mask clinically relevant biologic complexity and heterogeneity at the single-cell level. In our study, we found that disease activity in patients with RA was correlated with the frequency of DCs expressing particular transcriptional signatures. Patients with more severe inflammation had higher frequencies of CD1c+ cDCs expressing an “autoimmune” profile and lower frequencies of pDCs expressing a “healthy” transcriptional profile. These are promising findings that require validation in prospective studies. It will also be important to determine whether the changes in DC transcriptional profile are secondary to changes in the inflammatory environment, and therefore might provide an indirect measure of the degree of inflammation, or whether they reflect functional abnormalities that may affect the choice and outcome of treatment.

Single-cell gene expression analyses can identify heterogeneity and distinct cell populations within phenotypically similar cells. As these technologies improve and downstream analyses

become more robust and standardized, it is becoming more feasible to screen patients based on their immune cell transcriptional profiles. As we have shown in the present study, this approach may yield new disease markers and therapeutic targets in patients with autoimmune disease.

ACKNOWLEDGMENTS

We thank all of the participants who provided blood samples for this research.

AUTHOR CONTRIBUTIONS

All authors were involved in drafting the article or revising it critically for important intellectual content, and all authors approved the final version to be published. Dr. Bonifacio had full access to all of the data in the study and takes responsibility for the integrity of the data and the accuracy of the data analysis.

Study conception and design. Ashton, Eugster, Aringer, Bonifacio.

Acquisition of data. Ashton, Dietz, Loebel, Lindner, Kuehn, Taranko, Heschel, Gavrisan, Ziegler, Aringer, Bonifacio.

Analysis and interpretation of data. Ashton, Eugster, Aringer, Bonifacio.

REFERENCES

1. Cho JH, Feldman M. Heterogeneity of autoimmune diseases: pathophysiological insights from genetics and implications for new therapies. *Nat Med* 2015;21:730–8.
2. Bayry J, Gautier JF. Regulatory T cell immunotherapy for type 1 diabetes: a step closer to success? *Cell Metab* 2016;23:231–3.
3. Pozzilli P, Maddaloni E, Buzzetti R. Combination immunotherapies for type 1 diabetes mellitus. *Nat Rev Endocrinol* 2015;11:289–97.
4. Ziegler AG, Danne T, Dunger DB, Berner R, Puff R, Kiess W, et al. Primary prevention of β -cell autoimmunity and type 1 diabetes: the Global Platform for the Prevention of Autoimmune Diabetes (GPPAD) perspectives. *Mol Metab* 2016;5:255–62.
5. Steinman RM. Decisions about dendritic cells: past, present, and future. *Annu Rev Immunol* 2012;30:1–22.
6. Mildner A, Jung S. Development and function of dendritic cell subsets. *Immunity* 2014;40:642–56.
7. Coutant F, Miossec P. Altered dendritic cell functions in autoimmune diseases: distinct and overlapping profiles. *Nat Rev Rheumatol* 2016;12:703–15.
8. Ganguly D, Haak S, Sisirak V, Reizis B. The role of dendritic cells in autoimmunity. *Nat Rev Immunol* 2013;13:566–77.
9. Mollah ZU, Pai S, Moore C, O’Sullivan BJ, Harrison MJ, Peng J, et al. Abnormal NF- κ B function characterizes human type 1 diabetes dendritic cells and monocytes. *J Immunol* 2008;180:3166–75.
10. Thumer L, Adler K, Bonifacio E, Hofmann F, Keller M, Milz C, et al. German new onset diabetes in the young incident cohort study: DiMelli study design and first-year results. *Rev Diabet Stud* 2010;7:202–8.
11. Ziegler AG, Meier-Stiegen F, Winkler C, Bonifacio E. Prospective evaluation of risk factors for the development of islet autoimmunity and type 1 diabetes during puberty—TEENDIAB: study design. *Pediatr Diabetes* 2012;13:419–24.
12. Hochberg MC. Updating the American College of Rheumatology revised criteria for the classification of systemic lupus erythematosus. *Arthritis Rheum* 1997;40:1725.
13. Aletaha D, Neogi T, Silman AJ, Funovits J, Felson DT, Bingham CO III, et al. 2010 rheumatoid arthritis classification criteria: an American College of Rheumatology/European League Against Rheumatism collaborative initiative. *Arthritis Rheum* 2010;62:2569–81.

14. Heninger AK, Eugster A, Kuehn D, Buettner F, Kuhn M, Lindner A, et al. A divergent population of autoantigen-responsive CD4+ T cells in infants prior to β cell autoimmunity. *Sci Transl Med* 2017;9:eaaf8848.
15. Wei T, Simko V. Corrplot: visualization of a correlation matrix. 2016;R package version 0.77.
16. Van der Maaten L. Accelerating t-SNE using tree-based algorithms. *J Mach Learn Res* 2014;15:3221–45.
17. Krijthe J. Rtsne: T-distributed stochastic neighbor embedding using Barnes-Hut implementation. 2015;R package version 0.13.
18. McDavid A, Finak G, Yajima M. MAST: model-based analysis of single cell transcriptomics. 2015;R package version 0.931.
19. See P, Dutertre CA, Chen J, Gunther P, McGovern N, Irac SE, et al. Mapping the human DC lineage through the integration of high-dimensional techniques. *Science* 2017;356:eaag3009.
20. Villani AC, Satija R, Reynolds G, Sarkizova S, Shekhar K, Fletcher J, et al. Single-cell RNA-seq reveals new types of human blood dendritic cells, monocytes, and progenitors. *Science* 2017;356:eaah4573.
21. Birmachu W, Gleason RM, Bulbulian BJ, Riter CL, Vasilakos JP, Lipson KE, et al. Transcriptional networks in plasmacytoid dendritic cells stimulated with synthetic TLR 7 agonists. *BMC Immunol* 2007;8:26.
22. Hornung V, Rothenfusser S, Britsch S, Krug A, Jahrsdorfer B, Giese T, et al. Quantitative expression of Toll-like receptor 1-10 mRNA in cellular subsets of human peripheral blood mononuclear cells and sensitivity to CpG oligodeoxynucleotides. *J Immunol* 2002;168:4531–7.
23. Aletaha D, Nell VP, Stamm T, Uffmann M, Pflugbeil S, Machold K, et al. Acute phase reactants add little to composite disease activity indices for rheumatoid arthritis: validation of a clinical activity score. *Arthritis Res Ther* 2005;7:R796–806.
24. Crow MK. Type I interferon in the pathogenesis of lupus. *J Immunol* 2014;192:5459–68.
25. Mok CC, Lau CS. Pathogenesis of systemic lupus erythematosus. *J Clin Pathol* 2003;56:481–90.
26. Noack M, Miossec P. Selected cytokine pathways in rheumatoid arthritis. *Semin Immunopathol* 2017;39:365–83.
27. Blomberg S, Eloranta ML, Magnusson M, Alm GV, Rönnblom L. Expression of the markers BDCA-2 and BDCA-4 and production of interferon- α by plasmacytoid dendritic cells in systemic lupus erythematosus. *Arthritis Rheum* 2003;48:2524–32.
28. Conigliaro P, Perricone C, Benson RA, Garside P, Brewer JM, Perricone R, et al. The type I IFN system in rheumatoid arthritis. *Autoimmunity* 2010;43:220–5.
29. Crispin JC, Vargas-Rojas MI, Monsivais-Urenda A, Alcocer-Varela J. Phenotype and function of dendritic cells of patients with systemic lupus erythematosus. *Clin Immunol* 2012;143:45–50.
30. Obermoser G, Pascual V. The interferon- α signature of systemic lupus erythematosus. *Lupus* 2010;19:1012–9.
31. Ramos PS, Langefeld CD, Bera LA, Gaffney PM, Noble JA, Moser KL. Variation in the ATP-binding cassette transporter 2 gene is a separate risk factor for systemic lupus erythematosus within the MHC. *Genes Immun* 2009;10:350–5.
32. Chu CL, Yu YL, Shen KY, Lowell CA, Lanier LL, Hamerman JA. Increased TLR responses in dendritic cells lacking the ITAM-containing adapters DAP12 and FcR γ . *Eur J Immunol* 2008;38:166–73.
33. Dumitriu IE, Dunbar DR, Howie SE, Sethi T, Gregory CD. Human dendritic cells produce TGF- β 1 under the influence of lung carcinoma cells and prime the differentiation of CD4+CD25+Foxp3+ regulatory T cells. *J Immunol* 2009;182:2795–807.
34. Hall HT, Sjolín H, Brauner H, Tomasello E, Dalod M, Vivier E, et al. Increased diabetes development and decreased function of CD4+CD25+ Treg in the absence of a functional DAP12 adaptor protein. *Eur J Immunol* 2008;38:3191–9.
35. Kaneko T, Saito Y, Kotani T, Okazawa H, Iwamura H, Sato-Hashimoto M, et al. Dendritic cell-specific ablation of the protein tyrosine phosphatase Shp1 promotes Th1 cell differentiation and induces autoimmunity. *J Immunol* 2012;188:5397–407.
36. Melillo JA, Song L, Bhagat G, Blazquez AB, Plumlee CR, Lee C, et al. Dendritic cell (DC)-specific targeting reveals Stat3 as a negative regulator of DC function. *J Immunol* 2010;184:2638–45.
37. Sjolín H, Robbins SH, Bessou G, Hidmark A, Tomasello E, Johansson M, et al. DAP12 signaling regulates plasmacytoid dendritic cell homeostasis and down-modulates their function during viral infection. *J Immunol* 2006;177:2908–16.
38. Burska AN, Roget K, Blits M, Soto Gomez L, van de Loo F, Hazelwood LD, et al. Gene expression analysis in RA: towards personalized medicine. *Pharmacogenomics J* 2014;14:93–106.
39. Irvine KM, Gallego P, An X, Best SE, Thomas G, Wells C, et al. Peripheral blood monocyte gene expression profile clinically stratifies patients with recent-onset type 1 diabetes. *Diabetes* 2012;61:1281–90.
40. Nakamura S, Suzuki K, Iijima H, Hata Y, Lim CR, Ishizawa Y, et al. Identification of baseline gene expression signatures predicting therapeutic responses to three biologic agents in rheumatoid arthritis: a retrospective observational study. *Arthritis Res Ther* 2016;18:159.
41. Nikpour M, Dempsey AA, Urowitz MB, Gladman DD, Barnes DA. Association of a gene expression profile from whole blood with disease activity in systemic lupus erythematosus. *Ann Rheum Dis* 2008;67:1069–75.
42. Mostafavi S, Yoshida H, Moodley D, LeBoite H, Rothamel K, Raj T, et al. Parsing the interferon transcriptional network and its disease associations. *Cell* 2016;164:564–78.

CONCISE COMMUNICATION

DOI 10.1002/art.40805

Efficacy of baricitinib in the treatment of chilblains associated with Aicardi-Goutières syndrome, a type I interferonopathy

Aicardi-Goutières syndrome (AGS) is a rare, juvenile-onset autoinflammatory disease characterized by basal ganglia calcification, chronic cerebrospinal fluid (CSF) lymphocytosis, and elevated type I interferon (IFN) levels in the CSF (1,2). Typical clinical manifestations include developmental delay, intellectual impairment, chilblains, panniculitis, glaucoma, and autoimmunity overlapping with systemic lupus erythematosus (SLE) (1,3).

AGS is classified as a monogenic type I interferonopathy with autoinflammation resulting from constitutive up-regulation of type I IFN signaling (3). IFN-stimulated genes (ISGs) are constantly overexpressed in peripheral blood cells from AGS patients, and measurement of ISGs in these cells is a useful marker for disease activity (4,5). At least 7 distinct gene mutations have been reported for AGS, including mutations in *SAMHD1* (1). *SAMHD1* loss-of-function mutations are associated with dysfunctional cytosolic dNTP metabolism and overproduction of type I IFNs (1).

JAK/STAT activation is present in various autoimmune diseases, and treatment with specific JAK inhibitors in immune-mediated diseases has been increasingly reported (6). Recently, the oral JAK1/2 inhibitor baricitinib was approved for the treatment of active rheumatoid arthritis and was also found to be effective in the treatment of a patient with a *STAT1* gain-of-function mutation (7). In this report, we describe an AGS patient treated with baricitinib and demonstrate its potential clinical applications for the treatment of type I interferonopathies.

The patient, a 22-year-old Caucasian woman with a consanguineous family history, was diagnosed as having AGS at age 19 years based on a homozygous nonsense mutation in exon 4 of *SAMHD1* (c.490C>T [p.Arg164Ter]). This mutation has been described previously in AGS (8). Her medical history included subclinical hypothyroidism, basal ganglia calcifications, and mild intellectual disability. The most prominent clinical feature was severe chilblains, which had been active over many years. Scaly and crusted ulcers from chilblains persisted on both hands and feet (Figure 1A). Inflammation and pain were typically exacerbated after cold exposure.

Baricitinib treatment was initiated at a daily dose of 2 mg/kg. At the start of baricitinib therapy, the patient experienced active chilblains of the hands and feet. After 6 weeks of treatment, the lesions completely resolved. To date, there has been

no recurrence of chilblains after 18 months of treatment (Figure 1A). Lesions also did not reappear during winter, when the disease was usually more active. No occurrences of viral infections, opportunistic infections, or other complications were reported during treatment.

Peripheral blood samples were collected from the patient 4 weeks prior to the start of baricitinib therapy and after 2 and 6 weeks of treatment. Expression levels of 5 ISGs (*IFI44*, *IFI44L*, *IFIT3*, *LY6E*, and *MX1*) representing the gene signature for type I IFN activity (9) were measured in isolated CD14+ monocytes by quantitative reverse transcription–polymerase chain reaction and compared to the expression levels in 54 healthy controls. Prior to baricitinib therapy, monocytes from the patient displayed higher expression of all tested ISGs compared to healthy controls (Figure 1B). Expression of all 5 ISGs declined remarkably after initiation of baricitinib treatment (Figure 1B).

Furthermore, we measured total *STAT1* and phosphorylated *STAT1* in peripheral blood T lymphocytes by flow cytometry (7). Before and during treatment, T lymphocytes from the patient expressed higher levels of total *STAT1* than those observed in 2 age-, sex-, and race-matched healthy controls (Figure 1C). As shown in Figures 1D and E, T lymphocytes from the patient before and during baricitinib therapy displayed baseline levels of phosphorylated *STAT1* comparable to those in the healthy controls. However, T lymphocytes obtained from the patient before treatment displayed much higher levels of phosphorylated *STAT1* upon IFN α stimulation than healthy control T lymphocytes. The enhanced level of phosphorylated *STAT1* observed in patient T lymphocytes before baricitinib treatment was strongly reduced during treatment.

In summary, our findings suggest that baricitinib is a novel drug for the treatment of chilblains in AGS patients with a *SAMHD1* mutation and consequent up-regulation of type I IFN activity. The immunologic effects of JAK inhibitors depend on their selectivity and inhibitory capacity for the several JAK subtypes. Baricitinib displays a stronger inhibitory effect on cytokine-induced phosphorylated *STAT1* than ruxolitinib, which had been previously reported as successful in the treatment of STING-associated type I interferonopathy (6,10). Therefore, more in-depth research is warranted to evaluate baricitinib in the treatment of type I interferonopathies.

Supported by Erasmus University Medical Center, Rotterdam, The Netherlands, and the Chulalongkorn University Faculty of Medicine, Bangkok, Thailand. No potential conflicts of interest relevant to this article were reported.

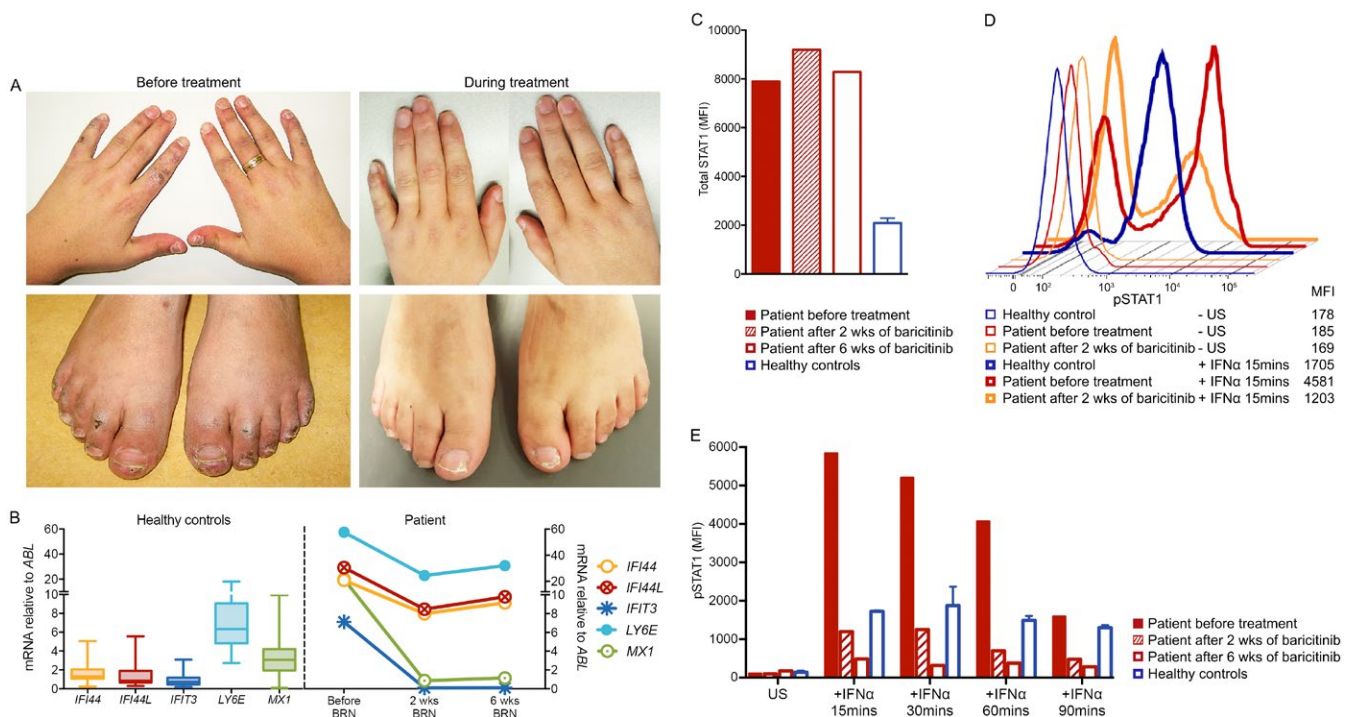


Figure 1. Clinical and immunologic response to baricitinib (BRN) treatment in a patient with Aicardi-Goutières syndrome (AGS). **A**, Dermatologic manifestations in the hands and feet before treatment (left), and clinical improvement during the fifth month of therapy (right). **B**, Expression of mRNA for interferon (IFN)-stimulated genes (ISGs) in monocytes from healthy controls (left) and from the patient before and during the treatment (right). Data were normalized to the housekeeping gene *ABL*. Data in the left panel are shown as box plots. Each box represents the 25th to 75th percentiles. Lines inside the boxes represent the median. Lines outside the boxes represent the 10th and 90th percentiles. **C**, Total *STAT1* levels in T lymphocytes from the patient and healthy controls. **D**, Phosphorylated *STAT1* levels in T lymphocytes upon IFN α induction. **E**, Kinetics of phosphorylated *STAT1* levels in T lymphocytes upon stimulation with IFN α for the indicated time periods. Values in **C** and **E** are the mean \pm SEM. MFI = mean fluorescence intensity; US = unstimulated.

Kornvalee Meesilpavikkai, MD
*Erasmus University Medical Center
 Rotterdam, The Netherlands
 and Chulalongkorn University
 Bangkok, Thailand*
 Willem A. Dik, PhD
 Benjamin Schrijver
 Cornelia G. van Helden-Meeuwse
 Marjan A. Versnel, PhD
 P. Martin van Hagen, MD, PhD
*Erasmus University Medical Center
 Rotterdam, The Netherlands*
 Emilia K. Bijlsma, MD, PhD
 Claudia A. L. Ruivenkamp, PhD
*Leiden University Medical Center
 Leiden, The Netherlands*
 Margreet J. Oele, MD
*Haaglanden Medical Centre,
 The Hague, The Netherlands*
 Virgil A. S. H. Dalm, MD, PhD
*Erasmus University Medical Center
 Rotterdam, The Netherlands*

AUTHOR CONTRIBUTIONS

All authors were involved in drafting the article or revising it critically for important intellectual content, and all authors approved the final version

to be published. Dr. Meesilpavikkai had full access to all of the data in the study and takes responsibility for the integrity of the data and the accuracy of the data analysis.

Study conception and design. Meesilpavikkai, Dik, Versnel, van Hagen, Dalm.

Acquisition of data. Meesilpavikkai, Dik, Schrijver, van Helden-Meeuwse, Dalm.

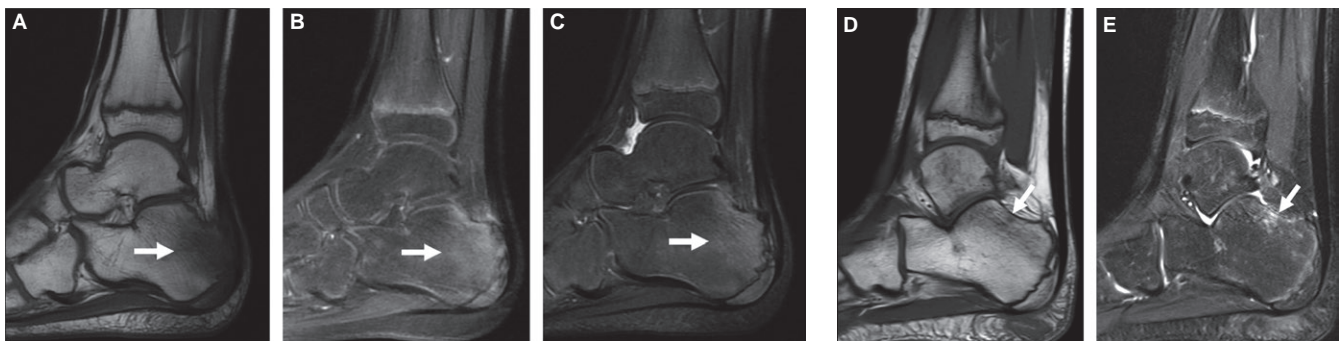
Analysis and interpretation of data. Meesilpavikkai, Dik, Bijlsma, Ruivenkamp, Oele, Dalm.

- Crow YJ, Manel N. Aicardi-Goutieres syndrome and the type I interferonopathies. *Nat Rev Immunol* 2015;15:429–40.
- Rice G, Patrick T, Parmar R, Taylor CF, Aeby A, Aicardi J, et al. Clinical and molecular phenotype of Aicardi-Goutieres syndrome. *Am J Hum Genet* 2007;81:713–25.
- Lee-Kirsch MA, Wolf C, Gunther C. Aicardi-Goutieres syndrome: a model disease for systemic autoimmunity. *Clin Exp Immunol* 2014;175:17–24.
- Wang BX, Grover SA, Kannu P, Yoon G, Laxer RM, Yeh EA, et al. Interferon-stimulated gene expression as a preferred biomarker for disease activity in Aicardi-Goutieres syndrome. *J Interferon Cytokine Res* 2017;37:147–52.
- Rice GI, Forte GM, Szykiewicz M, Chase DS, Aeby A, Abdel-Hamid MS, et al. Assessment of interferon-related biomarkers in Aicardi-Goutieres syndrome associated with mutations in *TREX1*, *RNASEH2A*, *RNASEH2B*, *RNASEH2C*, *SAMHD1*, and *ADAR*: a case-control study. *Lancet Neurol* 2013;12:1159–69.

6. Fremont ML, Rodero MP, Jeremiah N, Belot A, Jeziorski E, Duffy D, et al. Efficacy of the Janus kinase 1/2 inhibitor ruxolitinib in the treatment of vasculopathy associated with TMEM173-activating mutations in 3 children. *J Allergy Clin Immunol* 2016;138:1752–5.
7. Meesilpavikkai K, Dik WA, Schrijver B, Nagtzaam NM, Posthumus-van Sluijs SJ, van Hagen PM, et al. Baricitinib treatment in a patient with a gain-of-function mutation in signal transducer and activator of transcription 1 (STAT1). *J Allergy Clin Immunol* 2018;142:328–30.
8. Dale RC, Gornall H, Singh-Grewal D, Alcausin M, Rice GI, Crow YJ. Familial Aicardi-Goutieres syndrome due to SAMHD1 mutations is associated with chronic arthropathy and contractures. *Am J Med Genet A* 2010;152A:938–42.
9. Brkic Z, Maria NI, van Helden-Meeuwse CG, van de Merwe JP, van Daele PL, Dalm VA, et al. Prevalence of interferon type I signature in CD14 monocytes of patients with Sjogren's syndrome and association with disease activity and BAFF gene expression. *Ann Rheum Dis* 2013;72:728–35.
10. Clark JD, Flanagan ME, Telliez JB. Discovery and development of Janus kinase (JAK) inhibitors for inflammatory diseases. *J Med Chem* 2014;57:5023–38.

DOI 10.1002/art.40839

Clinical Images: Heel pain in a young patient—calcaneal involvement in juvenile spondyloarthritis



The patient, an 11-year-old boy, presented with left heel pain and mild fever. He had recently experienced diffuse arthralgias of the right knee, costochondral junctions, and both ankles. Laboratory findings were normal except for a slightly increased erythrocyte sedimentation rate. Magnetic resonance imaging (MRI) of the left heel was performed. On T1-weighted and fat-suppressed T2-weighted MRI sequences, bone marrow edema with indistinct margins was seen at the posterior margin of the calcaneus, above the growth plate, and below its posterior and superior cortex (**A** and **B**) (arrows). The shape of the apophysis was preserved. Enhancement was seen in the area of the bone marrow edema after gadolinium injection (**C**) (arrow), and the calcaneal bursa was also enhanced. This pattern of marrow changes differed from the thin high-signal-intensity strip normally seen along the growth plate at this age and from the normal variant of scattered patchy areas sometimes present in the posterior calcaneus (**D** and **E**) (arrows) (1). Sever's disease was ruled out as it mainly affects the secondary ossification center. Spondyloarthritis was diagnosed based on the calcaneal bone marrow edema and the involvement of the adjacent soft tissues below the Achilles tendon in a clinical context of diffuse arthralgias. This case illustrates calcaneal involvement in juvenile spondyloarthritis, which consisted of bone marrow edema and gadolinium enhancement involving the superior area of the posterior calcaneus above the secondary ossification center as well as the calcaneal bursa. Interestingly, in this patient, bone marrow changes predominated in the superior part of the posterior calcaneus at the level of the periosteal fibrocartilage located above the secondary ossification center and the Achilles entheses (2).

1. Rossi I, Rosenberg Z, Zember J. Normal skeletal development and imaging pitfalls of the calcaneal apophysis: MRI features. *Skeletal Radiol* 2016;45:483–93.
2. Benjamin M, McGonagle D. The anatomical basis for disease localisation in seronegative spondyloarthropathy at entheses and related sites. *J Anat* 2001;199:503–26.

Stacey Lallemand, MD
Jean-Denis Laredo, MD, MS
Lariboisière Hospital
Paris, France

LETTERS

DOI 10.1002/art.40823

Galectin 9: friend or foe of systemic lupus erythematosus? Comment on the article by Zeggar et al

To the Editor:

Systemic lupus erythematosus (SLE) is a complex, multisystem autoimmune disease with considerable clinical and immunologic heterogeneity. The hallmark of SLE is the presence of autoreactive antibodies. Available evidence suggests that genetic factors, immune dysregulation, and environmental factors (such as ultraviolet radiation) may be involved in the pathogenesis of SLE (1). However, the clear pathophysiology of SLE has not been elucidated.

We read with interest the recent article by Zeggar et al (2) describing their study which showed that galectin 9 (Gal-9) deficiency protects against lupus in mice, whereas in wild-type mice injected with pristane, lupus was induced, manifesting with glomerulonephritis, arthritis, and peritoneal lipogranuloma formation. The authors concluded that Gal-9 is required for lupus development, and antagonism of Gal-9 is beneficial for the treatment of lupus. In our opinion, the evidence is too preliminary to make this determination. Findings of current studies about the role of Gal-9 in lupus are inconsistent (2–6). Van den Hoogen et al showed that serum levels of Gal-9, CXCL10, and tumor necrosis factor receptor type II (TNFRII) were elevated in patients with SLE and correlated with disease activity and tissue factor expression (4). Gal-9 correlated more strongly than CXCL10 or TNFRII with the interferon (IFN) score and was superior to CXCL10 or TNFRII in detecting the IFN signature in patients with SLE, suggesting that it may be a biomarker for SLE (4). Similarly, Jiao et al reported that serum levels of Gal-9 were higher in SLE patients compared with healthy controls (5). Expression of Gal-9 on CD4+ T cells, CD8+ T cells, and CD56+ T cells was also elevated in SLE patients. Gal-9 expression was significantly related to Systemic Lupus Erythematosus Disease Activity Index scores (6). Gal-9–blocking antibody significantly inhibited CD3-stimulated peripheral blood mononuclear cell proliferation and the release of Th1-derived cytokines (interleukin-2 [IL-2], IFN γ , and TNF), Th2-derived cytokines (IL-4 and IL-10), and Th17-derived cytokine (IL-17A) in patients with SLE (5).

However, in a study by Moritoki et al, lupus-prone MRL/lpr mice injected intraperitoneally with Gal-9 had a reduced frequency of Th1, Th17, and activated CD8+ T cells (7). It suppressed anti–double-stranded DNA antibody production and decreased the number of plasma cells by inducing plasma cell apoptosis. BXSB/MpJ and (NZB \times NZW)F1 mice administered Gal-9 had reduced Toll-like receptor 7 (TLR-7)–mediated autoimmune manifestations, such as reduced splenomegaly, proteinuria, glomerular nephritis, and antinuclear autoantibody levels.

Gal-9 administration inhibited the phenotypic maturation of plasmacytoid dendritic cells and B cells and abrogated their ability to mount cytokine responses to TLR-7/TLR-9 ligands (3).

Therefore, the role of Gal-9 in lupus remains unclear. How it contributes to or inhibits lupus development, and whether it can be used as a biomarker for SLE, requires further investigation.

Supported by the National Natural Science Foundation of China (grant 81701606).

Wang-Dong Xu, MD
Southwest Medical University
Luzhou, China
Lin-Chong Su, MD
Affiliated Minda Hospital of Hubei
Institute for Nationalities
Enshi, China
An-Fang Huang, MD
Affiliated Hospital of Southwest
Medical University
Luzhou, China

1. Lisnevskaja L, Murphy G, Isenberg D. Systemic lupus erythematosus. *Lancet* 2014;384:1878–88.
2. Zeggar S, Watanabe KS, Teshigawara S, Hiramatsu S, Katsuyama T, Katsuyama E, et al. Role of Lgals9 deficiency in attenuating nephritis and arthritis in BALB/c mice in a pristane-induced lupus model. *Arthritis Rheumatol* 2018;70:1089–101.
3. Panda SK, Facchinetti V, Voynova E, Hanabuchi S, Karnell JL, Hanna RN, et al. Galectin-9 inhibits TLR7-mediated autoimmunity in murine lupus models. *J Clin Invest* 2018;128:1873–87.
4. Van den Hoogen LL, van Roon JAG, Mertens JS, Wienke J, Lopes AP, de Jager W, et al. Galectin-9 is an easy to measure biomarker for the interferon signature in systemic lupus erythematosus and antiphospholipid syndrome. *Ann Rheum Dis* 2018;77:1810–14.
5. Jiao Q, Qian Q, Zhao Z, Fang F, Hu X, An J, et al. Expression of human T cell immunoglobulin domain and mucin-3 (TIM-3) and TIM-3 ligands in peripheral blood from patients with systemic lupus erythematosus. *Arch Dermatol Res* 2016;308:553–61.
6. Bombardier C, Gladman DD, Urowitz MB, Caron D, Chang DH, and the Committee on Prognosis Studies in SLE. Derivation of the SLEDAI: a disease activity index for lupus patients. *Arthritis Rheum* 1992;35:630–40.
7. Moritoki M, Kadowaki T, Niki T, Nakano D, Soma G, Mori H, et al. Galectin-9 ameliorates clinical severity of MRL/lpr lupus-prone mice by inducing plasma cell apoptosis independently of Tim-3. *PLoS One* 2013;8:e60807.

DOI 10.1002/art.40822

Reply

To the Editor:


We thank Dr. Xu and colleagues for their interest in our study in which we observed beneficial effects of *Lgals9* deficiency in a

pristane-induced lupus model in BALB/c mice. Xu et al raised questions on the discrepancy of results between our study and previous publications reporting the protective effects of recombinant Gal-9 in MRL/lpr lupus-prone mice (1) and BXSB/MpJ and (NZB × NZW)F1 mice (2). Similar questions were also raised by others (3,4).

First, the dose-effect relationship of immune responses induced by physiologic, pathologic, and pharmacologic concentrations of Gal-9 may not be linear. Pathologically up-regulated concentrations of Gal-9 in SLE may efficiently crosslink the cell surface glycoprotein receptors, and Gal-9 promotes the survival and activation of immune-mediated cells such as Th1, Th17, and CD8+ T cells as well as plasmacytoid dendritic cells (PDCs) via the TLR-7/TLR-9 signaling pathway. A pharmacologic excess amount of Gal-9 completely occupies β -galactoside residues on cell surface glycoproteins and inhibits glycoprotein lattice formation, which may result in the inhibition of Th1, Th17, and CD8+ T cells and cytokine production in PDCs. Prominent reduction of lipogranuloma in pristane-injected *Lgals9*-deficient BALB/c mice suggests that Gal-9 is required for the development of autoimmune responses, at least in this model.

Second, the intervention studies in lupus animal models were conducted by injecting recombinant Gal-9 protein, and the extracellular application of Gal-9 has been specifically directed. In physiologic states, Gal-9 is abundantly expressed in cytoplasm and is secreted out as damage-associated molecular patterns, such as dengue virus-infected THP-1 cells (5). *Lgals9*-deficient BALB/c mice lack intracellular Gal-9, and inhibition of the intracellular function of Gal-9 may also be beneficial in the treatment of human SLE.

In view of the above, we speculate that inhibition of Gal-9 function, as well as administration of recombinant Gal-9 protein, may both be beneficial in the treatment of SLE. The reported plasma and serum concentrations of Gal-9 in human samples have varied considerably because some commercial enzyme-linked immunosorbent assay (ELISA) systems recognize degraded Gal-9 (6). Development of further accurate ELISAs would facilitate the evaluation of Gal-9 as a biomarker for SLE. In addition, we expect that the application of neutralizing antibodies against human Gal-9 (7) would facilitate drug discovery in autoimmune diseases.

Jun Wada, MD, PhD 
 Sonia Zeggar, MD, PhD
 Okayama University Graduate
 School of Medicine, Dentistry,
 and Pharmaceutical Sciences
 Okayama, Japan

1. Moritoki M, Kadowaki T, Niki T, Nakano D, Soma G, Mori H, et al. Galectin-9 ameliorates clinical severity of MRL/lpr lupus-prone mice by inducing plasma cell apoptosis independently of Tim-3. *PLoS One* 2013;8:e60807.

2. Panda SK, Facchinetti V, Voynova E, Hanabuchi S, Karnell JL, Hanna RN, et al. Galectin-9 inhibits TLR7-mediated autoimmunity in murine lupus models. *J Clin Invest* 2018;128:1873–87.
3. Panda AK, Das BK. Perplexing role of galectin 9 in experimental lupus models: comment on the article by Zeggar et al [letter]. *Arthritis Rheumatol* 2018;70:1530–1.
4. Wada J, Zeggar S. Reply [letter]. *Arthritis Rheumatol* 2018;70:1531–2.
5. Dapat IC, Pascapurnama DN, Iwasaki H, Labayo HK, Chagan-Yasutan H, Egawa S, et al. Secretion of galectin-9 as a DAMP during dengue virus infection in THP-1 Cells. *Int J Mol Sci* 2017;18:E1644.
6. Niki T, Fujita K, Rosen H, Hirashima M, Masaki T, Hattori T, et al. Plasma galectin-9 concentrations in normal and diseased condition. *Cell Physiol Biochem* 2018;50:1856–68.
7. Lhuillier C, Barjon C, Baloché V, Niki T, Gelin A, Mustapha R, et al. Characterization of neutralizing antibodies reacting with the 213-224 amino-acid segment of human galectin-9. *PLoS One* 2018;13:e0202512.

DOI 10.1002/art.40837

More comprehensive considerations in assessing the safety of treatments during pregnancy: comment on the editorial by Pope

To the Editor:

I read with interest a recent editorial by Dr. Pope reflecting on the hurdles in evaluating drug safety during pregnancy (1). In the same issue of *Arthritis & Rheumatology*, Clowse et al discussed updated data from a prospective follow-up of pregnant women exposed to certolizumab pegol (CZP) (2). Addressing weaknesses in surveillance data sources, Pope stresses the need for substantial improvements in assessment of treatment risks during pregnancy. I would like to further emphasize the need to approach exposure and risks from a new perspective, so patients can be more fully informed.

Observation of events is the principal instrument of epidemiologic studies on the impact of environmental toxins on large populations. However, given that most drugs considered for their use during pregnancy have been reasonably proved as nontoxic, different effects of exposure need to be explored. Moreover, there is a notable distinction between lack of toxicity and safety, the latter not measurable by epidemiologic methods alone, as Gabucio and I have commented on previously (3). Pregnancy outcomes, though meaningful, are not enough to ascertain safety. As discussed in Pope's editorial, we should aspire to measure not only malformations in a developing fetus, but also the impact of exposure on susceptibility to and occurrence of common conditions later in life (such as behavioral alterations, premature aging disorders, or infertility), that cannot be determined at the time of delivery.

Drugs, along with other bioactive compounds, may also elicit cell adaptation responses in a growing fetus, which has the plasticity to modify its epigenetic programming in response to environmental cues (4). Interestingly, cell adaptation responses can be triggered within a threshold lower than toxic actions, but prolonged exposure able to cause a stable environmental signal, such as long-term drug administration, is usually required. In the case of tumor necrosis factor inhibitors (TNFi), data drawn from preclinical models are reassuring, and a favorable risk profile can be forecast. Nonetheless, the benefit of TNF inhibition relies on increased cytokine activity in patients, though this effect cannot be translated to the abrogation of its homeostasis levels, as is probably the case in the patients' offspring. Indeed, TNF displays pleiotropic actions, including some specifically related to development (5), and its receptors have a widespread tissue distribution. At this time, not all of these actions have been completely deciphered, making it difficult to ascertain what consequences may be derived from in utero exposure to TNFi agents.

Perhaps the most relevant factor that requires investigation is whether placental transfer occurs (and if so, when), as this would provide an actual measure of exposure. Lack of placental transfer, at least during part of the pregnancy, might be the case with CZP treatment, and lack of transfer by itself would support the notion of its safety. Placental transfer makes timing of exposure critical, since exposed offspring are highly vulnerable from preconception to delivery (6). The complexity of human cell growth and differentiation programs is far from completely elucidated. Moreover, the conceptus is environment-sensitive and carries next-generation germ cells engaged in their own proliferation and migration programs, meaning that in fact there are 3 patients, and not just 2, to consider.

In order to have objective information about the full risks of drug exposure in pregnancy, we need more insight on the critical pharmacokinetic/pharmacodynamic aspects of exposure as well as further studies on the possible modifications of epigenetic patterns in embryonic tissue. To advance the assessment of drug safety in pregnancy, both clinicians and mothers should be aware of the importance of cord blood and cord tissue donation at delivery, as well as patient participation in surveillance registries. In the meantime, it would be preferable to limit prescription during pregnancy to patients with highly active disease and in whom the risk/benefit balance is unquestionably favorable.

Olga Sánchez-Pernaute, MD, PhD
*Jiménez Díaz Foundation University
 Hospital and Research Institute
 and Autonomia University
 Madrid, Spain*

1. Pope JE. Safety of tumor necrosis factor inhibitors in pregnancy [editorial]. *Arthritis Rheumatol* 2018;70:1359–63.
2. Clowse ME, Scheuerle AE, Chambers C, Afzali A, Kimball AB, Cush JJ, et al. Pregnancy outcomes after exposure to certolizumab pegol: updated results from a pharmacovigilance safety database. *Arthritis Rheumatol* 2018;70:1399–407.
3. Sánchez-Pernaute O, Gabucio A. Epigenetics and complex diseases: a new era in the assessment of exposure and risk? [editorial]. *Rheumatology (Oxford)* 2018;57:1693–4.
4. Feinberg AP, Fallin MD. Epigenetics at the crossroads of genes and the environment. *JAMA* 2015;314:1129–30.
5. AceView. Gene: TNF, a comprehensive annotation of human, mouse and worm genes with mRNA or ESTsAceView. URL: <https://www.ncbi.nlm.nih.gov/iebr/research/acembly/av.cgi?db=human&c=Gene&l=TNF>.
6. Hochberg Z, Feil R, Constancia M, Fraga M, Junien C, Carel JC, et al. Child health, developmental plasticity, and epigenetic programming. *Endocr Rev* 2011;32:159–224.

DOI 10.1002/art.40836

Reply

To the Editor:

I thank Dr. Sánchez-Pernaute for her interest in my editorial on safety of drugs in pregnancy. I agree in part that lack of toxicity in registries/databases does not imply full safety, as well as with other points raised in the discussion of the editorial and the report by Clowse et al about the safety of CZP in pregnancy (1). In fact, one cannot easily prove a cause-and-effect relationship involving drugs or rheumatic diseases causing harm to the fetus, or during later development.

Sir Austin Bradford Hill postulated that causality could be presumed using epidemiologic factors, such as strength of an association (a larger effect may be more likely, but not necessarily, causal), consistency of the literature, specificity (i.e., a specific exposure in a specific population yielding a result with no other likely explanation), temporality (the outcome occurs after the exposure), biologic gradient (dose response), plausibility of results, and coherence of epidemiologic and laboratory or in vitro data (2). These ideas are helpful in assessing cause and effect but cannot prove an association. For example, there may be a small exposure with a large effect occurring only rarely, such as pregnant women exposed to diethylstilbestrol (DES), an estrogen drug used to prevent abortions, and their daughters who were observed to have an increased chance of a rare vaginal carcinoma (transitional cell cancer); moreover, some offspring of the daughters of women exposed to DES also had some abnormalities (3). This is difficult to explain with a temporal association, and even biologic plausibility, of DES exposure in utero causing cancer decades later, which is very remote from the exposure. A recent editorial by Sánchez-Pernaute and Gabucio suggested that, considering epigenetic

changes that may occur with drug exposures in pregnant women, other studies to demonstrate safety to offspring in utero and during childhood are important (4). However, if an event from drug exposure in utero is quite latent, it is very challenging to determine cause and effect even with more advanced epigenetic studies.

The other difficulty of attributing causality when associations are found between mothers exposed to a certain medication or drug class and abnormalities in their babies is the lack of a diseased control group in cases where the association could be from the disease, drug, both, or neither.

When determining the safety of a medication during pregnancy, when many drug exposures could occur at once (such as use of nonsteroidal antiinflammatory drugs, glucocorticoids, immunosuppressive drugs, and biologic medications), there are multiple factors that could affect the ability to ascertain the true risk of one drug. Among those are the timing of the exposure, other factors contributing to risk (e.g., genetic risk, specific disease, disease activity), and even performance of assessments in which multiple drugs are analyzed as a group. For instance, the biologic agent infliximab differs from subcutaneous TNFi biologics, as it is dosed very differently and given intravenously, and other TNFi agents may or may not cross the placenta at different times during pregnancy. CZP does not result in any significant placental transfer, which may be related to its large size due to PEGylation (1).

In summary, there will never be enough data to fully rule out potential harm from many medications used in pregnancy, as there is potential confounding with respect to prescribing (channeling bias), and for ethical reasons, randomized trials will not be performed to study the safety of treatment versus no treatment for a rheumatic disease during pregnancy. Even if a trial was done, it could not be powered to fully rule out a small risk. However, it is important to balance the need for well-controlled disease to enable a fetus to grow and thrive while also allowing for the mother's quality of life during pregnancy, as opposed to complete avoidance of all medications during pregnancy. Mothers need to know, using the best data available, the risks and benefits of medications used in pregnancy (as well as prior to conception and during breastfeeding) in order to make informed choices with respect to treatment. As health care providers, it is our duty to be aware of guidelines to inform the choices of our patients and to champion research so as to answer questions about safety in pregnancy.

Janet E. Pope, MD, MPH, FRCPC
St. Joseph's Health Care London
London, Ontario, Canada

1. Clowse ME, Scheuerle AE, Chambers C, Afzali A, Kimball AB, Cush JJ, et al. Pregnancy outcomes after exposure to certolizumab pegol: updated results from a pharmacovigilance safety database. *Arthritis Rheumatol* 2018;70:1399–407.

2. Hill AB. The environment and disease: association or causation? *Proc R Soc Med* 1965;58:295–300.
3. Al Jishi T, Sergi C. Current perspective of diethylstilbestrol (DES) exposure in mothers and offspring. *Reprod Toxicol* 2017;71:71–7.
4. Sánchez-Pernaute O, Gabucio A. Epigenetics and complex diseases: a new era in the assessment of exposure and risk? [editorial]. *Rheumatology (Oxford)* 2018;57:1693–4.

DOI 10.1002/art.40825

Childhood- versus adult-onset Takayasu arteritis: are they really different? Comment on the article by Aeschlimann et al

To the Editor:

Takayasu arteritis (TAK) is a large vessel vasculitis of unknown origin that mainly occurs in young females and can manifest for the first time in childhood. Clinical expression of TAK may differ depending on the age at onset of disease. In a study recently published in *Arthritis & Rheumatology*, Aeschlimann et al compared clinical features and outcomes and efficacy and safety of immunosuppressive treatment in North American patients with childhood-onset ($n = 29$) and adult-onset ($n = 48$) TAK (1). Those with childhood-onset TAK were less frequently female, had more frequent involvement of the aorta and renal arteries, and had more arterial hypertension at presentation compared with those with adult-onset TAK. On the other hand, those with adult-onset TAK more frequently presented with subclavian artery lesions, claudication, decreased pulses of the upper extremities, and arthritis/arthralgia.

The clinical significance of the difference in the occurrence of arthritis/arthralgia between patients with childhood-onset TAK and those with adult-onset TAK (29% and 7%, respectively) is doubtful given the similar rate of constitutional symptoms (i.e., malaise, weight loss, fever, and night sweats) in the 2 cohorts. Laboratory signs of inflammation (increased erythrocyte sedimentation rate [ESR] and C-reactive protein level and anemia) were also found in similar proportions of pediatric and adult patients with TAK. Twenty-four percent of children with TAK were males, while all adult patients were females. The proportion of males was also high (up to 30%) in several other small cohorts of patients with childhood-onset TAK (2,3), while in adult populations it usually did not exceed 12–13% (4–6). However, the percentage of males was higher (16%) in our own cohort of 128 adult patients with TAK. A higher occurrence of renal artery stenosis and arterial hypertension were the most striking distinctive features of childhood-onset TAK in the study by Aeschlimann et al. Of note, similar data were reported by other investigators (2,3,7). It is difficult to explain the mechanism of difference in the pattern of vascular inflam-

mation between childhood-onset and adult-onset TAK if it is unrelated to bias.

The relapse rate within the first year of follow-up was high, both in pediatric patients with TAK and in adult patients with TAK. There was a trend toward a more severe and refractory course of disease in patients with childhood-onset TAK despite more aggressive initial immunosuppressive treatment that frequently included cyclophosphamide, methotrexate, and tumor necrosis factor (TNF) inhibitors. The course of childhood-onset TAK was also unfavorable in the largest study reported so far from South India. In this cohort, sustained remission at 5 years was achieved in only 29% of 40 pediatric patients, while new areas of vessel involvement developed in 38% of patients (2).

In summary, the study by Aeschlimann et al and several other studies suggest that childhood-onset TAK has certain distinctive clinical features differentiating it from the adult-onset phenotype, although apparent limitations of the studies (small samples, retrospective design, and relatively short follow-up periods) preclude any definite conclusions. Therefore, it is still unclear whether childhood-onset and adult-onset forms of TAK are really different from each other given the heterogeneity of disease presentation in general. It is particularly difficult to explain the difference between the distributions of affected arteries between pediatric and adult patients.

Any data should be interpreted from the perspective of treatment. Aeschlimann et al found a trend toward a more severe course of childhood-onset TAK compared with the adult-onset phenotype. These results may justify more aggressive initial immunosuppression in pediatric patients with TAK. Of note, 17% of children with TAK started treatment with cyclophosphamide in addition to glucocorticoids. In our opinion, the use of cyclophosphamide, even in more severe cases, should be avoided in children and can be replaced with less toxic medications like methotrexate, TNF inhibitors, or tocilizumab. A significant proportion of patients with TAK ultimately require biologic therapy. In our cohort, almost 20% of adult patients are currently treated with TNF inhibitors (infliximab, adalimumab, or certolizumab pegol) or tocilizumab. It is currently unknown whether biologic agents should be prescribed earlier (within the “window of opportunity”) or whether they should be reserved for second-line therapy in patients with disease refractory to standard immunosuppressive medications. In contrast to cyclophosphamide or methotrexate, TNF and interleukin-6 inhibitors do not impair reproductive potential and can be useful in younger patients with TAK. Certolizumab pegol seems to be a particularly promising treatment for young females with TAK given its very low potential to cross the placenta and the consequent safety of its use during a potential pregnancy (8).

TAK is an uncommon disease, and childhood-onset TAK occurs even more rarely. Therefore, we should not expect that larger studies will be conducted or that evidence-based guidelines

for treatment of TAK in children will be available in the near future. From a diagnostic perspective, the message is clear: pediatricians should include TAK in the evaluation of pediatric patients with arterial hypertension, particularly in the presence of elevated ESR and/or C-reactive protein level.

Supported by Russian Academic Excellence Project 5-100.

Sergey Moiseev, MD 
 Sechenov First Moscow State Medical University
 Ilya Smitienko, MD
 Medical Center K+31
 Alexander Kulikov, MD
 Lomonosov Moscow State University
 Pavel Novikov, MD
 Sechenov First Moscow State Medical University
 Moscow, Russia

1. Aeschlimann FA, Barra L, Alsolaimani R, Benseler SM, Hebert D, Khalidi N, et al. Presentation and disease course of childhood-onset versus adult-onset Takayasu arteritis. *Arthritis Rheumatol* 2019;71:315–23.
2. Goel R, Kumar TS, Danda D, Joseph G, Jeyaseelan V, Surin AK, et al. Childhood-onset Takayasu arteritis—experience from a tertiary care center in South India. *J Rheumatol* 2014;41:1183–9.
3. Eleftheriou D, Varnier G, Dolezalova P, McMahon AM, Al-Obaidi M, Brogan PA. Takayasu arteritis in childhood: retrospective experience from a tertiary referral centre in the United Kingdom. *Arthritis Res Ther* 2015;17:36.
4. Schmidt J, Kermani TA, Bacani AK, Crowson GS, Cooper LT, Matteson EL, et al. Diagnostic features, treatment, and outcomes of Takayasu arteritis in a US cohort of 126 patients. *Mayo Clin Proc* 2013;88:822–30.
5. Bicakcigil M, Aksu K, Kamali S, Ozbalkan Z, Ates A, Karadag O, et al. Takayasu's arteritis in Turkey—clinical and angiographic features of 248 patients. *Clin Exp Rheumatol* 2009;27 Suppl 52:S59–64.
6. Mirouse A, Biard L, Comarmond C, Lambert M, Mekinian A, Farfar Y, et al. Overall survival and mortality risk factors in Takayasu's arteritis: a multicenter study of 318 patients. *J Autoimmun* 2019;96:35–9.
7. Jales-Neto LH, Levy-Neto M, Bonfa E, de Carvalho JF, Pereira RM. Juvenile-onset Takayasu arteritis: peculiar vascular involvement and more refractory disease. *Scand J Rheumatol* 2010;39:506–10.
8. Novikov PI, Smitienko IO, Sokolova MV, Alibaz-Oner F, Kaymaz-Tahra S, Direskeneli H, et al. Certolizumab pegol in the treatment of Takayasu arteritis. *Rheumatology (Oxford)* 2018;57:2101–5.

DOI 10.1002/art.40824

Reply

To the Editor:

We thank Dr. Moiseev and colleagues for their interest in our article and for sharing their experience of 128 adult patients with TAK. Enabling a rapid diagnosis and making the best possible treatment decision at the bedside are the key motivating factors for the many dedicated teams of researchers around the world studying TAK in children and adults. In our series, we

explored the hypothesis that comparison of pediatric and adult TAK cohorts focusing on associated clinical phenotypes, vascular involvement, and treatment outcomes may provide additional insights into our understanding of TAK. We thank Dr. Moiseev and colleagues for summarizing the corresponding evidence generated by their team and in the published literature.

As with all studies of rare diseases, the specific study context is critically important, including the study time frame, the background population, exposures, patient comorbidities, and overall access of patients to care and medications. In our study, we reported the comparison of an ethnically diverse group of children and adults with TAK cared for at tertiary care centers in a health care system with equal access to health care, that of Canada. The difference in rates of arthritis may reflect a difference in TAK biology or it may be the result of bias, since the authors are pediatric rheumatologists and not cardiologists, or it may simply reflect the fact that joint symptoms are more uncommon in children than in adults overall.

Clinical symptoms paired with increased markers of inflammation typically prompt an evaluation for TAK, including vascular imaging. Additional symptoms such as arthritis may in fact be misleading; however, the documentation of their frequency in patients ultimately diagnosed as having TAK may be helpful for pediatric and adult rheumatology arthritis experts working their way through the differential diagnosis of primary inflammatory diseases with arthritis. In Canada, we are fortunate to be able to access advanced imaging modalities for all patients. We often require the setting of anesthesia and the capability to conduct serial lengthy, detailed studies to explore the extent of vascular involvement and its activity. We were hoping that sharing this information would be of value to the community of TAK care providers and researchers. As a result of our analysis, somewhat distinct vascular patterns appeared to evolve. This is supported by large cohort studies, including a recently reported series of 1,372 adult TAK patients, findings from which have suggested heterogeneity in vascular involvement and clinical features depending on age at onset, sex, and ethnic background (1–3). Consistent with our findings, a high prevalence of renal artery involvement and arterial hypertension has been observed throughout pediatric TAK series worldwide (4–9), while the reported prevalence is lower in adults (3,8,10). The cause of the heterogeneity observed between children and adults remains unclear.

The definition of distinct clinical and biologic phenotypes matters, particularly when it comes to treatment decisions. It would be desirable to match the severity of inflammation with the strength of the immunosuppressive medication, a treat-to-target approach that the entire TAK community is hoping to be able to use in the near future. On our way to treat-to-target, the search for clinical, biologic, and imaging biomarkers is critical, and we hope that our study has contributed to this search, sim-

ilar to the observations shared by Dr. Moiseev and the many other dedicated TAK researchers. We agree with Dr. Moiseev and colleagues that in the era of biologic therapies, the benefits and risks of cyclophosphamide should be carefully balanced. However, in real life TAK is often a relapsing–remitting disease in many patients, and failures of all available biologic agents are not infrequently seen, resulting in the need to revisit “older” medications. In our recently published single-center experience (11), cyclophosphamide was effective in controlling inflammation; however, methotrexate did not seem to control disease activity efficiently in childhood-onset TAK. Overall, biologic therapies (anti-TNF, anti-interleukin-6) resulted in higher rates of inactive disease.

In the future, multicenter collaborations, innovative trial designs, joint pediatric/adult cohorts, and associated biosamples may allow for better studies in TAK. The search for a better understanding of the biologic basis has to continue, and the reported differences in phenotypic presentation between childhood- and adult-onset TAK disease may serve as a nice launch point.

Florence A. Aeschlimann, MD, MPH
 Rae S. M. Yeung, MD, PhD
The Hospital for Sick Children
University of Toronto
 Toronto, Ontario, Canada
 Lillian Barra, MD, MPH
St. Joseph's Health Care London
University of Western Ontario
 London, Ontario, Canada
 Susanne M. Benseler, MD, PhD
Alberta Children's Hospital
University of Calgary
 Calgary, Alberta, Canada

1. Arnaud L, Haroche J, Limal N, Toledano D, Gambotti L, Costedoat Chalumeau N, et al. Takayasu arteritis in France: a single-center retrospective study of 82 cases comparing white, North African, and black patients. *Medicine (Baltimore)* 2010;89:1–17.
2. Cong XL, Dai SM, Feng X, Wang ZW, Lu QS, Yuan LX, et al. Takayasu's arteritis: clinical features and outcomes of 125 patients in China. *Clin Rheumatol* 2010;29:973–81.
3. Watanabe Y, Miyata T, Tanemoto K. Current clinical features of new patients with Takayasu arteritis observed from cross-country research in Japan: age and sex specificity. *Circulation* 2015;132:1701–9.
4. Brunner J, Feldman BM, Tyrrell PN, Kuemmerle-Deschner JB, Zimmerhackl LB, Gassner I, et al. Takayasu arteritis in children and adolescents. *Rheumatology (Oxford)* 2010;49:1806–14.
5. Eleftheriou D, Varnier G, Dolezalova P, McMahon AM, Al-Obaidi M, Brogan PA. Takayasu arteritis in childhood: retrospective experience from a tertiary referral centre in the United Kingdom. *Arthritis Res Ther* 2015;17:36.
6. Goel R, Kumar TS, Danda D, Joseph G, Jeyaseelan V, Surin AK, et al. Childhood-onset Takayasu arteritis—experience from a tertiary care center in South India. *J Rheumatol* 2014;41:1183–9.
7. Jales-Neto LH, Levy-Neto M, Bonfa E, de Carvalho JF, Pereira RM. Juvenile-onset Takayasu arteritis: peculiar vascular involvement and more refractory disease. *Scand J Rheumatol* 2010;39:506–10.

8. Schmidt J, Kermani TA, Bacani AK, Crowson CS, Cooper LT, Matteson EL, et al. Diagnostic features, treatment, and outcomes of Takayasu arteritis in a US cohort of 126 patients. *Mayo Clin Proc* 2013;88:822–30.
9. Szugye HS, Zeft AS, Spalding SJ. Takayasu Arteritis in the pediatric population: a contemporary United States-based single center cohort. *Pediatr Rheumatol Online J* 2014;12:21.
10. Park MC, Lee SW, Park YB, Lee SK. Serum cytokine profiles and their correlations with disease activity in Takayasu's arteritis. *Rheumatology (Oxford)* 2006;45:545–8.
11. Aeschlimann FA, Eng SW, Sheikh S, Laxer RM, Hebert D, Noone D, et al. Childhood Takayasu arteritis: disease course and response to therapy. *Arthritis Res Ther* 2017;19:255.

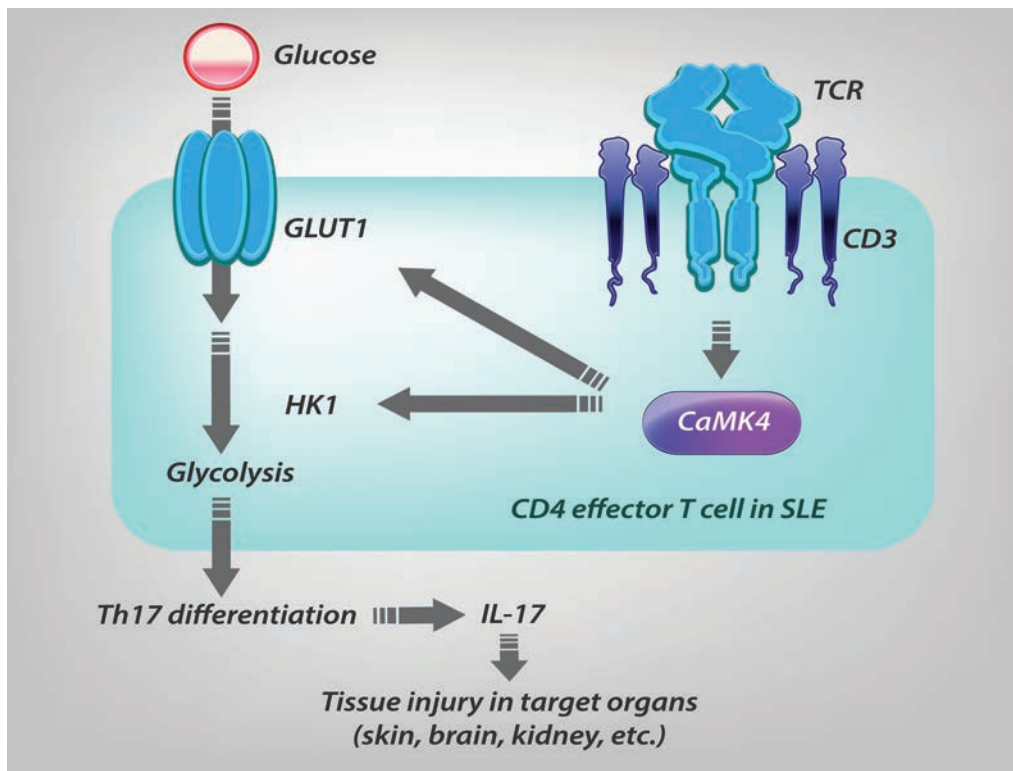
Clinical Connections

Promotion of Calcium/Calmodulin-Dependent Protein Kinase 4 by GLUT1-Dependent Glycolysis in Systemic Lupus Erythematosus

Koga et al, *Arthritis Rheumatol* 2019;71:766–772.

CORRESPONDENCE

Tomohiro Koga, MD, PhD: tkoga@nagasaki-u.ac.jp



KEY POINTS

- Glycolysis is critical for T cell effector functions, and increased glycolysis contributes to autoimmune responses.
- CaMK4 facilitates the glycolysis pathway during T cell activation.
- The expression of GLUT1 in effector memory CD4⁺ T cells was significantly higher in patients with active SLE.
- CaMK4 is a necessary element in GLUT1-dependent glycolysis, which promotes Th17 cell differentiation.

SUMMARY

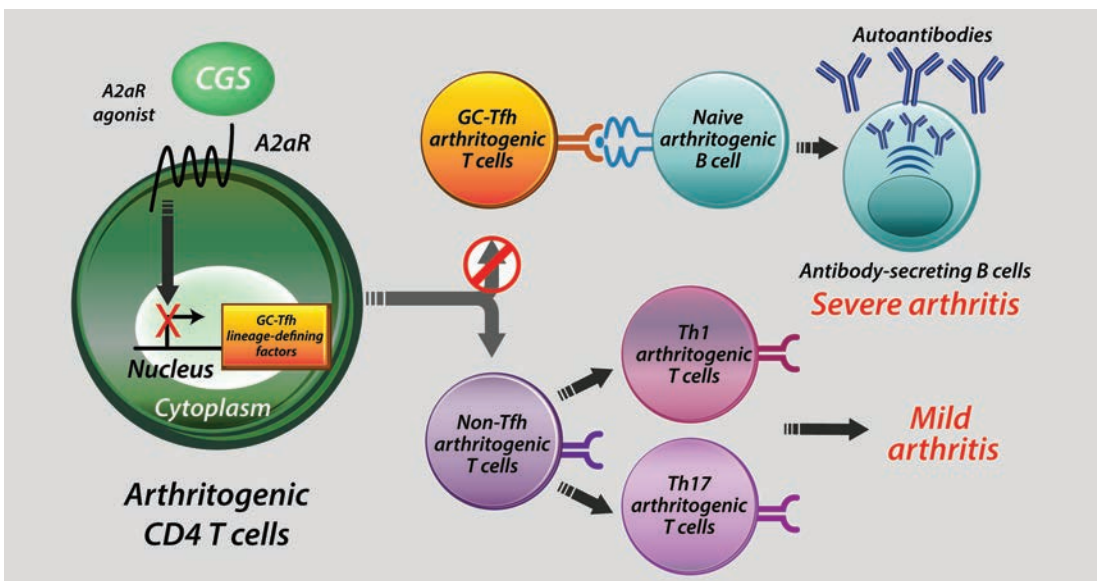
Patients with systemic lupus erythematosus (SLE) develop a T cell–driven immune response against ubiquitous autoantigens. For some time, it has been known that calcium/calmodulin-dependent protein kinase 4 (CaMK4) activity is abnormally increased in T cells from patients with SLE and lupus-prone mice. Metabolic pathways must be tightly regulated to allow normal proliferation and T cell effector function. In this study, Koga et al performed metabolomic profiling using capillary electrophoresis mass spectrometry in naive T cells from lupus-prone mice to explore the specific pathways involved in the CaMK4 signaling. The authors found that CaMK4 facilitated glycolysis but not the pentose phosphate pathway during T cell activation. CD4⁺ T cells treated with a CaMK4 inhibitor displayed decreased levels of glycolytic intermediates and suppression of the CaMK4–GLUT1 axis during T cell activation and Th17 cell differentiation. Importantly, the expression of GLUT1 and CaMK4 in CD4⁺ T cells correlated with disease activity in SLE, suggesting that CaMK4 may contribute to an aberrant expression of GLUT1 in T cells from patients with active SLE.

Adenosine 2a Receptor Signal Blockade of Murine Autoimmune Arthritis via Inhibition of Pathogenic Germinal Center–Follicular Helper T Cells

Schmiel et al, *Arthritis Rheumatol* 2019;71:773–783.

CORRESPONDENCE

Daniel L. Mueller, MD: muell002@umn.edu



SUMMARY

Methotrexate and sulfasalazine reduce chronic inflammatory arthritis symptoms and signs through the ability to enhance the extracellular accumulation of adenosine. An agonist (CGS-21680) of adenosine 2a receptors (A2aRs) also ameliorates disease activity in rodent models of arthritis. Nevertheless, the development of more targeted therapies designed to mimic A2aR signaling has been hindered by a lack of understanding regarding the identity of the adenosine-responsive cell. In this study, Schmiel et al demonstrate that CGS-21680 is shown to selectively interfere with the differentiation and accumulation of a germinal center (GC)–follicular helper T cell (Tfh) subset of CD4 T cells during the development of autoimmune arthritis. This A2aR-mediated block in GC-Tfh cell differentiation and protection from arthritis is accompanied by a decrease in the number of autoreactive B plasmablasts and a reduction in circulating autoantibody levels. Importantly, autoreactive CD4 T cells made genetically deficient for A2aRs still retain their ability to break immunologic tolerance in the autoreactive B cell compartment and elicit arthritis; however, the selective loss of A2aRs on CD4 T cells results in arthritogenic responses that are now resistant to CGS-21680. These data strongly suggest that binding of adenosine to A2aRs on autoreactive CD4 T cells abrogates the differentiation of a dangerous GC-Tfh cell subset, thus preventing the breakdown of B cell immune tolerance that underlies the development of autoimmune arthritis.

KEY POINTS

- Glucose-6-phosphate isomerase (GPI)–reactive GC-Tfh cells cooperate with GPI-specific B cells for the differentiation and expansion of GPI-binding plasmablasts, the secretion of anti-GPI antibody, and the development of disease activity in a mouse model of autoimmune arthritis.
- Treatment of mice with the A2aR agonist CGS-21680 inhibits the expression of Bcl-6 in autoreactive CD4 effector T cells, antagonizes their differentiation to the GC-Tfh fate, and limits their ability to cause arthritis.
- The presence of A2aRs on GPI-reactive CD4 T cells is necessary to achieve the immunosuppressive and antiarthritic effects of CGS-21680.

ACR Announcements

AMERICAN COLLEGE OF RHEUMATOLOGY
2200 Lake Boulevard NE, Atlanta, Georgia 30319-5312
www.rheumatology.org

ACR Meetings

Annual Meetings

November 8–13, 2019, Atlanta
November 6–11, 2020, Washington, DC

For additional information, contact the ACR office.

New ACR Journal Twitter Account (@ACR Journals) and Social Media Editor

The ACR journals are heightening our focus on social media, to benefit authors and readers. Among our first activities is the introduction of an official ACR Journals Twitter account: @ACR_Journals. Followers will enjoy special features and the opportunity to engage with authors and other fellow professionals about studies published in *Arthritis & Rheumatology*, *Arthritis Care & Research*, and *ACR Open Rheumatology*. Authors of published articles will have the opportunity to use @ACR_Journals to share their work and engage in dialogue with others interested in the research. The journals welcome Dr. Paul Sufka of Minneapolis as our first Social Media Editor.

Applications Invited for *Arthritis & Rheumatology* Editor-in-Chief (2020–2025 Term)

The American College of Rheumatology Committee on Journal Publications announces the search for the position of Editor, *Arthritis & Rheumatology*. The official term of the next *Arthritis & Rheumatology* editorship is July 1, 2020–June 30, 2025; however, some of the duties of the new Editor will begin during a transition period starting April 1, 2020. ACR members who are considering applying should submit a nonbinding letter of intent by May 1, 2019 to the Managing Editor, Jane Diamond, at jdiamond@rheumatology.org, and are also encouraged to contact the current Editor-in-Chief, Dr. Richard Bucala, to discuss details; initial contact should be made via e-mail to richard.bucala@yale.edu. Applications are due by June 21, 2019 and will be reviewed during the summer of 2019. Application materials are available on the ACR web site at <https://www.rheumatology.org/Learning-Center/Publications-Communications/Journals/A-R>.

Nominations for ACR Awards of Distinction and Masters Due May 15

The ACR has many Awards of Distinction, including the Presidential Gold Medal. Members who wish to nominate a colleague or

mentor for an Award of Distinction must complete the online form at www.rheumatology.org. The nomination process includes a letter of nomination, 2 additional letters of recommendation, and a copy of the nominee's curriculum vitae. Recognition as a Master of the American College of Rheumatology is one of the highest honors the ACR bestows. The designation of Master is conferred on ACR members age 65 or older who have made outstanding contributions to the field of rheumatology through scholarly achievements and/or service to their patients, students, and the profession. To nominate someone for a Master designation, members must complete the online nomination form at www.rheumatology.org and include a letter of nomination, 2 supporting letters from voting members of the ACR, and the nominee's curriculum vitae. Nominees for ACR Master must have reached the age of 65 before October 1, 2019.

ACR Invites Nominations for Volunteer Positions

The ACR encourages all members to participate in forming policy and conducting activities by assuming positions of leadership in the organization. Positions are available in all areas of the work of the American College of Rheumatology and the Rheumatology Research Foundation. Please visit www.rheumatology.org for information about nominating yourself or a colleague for a volunteer position with the College. The deadline for volunteer nominations is June 1, 2019. Letters of recommendation are not required but are preferred.

New Division Name

Rheumatology is truly a people specialty: We often develop lifelong relationships with our patients as well as our colleagues. We increasingly recognize that providing the best rheumatologic care requires a team effort. The collegial nature of our specialty is reflected in the ACR's mission statement: To empower rheumatology professionals to excel in their specialty.

In keeping with this mission, we are pleased to announce that our health professionals' membership division is changing its name to Association of Rheumatology Professionals (ARP). This name change highlights the dedication of the ACR to serve the entire rheumatology community. It also reflects our broadened base of interprofessional members (administrators, advanced practice nurses, health educators, nurses, occupational therapists, pharmacists, physical therapists, physician assistants, research teams, and more).

The name is new, but our commitment and promise remain the same: We are here for you, so you can be there for your patients.